THE ROLE OF THE BRAINSTEM AND CEREBELLUM IN AUTISM AND RELATED NEURODEVELOPMENTAL DISORDERS (DD)

EDITED BY: Eric London, Patricia Gaspar, Luis Puelles, Rubin Eduardo Jure and Randy J. Kulesza

PUBLISHED IN: Frontiers in Integrative Neuroscience

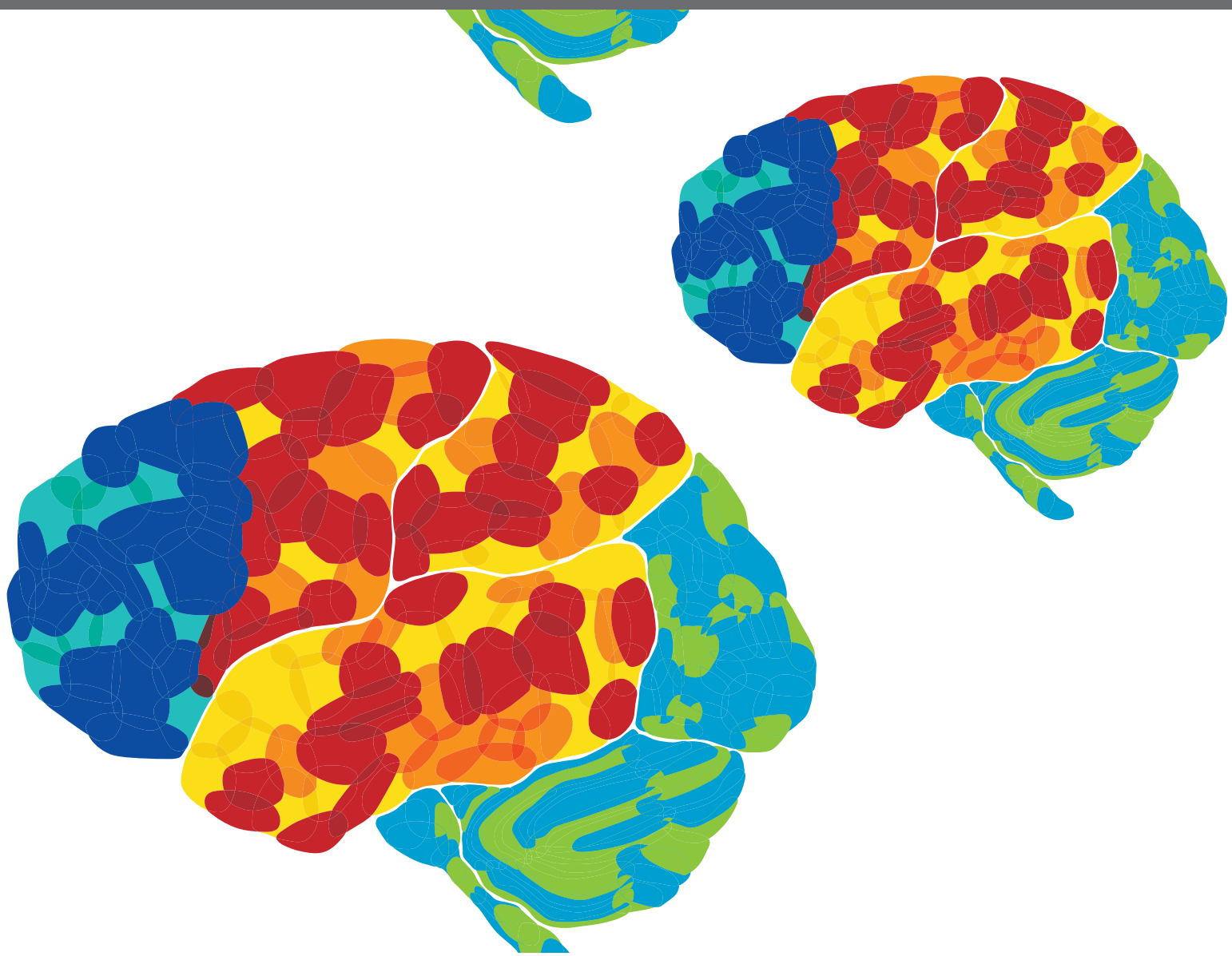

frontiers Research Topics

frontiers

ISSN 1664-8714
ISBN 978-2-83250-197-9
DOI 10.3389/978-2-83250-197-9

About Frontiers

Frontiers is more than just an open-access publisher of scholarly articles: it is a pioneering approach to the world of academia, radically improving the way scholarly research is managed. The grand vision of Frontiers is a world where all people have an equal opportunity to seek, share and generate knowledge. Frontiers provides immediate and permanent online open access to all its publications, but this alone is not enough to realize our grand goals.

Frontiers Journal Series

The Frontiers Journal Series is a multi-tier and interdisciplinary set of open-access, online journals, promising a paradigm shift from the current review, selection and dissemination processes in academic publishing. All Frontiers journals are driven by researchers for researchers; therefore, they constitute a service to the scholarly community. At the same time, the Frontiers Journal Series operates on a revolutionary invention, the tiered publishing system, initially addressing specific communities of scholars, and gradually climbing up to broader public understanding, thus serving the interests of the lay society, too.

Dedication to Quality

Each Frontiers article is a landmark of the highest quality, thanks to genuinely collaborative interactions between authors and review editors, who include some of the world's best academicians. Research must be certified by peers before entering a stream of knowledge that may eventually reach the public - and shape society; therefore, Frontiers only applies the most rigorous and unbiased reviews.
Frontiers revolutionizes research publishing by freely delivering the most outstanding research, evaluated with no bias from both the academic and social point of view. By applying the most advanced information technologies, Frontiers is catapulting scholarly publishing into a new generation.

What are Frontiers Research Topics?

Frontiers Research Topics are very popular trademarks of the Frontiers Journals Series: they are collections of at least ten articles, all centered on a particular subject. With their unique mix of varied contributions from Original Research to Review Articles, Frontiers Research Topics unify the most influential researchers, the latest key findings and historical advances in a hot research area! Find out more on how to host your own Frontiers Research Topic or contribute to one as an author by contacting the Frontiers Editorial Office: frontiersin.org/about/contact

THE ROLE OF THE BRAINSTEM AND CEREBELLUM IN AUTISM AND RELATED NEURODEVELOPMENTAL DISORDERS (DD)

Topic Editors:
Eric London, Institute for Basic Research in Developmental Disabilities (IBR), United States
Patricia Gaspar, Institut National de la Santé et de la Recherche Médicale (INSERM), France
Luis Puelles, University of Murcia, Spain
Rubin Eduardo Jure, Centro Privado de Neurología y Neuropsicología Infanto Juvenil WERNICKE, Argentina
Randy J. Kulesza, Lake Erie College of Osteopathic Medicine, United States

Citation: London, E., Gaspar, P., Puelles, L., Jure, R. E., Kulesza, R. J., eds. (2022). The Role of the Brainstem and Cerebellum in Autism and Related Neurodevelopmental Disorders (DD). Lausanne: Frontiers Media SA.
doi: 10.3389/978-2-83250-197-9

Table of Contents

frontiers | Frontiers in Integrative Neuroscience

TYPE Editorial
PUBLISHED 31 August 2022
DOI 10.3389/fnint.2022.957003

OPEN ACCESS

EDITED AND REVIEWED BY
Gerd Wagner,
University Hospital Jena, Germany

*CORRESPONDENCE
Eric London
naarlondon@gmail.com

RECEIVED 30 May 2022
ACCEPTED 27 July 2022
PUBLISHED 31 August 2022

CITATION
London E, Jure R, Gaspar P, Puelles L and Kulesza RJ (2022) Editorial: The role of the brainstem and cerebellum in autism and related neurodevelopmental disorders (DD). *Front. Integr. Neurosci.* 16:957003. doi: 10.3389/fnint.2022.957003

Editorial: The role of the brainstem and cerebellum in autism and related neurodevelopmental disorders (DD)

Eric London[1]*, Rubin Jure[2], Patricia Gaspar[3], Luis Puelles[4] and Randy J. Kulesza[5]

[1]Institute for Basic Research in Developmental Disabilities (IBR), Staten Island, NY, United States, [2]Centro Privado de Neurología y Neuropsicología Infanto Juvenil WERNICKE, Cordoba, Argentina, [3]INSERM U839 Institut du Fer à Moulin (IFM), Paris, France, [4]University of Murcia, Murcia, Spain, [5]Lake Erie College of Osteopathic Medicine, Erie, PA, United States

KEYWORDS

autism, brainstem, cerebellum, developmental disorders, hindbrain, midbrain

Editorial on the Research Topic
The role of the brainstem and cerebellum in autism and related neurodevelopmental disorders (DD)

An often-told story: One night, a man going into his favorite tavern saw a friend of his on all fours on the street in front of the tavern. "What are you doing?" "I lost my key" "Good luck finding it". Two hours later the man is leaving the tavern and his friend was still on all fours in the same place. "What are you doing?" "I lost my key" "I know, but you have been looking in the same place for 2 h it is not likely to be there" "I know, but I am under the only streetlight". Similarly, much of brain research chooses to look under the streetlight rather than where the key may be. The cortex and to some extent other forebrain structures are well lit. Large, near the surface, amenable to various types of scanning, imaging, and electrophysiology. The Brainstem until recently has been difficult to study in humans due to its small size, difficult to access location, and densely packed cells which have exuberant connectivity to all parts of the brain. As a phylogenetically persevered structure, it might seem that its role in a disorder of higher functioning which is unique to the human is unlikely. Recent as well as time-tested research, however, contradicts this, as hindbrain structures are known to be a crucial participant in nearly all cognitive functions. The brainstem, which is functioning early in fetal life, and is largely developed at birth, is crucial in the development of the higher centers (Joseph, 2000; Kohlmeier and Polli, 2020). Although once considered "hard wired" at birth, this isn't the case and the brainstem can exhibit high levels of plasticity itself (Kohlmeier and Polli, 2020). Speaking developmentally, cortical development could not proceed typically if there was aberrant functioning on the level of the hindbrain and midbrain structures. Despite research labeling various functions as belonging to some cortical area,

in reality, the circuits must include the brain stem and cerebellum. As the pathology and signs and symptoms of ASD and related developmental disorders remain largely unexplained, much like the lost key, we must broaden our search. The call for this special topic was generated by the desire to stimulate interest and research which includes these underexplored areas.

Of the midbrain and hindbrain structures, the cerebellum is the most studied in ASD and there is a growing literature to document cerebellar abnormalities in ASD. The role of the cerebellum in higher cognitive functions is no longer disputed. There is literature on the cerebellum's role in higher cognitive functioning dating back to the mid-19th century (Wang et al., 2014). Cerebellar abnormalities are among the most frequently reported findings in ASD and treatment directly aimed at cerebellar functioning is being explored (Stoodley et al., 2017). In this special topic, two studies expand on the role of the cerebellum in ASD. One endophenotype which has been advanced is the ability to integrate past experience into the predictive process in order to facilitate behavior including the complex behaviors needed for social skills. The role of the cerebellum in mediating these functions is reviewed in those with and without ASD by Frosch et al. Sensorimotor functioning is often not easily observable and also could be endophenotypes in ASD. Here McKinney et al. found increased force variability and saccade errors which correlated with localized cerebellar volumes.

Rather than conceptualizing ASD as a set of localized anomalous circuitry, many of the symptoms can be explained by deficits in neuromodulation (London, 2018). The brain's neuromodulators (dopamine, norepinephrine, serotonin, etc.) are centered in the brainstem their major centers such as the locus coeruleus, the ventral tegmental area, the substantia nigra, and the raphe nuclei. These areas have an extensive role in both brain function and development. Most of the medications which are used in psychiatry and in ASD mediate these neuromodulators. Dopamine neuron distribution and neurotransmission anomalies have been shown in several ASD animal models. Using valproic acid in embryonic domestic chicks, Adiletta et al., report that there is a rostro-caudal redistribution of dopamine neurons in the mesencephalon along with expression of genes linked to dopamine function in the septum, an area associated with social behavior. The Locus Coeruleus (LC) norepinephrine system has a growing body of literature to suggest its role in ASD. Keehn et al. report deficits in disengagement compared to typically developing peers, and this deficit was associated with increased resting pupil diameter suggestive of increased tonic activation of the LC.

The most highly developed literature on the brainstem in ASD pertains to the auditory system. A comprehensive review of the auditory and vestibular system by Mansour et al. with both anatomic and functional evidence makes a strong case for impairments in both systems at birth, and calls for tests of these two systems for as screenings to be done neonatally. The same group (Mansour and Kulesza), expanding on their previous work in which they found significant changes in neuron number and drastic dysmorphology in the superior olivary complex, found no changes in the Ventral Nucleus of the Trapezoid Body (VNTB) in ASD or the Valproate animal model. Here, they extended their work to show no changes in the ascending or descending tracts of the VNTB. Using the reports of sound localization deficits in ASD, which could lead to difficulty in the interpretation of complex sounds (language), Chokr et al. offer a hypothesis concerning the possibilities of the ASD-linked genes to cause developmental impairment of the Medial Nucleus of the Trapezoid Body. Möhrle et al. using the hypothesis of the excitation to inhibition ratio, and the Cntnap2 rat, measured auditory reactivity, filtering, and gating. They then treated with R-Baclofen (a GABA B agonist) and as a result, suggested that this medication could be useful for targeting sensory processing deficits in ASD. Chawla and McCullagh, reflecting on sensory sensitivities in the auditory system, specifically in Fragile X (in a knockout mouse), found that there is a deficit in high-frequency hearing and also an increased latency in the binaural interaction component in males, which is necessary for sound localization and could affect the processing of information.

Two papers suggest clinical tools for studying the brainstem in ASD. With the hypothesis of the centrality of brainstem functioning in ASD, Burstein and Geva present a review of brainstem-related markers which can be studied in early life. This would be able to anticipate the later occurring signs and symptoms which we are now using. These brainstem-related findings could serve to facilitate screening, prevention, and intervention. Acknowledging the difficulties in visualizing the brainstem and cerebellum, and therefore our inability to study brainstem in children (Guerrero-Gonzalez et al.) present a new scanning methodology which yields better visualization, improved microstructural property measurements, thus opening up the way for the study of the brainstem in ASD.

Two broad-based reviews of the role of the brainstem in ASD are in this special topic. In a systematic review of this topic, Seif et al. offer post-mortem studies, functional, neuroimaging, auditory brainstem response, pupillometry and eye tracking and cardiovascular autonomic monitoring is included, in addition to an array of animal models. In a review focusing on neuropathologic evidence for the brainstem's role in ASD (Baizer), three functions found in ASD were focused on; (1) motor control, (2) auditory and vestibular information processing and (3) control of affect. In addition to reviewing many of the structures which have been written about in connection with ASD, she introduces some structures not commonly associated with ASD such as the Pontine

Nuclei, the Arcuate Nucleus, and the Red Nucleus all of which could be key to understanding the circuitry involved in the communication between the cerebellum, cerebral cortex, and brainstem.

In a hypothesis paper (Jure) an extremely detailed account is given of how the Superior Colliculus' functioning is central to ASD. This paper creates a unique synthesis between an extensive array of clinical findings in ASD (well beyond the "core" symptoms), a list of many theories attempting to explain the findings in ASD, and the neuroscience background which can unify a great deal of these seemingly disparate findings and hypotheses. With so much evidence reviewed, the paper reminds us that these observations are yet to be tested with post-mortem or non-invasive functional human studies. One can easily observe that in a call for papers concerning the hind and midbrain's role in ASD, the majority of the papers are not original research. The goal of this special issue is to stimulate investigators to note the wealth of possibilities that exist if only they can find ways of searching for the key away from the streetlight.

Author contributions

All authors listed have made a substantial, direct, and intellectual contribution to the work and approved it for publication.

Conflict of interest

The authors declare that the research was conducted in the absence of any commercial or financial relationships that could be construed as a potential conflict of interest.

Publisher's note

All claims expressed in this article are solely those of the authors and do not necessarily represent those of their affiliated organizations, or those of the publisher, the editors and the reviewers. Any product that may be evaluated in this article, or claim that may be made by its manufacturer, is not guaranteed or endorsed by the publisher.

References

Joseph, R. (2000). Fetal brain behavior and cognitive development. *Dev. Rev.* 20, 81–98. doi: 10.1006/drev.1999.0486

Kohlmeier, K. A., and Polli, F. S. (2020). Plasticity in the brainstem: prenatal and postnatal experience can alter laterodorsal tegmental (LDT) structure and function. *Front. Synaptic Neurosci.* 12, 3. doi: 10.3389/fnsyn.2020.00003

London, E. (2018). Neuromodulation and a reconceptualization of autism spectrum disorders: using the locus coeruleus functioning as an exemplar. *Front Neurol.* 9, 1120. doi: 10.3389/fneur.2018.01120

Stoodley, C. J., D'Mello, A. M., Ellegood, J., Jakkamsetti, V., Liu, P., Nebel, M. B., et al. (2017). Altered cerebellar connectivity in autism and cerebellar-mediated rescue of autism-related behaviors in mice. *Nat Neurosci.* 1. doi: 10.1038/s41593-017-0004-1

Wang, S. S., Kloth, A. D., and Badura, A. (2014). The cerebellum, sensitive periods, and autism. *Neuron.* 83, 518–532. doi: 10.1016/j.neuron.2014.07.016

frontiers in Integrative Neuroscience

ORIGINAL RESEARCH
published: 20 August 2021
doi: 10.3389/fnint.2021.710593

$GABA_B$ Receptor Agonist R-Baclofen Reverses Altered Auditory Reactivity and Filtering in the *Cntnap2* Knock-Out Rat

Dorit Möhrle, Wenxuan Wang, Shawn N. Whitehead and Susanne Schmid*

Department of Anatomy and Cell Biology, Schulich School of Medicine & Dentistry, University of Western Ontario, London, ON, Canada

Altered sensory information processing, and auditory processing, in particular, is a common impairment in individuals with autism spectrum disorder (ASD). One prominent hypothesis for the etiology of ASD is an imbalance between neuronal excitation and inhibition. The selective $GABA_B$ receptor agonist R-Baclofen has been shown previously to improve social deficits and repetitive behaviors in several mouse models for neurodevelopmental disorders including ASD, and its formulation Arbaclofen has been shown to ameliorate social avoidance symptoms in some individuals with ASD. The present study investigated whether R-Baclofen can remediate ASD-related altered sensory processing reliant on excitation/inhibition imbalance in the auditory brainstem. To assess a possible excitation/inhibition imbalance in the startle-mediating brainstem underlying ASD-like auditory-evoked behaviors, we detected and quantified brain amino acid levels in the nucleus reticularis pontis caudalis (PnC) of rats with a homozygous loss-of-function mutation in the ASD-linked gene *Contactin-associated protein-like 2* (*Cntnap2*) and their wildtype (WT) littermates using Matrix-Assisted Laser Desorption Ionization Mass Spectrometry (MALDI MS). Abnormal behavioral read-outs of brainstem auditory signaling in *Cntnap2* KO rats were accompanied by increased levels of GABA, glutamate, and glutamine in the PnC. We then compared the effect of R-Baclofen on behavioral read-outs of brainstem auditory signaling in *Cntnap2* KO and WT rats. Auditory reactivity, sensory filtering, and sensorimotor gating were tested in form of acoustic startle response input-output functions, short-term habituation, and prepulse inhibition before and after acute administration of R-Baclofen (0.75, 1.5, and 3 mg/kg). Systemic R-Baclofen treatment improved disruptions in sensory filtering in *Cntnap2* KO rats and suppressed exaggerated auditory startle responses, in particular to moderately loud sounds. Lower ASR thresholds in *Cntnap2* KO rats were increased in a dose-dependent fashion, with the two higher doses bringing thresholds close to controls, whereas shorter ASR peak latencies at the threshold were further exacerbated. Impaired prepulse inhibition increased across various acoustic prepulse conditions after administration of

OPEN ACCESS

Edited by:
Randy J. Kulesza, Lake Erie College of Osteopathic Medicine, United States

Reviewed by:
Angel Nunez, Autonomous University of Madrid, Spain
Joseph A. McQuail, University of South Carolina, United States

***Correspondence:**
Dorit Möhrle
dorit.moehrle@googlemail.com

Received: *16 May 2021*
Accepted: *27 July 2021*
Published: *20 August 2021*

Citation:
Möhrle D, Wang W, Whitehead SN and Schmid S (2021) $GABA_B$ Receptor Agonist R-Baclofen Reverses Altered Auditory Reactivity and Filtering in the Cntnap2 Knock-Out Rat. Front. Integr. Neurosci. 15:710593. doi: 10.3389/fnint.2021.710593

R-Baclofen in *Cntnap2* KO rats, whereas R-Baclofen did not affect prepulse inhibition in WT rats. Our findings suggest that $GABA_B$ receptor agonists may be useful for pharmacologically targeting multiple aspects of sensory processing disruptions involving neuronal excitation/inhibition imbalances in ASD.

Keywords: autism spectrum disorders, sensory processing, startle, GABA, R-Baclofen, *CNTNAP2*, animal model

INTRODUCTION

Autism spectrum disorders (ASD) are neurodevelopmental disorders characterized by behavioral deficits in social interaction and unusual social communication as well as stereotyped, repetitive behaviors with restricted interests including sensory issues (DSM-5, 2013). Sensory abnormalities are present in over 90% of children with autism and can lead to great distress in everyday life settings (O'Neill and Jones, 1997; Leekam et al., 2007). Impairments in pre-attentive filtering of inundating sensory information, for example in noisy environments (Ornitz et al., 1993; Braff et al., 2001; Perry et al., 2007; Stevenson et al., 2017), are often accompanied by increased loudness perception (Khalfa et al., 2004; Danesh et al., 2015) and exaggerated reflexive responses to sudden sounds (Chamberlain et al., 2013; Kohl et al., 2014; Takahashi et al., 2016). The neural basis underlying ASD-related differences in sensory and other symptomatic behaviors has been hypothesized to be an imbalance in excitation and inhibition (E/I; Rubenstein and Merzenich, 2003). Indeed, alterations in biomarkers for GABA and glutamate (Glu) abundance and neurotransmission have been described in humans with ASD as well as in a multitude of rodent models with targeted mutations in risk genes for ASD (e.g., Yip et al., 2008; Blatt and Fatemi, 2011; Harada et al., 2011; Coghlan et al., 2012; Sgadò et al., 2013; Gaetz et al., 2014; Bridi et al., 2017; Horder et al., 2018b). Treatment options for ASD are currently limited, although pharmacological agents that modulate E/I balance showed promising preliminary results in clinical trials (for review, see Oberman, 2012; Port et al., 2019). As such, the selective $GABA_B$ receptor agonist Arbaclofen or its formulation R-Baclofen has been shown to ameliorate social avoidance symptoms in some individuals with ASD or the related genetic disorder Fragile X Syndrome (Berry-Kravis et al., 2012, 2017; Erickson et al., 2014; Veenstra-VanderWeele et al., 2017) and to improve social behavior deficits and repetitive behaviors in several corresponding genetic mouse models (Henderson et al., 2012; Silverman et al., 2015; Sinclair et al., 2017a; Stoppel et al., 2018). However, to the best of our knowledge, to date, no preclinical or clinical study has thoroughly investigated the potential of R-Baclofen for the treatment of behavioral outcomes of sensory abnormalities associated with ASD.

Homozygous loss-of-function mutations in the Contactin Associated Protein-like 2 (*Cntnap2*) gene have been identified as one of the rare single gene causes for ASD (Strauss et al., 2006; Poot, 2017). The protein encoded by *Cntnap2*, the neurexin CASPR2, shows enriched expression in sensory pathways of the brain (Gordon et al., 2016). CASPR2 is involved in neurotransmitter release and excitability through its clustering of voltage-gated potassium channels located at the juxtaparanodes of myelinated axons, at axonal segments, and synaptic terminals (Poliak et al., 2003; Scott et al., 2017). Rats and mice with knockout of the *Cntnap2* gene display alterations in sensory processing, both on the neuronal and behavioral level (Peñagarikano et al., 2011; Truong et al., 2015; Scott et al., 2017, 2020; Townsend and Smith, 2017; Dawes et al., 2018). In particular, alterations in brainstem auditory processing and auditory reactivity (Scott et al., 2018, 2020) reflect those reported in individuals with ASD (for review, see Sinclair et al., 2017b).

In the present study, we investigated if selective activation of $GABA_B$ receptors can remediate ASD-related altered sensory processing reliant on auditory brainstem function. We compared deficits in behavioral measures of auditory brainstem function from adult female and male *Cntnap2* knockout (KO) and wildtype (WT) controls after acute administration of vehicle (saline) or three different doses of R-Baclofen (0.75, 1.5, 3 mg/kg). Reflexive responses to startle-eliciting sounds were used to determine the efficacy of R-Baclofen to normalize acoustic reactivity, sensory filtering (i.e., short-term habituation), and sensorimotor gating (i.e., prepulse inhibition, PPI) in *Cntnap2* KO rats. The implicit (reflexive) reactivity to acoustic stimuli is mediated by a short primary pathway in the lower brainstem that activates spinal motor neurons to produce the startle response (**Figure 1**). An important element of the startle pathway is the nucleus reticularis pontis caudalis (PnC), the sensorimotor interface where cochlear root neurons (CRN) synapse on premotor neurons. Importantly, the transition of sensory input into the motor output can be directly influenced in the PnC by excitatory or inhibitory afferents (for review, see Koch, 1999; Simons-Weidenmaier et al., 2006). To further determine how R-Baclofen affects the transduction of sensory input into motor output within the brainstem startle circuit, we determined the threshold, effective stimulus (ES50), saturation, and slope of the startle input-output (ASR I-O) functions, as well as startle peak latencies. Finally, we quantified GABA, Glu, and glutamine (Gln) levels in the startle mediating PnC from *Cntnap2* KO and WT rats using Matrix-Assisted Laser Desorption Ionization Mass Spectrometry (MALDI MS) to determine if E/I imbalance underlies ASD-like deficits in brainstem auditory processing and behavior.

Overall, the present study provides preclinical evidence that acute, systemic R-Baclofen treatment reverses many disruptions in brainstem-mediated auditory processing and behavior associated with mutations in the autism-linked gene *Cntnap2*. These findings support further investigations of $GABA_B$ receptor agonists as promising pharmacological targets for the rescue of sensory processing deficits seen in neurodevelopmental disorders including ASD.

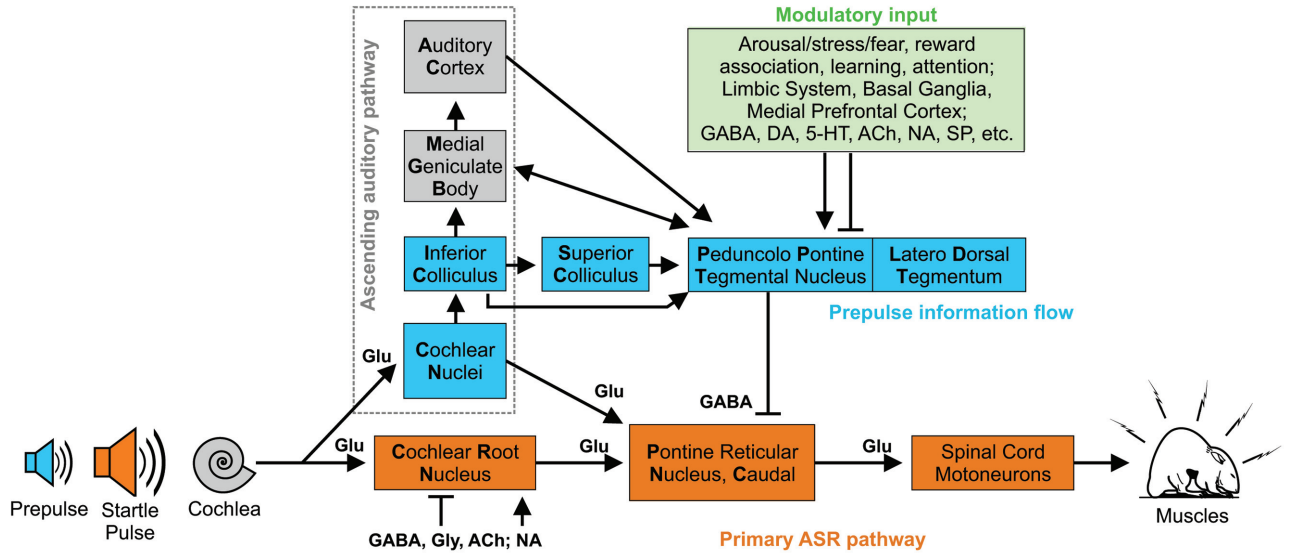

FIGURE 1 | Hypothetical simplified primary and modulatory neural circuitry underlying acoustic startle response and prepulse inhibition with presumed or confirmed neurotransmitters. In the primary ASR pathway (orange), the startle pulse sound information is transmitted *via* the auditory nerve to cochlear root neurons (CRN) in rodents which give short-latency input to the PnC (Pontine Reticular Nucleus, Caudal). These neurons project directly to cranial and spinal cord motoneurons to produce the motor response. Multiple pathways have been identified for sensorimotor gating modulating ASR. The acoustic prepulse is processed through the ascending auditory pathway (gray dotted frame) *via* the cochlear nucleus (CN) and the inferior colliculus. From there the prepulse information is transmitted directly or indirectly to the pedunculopontine tegmental nucleus (PPT) and neighboring region laterodorsal tegmental nucleus. Projections from the PPT to the PnC mediate PPI as a form of feed-forward inhibition. The PPT receives modulatory input (green pathway) from a variety of brain structures that can influence PPI e.g., linked with fear and arousal. Abbreviations: ACh, Acetyl choline; GABA, gamma aminobutyric acid; Glu, Glutamate; Gly, Glycine; DA, Dopamine; 5-HT, Serotonine; NA, Noradrenaline, SP, Substance P. Based on data and information from Lauer et al. (2017), Fulcher et al. (2020), and Gómez-Nieto et al. (2020).

MATERIALS AND METHODS

Animals

Male (M) and female (F) adult Sprague–Dawley wildtype (*Cntnap2* WT) and homozygous knockout (*Cntnap2* KO) rats were used in this study. Heterozygous breeders were obtained from Horizon Discovery (Boyertown, PA, USA), and all experimental animals were obtained from heterozygous crossings. Rats were housed in a temperature-controlled room on a 12 h light/dark cycle with *ad libitum* food and water. Behavioral testing was performed during the light phase of the cycle (lights on at 07:00 h). All procedures were approved by the University of Western Ontario Animal Care Committee and were in accordance with the guidelines established by the Canadian Council on Animal Care.

Acoustic Startle Responses (ASRs)

To investigate the effects of R-Baclofen on ASRs to startle-eliciting sounds, rats of the two genotypes (WT: 6 F, 5 M; KO: 6 F, 5 M) were tested after injection of 0.75, 1.5, and 3 mg/kg *i.p.* R-Baclofen at 8- to 11-months of age. The assessment of acoustic reactivity, sensory filtering, and sensorimotor gating was conducted in sound-attenuating startle boxes (LE116; Panlab) using the StartFear system (Panlab) and STARTLE software module (PACKWIN-CSST, PACKWIN version 2.0; Panlab) as described (Scott et al., 2018, 2020). In brief, using a pressure-sensitive platform, the rat's acoustic reactivity was measured as the magnitude of its startle response to acoustic stimuli (ASR I-O function) at varying intensities [pulse: 20 ms, 65–115 dB SPL in 5 dB steps, 10 stimuli of each in randomized order, inter-trial interval (ITI): 15, 17.5, or 20 s during a continuous background noise 60 dB SPL white noise]. To determine the startle threshold, effective stimulus ES50, and saturation (**Figure 2**) of each animal, we first scaled the ASR I-O function of a given animal and treatment between 0 and 1, then fit the scaled function with a GraphPad Prism 8.4.3 in-built model (Model: Standard curves to interpolate—Sigmoidal, 4PL, X is concentration; Method: Prism's default parameters; Compare: "Do the best-fit values of selected unshared parameters differ between data sets?," Comparison method: Extra sum-of-squares F test, Parameters: Bottom, Top, ES50, HillSlope; Constrain: constrain bottom to 0, top to 1; Initial values: choose automatically) with the following equation:

$$Y = Bottom + (X^{HillSlope}) * \frac{Top - Bottom}{X^{HillSlope} + ES50^{HillSlope}}$$

Y is the ASR magnitude

Bottom is the lower plateau of the startle pulse intensity (dB SPL) on the Y axis

Top is the upper plateau of the startle pulse intensity (dB SPL) on the Y axis

HillSlope is the steepness of the slope

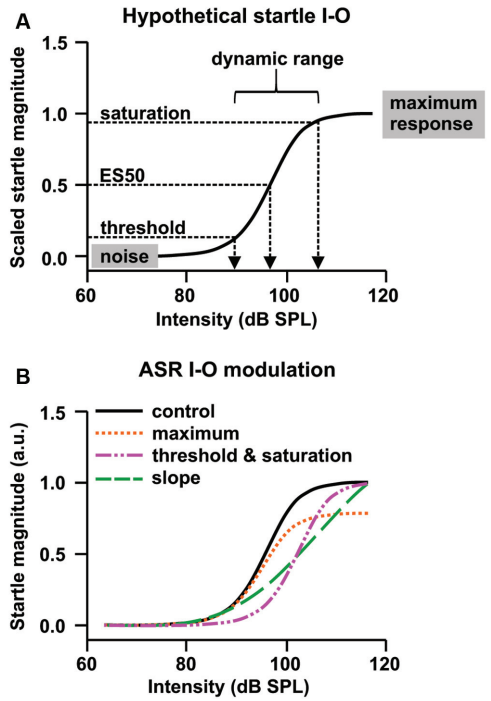

FIGURE 2 | Hypothetical plasticity of ASR input-output (I-O) functions. **(A)** The sigmoid function describing the relationship between startle stimulus (input) and startle response magnitude (output). The ASR threshold is a putative measure for ASR excitability, the efficient stimulus (ES) for the sound pulse potency, and the ASR maximum for motor capacity. Within the dynamic range of the I-O function, a small stimulus change can produce a large response change. The slope of the dynamic range can be used as metric for the reflex efficiency. **(B)** The control ASR I-O function (black solid line) could be altered through an increase or decrease in the maximum response to the loudest startle pulse (orange), a left- or right-shift of the curve, thereby increasing or decreasing ASR threshold, ES50, and saturation (pink), a steepening or flattening of the slope of the dynamic range of the function (green), or a combination of these effects (based on data and information from Hince and Martin-Iverson, 2005; Martin-Iverson and Stevenson, 2005). Normalization of the ASR I-O function to the individual startle magnitude at the loudest startle pulse allows analysis of threshold and slope without confounding effects of altered maximum response.

ES50 is the startle pulse intensity that gives an ASR magnitude halfway between Bottom and Top.

We then solved the above equation for X and calculated the ASR threshold and saturation for each animal from their individual curve fit parameters using MATLAB R2019a:

$$X = \sqrt[HillSlope]{\frac{(Y - Bottom) * ES50^{HillSlope}}{Top - Y}}$$

The ASR threshold X was defined at Y equal to 25% and the ASR saturation at Y equal to 90% of the span between the Top and Bottom plateau. We chose these values because the estimated ASR threshold and saturation after saline injection matched the between startle pulse intensity comparisons within genotype. ASR peak latencies were extracted within the I-O dynamic range (i.e., we rounded up threshold and rounded down saturation estimates to extract latencies of responses to actually measured sound pulse intensities).

Sensorimotor gating (expressed as the percentage of prepulse inhibition, %PPI) was determined by the extent that the rat's startle response to the 105 dB SPL pulse was attenuated when a brief prepulse was presented 30 or 100 ms prior to the startle stimulus (prepulse: 10 ms, 65, 75, or 85 dB SPL). Because startle reactivity can affect sensorimotor gating (Csomor et al., 2008), differences in baseline startle magnitude were calculated using the startle-only trials during PPI blocks and analyzed. The control startle stimulus (105 dB SPL) without prepulse and each combination of prepulse lead time and intensity was presented 10 times. The relative percentage of PPI was calculated using the maximum startle amplitudes as follows:

$$\%PPI = \left(1 - \frac{prepulse\ pulse}{pulse\ alone}\right) * 100\%$$

The latency of the startle response was also measured in trials with/without the prepulse, as an increase in startle latency in PPI trials is typical for sensorimotor gating (Ison et al., 1973; Hoffman and Ison, 1980). Relative changes in latency were calculated as the time to reach the maximum startle magnitude on startle pulse-alone trials subtracted from that during prepulse trials, i.e., positive values represented a latency increase (Lyall et al., 2009).

To determine the impact of R-Baclofen on sensory filtering, *Cntnap2* WT and KO rats were repeatedly presented a startle-eliciting stimulus (20 ms white noise at 105 dB SPL; 5 ms rise/fall time, ITI: 15, 17.5, or 20 s during a continuous background noise 60 dB SPL white noise) and the degree that their startle response habituated was compared across the genotypes and treatments. Habituation was assessed from the first eight trials with the startle magnitudes normalized to the magnitude at the first trial. A habituation score was calculated for each animal using the following formula (Scott et al., 2018):

$$Habituation\ score = \frac{average\ max\ startle\ magnitude\ trials\ 7\ and\ 8}{max\ startle\ magnitude\ trial\ 1}$$

A sensitization score was calculated for each animal using the following formula (Meincke et al., 2004):

$$Sensitization\ score = \frac{average\ max\ startle\ magnitude\ trials\ 2\ to\ 4}{max\ startle\ magnitude\ trial\ 1}$$

Before the behavioral procedures associated with the ASR (i.e., acoustic reactivity, sensory filtering, and sensorimotor gating), animals were handled and acclimated to the startle boxes over three 10 min sessions. During these acclimation sessions, only background noise (60 dB SPL, white noise) was presented to the animals.

Drug Application

R-Baclofen (provided by Simons Foundation Autism Research Initiative, SFARI through Clinical Research Assoc., LLC) was dissolved in 0.9% saline freshly on each experimental day and administered intraperitoneally (i.p., injection volume: 1 ml/kg)

1 h before the start of the test session in doses of 0.75, 1.5, and 3 mg/kg. Doses and injection time before testing were chosen in accordance with the literature (Henderson et al., 2012; Silverman et al., 2015; Lorrai et al., 2016). The vehicle condition was represented by the administration of an equal volume of saline. In the first experimental block (**Supplementary Figure 1**), each treatment was administered on two consecutive days in the following order: saline (Day 1&2), R-Baclofen at 0.75 mg/kg (Day 3&4), 1.5 mg/kg (Day 5&6), and 3 mg/kg (Day 7&8). We chose to inject R-Baclofen in increasing doses to avoid the need for week-long washout times between treatments (Henderson et al., 2012) and to keep behavioral testing as concise as possible. On the first day of each dose, injections of saline or R-Baclofen were followed by behavioral tests for sensory filtering (habituation) and acoustic reactivity (ASR I-O), and on the second day by the behavioral test for sensorimotor gating (PPI). After the first experimental block and a 1-week washout period, we repeated the same sequence of behavioral procedures over 8 days with saline injection. This second experimental block was used to control for effects of repeated testing. Over 2 days preceding either experimental block, rats were habituated to handling, behavioral testing, and intraperitoneal injections; specifically, rats received one injection of 1 ml/kg saline 1 h prior to testing on both days (not shown in **Supplementary Figure 1**). No statistical differences were found for either genotype between saline treatments across the two experimental blocks for habituation and acoustic reactivity and data were pooled across days for the most accurate genotype comparisons after saline. For PPI of ASR, genotype comparisons after saline were made based on Day 2 (**Supplementary Figure 1**) because there was a significant difference between the PPI of the two experimental blocks. Repeated testing within the second experimental block did not alter the PPI in *Cntnap2* WT and KO rats (**Supplementary Figure 2**) and we assumed that effects of repeated testing within the first experimental block were also negligible. For most consistent comparisons of R-Baclofen treatment effects within or between genotypes, data were compared within the first treatment block.

MALDI

In order to analyze if altered brain amino acid abundances underlie the *Cntnap2*-linked changes in auditory-evoked behaviors, 8 *Cntnap2* WT (4 F, 4 M) and 8 *Cntnap2* KO (4 F, 4 M) rats were deeply anesthetized with carbon dioxide and decapitated at 4- to 5-months-old. Brains were extracted and fresh frozen, and stored at −80°C, until cryosectioned at 10μm (Thermo-Fisher Scientific CryoStar NX50), and mounted on Indium tin oxide (ITO)-coated glass slides (Hudson Surface Technology Inc., Old Tappan, NJ, USA). Zinc oxide (Sigma-Aldrich, St. Louis, MO, USA) was selected as the MALDI matrix and prepared to 1 mg/ml in 50% ACN and 0.1% TFA (Fisher Scientific, Waltham, MA, USA) and applied onto the slides with TM-Sprayer^{TM} (HTX Technologies, LLC, Chapel Hill, NC, USA). Afterward, α-cyano-4-hydroxycinnamic acid standards were spotted onto the slides for internal mass calibration. ZnO matrix deposition using the TM Sprayer and MS data analysis of neurotransmitters were performed as previously described (Chen et al., 2021). MALDI-MS sample analyses were performed on a Sciex TOF/TOF 5800 MALDI mass spectrometer (Sciex, Framingham, MA, USA). Images were acquired in the positive ion reflectron mode at a mass range of 50–300 m/z using the TOF-TOF Series Explorer and Data Explorer were used for data acquisition and processing, respectively (Sciex). MS images were acquired at 70 μm raster with 50 shots/spectrum, and the laser energy was optimized based on the signal intensity, peak resolution and signal-to-noise ratio. MALDI MS images were visualized and analyzed through an experimentally blinded observer using Tissue View^{TM} Software IDL^{VM} (Sciex). PnC and superior olivary complex (SOC) region of interest in the brainstem were manually selected to generate the average mass spectra. Mass peaks corresponding to neurotransmitters and metabolites ($[GABA+K]^+$: 142m/z, $[Glu+K]^+$: 186m/z, $[Gln+K]^+$: 185m/z, $[Choline+K]^+$: 143m/z, $[Norepinephrine+K]^+$: 208m/z) were acquired from each mass spectra (Chen et al., 2021). Comparative analysis was performed based on the area under the curve (AUC) ratio (ratio between the peak of interest AUC to total AUC from 100 to 250m/z; Caughlin et al., 2017). Intensity values corresponding to the mass peaks were compared between respective WT-KO pairs on the slides. One female WT-KO pair had to be excluded due to significant tearing in the tissue that left the PnC region of interest unusable, resulting in three pairs of female and four pairs of male *Cntnap2* WT-KO rats. No significant differences between data from females and males were observed and data were pooled.

Statistical Analysis

Unless otherwise stated, data that followed normal distribution are presented as group mean with standard deviation (SD), and not normally distributed data as group median with interquartile range (IQR). Depending on the experimental design and distribution of the data, differences of the means were compared for statistical significance either by student's *t*-test, paired *t*-test, Welch *t*-test, one sample *t*-test, one sample Wilcoxon test, Mann–Whitney test, 2-way ANOVA, repeated measures (RM) ANOVA, Mixed-effect analysis, or Friedmann tests using GraphPad Prism 8.4.3 (La Jolla, USA). For 2-way ANOVA comparisons we did not assume sphericity because R-Baclofen was administered in consecutive, increasing doses (**Supplementary Figure 1**) and we used Greenhouse-Geisser correction where applicable. Two-way ANOVA, RM ANOVA, Mixed-effect analysis, or Friedmann tests were followed by multiple comparison tests with correction for type 1 error after Sidak's, Dunnett's, or Dunns's multiple comparisons test. The relative amount of prepulse inhibition was additionally analyzed by random permutation tests in consideration of small sample sizes to estimate the population mean from samples (resampling by bootstrapping, property mean, 10,000 random samples without replacement). Statistical significance level was $\alpha = 0.05$, and resulting p values are reported in the legends using: $(*)p < 0.1$, $*p \leq 0.05$; $**p \leq 0.01$; $***p \leq 0.001$; n.s., not significant.

RESULTS

Cntnap2 KO Rats Display Deficient Short-Term Habituation, Exaggerated Sensitization, and Increased Acoustic Reactivity

In order to investigate whether selective activation of $GABA_B$ receptors can remediate ASD-related altered sensory processing reliant on auditory brainstem function, we analyzed auditory reactivity, filtering, and sensorimotor gating in adult *Cntnap2* KO rats (n = 6 F, n = 5 M) in comparison to WT littermates (n = 6 F, n = 5 M) after acute administration of R-Baclofen (0.75, 1.5, and 3 mg/kg) or vehicle (saline).

To most accurately assess genotype-related differences between *Cntnap2* WT and KO rats in sensory filtering and acoustic reactivity (**Figure 3**), we first averaged the respective data from the five experimental days where short-term habituation and ASR I-O trials were measured 1 h after saline injection (Day # 1, 16, 18, 20, 22, see timeline in **Supplementary Figure 1**). To assess sensory filtering, short-term habituation of the startle response was measured across the first eight startle trials of the test day. Short-term habituation across the first eight startle trials of the test day revealed significantly less declined startle responses in *Cntnap2* KO compared with WT rats, in particular at trial number eight (*Cntnap2* WT: n = 11, *Cntnap2* KO: n = 11, two-way RM ANOVA, trial × genotype p = 0.0225, $F_{(7,140)}$ = 2.425, trial p = 0.0012, $F_{(4.714, 94.28)}$ = 4.528, genotype p = 0.0053, $F_{(1,20)}$ = 9.792, Sidak's multiple comparisons test, p = 0.0151, **Figure 3B**), indicating that KO rats do not habituate across trials. Habituation scores calculated from trial 7 and 8 in relation to trial 1 were significantly increased in *Cntnap2* KO rats compared with WT rats (**Figure 3C** Left, *Cntnap2* WT: 0.78 ± 0.11, KO: 0.97 ± 0.18 dB SPL, two-sided student's t-test p = 0.0082), confirming perturbed habituation across trials and indicating impaired sensory filtering in *Cntnap2* KO rats. Furthermore, *Cntnap2* KO rats displayed greater sensitization scores calculated from trial 2–4 in relation to trial 1 than *Cntnap2* WT rats (**Figure 3C** Right, *Cntnap2* WT:0.82 ± 0.15, KO:0.99 ± 0.16, two-sided student's t-test p = 0.0150).

To assess acoustic reactivity in *Cntnap2* WT and KO rats, startle response magnitudes to a series of startle pulses of increasing intensity (65–115 dB in 5 dB SPL increments) were measured and analyzed. Deficient short-term habituation and exaggerated sensitization in *Cntnap2* KO rats described above were accompanied by increased ASR magnitudes of the startle I-O growth function in both female (**Figure 3D**) and, even more so, in male (**Figure 3E**) *Cntnap2* KO rats compared with respective WT controls (F WT: n = 6, F KO: n = 6, two-way ANOVA, intensity × genotype p = 0.1598, $F_{(10,110)}$ = 1.471, intensity p < 0.0001, $F_{(10,110)}$ = 61.70, genotype p < 0.0001, $F_{(1,110)}$ = 28.83; M WT: n = 5, M KO: n = 5, two-way ANOVA, intensity × genotype p < 0.0001, $F_{(10,88)}$ = 14.97, intensity p < 0.0001, $F_{(10,88)}$ = 100.1, genotype p < 0.0001, $F_{(1,88)}$ = 301.7). ASR magnitudes were particularly increased at 105 dB SPL, and at 85–115 dB SPL startle pulse intensity in female and male *Cntnap2* KO rats, respectively (**Figure 3D**, WT F vs. KO F, Sidak's multiple comparisons test, 105 dB SPL: p = 0.0303, **Figure 3E**, WT M vs. KO M, Sidak's multiple comparisons test, 85–115 dB SPL: all p < 0.0001). While ASR magnitudes were similar in female and male *Cntnap2* WT rats (F WT: n = 6, M WT: n = 5, two-way ANOVA, intensity × sex p < 0.9551, $F_{(10,99)}$ = 0.3743, intensity p < 0.0001, $F_{(10,99)}$ = 59.17, sex p < 0.1054, $F_{(1,99)}$ = 2.670), exaggerated ASR magnitudes were more pronounced in male than female *Cntnap2* KO rats (note the higher startle magnitudes in *Cntnap2* KO males compared with KO females in **Figures 3E,D**, respectively, F: n = 6, M: n = 5, two-way ANOVA, intensity × sex p < 0.0001, $F_{(10,99)}$ = 6.864, intensity p < 0.0001, $F_{(10,99)}$ = 103.9, sex p < 0.0001, $F_{(1,99)}$ = 167.3).

To optimize the comparison of ASR magnitudes especially to moderate startle pulse intensities between animals (see hypothetical plasticity of ASR I-O in **Figure 2** and **Supplementary Figure 3**), ASR magnitudes of all animals were normalized to their individual magnitude at the loudest startle pulse intensity (115 dB SPL). Normalization of ASR I-O magnitudes eliminated sex differences and the data were pooled for male and female *Cntnap2* WT or KO rats, respectively (**Figure 3F**, *Cntnap2* WT F: n = 6, M: n = 5, *Cntnap2* KO F: n = 6, M: n = 6, three-way ANOVA, intensity × genotype × sex p = 0.4238, $F_{(10,198)}$ = 1.025, genotype × sex p = 0.1392, $F_{(1,198)}$ = 2.205, intensity × sex p = 0.6617, $F_{(10,198)}$ = 0.7657, intensity × genotype p < 0.0001, $F_{(10,198)}$ = 5.021, sex p = 0.8462, $F_{(1,198)}$ = 0.03771, genotype p < 0.0001, $F_{(1,198)}$ = 21.53, intensity p < 0.0001, $F_{(10,198)}$ = 307.1). Normalized startle magnitudes in *Cntnap2* KO rats were increased in comparison to *Cntnap2* WT rats, particularly at 90–100 dB SPL (**Figure 3F**, *Cntnap2* WT: n = 11, *Cntnap2* KO: n = 11, two-way ANOVA, intensity × genotype p < 0.0001, $F_{(10,220)}$ = 4.750, intensity p < 0.0001, $F_{(10,220)}$ = 313.5, genotype p < 0.0001, $F_{(1,220)}$ = 20.63, Sidak's multiple comparisons test, 90 dB SPL: p < 0.0001, 95 dB SPL: p = 0.0005, 100 dB SPL: p = 0.0069).

Besides the change in maximum startle response obtainable (ASR capacity, **Figures 3D,E**), the relationship between the startle pulse intensity and response magnitude could be altered in *Cntnap2* KO rats through several underlying mechanisms (**Figure 2**). To extract dynamic range characteristics including startle threshold and saturation from the startle I-O growth functions of individual animals, sigmoidal curves were fitted to the experimental data (scaled between 0 and 1). The ASR threshold was defined as 25%, and the ASR saturation as 90% of the scaled magnitude. The average fitted curves were significantly different between *Cntnap2* WT and KO rats, with fitted curves from KO rats showing both a steeper slope and a leftward shift of ES50 (startle pulse intensity that gives the half-maximal response, **Figure 3G** and **Table 1**, *Cntnap2* WT: n = 11 rats, *Cntnap2* KO: n = 11 rats, p < 0.0001). Increased startle magnitudes and altered dynamic range in *Cntnap2* KO rats (**Figures 3D–G**) were paralleled by a significantly lower startle threshold (**Figure 3H** Left, *Cntnap2* WT: 86.6 ± 4.29 dB SPL, KO: 82.7 ± 2.97 dB SPL, two-sided student's t-test: p = 0.0210) and saturation (**Figure 3H** Right, *Cntnap2* WT: 106.5 ± 6.8 dB SPL, KO: 97.8.7 ± 3.6 dB SPL, two-sided student's t-test: p = 0.0012).

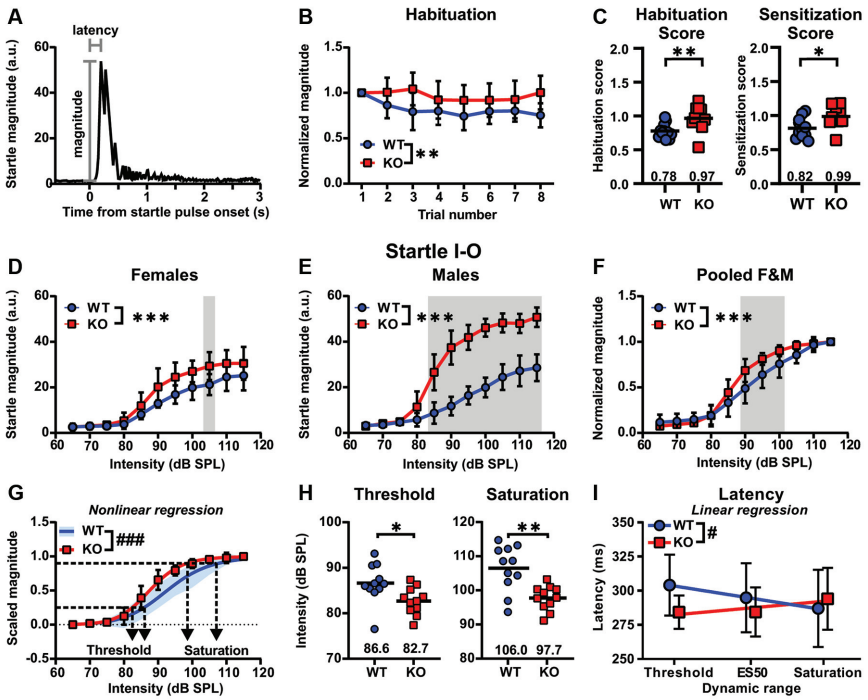

FIGURE 3 | Impaired short-term habituation and increased acoustic reactivity in *Cntnap2* KO compared with wildtype (WT) rats. **(A)** Schematic raw acoustic startle trace to a 115 dB SPL startle pulse. ASR peak magnitude and latency is determined within the recording window of 500 ms from startle pulse onset. **(B,C)** Sensory filtering as measured by short-term habituation is perturbed in *Cntnap2* KO rats. **(B)** Mean ± standard deviation (SD) startle response magnitudes across eight subsequent trials normalized to the first trial in *Cntnap2* WT and KO rats. Values <1 indicate habituation of the startle response. *Cntnap2* KO rats showed less declined startle responses than WT rats, indicating perturbed habituation, in particular at trial number eight (*Cntnap2* WT: $n = 11$, *Cntnap2* KO: $n = 11$, two-way repeated measures (RM) ANOVA, trial × genotype $p = 0.0225$, $F_{(7,140)} = 2.425$, trial $p = 0.0012$, $F_{(4.714,\ 94.28)} = 4.528$, genotype $p = 0.0053$, $F_{(1,20)} = 9.792$, Sidak's multiple comparisons test, $p = 0.0151$). **(C) Left**: Individual habituation scores calculated from the average of the last two trials divided by that of the first trial (WT: blue circles, KO: red squares, mean: horizontal black line). Values <1 indicate habituation of the startle response. *Cntnap2* KO rats had significantly greater habituation scores compared with WT rats (two-sided student's *t*-test $p = 0.0082$). **Right**: Individual sensitization scores calculated from the average of trials 2–4 divided by that of the first trial (WT: blue circles, KO: red squares, mean: horizontal black line). *Cntnap2* KO rats showed greater sensitization scores than WT rats (two-sided student's *t*-test $p = 0.0150$). **(D–F)** Mean ± SD startle responses in female (F) **(D)**, male (M) **(E)**, and pooled male and female **(C)** *Cntnap2* WT (blue circles) and KO (red squares) rats to startle pulses with sound intensities from 65 to 115 dB SPL in 5 dB steps. **(D)** Acoustic startle magnitudes were significantly increased in female *Cntnap2* KO (WT: $n = 6$, KO: $n = 6$, two-way ANOVA, intensity × genotype $p = 0.1598$, $F_{(10,110)} = 1.471$, intensity $p < 0.0001$, $F_{(10,110)} = 61.70$, genotype $p < 0.0001$, $F_{(1,110)} = 28.83$) and **(E)** male *Cntnap2* KO rats (WT: $n = 5$, KO: $n = 5$, two-way ANOVA, intensity × genotype $p < 0.0001$, $F_{(10,88)} = 14.97$, intensity $p < 0.0001$, $F_{(10,88)} = 100.1$, genotype $p < 0.0001$, $F_{(1,88)} = 301.7$) compared with WT littermates when collapsing over intensities, indicated by a leftward shift of the I-O ASR function. In particular, startle magnitudes were elevated in female *Cntnap2* KO at 105 dB SPL (Sidak's multiple comparisons test, $p = 0.0303$) and in male *Cntnap2* KO rats at 85–115 dB SPL (Sidak's multiple comparisons test, all $p < 0.0001$). **(F)** Normalized ASR I-O functions pooled for male and female *Cntnap2* WT and KO rats were significantly different (*Cntnap2* WT: $n = 11$, *Cntnap2* KO: $n = 11$, two-way ANOVA intensity × genotype $p < 0.0001$, $F_{(10,220)} = 4.750$, intensity $p < 0.0001$, $F_{(10,220)} = 313.5$, genotype $p < 0.0001$, $F_{(1,220)} = 20.63$). Normalized startle magnitudes in *Cntnap2* KO rats were particularly increased in comparison to *Cntnap2* WT rats at 90–100 dB SPL (Sidak's multiple comparisons test, 90 dB SPL: $p < 0.0001$, 95 dB SPL: $p = 0.0005$, 100 dB SPL: $p = 0.0069$). **(G)** Sigmoidal curves (lines) fitted to the startle magnitudes scaled between 0 and 1 were significantly different in *Cntnap2* WT (SD, blue area) and *Cntnap2* KO rats (mean ± SD, red squares and error bars; $p < 0.0001$, curve fit values see **Table 1**). Dotted horizontal line at 0.25 determined as ASR threshold and at 0.9 as ASR saturation. **(H)** Individual ASR thresholds (**Left**) and saturation (**Right**) extracted from individual sigmoidal curve fits were significantly lower in *Cntnap2* KO rats (blue squares, horizontal black lines: mean) compared with WT controls (red circles, horizontal black lines: mean; two-sided student's *t*-test, threshold: $p = 0.0210$, saturation: $p = 0.0012$). **(I)** Linear regression of ASR peak latencies across the dynamic range of *Cntnap2* WT (mean ± SD, blue circles and error bars, $Y = -8.537 * X + 312.4$, $r^2 = 0.9979$, blue line) and KO rats (mean ± SD, red squares and error bars, KO: $Y = 4.910 * X + 277.8$, $r^2 = 0.7576$, red line). The slopes of the regression lines were significantly different ($p = 0.0408$). ES50, acoustic startle pulse intensity that gives a startle magnitude at 50%. $^{*}p < 0.05$; $^{**}p < 0.01$; $^{***}p < 0.001$; $^{\#}p < 0.05$ (comparison of regression lines); $^{\#\#\#}p < 0.001$ (comparison of regression lines).

This means that, on average, *Cntnap2* KO rats reach the 25% and 90% criterion at lower startle pulse intensities than WT rats—further indicators for the left-shift of the ASR I-O function and increased acoustic reactivity in *Cntnap2* KO rats. Taken together, the ASR I-O functions and their parameters extracted from the sigmoidal curve fits demonstrated increased ASR capacity (maximal response possible), stimulus potency (ES50), ASR excitability (ASR threshold), dynamic range top plateau (ASR saturation), and ASR efficiency (slope) in *Cntnap2* KO rats.

ASR magnitude and latency are in general negatively correlated (i.e., the higher the magnitude, the shorter the latency; Hoffman and Searle, 1968). Peak latencies in *Cntnap2* WT and KO rats were investigated across the ASR dynamic range, in particular at near startle I-O threshold, at ES50, and

TABLE 1 | Comparison of sigmoidal curve fit of ASR I-O function with magnitude scaled between 0 and 1 in *Cntnap2* WT and KO rats corresponding to **Figure 3G**.

Best-fit values	*Cntnap2 WT*		*Cntnap2 KO*
Bottom	=0		=0
Top	=1		=1
ES50	92.64		87.49
HillSlope	14.55		18.41
Sy.x	0.1163		0.08851
Different curve fits?		<0.0001***	
Different slopes?		0.0088**	
Different ES50?		<0.0001***	

*Bottom plateau constraint to 0, Top plateau constraint to 1, ES50: acoustic pulse intensity (dB SPL) that gives a startle magnitude halfway between Bottom and Top, HillSlope: steepness of the curve, Sy.x: standard error of regression, Different curves: curve fit comparison between Cntnap2 WT and KO rats. p values, **p < 0.01, ***p < 0.001.*

saturation (**Figure 3I**). Thereby, we could compare individual latencies at startle pulse intensities that yielded similar ASR magnitudes in *Cntnap2* WT and KO rats relative to their dynamic range. As expected, *Cntnap2* WT rats showed a negative relationship between startle pulse intensities across the dynamic range and peak startle latency (**Figure 3I**, slope $m = -8.537$ ms/increment, deviation from zero $p = 0.0291$, $F_{(1,1)} = 479.3$), indicating shortening of latency with increasing ASR magnitudes across the dynamic range. In *Cntnap2* KO rats, however, no such negative relationship was found (**Figure 3I**, slope $m = 4.910$ ms/increment, deviation from zero $p = 0.3277$, $F_{(1,1)} = 3.126$, WT vs. KO $p = 0.0408$). In contrast to the WT controls, *Cntnap2* KO rats showed significantly shorter latencies near startle I-O threshold (*Cntnap2* WT: 304.1 ± 22.3 ms, KO: 284.31 ± 12.2 ms, two-sided student's *t*-test, $p = 0.0181$) and their startle peak latencies did not further decrease across the dynamic range (**Figure 3I**, deviation from zero $p = 0.3277$, $F_{(1,1)} = 3.126$). The shorter peak latencies near the threshold and the lack of further shortening of latency across the dynamic range are indicators for an overall increased response strength in *Cntnap2* KO rats. Taken together, our results show that *Cntnap2* KO rats have increased auditory reactivity and impaired habituation.

Excitatory and Inhibitory Neurotransmitter Levels Are Altered in the Startle-Mediating Brainstem From *Cntnap2* KO Rats

In order to assess possible alterations in neuronal excitation/inhibition within the startle-mediating brainstem circuitry that might underlie ASD-related sensory processing deficits (for review, see Sinclair et al., 2017b), we quantified GABA, glutamate, and glutamine amino acid levels ($[GABA+K]^+$: 142m/z, $[Glu+K]^+$: 186m/z, $[Gln+K]^+$: 185m/z) in the PnC (nucleus reticularis pontis caudalis) of fresh frozen coronal brain tissue sections from adult *Cntnap2* WT and KO rats using MALDI MS (**Figure 4**, **Table 2**). Visual inspection of the intensity map images showed an increase in signal intensity of all three amino acids in the brainstem and middle cerebellar peduncle region of *Cntnap2* KO (**Figure 4B**) compared with WT rats (**Figure 4A**). The AUC analysis of individual amino acid peaks in the mass spectra of the PnC region (**Figure 4C**) showed a significant increase in AUC ratio for GABA (**Figure 4D** Left, WT $n = 7$, KO $n = 7$, paired *t*-test $p = 0.0242$). AUC ratios of glutamate (**Figure 4D** Middle, paired *t*-test $p = 0.0858$) and glutamine (**Figure 4D** Right, paired *t*-test $p = 0.0703$) were slightly increased by statistical tendency. Comparative analysis (**Table 2**) showed a 2-fold increase in GABA in the PnC region from *Cntnap2* KO rats (one sample *t*-test $p = 0.0222$) and by tendency a 1.4-fold increase in both glutamate (one sample *t*-test $p = 0.0935$) and glutamine (one sample *t*-test $p = 0.0814$). Consequently, the ratio between Glu/Gln was similar in *Cntnap2* KO and WT rats (one sample *t*-test $p = 0.4051$), whereas GABA/Gln was significantly enhanced (one sample *t*-test $p = 0.0335$, **Table 2**). Finally, GABA was more enhanced than Glu, as evidenced by significantly decreased Glu/GABA ratio (one sample *t*-test $p = 0.0349$) and a slight, yet statistically insignificant, increase in GABA/Glu ratio (one sample *t*-test $p = 0.0853$). Importantly, the comparative analysis showed no differences in two other metabolite levels in the PnC region (**Table 2**), i.e., $[Choline+K]^+$: 143m/z (one sample *t*-test $p = 0.3336$) and $[Norepinephrine+K]^+$: 208m/z (one sample *t*-test $p = 0.1383$), indicating that the increases in Glu, GABA, and Gln levels were not based on a general impairment in metabolism or neurotransmission in *Cntnap2* KO rats. Furthermore, GABA, Glu, and Gln levels were not altered in the SOC within the auditory brainstem of *Cntnap2* KO rats (**Supplementary Figure 4**). This indicated that the amino acid level increases in the PnC in *Cntnap2* KO rats were not ubiquitous throughout the brain. Taken together, our findings indicate aberrant levels of GABA, Glu, and Gln in the PnC of *Cntnap2* KO rats. This suggests that altered implicit auditory-evoked behaviors linked with functional deletion of *Cntnap2* are associated with an imbalance of excitation and inhibition, particularly affecting the GABA neurotransmitter system.

R-Baclofen Treatment Improves Disruptions in Habituation in *Cntnap2* KO Rats

We first investigated the potential of R-Baclofen to remediate perturbed short-term habituation in *Cntnap2* KO rats. Short-term habituation of the startle response was measured across the first eight startle trials of the test day 1 h after systemic injection of 0.75, 1.5, or 3 mg/kg R-Baclofen (**Figure 5**). In both *Cntnap2* WT (**Figure 5A**) and KO rats (**Figure 5B**), the highest dose of R-Baclofen at 3 mg/kg led to a greater decline of startle magnitudes across the first eight trials in comparison with saline administration (**Figure 5A**, *Cntnap2* WT: $n = 11$, Two-way RM ANOVA, trial $p < 0.0001$, $F_{(7,80)} = 8.884$, treatment $p = 0.0071$, $F_{(2.647, 211.7)} = 4.397$, trial × treatment $p = 0.8352$, $F_{(21,240)} = 0.6965$, Dunnett's multiple comparisons test, saline vs. 0.75 mg/kg $p = 0.6549$, saline vs. 1.5 mg/kg $p = 0.1267$, saline vs. 3 mg/kg $p = 0.0084$, **Figure 5B**, *Cntnap2* KO: $n = 11$, Two-way RM ANOVA, trial $p = 0.6752$, $F_{(7,80)} = 0.6960$, treatment $p < 0.0001$, $F_{(2.864, 229.1)} = 10.16$, trial × treatment $p = 0.7925$, $F_{(21,240)} = 0.7925$, Dunnett's multiple comparisons test, saline vs. 0.75 mg/kg $p = 0.7085$, saline vs. 1.5 mg/kg $p = 0.0606$, saline vs. 3 mg/kg $p < 0.0001$). Habituation scores (**Figure 5C**) and sensitization scores (**Figure 5D**) were calculated and compared across R-Baclofen doses within genotype, and

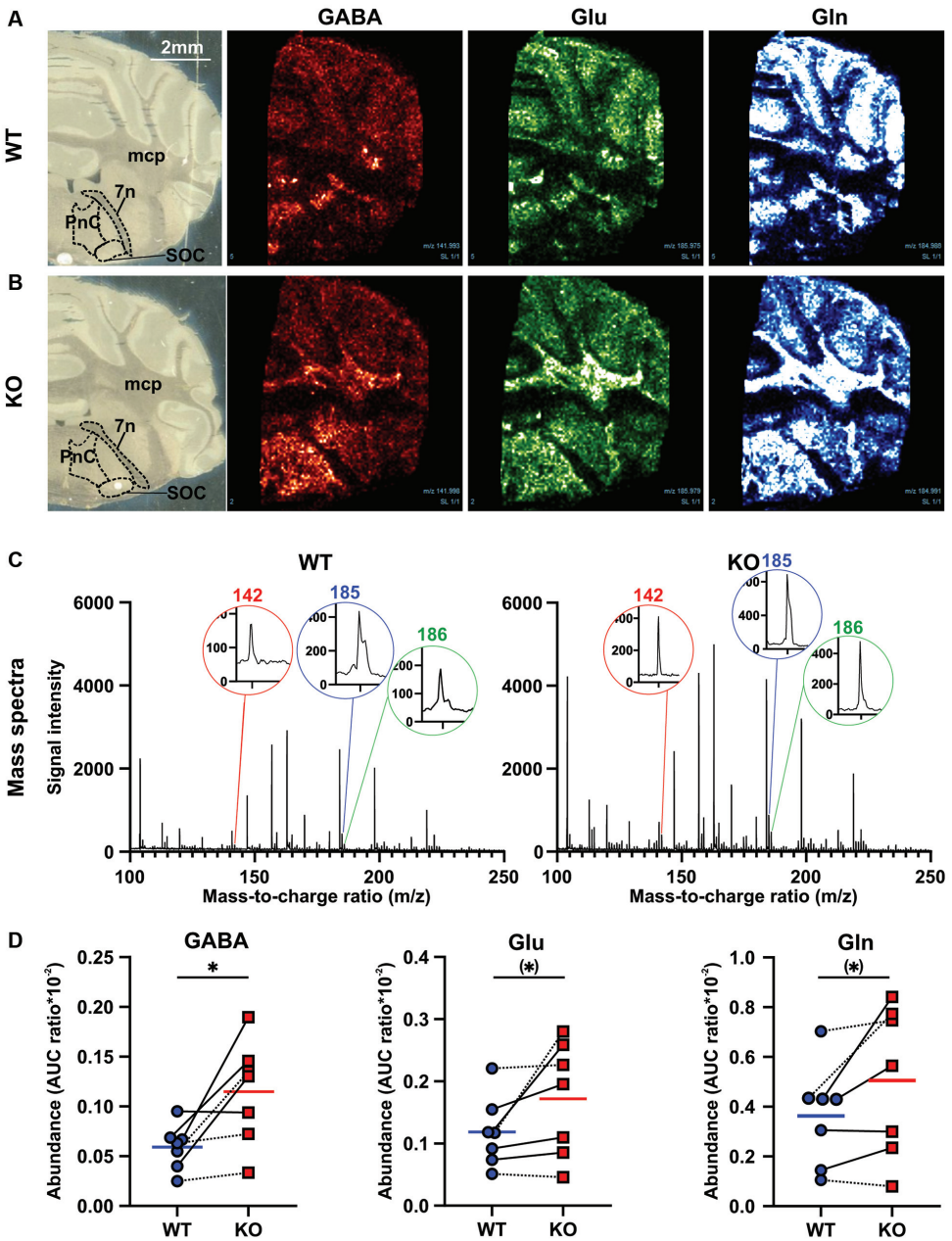

FIGURE 4 | Effect of *Cntnap2* knockout on the MALDI MS signals of amino acids in fresh frozen rat brain tissue. MALDI-MS generated intensity maps of GABA ([GABA+K]$^+$: 142m/z), glutamate ([Glu+K]$^+$: 186 m/z), and glutamine ([Gln+ K]$^+$: 185m/z) from a **(A)** *Cntnap2* WT and **(B)** KO rat. The signal of GABA, Glu, and Gln appears to be enhanced in the brainstem including and surrounding the PnC and in the mcp region in *Cntnap2* KO rats. **(C)** Mass spectra from the PnC region of interest acquired on a *Cntnap2* WT (**Left**) and KO (**Right**) rat coronal brain slice with ZnO in the mass region 100–250. Mass peaks corresponding to neurotransmitters ([GABA+K]$^+$: 142m/z, [Glu+K]$^+$: 186m/z, [Gln+ K]$^+$: 185m/z) were acquired from each mass spectra. **(D)** The degree of signal enhancement in the PnC region can be seen through pairwise comparative under the curve analysis for *Cntnap2* KO rats (n = 7, red squares and horizontal line) compared with WT controls (n = 7, blue circles and horizontal line). The area under the curve (AUC) ratio was significantly enhanced for GABA (**Left**, paired t-test p = 0.0242), and by tendency for Glu (**Middle**, paired t-test p = 0.0858) and Gln (**Right**, paired t-test p = 0.0703). Dotted lines denote female, solid lines male WT-KO pairs. Abbreviations: PnC, nucleus reticularis pontis caudalis; mcp, middle cerebellar peduncle; 7n, facial nerve. Scale bar: 2mm. $^{(*)}p < 0.1$, $^*p < 0.05$.

between equally treated *Cntnap2* WT and KO rats. Mixed-effects analysis showed significantly reduced habituation scores with 3 mg/kg R-Baclofen in comparison to saline in both genotypes, thereby confirming enhanced short-term habituation through R-Baclofen in *Cntnap2* WT and KO rats (**Figure 5C**, Mixed-effects analysis, *Cntnap2* WT: n = 9–11 rats, *Cntnap2* KO: n = 11 rats, genotype p = 0.0034, $F_{(1,20)}$ = 11.03, treatment p = 0.0005, $F_{(2.785, 53.84)}$ = 7.327, treatment × genotype p = 0.9632,

TABLE 2 | Statistical comparison of MALDI MS AUC ratio (AUC ratio*10^{-2}, paired *t*-test) and fold changes (one sample *t* test) for GABA, Glu, Gln, Choline, and Norepinephrine in the PnC region of experimentally naïve *Cntnap2* WT and KO rats.

	AUC ratio			Fold change							
Genotype	**GABA**	**Glu**	**Gln**	**GABA**	**Glu**	**Gln**	**Glu/GABA**	**GABA/Glu**	**Glu/Gln**	**GABA/Gln**	**Choline**	**Norepinephrine**
Cntnap2 WT	0.059	0.118	0.363	1	1	1	1	1	1	1	1	1
Cntnap2 KO	0.114	0.172	0.506	2.025	1.445	1.360	0.7671	1.442	1.066	1.487	1.108	1.485
t-test	0.0242*	0.0858(*)	0.0703(*)	0.0222*	0.0935(*)	0.0814(*)	0.0349*	0.0853(*)	0.4051$^{n.s.}$	0.0335*	0.3336$^{n.s.}$	0.1383$^{n.s.}$

*Post hoc t test: (*)$p < 0.1$, *$p < 0.05$, n.s.: not significant.*

$F_{(3,58)}$ = 0.09379, Dunnett's multiple comparison's test, WT: saline vs. 0.75 mg/kg p = 0.8601, saline vs. 1.5 mg/kg p = 0.2785, saline vs. 3 mg/kg: p = 0.0118; KO: saline vs. 0.75 mg/kg p = 0.9861, saline vs. 1.5 mg/kg p = 0.8595, saline vs. 3 mg/kg: p = 0.0205). To further analyze the effects of the three doses of R-Baclofen on short-term habituation between *Cntnap2* WT and KO rats, we performed straight-line regressions of the habituation scores depending on the treatment, and compared the slopes and elevations of the two regression lines (**Figure 5C**). The elevations of the regression lines were significantly different in *Cntnap2* KO compared with WT rats, resulting from the overall greater habituation scores across treatments in *Cntnap2* KO rats (**Figure 5C**, *Cntnap2* WT: n = 9–11 rats, elevation: c = 0.8004, *Cntnap2* KO: n = 11 rats, elevation: c = 1.073, p = 0.0093). The slopes were similar in *Cntnap2* WT and KO rats, showing a negative relationship between the R-Baclofen dose and habituation score in both genotypes (i.e., the higher the dose, the lower the habituation score, **Figure 5C**, *Cntnap2* WT: n = 9–11 rats, slope: m = −0.1273, *Cntnap2* KO: n = 11 rats, slope: m = −0.1514, p = 0.6940). This indicates that the selective activation of $GABA_B$ receptors by R-Baclofen had a similar suppressive mode of action on habituation scores in *Cntnap2* WT and KO rats. In contrast to short-term habituation, R-Baclofen did not induce a statistically significant reduction in sensitization scores, neither within nor between *Cntnap2* WT and KO rats (**Figure 5D**, two-way RM-ANOVA, *Cntnap2* WT: n = 11 rats, *Cntnap2* KO: n = 11 rats, genotype p = 0.0966, $F_{(1,20)}$ = 3.040, treatment p = 0.1430, $F_{(2.628, 52.56)}$ = 1.930, treatment × genotype p = 0.5867, $F_{(3,60)}$ = 0.6490; Linear regression, *Cntnap2* WT: Y = −0.04851 * X + 0.8589, Sy.x = 0.05019, *Cntnap2* KO: Y = −0.08989 * X + 1.014, Sy.x = 0.05991, WT vs. KO: slopes p = 0.3053, elevation p = 0.0548). Taken together, our results suggest that higher doses of R-Baclofen have the potential to improve deficient sensory filtering in *Cntnap2* KO rats by enhancing short-term habituation. Sensitization of the ASR, however, appeared insensitive to the influence of R-Baclofen. This indicates that the cellular mechanisms or neural circuits controlling short-term habituation and sensitization are not affected the same way by selective activation of $GABA_B$ receptors though systemic administration of R-Baclofen.

R-Baclofen Ameliorates Exaggerated ASRs in *Cntnap2* KO Rats to Moderate, but Not to High Startle Pulse Intensities

The relationship between startle pulse intensities and ASR magnitudes can be altered through a number of variables, such as the genotype and pharmaceuticals (**Figure 2**; for review, see Koch, 1999). We next aimed to test if R-Baclofen could decrease the enhanced ASR magnitudes and ASR capacity in *Cntnap2* KO rats. We first compared the effects of R-Baclofen on the ASR I-O function and maximal response magnitudes within genotype and sex (**Figure 6**). In *Cntnap2* WT rats, all three doses of R-Baclofen (0.75, 1.5, 3 mg/kg) significantly decreased the ASR magnitudes to startle pulses of increasing intensity compared with saline in both females and males (**Figure 6A** Left, *Cntnap2* WT F: n = 6, Two-way RM ANOVA, intensity p < 0.0001, $F_{(10,55)}$ = 44.28,

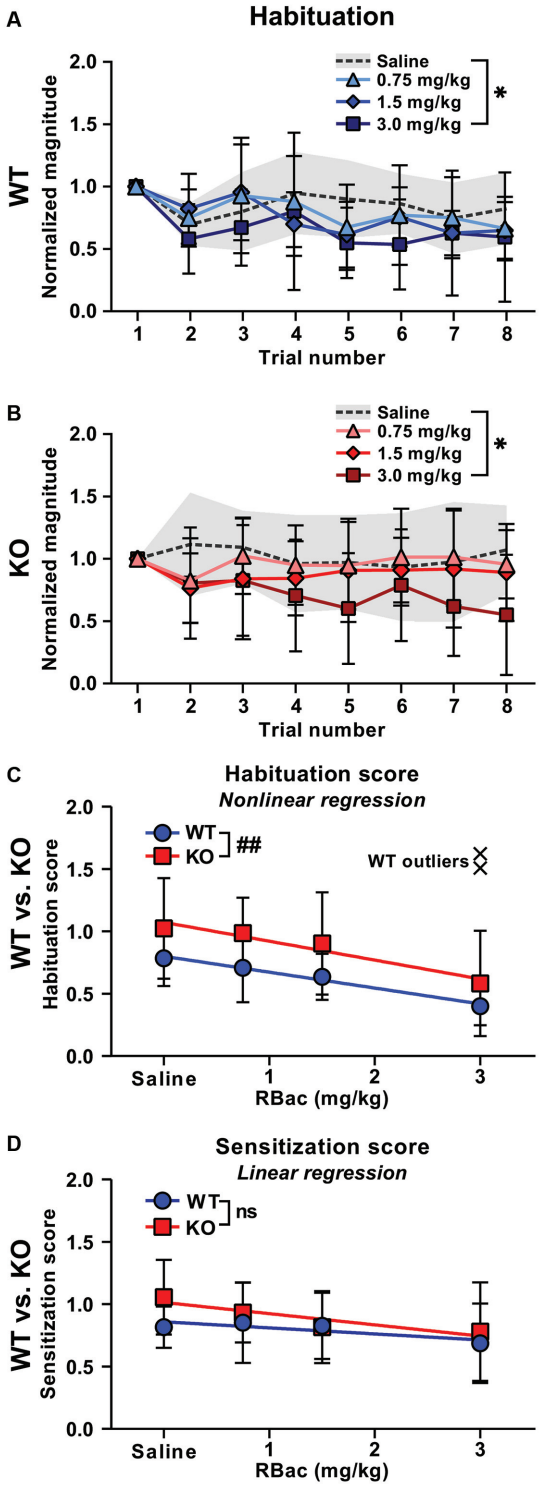

FIGURE 5 | Higher doses of R-Baclofen (RBac) normalize habituation in *Cntnap2* KO rats. **(A,B)** Mean ± SD startle response magnitudes across eight subsequent trials normalized to the first trial in *Cntnap2* WT (**A**, blue symbols) and KO rats (**B**, red symbols) 1 h after injection of 0.75 mg/kg (triangles and error bars), 1.5 mg/kg (diamonds and error bars), or 3.0 mg/kg (squares and error bars) R-Baclofen compared with vehicle (saline, dotted line and gray

(*Continued*)

FIGURE 5 | Continued

area). Values <1 indicate habituation of the startle response. 3 mg/kg R-Baclofen led to a greater decline of startle magnitudes across the first eigth trials in comparison with saline administration in both *Cntnap2* WT (**A**, $n = 11$, Two-way RM ANOVA, trial $p < 0.0001$, $F_{(7,80)} = 8.884$, treatment $p = 0.0071$, $F_{(2.647, 211.7)} = 4.397$, trial × treatment $p = 0.8352$, $F_{(21,240)} = 0.6965$, Dunnett's multiple comparisons test, saline vs. 0.75 mg/kg $p = 0.6549$, saline vs. 1.5 mg/kg $p = 0.1267$, saline vs. 3 mg/kg $p = 0.0084$) and *Cntnap2* KO rats (**B**, $n = 11$, Two-way RM ANOVA, trial $p = 0.6752$, $F_{(7,80)} = 0.6960$, treatment $p < 0.0001$, $F_{(2.864, 229.1)} = 10.16$, trial × treatment $p = 0.7925$, $F_{(21,240)} = 0.7925$, Dunnett's multiple comparisons test, saline vs. 0.75 mg/kg $p = 0.7085$, saline vs. 1.5 mg/kg $p = 0.0606$, saline vs. 3 mg/kg $p < 0.0001$). **(C)** Straight-line regression of the habituation scores in *Cntnap2* WT (blue circles and error bars, mean ± SD) and KO rats (red squares and error bars, mean ± SD). Mixed-effects analysis showed significantly reduced habituation scores with 3 mg/kg R-Baclofen in comparison to saline in both genotypes (*Cntnap2* WT: $n = 9$–11 rats, *Cntnap2* KO: $n = 11$ rats, genotype $p = 0.0034$, $F_{(1,20)} = 11.03$, treatment $p = 0.0005$, $F_{(2.785, 53.84)} = 7.327$, treatment × genotype $p = 0.9632$, $F_{(3,58)} = 0.09379$, Dunnett's multiple comparison's test, WT: saline vs. 0.75 mg/kg $p = 0.8601$, saline vs. 1.5 mg/kg $p = 0.2785$, saline vs. 3 mg/kg: $p = 0.0118$; KO: saline vs. 0.75 mg/kg $p = 0.9861$, saline vs. 1.5 mg/kg $p = 0.8595$, saline vs. 3 mg/kg: $p = 0.0205$). The slopes of the regression lines showed no R-Baclofen dose-dependent differences in *Cntnap2* WT ($n = 9$–11 rats, $Y = -0.1273 * X + 0.8004$, $Sy.x = 0.2131$) and KO rats ($n = 11$ rats, $Y = -0.1514 * X + 1.073$, $Sy.x = 0.3777$), whereas the elevations of the regression lines were significantly different ($p = 0.0093$). Two *Cntnap2* WT outliers at 3 mg/kg R-Baclofen (black crosses) were excluded from the straight-line regression and mixed-effects analysis using Prism GraphPad's "Detect and eliminate outliers" method. **(D)** R-Baclofen treatment did not induce a statistically significant reduction in sensitization scores, neither in *Cntnap2* WT nor KO rats (two-way RM-ANOVA, *Cntnap2* WT: $n = 11$ rats, *Cntnap2* KO: $n = 11$ rats, genotype $p = 0.0966$, $F_{(1,20)} = 3.040$, treatment $p = 0.1430$, $F_{(2.628, 52.56)} = 1.930$, treatment × genotype $p = 0.5867$, $F_{(3,60)} = 0.6490$). Regression lines were similar in both genotypes (*Cntnap2* WT: $Y = -0.04851 * X + 0.8589$, $Sy.x = 0.05019$, *Cntnap2* KO: $Y = -0.08989 * X + 1.014$, $Sy.x = 0.05991$, WT vs. KO: slopes $p = 0.3053$, elevation $p = 0.0548$). $^{*}p < 0.05$; $^{\#\#}p < 0.01$ (comparison of regression lines); n.s.: not significant.

treatment $p < 0.0001$, $F_{(2.453, 134.9)} = 86.07$, intensity × treatment $p < 0.0001$, $F_{(30,165)} = 4.390$, Dunnett's multiple comparisons test, saline vs. 0.75 mg/kg $p < 0.0001$, saline vs. 1.5 mg/kg $p < 0.0001$, saline vs. 3 mg/kg: $p < 0.0001$; Right, *Cntnap2* WT M: $n = 5$, Two-way RM ANOVA, intensity $p < 0.0001$, $F_{(10,44)} = 21.39$, treatment $p < 0.0001$, $F_{(2.511, 110.5)} = 63.83$, intensity × treatment $p < 0.0001$, $F_{(30,132)} = 2.847$, Dunnett's multiple comparisons test, saline vs. 0.75 mg/kg $p = 0.0002$, saline vs. 1.5 mg/kg $p < 0.0001$, saline vs. 3 mg/kg: $p < 0.0001$). This decrease in ASR magnitudes was evident across a wide range of startle pulse intensities after injection of 1.5 and 3 mg/kg R-Baclofen in female and male *Cntnap2* WT rats (*post hoc* comparisons matched for startle pulse intensities see **Supplementary Table 1**). In *Cntnap2* KO rats, 1.5 and 3 mg/kg R-Baclofen significantly reduced ASR magnitudes in both females and males, whereas the lowest dose of R-Baclofen (0.75 mg/kg) did not (**Figure 6B** Left, *Cntnap2* KO F: $n = 6$, Two-way RM ANOVA, intensity $p < 0.0001$, $F_{(10,55)} = 17.99$, treatment $p < 0.0001$, $F_{(1.911, 105.1)} = 29.81$, intensity × treatment $p = 0.0405$, $F_{(30,165)} = 1.568$, Dunnett's multiple comparisons test, saline vs. 0.75 mg/kg $p > 0.9999$, saline vs. 1.5 mg/kg $p = 0.0309$, saline vs. 3 mg/kg: $p < 0.0001$; Right, *Cntnap2* KO M: $n = 5$, Two-way RM ANOVA, intensity $p < 0.0001$, $F_{(10,44)} = 77.47$,

treatment $p < 0.0001$, $F_{(2.137, 94.04)} = 20.74$, intensity × treatment $p = 0.1091$, $F_{(30,132)} = 1.384$, Dunnett's multiple comparisons test, saline vs. 0.75 mg/kg $p = 0.9802$, saline vs. 1.5 mg/kg $p = 0.0003$, saline vs. 3 mg/kg: $p < 0.0001$). Interestingly, in both female and male *Cntnap2* KO rats, the reduction in ASR magnitude was only present in response to weaker, but not to higher startle pulse intensities (*post hoc* comparisons matched for startle pulse intensities see **Supplementary Table 1**). To further investigate the effect of R-Baclofen on maximum ASR capacity, we compared the ASR magnitudes at the loudest startle pulse (115 dB SPL) relative to respective saline controls (**Figures 6C,D**). In female and male *Cntnap2* WT rats, R-Baclofen induced a dose-dependent reduction in maximal ASR magnitude [**Figure 6C**, median (IQR), WT F: $n = 6$ rats, 0.75 mg/kg re saline: 0.79 (0.49–1.06), 1.5 mg/kg re saline: 0.70 (0.60–0.88), 3 mg/kg re saline: 0.38 (0.30–0.52), Friedman test, $p = 0.0085$, Dunn's multiple comparisons test, 0.75 mg/kg vs. saline: $p > 0.9999$, 1.5 mg/kg vs. saline: $p = 0.5391$, 3 mg/kg vs. saline: $p = 0.0052$; WT M: $n = 5$ rats, 0.75 mg/kg re saline: 0.71 (0.64–0.99), 1.5 mg/kg re saline: 0.66 (0.39–0.74), 3 mg/kg re saline: 0.52 (0.35–0.68), Friedman test, $p = 0.0120$, Dunn's multiple comparisons test, 0.75 mg/kg vs. saline: $p = 0.6620$, 1.5 mg/kg vs. saline: $p = 0.0825$, 3.0 mg/kg vs. saline: $p = 0.0099$]. In contrast, maximal ASR magnitudes were similar irrespective of treatment in both female and male *Cntnap2* KO rats (**Figure 6D**, median (IQR), KO F: $n = 6$ rats, 0.75 mg/kg re saline: 1.04 (0.85–1.26), 1.5 mg/kg re saline: 1.19 (0.91–1.42), 3 mg/kg re saline: 0.59 (0.42–0.79), Friedman test, $p = 0.1268$; KO M: $n = 5$ rats, 0.75 mg/kg re saline: 1.00 (0.94–1.17), 1.5 mg/kg re saline: 1.02 (0.88–1.09), 3 mg/kg re saline: 0.98 (0.83–1.02), Friedman test, $p = 0.3720$). In summary, as expected, R-Baclofen decreased magnitudes in the ASR I-O growth functions. In doing so, *Cntnap2* KO rats showed a higher minimal effective dose (1.5 mg/kg) than WT rats (0.75 mg/kg). The reduction in ASR magnitudes in *Cntnap2* KO rats was restricted to lower startle pulse intensities, whereas the increased maximal ASR capacity was not ameliorated by R-Baclofen. This notion was further corroborated by between genotype comparisons, in particular, ASR magnitudes in *Cntnap2* KO males after R-Baclofen treatment compared to saline-injected WT males (**Supplementary Figures 5D–F**). R-Baclofen dose-dependently reduced ASR magnitudes in *Cntnap2* KO males and brought them closer to WT control levels. However, ASR magnitudes were most notably downregulated for low to medium startle pulse intensities, but not for the highest startle pulse intensities tested (**Supplementary Figures 5D–F**). Furthermore, *post hoc* testing of normalized ASR I-O functions matched for startle pulse intensities did not find statistically significant differences between treatments in *Cntnap2* WT rats, whereas in *Cntnap2* KO rats ASR magnitudes were reduced in particular at 85 and 90 dB SPL after 1.5 mg/kg R-Baclofen and at 90 dB SPL after 3 mg/kg R-Baclofen administration (Dunnett's multiple comparisons test, saline vs. 1.5 mg/kg: 85 dB SPL: $p = 0.0105$, 90 dB SPL: $p = 0.0322$; saline vs. 3 mg/kg: 90 dB SPL: $p = 0.0375$, **Supplementary Figure 6**). The minimal effective dose of R-Baclofen in *Cntnap2* KO rats determined from their normalized ASR magnitudes after treatment with R-Baclofen compared to those in WT rats after saline injection was 1.5 mg/kg (**Supplementary Figures 6C–E**). These differences between *Cntnap2* WT and KO rats after normalizing magnitudes to the individual ASR capacities further emphasize the differential effect of R-Baclofen on ASR I-O growth functions in the two genotypes. It suggests that the R-Baclofen effect was distinctly suppressive on ASRs to weaker startle pulse intensities in KO rats. In contrast, lack of such a suppression indicated that in WT rats R-Baclofen particularly impacted their ASRs to higher startle pulse intensities.

R-Baclofen Treatment Normalizes ASR I-O Threshold and Saturation in *Cntnap2* KO Rats, but Exacerbates Shorter ASR Peak Latencies

Sigmoidal curves were fitted to the ASR I-O data scaled between 0 and 1 for individual animals of both genotypes and all treatments. Average curve fits were significantly different between *Cntnap2* KO rats treated with 0.75 mg/kg R-Baclofen and *Cntnap2* WT rats after saline injection (**Figure 7A** and **Table 3**, $p < 0.0001$, $F_{(2,238)} = 12.12$). In contrast to this, average curve fits were similar between *Cntnap2* KO rats treated with 1.5 mg/kg (**Figure 7B** and **Table 3**, $p = 0.6048$, $F_{(2,238)} = 0.5039$) or 3 mg/kg R-Baclofen (**Figure 7C** and **Table 3**, $p = 0.7751$, $F_{(2,238)} = 0.2550$) compared with *Cntnap2* WT rats after saline injection. ASR thresholds extracted at the 25% scaled magnitude generally increased with the dose of R-Baclofen (**Figure 7D** and **Supplementary Table 2**). This increase was significant in *Cntnap2* KO rats in particular with 1.5 mg/kg R-Baclofen in comparison with saline, but not in WT rats (**Figure 7D** Left, *Cntnap2* WT rats ($n = 11$), mean ± SD saline: 87.9 ± 5.1 dB SPL, 0.75 mg/kg: 88.1 ± 5.0 dB SPL, 1.5 mg/kg: 89.4 ± 4.3 dB SPL, 3 mg/kg: 92.2 ± 5.8 dB SPL, RM ANOVA, $p = 0.0685$, **Figure 7D** Middle, *Cntnap2* KO rats ($n = 11$), saline: 82.8 ± 4.7 dB SPL, 0.75 mg/kg: 84.3 ± 3.4 dB SPL, 1.5 mg/kg: 86.5 ± 3.9 dB SPL, 3 mg/kg: 88.8 ± 5.4 dB SPL, RM ANOVA, $p = 0.0291$, Dunnett's multiple comparisons test, saline vs. 0.75 mg/kg $p = 0.5583$, saline vs. 1.5 mg/kg $p = 0.0315$, saline vs. 3 mg/kg: $p = 0.0784$). Comparison of ASR thresholds in R-Baclofen-treated *Cntnap2* KO rats with saline-treated WT rats showed that thresholds were increased to control level after injection of 1.5 and 3 mg/kg R-Baclofen, while they were by tendency still lower than in controls with 0.75 mg/kg R-Baclofen (**Figure 7D** Right, two-sided student's *t*-test, WT—Saline vs. KO–0.75 mg/kg: $p = 0.0690$, WT—Saline vs. KO–1.5 mg/kg: $p = 0.4839$, WT—Saline vs. KO–3 mg/kg: $p = 0.6819$). Saturation of the ASR I-O function extracted at the 90% scaled magnitude was significantly altered through R-Baclofen in *Cntnap2* KO rats, but not in WT rats (**Figure 7E** and **Supplementary Table 2**). In particular, 3 mg/kg R-Baclofen increased ASR I-O saturation in *Cntnap2* KO rats compared with saline [**Figure 7E** Left, *Cntnap2* WT rats ($n = 11$), median (IQR), saline: 109.3 (97.4-115.0) dB SPL, 0.75 mg/kg: 100.7 (99.1-106.7) dB SPL, 1.5 mg/kg: 104.3 (98.5-112.8) dB SPL, 3 mg/kg: 111.3 (97.7-112.2) dB SPL, Friedman test, $p = 0.5915$, **Figure 7E** Middle, *Cntnap2* KO rats ($n = 11$), saline: 100.8 (94.2-102.3) dB SPL, 0.75 mg/kg: 97.2 (95.3-103.1) dB SPL, 1.5 mg/kg:

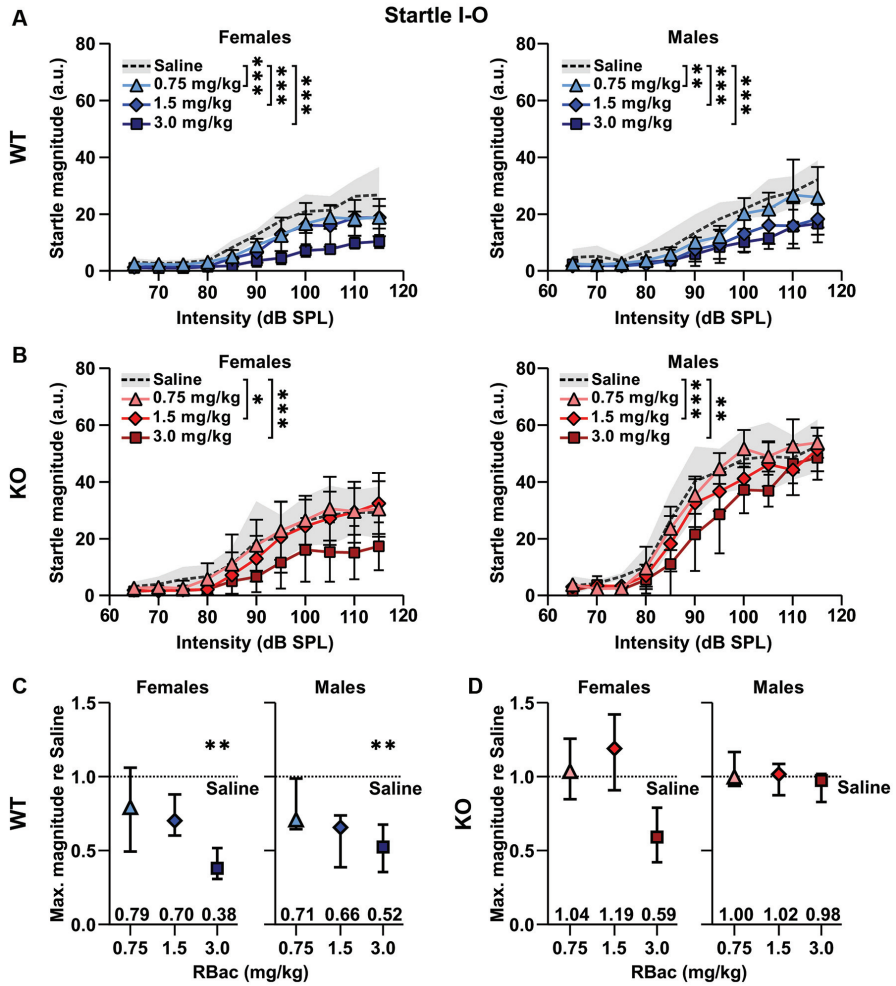

FIGURE 6 | Medium and high doses of R-Baclofen decrease ASR magnitudes in *Cntnap2* KO rats to control levels. **(A,B)** Mean ± SD startle response magnitudes to increasing startle pulse intensities after injection of saline (dotted line and gray area), 0.75 mg/kg (triangles), 1.5 mg/kg (diamonds), 3 mg/kg R-Baclofen (squares) in *Cntnap2* WT rats (**A**, blue symbols) and *Cntnap2* KO rats (**B**, red symbols). Startle magnitudes were significantly reduced after injection of 0.75, 1.5, or 3 mg/kg R-Baclofen in comparison with injection of saline in female **(A, Left)** and male **(A, Right)** *Cntnap2* WT rats (**A, Left**, *Cntnap2* WT F: $n = 6$, two-way RM ANOVA, intensity $p < 0.0001$, $F_{(10,55)} = 44.28$, treatment $p < 0.0001$, $F_{(2.453,\ 134.9)} = 86.07$, intensity × treatment $p < 0.0001$, $F_{(30,165)} = 4.390$, Dunnett's multiple comparisons test, saline vs. 0.75 mg/kg $p < 0.0001$, saline vs. 1.5 mg/kg $p < 0.0001$, saline vs. 3 mg/kg: $p < 0.0001$; **A, Right**, *Cntnap2* WT M: $n = 5$, two-way RM ANOVA, intensity $p < 0.0001$, $F_{(10,44)} = 21.39$, treatment $p < 0.0001$, $F_{(2.511,\ 110.5)} = 63.83$, intensity × treatment $p < 0.0001$, $F_{(30,132)} = 2.847$, Dunnett's multiple comparisons test, saline vs. 0.75 mg/kg $p = 0.0002$, saline vs. 1.5 mg/kg $p < 0.0001$, saline vs. 3 mg/kg: $p < 0.0001$). **(B)** Startle magnitudes in female **(B, Left)** and male **(B, Right)** *Cntnap2* KO rats were significantly reduced after injection of 1.5, or 3 mg/kg, but not with 0.75 mg/kg, R-Baclofen in comparison with saline injection (**B, Left**, *Cntnap2* KO F: $n = 6$, Two-way RM ANOVA, intensity $p < 0.0001$, $F_{(10,55)} = 17.99$, treatment $p < 0.0001$, $F_{(1.911,\ 105.1)} = 29.81$, intensity × treatment $p = 0.0405$, $F_{(30,165)} = 1.568$, Dunnett's multiple comparisons test, saline vs. 0.75 mg/kg $p > 0.9999$, saline vs. 1.5 mg/kg $p = 0.0309$, saline vs. 3 mg/kg: $p < 0.0001$; **B, Right**, *Cntnap2* KO M: $n = 5$, Two-way RM ANOVA, intensity $p < 0.0001$, $F_{(10,44)} = 77.47$, treatment $p < 0.0001$, $F_{(2.137,\ 94.04)} = 20.74$, intensity × treatment $p = 0.1091$, $F_{(30,132)} = 1.384$, Dunnett's multiple comparisons test, saline vs. 0.75 mg/kg $p = 0.9802$, saline vs. 1.5 mg/kg $p = 0.0003$, saline vs. 3 mg/kg: $p < 0.0001$). **(C,D)** Comparison of ASR maximum response. **(C)** In both female (**Left**) and male (**Right**) *Cntnap2* WT rats, R-Baclofen induced a significant decrease in the maximum ASR capacity at 115 dB SPL (WT F: Friedman test, $p = 0.0085$, Dunn's multiple comparisons test, 0.75 mg/kg $p > 0.9999$, 1.5 mg/kg $p = 0.5391$, 3.0 mg/kg $p = 0.0052$; WT M: Friedman test, $p = 0.0120$, Dunn's multiple comparisons test, 0.75 mg/kg $p = 0.6620$, 1.5 mg/kg $p = 0.0825$, 3.0 mg/kg $p = 0.0099$). **(D)** R-Baclofen did not induce a decrease in maximum ASR capacity from female (**Left**) nor male (**Right**) *Cntnap2* KO rats (KO F: Friedman test, $p = 0.1268$; KO M: Friedman test, $p = 0.3720$). $^{*}p < 0.05$; $^{**}p < 0.01$; $^{***}p < 0.001$.

109.3 (99.4-110.2) dB SPL, 3 mg/kg: 104.0 (97.9-115.5) dB SPL, Friedman test, $p = 0.0240$, Dunn's multiple comparisons test, saline vs. 0.75 mg/kg: $p > 0.9999$, saline vs. 1.5 mg/kg: $p = 0.2959$, saline vs. 3 mg/kg: $p = 0.0150$]. Comparison between genotypes showed that ASR I-O saturation in *Cntnap2* KO rats with 1.5 and 3 mg/kg R-Baclofen was similar to saturation in WT rats after saline injection, while there was a slight, yet not quite significant, difference with 0.75 mg/kg (**Figure 7E** Right, Mann–Whitney test, WT—Saline vs. KO–0.75 mg/kg: $p = 0.0879$, WT—Saline vs. KO–1.5 mg/kg: $p = 0.7477$, WT—Saline vs. KO–3 mg/kg: $p = 0.8470$). Taken together, our results suggest that selective activation of $GABA_B$ receptors by 1.5 mg/kg and 3 mg/kg

R-Baclofen can normalize acoustic reactivity in *Cntnap2* KO rats through a right-shift in ASR I-O function and an increase in ASR threshold and saturation sound levels to control levels.

We next investigated R-Baclofen-related changes in ASR peak latencies in *Cntnap2* WT and KO rats across the ASR dynamic range (**Figures 7F–H** and **Table 4**). In *Cntnap2* WT rats, R-Baclofen increased the ASR peak latencies across the dynamic range by means of greater regression line elevations in comparison with saline (most notably at 0.75 and 3 mg/kg, **Figure 7F** and **Table 4**, elevation: $p = 0.0034$). In contrast to this, R-Baclofen decreased the ASR peak latencies across the dynamic range by means of smaller regression line elevations in *Cntnap2* KO rats compared with saline (most notably at 1.5 and 3 mg/kg, **Figure 7G** and **Table 4**, elevation: $p = 0.0336$). Slopes of the peak latency regression lines across the ASR dynamic range were not altered through R-Baclofen in comparison with saline within genotypes, neither in *Cntnap2* WT nor KO rats (**Figures 7F–G** and **Table 4**, slopes: WT $p = 0.8086$, KO $p = 0.7055$).

As shown in **Figure 7** and **Supplementary Figures 5, 6**, R-Baclofen decreased ASR magnitudes in *Cntnap2* KO rats particularly at lower startle pulse intensities near ASR I-O threshold. To further analyze the effects of the three doses of R-Baclofen on peak latencies near ASR threshold, we performed linear regressions of the peak latencies at ASR I-O threshold across treatments (**Figure 7H**). Comparison of the two regression lines from *Cntnap2* WT and KO rats showed that the slopes were significantly different (**Figure 7H**, WT: $Y = 5.893 * X + 306.6$, Sy.$x = 7.147$; KO: $Y = -8.876 * X + 295.3$, Sy.$x = 2.057$, slopes $p = 0.0116$). In *Cntnap2* KO rats, the ASR peak latency at I-O threshold was negatively related to the R-Baclofen dose (i.e., the higher the dose, the shorter the latency, **Figure 7H**, slope $m = -8.876$ ms/increment, deviation from zero $p = 0.0107$, $F_{(1,2)} = 91.68$). No such relationship between latency and R-Baclofen dose was found in *Cntnap2* WT rats (**Figure 7H**, slope $m = 5.893$ ms/increment, deviation from zero $p = 0.2088$, $F_{(1,2)} = 3.347$). The differential effects of R-Baclofen on startle peak latencies at threshold in *Cntnap2* WT and KO rats became especially prominent at 3 mg/kg (**Figure 7H**, two-way RM ANOVA, treatment $p = 0.8260$, $F_{(2.290, 45.79)} = 0.2271$, genotype $p = 0.0152$, $F_{(1,20)} = 7.050$, treatment × genotype $p = 0.1859$, $F_{(3,60)} = 1.657$, Sidak's multiple comparisons test, WT vs. KO: Saline $p = 0.9991$, 0.75 mg/kg $p = 0.3525$, 1.5 mg/kg $p = 0.2288$, 3 mg/kg $p = 0.0021$). This indicates that the cellular mechanisms or neural circuits controlling ASR peak latencies near ASR thresholds are affected differently by selective activation of $GABA_B$ receptors through systemic administration of R-Baclofen in *Cntnap2* WT and KO rats.

R-Baclofen Improves Sensorimotor Gating in *Cntnap2* KO Rats by Means of Increasing the Relative Amount and Relative Latencies of Startle in PPI Trials

The effect of R-Baclofen on sensorimotor gating in *Cntnap2* WT and KO rats was assessed using the PPI of the startle. The relative amount of PPI (%PPI) elicited by three prepulse stimulus levels (65, 75, and 85 dB SPL) at two different ISIs (30 and 100 ms) was first compared between *Cntnap2* WT and KO rats after injection of saline. *Cntnap2* KO rats had robust, but statistically nonsignificant, lower %PPI than WT rats for all prepulse conditions (**Figure 8A** and **Table 5**). Random permutation tests of %PPI for prepulses with 75 dB SPL, 100 ms, as well as 85 dB SPL, 30 ms between *Cntnap2* WT and KO rats gave estimated p values of $p = 0.0017$ and $p = 0.0163$ (40 repetitions of 10,000 random samples without replacement, see **Table 5**), indicating a significant PPI deficit in *Cntnap2* KO rats for these two prepulse types (**Figure 8A** and **Table 5**). In *Cntnap2* WT rats, R-Baclofen showed no significant effect on %PPI elicited by any of the six prepulse types (**Figure 8B**, statistical comparisons see **Table 6**). In contrast, KO rats showed a significant increase in %PPI in four of the six prepulse conditions through R-Baclofen (intensity, ISI: 75 dB SPL, 30 ms, 75 dB SPL, 100 ms, 85 dB SPL, 30 ms; 85 dB SPL, 100 ms, **Figure 8C**, for statistical comparisons see **Table 6**). In particular, %PPI in *Cntnap2* KO rats was increased with 1.5 mg/kg (prepulse 85 dB SPL, 100 ms) or 3 mg/kg R-Baclofen (prepulse 75 dB SPL, 30 ms, 75 dB SPL, 100 ms, 85 dB SPL, 30 ms; **Figure 8C**, for statistical comparisons see **Table 6**). Taken together, our results suggest that $GABA_B$ receptor agonist R-Baclofen can improve deficient sensorimotor gating in *Cntnap2* KO rats by increasing the relative amount of PPI.

To analyze the influence of R-Baclofen on temporal properties of sensorimotor gating, we compared the change in latency to the maximum startle response in trials with and without a prepulse between *Cntnap2* WT and KO rats (**Figure 9**). After injection of saline, *Cntnap2* KO rats showed generally shorter relative latencies than WT rats. The difference was significant for relative latencies to the prepulse type with 85 dB SPL, 30 ms (**Figure 9A**, two-sided student's t-test $p = 0.0195$). The shorter relative latencies in trials that included a prepulse indicated impaired temporal characteristics of sensorimotor gating in *Cntnap2* KO rats compared to WT rats. Within genotype, comparisons showed that R-Baclofen did not significantly increase the relative latencies in either *Cntnap2* WT or KO rats for any of the six prepulse types, even though there appeared to be a slight increase in relative latency for some prepulse conditions in *Cntnap2* KO rats (shown for prepulse condition 85 dB SPL, 30 ms in **Figure 9B**, Left: WT, RM ANOVA, $p = 0.9282$, $F = 0.1226$; Right: KO, RM ANOVA, $p = 0.5611$, $F = 0.6374$; for statistical results of all six prepulse conditions see **Supplementary Figure 8**). Therefore, we aimed to analyze if subtle changes in relative latency through R-Baclofen had the potential to increase latencies in *Cntnap2* KO rats to WT control levels after saline injection. Indeed, all three doses of R-Baclofen increased the relative latency in *Cntnap2* KO rats to levels similar to WT controls for prepulse type 85 dB SPL, 30 ms (**Figure 9C**, two-sided student's t-test, WT—Saline vs. KO–0.75 mg/kg: $p = 0.4381$, WT—Saline vs. KO–1.5 mg/kg: $p = 0.2627$, WT—Saline vs. KO–3 mg/kg: $p = 0.3069$). This indicates that $GABA_B$

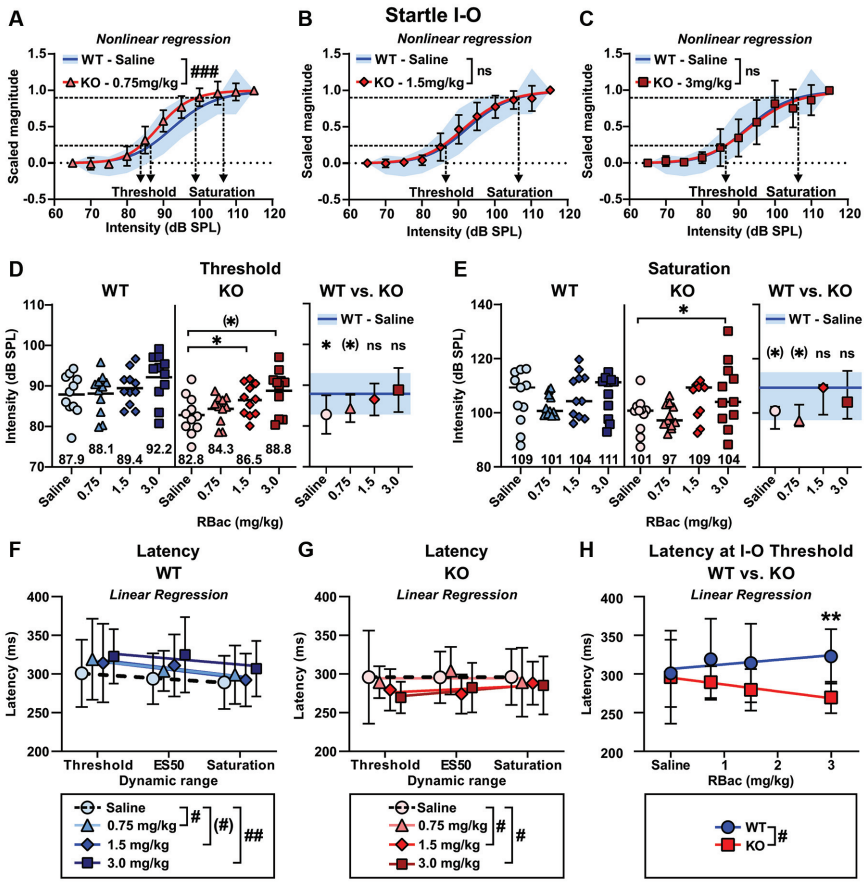

FIGURE 7 | Medium and high doses of R-Baclofen increase ASR I-O threshold and saturation in *Cntnap2* KO rats close to controls but shorten ASR peak latencies. **(A–C)** Sigmoidal curves (lines) fitted to the startle magnitudes scaled between 0 and 1 in *Cntnap2* WT rats with saline (SD, blue area) and *Cntnap2* KO rats (mean ± SD) with 0.75 mg/kg (**A**, red triangles and error bars), 1.5 mg/kg (**B**, red diamonds and error bars), and 3 mg/kg R-Baclofen (**C**, red squares and error bars). Dotted horizontal line at 0.25 determined as ASR threshold and at 0.9 as ASR saturation (curve fit values see **Table 3**). The average curve fit was significantly different from controls in *Cntnap2* KO rats after administration of 0.75 mg/kg (**A**, $p < 0.0001$, $F_{(2,238)} = 12.12$), but similar to controls with 1.5 mg/kg (**B**, $p = 0.6048$, $F_{(2,238)} = 0.5039$), and 3 mg/kg R-Baclofen (**C**, $p = 0.7751$, $F_{(2,238)} = 0.2550$). **(D)** Individual ASR thresholds in *Cntnap2* WT (**Left**), KO (**Middle**), and WT vs. KO rats (**Right**) extracted from individual sigmoidal curve fits (ASR threshold values see **Supplementary Table 2**). **(D, Left)** Mean ASR thresholds were not significantly increased in *Cntnap2* WT rats with R-Baclofen (0.75 mg/kg: light blue triangles and horizontal black line, 1.5 mg/kg: blue diamonds and horizontal black line, 3 mg/kg: dark blue squares and horizontal black line) compared to saline (circles and horizontal black line, RM ANOVA, $p = 0.0685$). **(D, Middle)** Mean ASR thresholds were significantly increased in *Cntnap2* KO rats with R-Baclofen compared to saline (saline: circles and horizontal black line, 0.75 mg/kg: light red triangles and horizontal black line, 1.5 mg/kg: red diamonds and horizontal black line, 3 mg/kg: dark red squares and horizontal black line, RM ANOVA, $p = 0.0291$, Dunnett's multiple comparisons test, saline vs. 0.75 mg/kg: $p = 0.5583$, saline vs. 1.5 mg/kg: $p = 0.0315$, saline vs. 3 mg/kg: $p = 0.0784$). **(D, Right)** Mean ± SD ASR thresholds in *Cntnap2* KO rats were significantly different from WT controls (after saline, blue line and area) with saline (two-sided student's *t*-test, $p = 0.0244$), not quite significantly different with 0.75 mg/kg (two-sided student's *t*-test, $p = 0.0690$), and similar to controls with 1.5 mg/kg (two-sided student's *t*-test, $p = 0.4839$) and 3 mg/kg R-Baclofen (two-sided student's *t*-test, $p = 0.6819$). **(E)** Individual ASR saturation levels in *Cntnap2* WT (**Left**), KO (**Middle**), and WT vs. KO rats (**Right**) extracted from individual sigmoidal curve fits (ASR saturation values see **Supplementary Table 2**). **(E, Left)** Median ASR saturation levels were not significantly altered in *Cntnap2* WT rats with R-Baclofen (0.75 mg/kg: light blue triangles and horizontal black line, 1.5 mg/kg: blue diamonds and horizontal black line, 3 mg/kg: dark blue squares and horizontal black line) compared to saline (circles and horizontal black line, Friedman test, $p = 0.5915$). **(E, Middle)** Median ASR saturation levels were significantly increased in *Cntnap2* KO rats with R-Baclofen compared to saline (saline: circles and horizontal black line, 0.75 mg/kg: light red triangles and horizontal black line, 1.5 mg/kg: red diamonds and horizontal black line, 3 mg/kg: dark red squares and horizontal black line, Friedman test, $p = 0.0240$, Dunn's multiple comparisons test, saline vs. 0.75 mg/kg: $p > 0.9999$, saline vs. 1.5 mg/kg: $p = 0.2959$, saline vs. 3 mg/kg: $p = 0.0150$). **(E, Right)** Median ± interquartile range (IQR) ASR saturation levels in *Cntnap2* KO rats were by tendency different from WT controls (after saline, blue line and area) with saline (Mann–Whitney test, $p = 0.0879$) and 0.75 mg/kg (Mann–Whitney test, $p = 0.0879$), and similar to controls with 1.5 mg/kg (Mann–Whitney test, $p = 0.7477$) and 3 mg/kg R-Baclofen (Mann–Whitney test, $p = 0.8470$). **(F,G)** Linear regression of ASR peak latencies across the dynamic range of *Cntnap2* WT **(F)** and KO **(G)** rats with saline or R-Baclofen (mean ± SD, linear regression fits see **Table 4**). Elevations of the regression lines were significantly different in *Cntnap2* WT (**F**, $p = 0.0034$, $F_{(3,7)} = 12.46$; saline vs. 0.75 mg/kg: $p = 0.0202$, $F_{(1,3)} = 20.50$; saline vs. 1.5 mg/kg: $p = 0.0620$, $F_{(1,3)} = 8.468$; saline vs. 3 mg/kg: $p = 0.0099$, $F_{(1,3)} = 34.45$) and KO rats **(G**; $p = 0.0336$, $F_{(3,7)} = 5.192$; saline vs. 0.75 mg/kg: $p = 0.8075$, $F_{(1,3)} = 0.07070$; saline vs. 1.5 mg/kg: $p = 0.0375$, $F_{(1,3)} = 12.76$; saline vs. 3 mg/kg: $p = 0.0272$, $F_{(1,3)} = 16.37$). **(H)** Linear regression of ASR peak latencies near threshold across treatment in *Cntnap2* WT (blue circles and error bars, mean ± SD) and KO rats (red squares and error bars, mean ± SD). Slopes of the regression lines were significantly different ($p = 0.0116$, $F_{(1,4)} = 19.41$; WT: blue line, $Y = 5.893 * X + 306.6$, Sy.$x = 7.147$; KO: red line, $Y = -8.876 * X + 295.3$, Sy.$x = 2.057$). $^{(*)}p < 0.1$; $^{*}p < 0.05$; $^{**}p < 0.01$; comparison of regression lines: $^{(\#)}p < 0.1$; $^{\#}p < 0.05$; $^{\#\#}p < 0.01$; $^{\#\#\#}p < 0.001$, n.s., not significant.

TABLE 3 | Comparison of sigmoidal regression fit of ASR I-O function with magnitude scaled between 0 and 1 in *Cntnap2* WT and KO rats.

	RBac (mg/kg)	Saline	0.75	1.5	3
Cntnap2 WT	Bottom	=0	=0	=0	=0
	Top	=1	=1	=1	=1
	ES50	92.92	92.87	94.10	96.67
	HillSlope	15.92	19.96	17.41	16.52
	Sy.x	0.1978	0.1400	15.06	0.1809
Cntnap2 KO	Bottom	=0	=0	=0	=0
	Top	=1	=1	=1	=1
	ES50	87.96	88.82	91.97	93.47
	HillSlope	16.31	19.85	15.70	14.60
	Sy.x	0.1688	0.1184	0.1304	0.1999
KO vs. WT—Saline	Different curve fits?	<0.0001***	<0.0001***	$0.6048^{n.s.}$	$0.7751^{n.s.}$
	Different slopes?	$0.8760^{n.s.}$	$0.1152^{n.s.}$	$0.9173^{n.s.}$	$0.5915^{n.s.}$
	Different ES50?	<0.0001***	<0.0001***	$0.3218^{n.s.}$	$0.6345^{n.s.}$

*Bottom plateau constraint to 0, Top plateau constraint to 1, ES50: acoustic pulse intensity (dB SPL) that gives a startle magnitude halfway between Bottom and Top, HillSlope: steepness of the curve, Sy.x: standard error of regression, KO vs. WT—Saline: curve fit comparison between Cntnap2 KO rats treated with saline, 0.75, 1.5, or 3 mg/kg R-Baclofen and WT rats with saline. p values, ***p < 0.001, n.s.: not significant.*

TABLE 4 | Linear regression of ASR peak latencies in *Cntnap2* WT and KO rats after treatment with saline or R-Baclofen (0.75, 1.5, 3 mg/kg).

	RBac (mg/kg)	Saline	0.75	1.5	3
Cntnap2 WT	m	−5.900	−10.08	−10.92	−7.886
	c	306.5	327.6	327.7	334.0
	Sy.x	0.9501	4.142	6.339	8.221
RBac vs. Saline	m	N/A	$0.2986^{n.s.}$	$0.3836^{n.s.}$	$0.7666^{n.s.}$
	c	N/A	0.0202^{*}	$0.0620^{(*)}$	0.0099^{**}
Cntnap2 KO	m	0.05455	−0.004545	4.377	7.809
	c	295.8	294.4	271.8	263.6
	Sy.x	0.3860	12.25	7.991	4.045
RBac vs. Saline	m	N/A	$0.9952^{n.s.}$	$0.5246^{n.s.}$	$0.1143^{n.s.}$
	c	N/A	$0.8075^{n.s.}$	0.0375^{*}	0.0272^{*}

*m: slope, c: Y-intercept, Sy.x: standard error of regression, RBac vs. Saline: within genotype comparison of regression lines after saline and R-Baclofen administration. p values, $^{(*)}$p < 0.1, *p < 0.05, **p < 0.01, n.s., not significant.*

TABLE 5 | Statistical comparison and estimated *p* values through resampling of %PPI elicited by six prepulse conditions in *Cntnap2* WT and KO rats after injection of saline.

Prepulse intensity, ISI	65 dB SPL, 30 ms	65 dB SPL, 100 ms	75 dB SPL, 30 ms	75 dB SPL, 100 ms	85 dB SPL, 30 ms	85 dB SPL, 100 ms
Cntnap2 WT	5.03 (−7.95–13.4)	15.3 (6.29–29.5)	31.0 (24.2–48.8)	38.2 (19.6–40.4)	57.6 (39.4–64.9)	54.9 (29.5–62.4)
Cntnap2 KO	2.30 (−13.0–11.5)	9.67 (−1.99–38.0)	21.2 (0.308–53.0)	11.9 (9.82–38.9)	39.0 (25.4–52.2)	44.5 (27.4–59.0)
WT vs. KO Mann–Whitney test	$0.4779^{n.s.}$	$0.8977^{n.s.}$	$0.1513^{n.s.}$	$0.1513^{n.s.}$	$0.1932^{n.s.}$	$0.3316^{n.s.}$
WT vs. KO Estimated p value	$0.4290^{n.s.}$	$0.4599^{n.s.}$	$0.1125^{n.s.}$	0.0017**	0.0163*	$0.2869^{n.s.}$

*Median (IQR); *p < 0.05, **p < 0.01, n.s.: not significant.*

TABLE 6 | Statistical comparison of %PPI within *Cntnap2* WT or KO rats after injection of saline, and 0.75, 1.5, and 3 g/kg R-Baclofen.

		Prepulse intensity (dB SPL), ISI (ms)					
Genotype	**Comparison**	**65 dB SPL, 30 ms**	**65 dB SPL, 100 ms**	**75 dB SPL, 30 ms**	**75 dB SPL, 100 ms**	**85 dB SPL, 30 ms**	**85 dB SPL, 100 ms**
Cntnap2 WT	Friedman test	$0.1828^{n.s.}$	$0.6886^{n.s.}$	$0.9209^{n.s.}$	$0.2197^{n.s.}$	$0.4088^{n.s.}$	$0.5248^{n.s.}$
Cntnap2 KO	Friedman test	$0.1039^{n.s.}$	$0.5915^{n.s.}$	0.0394^{*}	0.0017^{**}	0.0456^{*}	0.0252^{*}
	Saline vs. 0.75 mg/kg	N/A	N/A	$>0.9999^{n.s.}$	$>0.9999^{n.s.}$	$0.9653^{n.s.}$	$0.1425^{n.s.}$
	Saline vs. 1.5 mg/kg	N/A	N/A	$0.1425^{n.s.}$	$0.4116^{n.s.}$	$0.1425^{n.s.}$	0.0089^{**}
	Saline vs. 3 mg/kg	N/A	N/A	0.0397^{*}	0.0051^{**}	0.0247^{*}	$0.1425^{n.s.}$

*Post hoc test: Dunn's multiple comparisons test; *p < 0.05, **p < 0.01, n.s.: not significant.*

receptor agonist R-Baclofen can improve deficient sensorimotor gating in *Cntnap2* KO rats by subtle increases of the relative latency of startle in PPI trials with a minimal dose of 0.75 mg/kg R-Baclofen.

DISCUSSION

The present study sought to investigate whether selective activation of $GABA_B$ receptors can remediate ASD-related

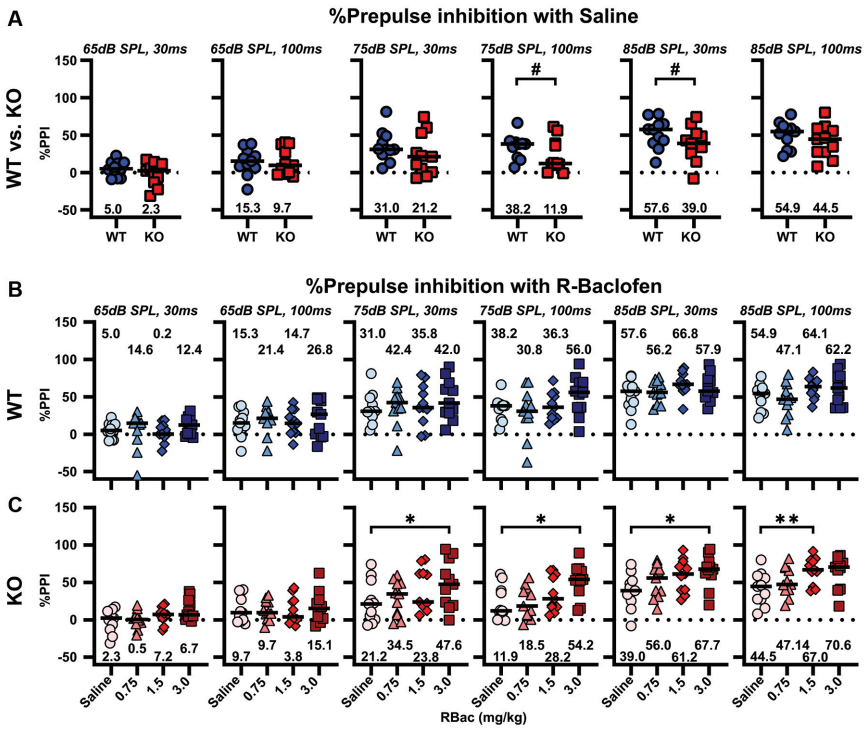

FIGURE 8 | R-Baclofen increases the relative amount of PPI (%PPI) in *Cntnap2* KO rats. **(A–C)** %PPI was elicited by six different prepulse conditions with three stimulus levels at two different ISIs (from left to right: 65 dB SPL, 30 ms; 65 dB SPL, 100 ms; 75 dB SPL, 30 ms; 75 dB SPL, 100 ms; 85 dB SPL, 30 ms; 85 dB SPL, 100 ms). Scatter plots depict individual %PPI for each prepulse condition and black horizontal lines represent the median %PPI. **(A)** %PPI for each prepulse condition in *Cntnap2* WT (blue circles) and KO rats (red squares) after saline injection. *Cntnap2* KO rats had consistently, but statistically nonsignificant, lower %PPI than WT rats. Estimated p values of $p = 0.0017$ and $p = 0.0163$ indicate a significant PPI deficit in *Cntnap2* KO rats for prepulses with 75 dB SPL, 100 ms, and 85 dB SPL, 30 ms (for statistical comparisons and estimated p values through resampling see **Table 5**). **(B)** There were no significant differences in %PPI in *Cntnap2* WT rats between saline (circles), and 0.75 mg/kg (light blue triangles), 1.5 mg/kg (blue diamonds), and 3 mg/kg R-Baclofen (dark blue squares) for any of the six prepulse conditions (for statistical comparisons see **Table 6**). **(C)** In *Cntnap2* KO rats, %PPI was significantly increased through R-Baclofen (0.75 mg/kg: light red triangles, 1.5 mg/kg: red diamonds, 3 mg/kg R-Baclofen: dark red squares) compared with saline (circles), in particular with prepulses of 75 dB SPL, 30 ms; 75 dB SPL, 100 ms; 85 dB SPL, 30 ms (3 mg/kg); and 85 dB SPL, 100 ms (1.5 mg/kg). For statistical comparisons see **Table 6**. Dotted horizontal lines at 0%PPI represent no PPI of the startle. $^{*}p < 0.05$; $^{**}p < 0.01$; $^{\#}p < 0.05$ estimated p-value through resampling.

altered sensory processing reliant on auditory brainstem function. We, therefore, compared behavioral read-outs of brainstem auditory signaling from rats with the homozygous knockout of *Cntnap2* to their WT littermates, with and without administration of R-Baclofen. Homozygous loss-of-function of *Cntnap2* leads to characteristic changes in brainstem-mediated auditory processing and behavior (Scott et al., 2018, 2020). Here, we demonstrate that these functional changes are accompanied by increased levels of excitatory and inhibitory neurotransmitters in the startle-mediating PnC and that they can largely be remediated by selective activation of $GABA_B$ receptors through R-Baclofen. In the present study, R-Baclofen: (1) improved deficient sensory filtering by enhancing short-term habituation; (2) suppressed exaggerated responses to moderately loud startling sounds; (3) rectified dynamic range response characteristics including ASR threshold, half-maximal response, and saturation; (4) improved sensorimotor gating by means of the relative amount of PPI and latency of startle in PPI trials; (5) but did not improve startle sensitization and peak response latency at ASR threshold in *Cntnap2* KO rats. Therefore, our results provide evidence that $GABA_B$ receptor agonists may be useful for pharmacologically targeting multiple aspects of sensory processing disruptions in ASD.

E/I Imbalance in *Cntnap2* KO Rats

Perturbed balance in neuronal excitation and inhibition is commonly assumed a possible final shared mechanism in autism (for review, see Rubenstein and Merzenich, 2003) that might underlie altered auditory processing in ASD (for review, see Sinclair et al., 2017b). *Cntnap2* is suggested to be involved in the regulation of neuronal circuit E/I balance, evidenced by decreased dendritic arborization and spine development after *Cntnap2* knockdown in cortical neurons (Anderson et al., 2012), and by increased excitatory synaptic input (Scott et al., 2017) and disrupted maturation of GABAergic inhibitory transmission in the cortex of *Cntnap2* KO mice (Bridi et al., 2017). Given the expression of *Cntnap2* along the ascending auditory and startle-mediating pathways (**Figure 1**)—including auditory nerve, dorsal, ventral, and granular layers of the cochlear nucleus (CN), SOC, dorsal nucleus of the lateral lemniscus, inferior colliculus,

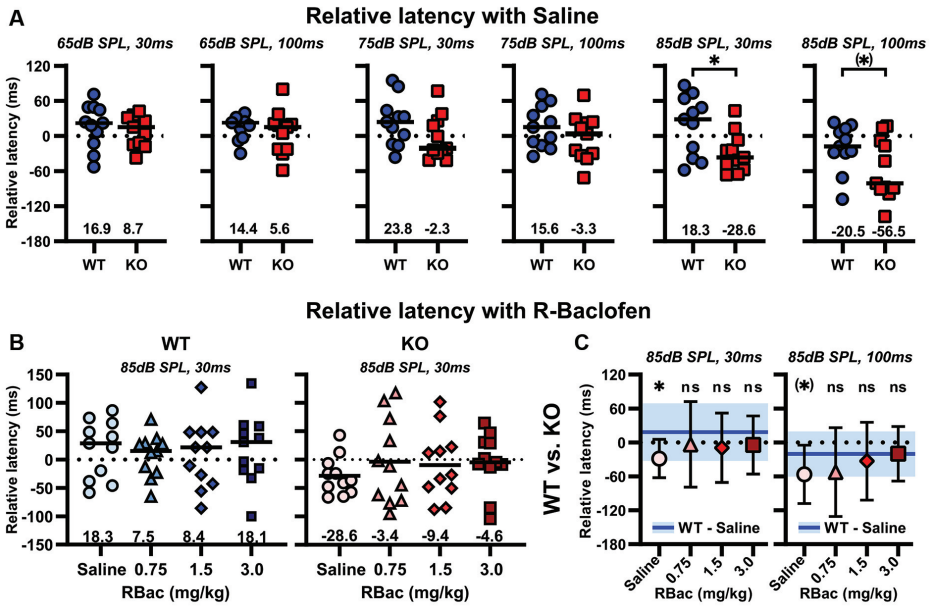

FIGURE 9 | R-Baclofen increases the relative latencies of startle in PPI trials (ms) in *Cntnap2* KO rats compared with WT controls. **(A)** Relative latencies of startle in PPI trials for six different prepulse conditions with three stimulus levels at two different ISIs. Scatter plots depict individual relative latencies of startle in PPI trials for each prepulse condition and black horizontal lines represent the mean relative latency of startle. After saline injection, *Cntnap2* KO rats (red squares) had consistently shorter relative latencies of startle in PPI trials than WT rats (blue circles), with a significant difference for the prepulse condition 85 dB SPL, 30 ms and a tendency for the prepulse condition 85 dB SPL, 100 ms (two-sided student's *t*-test, from left to right: 65 dB SPL, 30 ms; $p = 0.5569$; 65 dB SPL, 100 ms; $p = 0.5043$; 75 dB SPL, 30 ms; $p = 0.1335$; 75 dB SPL, 100 ms; $p = 0.2566$; 85 dB SPL, 30 ms; $p = 0.0195$; 85 dB SPL, 100 ms; $p = 0.0819$). **(B)** Scatter plots depicting individual (symbols) and mean relative latencies of startle in PPI trials (black horizontal lines) for prepulse condition 85 dB SPL, 30 ms in *Cntnap2* WT (**Left**, blue) and KO rats (**Right**, red) after injection of saline (circles), 0.75 mg/kg (triangles), 1.5 mg/kg (diamonds), and 3 mg/kg R-Baclofen (squares). R-Baclofen did not significantly increase relative latencies in *Cntnap2* WT (**Left**: WT, RM ANOVA, $p = 0.9282$, $F = 0.1226$). There was a slight, yet statistically not significant, increase in KO rats **(Right**: KO, RM ANOVA, $p = 0.5611$, $F = 0.6374$). **(C, Left)** Mean ± SD relative latency to prepulse condition 85 dB SPL, 30 ms in *Cntnap2* KO rats was significantly different from WT controls (after saline, blue line and area) with saline (two-sided student's *t*-test, $p = 0.0195$), and similar to controls with 0.75 mg/kg (two-sided student's *t*-test, $p = 0.4381$), 1.5 mg/kg (two-sided student's *t*-test, $p = 0.2627$) and 3 mg/kg R-Baclofen (two-sided student's *t*-test, $p = 0.3069$). **(C, Right)** Mean ± SD relative latency to prepulse condition 85 dB SPL, 100 ms in *Cntnap2* KO rats was by tendency different from WT controls (after saline, blue line and area) with saline (two-sided student's *t*-test, $p = 0.0819$), and similar to controls with 0.75 mg/kg (Welch's *t*-test, $p = 0.2479$), 1.5 mg/kg (two-sided student's *t*-test, $p = 0.6028$) and 3 mg/kg R-Baclofen (two-sided student's *t*-test, $p = 0.9833$). Dotted horizontal lines at 0 Relative Latency (ms) represent similar latency to the maximum startle response in trials with vs. without a prepulse. $^{(*)}p < 0.1$, $^{*}p < 0.05$; n.s.: not significant.

medial geniculate body, CRN, PnC, and pedunculopontine tegmental nucleus (PPT; Gordon et al., 2016; Scott et al., 2018)—it is plausible to assume that an irregular E/I balance in the auditory brainstem from *Cntnap2* KO rats is underlying the ASD-like altered implicit auditory-evoked behaviors observed in the present study (**Figures 3**, **8A**, **9A**). Indeed, quantification of amino acid levels through MALDI MS imaging demonstrated an increase in glutamine, glutamate, and GABA in the PnC from *Cntnap2* KO rats (**Figure 4**). Herein, GABA appeared to be disproportionally elevated, evidenced by lower Glu/GABA, increased GABA/Glu, but similar Glu/Gln ratio compared with WT controls. Due to the limited spatial resolution of MALDI imaging (80 μm), we can neither draw conclusions about the (sub-) cellular localization (extra- or intracellular, neuronal or glial, vesicular or cytoplasmic) of the detected amino acids, nor about the availability of the neurotransmitters for synaptic signaling (Waagepetersen et al., 2001; for reviews see Choudhury et al., 2011; Coghlan et al., 2012). Astrocytic-derived glutamine is the precursor of both glutamate and GABA. Normally, more glutamine is transferred from astrocytes to glutamatergic neurons, since GABAergic neurons have a greater capability of re-utilizing their neurotransmitter by re-uptake (for review, see Walls et al., 2015). The perturbed relations between Gln, Glu, and GABA in the PnC from *Cntnap2* KO rats indicate a dysregulation in the glutamine-glutamate/GABA re-uptake and/or synthetization cycle that might result in disturbance of the functional E/I homeostasis and underlie ASD pathogenesis (Van Elst et al., 2014). These alterations could be the result of a compensatory upregulation of neurotransmitter levels in response to decreased postsynaptic receptor availability, as has been observed in form of decreased glutamate receptor expression in the PFC from *Cntnap2* KO mice (Kim et al., 2019), impaired glutamate receptor trafficking to the cell surface of hippocampal *Cntnap2* KO neurons (Varea et al., 2015), and reduced GABA receptor subunit expression in autistic human brain samples (Fatemi et al., 2009; Blatt and Fatemi, 2011). A compensatory upregulation of GAD67, one of the isoforms of the key synthesizing enzymes for GABA, has been observed in ASD brains, possibly to provide increased GABAergic feed-forward inhibition to compensate for the loss of cerebellar neurons

(Yip et al., 2008). Interestingly, reduced numbers of cortical GABAergic interneurons have also been observed in *Cntnap2* KO mice (Peñagarikano et al., 2011) and reduced numbers of neurons in the auditory brainstem of humans with ASD (Kulesza et al., 2011). It remains to be elucidated whether *Cntnap2* KO rats have reduced numbers of neurons in the PnC and whether the elevated GABA level observed in our study is correlated with (insufficient) compensatory upregulation (Antoine et al., 2019) of GABAergic feedforward inhibition from the PPT to the PnC (Yeomans et al., 2010; Fulcher et al., 2020). It should be noted that abnormalities in glutamine, glutamate, and GABA levels appear to be highly age-, species-, strain-, and brain region/circuit-specific (Horder et al., 2013, 2018a,b; Van Elst et al., 2014). Interestingly, GABA, Glu, and Gln levels were not altered in the SOC within the auditory brainstem of *Cntnap2* KO rats (**Supplementary Figure 4**). This indicates that *Cntnap2* might not generally interact with the Glu-Gln/GABA system throughout the brain. It rather suggests that Glu-Gln/GABA system dysregulation might be a secondary effect of functional *Cntnap2* deletion that is confined to certain brain regions or neural circuits. Analogous to our findings in the PnC from *Cntnap2* KO rats, BTBR T+tf/J mice show increases in all three amino acids particularly in the striatum, but not in the PFC (Horder et al., 2018b). Several other rodent models of ASD presented with other distinct Glu, Gln, and GABA concentration profiles, three of them recapitulating the reduction in striatal Glu from the adult autistic human cohort (Horder et al., 2018b). Higher absolute concentrations of GABA and glutamate, as well as lower Glu/GABA ratios, on the other hand, have been described in blood plasma from pediatric and adolescent autistic patients (El-Ansary and Al-Ayadhi, 2014; Al-Otaish et al., 2018). Increased combined Gln and Glu signals in the anterior cingulate from children and adolescents with ASD have been interpreted as an indicator of neuronal overexcitation (Bejjani et al., 2012; Van Elst et al., 2014), and increased GABA—a product of glutamate metabolism—as a consequence of significantly elevated glutamate and/or decreased breakdown of GABA into glutamate (El-Ansary and Al-Ayadhi, 2014; for review, see Walls et al., 2015; Zheng et al., 2019). Given that baseline ASRs rely on the glutamatergic excitation of PnC giant neurons (Ebert and Koch, 1992), and GABA receptors on PnC giant neurons mediate a substantial part of PPI (Yeomans et al., 2010), the dysregulation of the Glu-Gln/GABA system likely perturbs acoustic startle circuitry and behavior in *Cntnap2* KO rats. Even though future immunohistochemical and electrophysiological studies are needed to investigate the anatomical distribution and functional correlation of amino acid levels in the startle-mediating pathway in closer detail, our results strongly indicate that altered implicit auditory-evoked behaviors commonly observed in ASD (Chamberlain et al., 2013; Kohl et al., 2014; Takahashi et al., 2016) might result from disturbed E/I balance within the neuronal startle circuit.

R-Baclofen Mechanism of Action

At this point, we can only speculate how *R*-Baclofen treatment improves the behavioral read-outs of sensory processing in *Cntnap2* KO rats. The efficacy of R-Baclofen could result from its ability to dampen hyperexcitability *via* pre- and postsynaptic mechanisms. Baclofen stimulates metabotropic $GABA_B$ receptors which function as presynaptic auto- or heteroreceptors to inhibit the vesicular release of GABA or glutamate, respectively (Waldmeier et al., 2008; Delaney et al., 2018). Postsynaptically, R-Baclofen activates inward-rectifying potassium channels that cause neuronal hyperpolarization. Together, these mechanisms serve to tonically hyperpolarize neurons, decrease resting membrane potential, and reduce cell firing (Gandal et al., 2012; for review, see Wu and Sun, 2015). R-Baclofen may be beneficial in *Cntnap2* KO animals by counteracting the reported reduction in the number of GABAergic interneurons and asynchronous neuronal firing (Peñagarikano et al., 2011; Vogt et al., 2017), decreased GABAergic phasic and tonic inhibition (Bridi et al., 2017), increased neurotransmitter release and increased postsynaptic excitatory responses in *Cntnap2* KO animals (Scott et al., 2017), and the dysregulated glutamine-glutamate/GABA cycle indicated by the lacking rebalance of Glu/GABA ratios in the present study.

In the auditory system, Baclofen has been shown to have large effects on overall excitability (Szczepaniak and Møller, 1995), including the suppression of sound-evoked activity and/or hyperexcitability in the CN (Martin, 1982; Caspary et al., 1984), inferior colliculus (Szczepaniak and Møller, 1996; Sun et al., 2006) and auditory cortex (Lu et al., 2011). In a genetic mouse model of E/I dysfunction, Baclofen dose-dependently normalized auditory-evoked potentials, elevated ASRs, and deficient PPI of ASRs. This was linked to the improvement of several elements of E/I homeostasis such as circuit excitability, neural synchrony, and signal-to-noise ratio (Gandal et al., 2012).

ASR amplitudes are the sum of habituation and the parallel independent process of sensitization, with habituation being the decrease and sensitization the initial increase in magnitude to a series of sound pulses (Payne and Anderson, 1967; Groves and Thompson, 1970; Geyer and Braff, 1982; Pilz and Schnitzler, 1996; Rankin et al., 2009). Impaired habituation and increased sensitization apparent in our study in *Cntnap2* KO rats (**Figures 3B,C**) are also associated with ASD in humans (Perry et al., 2007; Chamberlain et al., 2013; Madsen et al., 2014). Short-term habituation relies on synaptic depression at the axon terminals of the CRN sensory afferents in the PnC (**Figure 1**), likely mediated by activation of voltage- and calcium-dependent potassium channels (Ebert and Koch, 1992; Weber et al., 2002; Simons-Weidenmaier et al., 2006; Zaman et al., 2017). Lack of *Cntnap2* in KO rats might interfere directly with startle habituation through its function in clustering of voltage-gated potassium channels (Poliak et al., 2003; Dawes et al., 2018; Scott et al., 2018). At an auditory glutamatergic synapse featuring strong synaptic depression, Baclofen modulated transmitter release in an activity-dependent manner (Brenowitz et al., 1998) which might explain the improvement of short-term habituation in *Cntnap2* WT and KO rats with R-Baclofen (**Figures 5A–C**). Sensitization, on the other hand, is caused by extrinsic modulation of the startle pathway (**Figure 1**) by structures including the periaqueductal gray, the amygdala, and the bed nucleus of the stria terminalis (Leaton and Supple,

1986; Fendt et al., 1994a,b; Davis et al., 1997)—structures that all express *Cntnap2* (Alarcón et al., 2008; Gordon et al., 2016). The ineffectiveness of R-Baclofen to suppress increased ASR sensitization in *Cntnap2* KO rats or sensitization in WT controls (**Figure 5D**) might be due to the fact that the modulatory input from these structures altering sensitization includes several neurotransmitters other than GABA or Glu, such as noradrenaline (Fendt et al., 1994a), substance P (Krase et al., 1994), glycine (Plappert et al., 2001), or dopamine (Halberstadt and Geyer, 2009). In support of this notion, Baclofen was also unable to reverse dopamine receptor agonist apomorphine-induced disruptions in sensorimotor gating, while it did reverse NMDA receptor antagonist effects (Bortolato et al., 2004).

Baclofen and its formulations R- and S-Baclofen are well known to suppress ASRs in controls and in animals with proposed E/I dysfunction, either genetically or pharmacologically induced (e.g., Bortolato et al., 2004; Lu et al., 2011; Gandal et al., 2012). In our hands, R-Baclofen was more potent in *Cntnap2* WT rats (effective dose of 0.75 mg/kg) than in *Cntnap2* KO rats (effective dose of 1.5 mg/kg, **Figure 6**) and more effective in female than in male KO rats (**Supplementary Figure 5**). This sex-dependent effect of R-Baclofen on the ASR I-O function is probably due to the fact that *Cntnap2* KO males had higher ASR magnitudes than females to begin with (i.e., without R-Baclofen, **Figures 3D,E**). Sex effects on ASR I-O function in untreated rats from the *Cntnap2* model have been described before (Scott et al., 2018). In humans, the male prevalence of ASD symptoms has been attributed to sex-differential factors such as reduced susceptibility in females, or lower mutational burden threshold in males. In this regard, mutations affecting GABA signaling appear to be particularly pervasive in males (for reviews, see Werling and Geschwind, 2013; Rylaarsdam and Guemez-Gamboa, 2019), and *Cntnap2* mutations affect functional responses of cortical circuitry more strongly in male than in female mice (Townsend and Smith, 2017). Interestingly, the *Cntnap2* gene is differentially expressed in sexually dimorphic song nuclei essential for vocal learning in songbirds (Panaitof et al., 2010) in accordance with the sexual dimorphism of neural circuitry in vocal control areas (Nottebohm and Arnold, 1976); and genetic variants in the *CNTNAP2* gene are associated with gender differences among dyslexic children (Gu et al., 2018). Exploring in more detail the neurobiological basis of sex-dependent differences in startle responses and efficacy of R-Baclofen found in *Cntnap2* KO rats should be considered in future studies.

In addition to differences in the effective dose, R-Baclofen suppressed ASR magnitudes across a wide range of startle pulse intensities in *Cntnap2* WT rats, whereas in KO rats the maximum ASR capacity was unaltered (**Figure 6**). A similar phenomenon has been described in rats after treatment with S-Baclofen to suppress salicylate-induced enhancement of ASRs (Lu et al., 2011). The robustly increased ASRs to high sound intensities in *Cntnap2* KO rats might be due to increased excitatory input from the CN to the PnC (**Figure 1**). Behavioral studies showed that electrolytic lesions of the CN reduced ASRs particularly to loud sound intensities of 110 and 115 dB SPL (Meloni and Davis, 1998). In contrast, chemical lesions of CRNs or the PnC blocked ASRs at all intensities (Lee et al., 1996). Interestingly, Flores et al. (2015) identified an alternative pathway from the cochlea to the CN for the detection of loud, potentially tissue-damaging, auditory stimuli. One might speculate if this form of sensation (termed "auditory nociception") is increased in *Cntnap2* KO rats and contributes to their exaggerated ASRs (**Figure 3**) as well as greater active sound avoidance (Scott et al., 2020). "Auditory nociception" would have similarities to C-fiber nociception (Flores et al., 2015) which is indeed enhanced in *Cntnap2* KO animals (Dawes et al., 2018). Taken together, the dramatically reduced ASRs including maximum capacity in *Cntnap2* WT rats by R-Baclofen (**Figure 6**) might be predominantly due to reduced excitability in CRNs and/or the PnC. In contrast, in *Cntnap2* KO rats, the R-Baclofen-induced suppression of exaggerated responses to moderate startling sounds might be the behavioral outcome of an interaction between reduction in CRNs and/or PnC hyperexcitability, and unproportionally high excitatory input from the CN to PnC.

The decrease of ASRs to moderate startle pulse intensities through R-Baclofen in *Cntnap2* KO rats was accompanied by the normalization of their ASR thresholds to control levels, indicated by an increase of the minimum sound intensity required to elicit a response (from about 83–89 dB SPL at the 25% response magnitude, **Figure 7**, **Supplementary Table 2**). The high acoustic input required to reach the ASR threshold and elicit a motor response is likely determined by a high firing threshold in the CRNs. In contrast, electrophysiological data have shown that PnC neurons, that receive rapid input from the CRNs, have a relatively low firing threshold (Wagner and Mack, 1998; Brosda et al., 2011). Given the expression of *Cntnap2* in CRNs from WT rats (Scott et al., 2018), its lack in *Cntnap2* KO rats may result in neuronal hyperexcitability in the CRNs, leading to lower ASR thresholds (**Figure 3H**). CRN neurons receive inhibitory GABAergic input that modulates their neuronal responses and consequently the ASR output (for review, see Osen et al., 1991; Gómez-Nieto et al., 2008). Therefore, R-Baclofen might attenuate intrinsic excitability and increase firing thresholds of CRNs, and thereby normalize ASR thresholds in *Cntnap2* KO rats. Alternatively, R-Baclofen might take effect by blocking the glutamate release from the auditory nerve fibers (Martin, 1982) synapsing onto CRNs (Gómez-Nieto et al., 2014).

The normalization of the ASR threshold in *Cntnap2* KO rats through R-Baclofen was correlated with a parallel rightward shift of the I-O function, determined by an increase in the half-maximal response (ES50) and ASR saturation (90% response magnitude, **Figure 7**, **Table 3**). This means that—while the extent of the I-O dynamic range remained similar—the I-O dynamic range was shifted to higher startle pulse intensities. Conversely, this indicates that the acoustic stimulus potency was decreased by R-Baclofen. In the dynamic range of the I-O function, a small stimulus change can produce a large response change (Stoddart et al., 2008) and the slope is an important aspect of the ASR I-O function as it directly reflects the sensorimotor integration process (Hince and Martin-Iverson, 2005). R-Baclofen did not induce a change in ASR I-O slope within the genotype (**Supplementary Figure 7** and

Supplementary Table 3). Therefore, it can be assumed that in *Cntnap2* KO rats the ASR efficiency, i.e., the transduction of sensory information into motor output, remained at a similar rate (**Figure 2**). This speaks against a generalized increase in inhibition of the ASR system through R-Baclofen, as this would also predict a change in slope (Hince and Martin-Iverson, 2005). Interestingly, Martin-Iverson and Stevenson (2005) found a change in ASR I-O slope through emotional modulatory input such as fear, modified by dopaminergic signaling (**Figure 1**). It should be pointed out that R-Baclofen normalized the ASR I-O fitted curves from *Cntnap2* KO rats to control levels, despite the unaltered slope in the within genotype comparisons (**Figures 7A–C**, **Supplementary Figure 7**).

ASR magnitude and latency are in general negatively correlated (i.e., the higher the magnitude, the shorter the latency; Hoffman and Searle, 1968). In a unique approach, we analyzed ASR peak latencies from individual animals relative to their dynamic range characteristics (i.e., threshold, ES50, saturation, **Figures 7F–H**). This allowed us to investigate the processing speed between sensory (acoustic) input and maximum ASR motor output without the confounding effect of genotype-related differences in startle magnitudes. Peak latencies were significantly shorter in *Cntnap2* KO than in WT rats, specifically at the ASR threshold. Surprisingly, R-Baclofen led to even shorter, rather than longer, ASR peak latencies in *Cntnap2* KO rats. As outlined above, motor responses to low, near-threshold, acoustic inputs are likely gated by CRN activity (Wagner and Mack, 1998; Brosda et al., 2011). It might be possible that the shift in threshold to higher sound intensities in *Cntnap2* KO rats with R-Baclofen goes along with more synchronous short-latency inputs to the PnC, thereby speeding up temporal processing (Gandal et al., 2012; Harris and Dubno, 2017). In contrast to $GABA_B$ receptor activation through R-Baclofen, pharmacological modulation of other neurotransmitter receptors targeting ASR sensitization might have shown normalizing effects on ASR latency, since the course of response latency is dominated by ASR sensitization (Pilz and Schnitzler, 1996).

In addition to increased acoustic reactivity, *Cntnap2* KO rats consistently presented with disrupted sensorimotor gating in two of our previous studies, despite differences in the acoustic prepulse conditions (Scott et al., 2020) or breeding scheme (Scott et al., 2018). In line with these previous results, *Cntnap2* KO rats in the present study also displayed robustly lower PPI of ASRs than WT controls (**Figure 8A**). These differences were statistically significant for two prepulse conditions (75 dB SPL, 100 ms and 85 dB SPL, 30 ms ISI) with a random permutation test for small sample sizes. R-Baclofen improved sensorimotor gating in *Cntnap2* KO rats as shown by a dose-dependent increase in PPI for four prepulse conditions (75 dB SPL, 30 ms; 75 dB SPL, 100 ms; 85 dB SPL, 30 ms; 85 dB SPL, 100 ms, **Figure 8C**). Likewise, enhancing GABAergic inhibition through Baclofen previously rescued PPI disrupted by pharmacological NMDA receptor blockade (Bortolato et al., 2004; Arai et al., 2008; Fejgin et al., 2009) or hypofunction (Gandal et al., 2012). In control animals, Baclofen *per se* produced no significant changes in PPI at any given dose in these previous studies (Bortolato et al., 2004), similar to *Cntnap2* WT rats in our study (**Figure 8B**). This was due to the uniform suppression of response magnitudes in trials with and without a prepulse (**Supplementary Figure 9A**). In contrast, in *Cntnap2* KO rats the response magnitudes to the prepulse + startle pulse condition were suppressed more strongly by R-Baclofen than the ones to the startle pulse alone condition (**Supplementary Figure 9B**). Previous studies have demonstrated the involvement of $GABA_B$ receptors in prepulse processing and sensorimotor gating (Koch et al., 2000; Takahashi et al., 2007; Yeomans et al., 2010). R-Baclofen might improve the behavioral salience of weak acoustic prepulses through increased feedforward inhibition onto the PnC (Carlson and Willott, 1996; Price et al., 2008; Antoine et al., 2019) achieved by decreased spontaneous firing ("neuronal noise") and improved neural synchrony in response to the prepulse (Gandal et al., 2012) within the PPI circuitry (**Figure 1**). It is unlikely that the improved sensorimotor gating was due to changes in detectability of the prepulse in the auditory periphery (i.e., hearing thresholds) since Baclofen does not affect the sound-evoked cochlear output and summed auditory nerve potentials (Martin, 1982). In addition, the prepulse elicited response (at 100 ms, **Supplementary Figure 10**) was not increased with R-Baclofen, which is different from a pharmacologically induced rodent model of schizophrenia-like sensorimotor gating deficits (Yee et al., 2004).

In line with our previous results (Scott et al., 2018), *Cntnap2* KO rats did not only show disrupted PPI in terms of amplitudes but also a lack of the typical increase in startle latency in PPI trials (**Figure 9A**; Ison et al., 1973; Hoffman and Ison, 1980). However, in contrast to ASR peak latencies (at the threshold, **Figures 7F–H**), R-Baclofen prolonged and normalized the startle latency in PPI trials from *Cntnap2* KO rats (**Figure 9C**). This might underscore that the changes in neuronal transmission rectifying not only PPI amplitudes but also latencies mainly lie within the circuit branch processing prepulse information and take effect downstream of the CRN (i.e., GABAergic PPT projections onto PnC).

Model Validity and Clinical Implications

Even though we cannot fully exclude dose-dependent myorelaxant properties of R-Baclofen (Davidoff, 1985; Nevins et al., 1993), it is reasonable to assume that the changes we observed in *Cntnap2* KO rats were mostly due to the brainstem processing involved in ASR generation. This is because the maximum ASR as a putative index for motor capacity (Hince and Martin-Iverson, 2005) was not altered in *Cntnap2* KO rats even with 3 mg/kg R-Baclofen, and ASR peak latencies at the threshold were shortened, not prolonged. Importantly, intrathecal administration of Baclofen reversed enhanced ASRs and restored reduced PPI of the blink reflex in patients with spinal cord injury, strongly suggesting a muscle tone regulating effect of Baclofen at the brainstem level (Kumru et al., 2009; Kumru and Kofler, 2012). Future studies should address in more detail the sites and mechanisms of R-Baclofen action. The most promising target of R-Baclofen action is the PnC as it is the sensorimotor interface of the startle circuit (**Figure 1**), where the transition of sensory input into the motor output can be directly influenced (for review, see

Koch, 1999). Using cannulated microelectrodes, R-Baclofen infusions into the PnC and simultaneous electrophysiological recordings in behaving *Cntnap2* WT and KO rats would allow to assess changes in startle responses correlated to changes in PnC neuronal activity without possible systemic effects of R-Baclofen. Suppression of the speculated PnC hyperexcitability in *Cntnap2* KO rats through local application of R-Baclofen might attenuate their exaggerated startle responses, in particular to moderate startling sounds. Furthermore, microinfusions of R-Baclofen to the cochlear round window membrane might be a useful tool to dissect the contribution of the sensory (as opposed to motor) branch in the ASR pathway to effects observed in our study. The round window membrane delivery approach of R-Baclofen to the inner ear might reduce glutamate release from the auditory nerve fibers synapsing onto CRNs (Gómez-Nieto et al., 2014), resulting in less sound-evoked PnC activity, and possibly a shift in ASR thresholds as well as reduced startle response magnitudes. Lastly, R-Baclofen-induced alterations in modulatory input to the PnC might be identified through local application to the PPT. Simultaneous electrophysiological recordings of sound-evoked activity in PnC neurons to a prepulse+startle pulse sound paradigm would help scrutinize R-Baclofen-induced changes in GABAergic feedforward inhibition from the PPT to the PnC that might underlie altered PPI of startle in *Cntnap2* KO rats in the present study. On a cellular level, R-Baclofen actions on excitatory and inhibitory transmission (mediated by presynaptic $GABA_B$ heteroreceptors or autoreceptors, respectively) could be addressed by examining its effects on excitatory (glutamatergic) and inhibitory (GABAergic) postsynaptic currents using whole-cell voltage clamp recordings in PnC giant neurons from *Cntnap2* WT and KO rats.

Rats with homozygous, and to a lesser extent heterozygous, functional deletion of the *Cntnap2* gene display behavioral alterations that parallel core symptoms of ASD, including deficits in sociability, repetitive stereotypy, and sensory abnormalities (Scott et al., 2018, 2020). Therefore, the *Cntnap2* rat model for autism does not only have a high construct but also face validity. This is particularly important considering that ASD diagnosis and consequently validation of treatments rely on evaluating behavioral traits both in clinical testing and in preclinical models that seek to recapitulate those behavioral traits from humans (for reviews, see Servadio et al., 2015; Kazdoba et al., 2016; Möhrle et al., 2020; Scott et al., 2021). One limitation of our study might be that single gene mutations such as *Cntnap2* account for no more than 1% of ASD cases (for review, see Yoo, 2015). However, the majority of ASD susceptibility genes seem to converge in shared or interacting biological pathways that are typically involved in synapse formation and function, transcriptional control, and chromatin-remodeling (De Rubeis et al., 2014; Iossifov et al., 2014; Pinto et al., 2014). Therefore, monogenic rodent models including *Cntnap2* are useful tools in the search of standardized objective biomarkers for the neurological basis, and the utility of diagnosis and treatment of ASD.

Exaggerated acoustic reactivity and impaired sensorimotor gating have been described in individuals with autism (Perry et al., 2007; Chamberlain et al., 2013; Kohl et al., 2014; Takahashi et al., 2016) along with other sensory alterations affecting the auditory, visual, touch, smell/taste and pain domain. Exploring the usefulness of therapeutic approaches to rectify sensory alterations might be of particular importance considering that atypical low-level sensory processing might exacerbate or interact with other, higher-level, symptoms in individuals with ASD (O'Neill and Jones, 1997; Leekam et al., 2007). For example, regarding the auditory system, timing deficits within the brainstem negatively impact rapid acoustic processing, predictive of a higher risk for developing speech processing issues and language disorders (Benasich et al., 2002; Wible et al., 2004; Abrams et al., 2006), representing core symptoms of ASD (for review, see Alarcón et al., 2008; Mody and Belliveau, 2013; Rodenas-Cuadrado et al., 2016). Interestingly, rodent models with mutations in *Cntnap2* parallel slowed neurotransmission along the ascending auditory brainstem reported in ASD (Rosenhall et al., 2003; Kwon et al., 2007; Miron et al., 2016; Scott et al., 2018), and deficient language-relevant rapid auditory processing seen in infants carrying variants of *Cntnap2* (Truong et al., 2015; Riva et al., 2018). Targeting E/I balance to modulate more spectrotemporally complex auditory processes such as brainstem representation and higher-level perception of speech-like sounds in *Cntnap2* KO rats is an exciting consideration for future studies.

CONCLUSION

In conclusion, this study demonstrated a relationship between *Cntnap2* gene deletion, disrupted excitatory/inhibitory homeostasis, auditory brainstem-mediated sensory processing, and symptoms of ASD. Increasing GABAergic signaling *via* the $GABA_B$ receptor agonist R-Baclofen improved many aspects of acoustic reactivity, sensory filtering, and sensorimotor gating in *Cntnap2* KO rats. These findings encourage further efforts to establish translatable paradigms based on auditory-evoked behaviors for preclinical and clinical therapeutic screening for neurodevelopmental disorders. Our results support the hypothesis that enhancing inhibitory transmission improves ASD relevant deficits and that $GABA_B$ receptors are a promising therapeutic target for restoring neural circuit and behavioral abnormalities in disorders characterized by E/I imbalance.

DATA AVAILABILITY STATEMENT

The raw data supporting the conclusions of this article will be made available by the authors, without undue reservation.

ETHICS STATEMENT

The animal study was reviewed and approved by the University of Western Ontario Animal Care Committee, and all procedures were in accordance with the guidelines established by the Canadian Council on Animal Care.

AUTHOR CONTRIBUTIONS

DM, SW, and SS: participated in research design. DM and WW: conducted experiments. DM: performed data analysis. DM, WW, SW, and SS: wrote or contributed to the writing of the manuscript. All authors contributed to the article and approved the submitted version.

FUNDING

This research was supported by Canadian Institutes of Health Research (CIHR), Natural Sciences and Engineering Research Council of Canada (NSERC), BrainsCAN (Rat Behavioral Facility), and the Deutsche Forschungsgemeinschaft (DFG, German Research Foundation)—project number 442662585.

ACKNOWLEDGMENTS

We thank SFARI for providing R-Baclofen.

SUPPLEMENTARY MATERIAL

The Supplementary Material for this article can be found online at: https://www.frontiersin.org/articles/10.3389/fnint.2021.710593/full#supplementary-material.

REFERENCES

Abrams, D. A., Nicol, T., Zecker, S. G., and Kraus, N. (2006). Auditory brainstem timing predicts cerebral asymmetry for speech. *J. Neurosci.* 26, 11131–11137. doi: 10.1523/JNEUROSCI.2744-06.2006

Alarcón, M., Abrahams, B. S., Stone, J. L., Duvall, J. A., Perederiy, J. V., Bomar, J. M., et al. (2008). Linkage, association and gene-expression analyses identify *Cntnap2* as an autism-susceptibility gene. *Am. J. Hum. Genet.* 82, 150–159. doi: 10.1016/j.ajhg.2007.09.005

Al-Otaish, H., Al-Ayadhi, L., Bjørklund, G., Chirumbolo, S., Urbina, M. A., El-Ansary, A., et al. (2018). Relationship between absolute and relative ratios of glutamate, glutamine and GABA and severity of autism spectrum disorder. *Metab. Brain Dis.* 33, 843–854. doi: 10.1007/s11011-018-0186-6

Anderson, G. R., Galfin, T., Xu, W., Aoto, J., Malenka, R. C., Südhof, T. C., et al. (2012). Candidate autism gene screen identifies critical role for cell-adhesion molecule CASPR2 in dendritic arborization and spine development. *Proc. Natl. Acad. Sci. U S A* 109, 18120–18125. doi: 10.1073/pnas.1216398109

Antoine, M. W., Langberg, T., Schnepel, P., and Feldman, D. E. (2019). Increased excitation-inhibition ratio stabilizes synapse and circuit excitability in four autism mouse models. *Neuron* 101, 648–661.e644. doi: 10.1016/j.neuron.2018.12.026

Arai, S., Takuma, K., Mizoguchi, H., Ibi, D., Nagai, T., Takahashi, K., et al. (2008). Involvement of pallidotegmental neurons in methamphetamine- and MK-801-induced impairment of prepulse inhibition of the acoustic startle reflex in mice: reversal by $GABA_B$ receptor agonist baclofen. *Neuropsychopharmacology* 33, 3164–3175. doi: 10.1038/npp.2008.41

Bejjani, A., O'Neill, J., Kim, J. A., Frew, A. J., Yee, V. W., Ly, R., et al. (2012). Elevated glutamatergic compounds in pregenual anterior cingulate in pediatric autism spectrum disorder demonstrated by 1H MRS and 1H MRSI. *PLoS One* 7:e38786. doi: 10.1371/journal.pone.0038786

Benasich, A. A., Thomas, J. J., Choudhury, N., and Leppänen, P. H. T. (2002). The importance of rapid auditory processing abilities to early language development: evidence from converging methodologies. *Dev. Psychobiol.* 40, 278–292. doi: 10.1002/dev.10032

Berry-Kravis, E., Hagerman, R., Visootsak, J., Budimirovic, D., Kaufmann, W. E., Cherubini, M., et al. (2017). Arbaclofen in fragile X syndrome: results of phase 3 trials. *J. Neurodev. Disord.* 9:3. doi: 10.1186/s11689-016-9181-6

Berry-Kravis, E. M., Hessl, D., Rathmell, B., Zarevics, P., Cherubini, M., Walton-Bowen, K., et al. (2012). Effects of STX209 (arbaclofen) on neurobehavioral function in children and adults with fragile X syndrome: a randomized, controlled, phase 2 trial. *Sci. Transl. Med.* 4:152ra127. doi: 10.1126/scitranslmed.3004214

Blatt, G. J., and Fatemi, S. H. (2011). Alterations in GABAergic biomarkers in the autism brain: research findings and clinical implications. *Anat. Rec. (Hoboken)* 294, 1646–1652. doi: 10.1002/ar.21252

Bortolato, M., Frau, R., Aru, G. N., Orrù, M., and Gessa, G. L. (2004). Baclofen reverses the reduction in prepulse inhibition of the acoustic startle response induced by dizocilpine, but not by apomorphine. *Psychopharmacology* 171, 322–330. doi: 10.1007/s00213-003-1589-5

Braff, D. L., Geyer, M. A., and Swerdlow, N. R. (2001). Human studies of prepulse inhibition of startle: normal subjects, patient groups and pharmacological studies. *Psychopharmacology (Berl)* 156, 234–258. doi: 10.1007/s002130100810

Brenowitz, S., David, J., and Trussell, L. (1998). Enhancement of synaptic efficacy by presynaptic $GABA_B$ receptors. *Neuron* 20, 135–141. doi: 10.1016/s0896-6273(00)80441-9

Bridi, M. S., Park, S. M., and Huang, S. (2017). Developmental diisruption of $GABA_A$ R-meditated inhibition in *Cntnap2* KO mice. *eNeuro* 4:ENEURO.0162–0117.2017. doi: 10.1523/ENEURO.0162-17.2017

Brosda, J., Hayn, L., Klein, C., Koch, M., Meyer, C., Schallhorn, R., et al. (2011). Pharmacological and parametrical investigation of prepulse inhibition of startle and prepulse elicited reactions in wistar rats. *Pharmacol. Biochem. Behav.* 99, 22–28. doi: 10.1016/j.pbb.2011.03.017

Carlson, S., and Willott, J. F. (1996). The behavioral salience of tones as indicated by prepulse inhibition of the startle response: relationship to hearing loss and central neural plasticity in C57BL/6J mice. *Hear. Res.* 99, 168–175. doi: 10.1016/s0378-5955(96)00098-6

Caspary, D. M., Rybak, L. P., and Faingold, C. L. (1984). Baclofen reduces tone-evoked activity of cochlear nucleus neurons. *Hear. Res.* 13, 113–122. doi: 10.1016/0378-5955(84)90102-3

Caughlin, S., Park, D. H., Yeung, K. K., Cechetto, D. F., and Whitehead, S. N. (2017). Sublimation of DAN matrix for the detection and visualization of gangliosides in rat brain tissue for MALDI imaging mass spectrometry. *J. Vis. Exp.* 121:55254. doi: 10.3791/55254

Chamberlain, P. D., Rodgers, J., Crowley, M. J., White, S. E., Freeston, M. H., South, M., et al. (2013). A potentiated startle study of uncertainty and contextual anxiety in adolescents diagnosed with autism spectrum disorder. *Mol. Autism* 4:31. doi: 10.1186/2040-2392-4-31

Chen, C., Laviolette, S. R., Whitehead, S. N., Renaud, J. B., and Yeung, K. K. (2021). Imaging of neurotransmitters and small molecules in brain tissues using laser desorption/ionization mass spectrometry assisted with zinc oxide nanoparticles. *J. Am. Soc. Mass Spectrom.* 32, 1065–1079. doi: 10.1021/jasms.1c00021

Choudhury, P., Lahiri, S., and Rajamma, U. (2011). Glutamate mediated signaling in the pathophysiology of autism spectrum disorders. *Pharmacol. Biochem. Behav.* 100, 841–849. doi: 10.1016/j.pbb.2011.06.023

Coghlan, S., Horder, J., Inkster, B., Mendez, M. A., Murphy, D. G., Nutt, D. J., et al. (2012). GABA system dysfunction in autism and related disorders: from synapse to symptoms. *Neurosci. Biobehav. Rev.* 36, 2044–2055. doi: 10.1016/j.neubiorev.2012.07.005

Csomor, P. A., Yee, B. K., Vollenweider, F. X., Feldon, J., Nicolet, T., and Quednow, B. B. (2008). On the influence of baseline startle reactivity on the indexation of prepulse inhibition. *Behav. Neurosci.* 122, 885–900. doi: 10.1037/0735-7044.122.4.885

Danesh, A. A., Lang, D., Kaf, W., Andreassen, W. D., Scott, J., Eshraghi, A. A., et al. (2015). Tinnitus and hyperacusis in autism spectrum disorders with emphasis on high functioning individuals diagnosed with Asperger's Syndrome. *Int. J. Pediatr. Otorhinolaryngol.* 79, 1683–1688. doi: 10.1016/j.ijporl.2015.07.024

Davidoff, R. A. (1985). Antispasticity drugs: mechanisms of action. *Ann. Neurol.* 17, 107–116. doi: 10.1002/ana.410170202

Davis, M., Walker, D. L., and Lee, Y. (1997). Roles of the amygdala and bed nucleus of the stria terminalis in fear and anxiety measured with the acoustic startle reflex. *Ann. N.Y. Acad. Sci.* 821, 305–331. doi: 10.1111/j.1749-6632.1997.tb48289.x

Dawes, J. M., Weir, G. A., Middleton, S. J., Patel, R., Chisholm, K. I., Pettingill, P., et al. (2018). Immune or genetic-mediated disruption of CASPR2 causes pain hypersensitivity due to enhanced primary afferent excitability. *Neuron* 97, 806–822.e810. doi: 10.1016/j.neuron.2018.01.033

De Rubeis, S., He, X., Goldberg, A. P., Poultney, C. S., Samocha, K., Ercument Cicek, A., et al. (2014). Synaptic, transcriptional and chromatin genes disrupted in autism. *Nature* 515, 209–215. doi: 10.1038/nature13772

Delaney, A. J., Crane, J. W., Holmes, N. M., Fam, J., and Westbrook, R. F. (2018). Baclofen acts in the central amygdala to reduce synaptic transmission and impair context fear conditioning. *Sci. Rep.* 8:9908. doi: 10.1038/s41598-018-28321-0

DSM-5, American Psychiatric Association. (2013). *Diagnostic and Statistical Manual of Mental Disorders (DSM-5)*, 5th Edn. Washington, DC: American Psychiatric Publishing.

Ebert, U., and Koch, M. (1992). Glutamate receptors mediate acoustic input to the reticular brain stem. *NeuroReport* 3, 429–432. doi: 10.1097/00001756-199205000-00013

El-Ansary, A., and Al-Ayadhi, L. (2014). GABAergic/glutamatergic imbalance relative to excessive neuroinflammation in autism spectrum disorders. *J. Neuroinflammation* 11:189. doi: 10.1186/s12974-014-0189-0

Erickson, C. A., Veenstra-Vanderweele, J. M., Melmed, R. D., McCracken, J. T., Ginsberg, L. D., Sikich, L., et al. (2014). STX209 (arbaclofen) for autism spectrum disorders: an 8-week open-label study. *J. Autism Dev. Disord.* 44, 958–964. doi: 10.1007/s10803-013-1963-z

Fatemi, S. H., Folsom, T. D., Reutiman, T. J., and Thuras, P. D. (2009). Expression of $GABA_B$ receptors is altered in brains of subjects with autism. *Cerebellum (London, England)* 8, 64–69. doi: 10.1007/s12311-008-0075-3

Fejgin, K., Pålsson, E., Wass, C., Finnerty, N., Lowry, J., Klamer, D., et al. (2009). Prefrontal $GABA_B$ receptor activation attenuates phencyclidine-induced impairments of prepulse inhibition: involvement of nitric oxide. *Neuropsychopharmacology* 34, 1673–1684. doi: 10.1038/npp.2008.225

Fendt, M., Koch, M., and Schnitzler, H.-U. (1994a). Amygdaloid noradrenaline is involved in the sensitization of the acoustic startle response in rats. *Pharmacol. Biochem. Behav.* 48, 307–314. doi: 10.1016/0091-3057(94)90532-0

Fendt, M., Koch, M., and Schnitzler, H.-U. (1994b). Lesions of the central gray block the sensitization of the acoustic startle response in rats. *Brain Res.* 661, 163–173. doi: 10.1016/0006-8993(94)91193-2

Flores, E. N., Duggan, A., Madathany, T., Hogan, A. K., Márquez, F. G., Kumar, G., et al. (2015). A non-canonical pathway from cochlea to brain signals tissue-damaging noise. *Curr. Biol.* 25, 606–612. doi: 10.1016/j.cub.2015.01.009

Fulcher, N., Azzopardi, E., De Oliveira, C., Hudson, R., Schormans, A. L., Zaman, T., et al. (2020). Deciphering midbrain mechanisms underlying prepulse inhibition of startle. *Prog. Neurobiol.* 185:101734. doi: 10.1016/j.pneurobio.2019.101734

Gaetz, W., Bloy, L., Wang, D. J., Port, R. G., Blaskey, L., Levy, S. E., et al. (2014). GABA estimation in the brains of children on the autism spectrum: measurement precision and regional cortical variation. *NeuroImage* 86, 1–9. doi: 10.1016/j.neuroimage.2013.05.068

Gandal, M. J., Sisti, J., Klook, K., Ortinski, P. I., Leitman, V., Liang, Y., et al. (2012). $GABA_B$-mediated rescue of altered excitatory-inhibitory balance, gamma synchrony and behavioral deficits following constitutive NMDAR-hypofunction. *Transl. Psychiatry* 2:e142. doi: 10.1038/tp.2012.69

Geyer, M. A., and Braff, D. L. (1982). Habituation of the blink reflex in normals and schizophrenic patients. *Psychophysiology* 19, 1–6. doi: 10.1111/j.1469-8986.1982.tb02589.x

Gómez-Nieto, R., Hormigo, S., and López, D. (2020). Prepulse inhibition of the auditory startle reflex assessment as a hallmark of brainstem sensorimotor gating mechanisms. *Brain Res.* 10:639. doi: 10.3390/brainsci10090639

Gómez-Nieto, R., Horta-Junior, J. A. C., Castellano, O., Herrero-Turrión, M. J., Rubio, M. E., López, D. E., et al. (2008). Neurochemistry of the afferents to the rat cochlear root nucleus: Possible synaptic modulation of the acoustic startle. *Neuroscience* 154, 51–64. doi: 10.1016/j.neuroscience.2008.01.079

Gómez-Nieto, R., Horta-Júnior, J. D. A. C., Castellano, O., Millian-Morell, L., Rubio, M. E., López, D. E., et al. (2014). Origin and function of short-latency inputs to the neural substrates underlying the acoustic startle reflex. *Front. Neurosci.* 8:216. doi: 10.3389/fnins.2014.00216

Gordon, A., Salomon, D., Barak, N., Pen, Y., Tsoory, M., Kimchi, T., et al. (2016). Expression of *Cntnap2* (Caspr2) in multiple levels of sensory systems. *Mol. Cell. Neurosci.* 70, 42–53. doi: 10.1016/j.mcn.2015.11.012

Groves, P. M., and Thompson, R. F. (1970). Habituation: a dual-process theory. *Psychol. Rev.* 77, 419–450. doi: 10.1037/h0029810

Gu, H., Hou, F., Liu, L., Luo, X., Nkomola, P. D., Xie, X., et al. (2018). Genetic variants in the *Cntnap2* gene are associated with gender differences among dyslexic children in China. *EBioMedicine* 34, 165–170. doi: 10.1016/j.ebiom.2018.07.007

Halberstadt, A. L., and Geyer, M. A. (2009). Habituation and sensitization of acoustic startle: opposite influences of dopamine D1 and D2-family receptors. *Neurobiol. Learn Mem.* 92, 243–248. doi: 10.1016/j.nlm.2008.05.015

Harada, M., Taki, M. M., Nose, A., Kubo, H., Mori, K., Nishitani, H., et al. (2011). Non-invasive evaluation of the GABAergic/glutamatergic system in autistic patients observed by MEGA-editing proton MR spectroscopy using a clinical 3 Tesla instrument. *J. Autism Dev. Disord.* 41, 447–454. doi: 10.1007/s10803-010-1065-0

Harris, K. C., and Dubno, J. R. (2017). Age-related deficits in auditory temporal processing: unique contributions of neural dyssynchrony and slowed neuronal processing. *Neurobiol. Aging* 53, 150–158. doi: 10.1016/j.neurobiolaging.2017.01.008

Henderson, C., Wijetunge, L., Kinoshita, M. N., Shumway, M., Hammond, R. S., Postma, F. R., et al. (2012). Reversal of disease-related pathologies in the fragile X mouse model by selective activation of $GABA_B$ receptors with Arbaclofen. *Sci. Transl. Med.* 4:152ra128. doi: 10.1126/scitranslmed.3004218

Hince, D. A., and Martin-Iverson, M. T. (2005). Differences in prepulse inhibition (PPI) between wistar and sprague-dawley rats clarified by a new method of PPI standardization. *Behav. Neurosci.* 119, 66–77. doi: 10.1037/0735-7044.119.1.66

Hoffman, H. S., and Ison, J. R. (1980). Reflex modification in the domain of startle: I. Some empirical findings and their implications for how the nervous system processes sensory input. *Psychol. Rev.* 87, 175–189.

Hoffman, H. S., and Searle, J. L. (1968). Acoustic and temporal factors in the evocation of startle. *J. Acoust. Soc. Am.* 43, 269–282. doi: 10.1121/1.1910776

Horder, J., Andersson, M., Mendez, M. A., Singh, N., Tangen, Ä., Lundberg, J., et al. (2018a). $GABA_A$ receptor availability is not altered in adults with autism spectrum disorder or in mouse models. *Sci. Transl. Med.* 10:eaam8434. doi: 10.1126/scitranslmed.aam8434

Horder, J., Lavender, T., Mendez, M., O'gorman, R., Daly, E., Craig, M., et al. (2013). Reduced subcortical glutamate/glutamine in adults with autism spectrum disorders: a [1 H] MRS study. *Transl. Psychiatry* 3:e279. doi: 10.1038/tp.2013.53

Horder, J., Petrinovic, M. M., Mendez, M. A., Bruns, A., Takumi, T., Spooren, W., et al. (2018b). Glutamate and GABA in autism spectrum disorder-a translational magnetic resonance spectroscopy study in man and rodent models. *Transl. Psychiatry* 8:106. doi: 10.1038/s41398-018-0155-1

Iossifov, I., O'Roak, B. J., Sanders, S. J., Ronemus, M., Krumm, N., Levy, D., et al. (2014). The contribution of de novo coding mutations to autism spectrum disorder. *Nature* 515:216. doi: 10.1038/nature13908

Ison, J. R., McAdam, D. W., and Hammond, G. R. (1973). Latency and amplitude changes in the acoustic startle reflex of the rat produced by variation in auditory prestimulation. *Physiol. Behav.* 10, 1035–1039. doi: 10.1016/0031-9384(73)90185-6

Kazdoba, T. M., Leach, P. T., and Crawley, J. N. (2016). Behavioral phenotypes of genetic mouse models of autism. *Genes Brain Behav.* 15, 7–26. doi: 10.1111/gbb.12256

Khalfa, S., Bruneau, N., Rogé, B., Georgieff, N., Veuillet, E., Adrien, J. L., et al. (2004). Increased perception of loudness in autism. *Hear. Res.* 198, 87–92. doi: 10.1016/j.heares.2004.07.006

Kim, J.-W., Park, K., Kang, R. J., Gonzales, E. L. T., Kim, D. G., Oh, H. A., et al. (2019). Pharmacological modulation of AMPA receptor rescues social impairments in animal models of autism. *Neuropsychopharmacology* 44, 314–323. doi: 10.1038/s41386-018-0098-5

Koch, M. (1999). The neurobiology of startle. *Prog. Neurobiol.* 59, 107–128. doi: 10.1016/s0301-0082(98)00098-7

Koch, M., Fendt, M., and Kretschmer, B. D. (2000). Role of the substantia nigra pars reticulata in sensorimotor gating, measured by prepulse inhibition of startle in rats. *Behav. Brain Res.* 117, 153–162. doi: 10.1016/s0166-4328(00)00299-0

Kohl, S., Wolters, C., Gruendler, T. O. J., Vogeley, K., Klosterkötter, J., Kuhn, J., et al. (2014). Prepulse inhibition of the acoustic startle reflex in high functioning autism. *PLoS One* 9:e92372. doi: 10.1371/journal.pone.0092372

Krase, W., Koch, M., and Schnitzler, H.-U. (1994). Substance P is involved in the sensitization of the acoustic startle response by footshocks in rats. *Behav. Brain Res.* 63, 81–88. doi: 10.1016/0166-4328(94)90053-1

Kulesza, R. J. Jr., Lukose, R., and Stevens, L. V. (2011). Malformation of the human superior olive in autistic spectrum disorders. *Brain Res.* 1367, 360–371. doi: 10.1016/j.brainres.2010.10.015

Kumru, H., and Kofler, M. (2012). Effect of spinal cord injury and of intrathecal baclofen on brainstem reflexes. *Clin. Neurophysiol.* 123, 45–53. doi: 10.1016/j.clinph.2011.06.036

Kumru, H., Kofler, M., Valls-Solé, J., Portell, E., and Vidal, J. (2009). Brainstem reflexes are enhanced following severe spinal cord injury and reduced by continuous intrathecal baclofen. *Neurorehabil. Neural Repair* 23, 921–927. doi: 10.1177/1545968309335979

Kwon, S., Kim, J., Choe, B. H., Ko, C., and Park, S. (2007). Electrophysiologic assessment of central auditory processing by auditory brainstem responses in children with autism spectrum disorders. *J. Korean Med. Sci.* 22, 656–659. doi: 10.3346/jkms.2007.22.4.656

Lauer, A. M., Behrens, D., and Klump, G. (2017). Acoustic startle modification as a tool for evaluating auditory function of the mouse: Progress, pitfalls and potential. *Neurosci. Biobehav. Rev.* 77, 194–208. doi: 10.1016/j.neubiorev.2017.03.009

Leaton, R. N., and Supple, W. F. Jr. (1986). Cerebellar vermis: essential for long-term habituation of the acoustic startle response. *Science* 232, 513–515. doi: 10.1126/science.3961494

Lee, Y., López, D. E., Meloni, E. G., and Davis, M. (1996). A primary acoustic startle pathway: obligatory role of cochlear root neurons and the nucleus reticularis pontis caudalis. *J. Neurosci.* 16, 3775–3789. doi: 10.1523/JNEUROSCI.16-11-03775.1996

Leekam, S. R., Nieto, C., Libby, S. J., Wing, L., and Gould, J. (2007). Describing the sensory abnormalities of children and adults with autism. *J. Autism Dev. Disord.* 37, 894–910. doi: 10.1007/s10803-006-0218-7

Lorrai, I., Maccioni, P., Gessa, G. L., and Colombo, G. (2016). R(+)-Baclofen, but not S(−)-Baclofen, alters alcohol self-administration in alcohol-preferring rats. *Front. Psychiatry* 7:68. doi: 10.3389/fpsyt.2016.00068

Lu, J., Lobarinas, E., Deng, A., Goodey, R., Stolzberg, D., Salvi, R. J., et al. (2011). GABAergic neural activity involved in salicylate-induced auditory cortex gain enhancement. *Neuroscience* 189, 187–198. doi: 10.1016/j.neuroscience.2011.04.073

Lyall, A., Swanson, J., Liu, C., Blumenthal, T. D., and Turner, C. P. (2009). Neonatal exposure to MK801 promotes prepulse-induced delay in startle response time in adult rats. *Exp. Brain Res.* 197, 215–222. doi: 10.1007/s00221-009-1906-2

Madsen, G. F., Bilenberg, N., Cantio, C., and Oranje, B. (2014). Increased prepulse inhibition and sensitization of the startle reflex in autistic children. *Autism Res.* 7, 94–103. doi: 10.1002/aur.1337

Martin, M. R. (1982). Baclofen and the brain stem auditory evoked potential. *Exp. Neurol.* 76, 675–680. doi: 10.1016/0014-4886(82)90135-2

Martin-Iverson, M. T., and Stevenson, K. N. (2005). Apomorphine effects on emotional modulation of the startle reflex in rats. *Psychopharmacology (Berl)* 181, 60–70. doi: 10.1007/s00213-005-2217-3

Meincke, U., Light, G. A., Geyer, M. A., Braff, D. L., and Gouzoulis-Mayfrank, E. (2004). Sensitization and habituation of the acoustic startle reflex in patients with schizophrenia. *Psychiatry Res.* 126, 51–61. doi: 10.1016/j.psychres.2004.01.003

Meloni, E. G., and Davis, M. (1998). The dorsal cochlear nucleus contributes to a high intensity component of the acoustic startle reflex in rats. *Hear. Res.* 119, 69–80. doi: 10.1016/s0378-5955(98)00040-9

Miron, O., Ari-Even Roth, D., Gabis, L. V., Henkin, Y., Shefer, S., Dinstein, I., et al. (2016). Prolonged auditory brainstem responses in infants with autism. *Autism Res.* 9, 689–695. doi: 10.1002/aur.1561

Mody, M., and Belliveau, J. W. (2013). Speech and language impairments in autism: insights from behavior and neuroimaging. *N. Am. J. Med. Sci. (Boston)* 5, 157–161. doi: 10.7156/v5i3p157

Möhrle, D., Fernández, M., Peñagarikano, O., Frick, A., Allman, B., Schmid, S., et al. (2020). What we can learn from a genetic rodent model about autism. *Neurosci. Biobehav. Rev.* 109, 29–53. doi: 10.1016/j.neubiorev.2019.12.015

Nevins, M. E., Nash, S. A., and Beardsley, P. M. (1993). Quantitative grip strength assessment as a means of evaluating muscle relaxation in mice. *Psychopharmacology* 110, 92–96. doi: 10.1007/BF02246955

Nottebohm, F., and Arnold, A. P. (1976). Sexual dimorphism in vocal control areas of the songbird brain. *Science* 194, 211–213. doi: 10.1126/science.959852

Oberman, L. M. (2012). mGluR antagonists and GABA agonists as novel pharmacological agents for the treatment of autism spectrum disorders. *Expert Opin. Investig. Drugs* 21, 1819–1825. doi: 10.1517/13543784.2012.729819

O'Neill, M., and Jones, R. S. (1997). Sensory-perceptual abnormalities in autism: a case for more research? *J. Autism Dev. Disord.* 27, 283–293. doi: 10.1023/a:1025850431170

Ornitz, E. M., Lane, S. J., Sugiyama, T., and de Traversay, J. (1993). Startle modulation studies in autism. *J. Autism Dev. Disord.* 23, 619–637. doi: 10.1007/BF01046105

Osen, K., López, D., Slyngstad, T., Ottersen, O., and Storm-Mathisen, J. (1991). GABA-like and glycine-like immunoreactivities of the cochlear root nucleus in rat. *J. Neurocytol.* 20, 17–25. doi: 10.1007/BF01187131

Panaitof, S. C., Abrahams, B. S., Dong, H., Geschwind, D. H., and White, S. A. (2010). Language-related *Cntnap2* gene is differentially expressed in sexually dimorphic song nuclei essential for vocal learning in songbirds. *J. Comp. Neurol.* 518, 1995–2018. doi: 10.1002/cne.22318

Payne, R., and Anderson, D. C. (1967). Scopolamine-produced changes in activity and in the startle response: implications for behavioral activation. *Psychopharmacologia* 12, 83–90. doi: 10.1007/BF00402758

Peñagarikano, O., Abrahams, B. S., Herman, E. I., Winden, K. D., Gdalyahu, A., Dong, H., et al. (2011). Absence of *Cntnap2* leads to epilepsy, neuronal migration abnormalities and core autism-related deficits. *Cell* 147, 235–246. doi: 10.1016/j.cell.2011.08.040

Perry, W., Minassian, A., Lopez, B., Maron, L., and Lincoln, A. (2007). Sensorimotor gating deficits in adults with autism. *Biol. Psychiatry* 61, 482–486. doi: 10.1016/j.biopsych.2005.09.025

Pilz, P. K. D., and Schnitzler, H.-U. (1996). Habituation and sensitization of the acoustic startle response in rats: Amplitude, threshold and latency measures. *Neurobiol. Learn. Mem.* 66, 67–79. doi: 10.1006/nlme.1996.0044

Pinto, D., Delaby, E., Merico, D., Barbosa, M., Merikangas, A., Klei, L., et al. (2014). Convergence of genes and cellular pathways dysregulated in autism spectrum disorders. *Am. J. Hum. Genet.* 94, 677–694. doi: 10.1016/j.ajhg.2014.03.018

Plappert, C. F., Pilz, P. K., Becker, K., Becker, C. M., and Schnitzler, H. U. (2001). Increased sensitization of acoustic startle response in spasmodic mice with a mutation of the glycine receptor alpha1-subunit gene. *Behav. Brain Res.* 121, 57–67. doi: 10.1016/s0166-4328(00)00385-5

Poliak, S., Salomon, D., Elhanany, H., Sabanay, H., Kiernan, B., Pevny, L., et al. (2003). Juxtaparanodal clustering of Shaker-like K^+ channels in myelinated axons depends on Caspr2 and TAG-1. *J. Cell. Biol.* 162, 1149–1160. doi: 10.1083/jcb.200305018

Poot, M. (2017). Intragenic *Cntnap2* deletions: a bridge too far? *Mol. Syndromol.* 8, 118–130. doi: 10.1159/000456021

Port, R. G., Oberman, L. M., and Roberts, T. P. (2019). Revisiting the excitation/inhibition imbalance hypothesis of ASD through a clinical lens. *Br. J. Radiol.* 92:20180944. doi: 10.1259/bjr.20180944

Price, C. J., Scott, R., Rusakov, D. A., and Capogna, M. (2008). $GABA_B$ receptor modulation of feedforward inhibition through hippocampal neurogliaform cells. *J. Neurosci.* 28, 6974–6982. doi: 10.1523/JNEUROSCI.4673-07.2008

Rankin, C. H., Abrams, T., Barry, R. J., Bhatnagar, S., Clayton, D. F., Colombo, J., et al. (2009). Habituation revisited: an updated and revised description of the behavioral characteristics of habituation. *Neurobiol. Learn. Mem.* 92, 135–138. doi: 10.1016/j.nlm.2008.09.012

Riva, V., Cantiani, C., Benasich, A. A., Molteni, M., Piazza, C., Giorda, R., et al. (2018). From *Cntnap2* to early expressive language in infancy: The mediation role of rapid auditory processing. *Cereb. Cortex* 28, 2100–2108. doi: 10.1093/cercor/bhx115

Rodenas-Cuadrado, P., Pietrafusa, N., Francavilla, T., La Neve, A., Striano, P., Vernes, S.C., et al. (2016). Characterisation of CASPR2 deficiency disorder—a syndrome involving autism, epilepsy and language impairment. *BMC Med. Genet.* 17:8. doi: 10.1186/s12881-016-0272-8

Rosenhall, U., Nordin, V., Brantberg, K., and Gillberg, C. (2003). Autism and auditory brain stem responses. *Ear Hear.* 24, 206–214. doi: 10.1097/01.AUD.0000069326.11466.7E

Rubenstein, J. L., and Merzenich, M. M. (2003). Model of autism: increased ratio of excitation/inhibition in key neural systems. *Genes Brain Behav.* 2, 255–267. doi: 10.1034/j.1601-183x.2003.00037.x

Rylaarsdam, L., and Guemez-Gamboa, A. (2019). Genetic causes and modifiers of autism spectrum disorder. *Front. Cell. Neurosci.* 13:385. doi: 10.3389/fncel.2019.00385

Scott, K. E., Kazazian, K., Mann, R. S., Möhrle, D., Schormans, A. L., Schmid, S., et al. (2020). Loss of *Cntnap2* in the rat causes autism-related alterations in social interactions, stereotypic behavior and sensory processing. *Autism Res.* 13, 1698–1717. doi: 10.1002/aur.2364

Scott, K. E., Schormans, A. L., Pacoli, K. Y., De Oliveira, C., Allman, B. L., Schmid, S., et al. (2018). Altered auditory processing, filtering and reactivity in the *Cntnap2* knock-out rat model for neurodevelopmental disorders. *J. Neurosci.* 38, 8588–8604. doi: 10.1523/JNEUROSCI.0759-18.2018

Scott, K. E., Schulz, S. E., Moehrle, D., Allman, B. L., Oram Cardy, J. E., Stevenson, R. A., et al. (2021). Closing the species gap: translational approaches to studying sensory processing differences relevant for autism spectrum disorder. *Autism Res.* 14, 1322–1331. doi: 10.1002/aur.2533

Scott, R., Sánchez-Aguilera, A., van Elst, K., Lim, L., Dehorter, N., Bae, S. E., et al. (2017). Loss of *Cntnap2* causes axonal excitability deficits, developmental delay in cortical myelination and abnormal stereotyped motor behavior. *Cereb. Cortex* 29, 586–597. doi: 10.1093/cercor/bhx341

Servadio, M., Vanderschuren, L. J., and Trezza, V. (2015). Modeling autism-relevant behavioral phenotypes in rats and mice: Do 'autistic' rodents exist? *Behav. Pharmacol.* 26, 522–540. doi: 10.1097/FBP.0000000000000163

Sgadò, P., Genovesi, S., Kalinovsky, A., Zunino, G., Macchi, F., Allegra, M., et al. (2013). Loss of GABAergic neurons in the hippocampus and cerebral cortex of Engrailed-2 null mutant mice: implications for autism spectrum disorders. *Exp. Neurol.* 247, 496–505. doi: 10.1016/j.expneurol.2013.01.021

Silverman, J. L., Pride, M. C., Hayes, J. E., Puhger, K. R., Butler-Struben, H. M., Baker, S., et al. (2015). $GABA_B$ receptor agonist R-Baclofen reverses social deficits and reduces repetitive behavior in two mouse models of autism. *Neuropsychopharmacology* 40, 2228–2239. doi: 10.1038/npp.2015.66

Simons-Weidenmaier, N. S., Weber, M., Plappert, C. F., Pilz, P. K., and Schmid, S. (2006). Synaptic depression and short-term habituation are located in the sensory part of the mammalian startle pathway. *BMC Neurosci.* 7:38. doi: 10.1186/1471-2202-7-38

Sinclair, D., Featherstone, R., Naschek, M., Nam, J., Du, A., Wright, S., et al. (2017a). $GABA_B$ agonist Baclofen normalizes auditory-evoked neural oscillations and behavioral deficits in the Fmr1 knockout mouse model of fragile X syndrome. *eNeuro* 4:ENEURO.0380–0316.2017. doi: 10.1523/ENEURO.0380-16.2017

Sinclair, D., Oranje, B., Razak, K. A., Siegel, S. J., and Schmid, S. (2017b). Sensory processing in autism spectrum disorders and Fragile X syndrome-From the clinic to animal models. *Neurosci. Biobehav. Rev.* 76, 235–253. doi: 10.1016/j.neubiorev.2016.05.029

Stevenson, R. A., Baum, S. H., Segers, M., Ferber, S., Barense, M. D., Wallace, M. T., et al. (2017). Multisensory speech perception in autism spectrum disorder: from phoneme to whole-word perception. *Autism Res.* 10, 1280–1290. doi: 10.1002/aur.1776

Stoddart, C. W., Noonan, J., and Martin-Iverson, M. T. (2008). Stimulus quality affects expression of the acoustic startle response and prepulse inhibition in mice. *Behav. Neurosci.* 122, 516–526. doi: 10.1037/0735-7044.122.3.516

Stoppel, L. J., Kazdoba, T. M., Schaffler, M. D., Preza, A. R., Heynen, A., Crawley, J. N., et al. (2018). R-Baclofen reverses cognitive deficits and improves social interactions in two lines of 16p11.2 deletion mice. *Neuropsychopharmacology* 43, 513–524. doi: 10.1038/npp.2017.236

Strauss, K. A., Puffenberger, E. G., Huentelman, M. J., Gottlieb, S., Dobrin, S. E., Parod, J. M., et al. (2006). Recessive symptomatic focal epilepsy and mutant contactin-associated protein-like 2. *N. Engl. J. Med.* 354, 1370–1377. doi: 10.1056/NEJMoa052773

Sun, H., Ma, C. L., Kelly, J. B., and Wu, S. H. (2006). $GABA_B$ receptor-mediated presynaptic inhibition of glutamatergic transmission in the inferior colliculus. *Neurosci. Lett.* 399, 151–156. doi: 10.1016/j.neulet.2006.01.049

Szczepaniak, W. S., and Møller, A. (1995). Effects of L-Baclofen and D-Baclofen on the auditory system: A study of click-evoked potentials from the inferior colliculus in the rat. *Ann. Otol. Rhinol. Laryngol.* 104, 399–404. doi: 10.1177/000348949510400511

Szczepaniak, W. S., and Møller, A. R. (1996). Effects of (−)-baclofen, clonazepam and diazepam on tone exposure-induced hyperexcitability of the inferior colliculus in the rat: possible therapeutic implications for pharmacological management of tinnitus and hyperacusis. *Hear. Res.* 97, 46–53. doi: 10.1016/s0378-5955(96)80006-2

Takahashi, H., Komatsu, S., Nakahachi, T., Ogino, K., and Kamio, Y. (2016). Relationship of the acoustic startle Rresponse and its modulation to emotional and behavioral problems in typical development children and those with autism spectrum disorders. *J. Autism Dev. Disord.* 46, 534–543. doi: 10.1007/s10803-015-2593-4

Takahashi, K., Nagai, T., Kamei, H., Maeda, K., Matsuya, T., Arai, S., et al. (2007). Neural circuits containing pallidotegmental GABAergic neurons are involved in the prepulse inhibition of the startle reflex in mice. *Biol. Psychiatry* 62, 148–157. doi: 10.1016/j.biopsych.2006.06.035

Townsend, L. B., and Smith, S. L. (2017). Genotype- and sex-dependent effects of altered *Cntnap2* expression on the function of visual cortical areas. *J. Neurodev. Disord.* 9:2. doi: 10.1186/s11689-016-9182-5

Truong, D. T., Rendall, A. R., Castelluccio, B. C., Eigsti, I. M., and Fitch, R. H. (2015). Auditory processing and morphological anomalies in medial geniculate nucleus of *Cntnap2* mutant mice. *Behav. Neurosci.* 129, 731–743. doi: 10.1037/bne0000096

Van Elst, L. T., Maier, S., Fangmeier, T., Endres, D., Mueller, G., Nickel, K., et al. (2014). Disturbed cingulate glutamate metabolism in adults with high-functioning autism spectrum disorder: evidence in support of the excitatory/inhibitory imbalance hypothesis. *Mol. Psychiatry* 19, 1314–1325. doi: 10.1038/mp.2014.62

Varea, O., Martin-de-Saavedra, M. D., Kopeikina, K. J., Schürmann, B., Fleming, H. J., Fawcett-Patel, J. M., et al. (2015). Synaptic abnormalities and cytoplasmic glutamate receptor aggregates in contactin associated protein-like 2/Caspr2 knockout neurons. *Proc. Natl. Acad. Sci. U S A* 112, 6176–6181. doi: 10.1073/pnas.1423205112

Veenstra-VanderWeele, J., Cook, E. H., King, B. H., Zarevics, P., Cherubini, M., Walton-Bowen, K., et al. (2017). Arbaclofen in children and Aadolescents with autism spectrum disorder: a randomized, controlled, phase 2 trial. *Neuropsychopharmacology* 42, 1390–1398. doi: 10.1038/npp.2016.237

Vogt, D., Cho, K. K. A., Shelton, S. M., Paul, A., Huang, Z. J., Sohal, V. S., et al. (2017). Mouse *Cntnap2* and human *Cntnap2* ASD alleles cell autonomously regulate PV^+ cortical interneurons. *Cereb. Cortex* 28, 3868–3879. doi: 10.1093/cercor/bhx248

Waagepetersen, H. S., Sonnewald, U., Gegelashvili, G., Larsson, O. M., and Schousboe, A. (2001). Metabolic distinction between vesicular and cytosolic GABA in cultured GABAergic neurons using 13C magnetic resonance spectroscopy. *J. Neurosci. Res.* 63, 347–355. doi: 10.1002/1097-4547(20010215)63:4<347::AID-JNR1029>3.0.CO;2-G

Wagner, T., and Mack, A. (1998). Membrane properties of giant neurons in the caudal pontine reticular formation in vitro. *NeuroReport* 9, 1211–1215. doi: 10.1097/00001756-199804200-00046

Waldmeier, P. C., Kaupmann, K., and Urwyler, S. (2008). Roles of $GABA_B$ receptor subtypes in presynaptic auto- and heteroreceptor function regulating GABA and glutamate release. *J. Neural Transm. (Vienna)* 115, 1401–1411. doi: 10.1007/s00702-008-0095-7

Walls, A. B., Waagepetersen, H. S., Bak, L. K., Schousboe, A., and Sonnewald, U. (2015). The glutamine-glutamate/GABA cycle: function, regional differences in glutamate and GABA production and effects of interference with GABA metabolism. *Neurochem. Res.* 40, 402–409. doi: 10.1007/s11064-014-1473-1

Weber, M., Schnitzler, H. U., and Schmid, S. (2002). Synaptic plasticity in the acoustic startle pathway: the neuronal basis for short-term habituation? *Eur. J. Neurosci.* 16, 1325–1332. doi: 10.1046/j.1460-9568.2002.02194.x

Werling, D. M., and Geschwind, D. H. (2013). Sex differences in autism spectrum disorders. *Curr. Opin. Neurol.* 26, 146–153. doi: 10.1097/WCO.0b013e32835ee548

Wible, B., Nicol, T., and Kraus, N. (2004). Atypical brainstem representation of onset and formant structure of speech sounds in children with language-based learning problems. *Biol. Psychol.* 67, 299–317. doi: 10.1016/j.biopsycho.2004.02.002

Wu, C., and Sun, D. (2015). GABA receptors in brain development, function and injury. *Metab. Brain Dis.* 30, 367–379. doi: 10.1007/s11011-014-9560-1

Yee, B. K., Chang, D. T., and Feldon, J. (2004). The effects of dizocilpine and phencyclidine on prepulse inhibition of the acoustic startle reflex and on prepulse-elicited reactivity in C57BL6 mice. *Neuropsychopharmacology* 29, 1865–1877. doi: 10.1038/sj.npp.1300480

Yeomans, J. S., Bosch, D., Alves, N., Daros, A., Ure, R. J., Schmid, S., et al. (2010). GABA receptors and prepulse inhibition of acoustic startle in mice and rats. *Eur. J. Neurosci.* 31, 2053–2061. doi: 10.1111/j.1460-9568.2010.07236.x

Yip, J., Soghomonian, J. J., and Blatt, G. J. (2008). Increased GAD67 mRNA expression in cerebellar interneurons in autism: implications for Purkinje cell dysfunction. *J. Neurosci. Res.* 86, 525–530. doi: 10.1002/jnr.21520

Yoo, H. (2015). Genetics of autism spectrum disorder: Current status and possible clinical applications. *Exp. Neurobiol.* 24, 257–272. doi: 10.5607/en.2015.24.4.257

Zaman, T., De Oliveira, C., Smoka, M., Narla, C., Poulter, M. O., Schmid, S., et al. (2017). BK channels mediate synaptic plasticity underlying habituation in rats. *J. Neurosci.* 37, 4540–4551. doi: 10.1523/JNEUROSCI.3699-16.2017

Zheng, P., Zeng, B., Liu, M., Chen, J., Pan, J., Han, Y., et al. (2019). The gut microbiome from patients with schizophrenia modulates the glutamate-glutamine-GABA cycle and schizophrenia-relevant behaviors in mice. *Sci. Adv.* 5:eaau8317. doi: 10.1126/sciadv.aau8317

Conflict of Interest: The authors declare that the research was conducted in the absence of any commercial or financial relationships that could be construed as a potential conflict of interest.

Publisher's Note: All claims expressed in this article are solely those of the authors and do not necessarily represent those of their affiliated organizations, or those of the publisher, the editors and the reviewers. Any product that may be evaluated in this article, or claim that may be made by its manufacturer, is not guaranteed or endorsed by the publisher.

frontiers in Integrative Neuroscience

ORIGINAL RESEARCH
published: 31 August 2021
doi: 10.3389/fnint.2021.716447

Attentional Disengagement and the Locus Coeruleus – Norepinephrine System in Children With Autism Spectrum Disorder

Brandon Keehn[1,2], Girija Kadlaskar[1], Sophia Bergmann[1], Rebecca McNally Keehn[3] and Alexander Francis[1]*

[1] Department of Speech, Language, and Hearing Sciences, Purdue University, West Lafayette, IN, United States, [2] Department of Psychological Sciences, Purdue University, West Lafayette, IN, United States, [3] Department of Pediatrics, Indiana University School of Medicine, Indianapolis, IN, United States

Background: Differences in non-social attentional functions have been identified as among the earliest features that distinguish infants later diagnosed with autism spectrum disorder (ASD), and may contribute to the emergence of core ASD symptoms. Specifically, slowed attentional disengagement and difficulty reorienting attention have been found across the lifespan in those at risk for, or diagnosed with, ASD. Additionally, the locus coeruleus-norepinephrine (LC-NE) system, which plays a critical role in arousal regulation and selective attention, has been shown to function atypically in ASD. While activity of the LC-NE system is associated with attentional disengagement and reorienting in typically developing (TD) individuals, it has not been determined whether atypical LC-NE activity relates to attentional disengagement impairments observed in ASD.

Objective: To examine the relationship between resting pupil diameter (an indirect measure of tonic LC-NE activation) and attentional disengagement in children with ASD.

Methods: Participants were 21 school-aged children with ASD and 20 age- and IQ-matched TD children. The study consisted of three separate experiments: a resting eye-tracking task and visual and auditory gap-overlap paradigms. For the resting eye-tracking task, pupil diameter was monitored while participants fixated a central crosshair. In the gap-overlap paradigms, participants were instructed to fixate on a central stimulus and then move their eyes to peripherally presented visual or auditory targets. Saccadic reaction times (SRT), percentage of no-shift trials, and disengagement efficiency were measured.

Results: Children with ASD had significantly larger resting pupil size compared to their TD peers. The groups did not differ for overall SRT, nor were there differences in SRT for overlap and gap conditions between groups. However, the ASD group did evidence impairments in disengagement (larger step/gap effects, higher percentage of no-shift trials, and reduced disengagement efficiency) compared to their TD peers. Correlational analyses showed that slower, less efficient disengagement was associated with increased pupil diameter.

OPEN ACCESS

Edited by:
Eric London, Institute for Basic Research in Developmental Disabilities (IBR), United States

Reviewed by:
David Quentin Beversdorf, University of Missouri, United States
Nico Bast, Goethe University Frankfurt, Germany

***Correspondence:**
Brandon Keehn
bkeehn@purdue.edu

Received: *28 May 2021*
Accepted: *10 August 2021*
Published: *31 August 2021*

Citation:
Keehn B, Kadlaskar G, Bergmann S, McNally Keehn R and Francis A (2021) Attentional Disengagement and the Locus Coeruleus – Norepinephrine System in Children With Autism Spectrum Disorder. Front. Integr. Neurosci. 15:716447. doi: 10.3389/fnint.2021.716447

Conclusion: Consistent with prior reports, children with ASD show significantly larger resting pupil diameter, indicative of atypically elevated tonic LC-NE activity. Associations between pupil size and measures of attentional disengagement suggest that atypically increased tonic activation of the LC-NE system may be associated with poorer attentional disengagement in children with ASD.

Keywords: autism spectrum disorder, locus coeruleus, attention, disengagement, norepinephrine, pupil

INTRODUCTION

Differences in non-social attentional functions have been identified as among the earliest features that distinguish infants who develop autism spectrum disorder (ASD), and may play a critical role in the emergence of core ASD symptoms (Keehn et al., 2013). In particular, slowed attentional disengagement and difficulty reorienting attention (i.e., "sticky attention") have been found across the lifespan in those at risk for, or diagnosed with, ASD (Sacrey et al., 2014). However, despite research highlighting these early emerging non-social attentional differences and their association with ASD symptomatology and later ASD diagnosis (Zwaigenbaum et al., 2005; Elison et al., 2013; Elsabbagh et al., 2013), the mechanism(s) underlying atypical attentional disengagement remain unknown.

To date, evidence of impaired attentional disengagement in ASD has been primarily demonstrated using gap-overlap paradigms, which have been employed from infancy through adulthood (see Sacrey et al., 2014, for review). Generally, these tasks examine differences in the latency of eye movements to peripheral targets, which appear with, or without, the presence of a central stimulus. Latency to execute saccadic eye movements (i.e., saccadic reaction time; SRT) is reduced when the fixated central stimulus is removed simultaneously with or prior to (e.g., 200 ms) the onset of a peripheral target compared to saccades generated when the central stimulus remains present (Saslow, 1967). The resulting difference in SRT is referred to as the gap (or step) effect, and is thought to result from two separate sources: (1) a generalized warning effect as a consequence of the central stimulus offset (i.e., an alerting cue), and (2) the release of ocular inhibition due to (a) the disappearance of a foveal stimulus, and (b) the top-down preparation of a saccadic response (Kingstone and Klein, 1993; Taylor et al., 1998). Although a large body of research has examined the neural circuitry associated with the generation of saccadic eye movements (see Liversedge et al., 2011, for example), a limited number of studies have investigated the neural substrates specifically associated with the gap effect.

Early evidence from studies investigating the neural mechanisms associated with latency differences between gap and overlap conditions has predominantly come from research with non-human primates. Unique patterns of gap-period activation in neurons of the superior colliculus have been linked to faster SRTs and increased frequency of express saccades [i.e., fast latency saccades (RT $<$ 140 ms); Fischer and Weber, 1993) in the gap condition (Dorris and Munoz, 1995; Dorris et al., 1997)]. Other work has shown that neurons in the frontal eye fields (FEF) may increase their firing rate during the gap period (Dias and Bruce, 1994). Research investigating attentional disengagement in human adults with focal brain lesions has shown that increased saccadic latency for the overlap (but not the gap) condition is associated with lesions in both the frontal eye fields (FEF; Rivaud et al., 1994) and the posterior region of the anterior cingulate cortex (ACC; Gaymard et al., 1998). More recently, an fMRI investigation of gap-overlap performance in neurotypical adults showed that slower SRT for the overlap condition was associated with decreased activation in the bilateral inferior frontal junction (Ozyurt and Greenlee, 2011). These authors hypothesize that saccade generation while maintaining an active fixation on the central stimulus may require greater processing effort (especially compared to gap trials), and that efficient responding for overlap trials may require increased activation of this area, which is involved in task switching and set shifting. Together, these results suggest that the gap effect is generated by a combination of cortical and subcortical sources associated with condition-specific changes in SRT.

Although experimental parameters vary widely across previous studies (see Sacrey et al., 2014, for discussion), when ASD-related differences in task performance are present these tend to be exhibited as disproportionally longer SRT to *overlap trials* relative to gap trials compared to their typically developing (TD) peers. To date, only one study has examined the neurofunctional correlates of gap effect in ASD. Kawakubo et al. (2007) measured event-related potentials (ERP) during a gap-overlap task to investigate the neurophysiological indices of attentional disengagement. Compared to both TD adults and adults with intellectual disability, adults with ASD showed greater pre-saccadic positivity (PSP) for overlap but not gap trials. Prior work in neurotypical adults has shown that the PSP is greater for overlap compared to gap trials and may reflect greater activation of cortical eye-movement control network necessary to disinhibit the collicular system in overlap trials (Gomez et al., 1996; Csibra et al., 1997). Thus, larger PSP in ASD may reflect increased cortical activation necessary to initiate saccades in circumstances when individuals are engaged or fixating on a central stimulus (i.e., overlap trials).

Additionally, based on the pattern of prior gap-overlap findings in ASD, Keehn et al. (2019) hypothesized that disengagement impairments may reflect atypical activation of the locus coeruleus – norephinephrine (LC-NE) system. The LC-NE system is known to play a key role in arousal regulation and selective attention (Berridge and Waterhouse, 2003), and is an important node in two influential models of attention (Corbetta et al., 2008; Petersen and Posner, 2012). Norepinephrine functions to inhibit spontaneous neural

activity, thereby permitting increased neural responses to sensory stimulation, thus increasing signal-to-noise, especially in sensory areas (Foote et al., 1975). Tonic (i.e., resting or baseline) activation of the LC-NE system is associated with regulation of the sleep-wake cycle, with lower tonic activation seen in sleep and greater tonic activity with increased arousal during the awake state; phasic activation of LC neurons occurs in response to salient or behaviorally relevant stimuli (Aston-Jones and Cohen, 2005). According to the adaptive gain model (Aston-Jones and Cohen, 2005), intermediate levels of tonic LC-NE activity are associated with robust phasic LC activation to task-relevant stimuli and superior task performance, whereas elevated tonic LC-NE activity is related to decreased phasic LC responses as well as poorer task performance and greater levels of distractibility.

Prior work has hypothesized that the LC-NE system may be implicated more generally in the pathophysiology of ASD (London, 2018) and more specifically related to differences in attention present in ASD (Bast et al., 2018). While previous findings based on plasma NE metabolites suggests that NE may be elevated in individuals with ASD (Lam et al., 2006), histological (Martchek et al., 2006) and positron emission tomography (PET; Kubota et al., 2020) findings suggest equivalent LC volume and cell counts as well as norepinephrine transport binding in ASD. However, the size and location of the LC (a small nucleus located adjacent to the fourth ventricle in the rostral pons) has made the study of LC activity difficult. More recently, pupil diameter has been shown to be an indirect index of LC-NE activity (see Joshi and Gold, 2020, for review). For example, several studies have shown that LC activity is associated with resting pupil size (Joshi et al., 2016; Reimer et al., 2016). Together, these results suggest that resting pupil diameter is valid proxy measurement for tonic LC-NE activity. However, only a limited number of studies (n = 5) have examined resting tonic pupil size in ASD (see Arora et al., 2021, for review). Of these, half have reported significantly increased pupil diameter in ASD, which may reflect increased tonic activity of the LC-NE system. Arora et al. (2021) note that measurement of autonomic indices (including pupil diameter) during resting state without stimulation (i.e., maintaining fixation to a central stimulus, not passively attending to multiple images or flashes) is more likely to produce significant group differences. For example, multiple studies that have recorded pupil diameter during extended periods of *rest* while maintaining fixation to a centrally presented crosshair have provided evidence of increased pupil diameter in ASD (Anderson and Colombo, 2009; Anderson et al., 2013; Top et al., 2018), whereas studies examining *baseline* pupil diameter within the context of stimulus presentation have not (de Vries et al., 2021). According to the adaptive gain model (Aston-Jones and Cohen, 2005), atypically increased resting, tonic LC-NE activity in individuals with ASD may be associated with reductions in phasic responsiveness; this may lead to slower, more variable, attentional disengagement, as the onset of peripheral targets does not result in robust phasic activity when attending to the fixation. For example, failure to make a saccade (i.e., a no-shift trial) and/or slower SRTs in the overlap condition may result from a more general inability to detect and respond to behaviorally relevant events (i.e., the target), especially when targets are not preceded by a cue (i.e., the offset of the fixation). Thus, increased tonic activation and associated reductions in phasic LC responsiveness may contribute to the presence of disengagement impairments in ASD.

The objectives of the present study were to investigate tonic LC-NE activity in ASD (as indexed by resting pupil diameter), and to test the hypothesis that elevated tonic LC-NE activity is associated with impairments in attentional disengagement in children with ASD. To examine this association, a resting pupillometry experiment was conducted in conjunction with two gap-overlap paradigms: one auditory (Keehn et al., 2019) and one visual. Additionally, given that ASD may be associated with impaired zooming out of attention (Mann and Walker, 2003; Ronconi et al., 2013, 2018), we examined disengagement and shifting attention to targets occurring at both near and far distances from the central fixation. Our previous report (Keehn et al., 2019) showed that deficits in auditory attentional disengagement are present in children with ASD; however, in the present study, we expand our investigation to focus on a potential mechanism related to auditory and visual attentional disengagement impairments in ASD – atypical LC-NE activation. We hypothesized that children with ASD would evidence atypically increased resting pupil size (indicative of greater tonic LC-NE activation) and impaired auditory and visual attentional disengagement (which would be greater for targets occurring at larger distances from the central fixation), and that elevated LC-NE activation would be associated with poorer attentional disengagement in ASD in both sensory modalities.

MATERIALS AND METHODS

Participants

Twenty-one children with ASD and 20 age- and IQ-matched TD children participated in the study (see **Table 1**). The current manuscript includes the same participants from Keehn et al. (2019). Clinical diagnoses were confirmed using the Autism Diagnostic Observation Schedule, Second Edition (ADOS-2; Lord et al., 2012), Social Communication Questionnaire (SCQ; Rutter et al., 2003), and expert clinical judgment according to DSM-5 criteria. Children with ASD-related medical conditions (e.g., Fragile-X syndrome, tuberous sclerosis) were excluded. Participants in the TD group had no reported family history of ASD and were confirmed via parent report to be below clinical cutoffs on the Social Responsiveness Scale, Second Edition (Constantino and Gruber, 2012). Informed assent and consent were obtained from all participants and their caregivers in accordance with the Purdue University Institutional Review Board.

Resting Pupil Dilation

Apparatus

The experiment was presented using SR Research Experiment Builder 2.1 on a 17-inch LCD monitor. Participants were seated approximately 60 cm from the display. Eye movements and pupil diameter were recorded (500Hz; monocular) using an

EyeLink 1000 Plus remote eye-tracking system (SR Research, Ontario, Canada).

Procedure

Participants first completed a nine-point calibration and validation procedure. Next, participants completed a total of six minutes of eyes-open resting eye tracking (3, 2-minute blocks with breaks in between). A black central fixation was presented on a gray background, and participants were instructed to relax, look at the crosshair, and remain as still as possible. Background illumination of the room was fixed (450 lux).

Preprocessing and Analysis

A procedure similar to that described by Steiner and Barry (2011) was used to convert arbitrary units reported by Eyelink eye tracker to millimeters. Briefly, prior to data collection, an array of simulated pupils (2–10 mm) were placed at multiple distances (550–700 mm) from the eye tracker, using multiple thresholds. These measurements were entered into a multiple linear regression and coefficients from this analysis were used to predict absolute pupil size for the current data set.

Periods in which the eye tracker did not record pupil diameter were considered artifacts and excluded (e.g., blinks and saccades). Furthermore, instances in which the pupil size exceeded 1.5× interquartile range were considered outliers and were removed from the data. Lastly, data 200 ms before and after periods of missing or excluded data were removed. Missing and excluded data were corrected using linear interpolation.

In addition, the distance between the eye tracker and the forehead of the participant was used to monitor participant movement. Specifically, the root mean square of the first temporal derivative of the distance measurement was used a metric of overall head movement during resting pupil recording.

Visual Gap-Overlap Experiment

Apparatus and Stimuli

Eye-tracking equipment and participant setup were identical to the resting pupil paradigm. The central fixation was a crosshair ("+") and the target was an annulus. At a viewing distance of 60 cm, the crosshair and annulus were approximately 1° by 1° visual angle. White fixation and target were displayed on a black background. There were 16 target locations arranged on two invisible concentric circles (8 per circle); circles surrounded the fixation cross at eccentricities of 4.9° (near) and 9.8° (far; see **Figure 1B**). For each trial, a single target was randomly presented in one of these locations.

TABLE 1 | Participant characteristics.

		ASD	TD	Statistic	*p*
n (M:F)		21 (17:4)	20 (15:5)	χ = 0.2	0.65
Age (years)		11.5 (1.3); 9.2–14.5	11.2 (1.5); 9.3–15.0	*t* = 0.6	0.57
Verbal IQ		102 (19); 69–154	110 (11); 95–127	*t* = -1.5	0.14
Non-verbal IQ		101 (20); 52–132	111 (13); 87–134	*t* = -1.9	0.07
SRS-2 total score		75 (11); 57–90	44 (5); 37–55	*t* = 11.6	<0.001
ADOS-2	Social affect	11 (4); 5–17	–	–	–
	Repetitive behavior	2 (1); 0–5	–	–	–

IQ determined using the Wechsler Abbreviated Scale of Intelligence, Second Edition (WASI-II; Wechsler, 2011). Mean (SD); range.

Procedure

Participants first completed a nine-point calibration and validation procedure. As illustrated in **Figure 1A**, each trial began with the central crosshair presented alone for a random duration between 1000 and 1500 ms. Next, the peripheral target appeared either: (1) with the central fixation remaining onscreen (overlap condition), (2) 200 ms after the central fixation disappeared (gap condition), or (3) with the simultaneous offset of the central fixation (baseline condition). The target (and the central crosshair for overlap trials) remained onscreen for 2000 ms or until a target fixation had been made (minimum 200 ms). Then a 1000 ms inter-trial interval occurred during which only a blank black screen was presented. Prior to beginning the experiment, participants were instructed to look at the center fixation at the start of each trial, and then to move only their eyes to the target once it appeared. Participants completed a series of twelve practice trials prior to beginning the experiment.

Design

The experiment consisted of 144 trials, divided into three blocks of 48 trials. Within each block, condition (gap, baseline, and overlap), distance (near, far), and location (16 possible) were varied in pseudorandom order. All trial types were presented an equal number of times within each block and across the experiment.

Preprocessing and Analysis

To be considered a valid trial for subsequent analysis the following criteria had to be met: (1) at the onset of the target, participant's gaze must be on the central fixation location, and (2) the endpoint of the initial saccade after target onset was located within approximately 2° of the target (anticipatory saccades [<100 ms] were removed; see **Figure 1C**). Saccadic reaction time (SRT) was defined as duration between the presentation of the peripheral target and the onset of the initial saccadic eye movement. No-shift trials required that no saccade was made within 2000 ms after target onset, and that fixation was maintained on the central crosshair. Percentage of no-shift trials was calculated as the number of no-shifts trials divided by the total number of usable trials. Finally, to simultaneously account for saccadic latency and no-shift percentage, disengagement efficiency was calculated [SRT/(1 – no-shift%)].

Auditory Gap-Overlap Experiment

As noted above, methods and results from this experiment have previously been reported in Keehn et al. (2019). Thus, only an abbreviated description is reported below.

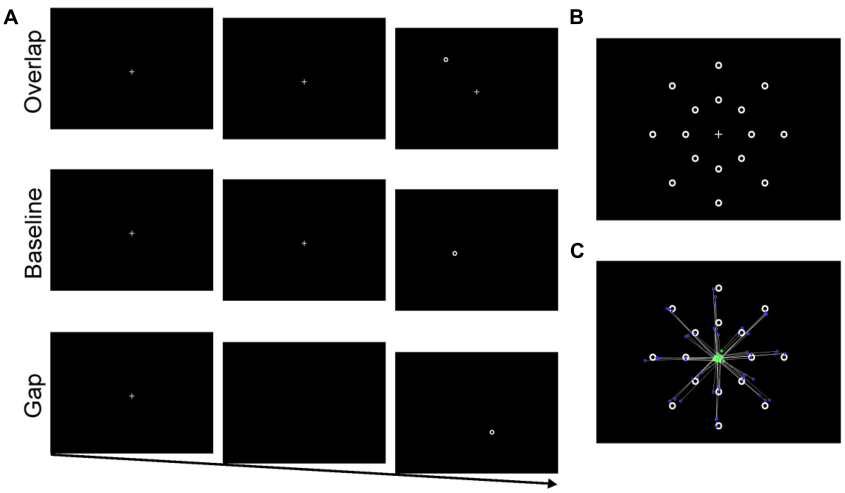

FIGURE 1 | (A) Stimulus sequence for overlap, baseline, and gap conditions. **(B)** Stimulus array with 16 possible target locations (only one target was present for each trial). **(C)** An example of saccades from one participant (one block) included in the latency analysis. Green dots represent individual saccade start location and blue dots represent saccadic endpoint.

Apparatus and Stimuli

Participants were tested in a sound attenuated, darkened room, and seated comfortably approximately 1.5 m directly in front of five speakers (Hafler M5 Reference) positioned on stands at approximately eye-level. Speakers were positioned in a semi-circular array at 0° (i.e., directly in front of) and at 15° and 30° to the left and right of participant. Auditory fixation at the central location was a 500 Hz pure tone, and peripheral targets emitted from side speakers were white noise (similar to Shafiq et al., 1998). All stimuli were played at a comfortable listening level (approximately 60 dBA).

Saccadic eye movements were recorded using electrooculography (EOG) via a Biopac EOG100C amplifier at a sampling rate of 500 Hz. Two 4mm reusable Ag/AgCL shielded electrodes (Biopac EL254S) filled with conductive gel (5% NaCl, 0.85 molar NaCl) were applied at the lateral canthi of the left and right eye. Hardware gain was set to 5000 (corresponding to an input gain of ±2 mV), and filter bandwidth was set to 0.05–35Hz prior to digitization. Data were acquired using AcqKnowledge 4.3 software (Biopac Systems, Inc).

Procedure

First, an EOG calibration procedure was completed. Participants were instructed to keep their head still and to move their eyes to each speaker, which were visible during calibration, when a sound was presented. No visual stimulus (e.g., a light) was presented in association with the sound. Prior to the start of the gap-overlap task, a black curtain was drawn in front of the speaker array approximately 1.2m from the participant, thus visually occluding speakers. Therefore, rather than fixate on a specific object (e.g., central crosshair in the visual gap-overlap task), participants fixated on a specific location (i.e., the source of the sound). Each trial began with a tone presented alone from the center speaker for a random duration between 1300 and 1500 ms. Next, a peripheral noise was played from one of the side speakers for 1200 ms either: (1) with the tone continuing to play for the duration of the peripheral noise from the center speaker (overlap condition), (2) 200 ms after the central tone stopped (gap condition), or (3) with the simultaneous offset of the central tone (baseline condition). Finally, there was a 2000 ms inter-stimulus interval during which time no sound was presented. Prior to beginning the experiment, participants were told they were going to play the "find the noise" game. They were instructed to look at the center location when the tone was playing, then to move only their eyes to location of the sound once the peripheral noise played, and then to look back toward the central location to wait for the tone. Finally, participants completed a series of six practice trials.

Design

The experiment consisted of 108 trials, divided into three blocks of 36 trials. Within each block, condition (gap, baseline, and overlap), distance (near and far), and side (left and right) were varied in pseudorandom order. All trial types were presented an equal number of times within each block and across the experiment.

Preprocessing and Analysis

Horizontal saccadic eye movements to the target locations were detected as abrupt changes in the EOG with a peak velocity greater than 50°/s for a duration of at least 20 ms for the duration of the peripheral noise (1200 ms). In addition, data from each trial were visually inspected by trained research assistants blind to group membership. To be included, initial saccadic eye movements were required to follow a steady fixation at the central location for at least 200 ms prior to target presentation. Trials in which there was no stable fixation at the central location (due to movements or noise) or trials in which the initial saccade was directed toward the incorrect side (e.g., saccade to left with

target on right) were excluded. Saccadic reaction time (SRT) was defined as duration between the presentation of the peripheral noise and the onset of the first saccadic eye movement directed toward the side of the noise. Trials with SRTs less than 80 ms were considered anticipatory and excluded. Trials on which no saccade occurred but where fixation was maintained at the central location were coded as no-shift trials. Percentage of no-shift trials was calculated as the number of no-shifts trials divided by the total number of usable trials. Finally, to simultaneously account for saccadic latency and no-shift percentage, disengagement efficiency (DE) was calculated [SRT/(1 – no-shift%)].

RESULTS

As shown in **Table 1**, groups did not differ significantly on age, sex, or non-verbal IQ. Compared to the TD group, the ASD group did have significantly lower verbal IQ.

Resting Pupil Dilation

Independent-samples *t*-tests were used to compare pupil diameter, head motion, and percentage of excluded data across groups. As illustrated in **Figure 2**, children with ASD (M = 4.18; SD = 0.71) showed significantly larger pupil diameter compared to their TD peers (M = 3.71; SD = 0.48), $t(39) = 2.503$, $p = 0.017$. Groups did not differ in head movement (ASD: M = 0.11; SD = 0.10; TD: M = 0.08; SD = 0.03), $t(39) = 1.11$, $p = 0.275$, but the ASD group had significantly more data excluded (ASD: M = 26.3%; SD = 9.9; TD: M = 10.1%; SD = 7.5), $t(39) = 5.893$, $p < 0.001$. However, percentage of data excluded was not associated with pupil diameter for either the ASD, $r(20) = 0.084$, $p = 0.717$, or the TD, $r(19) = 0.362$, $p = 0.117$, group. Additionally, to confirm that variability in age and IQ did not contribute to differences in pupil diameter across groups, separate ANCOVAs were conducted that included age and IQ as covariates. Children with ASD exhibited significantly larger resting pupil diameter when both age, $F(1,38) = 7.58$, $p = 0.009$, and non-verbal IQ, $F(1,38) = 5.43$, $p = 0.025$, were entered as covariates.

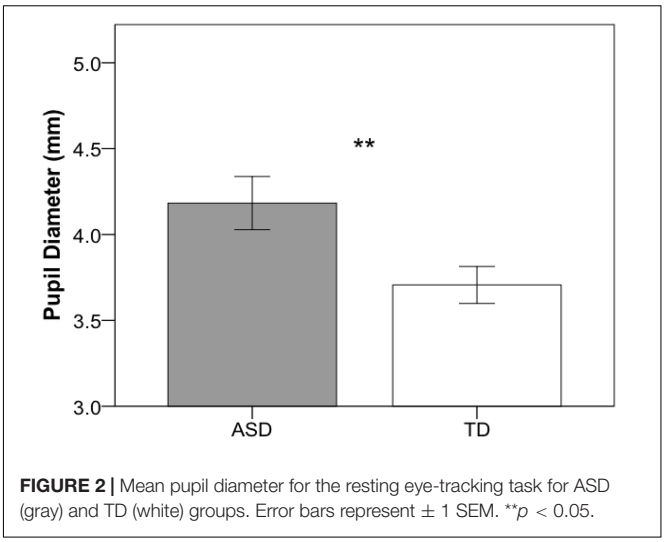

FIGURE 2 | Mean pupil diameter for the resting eye-tracking task for ASD (gray) and TD (white) groups. Error bars represent ± 1 SEM. $^{**}p < 0.05$.

Visual Gap-Overlap

Number of usable trials, saccadic reaction time (SRT), percentage of no-shift trials, and disengagement efficiency were analyzed using mixed-model repeated-measures ANOVA with between-subject factor group (ASD and TD) and within-subjects factors condition (gap, baseline, and overlap) and distance (near and far). In addition, the gap effect was calculated by subtracting SRT (or DE) for gap from overlap (overlap-gap) conditions and the step effect was calculated by subtracting SRT (or DE) for baseline from overlap (overlap-baseline) conditions for near, far, and combined target distances, and were analyzed using a repeated-measures ANOVA with between-subjects factor group (ASD and TD) and within-subjects factor distance (near and far).

Children with ASD (M = 90; SD = 23) did provide fewer usable trials compared to TD children (M = 114; SD = 17), $F(1,39) = 13.660$, $p = 0.001$, $\eta_p^2 = 0.26$; however, there were no significant interactions between group and any factor for usable trials (all p-values > 0.4). For SRT, as expected, there were was a significant main effect of condition, $F(2,78) = 22.295$, $p < 0.001$, $\eta_p^2 = 0.36$ (gap < baseline < overlap; $p < 0.001$; gap: M = 158 ms; SD = 29; baseline: M = 175 ms; SD = 29; overlap: M = 213 ms; SD = 77). There was no main effect of group, $F(1,39) = 1.111$, $p = 0.298$, $\eta_p^2 = 0.03$, nor was there a significant interaction between group and any other factor (all p-values > 0.108). For the gap effect, children with ASD (M = 72 ms; SD = 86) showed a marginally significant increase compared to their TD peers (M = 36 ms; SD = 39), $F(1,39) = 2.846$, $p = 0.0996$; however, there was no significant interaction between group and distance, $F(1,39) = 0.044$, $p = 0.834$, $\eta_p^2 = 0.00$ (see **Figure 3**). For the step effect, there was a significant main effect of group (ASD: M = 25 ms; SD = 21; TD: M = 9 ms; SD = 24), $F(1,39) = 5.381$, $p = 0.26$, $\eta_p^2 = 0.12$, as the ASD group had a larger step effect compared to the TD group. There was no significant interaction between group and distance, $F(1,39) = 0.099$, $p = 0.754$, $\eta_p^2 = 0.00$.

No-shift percentage was non-normally distributed; thus, data were square-root transformed. For the percentage of no-shift trials, there was a significant main effect of condition, $F(2,78) = 5.289$, $p = 0.007$, $\eta_p^2 = 0.12$, as no-shift trials were most common in the overlap condition (gap < baseline < overlap; all p-values < 0.05). There was no main effect of group, $F(1,39) = 0.837$, $p = 0.366$, $\eta_p^2 = 0.02$, and no significant interaction between group and any factor (all p-values > 0.321).

Results for disengagement efficiency were similar; there was a main effect of condition, $F(2,78) = 10.308$, $p < 0.001$, $\eta_p^2 = 0.21$ (gap = baseline < overlap; $p < 0.01$), but no main effect of group, $F(1,39) = 2.161$, $p = 0.150$, $\eta_p^2 = 0.05$, or any significant interaction between group and any other factor (all p-values > 0.277). Finally, there were no significant main effects for disengagement efficiency gap or step effects (all p-values > 0.2).

Auditory Gap-Overlap

Results have previously been reported in Keehn et al. (2019). Briefly, main findings involving group included: no main effect

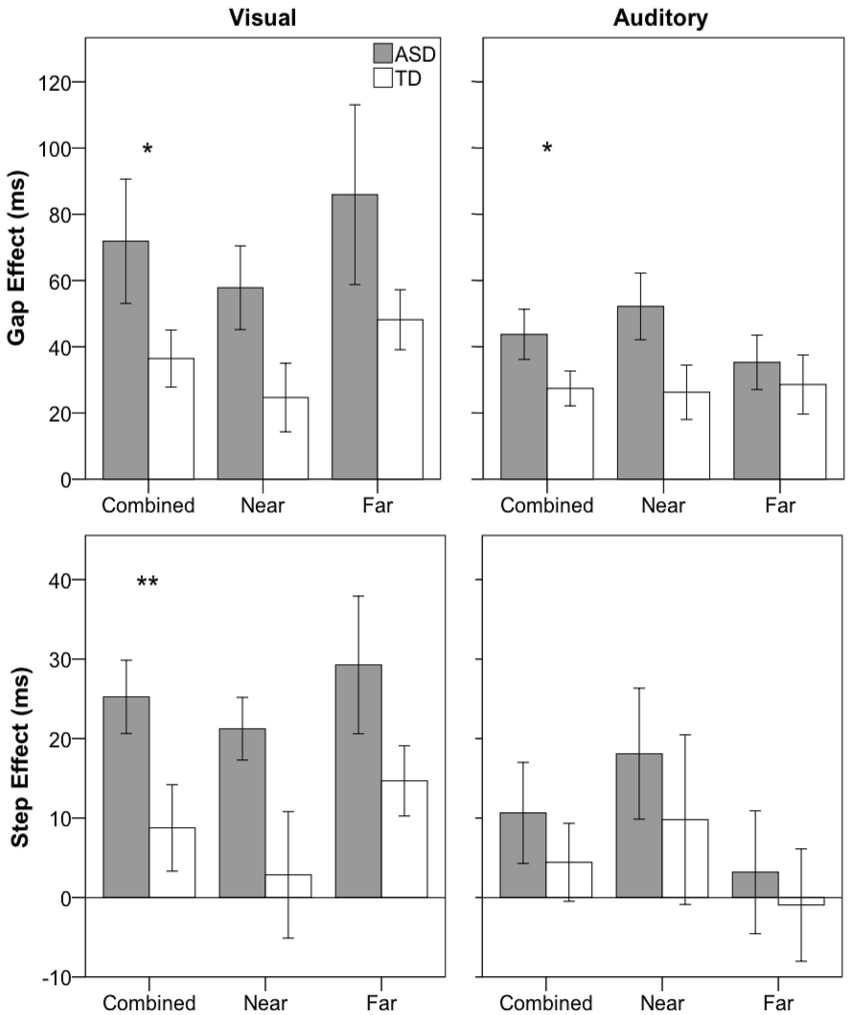

FIGURE 3 | Saccadic reaction time gap (overlap-gap; top row) and step (overlap-baseline; bottom row) effects for visual **(left column)** and auditory **(right column)** for ASD (gray) and TD (white) groups. Error bars represent ± 1 SEM. $^{**}p < 0.05$, $^{*}p < 0.1$.

TABLE 2 | Visual gap-overlap correlations with pupil diameter.

		Gap effect			Step effect			% No-shift			
		All	**Near**	**Far**	**All**	**Near**	**Far**	**All**	**Gap**	**Baseline**	**Overlap**
All	SRT	0.130	0.058	0.256	−0.012	−0.062	0.102	0.330*	0.206	0.143	0.376*
	DE	0.232	0.164	0.212	0.264	0.211	0.338*				
ASD	SRT	0.198	0.116	0.264	−0.077	−0.284	0.089	0.419	0.237	0.277	0.464*
	DE	0.289	0.216	0.219	0.324	0.281	0.353				
TD	SRT	−0.374	−0.415	−0.066	−0.263	−0.195	−0.202	0.044	−0.136	0.001	0.111
	DE	−0.320	−0.454*	−0.001	−0.190	−0.429	0.102				

$^{*}p < 0.05$, $^{**}p < 0.01$; SRT, Saccadic reaction time; DE, disengagement efficiency.

of group, $F(1,39) < 1$, nor were there any significant interactions between group and other experimental factors for number of usable trials (all p-values > 0.2), no significant main effect of group for SRT, $F(1,39) < 1$, and no significant interactions between group and any other factor (all p-values > 0.17). Similar to the visual paradigm, there was a marginally significant main effect of group for the gap effect (ASD: $M = 44$ ms; $SD = 35$; TD: $M = 27$; $SD = 23$), $F(1,39) = 3.078$, $p = 0.087$, $\eta_p^2 = 0.03$, but no significant interaction between group and distance, $F(1,39) = 1.278$, $p = 0.265$, $\eta_p^2 = 0.03$. Additionally, there was no significant main effect of group, or group by distance interaction for the step effect (all p-values > 0.4).

No-shift percentage was non-normally distributed; thus, data were square-root transformed. For percentage of no-shift trials, there was a significant interaction between group and condition, $F(2,78) = 4.781$, $p = 0.011$, $\eta_p^2 = 0.11$, and follow-up independent-samples *t*-tests showed that the ASD group had a significantly higher no-shift percentage for the overlap, $t(39) = 2.336$, $p = 0.025$, but not the gap, $t(39) = 0.866$, $p = 0.392$, or baseline condition, $t(39) = -0.178$, $p = 0.860$, compared to the TD group.

Significantly increased no-shift percentage and slower SRTs in the ASD group resulted in significantly decreased disengagement efficiency in the ASD group. Specifically, the group by condition interaction was significant, $F(2,78) = 3.942$, $p = 0.023$, $\eta_p^2 = 0.09$. For disengagement efficiency gap effect, there was a significant main effect of group, $F(1,39) = 5.693$, $p = 0.022$, $\eta_p^2 = 0.12$, with larger gap effects in the ASD ($M = 53$ ms; $SD = 45$) as compared to the TD ($M = 27$ ms; $SD = 20$) group; however, there was no significant interaction between group and distance, $F(1,39) = 1.041$, $p = 0.314$, $\eta_p^2 = 0.03$. For disengagement efficiency step effect, children with ASD showed marginally increased scores compared to TD children, $F(1,39) = 3.916$, $p = 0.055$, $\eta_p^2 = 0.091$, but no significant interaction between group and distance, $F(1,39) = 0.795$, $p = 0.378$, $\eta_p^2 = 0.02$.

Associations Between Pupil Dilation and Disengagement Measures

Pearson's correlations were used to investigate the association between resting pupil diameter and disengagement metrics (i.e., gap/step effects and percentage no-shift trials). For the visual gap-overlap experiment, across all participants there was a significant association between pupil diameter and overall percentage no-shift trials (see **Table 2**), which was due primarily to the association between pupil size and no-shift percentage for overlap, but not gap or baseline conditions. This pattern was present in the ASD group, but not the TD group (see **Figure 4A**). No other correlations were significant for the ASD group for the visual gap-overlap experiment.

For the auditory gap-overlap paradigm, there were significant correlations for all participants between pupil size and combined and near SRT and disengagement efficiency gap effects (see **Table 3**). Again, this pattern was present in the ASD but not the TD group. For the ASD group there were significant correlations between combined, near, and far SRT gap effects and combined and far disengagement efficiency gap effects (see **Figure 4B**).

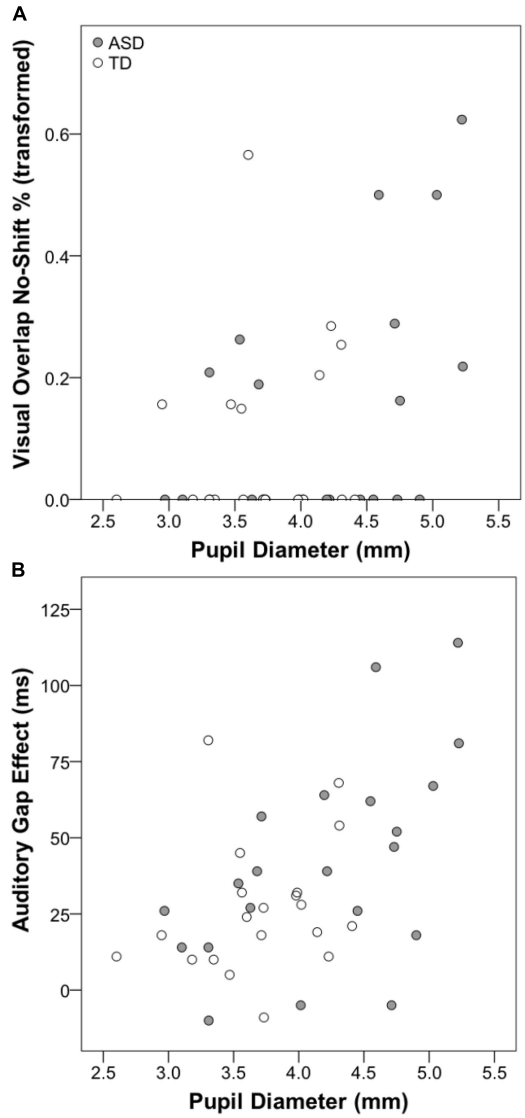

FIGURE 4 | Scatterplots displaying associations between resting pupil diameter and visual gap-overlap task no-shift percentage **(A)** and auditory gap-overlap task gap effect score **(B)**.

DISCUSSION

The goals of the current study were to investigate whether tonic activation of the LC-NE system (as indexed by resting pupil diameter) is atypical in ASD, and to determine whether differences in attentional disengagement are associated with atypical tonic activity of the LC-NE system in children with ASD. In accord with previous reports, children with ASD exhibited significantly larger resting pupil diameter compared to their TD peers, which is indicative of increased tonic LC-NE activity. Furthermore, similar to prior findings, children with ASD showed subtle impairments in attentional disengagement in both visual and auditory gap-overlap tasks. Importantly, measures of disengagement were associated with our index of tonic LC-NE activity. Together, these results suggest that atypically increased tonic LC-NE activation may contribute to disengagement deficits in children with ASD.

First, our finding of significantly larger resting pupil diameter in ASD is in agreement with and extends earlier findings suggesting elevated tonic LC-NE activity in ASD (Anderson and Colombo, 2009; Anderson et al., 2013; Blaser et al., 2014; Top et al., 2018). Previous studies have shown larger pupil sizes in toddlers and young children (Anderson and Colombo, 2009; Anderson et al., 2013; Blaser et al., 2014) as well as adults with ASD (Top et al., 2018). The results of the present study extend these findings to older school-aged children and

TABLE 3 | Auditory gap-overlap correlations with pupil diameter.

		Gap effect			Step effect			% No-shift			
		All	**Near**	**Far**	**All**	**Near**	**Far**	**All**	**Gap**	**Baseline**	**Overlap**
All	SRT	0.509**	0.373*	0.265	0.086	−0.087	0.509**	0.051	0.143	−0.179	0.126
	DE	0.533**	0.393*	0.304	0.309*	0.102	0.405**				
ASD	SRT	0.558**	0.479*	0.444*	0.196	0.083	0.243	0.120	0.233	−0.087	0.201
	DE	0.554**	0.387	0.484*	0.382	0.209	0.374				
TD	SRT	0.232	−0.061	−0.013	−0.116	−0.414	0.490*	−0.317	−0.137	−0.332	−0.619**
	DE	0.190	0.079	−0.222	−0.089	−0.394	0.408				

*$p < 0.05$, **$p < 0.01$; SRT, Saccadic reaction time; DE, disengagement efficiency.*

younger adolescents and suggest that atypically increased tonic LC activation may be present across the lifespan in individuals with ASD. Additionally, these findings are consistent with preliminary neuropharmacological research, which suggests that β-adrenergic antagonists (e.g., Propranolol), which block the action of norepinephrine, may improve functioning in a variety of behavioral domains in individuals with ASD (Beversdorf, 2020).

In addition to previously reported impairments in attentional disengagement for the auditory gap-overlap task (Keehn et al., 2019), results from the visual gap-overlap paradigm also suggest subtle deficits in visual attentional disengagement. Specifically, the gap effect was marginally increased and step effect scores were significantly larger in the ASD group. In both cases, these were due to disproportionally longer SRTs to overlap trials. However, contrary to our hypothesis, these group differences in disengagement did not vary based on the location (near or far) of the peripheral target. Prior findings of impaired disengagement from gap-overlap paradigms are mixed in ASD; however, our results add to the growing body of evidence that suggests that children with ASD exhibit impairments in disengaging attention.

The primary objective of the present report was to examine the associations between measures of tonic LC-NE activation and attentional disengagement. For both the visual and auditory gap-overlap tasks, the percentage of no-shift trials was significantly greater for overlap compared to other conditions, consistent with the premise that disengaging attention is more difficult when the central stimulus is present. For the visual task, we found that greater tonic activation of the LC-NE system was associated with increased overlap no-shift percentage for all participants; group-level analyses showed that this association was present for the ASD group, but not the TD group. For the auditory task, we found that greater tonic LC-NE activity was associated with both increased SRT and disengagement efficiency gap effect scores. Similarly, group-level analyses showed that this association was specific to the ASD group. ASD-specific correlations may be due to increased variability within the ASD group, which is likely associated with elevated resting pupil size and disengagement impairments in some, but not all, children with ASD. Furthermore, although the associations with specific disengagement indices varied across task, the direction of these relationships was consistent. For children with ASD, greater tonic LC-NE activation was associated with increased difficulty disengaging attention.

As highlighted previously (Forman et al., 1993), condition-specific changes in latency in gap-overlap paradigms are determined by more than one pathway. Much of the neurophysiological research investigating the gap effect has focused on the presence of faster SRTs and frequency of express saccades for the gap condition. However, in the current study and for the majority of previous findings, individuals with ASD show statistically equivalent and numerically faster SRT for gap trials. These findings suggest that the mechanism underlying group differences in disengagement may be unrelated to pathways responsible for gap-related changes in eye-movement dynamics.

Rather, findings from the present study suggest that atypically elevated tonic activation of the LC-NE system may contribute to poorer gap-overlap performance in children with ASD; although speculative, several interrelated theories of LC-NE function may explain this relationship. First, the adaptive gain model (Aston-Jones and Cohen, 2005) proposes that the LC operates in two modes: phasic and tonic. The phasic mode is associated with moderate levels of tonic activation, and reliable phasic responsivity to task-related stimuli, whereas the tonic mode is related to elevated levels of tonic activation with reduced phasic responsivity. Larger pupil dilation results from the resting eye-tracking task suggest that individuals with ASD may operate in the tonic LC-NE mode. Thus, one potential explanation for the association between atypically increased tonic LC-NE activation and disengagement impairments (increased overlap no-shift percentage and larger gap effects) is that, in the absence of a cue (fixation offset in gap trials), peripheral targets do not elicit significant phasic LC activation. Decreased or absent phasic LC activation to the onset of peripheral targets, due to elevated tonic LC activity, would likely result in increased saccade latency and/or more frequent no-shift trials. These findings are consistent with a recent report by Bast et al. (2021a), who showed altered LC-NE activity and slower reaction time in children and adolescents with ASD. These authors suggest that LC-NE tonic upregulation may decrease sensory selectivity contributing to increased reaction time latency in ASD.

The LC-NE system also plays a critical role in managing environmental uncertainty, acting as an interrupt signal in response to unexpected events (Yu and Dayan, 2005; Dayan and Yu, 2006). Similar to previous studies that have shown disengagement impairments in ASD, both visual and auditory gap-overlap tasks included variable duration for the fixation

stimulus and randomized presentation of trial types (i.e., gap, baseline, and overlap presented within the same block). Prior research on neurotypical adults has shown larger switch costs associated with mixed (i.e., gap and overlap presented within the same block) compared to pure (i.e., just gap or overlap presented in each block) for SRT (Vernet et al., 2009). Moreover, the number of target locations used in the study tasks (16 for visual; 4 for auditory) is greater than most prior studies (typically two). As discussed previously (Keehn et al., 2019), these factors increase the unpredictable nature of the current paradigms and may contribute to disengagement differences, specifically slower SRTs and increased no-shift percentage for overlap trials, observed in the ASD group. According to Dayan and Yu (2006), changes in an individual's task state in response to unexpected events are triggered by phasic NE responses, which act as an interrupt signals. Thus, similar to the adaptive gain model, elevated tonic LC-NE activity may disrupt phasic LC responsivity to unpredictable events (i.e., overlap trials; 33% of trials), resulting in disengagement differences in ASD.

Relatedly, in the current and previous gap-overlap tasks, participants were instructed to fixate the central stimulus and then to make an eye movement to the target once it appears; they were not explicitly told that fixation offsets cue impending targets. Nevertheless, participants learn the cue-target association and as a result SRTs to cued targets (i.e., gap and/or baseline conditions) are accelerated. However, overlap trials violate this antecedent-response expectation as overlap targets appear without fixation offset. Previous research in non-human primates has shown that atomoxetine, an NE-reuptake inhibitor that boosts the levels of NE, is associated with improved orienting in *predictive contexts*, but slower responses in non-cued conditions (Reynaud et al., 2019). These results suggest that NE may affect behavioral response patterns in a context-specific manner, speeding orienting to predictive cues (such as fixation offset in gap/baseline trials) and slowing reaction time to non-cued targets (such as in overlap trials). Furthermore, research by Gonzalez-Gadea et al. (2015) has shown reduced P3 amplitude, an indirect index of phasic LC-NE activation (Nieuwenhuis et al., 2005), to unexpected events in children with ASD. Additionally, findings from Goris et al. (2018) demonstrated that context-dependent modulations of the mis-match negativity (MMN) were also reduced in adults with ASD compared to the TD peers. Together, these results suggest that atypical responsivity to overlap trials in people with ASD may result from impairments in the ability to adjust precision when faced with uncertainty. In the context of the current study, strict application of a fixation offset – target onset expectancy may result in behavioral costs for conditions that violate that prediction, and this predictive processing may rely, in part, on LC-NE activation. More recently research by Bast et al. (2021b) showed differences in oculomotor function in individuals with ASD, specifically decreased saccade duration and amplitude, which may be associated with reduced visual exploration. These authors hypothesized that the underlying mechanism associated with atypically clustered fixations may be altered pontocerebellar circuitry. Although the present study focused on attentional disengagement and not basic saccade dynamics, the LC does project to (oculo)motor neurons of the brainstem and cerebellum (Samuels and Szabadi, 2008), and may also contribute to atypical oculomotor/attentional function in individuals with ASD.

Locus coeruleus – norepinephrine disruption is not unique to ASD and has also been shown to be present in conditions such as ADHD (Del Campo et al., 2011) and anxiety (Morris et al., 2020), which are both frequently comorbid with ASD (Lai et al., 2019). Related to the present study, anxiety has been associated with impairments in attentional disengagement (e.g., from threat-related stimuli; Richards et al., 2014). Future research should use a transdiagnostic approach to examine the LC-NE system and attentional dysfunction in children with ASD, ADHD, anxiety, and other conditions, which may share overlapping genotypic and phenotypic features.

Finally, there are several limitations to the present study. Although groups were age-, IQ-, and sex-matched, they did differ on the percentage of usable data on resting pupil and visual disengagement paradigms. However, for resting pupil task, the amount of usable data was not associated with pupil diameter across all participants or within each group, suggesting that increased missing data in the ASD may not have contributed to larger pupil size in ASD. Additionally, our resting state pupil diameter analyses did not control for differences in gaze deviations from central fixation, and thus we cannot rule out whether systematic differences in fixation patterns across group contributed to the presence of pupil diameter differences. Lastly, although increased in the overlap relative to the gap and baseline conditions, no-shift trials were rare and did not occur frequently in participants. As such, correlations between tonic pupil size and no-shift percentage may have resulted from a small subgroup of participants with increased no-shift percentages.

CONCLUSION

Difficulties in disengaging and shifting attention are present early and persist across the lifespan in individuals with ASD. These early fundamental differences in attention are associated with subsequent ASD diagnosis and may contribute to the emergence of the ASD phenotype. However, thus far, the neural mechanism(s) underlying impaired attentional disengagement in ASD remain unclear. Results from the present study confirm prior reports of larger resting pupil size in individuals with ASD, indicative of atypically increased tonic LC-NE activation. Furthermore, consistent with our hypothesis, we also found that individuals with ASD showed slower attentional disengagement, and differences in attentional disengagement in individuals with ASD were associated with elevated levels of tonic LC-NE activity. Together, these results suggest that atypical tonic activation of the LC-NE system is present in ASD and may contribute to difficulties in disengaging and orienting attention. Future research aimed at understanding the role of the LC-NE system in context-specific patterns of responsivity in ASD

will further inform our understanding the neural bases of these attentional differences, and have the potential to contribute to the development of novel biobehavioral markers and behavioral and pharmacological intervention targets.

DATA AVAILABILITY STATEMENT

The raw data supporting the conclusions of this article will be made available by the authors, without undue reservation.

ETHICS STATEMENT

The studies involving human participants were reviewed and approved by Purdue University Institutional Review Board. Written informed assent and consent to participate in this study were provided by all participants and participants' legal guardian/next of kin.

AUTHOR CONTRIBUTIONS

BK conceived of and designed the study, performed the statistical analyses, and drafted the manuscript. AF participated in the design of the study. BK, GK, SB, and RM acquired the data. GK, RM, and AF helped to revise the manuscript. All authors read and approved the final version of the manuscript.

FUNDING

This research was supported in part by NIH R21-MH114095 (BK).

ACKNOWLEDGMENTS

Special thanks to the children and families who generously participated.

REFERENCES

Anderson, C. J., and Colombo, J. (2009). Larger tonic pupil size in young children with autism spectrum disorder. *Dev. Psychobiol.* 51, 207–211. doi: 10.1002/dev.20352

Anderson, C. J., Colombo, J., and Unruh, K. E. (2013). Pupil and salivary indicators of autonomic dysfunction in autism spectrum disorder. *Dev. Psychobiol.* 55, 465–482. doi: 10.1002/dev.21051

Arora, I., Bellato, A., Ropar, D., Hollis, C., and Groom, M. J. (2021). Is autonomic function during resting-state atypical in Autism: A systematic review of evidence. *Neurosci. Biobehav. Rev.* 125, 417–441. doi: 10.1016/j.neubiorev.2021.02.041

Aston-Jones, G., and Cohen, J. D. (2005). An integrative theory of locus coeruleus-norepinephrine function: Adaptive gain and optimal performance. *Annu. Rev. Neurosci.* 28, 403–450. doi: 10.1146/annurev.neuro.28.061604.135709

Bast, N., Boxhoorn, S., Super, H., Helfer, B., Polzer, L., Klein, C., et al. (2021a). Atypical Arousal Regulation in Children With Autism but Not With Attention-Deficit/Hyperactivity Disorder as Indicated by Pupillometric Measures of Locus Coeruleus Activity. *Biol. Psychiatry Cogn. Neurosci. Neuroimaging* 2021:10.

Bast, N., Mason, L., Freitag, C. M., Smith, T., Portugal, A. M., Poustka, L., et al. (2021b). Saccade dysmetria indicates attenuated visual exploration in autism spectrum disorder. *J. Child Psychol. Psychiatry* 62, 149–159. doi: 10.1111/jcpp.13267

Bast, N., Poustka, L., and Freitag, C. M. (2018). The locus coeruleus-norepinephrine system as pacemaker of attention - a developmental mechanism of derailed attentional function in autism spectrum disorder. *Eur. J. Neurosci.* 47, 115–125. doi: 10.1111/ejn.13795

Berridge, C. W., and Waterhouse, B. D. (2003). The locus coeruleus-noradrenergic system: modulation of behavioral state and state-dependent cognitive processes. *Brain Res. Brain Res. Rev.* 42, 33–84. doi: 10.1016/s0165-0173(03)00143-7

Beversdorf, D. Q. (2020). The Role of the Noradrenergic System in Autism Spectrum Disorders, Implications for Treatment. *Semin Pediatr. Neurol.* 35:100834. doi: 10.1016/j.spen.2020.100834

Blaser, E., Eglington, L., Carter, A. S., and Kaldy, Z. (2014). Pupillometry reveals a mechanism for the Autism Spectrum Disorder (ASD) advantage in visual tasks. *Sci. Rep.* 4:4301.

Constantino, J. M., and Gruber, C. P. (2012). *Social Responsiveness Scale - Second Edition (SRS-2)*. Torrance, CA: Western Psychological Services.

Corbetta, M., Patel, G., and Shulman, G. L. (2008). The reorienting system of the human brain: From environment to theory of mind. *Neuron* 58, 306–324. doi: 10.1016/j.neuron.2008.04.017

Csibra, G., Johnson, M. H., and Tucker, L. A. (1997). Attention and oculomotor control: a high-density ERP study of the gap effect. *Neuropsychologia* 35, 855–865. doi: 10.1016/s0028-3932(97)00016-x

Dayan, P., and Yu, A. J. (2006). Phasic norepinephrine: a neural interrupt signal for unexpected events. *Network* 17, 335–350. doi: 10.1080/09548980601004024

de Vries, L., Fouquaet, I., Boets, B., Naulaers, G., and Steyaert, J. (2021). Autism spectrum disorder and pupillometry: A systematic review and meta-analysis. *Neurosci. Biobehav. Rev.* 120, 479–508. doi: 10.1016/j.neubiorev.2020.09.032

Del Campo, N., Chamberlain, S. R., Sahakian, B. J., and Robbins, T. W. (2011). The roles of dopamine and noradrenaline in the pathophysiology and treatment of attention-deficit/hyperactivity disorder. *Biol. Psychiatry* 69, e145–e157.

Dias, E. C., and Bruce, C. J. (1994). Physiological correlate of fixation disengagement in the primate's frontal eye field. *J. Neurophysiol.* 72, 2532–2537. doi: 10.1152/jn.1994.72.5.2532

Dorris, M. C., and Munoz, D. P. (1995). A neural correlate for the gap effect on saccadic reaction times in monkey. *J. Neurophysiol.* 73, 2558–2562. doi: 10.1152/jn.1995.73.6.2558

Dorris, M. C., Pare, M., and Munoz, D. P. (1997). Neuronal activity in monkey superior colliculus related to the initiation of saccadic eye movements. *J. Neurosci.* 17, 8566–8579. doi: 10.1523/jneurosci.17-21-08566.1997

Elison, J. T., Paterson, S. J., Wolff, J. J., Reznick, J. S., Sasson, N. J., Gu, H., et al. (2013). White matter microstructure and atypical visual orienting in 7-month-olds at risk for autism. *Am. J. Psychiatry* 170, 899–908. doi: 10.1176/appi.ajp.2012.12091150

Elsabbagh, M., Fernandes, J., Jane Webb, S., Dawson, G., Charman, T., and Johnson, M. H. (2013). Disengagement of Visual Attention in Infancy Is Associated with Emerging Autism in Toddlerhood. *Biolog. Psychiatry* 74, 189–194. doi: 10.1016/j.biopsych.2012.11.030

Fischer, B., and Weber, H. (1993). Express Saccades and Visual-Attention. *Behav. Brain Sci.* 16, 553–567. doi: 10.1017/s0140525x00031575

Foote, S. L., Freedman, R., and Oliver, A. P. (1975). Effects of putative neurotransmitters on neuronal activity in monkey auditory cortex. *Brain Res.* 86, 229–242. doi: 10.1016/0006-8993(75)90699-x

Forman, S. D., Cohen, J. D., and Johnson, M. H. (1993). Frontal Eye Fields - Inhibition through Competition. *Behav. Brain Sci.* 16, 578–578. doi: 10.1017/s0140525x00031708

Gaymard, B., Rivaud, S., Cassarini, J. F., Dubard, T., Rancurel, G., Agid, Y., et al. (1998). Effects of anterior cingulate cortex lesions on ocular saccades in humans. *Exp. Brain Res.* 120, 173–183. doi: 10.1007/s002210050391

Gomez, C., Atienza, M., Gomez, G. J., and Vazquez, M. (1996). Response latencies and event-related potentials during the gap paradigm using saccadic responses in human subjects. *Int. J. Psychophysiol.* 23, 91–99. doi: 10.1016/0167-8760(96)00034-7

Gonzalez-Gadea, M. L., Chennu, S., Bekinschtein, T. A., Rattazzi, A., Beraudi, A., Tripicchio, P., et al. (2015). Predictive coding in autism spectrum disorder and attention deficit hyperactivity disorder. *J. Neurophysiol.* 114, 2625–2636.

Goris, J., Braem, S., Nijhof, A. D., Rigoni, D., Deschrijver, E., Van de Cruys, S., et al. (2018). Sensory Prediction Errors Are Less Modulated by Global Context in Autism Spectrum Disorder. *Biol. Psychiatry Cogn. Neurosci. Neuroimaging* 3, 667–674. doi: 10.1016/j.bpsc.2018.02.003

Joshi, S., and Gold, J. I. (2020). Pupil Size as a Window on Neural Substrates of Cognition. *Trends Cogn. Sci.* 24, 466–480. doi: 10.1016/j.tics.2020.03.005

Joshi, S., Li, Y., Kalwani, R. M., and Gold, J. I. (2016). Relationships between Pupil Diameter and Neuronal Activity in the Locus Coeruleus, Colliculi, and Cingulate Cortex. *Neuron* 89, 221–234. doi: 10.1016/j.neuron.2015.11.028

Kawakubo, Y., Kasai, K., Okazaki, S., Hosokawa-Kakurai, M., Watanabe, K., Kuwabara, H., et al. (2007). Electrophysiological abnormalities of spatial attention in adults with autism during the gap overlap task. *Clin. Neurophys.* 118, 1464–1471. doi: 10.1016/j.clinph.2007.04.015

Keehn, B., Kadlaskar, G., McNally Keehn, R., and Francis, A. L. (2019). Auditory Attentional Disengagement in Children with Autism Spectrum Disorder. *J. Autism. Dev. Disord* 49, 3999–4008. doi: 10.1007/s10803-019-04111-z

Keehn, B., Muller, R. A., and Townsend, J. (2013). Atypical attentional networks and the emergence of autism. *Neurosci. Biobehav. Rev.* 37, 164–183. doi: 10.1016/j.neubiorev.2012.11.014

Kingstone, A., and Klein, R. M. (1993). Visual offsets facilitate saccadic latency: Does predisengagement of visuospatial attention mediate this gap effect? *J. Exp. Psychol.* 19, 1251–1265. doi: 10.1037/0096-1523.19.6.1251

Kubota, M., Fujino, J., Tei, S., Takahata, K., Matsuoka, K., Tagai, K., et al. (2020). Binding of Dopamine D1 Receptor and Noradrenaline Transporter in Individuals with Autism Spectrum Disorder: A PET Study. *Cereb Cortex* 30, 6458–6468. doi: 10.1093/cercor/bhaa211

Lai, M. C., Kassee, C., Besney, R., Bonato, S., Hull, L., Mandy, W., et al. (2019). Prevalence of co-occurring mental health diagnoses in the autism population: a systematic review and meta-analysis. *Lancet Psychiatry* 6, 819–829. doi: 10.1016/s2215-0366(19)30289-5

Lam, K. S., Aman, M. G., and Arnold, L. E. (2006). Neurochemical correlates of autistic disorder: A review of the literature. *Res. Dev. Disabil.* 27, 254–289. doi: 10.1016/j.ridd.2005.03.003

Liversedge, S. P., Gilchrist, I. D., and Everling, S. (eds) (2011). *The Oxford Handbook of Eye Movements*. Oxford, UK: Oxford University Press.

London, E. B. (2018). Neuromodulation and a Reconceptualization of Autism Spectrum Disorders: Using the Locus Coeruleus Functioning as an Exemplar. *Front. Neurol.* 9:1120.

Lord, C., Rutter, M., DiLavore, P. C., Risi, S., Gotham, K., and Bishop, S. (2012). *Autism Diagnostic Obervation Schedule, Second Edition*. Torrance, CA: Western Psychological Services.

Mann, T. A., and Walker, P. (2003). Autism and a deficit in broadening the spread of visual attention. *J. Child Psychol. Psychiatry* 44, 274–284. doi: 10.1111/1469-7610.00120

Martchek, M., Thevarkunnel, S., Bauman, M., Blatt, G., and Kemper, T. (2006). Lack of evidence of neuropathology in the locus coeruleus in autism. *Acta Neuropathol.* 111, 497–499. doi: 10.1007/s00401-006-0061-0

Morris, L. S., McCall, J. G., Charney, D. S., and Murrough, J. W. (2020). The role of the locus coeruleus in the generation of pathological anxiety. *Brain Neurosci. Adv.* 4:2398212820930321.

Nieuwenhuis, S., Aston-Jones, G., and Cohen, J. D. (2005). Decision making, the P3, and the locus coeruleus-norepinephrine system. *Psychological. Bull.* 131, 510–532. doi: 10.1037/0033-2909.131.4.510

Ozyurt, J., and Greenlee, M. W. (2011). Neural correlates of inter- and intra-individual saccadic reaction time differences in the gap/overlap paradigm. *J. Neurophysiol.* 105, 2438–2447. doi: 10.1152/jn.00660.2009

Petersen, S. E., and Posner, M. I. (2012). The attention system of the human brain: 20 years after. *Annu. Rev. Neurosci.* 35, 73–89. doi: 10.1146/annurev-neuro-062111-150525

Reimer, J., McGinley, M. J., Liu, Y., Rodenkirch, C., Wang, Q., McCormick, D. A., et al. (2016). Pupil fluctuations track rapid changes in adrenergic and cholinergic activity in cortex. *Nat. Commun.* 7:13289.

Reynaud, A. J., Froesel, M., Guedj, C., Ben Hadj Hassen, S., Clery, J., Meunier, M., et al. (2019). Atomoxetine improves attentional orienting in a predictive context. *Neuropharmacology* 150, 59–69. doi: 10.1016/j.neuropharm.2019.03.012

Richards, H. J., Benson, V., Donnelly, N., and Hadwin, J. A. (2014). Exploring the function of selective attention and hypervigilance for threat in anxiety. *Clin. Psychol. Rev.* 34, 1–13. doi: 10.1016/j.cpr.2013.10.006

Rivaud, S., Muri, R. M., Gaymard, B., Vermersch, A. I., and Pierrot-Deseilligny, C. (1994). Eye movement disorders after frontal eye field lesions in humans. *Exp. Brain Res.* 102, 110–120.

Ronconi, L., Devita, M., Molteni, M., Gori, S., and Facoetti, A. (2018). Brief Report: When Large Becomes Slow: Zooming-Out Visual Attention Is Associated to Orienting Deficits in Autism. *J. Autism. Dev. Disord* 48, 2577–2584. doi: 10.1007/s10803-018-3506-0

Ronconi, L., Gori, S., Ruffino, M., Molteni, M., and Facoetti, A. (2013). Zoom-out attentional impairment in children with autism spectrum disorder. *Cortex* 49, 1025–1033. doi: 10.1016/j.cortex.2012.03.005

Rutter, M., Bailey, A., and Lord, C. (2003). *Social Communication Questionnaire (SCQ)*. Los Angeles, CA: Western Psychological Services.

Sacrey, L. A., Armstrong, V. L., Bryson, S. E., and Zwaigenbaum, L. (2014). Impairments to visual disengagement in autism spectrum disorder: a review of experimental studies from infancy to adulthood. *Neurosci. Biobehav. Rev.* 47, 559–577. doi: 10.1016/j.neubiorev.2014.10.011

Samuels, E. R., and Szabadi, E. (2008). Functional neuroanatomy of the noradrenergic locus coeruleus: its roles in the regulation of arousal and autonomic function part I: principles of functional organisation. *Curr. Neuropharmacol.* 6, 235–253. doi: 10.2174/157015908785777229

Saslow, M. G. (1967). Effects of components of displacement-step stimuli upon latency for saccadic eye movement. *J. Opt. Soc. Am.* 57, 1024–1029. doi: 10.1364/josa.57.001024

Shafiq, R., Stuart, G. W., Sandbach, J., Maruff, P., and Currie, J. (1998). The gap effect and express saccades in the auditory modality. *Exp. Brain Res.* 118, 221–229. doi: 10.1007/s002210050275

Steiner, G. Z., and Barry, R. J. (2011). Pupillary responses and event-related potentials as indices of the orienting reflex. *Psychophysiology* 48, 1648–1655. doi: 10.1111/j.1469-8986.2011.01271.x

Taylor, T. L., Kingstone, A., and Klein, R. M. (1998). The disapperance of foveal and nonfoveal stimuli: Decomposing the gap effect. *Can. J. Exp. Psychol.* 52, 192–199. doi: 10.1037/h0087292

Top, D. N. Jr., Luke, S. G., Stephenson, K. G., and South, M. (2018). Psychophysiological Arousal and Auditory Sensitivity in a Cross-Clinical Sample of Autistic and Non-autistic Anxious Adults. *Front. Psychiatry* 9:783.

Vernet, M., Yang, Q., Gruselle, M., Trams, M., and Kapoula, Z. (2009). Switching between gap and overlap pro-saccades: cost or benefit? *Exp. Brain Res.* 197, 49–58. doi: 10.1007/s00221-009-1887-1

Wechsler, D. (2011). *Wechsler's Abbreviated Scale of Intelligence - Second Edition (WASI-II)*. San Antonio, TX: NCS Pearson.

Yu, A. J., and Dayan, P. (2005). Uncertainty, neuromodulation, and attention. *Neuron* 46, 681–692. doi: 10.1016/j.neuron.2005.04.026

Zwaigenbaum, L., Bryson, S., Rogers, T., Roberts, W., Brian, J., and Szatmari, P. (2005). Behavioral manifestations of autism in the first year of life. *Internat. J. Dev. Neurosci.* 23, 143–152. doi: 10.1016/j.ijdevneu.2004.05.001

Conflict of Interest: The authors declare that the research was conducted in the absence of any commercial or financial relationships that could be construed as a potential conflict of interest.

frontiers in Integrative Neuroscience

ORIGINAL RESEARCH
published: 29 September 2021
doi: 10.3389/fnint.2021.730439

The Untouchable Ventral Nucleus of the Trapezoid Body: Preservation of a Nucleus in an Animal Model of Autism Spectrum Disorder

Yusra Mansour[1,2] *and Randy J. Kulesza*[2]*

[1] Department of Otolaryngology, Henry Ford Macomb Hospital, Clinton Township, MI, United States, [2] Department of Anatomy, Lake Erie College of Osteopathic Medicine, Erie, PA, United States

Autism spectrum disorder (ASD) is a neurodevelopmental condition characterized by repetitive behaviors, poor social skills, and difficulties with communication and hearing. The hearing deficits in ASD range from deafness to extreme sensitivity to routine environmental sounds. Previous research from our lab has shown drastic hypoplasia in the superior olivary complex (SOC) in both human cases of ASD and in an animal model of autism. However, in our study of the human SOC, we failed to find any changes in the total number of neurons in the ventral nucleus of the trapezoid body (VNTB) or any changes in cell body size or shape. Similarly, in animals prenatally exposed to the antiepileptic valproic acid (VPA), we failed to find any changes in the total number, size or shape of VNTB neurons. Based on these findings, we hypothesized that the neurotransmitter profiles, ascending and descending axonal projections of the VNTB are also preserved in these neurodevelopmental conditions. We investigated this hypothesis using a combination of immunohistochemistry and retrograde tract tracing. We found no difference between control and VPA-exposed animals in the number of VNTB neurons immunoreactive for choline acetyltransferase (ChAT). Additionally, we investigated the ascending projections from the VNTB to both the central nucleus of the inferior colliculus (CNIC) and medial geniculate (MG) and descending projections to the cochlea. Our results indicate no significant differences in the ascending and descending projections from the VNTB between control and VPA-exposed animals despite drastic changes in these projections from surrounding nuclei. These findings provide evidence that certain neuronal populations and circuits may be protected against the effects of neurodevelopmental disorders.

Keywords: autism, hearing – disorders, brainstem, olivocochlear, valproate

Edited by:
Martin Ralph,
University of Toronto, Canada

Reviewed by:
Richardson N. Leão,
Federal University of Rio Grande do Norte, Brazil
Adrian Rodriguez-Contreras,
The City College of New York (CUNY), United States
Kirupa Suthakar,
National Institute on Deafness and Other Communication Disorders (NIDCD), United States

***Correspondence:**
Randy J. Kulesza
rkulesza@lecom.edu

Received: *24 June 2021*
Accepted: *08 September 2021*
Published: *29 September 2021*

Citation:
Mansour Y and Kulesza RJ (2021) The Untouchable Ventral Nucleus of the Trapezoid Body: Preservation of a Nucleus in an Animal Model of Autism Spectrum Disorder. Front. Integr. Neurosci. 15:730439. doi: 10.3389/fnint.2021.730439

Abbreviations: +, positive; AN, auditory nerve; ASD, autism spectrum disorder; ChAT, choline acetyltransferase; CI, confidence interval; CL, contralateral; CN, cochlear nucleus; CNIC, central nucleus of the inferior colliculus; D, dorsal; DMW, dorsal medial wedge; DNLL, dorsal nucleus of the lateral lemniscus; E, embryonic; FB, Fast Blue; FG, Fluorogold; FN, facial nerve; GABA, gamma amino butyric acid; GAD, glutamate decarboxylase; IL, ipsilateral; LNTB, lateral nucleus of the trapezoid body; LSO, lateral superior olive; M, medial; MG, medial geniculate; mMG, medial nucleus of the medial geniculate; MNTB, medial nucleus of the trapezoid body; MSO, medial superior olive; NHS, normal horse serum; nl, nanoliter; NTR, Neurotrace Red; OC, olivocochlear; OCB, olivocochlear bundle; P, postnatal; PBS, phosphate buffered saline; PFA, paraformaldehyde; SC, superior colliculus; SOC, superior olivary complex; SPON, superior paraolivary nucleus; tz, trapezoid body; VCN, ventral cochlear nucleus; vMG, ventral nucleus of the medial geniculate; VNLL, ventral nucleus of the lateral lemniscus; VNTB, ventral nucleus of the trapezoid body; VPA, valproic acid.

INTRODUCTION

The ventral nucleus of the trapezoid body (VNTB) is one of the periolivary nuclei within the superior olivary complex (SOC) – a multichannel processing station along the mammalian auditory pathway. VNTB neurons reside within the decussating axons of the trapezoid body that originate from neurons in the ventral cochlear nucleus (VCN) and are directed largely toward the SOC and nuclei of the lateral lemniscus. The VNTB includes about 4,500 neurons in rat (Kulesza et al., 2002) and 1,400 neurons in human (Kulesza, 2008). The VNTB includes a number of distinct neurochemical populations. There are populations of both large and small cholinergic neurons (see below; Warr, 1975; Sherriff and Henderson, 1994; Warr and Beck, 1996). There are also glycinergic (Saint Marie and Baker, 1990) and GABAergic populations (Roberts and Ribak, 1987; Albrecht et al., 2014) and a population that likely co-localizes these neurotransmitters (Albrecht et al., 2014). In fact, during the early postnatal period VNTB neurons transition from using gamma amino butyric acid (GABA) to glycine as a neurotransmitter (Albrecht et al., 2014).

The VNTB receives ascending input from globular bushy cells, octopus cells, and multipolar cells in the contralateral (CL) VCN (Warr, 1972; Friauf and Ostwald, 1988; Kuwabara and Zook, 1991; Smith et al., 1991; Thompson, 1998) and smaller projections from the ipsilateral (IL) VCN. The VNTB also receives input from the IL medial nucleus of the trapezoid body (MNTB; Kuwabara and Zook, 1991). There is also a descending projection from the IL central nucleus of the inferior colliculus (CNIC; Caicedo and Herbert, 1993; Vetter et al., 1993). Consistent with such a wide range of inputs, the VNTB projects extensively throughout the auditory brainstem. The best characterized projection is part of the olivocochlear (OC) system that projections *via* the olivocochlear bundle (OCB) to outer hair cells in the cochlea; this is a bilateral projection with a contralateral (CL) predominance (rat – White and Warr, 1983; cat – Warr et al., 2002). This vast majority of VNTB neurons projecting to the cochlear nucleus (CN) and cochlea are cholinergic (Dannhof et al., 1991; Vetter et al., 1991). While OC neurons in the VNTB may send collateral projections to the CN, there are some smaller neurons that are choline acetyltransferase positive (ChAT+) neurons that project to the dorsal and ventral cochlear nuclei and cochlear root neurons *via* the trapezoid body (Osen et al., 1984; Godfrey et al., 1987; Benson and Brown, 1990; Sherriff and Henderson, 1994; Warr and Beck, 1996; Gómez-Nieto et al., 2008). The VNTB makes a glycinergic projection *via* the lateral lemniscus to the IL inferior colliculus (Saint Marie and Baker, 1990; Warr and Beck, 1996). Finally, there are local projections within the SOC to the MNTB, lateral nucleus of the trapezoid body (LNTB) and lateral superior olive (LSO; Warr and Beck, 1996; Albrecht et al., 2014). Based on these observations, the VNTB is a heterogeneous nucleus that receives both ascending and descending inputs. It forms a major component of the medial olivocochlear system that modulates the sensitivity of the organ of Corti and projects to cochlear root neurons to influence the acoustic startle reflex. The VNTB projects locally within the SOC and along the ascending auditory pathway where it functions in sound localization and coding spectral and temporal features of sound. Indeed, the VNTB is situated to function in a number of important aspects of brainstem auditory processing.

Auditory processing deficits are common in subjects with autism spectrum disorders (ASD) and in animal models of ASD (Greenspan and Wieder, 1997; Tomchek and Dunn, 2007; Gomes et al., 2008; Bolton et al., 2012; Danesh and Kaf, 2012; O'Connor, 2012). In fact, human subjects with ASD have auditory brainstem responses (ABR) and stapedial reflexes with longer latency, decreased amplitude, and right-left asymmetry (Skoff et al., 1980; Rumsey et al., 1984; McClelland et al., 1992; Klin, 1993; Kwon et al., 2007; Roth et al., 2012; Lukose et al., 2013). *In utero* exposure to the antiepileptic valproic acid (VPA) results in increased risk of an ASD diagnosis in humans and is a validated animal model of ASD (Rodier et al., 1996; Moore et al., 2000; Williams et al., 2001; Rasalam et al., 2005; Koren et al., 2006; Bromley et al., 2013; Christensen et al., 2013; Mabunga et al., 2015).

Our previous research has revealed significantly fewer neurons in the SOC of both human subjects (ranging in age from 2 to 52 years of age) diagnosed with ASD and in VPA-exposed animals (Kulesza and Mangunay, 2008; Kulesza et al., 2011; Lukose et al., 2015). In fact, in both human cases of ASD and VPA-exposed animals, we found significantly fewer neurons in the medial superior olive (MSO), LSO, MNTB, LNTB, and superior paraolivary nucleus (SPON; Kulesza et al., 2011; Lukose et al., 2015). However, morphology of VNTB neurons was not significantly different in our study of over 56 human subjects with ASD and in our study of VPA-exposed animals (Kulesza and Mangunay, 2008; Kulesza et al., 2011; Lukose et al., 2015; Zimmerman et al., 2018). Specifically, we found no differences in the total number of neurons and no differences in the size or shape of VNTB neurons, even when split by cell type (Kulesza et al., 2011; Lukose et al., 2015; Zimmerman et al., 2018). These observations led us to consider that despite the drastic changes in the surrounding SOC nuclei, the VNTB is spared in ASD and animal models of this condition. Further, 3D volumetric models of the human SOC revealed all SOC nuclei were significantly smaller, except for the VNTB (Mansour and Kulesza, 2020).

These observations led us to hypothesize that VPA exposure does not impact ascending or descending projections or neurotransmitter profiles in the VNTB. To examine this hypothesis, we undertook retrograde tract tracing experiments using Fluorogold (FG) or Fast Blue (FB). We examined ascending projections to the medial geniculate body (MG), or CNIC and examined descending projections to the cochlea by injections of FG at the round window. We finally correlated retrogradely labeled neurons with neurotransmitter profile in double-labeling experiments for choline acetyltransferase (ChAT).

MATERIALS AND METHODS

Valproic Acid Exposure

All handling and surgical procedures were approved by the LECOM Institutional Animal Care and Use Committee (protocols #16-02, 18-03, 19-04, and 20-02) and conducted in

accordance with the National Institute of Health Guide for the Care and Use of Laboratory Animals. Sprague–Dawley rats were maintained on a 12 h light/dark cycle with *ad libitum* access to food and water. *In utero* exposure to VPA was performed as previously described (**Figure 1A**; Main and Kulesza, 2017; Zimmerman et al., 2018, 2020; Mansour et al., 2019, 2021). Briefly, dams were fed 3.1 g of peanut butter on embryonic days (E) 7–12. On E10 and E12, dams in the VPA group were fed peanut butter mixed with 800 mg/kg of VPA (**Figure 1A**). Control animals were fed peanut butter meals without VPA. Both control and VPA-exposed dams were permitted to deliver pups without interference (litters were not culled). On postnatal day (P) 21, litters were weaned and only male pups were included in the study since gender-specific effects of VPA exposure are established (Schneider et al., 2008). We conducted this study under the assumption that all male pups in a given litter were equally affected by VPA exposure; our previous studies provide data consistent with this strategy (Main and Kulesza, 2017; Zimmerman et al., 2018, 2020; Mansour et al., 2019, 2021). We additionally utilized archival collections of Giemsa-stained tissue sections (i.e., every 3rd tissue section at a thickness of 40 μm) from previous investigations as reference for morphological features of the VNTB (Zimmerman et al., 2018; Mansour et al., 2019). While our previous work provides evidence for abnormal tonotopic maps and/or hyperactivation of brainstem centers in VPA-exposed animals (Dubiel and Kulesza, 2016) and abnormal ascending projections to the midbrain and thalamus (Zimmerman et al., 2020; Mansour et al., 2021), we did not perform any hearing tests or audiometric screening on the animals used in this study.

Surgery and Tracer Injections

Cochlear injections were made on P28 (**Figure 1B**). Animals were placed in an induction chamber and anesthetized with vaporized isoflurane (5% induction, 2.5–3% maintenance, O_2: 1.2 l/min). Once animals were unresponsive, they were removed from the chamber, fit with a custom face mask providing continuous anesthesia and secured in a custom foam support. Body temperature was maintained *via* a heating pad. The scalp was disinfected with 70% ethanol and washed with iodine solution. A retroauricular approach was taken to the cochlea. After cutting through the skin, blunt dissection was used to reach the bulla; the bulla was opened along the caudal aspect sufficient to visualize the stapedial artery and round window. A 1 μl Hamilton syringe (32 gauge and 4 point) was used to inject 800 nl of 4% FG (Fluorochrome). We did not observe any abnormalities of the auditory bulla, cochlear promontory or oval window in VPA-exposed animals. After the injection, the wound was closed and the animal was returned to their home cage and permitted to recover for 6 days. Injections into the CNIC or MG nuclei were made between P50 and P63 *via* stereotaxic craniotomy as previously described (**Figure 1**; Zimmerman et al., 2020; Mansour et al., 2021). Animals receiving these injections were anesthetized as above but were secured in a stereotaxic frame with non-rupture ear bars (Kopf Instruments). A midline incision was made in the scalp to expose the dorsal aspect of the skull. The coordinates for CNIC injections were: 0.2 mm rostral to lambda (as indicated by Paxinos and Watson, 2007), 1.5 mm right of the midline. Injections of FB (2.5% in water; Polysciences, Inc.) were made into the CNIC using a 1 μl Hamilton KH Neuros syringe (32 gauge and 4 point; **Figure 1B**). A depth measurement was taken from the surface of the dura mater and deposits of 100 nl of FB were made at depths of −3.6, −3.2, and −2.6 mm for a total injected volume of 300 nl. The coordinates for MG injections were: 5.6 mm caudal to bregma and 3.4 mm right of the midline (as indicated by Paxinos and Watson, 2007). Injections of FG (4.0% in saline; Fluorochrome) were made using a 1 μl Hamilton KH Neuros syringe (32 gauge and 4 point; **Figure 1B**). A depth measurement was taken from the surface of the dura mater and deposits of 100 nl of FG were made at depths of −5.8 and −5.0 mm for a total injected volume of 200 nl. After the final injection, the needle was left in place for 10 min. The needle was removed, the bony defect was filled with dental wax and the incision sutured. The wound was injected with lidocaine and the animal taken off isoflurane, returned to their homecage, and monitored until they were able to stand on all fours.

For this study, a stereotaxic injection of FB was made into the CNIC of 10 control animals (from 4 L) and 6 VPA-exposed animals (from 4 L), a stereotaxic injection of FG was made into the MG of 6 control animals (from 6 L) and 5 VPA-exposed animals (from 4 L), and an injection of FG was made into the cochlea of 4 control animals (from 4 L) and 4 VPA-exposed animals (from 4 L). Each animal received only a single injection; we did not attempt any double retrograde labeling experiments.

Perfusion and Sectioning

Six days following tracer injections, animals were anesthetized with isoflurane and perfused through the ascending aorta with saline followed by 4% paraformaldehyde (PFA) in 0.1 M sodium phosphate buffer (PB). Brains were removed from the skull and the right side was marked with a register pin. Accordingly, the right side is ipsilateral (IL) to the injection and the left side is contralateral (CL). Brains were postfixed in 4% PFA and placed in cryoprotectant (30% sucrose in 4% PFA) 24 h before frozen sectioning. Brains were sectioned in the coronal plane at 50 μm and collected into three wells. Sections from well 1 were archived. Sections from well 2 were used to reconstruct CNIC or MG injection sites. For counting of FB and FG+ neurons, all sections from well 3 were counterstained with Neurotrace Red (a fluorescent Nissl stain; NTR, Invitrogen) and/or processed for immunohistochemistry (see next).

Immunohistochemistry

Free-floating sections were rinsed in phosphate buffered saline (PBS), blocked in 1% normal horse serum (NHS; Abcam), 0.5% triton X in PBS for 1 h. Sections processed for ChAT were incubated in primary antisera (rabbit anti-ChAT, 1:1000 with 1% NHS; Abcam, catalog #: ab178850) overnight, rinsed in PBS and incubated for 2 h in goat anti-rabbit Dylight 488 (1:100; Vector Labs). Sections processed for glutamate decarboxylase (GAD) were incubated in primary antisera (mouse anti-GAD, 1:250 with 1% NHS; Abcam, catalog #: ab26116) overnight. These sections were then incubated with biotinylated Gt anti-mouse (1:100, Vector Labs) for at least 6 h and then

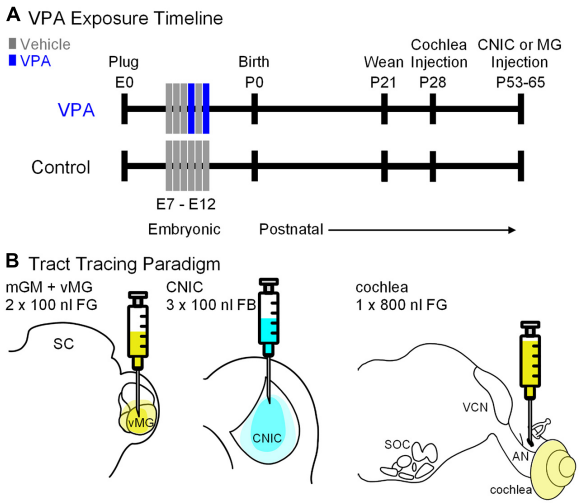

FIGURE 1 | Study design. Shown in **(A)** is the timeline for the study. Pregnant females were fed peanut butter on E7–12 and animals in the VPA group received peanut butter with VPA on E10 and 12. Pups were weaned on P21. Cochlear injections were made on P28. Injections into the CNIC or MG were made between P53–65. Shown in **(B)** is the tracer and volume injected into each target.

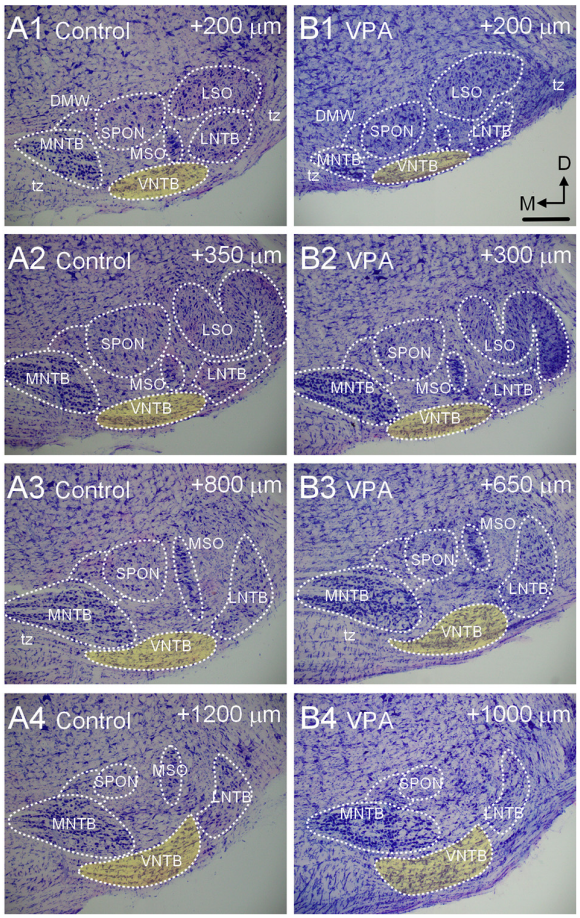

FIGURE 2 | Morphology of the VNTB. Shown in **(A1–4)** is a caudal to rostral series of Giemsa-stained sections through the SOC of a P28 control animal. The VNTB is indicated in yellow. The numbers in the upper right corner of each image indicates how far the section is rostral to the beginning of the SOC in the series. Shown in **(B1–4)** is a similar series through the SOC of a VPA-exposed animal. The SOC in VPA-exposed animals is shorter in the rostrocaudal dimension and besides the VNTB, other nuclei are smaller. The scale bar in **(B1)** is equal to 300 µm.

incubated overnight with Streptavidin Dylight 488 (Vector Labs). After the final antibody step, tissue sections were rinsed, and counterstained with Neurotrace Red (Thermo Fisher Scientific), mounted onto glass slides, dried and coverslipped with Entellan (Millipore Sigma).

Quantification

Injection sites were confirmed and quantified as previously described (Zimmerman et al., 2020; Mansour et al., 2021). Injection sites in the CNIC are the same as published in figures 2 and 3 in Zimmerman et al. (2020) and injection sites in the MG are the same as published in figure 5 in Mansour et al. (2021). Nuclear boundaries of the VNTB were as per previous work on the rat SOC (Kulesza et al., 2002). Photomicrographs were taken with a DP71 digital camera on an Olympus CKX41 microscope or a Leica TCS SP5 confocal microscope. Depending on the experiment, we took photographs of NTR, FG/FB, and ChAT/GAD. Images were overlaid using the stack and z project features in ImageJ (Schindelin et al., 2012). Counts of FG and NTR labeled VNTB neurons were made in at least 3 tissue sections per animal, per CNIC or MG injection. We counted the total number of NTR, FB/FG and ChAT/GAD-labeled neuronal profiles (i.e., triple labeled neurons) in at least two randomly selected sections per animal. Our labeling paradigms revealed no obvious gradients of FG labeled neurons from the CNIC, MG or cochlea and no apparent gradient of ChAT or GAD+ neurons in the VNTB of control or VPA-exposed neurons. All counts were made in ImageJ (Schindelin et al., 2012) using the cell counting feature by an observer blind to experimental condition. Counts were combined for each animal; the analyses are based on combined proportions of retrogradely labeled neurons in each nucleus.

Statistical Analysis

Descriptive statistics were generated for each control and VPA group using GraphPad Prism 7.03 (GraphPad Software, La Jolla, CA, United States). All data sets were tested against a normal distribution using the D'Agostino and Pearson omnibus normality test. If a data set was too small for normality testing, non-parametric tests were used (i.e., Mann–Whitney *U* test) and data are presented in the text as median with the 95% confidence interval (CI) of the median. The proportions of IL and CL labeled neurons were compared using Fisher's exact test. Differences were considered statistically significant if p-values were <0.05.

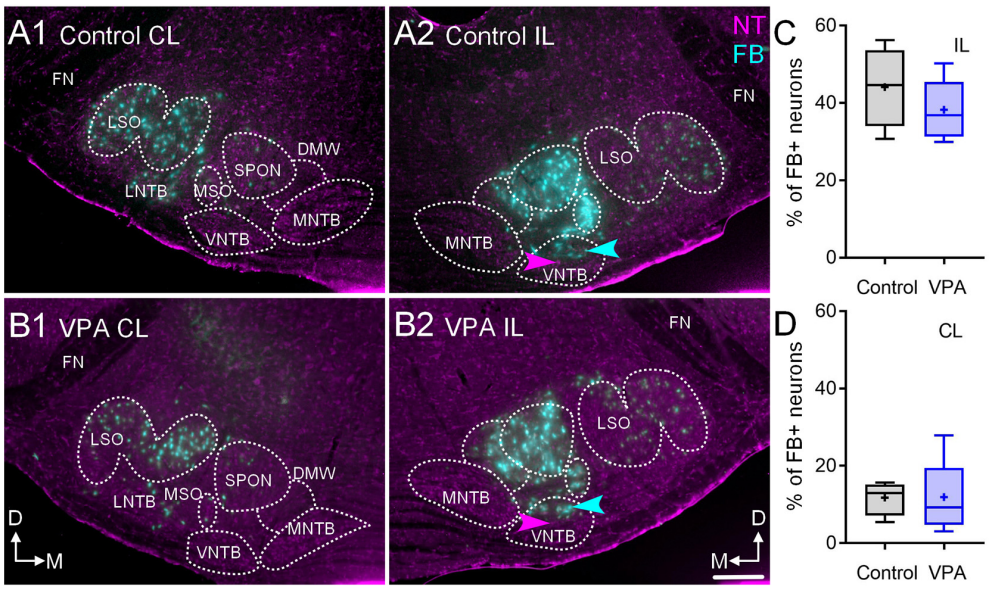

FIGURE 3 | Retrograde labeling after FB injection in the CNIC. Shown in **(A1–2)** are sections through the SOC after FB injection in the CNIC of a control animal (**A1**, CL and **A2**, IL) and **(B)** shows sections from a VPA-exposed animal (**B1**, CL and **B2**, IL). While there are fewer FB+ neurons in the VPA-exposed animal, there was no difference in the number of FB+ neurons in the VNTB IL or CL to the injection. The proportions of FB+ neurons IL to the injection are shown in (**C**) and those CL to the injection are shown in **(D)**. The scale bar in **(B2)** is equal to 100 μm.

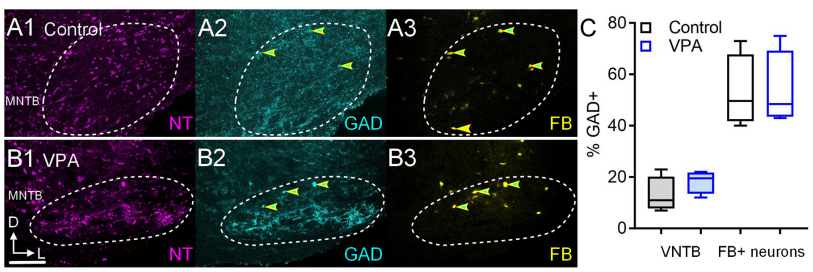

FIGURE 4 | GAD+ VNTB neurons projecting to the CNIC. Shown in **(A1–3)** are sections through the VNTB after a FB injection in the CNIC of a control animal and similar sections are shown from a VPA-exposed animal in **(B1–3)**. GAD immunolabeling is shown in cyan (2) and FB is shown in yellow (3). Neurons that are both GAD and FB+ are indicated by the yellow and cyan arrowheads. The scale bar in **(B2)** is equal to 250 μm. The percentage of GAD+ VNTB neurons is shown in **(C left)** and the percentage of neurons that were GAD and FB+ are shown in **(C right)**.

RESULTS

Features of the Ventral Nucleus of the Trapezoid Body

The VNTB is situated within the SOC along the ventral aspect of the pons amongst the decussating axons of the trapezoid body (**Figure 2**). The VNTB extends rostrocaudally along nearly the entire extent of the SOC (**Figures 2A1–4**). Consistent with smaller brains and brainstems in VPA-exposed animals (Zimmerman et al., 2018; Mansour et al., 2019), the SOC is shorter in the rostrocaudal dimension, the constituent nuclei contain significantly fewer neurons and surviving neurons exhibit dysmorphology (Zimmerman et al., 2018). Specifically, in control animals the SOC extends a rostrocaudal distance of 1,457 ± 142 μm and in VPA-exposed animals this is significantly reduced to 1,160 ± 98 μm [$t(11) = 4.3$, $p = 0.0012$]. Consistent with this shortened rostrocaudal distance, the VNTB extends a significantly shorter distance in VPA exposed animals {control = 1,371 ± 98, VPA = 1,040 ± 98 μm; [$t(11) = 5.22$, $p = 0.0003$]}. Despite the significant change in rostrocaudal length and drastic changes in the surrounding SOC nuclei, the VNTB exhibits no significant changes in total nuclear volume, neuron number, or neuronal morphology along its rostrocaudal dimension (Zimmerman et al., 2018; **Figures 2B1–4**).

Ascending Projections

After injections of FB in the right CNIC, we found that in control animals 47% (CI 31–56%) of neurons in the IL VNTB and 12.95% (CI 6–17%) of neurons in the CL VNTB were FB+ (**Figures 3A1,A2,C,D**). In VPA-exposed animals, we found that 37% (CI 30–50%) of neurons in the IL VNTB and 9.28% (CI 3–28%) of neurons in the CL VNTB were FB+ (**Figures 3B1,B2,C,D**). These differences were not

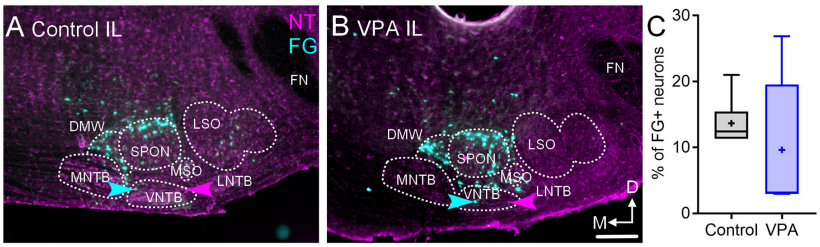

FIGURE 5 | Retrograde labeling after FG injection in the MG. Shown in **(A)** is a section through the IL SOC after FG injection in the MG of a control animal and **(B)** shows a section from a VPA-exposed animal. While there are fewer FG+ neurons in the SOC of VPA-exposed animals, there was no difference in the number of FG+ neurons in the VNTB IL to the injection. The proportions of FG+ neurons IL to the injection are shown in **C**. The scale bar in B2 is equal to 100 μm.

significant [CL: $U(4,6) = 11$, $p = 0.91$; IL: $U(4,6) = 8$, $p = 0.47$] (**Figures 3C,D**). The difference in proportions of CL/IL projections from the VNTB was similar between control and VPA-exposed animals (Fisher's exact, $p > 0.99$).

We also examined the number of VNTB neurons that were GABAergic and the number of FB+/GAD+ after injections in the IL CNIC (**Figure 4**). In control animals 11% (CI 7–23%) of VNTB neurons were GAD+ and in VPA-exposed animals 19% (CI 12–22%) of VNTB neurons were GAD+ and this was not significant [$U(4,4) = 4.5$, $p = 0.37$; **Figure 4C**]. After injection of FB in the IL CNIC, 50% (CI 40–73%) of FB+ neurons in the VNTB were GAD+ (**Figures 4A1–3**). In VPA-exposed animals, 49% (CI 43–75%) of FB+ neurons in the VNTB were GAD+ (**Figures 4B1–3**). This difference was not significant [$U(4,4) = 8$, $p > 0.99$; **Figure 4C**]. In both control and VPA-exposed animals, none of the neurons retrogradely labeled from injection of FB in the CNIC were ChAT+ (0/26 control; 0/19 VPA).

After injections of FG in the right MG, 12% (CI 11–21%) of neurons in the IL VNTB were FG+ in control animals and 10% (CI 3–26%) were FG+ in VPA-exposed animals (**Figures 5A–C**). This difference was not significant [$U(6,5) = 9$, $p = 0.30$; **Figure 5C**]. In both control and VPA-exposed animals less than 1% of neurons in the CL VNTB were FG+.

Cochlea Injections

After FG deposits through the right round window in control animals, 5.31% (CI 2–7%) of VNTB neurons CL to the injection were FG+ and 3.2% (CI 1–5%) were FG+ IL to the injection (**Figure 6C**). After similar injections in VPA-exposed animals, 4.5% (CI 2–9%) of VNTB neurons CL to the injection were FG+ and 3.4% (CI 3–4%) were FG+ IL to the injection (**Figure 6C**). Neither of these differences were significant [CL: $U(4,4) = 3$, $p = 0.20$; IL: $U(4,4) = 4$, $p = 0.34$]. The ratio of IL/CL FG+ neurons was 0.60 in control and 0.75 in VPA-exposed animals. The difference in proportions of CL/IL projections from the VNTB to the cochlea was similar between control and VPA-exposed animals (Fisher's exact, $p > 0.99$).

In control animals, 5% (CI 2–8%) of VNTB neurons were ChAT+ and 7.6% (CI 2–9%) of VNTB neurons were ChAT+ in VPA-exposed animals. This difference was not significant [$U(6,7) = 10$, $p = 0.13$]. CL to the cochlear injection, we found that in control animals 61% (CI 27–77%) of FG+ neurons in the

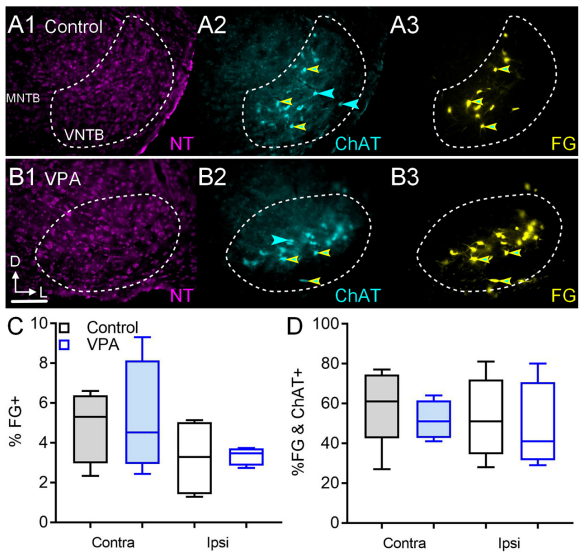

FIGURE 6 | Retrograde labeling after FG injection in the cochlea. Shown in **(A1–3)** are sections through the VNTB after FG injection in the cochlea of a control animal with immunolabeling for ChAT (2). **(B1–3)** shows the VNTB from a VPA-exposed animal. The percentage of FG+ neurons IL and CL to the injection are shown in **(C)**. The percentage of VNTB neurons that were FG and ChAT+ after a cochlear injection are shown in **(D)**. The scale bar in **(B1)** is equal to 250 μm.

VNTB were ChAT+ (double labeled; **Figures 6A1–3**). In VPA-exposed animals 51% (CI 41–64%) of FG+ neurons in the VNTB were ChAT+ (**Figures 6B1–3**). This difference was not significant [$U(5,4) = 6$, $p = 0.41$; **Figure 6D**]. IL to the cochlear injection, 51% (CI 28–81%) of FG+ neurons in the VNTB were ChAT+ (double labeled) in control animals. In VPA-exposed animals 41% (CI 29–80%) of FG+ neurons in the VNTB were ChAT+. This difference was not significant [$U(5,4) = 8$, $p = 0.73$; **Figure 6D**].

DISCUSSION

This study was motivated by the observations that the VNTB was preserved in both human subjects with ASD and VPA-exposed animals despite well documented auditory processing

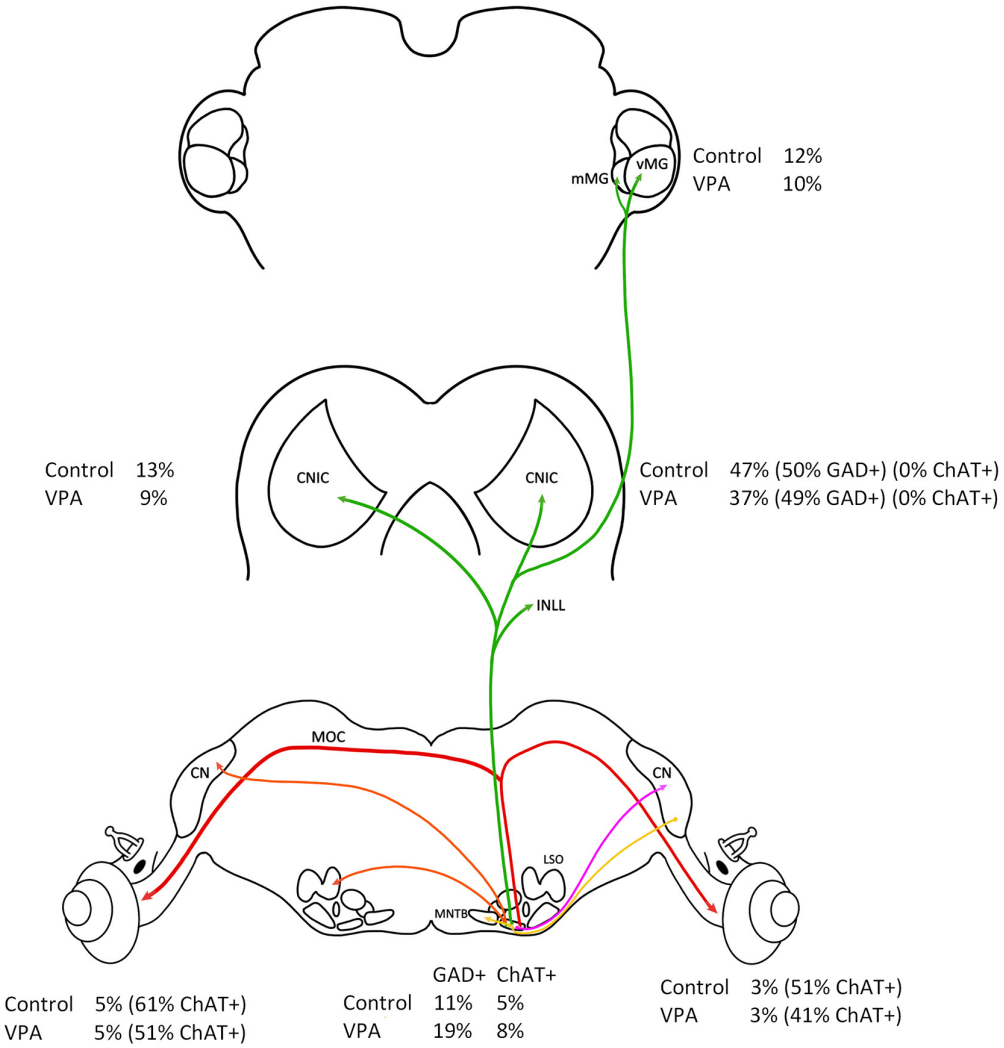

FIGURE 7 | Summary of results. This figure shows a summary of all results presented in this study. All values are relative to the right (IL) VNTB. There was no difference in the percentage of VNTB neurons projecting to the IL or CL cochlea (red line) and no difference in the number of ChAT+ neurons in the VNTB. There was also no difference in the percentage of neurons projecting to the CNIC and MG (green line) and no difference in the number of GAD+ neurons.

issues in ASD and significantly hypotrophy and dysmorphology throughout the auditory brainstem in ASD and VPA-exposed animals. Our initial observations that the VNTB was unaffected in these conditions was intriguing since VNTB neurons share a number of developmental features with other SOC nuclei, including origin, lineage and birthday (Altman and Bayer, 1980; Maricich et al., 2009; Marrs et al., 2013). It is important to emphasize that the VNTB is a heterogeneous nucleus in neuronal morphologies, functions and projections but also by origin. Specifically, the majority of VNTB neurons are derived from rhombomeres 3 and 5 while MOC neurons are unique in the SOC in their origin from rhombomere 4 (Di Bonito et al., 2013; Marrs et al., 2013; Altieri et al., 2016). Regardless, our previous work showed that in VPA-exposed animals the VNTB had the same total number of neurons, and these neurons had the same cell body size and shape (Zimmerman et al., 2018). Specifically, there was no difference in the proportions of neuronal morphologies in the VNTB between control and VPA-exposed animals (62–69% round/oval neurons, 18–26% stellate, and 12–13% fusiform; Zimmerman et al., 2018). Furthermore, there was no difference in cell body size in VNTB neurons between control and VPA-exposed animals even when split by cell body shape (Zimmerman et al., 2018). The results presented in this report show there is no significant difference in the proportion of VNTB neurons projecting to the CNIC, MG, and cochlea (**Figure 7**). Transport of FG from the injection site requires uptake and retrograde transport from axon terminals to the cell body. We worked with the assumption that these processes are normal in VPA-exposed animals. Additionally, we recognize that our tract tracing paradigms may not label all VNTB neurons projecting to these targets, but we expected to label the vast majority of these neurons. We also found no change in the number of VNTB

neurons that were GAD+ or ChAT+ and there were no changes in the number of retrogradely labeled VNTB neurons that were GAD+ or ChAT+ (**Figure 7**). It is possible that some GAD or ChAT immunonegative neurons contain levels of these proteins below the detection levels of our imaging equipment. Further, it is possible our counting paradigm under sampled neuron profiles – however this would have affected counts from both control and VPA-exposed animals. After cochlear injections of FG, we found a number of ChAT+ neurons that were FG negative – these likely represent neurons projecting to the CL cochlea. Based on these observations, we still have no evidence that the VNTB is impacted in ASD or in our animal model of ASD. Below we review the impact of VPA exposure on the SOC and discuss possible features of the VNTB that may subserve its protection in these conditions.

We have examined the SOC in 43 subjects diagnosed with ASD ranging in age from 2 to 56 years of age (Kulesza and Mangunay, 2008; Kulesza et al., 2011; Lukose et al., 2015) and we recently constructed 3D models of the SOC nuclei from seven subjects with ASD (2–11 years of age; Mansour and Kulesza, 2020). We found significant changes in the number of neurons in the surrounding SOC nuclei and drastic dysmorphology in the MSO. However, we found no differences in the volume or number of neurons in the VNTB and there were no changes in neuron size or morphology in subjects with ASD. Additionally, we have studied the structure and connectivity of the SOC in animals exposed to VPA *in utero*. After VPA exposure, we find significantly fewer neurons in all SOC nuclei except the LNTB and VNTB and we find significantly smaller neurons in all SOC nuclei except the VNTB (Zimmerman et al., 2018). Furthermore, there was no change in the proportions of stellate or fusiform neurons in the VNTB (Zimmerman et al., 2018). It is important to note that efferent innervation of outer hair cells in human is relatively sparse and attenuates with age (Liberman and Liberman, 2019). Accordingly, the contribution of the different VNTB subpopulations to the repertoire of VNTB functions may vary from rodent to humans. Besides changes in neuron number and morphology, VPA exposure results in abnormal tonotopic maps (Dubiel and Kulesza, 2016), reduced immunolabeling for the calcium binding proteins calbindin in octopus cells in the VCN, MNTB, and dorsal nucleus of the lateral lemniscus (DNLL; Zimmerman et al., 2018; Mansour et al., 2019) and calretinin in globular bushy cells and calyceal axons (Zimmerman et al., 2018). VPA exposure also results in significantly smaller axon diameters in the trapezoid body and lateral lemniscus (Zimmerman et al., 2018; Mansour et al., 2019). Recently we have examined the impact of VPA exposure on ascending projections to the midbrain and thalamus. VPA exposure resulted in not only fewer neurons in the LSO, MSO, and SPON but also a lower proportion of these neurons in these nuclei were retrogradely labeled from injections of FB in the CNIC (Zimmerman et al., 2020). In fact, the MSO projection was the most severely impacted among the ascending projections to the CNIC. Further, VPA exposure resulted in 31% fewer CNIC neurons (Mansour et al., 2019), 50% fewer neurons in the ventral nucleus of the medial geniculate (vMG) and 55% fewer neurons in the medial nucleus of the medial geniculate (mMG; Mansour et al., 2021). Like the ascending projections to the CNIC, VPA exposure resulted in significantly reduced projections to the MG from the CN, SOC, and CNIC (Mansour et al., 2021). In the SOC, we found both overall and proportionally reduced projections to the MG from the IL LSO, MSO, SPON, and dorsal medial wedge (DMW). In both of these retrograde tracing studies, we found not only reduced projections but abnormal patterns of inputs from the SOC and VCN to the CNIC and MG (see figure 11 in Mansour et al., 2021). The current study provides data showing that the major ascending projections to the CNIC and MG and descending projections to the cochlea from the VNTB are not impacted by VPA exposure. Not only does VPA not impact the projections of the VNTB, but it also does not appear to impact the neurotransmitter profile of these neurons (**Figure 7**). We found significantly fewer neurons in the CNIC and MG after VPA exposure, but the VNTB projections were normal. It is unclear how VNTB axons terminate in these locations. Specifically, does a single VNTB axon contact more neurons or spread across larger territories in the CNIC and MG of VPA-exposed animals? We will attempt to investigate this question with a combination of anterograde tract tracing and immunohistochemistry. The circuitry of the VNTB is complex and it is important to recognize that we have not examined all projections. Small, focal injections of tracers into the SOC and cochlear nuclei would be required to study these connections, but we hypothesize that these connections are unaffected as well. It is important to note that we have utilized morphometric techniques, immunohistochemistry, and tract tracing strategies to study the VNTB. We have not directly examined function of these neurons and it is possible that sound-evoked responses of VNTB neurons are impaired and/or that function of these neurons is disrupted by abnormal features of target cells in the cochlea, IC, and MG. Notwithstanding, the reason the VNTB is preserved in ASD and in VPA exposures is unclear. However, given these are neurodevelopmental conditions, we propose a mechanism related to developmental origins and protein expression.

The VNTB, along with the MNTB, LNTB, and SPON are most likely derived from the basal plate between E12 and 16 and among the SOC nuclei, have a unique expression pattern of transcription factors (Altman and Bayer, 1980; Kudo et al., 2000; Marrs et al., 2013). Specifically, about 80% of VNTB neurons express *En1* with smaller populations that express *FoxP1* and co-express these markers (Marrs et al., 2013). This pattern is not found in any of the other SOC nuclei but is most closely matched by the LNTB, but only about 45% of LNTB neurons express *En1* (Marrs et al., 2013). Our VPA exposure occurs between E10 and 12, primordial SOC neurons express *En1* as early as E12.5 and the VNTB, MNTB, and LNTB appear to express *En1* until at least P10 (Marrs et al., 2013). *En1* is mainly expressed during development, promotes cell survival through a mitochondrial cascade and protects neurons against cell death (Beltran et al., 2013). *En2* has been implicated in ASD and in the hindbrain this gene is primarily expressed by monoaminergic neurons projecting to the forebrain (Genestine et al., 2015). Dopaminergic neurons in the midbrain substantia nigra express *En1* and in animals heterozygous for *En1* more

of these neurons show pathological changes and progressively degenerate (Simon et al., 2001; Alberi et al., 2004; Sonnier et al., 2007; Chatterjee et al., 2019). Furthermore, infusion of engrailed protein into the midbrain protects dopaminergic neurons in the substantia nigra from cell death in animal models of exposure-based Parkinson's disease (Chatterjee et al., 2019). Interestingly, *En1* is also overexpressed in aggressive forms of breast cancer (Beltran et al., 2013). It would appear then that *En1* plays an important role in cell survival. In mouse models with an *En1* deletion, the MNTB, VNTB do not form and no GABA/glycinergic neurons form in the ventral nucleus of the lateral lemniscus (VNLL; Jalabi et al., 2013; Altieri et al., 2016). As such, it appears that *En1* expression is essential for development of the vast majority of VNTB neurons. Given that nearly all VNTB neurons express *En1* (except MOC neurons derived from rhombomere 4), we interpret our results to suggest this transcription factor, and/or signaling cascades downstream of *En1*, serves to protect the non-MOC VNTB neurons from the *in utero* effects of VPA and neuropathological sequelae of ASD. Since non-MOC VNTB neurons do not form in *En1* knockout animals (Altieri et al., 2016), it would be difficult to examine the impact of *in utero* VPA exposure on this nucleus. However, we hypothesize that VPA exposure in *En1* deficient/heterozygous animals would have much more drastic effects. It is unclear if the VNTB is intact in *En1* ± animals, but if it is, we suspect VPA exposure would result in significantly fewer neurons and dysmorphology. Since MOC neurons in the VNTB are not derived from the *En1* lineage, some other transcription factors or mechanism must protect these neurons (Di Bonito et al., 2013; Marrs et al., 2013; Altieri et al., 2016). Our results suggests that less than 10% of VNTB neurons are ChAT+ and so MOC neurons are a minor component of the VNTB. Our study of brainstem oropharyngeal motor neurons in VPA-exposed animals revealed no changes in the total number of neurons in the facial nucleus, glossopharyngeal nucleus, trigeminal nucleus, or nucleus ambiguous (Alhelo and Kulesza, 2021) suggesting their motor/cholinergic lineage provides protection against premature cell death by *in utero* VPA exposure. Additionally, this minor populations of VNTB neurons may be protected through the local milieu and involve local signaling. VPA, through a number of mechanisms, increases GABA levels in the brain but also acts as a histone deacetylase inhibitor, through which it impacts expression of numerous genes (Göttlicher, 2004). It is unclear what role elevated GABA levels might play in the SOC and VNTB at E10 and E12.5, although GABA receptors are present as early as E11.5 in cortical neurons (Li et al., 2006).

The protective role of *En1* for the VNTB in ASD/VPA exposure is complicated by the fact that other SOC neurons express *En1* (Marrs et al., 2013). Nearly 50% of LNTB neurons express *En1* but ∼90% of MNTB neurons express *En1* and *FoxP1* (Marrs et al., 2013). Again, it may be signaling pathways downstream of engrailed that protect VNTB neurons and/or expression in targets of VNTB axons. Additionally, the timeframe for *En1* expression in the VNTB is unclear. Since the vast majority of VNTB neurons express *En1* it seems these neuronal subtypes (with the exception of MOC neurons) share the same *En1*/engrailed protection. Regardless, our results provide evidence that neurons derived from certain neuronal lineages may be less susceptible to the effects of neurodevelopmental or neurodegenerative conditions and serve as an important foundation into such protective mechanisms.

DATA AVAILABILITY STATEMENT

The raw data supporting the conclusions of this article will be made available by the authors, without undue reservation.

ETHICS STATEMENT

The animal study was reviewed and approved by the LECOM Institutional Animal Care and Use Committee.

AUTHOR CONTRIBUTIONS

YM designed the study, performed the experiments, collected and analyzed the data, created the figures, and edited and approved the manuscript. RK designed the study, provided the resources, performed the experiments, analyzed the data, created the figures, drafted the manuscript, edited and approved the manuscript. Both authors contributed to the article and approved the submitted version.

REFERENCES

Alberi, L., Sgado, P., and Simon, H. H. (2004). Engrailed genes are cell autonomously required to prevent apoptosis in mesencephalic dopaminergic neurons. *Development* 131, 3229–3236. doi: 10.1242/dev.01128

Albrecht, O., Dondzillo, A., Mayer, F., Thompson, J. A., and Klug, A. (2014). Inhibitory projections from the ventral nucleus of the trapezoid body to the medial nucleus of the trapezoid body in the mouse. *Front. Neural Circuits* 8:83. doi: 10.3389/fncir.2014.00083

Alhelo, H., and Kulesza, R. (2021). Brainstem motor neuron dysmorphology and excitatory/inhibitory imbalance in an animal model of autism. *Folia Morphol.* (in press).

Altieri, S. C., Zhao, T., Jalabi, W., Romito-DiGiacomo, R. R., and Maricich, S. M. (2016). En1 is necessary for survival of neurons in the ventral nuclei of the lateral lemniscus. *Dev. Neurobiol.* 76, 1266–1274. doi: 10.1002/dneu.22388

Altman, J., and Bayer, S. A. (1980). Development of the brain stem in the rat. III. Thymidine-radiographic study of the time of origin of neurons of the vestibular and auditory nuclei of the upper medulla. *J. Comp. Neurol.* 194, 877–904. doi: 10.1002/cne.901940410

Beltran, A. S., Graves, L. M., and Blancafort, P. (2013). Novel role of Engrailed 1 as a prosurvival transcription factor in basal-like breast cancer and engineering of interference peptides block its oncogenic function. *Oncogene* 33, 4767–4777. doi: 10.1038/onc.2013.422

Benson, T. E., and Brown, M. C. (1990). Synapses formed by olivocochlear axon branches in the mouse cochlear nucleus. *J. Comp. Neurol.* 295, 52–70. doi: 10.1002/cne.902950106

Bolton, P. F., Golding, J., Emond, A., and Steer, C. D. (2012). Autism spectrum disorder and autistic traits in the Avon Longitudinal Study of Parents and

Children: precursors and early signs. *J. Am. Acad. Child Adolesc. Psychiatry* 51, 249–260.e25. doi: 10.1016/j.jaac.2011.12.009

Bromley, R. L., Mawer, G. E., Briggs, M., Cheyne, C., Clayton-Smith, J., García-Fiñana, M., et al. (2013). Liverpool and Manchester Neurodevelopment Group. The prevalence of neurodevelopmental disorders in children prenatally exposed to antiepileptic drugs. *J. Neurol. Neurosurg. Psychiatry* 84, 637–643. doi: 10.1136/jnnp-2012-304270

Caicedo, A., and Herbert, H. (1993). Topography of descending projections from the inferior colliculus to auditory brainstem nuclei in the rat. *J. Comp. Neurol.* 328, 377–392. doi: 10.1002/cne.903280305

Chatterjee, D., Sanchez, D. S., Quansah, E., Rey, N. L., George, S., Becker, K., et al. (2019). Loss of One Engrailed1 Allele Enhances Induced α-Synucleinopathy. *J. Parkinsons Dis.* 9, 315–326. doi: 10.3233/JPD-191590

Christensen, J., Gronborg, T. K., and Sorensen, M. J. (2013). Prenatal valproate exposure and risk of autism spectrum disorders and childhood autism. *JAMA* 309, 1696–1703. doi: 10.1001/jama.2013.2270

Danesh, A. A., and Kaf, W. A. (2012). DPOAEs and contralateral acoustic stimulation and their link to sound hypersensitivity in children with autism. *Int. J. Audiol.* 51, 345–352. doi: 10.3109/14992027.2011.626202

Dannhof, B. J., Roth, B., and Bruns, V. (1991). Anatomical mapping of choline acetyltransferase (ChAT)-like and glutamate decarboxylase (GAD)-like immunoreactivity in outer hair cell efferents in adult rats. *Cell Tissue Res.* 266, 89–95. doi: 10.1007/BF00678715

Di Bonito, M., Narita, Y., Avallone, B., Sequino, L., Mancuso, M., Andolfi, G., et al. (2013). Assembly of the auditory circuitry by a Hox genetic network in the mouse brainstem. *PLoS Genet.* 9:e1003249. doi: 10.1371/journal.pgen.1003249

Dubiel, A., and Kulesza, R. J. (2016). Prenatal valproic acid exposure disrupts tonotopic c-Fos expression in the rat brainstem. *Neuroscience* 324, 511–523. doi: 10.1016/j.neuroscience.2016.01.030

Friauf, E., and Ostwald, J. (1988). Divergent projections of physiologically characterized rat ventral cochlear nucleus neurons as shown by intra-axonal injection of horseradish peroxidase. *Exp. Brain Res.* 73, 263–284. doi: 10.1007/BF00248219

Genestine, M., Lin, L., Durens, M., Yan, Y., Jiang, Y., Prem, S., et al. (2015). Engrailed-2 (En2) deletion produces multiple neurodevelopmental defects in monoamine systems, forebrain structures and neurogenesis and behavior. *Hum. Mol. Genet.* 24, 5805–5827. doi: 10.1093/hmg/ddv301

Godfrey, D. A., Park-Hellendall, J. L., Dunn, J. D., and Ross, C. D. (1987). Effect of olivocochlear bundle transection on choline acetyltransferase activity in the rat cochlear nucleus. *Hear. Res.* 28, 237–251. doi: 10.1016/0378-5955(87)90052-9

Gomes, E., Pedroso, F. S., and Wagner, M. B. (2008). Auditory hypersensitivity in the autistic spectrum disorder. *Pro Fono* 20, 279–284. doi: 10.1590/S0104-56872008000400013

Gómez-Nieto, R., Rubio, M. E., and López, D. E. (2008). Cholinergic input from the ventral nucleus of the trapezoid body to cochlear root neurons in rats. *J. Comp. Neurol.* 506, 452–468. doi: 10.1002/cne.21554

Göttlicher, M. (2004). Valproic acid: an old drug newly discovered as inhibitor of histone deacetylases. *Ann. Hematol.* 83, S91–S92.

Greenspan, S. I., and Wieder, S. (1997). Developmental patterns and outcomes in infants and children with disorders in relating and communicating: a chart review of 200 cases of children with autistic spectrum diagnoses. *J. Dev. Learn. Dis.* 1, 87–141.

Jalabi, W., Kopp-Scheinpflug, C., Allen, P. D., Schiavon, E., DiGiacomo, R. R., Forsythe, I. D., et al. (2013). Sound localization ability and glycinergic innervation of the superior olivary complex persist after genetic deletion of the medial nucleus of the trapezoid body. *J. Neurosci.* 33, 15044–15049. doi: 10.1523/JNEUROSCI.2604-13.2013

Klin, A. (1993). Auditory brainstem responses in autism: brainstem dysfunction or peripheral hearing loss?. *J. Autism Dev. Disord.* 23, 15–35. doi: 10.1007/BF01066416

Koren, G., Nava-Ocampo, A. A., Moretti, M. E., Sussman, R., and Nulman, I. (2006). Major malformations with valproic acid. *Can. Fam. Physician* 52, 441–447.

Kudo, M., Sakurai, H., Kurokawa, K., and Yamada, H. (2000). Neurogenesis in the superior olivary complex in the rat. *Hear. Res.* 139, 144–152. doi: 10.1016/S0378-5955(99)00172-0

Kulesza, R. J. Jr. (2008). Cytoarchitecture of the human superior olivary complex: nuclei of the trapezoid body and posterior tier. *Hear Res.* 241, 52–63. doi: 10.1016/j.heares.2008.04.010

Kulesza, R. J. Jr., Lukose, R., and Stevens, L. V. (2011). Malformation of the human superior olive in autistic spectrum disorders. *Brain Res.* 1367, 360–371. doi: 10.1016/j.brainres.2010.10.015

Kulesza, R. J., and Mangunay, K. (2008). Morphological features of the medial superior olive in autism. *Brain Res.* 1200, 132–137. doi: 10.1016/j.brainres.2008.01.009

Kulesza, R. J., Viñuela, A., Saldaña, E., and Berrebi, A. S. (2002). Unbiased stereological estimates of neuron number in subcortical auditory nuclei of the rat. *Hear. Res.* 168, 12–24. doi: 10.1016/S0378-5955(02)00374-X

Kuwabara, N., and Zook, J. M. (1991). Classification of the principal cells of the medial nucleus of the trapezoid body. *J. Comp. Neurol.* 314, 707–720. doi: 10.1002/cne.903140406

Kwon, S., Kim, J., Choe, B. H., Ko, C., and Park, S. (2007). Electrophysiologic assessment of central auditory processing by auditory brainstem responses in children with autism spectrum disorders. *J. Korean Med. Sci.* 22, 656–659. doi: 10.3346/jkms.2007.22.4.656

Li, S. P., Lee, H. Y., Park, M. S., Bahk, J. Y., Chung, B. C., and Kim, M. O. (2006). Prenatal GABAB1 and GABAB2 receptors: cellular and subcellular organelle localization in early fetal rat cortical neurons. *Synapse* 60, 557–566. doi: 10.1002/syn.20332

Liberman, L. D., and Liberman, M. C. (2019). Cochlear Efferent Innervation Is Sparse in Humans and Decreases with Age. *J. Neurosci.* 39, 9560–9569. doi: 10.1523/JNEUROSCI.3004-18.2019

Lukose, R., Beebe, K., and Kulesza, R. J. Jr. (2015). Organization of the human superior olivary complex in 15q duplication syndromes and autism spectrum disorders. *Neuroscience* 286, 216–230. doi: 10.1016/j.neuroscience.2014.11.033

Lukose, R., Brown, K., Barber, C. M., and Kulesza, R. J. Jr. (2013). Quantification of the stapedial reflex reveals delayed responses in autism. *Autism Res.* 6, 344–353. doi: 10.1002/aur.1297

Mabunga, D. F., Gonzales, E. L., Kim, J. W., Kim, K. C., and Shin, C. Y. (2015). Exploring the Validity of Valproic Acid Animal Model of Autism. *Exp. Neurobiol.* 24, 285–300. doi: 10.5607/en.2015.24.4.285

Main, S., and Kulesza, R. J. (2017). Repeated prenatal exposure to valproic acid results in cerebellar hypoplasia and ataxia. *Neuroscience* 340, 34–47. doi: 10.1016/j.neuroscience.2016.10.052

Mansour, Y., Ahmed, S. N., and Kulesza, R. (2021). Abnormal morphology and subcortical projections to the medial geniculate in an animal model of autism. *Exp. Brain Res.* 239, 381–400. doi: 10.1007/s00221-020-05982-w

Mansour, Y., and Kulesza, R. (2020). Three dimensional reconstructions of the superior olivary complex from children with autism spectrum disorder. *Hear. Res.* 393:107974. doi: 10.1016/j.heares.2020.107974

Mansour, Y., Mangold, S., Chosky, D., and Kulesza, R. J. Jr. (2019). Auditory Midbrain Hypoplasia and Dysmorphology after Prenatal Valproic Acid Exposure. *Neuroscience* 396, 79–93. doi: 10.1016/j.neuroscience.2018.11.016

Maricich, S. M., Xia, A., Mathes, E. L., Wang, V. Y., Oghalai, J. S., Fritzsch, B., et al. (2009). Atoh1-lineal neurons are required for hearing and for the survival of neurons in the spiral ganglion and brainstem accessory auditory nuclei. *J. Neurosci.* 29, 11123–11133. doi: 10.1523/JNEUROSCI.2232-09.2009

Marrs, G. S., Morgan, W. J., Howell, D. M., Spirou, G. A., and Mathers, P. H. (2013). Embryonic origins of the mouse superior olivary complex. *Dev. Neurobiol.* 73, 384–398. doi: 10.1002/dneu.22069

McClelland, R. J., Eyre, D. G., Watson, D., Calvert, G. J., and Sherrard, E. (1992). Central conduction time in childhood autism. *Br. J. Psychiatry* 160, 659–663. doi: 10.1192/bjp.160.5.659

Moore, S. J., Turnpenny, P., Quinn, A., Glover, S., Lloyd, D. J., Montgomery, T., et al. (2000). A clinical study of 57 children with fetal anticonvulsant syndromes. *J. Med. Genet.* 37, 489–497. doi: 10.1136/jmg.37.7.489

O'Connor, K. (2012). Auditory processing in autism spectrum disorder: a review. *Neurosci. Biobehav. Rev.* 36, 836–854. doi: 10.1016/j.neubiorev.2011.11.008

Osen, K. K., Mugnaini, E., Dahl, A. L., and Christiansen, A. H. (1984). Histochemical localization of acetylcholinesterase in the cochlear and superior olivary nuclei. A reappraisal with emphasis on the cochlear granule cell system. *Arch. Ital. Biol.* 122, 169–212.

Paxinos, G., and Watson, C. (2007). *The Rat Brain in Stereotaxic Coordinates*. London: Academic Press.

Rasalam, A. D., Hailey, H., Williams, J. H., Moore, S. J., Turnpenny, P. D., Lloyd, D. J., et al. (2005). Characteristics of fetal anticonvulsant syndrome associated autistic disorder. *Dev. Med. Child Neurol.* 47, 551–555. doi: 10.1017/S0012162205001076

Roberts, R. C., and Ribak, C. E. (1987). GABAergic neurons and axon terminals in the brainstem auditory nuclei of the gerbil. *J. Comp. Neurol.* 258, 267–280. doi: 10.1002/cne.902580207

Rodier, P. M., Ingram, J. L., Tisdale, B., Nelson, S., and Romano, J. (1996). Embryological origin for autism: developmental anomalies of the cranial nerve motor nuclei. *J. Comp. Neurol.* 370, 247–261. doi: 10.1002/(SICI)1096-9861(19960624)370:2<247::AID-CNE8>3.0.CO;2-2

Roth, D. A., Muchnik, C., Shabtai, E., Hildesheimer, M., and Henkin, Y. (2012). Evidence for atypical auditory brainstem responses in young children with suspected autism spectrum disorders. *Dev. Med. Child Neurol.* 54, 23–29. doi: 10.1111/j.1469-8749.2011.04149.x

Rumsey, J. M., Grimes, A. M., Pikus, A. M., Duara, R., and Ismond, D. R. (1984). Auditory brainstem responses in pervasive developmental disorders. *Biol. Psychiatry* 19, 1403–1418.

Saint Marie, R. L., and Baker, R. A. (1990). Neurotransmitter-specific uptake and retrograde transport of [3H]glycine from the inferior colliculus by ipsilateral projections of the superior olivary complex and nuclei of the lateral lemniscus. *Brain Res.* 524, 244–253. doi: 10.1016/0006-8993(90)90698-B

Schindelin, J., Arganda-Carreras, I., Frise, E., Kaynig, V., Longair, M., Pietzsch, T., et al. (2012). Fiji: an open-source platform for biological-image analysis. *Nat. Methods* 9, 676–682. doi: 10.1038/nmeth.2019

Schneider, T., Roman, A., Basta-Kaim, A., Kubera, M., Budziszewska, B., Schneider, K., et al. (2008). Gender-specific behavioral and immunological alterations in an animal model of autism induced by prenatal exposure to valproic acid. *Psychoneuroendocrinology* 33, 728–740. doi: 10.1016/j.psyneuen.2008.02.011

Sherriff, F. E., and Henderson, Z. (1994). Cholinergic neurons in the ventral trapezoid nucleus project to the cochlear nuclei in the rat. *Neuroscience* 58, 627–633. doi: 10.1016/0306-4522(94)90086-8

Simon, H. H., Saueressig, H., Wurst, W., Goulding, M. D., and O'Leary, D. D. (2001). Fate of midbrain dopaminergic neurons controlled by the engrailed genes. *J. Neurosci.* 21, 3126–3134. doi: 10.1523/JNEUROSCI.21-09-03126.2001

Skoff, B. F., Mirsky, A. F., and Turner, D. (1980). Prolonged brainstem transmission time in autism. *Psychiatry Res.* 2, 157–166. doi: 10.1016/0165-1781(80)90072-4

Smith, P. H., Joris, P. X., Carney, L. H., and Yin, T. C. (1991). Projections of physiologically characterized globular bushy cell axons from the cochlear nucleus of the cat. *J. Comp. Neurol.* 304, 387–407. doi: 10.1002/cne.903040305

Sonnier, L., Le Pen, G., Hartmann, A., Bizot, J. C., Trovero, F., Krebs, M. O., et al. (2007). Progressive loss of dopaminergic neurons in the ventral midbrain of adult mice heterozygote for Engrailed1. *J. Neurosci.* 27, 1063–1071. doi: 10.1523/JNEUROSCI.4583-06.2007

Thompson, A. M. (1998). Heterogeneous projections of the cat posteroventral cochlear nucleus. *J. Comp. Neurol.* 390, 439–453. doi: 10.1002/(SICI)1096-9861(19980119)390:3<439::AID-CNE10>3.0.CO;2-J

Tomchek, S. D., and Dunn, W. (2007). Sensory processing in children with and without autism: a comparative study using the short sensory profile. *Am. J. Occup. Ther.* 61, 190–200. doi: 10.5014/ajot.61.2.190

Vetter, D. E., Adams, J. C., and Mugnaini, E. (1991). Chemically distinct rat olivocochlear neurons. *Synapse* 7, 21–43. doi: 10.1002/syn.890070104

Vetter, D. E., Saldaña, E., and Mugnaini, E. (1993). Input from the inferior colliculus to medial olivocochlear neurons in the rat: a double label study with PHA-L and cholera toxin. *Hear. Res.* 70, 173–186. doi: 10.1016/0378-5955(93)90156-U

Warr, W. B. (1972). Fiber degeneration following lesions in the multipolar and globular cell areas in the ventral cochlear nucleus of the cat. *Brain Res.* 40, 247–270. doi: 10.1016/0006-8993(72)90132-1

Warr, W. B. (1975). Olivocochlear and vestibular efferent neurons of the feline brain stem: their location, morphology and number determined by retrograde axonal transport and acetylcholinesterase histochemistry. *J. Comp. Neurol.* 161, 159–181. doi: 10.1002/cne.901610203

Warr, W. B., and Beck, J. E. (1996). Multiple projections from the ventral nucleus of the trapezoid body in the rat. *Hear. Res.* 93, 83–101. doi: 10.1016/0378-5955(95)00198-0

Warr, W. B., Beck Boche, J. E., Ye, Y., and Kim, D. O. (2002). Organization of olivocochlear neurons in the cat studied with the retrograde tracer cholera toxin-B. *J. Assoc. Res. Otolaryngol.* 3, 457–478. doi: 10.1007/s10162-002-2046-6

White, J. S., and Warr, W. B. (1983). The dual origins of the olivocochlear bundle in the albino rat. *J. Comp. Neurol.* 219, 203–214. doi: 10.1002/cne.902190206

Williams, G., King, J., Cunningham, M., Stephan, M., Kerr, B., and Hersh, J. H. (2001). Fetal valproate syndrome and autism: additional evidence of an association. *Dev. Med. Child Neurol.* 43, 202–206. (Mar)., doi: 10.1111/j.1469-8749.2001.tb00188.x

Zimmerman, R., Patel, R., Smith, A., Pasos, J., and Kulesza, R. J. Jr. (2018). Repeated Prenatal Exposure to Valproic Acid Results in Auditory Brainstem Hypoplasia and Reduced Calcium Binding Protein Immunolabeling. *Neuroscience* 377, 53–68. doi: 10.1016/j.neuroscience.2018.02.030

Zimmerman, R., Smith, A., Fech, T., Mansour, Y., and Kulesza, R. J. Jr. (2020). In utero exposure to valproic acid disrupts ascending projections to the central nucleus of the inferior colliculus from the auditory brainstem. *Exp. Brain Res.* 238, 551–563. doi: 10.1007/s00221-020-05729-7

Conflict of Interest: The authors declare that the research was conducted in the absence of any commercial or financial relationships that could be construed as a potential conflict of interest.

Publisher's Note: All claims expressed in this article are solely those of the authors and do not necessarily represent those of their affiliated organizations, or those of the publisher, the editors and the reviewers. Any product that may be evaluated in this article, or claim that may be made by its manufacturer, is not guaranteed or endorsed by the publisher.

frontiers in Integrative Neuroscience

REVIEW
published: 29 September 2021
doi: 10.3389/fnint.2021.743561

Central Auditory and Vestibular Dysfunction Are Key Features of Autism Spectrum Disorder

Yusra Mansour[1,2], *Alyson Burchell*[2] *and Randy J. Kulesza*[2]*

[1]*Department of Otolaryngology, Henry Ford Macomb Hospital, Detroit, MI, United States,* [2]*Department of Anatomy, Lake Erie College of Osteopathic Medicine, Erie, PA, United States*

Autism spectrum disorder (ASD) is a neurodevelopmental disorder characterized by repetitive behaviors, poor social skills, and difficulties with communication. Beyond these core signs and symptoms, the majority of subjects with ASD have some degree of auditory and vestibular dysfunction. Dysfunction in these sensory modalities is significant as normal cognitive development depends on an accurate representation of our environment. The hearing difficulties in ASD range from deafness to hypersensitivity and subjects with ASD have abnormal sound-evoked brainstem reflexes and brainstem auditory evoked potentials. Vestibular dysfunction in ASD includes postural instability, gait dysfunction, and impaired gaze. Untreated vestibular dysfunction in children can lead to delayed milestones such as sitting and walking and poor motor coordination later in life. Histopathological studies have revealed that subjects with ASD have significantly fewer neurons in the auditory hindbrain and surviving neurons are smaller and dysmorphic. These findings are consistent with auditory dysfunction. Further, the cerebellum was one of the first brain structures implicated in ASD and studies have revealed loss of Purkinje cells and the presence of ectopic neurons. Together, these studies suggest that normal auditory and vestibular function play major roles in the development of language and social abilities, and dysfunction in these systems may contribute to the core symptoms of ASD. Further, auditory and vestibular dysfunction in children may be overlooked or attributed to other neurodevelopmental disorders. Herein we review the literature on auditory and vestibular dysfunction in ASD. Based on these results we developed a brainstem model of central auditory and vestibular dysfunction in ASD and propose that simple, non-invasive but quantitative testing of hearing and vestibular function be added to newborn screening protocols.

Keywords: brainstem, hearing, vestibuar sytem, autism, screening tools

OPEN ACCESS

Edited by:
Srdjan Vlajkovic,
The University of Auckland,
New Zealand

Reviewed by:
Juliette Elizabeth Cheyne,
The University of Auckland,
New Zealand
Carly Demopoulos,
University of California,
San Francisco, United States

***Correspondence:**
Randy J. Kulesza
rkulesza@lecom.edu

Received: *18 July 2021*
Accepted: *07 September 2021*
Published: *29 September 2021*

Citation:
Mansour Y, Burchell A and Kulesza RJ (2021) Central Auditory and Vestibular Dysfunction Are Key Features of Autism Spectrum Disorder.
Front. Integr. Neurosci. 15:743561.
doi: 10.3389/fnint.2021.743561

Abbreviations: A1, primary auditory cortex; ABR, auditory brainstem response; AN, auditory nerve; ASD, autism spectrum disorder; ASR, acoustic stapedial reflex; BIC, binaural interaction components; CNIC, central nucleus of the inferior colliculus; CN, cochlear nuclei; DCN, dorsal cochlear nucleus; DNLL, dorsal nucleus of the lateral lemniscus; DPOAE, distortion product otoacoustic emission; IC, inferior colliculus; INLL, intermediate nucleus of the lateral lemniscus; ITD, interaural timing difference; LL, lateral lemniscus; LOC, lateral olivocochlear; LSO, lateral superior olive; MOC, medial olivocochlear; MSO, medial superior olive; NT, neurotypical; OAE, otoacoustic emission; SOC, superior olivary complex; SPON, superior paraolivary nucleus; Tz, trapezoid body; VCN, ventral cochlear nucleus; vMG, ventral nucleus of the medial geniculate; VNLL, ventral nucleus of the lateral lemniscus; VNTB, ventral nucleus of the trapezoid body; VOR, vestibulo-ocular reflex.

INTRODUCTION

Autism Spectrum Disorder

Autism spectrum disorder (ASD) is a developmental disability associated with impairment in social, communicative, and behavioral domains (CDC.gov, 2021). ASD affects approximately one in 54 children and is four times more common in males. While difficulties with hearing and balance are not diagnostic signs or symptoms, children or adults with a diagnosis of ASD may have difficulty hearing or attending to speech or vocalizations despite being able to hear other environmental sounds and they may have abnormal responses to sounds. Further, large scale studies suggest that most if not all individuals with ASD have some degree of auditory dysfunction (Greenspan and Wieder, 1997) and several studies indicate brainstem and cerebellar pathological changes in ASD (Ornitz, 1969; Bauman and Kemper, 1985; Courchesne et al., 1987, 1988, 1994a,b; Ogawa, 1989; Scott et al., 2009). Herein, we review auditory and vestibular dysfunction in ASD and propose the incorporation of these modalities into screening for ASD.

The Auditory System

The mammalian auditory system begins with bilaterally situated external ears or pinnae, that serve to collect and funnel sound pressure waves through the external auditory meatus towards the tympanic membrane. Vibrations of the tympanic membrane are transferred through the ossicles in the middle ear (tympanic cavity) to the oval window. Mechanical vibrations at the oval window transduce this energy to fluid waves of endolymph in the cochlear duct. These fluid waves activate mechanoreceptive inner hair cells in the organ of Corti in the cochlea. The central auditory pathway originates with bipolar neurons in the spiral ganglion. These neurons collect information from inner hair cells through their peripheral processes and relay this information via central axons to both the dorsal and ventral cochlear nuclei (DCN and VCN, respectively) in the rostral medulla (**Figures 1A–C**). Neurons in the VCN project bilaterally to the superior olivary complex (SOC; in the caudal pons) through the trapezoid body (Tz) and the contralateral inferior colliculus (IC; midbrain) through the lateral lemniscus (LL; **Figures 1A–C**). The SOC is a collection of brainstem nuclei, and each nucleus contributes a unique circuit subserving a specific function. As a group, the SOC plays prominent roles in localization of sound sources, coding temporal and spectral features of sound, and descending modulation of the organ of Corti. Along the LL, there are ventral, intermediate, and dorsal nuclei of the lateral lemniscus (VNLL, INLL, and DNLL, respectively) that receive input from the VCN and SOC and project to the inferior colliculus (IC). The IC includes a central nucleus (CNIC), a dorsal cortex, and an external cortex. The CNIC forms an essential component of the ascending auditory pathway and sends a major projection to the medial geniculate in the thalamus and specifically the ventral nucleus of the medial geniculate (vMG). The vMG projects through the internal capsule to the primary auditory cortex (A1).

Humans have a comparatively narrow range of hearing sensitivity but are excellent low-frequency listeners. The SOC is subject to sometimes drastic interspecies variation but the core nuclei are modified to meet the specific hearing needs of the animal; accordingly, the human SOC is specialized for encoding and localizing lower frequency sounds and includes a prominent medial superior olive (MSO; Kulesza, 2007). The human MSO is composed of a thin column of neurons and each neuron forms both a medial and lateral dendrite (Kulesza, 2007; Mansour and Kulesza, 2021). Human MSO dendrites are symmetric and are distributed into the peri-MSO fields (Mansour and Kulesza, 2020, 2021). These dendrites serve to collect information from both ears: the lateral dendrite receives input from the ipsilateral ear and the medial dendrite receives input from the contralateral ear. Neurons of the MSO are often referred to as coincidence detector neurons since they function to encode differences in arrival time of sounds between the two ears—this is known as the interaural time difference (ITD). Therefore, the normal number and morphology of MSO neurons and their dendrites are required for normal ITD coding.

Along with the ascending auditory pathway described above, there is a descending pathway that begins in the cerebral cortex that includes neurons at each level of the pathway, and terminates in the cochlea (see Schofield, 2010 for a detailed review). This descending circuit is complex and integrates auditory and non-auditory inputs. The final neurons in this descending pathway are situated in the SOC and comprise two unique circuits: a medial olivocochlear system (MOC) and a lateral olivocochlear system (LOC). Neurons compromising the MOC reside mainly in the ventral nucleus of the trapezoid body (VNTB) and these neurons project to outer hair cells in the organ of Corti. This projection results in the contraction of outer hair cells, serving to reduce cochlear output to filter out background noises when listening in noisy environments. Neurons of the LOC are situated in and around the lateral superior olive (LSO). LOC neurons send axons to the ipsilateral cochlea and innervate auditory nerve axons that innervate inner hair cells. Together, olivocochlear neurons modulate the function of the cochlea to protect the cochlea from damage by loud sounds and for selective listening in background noise.

The Vestibular System

The mammalian vestibular system begins with delicate, endolymph-filled membranous labyrinths encased in each temporal bone (Lysakowski and Goldeberg, 2004). Each membranous labyrinth includes a cochlear duct, two enlarged sac-like structures—the utricle and saccule, and three semicircular canals (**Figure 2**). The utricle and saccule include collections of mechanoreceptive hair cells arranged in maculae (Lysakowski and Goldeberg, 2004). The stereocilia of the macular hair cells are embedded in an otolith membrane. Movements of the head (e.g., up and down) cause inertial movements of the otolith and mechanical activation of macular hair cells. This serves to encode linear motion and orientation of the head relative to gravity. The base of each semicircular canal includes an ampulla where it joins the utricle and each ampulla contains a crista ampullaris. The cristae are composed of mechanoreceptive hair cells with stereocilia embedded in a gelatinous matrix known as the cupula. Movements of

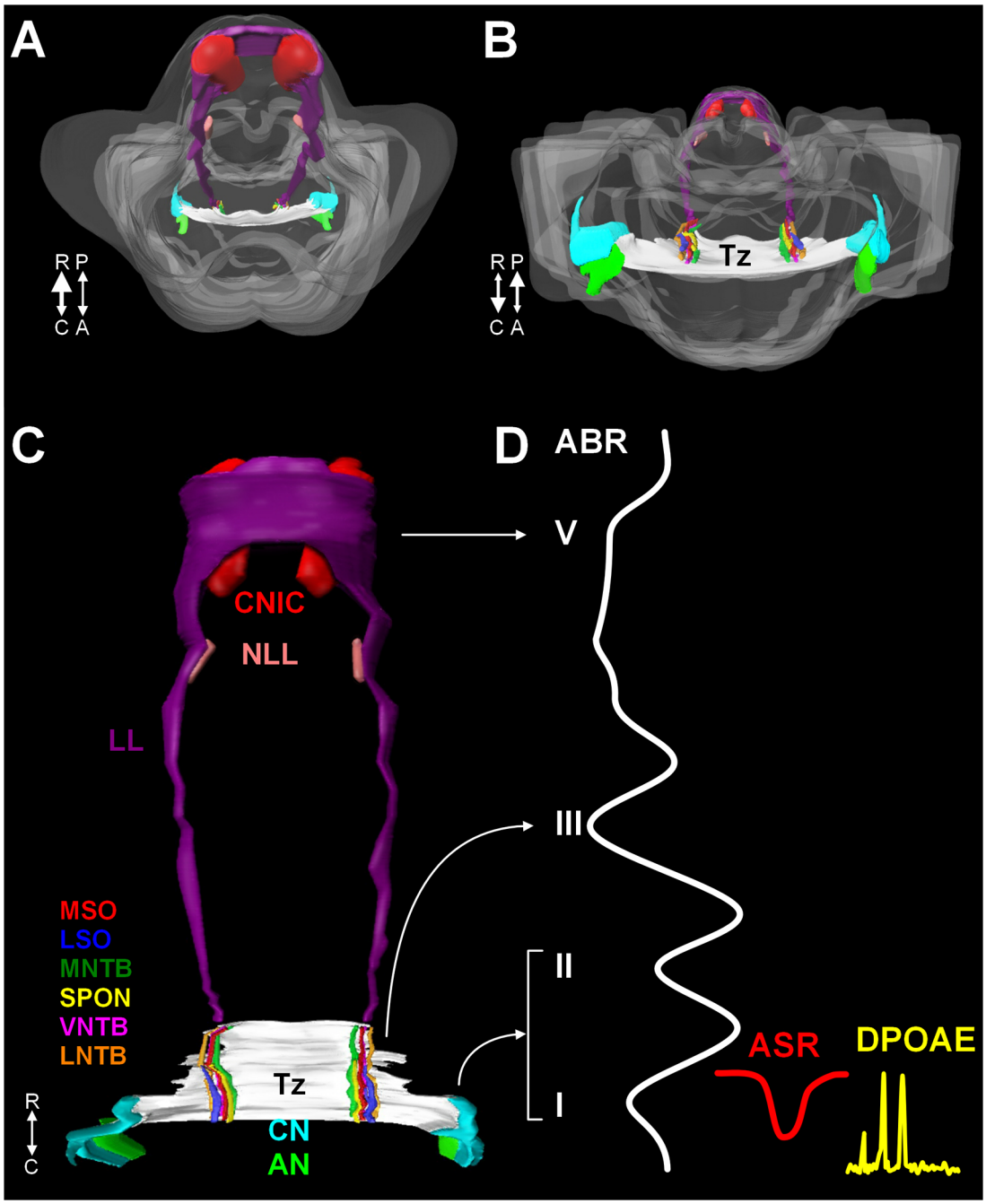

FIGURE 1 | A 3D reconstruction of the human auditory brainstem. Images **(A)** through **(C)** show 3D volume renderings of nuclei and tracts of the human auditory brainstem. Image **(A)** shows a rostral to caudal view (from midbrain down to the medulla) and **(B)** shows a caudal to rostral view (from medulla up to midbrain). Image **(C)** shows a posterior view (viewed from posterior to anterior). In **(A)** and **(B)**, the contour of the brainstem is indicated in gray. A key to the colors and nuclei/tracts is shown in figure **(C)**. The CN and SOC nuclei are limited to the rostral medulla and caudal pons. The LL extends from the caudal pons to the CNIC. Figure **(D)** shows examples of ABR, ASR, and distortion product DPOAE recordings juxtaposed to the levels of the auditory pathway they measure. Numbers in roman numerals indicate specific waves of the ABR. ABR waves I and II correspond to the AN and CN, wave III corresponds to the SOC. Waves IV and V correspond to the LL and CNIC respectively. Abbreviations: R, rostral; C, caudal; P, posterior; A, anterior; DPOAE, distortion product otoacoustic emission.

the cupula coincide with rotational movements of the head. Vestibular hair cells are innervated by peripheral processes of bipolar neurons located in the vestibular (Scarpa's) ganglion. Neurons in the vestibular ganglion send central projections to the cerebellum and four vestibular nuclei residing along the floor of the fourth ventricle in the medulla and pons (**Figure 2**). The

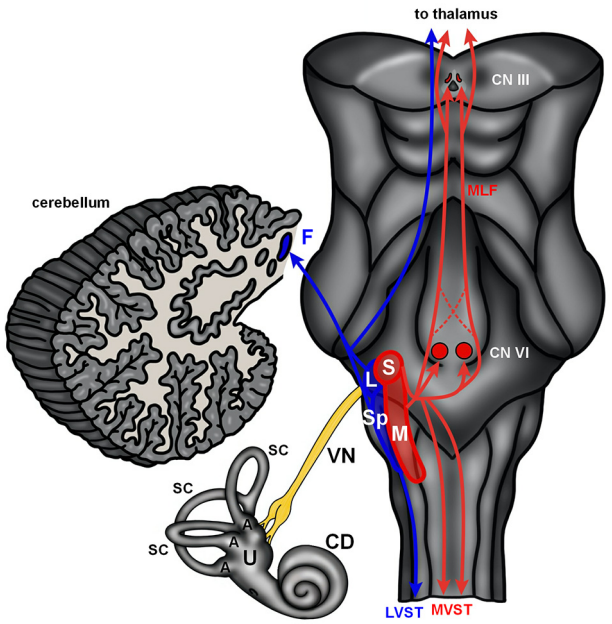

FIGURE 2 | The human vestibular brainstem. A schematic of the human vestibular pathway and vestibulocerebellum is shown. Vestibular hair cells are housed in cristae found in the ampulla (A) of the three semicircular canals (SC), and macula situated in both the utricle (U) and saccule. These hair cell collections are innervated by the vestibular division of the vestibulocochlear nerve. The vestibular nerve (VN) projects to the vestibular nuclei (red and blue contours) that extend from the medulla into the caudal pons. The lateral (L) and spinal (Sp) vestibular nuclei project to the fastigial nucleus (F) in the cerebellum and spinal cord *via* the lateral vestibulospinal tract (LVST). The superior (S) and medial (M) nucleus project to the spinal cord *via* the medial vestibular spinal tract (MVST) and nuclei controlling extraocular muscles (CN VI—abducens nucleus; CN III—oculomotor nucleus) *via* the medial longitudinal fasciculus (MLF). The vestibular nuclei also send projections to the thalamus. Abbreviations: CD, cochlear duct.

superior and medial vestibular nuclei (**Figure 2**, red) receive their major inputs from the cristae and project along the medial vestibulospinal tracts and medial longitudinal fasciculus to nuclei controlling the extraocular muscles and to the cervical spinal cord to control gaze and maintain a stable platform for the eyes. The lateral vestibular nucleus (Deiters' nucleus) receives input from the cristae and macula and projects through the lateral vestibulospinal tract to influence postural reflexes (**Figure 2**, blue). The spinal (descending) nucleus receives input from the otolith organs and projects to the cerebellum, reticular formation, and spinal cord to regulate posture. Information from the vestibular ganglion and vestibular nuclei target the fastigial nucleus and flocculonodular lobe of the cerebellum (**Figure 2**, blue). Together, the vestibular apparatus and associated central connections encode movements of the head and direct adjustments to eye position, muscle tone, and body posture (Lysakowski and Goldeberg, 2004). Like the auditory hair cells, the vestibular sensory organs receive efferent innervation from cholinergic neurons near the genu of the facial nerve (Warr, 1975).

Autism Spectrum Disorder and CN VIII Dysfunction

Auditory Dysfunction in ASD

Autism spectrum disorder (ASD) is a neurodevelopmental disorder characterized by difficulties in social, communicative, and behavioral domains (CDC.gov, 2021). The most recent reports indicate that ASD impacts one in 54 children with a strong predilection for males (CDC.gov, 2021). One of the key signs/symptoms of ASD is abnormal responses to sensory stimuli. This can manifest as hypersensitivity or overreactions involving somatic sensations (touch) or special senses (smell, vision, and hearing). Beyond abnormal responses to sound, auditory dysfunction is present in most, if not all individuals with ASD (Greenspan and Wieder, 1997; Tomchek and Dunn, 2007; Bolton et al., 2012). This dysfunction ranges from deafness to hyperacusis and often includes difficulty listening to background noise and understanding speech (Roper et al., 2003; Alcántara et al., 2004; Khalfa et al., 2004; Szelag et al., 2004; Teder-Sälejärvi et al., 2005; Gravel et al., 2006; Tharpe et al., 2006; Russo et al., 2009). Collet et al. (1993) were the first to suggest the hyperacusis observed in ASD might be related to abnormalities in the MOC system. Consistent with these reports, hearing difficulties have been proposed as a cardinal indicator of ASD (Osterling and Dawson, 1994).

Interestingly, involvement of the auditory system in ASD was suspected in the original report of autistic children in 1943. One of the common findings in these children was difficulty with language and hypersensitivity to loud noises (Kanner, 1943). Observations from a study of auditory-evoked potentials further supported the idea of auditory involvement (Ornitz et al., 1968). Additional studies of individuals with ASD implicated problems with processing language (Hermelin and Frith, 1971), focusing on multiple sounds or stimuli (Reynolds et al., 1974), conductive hearing loss (Smith et al., 1988) and hyposensitivity, or hypersensitivity depending on the stimulus modality (Ornitz et al., 1968; Hayes and Gordon, 1977; Rosenhall et al., 1999). A number of studies also suggested difficulties in processing complex sounds such as speech. Specifically, (Koegel and Schreibman, 1976) reported on a child with ASD who appeared to be deaf for complex sounds (white noise) but responded to environmental sounds at normal thresholds. A review of 1st birthday home videos revealed that children with ASD often failed to orient to their name being called (Osterling and Dawson, 1994), have a clear preference for noise or non-verbal sounds over speech and vocalizations (Klin, 1991, 1993) or frank impairment for speech sounds (Ceponiene et al., 2003; Jeste and Nelson, 2009; Bidet-Caulet et al., 2017; Jayanath and Ozonoff, 2020).

The auditory dysfunction in ASD has been studied and characterized by numerous researchers using fairly simple, non-invasive techniques. The acoustic stapedial reflex (ASR) has been utilized to examine the function of the lower auditory brainstem, facial nucleus, and contraction of the stapedius muscle in subjects with ASD with some conflicting results (**Figure 1D**; Gravel et al., 2006; Tharpe et al., 2006; Gomes et al., 2008). Specifically, only Gomes found that subjects with ASD

had lower thresholds relative to neurotypical (NT) individuals. (Gravel et al., 2006) found no significant differences between control children and subjects with ASD in cohorts that were matched by age and hearing threshold. We examined the ASR in a group of 29 neurotypical children (ages 7–17 years) and 54 children and young adults with high-functioning ASD (ages 4–23 years; Lukose et al., 2013). The subjects with ASD had significantly lower thresholds (i.e., hypersensitivity), and significantly longer response latencies. The longer latencies were most commonly observed in response to a 1 kHz tone presented in the ipsilateral ear. In all NT subjects, ipsilateral reflex responses always occurred at shorter latencies compared to contralateral reflex responses regardless of tone frequency. However, in subjects with ASD, this clear and predictable pattern of slower ipsilateral responses was not always found. Specifically, when we stimulated the left ear of subjects with ASD, the ipsilateral reflex responses occurred at a significantly longer latency compared to the contralateral response. Finally, in our study of the ASR, 97% of subjects with ASD had at least one response outside the 95% confidence interval of NT responses. Regardless, our results are based on a relatively small group of children and young adults—whether these findings can be generally extended to subjects with ASD will require further investigation.

The ABR is a sound-evoked response of synchronized brain activity and each peak or wave corresponds to a particular level of the auditory brainstem pathway (**Figure 1D**). The ABR has provided the most insight into the function of brainstem centers in ASD. The majority of studies of the ABR in subjects with ASD over the past 40 years provide evidence that subjects with ASD have smaller amplitudes in waves I, II, III, IV, and V (Ornitz et al., 1972; Gillberg et al., 1983; Martineau et al., 1987, 1992; Klin, 1993), longer latencies between waves I-III and waves I-V (Taylor et al., 1982), and longer latencies/slower responses (Ornitz, 1969; Student and Sohmer, 1978; Rosenblum et al., 1980; Sohmer, 1982; Tanguay et al., 1982; Gillberg et al., 1983; Sersen et al., 1990; Thivierge et al., 1990; Wong and Wong, 1991; Maziade et al., 2000; Kwon et al., 2007; Roth et al., 2012; Azouz et al., 2014; Taş et al., 2017; Miron et al., 2018, 2021; Ramezani et al., 2019; Delgado et al., 2021; reviewed in Talge et al., 2018). These longer latency and lower amplitude responses have been attributed to the immaturity of brainstem circuits (Li et al., 2020). A recent study showed delays in speech-based ABRs (Chen et al., 2019) and reduced binaural interaction components (BIC) of the ABR in subjects with ASD (ElMoazen et al., 2020). The latter study also found a significant positive correlation between the amplitude of the BIC ABR waveform and both language and social scores in subjects with ASD (ElMoazen et al., 2020).

The literature provides convincing evidence that ABRs can be used as a screening instrument for the risk of ASD and/or other neurodevelopmental disorders. Specifically, a prospective study of ABRs found that young children (birth to 3 months) with longer wave V latencies and I-V interpeak latencies were later diagnosed with ASD (Miron et al., 2016). Consistent with observed asymmetries in ASR and otoacoustic emissions (OAEs; see below), these authors found longer III-V interpeak latencies when stimulating the right ear only. In fact, these changes in wave V have a positive predictive value of 78% and a negative predictive value of 73% for wave V. These differences in subjects with ASD can be further illustrated with masking experiments. Such paradigms revealed abnormal interpeak latencies between waves I-V and III-V (Thivierge et al., 1990), the reduced amplitude of wave III (Källstrand et al., 2010), and asymmetric masking by contralateral noise (Khalfa et al., 2001).

While ASR and ABRs examine brainstem circuits, the function of the cochlea can be evaluated using otoacoustic emissions (OAEs). Similar to the asymmetry seen in ASR testing, subjects with ASD exhibited abnormal OAEs with marked asymmetry (Khalfa et al., 2001) and significantly reduced responses in the 1 kHz ranges (Bennetto et al., 2017). However, other researchers have found hypersensitivity or elevated responses (Danesh and Kaf, 2012; Taş et al., 2017). These conflicting results might be attributed to differences in subjects, equipment, and/or interpretation of the data. Also, the direct involvement of the cochlea in ASD is unclear. While OAEs provide an objective measure of the auditory function, its value as a screening tool is unclear. Beyond differences in ASR, OAEs, and ABRs, there is abundant evidence for additional problems in auditory processing in ASD. Specifically, subjects with ASD have difficulties with temporal processing (Russo et al., 2008; Bhatara et al., 2013; Foss-Feig et al., 2017), difficulties listening in the presence of background noise (Alcántara et al., 2004; Teder-Sälejärvi et al., 2005) and problems with sound localization tasks (Osterling and Dawson, 1994; Baranek, 1999; Werner et al., 2000; Dawson et al., 2004; Lodhia et al., 2014, 2018). Finally, there are reports of dysfunction in the auditory forebrain. This includes weaker interhemispheric projections, stronger projections from the thalamus to the cortex in subjects with ASD (Linke et al., 2018), and right-left asymmetries of the secondary auditory cortex (Orekhova et al., 2012; Azouz et al., 2014). Additionally, there is evidence for abnormalities in cortical evoked auditory potentials (reviewed in O'Connor, 2012). It is unclear if these forebrain abnormalities result from dysfunction of brainstem centers or if the auditory forebrain is an additional primary site of injury in ASD. Therefore, it seems very likely that the difficulties children with ASD have developing language is intimately related to problems encoding and understanding the complex temporal and spectral features of speech.

Taken together, these studies implicate the lower auditory brainstem as a key site, if not the origin of abnormal circuitry and dysfunction in ASD. These changes can be identified in young children and can be assessed at birth. It is important to recognize that identification of these differences requires careful analysis of the responses. Newborn hearing screenings are often superficial and many children with auditory dysfunction pass these newborn screens or are missed on follow-up testing. In fact, a recent study demonstrates that childred who failed newborn ABR screens but were diagnosed with normal hearing at follow-up were five to 10 times more likely to be diagnosed with ASD (Tu et al., 2020). We hypothesize the majority of children that will be diagnosed with ASD have these hearing issues at birth and are missed by routine newborn screening because they have clinically normal hearing thresholds. Consistent with this hypothesis, only a small number of children with ASD have

abnormal pure tone audiometry results, but when combined with comprehensive auditory screening (including audiometry, tympanometry, acoustic reflexes, OAE, and ABR) more than half of the subjects have an abnormal result; regardless subjects with ASD who pass these screens can still have difficulty with speech and language tasks (Demopoulos and Lewine, 2016).

Auditory Brainstem Dysmorphology in ASD

A number of imaging studies revealed smaller cerebella and brainstems in subjects with ASD (Courchesne et al., 1988, 1994a,b; Gaffney et al., 1988; Murakami et al., 1989; Ciesielski et al., 1990; Hashimoto et al., 1992, 1993, 1995; Kleiman et al., 1992; Piven et al., 1992). Postmortem neuropathological studies confirmed that subjects with ASD have consistent dysmorphology in the brainstem and cerebellum (Williams et al., 1980; Bauman and Kemper, 1985; Bauman, 1991; Ritvo et al., 1986; Arin et al., 1991; Rodier et al., 1996; Bailey et al., 1998; Kulesza and Mangunay, 2008; Kulesza et al., 2011; Lukose et al., 2015; Mansour and Kulesza, 2020). Specifically, these studies revealed fewer cerebellar Purkinje cells and hypoplasia of the facial nucleus and SOC. Further investigations by Wegiel and coworkers revealed multifocal heterotopias and dysplasias in the forebrain and cerebellum and significantly fewer cerebellar Purkinje cells (Wegiel et al., 2010, 2014). Together, these findings support multiple sites of impaired neurogenesis, neuronal migration, and/or neuron survival in ASD (Wegiel et al., 2010, 2014).

Some of the first evidence for focal brainstem deficits in ASD was the work of Rodier and colleagues (Rodier et al., 1996). These researchers found significant hypoplasia of the facial nucleus and SOC, abnormal bundles of axons related to the hypoglossal nucleus, and significant reduction in the rostrocaudal length of the pons. Based on their finding of changes in the SOC, together with reports of gross brainstem dysmorphology and hearing difficulties in ASD, we hypothesized these hearing difficulties are directly related to dysmorphology of lower auditory brainstem centers. We investigated this hypothesis first by studying the brainstems of five subjects with ASD (8–32 years of age) and two typical developing controls (26–29 years of age; Kulesza and Mangunay, 2008). A preliminary study of these specimens revealed noticeable changes in the MSO and we, therefore, focused our analysis on this nucleus. Our previous study of over 85 brainstems from NT subjects revealed the human MSO is composed of a thin column of 13–14,000 neurons (Kulesza, 2007; Lukose et al., 2015; Mansour and Kulesza, 2021) each emitting medial and lateral dendrites collecting input from the contralateral and ipsilateral ears, respectively (Mansour and Kulesza, 2021). The structure and arrangement of MSO neurons is essential to their function of encoding ITDs. We discovered that the MSO from subjects with ASD have significantly smaller neurons and the majority of these neurons have round/oval soma. We also found these neurons are abnormally oriented within the MSO. We then studied a larger cohort of brainstems, from nine subjects with ASD (2–36 years of age) and four NT individuals (4–32 years of age; Kulesza et al., 2011). In this study we analyzed all six SOC nuclei and found fewer and significantly smaller neurons in five of the six constituent nuclei; only the VNTB was unaffected (Lukose et al., 2011). Subjects with ASD also had extracellular eosinophilic fibers, hypergliosis around the MSO, and in two subjects (two of nine; ∼22%) clusters of ectopic neurons in the pontine tegmentum. We then extended this to an even larger cohort including 10 NT subjects (3–32 years of age), 16 subjects with ASD (5–56 years of age) and 12 subjects with ASD and a duplication of the *q* region of chromosome 15 [dup(15q)] (5–39 years of age; Lukose et al., 2015). In this cohort, we found fewer and smaller neurons in all SOC nuclei except the VNTB. Consistent with our previous studies, the MSO was the most severely affected nucleus in the SOC. In NT subjects, the MSO included about 13,000 neurons. In subjects with ASD or ASD + dup(15q), there were only about 5,400 neurons in the MSO and these neurons were significantly smaller, more round, and abnormally arranged in the nucleus. The peri-MSO was also significantly smaller in subjects with ASD (Mansour and Kulesza, 2020) and we interpret this finding to suggest that dendrites of MSO neurons are significantly shorter and less complex than NT subjects. Consistent with this hypothesis, human MSO neurons from subjects with ASD are smaller, more circular, and emit smaller caliber primary dendrites (Kulesza et al., 2011; Lukose et al., 2015). In this cohort, we compared the total number of MSO neurons with the subject's Autism Diagnostic Interview-Revised (combined social, communication, and behaviors scores); however, there was no relationship between these values. Our previous studies of the human MSO from NT subjects revealed round/oval neurons are more common in younger subjects (<10 years of age). Therefore, we interpret the presence of round/oval neurons in the adult MSO of subjects with ASD to indicate brainstem immaturity or arrested development. In this study, we also found ectopic clusters of neurons in the caudal pontine tegmentum. We believe these ectopic cells to be neurons lost during migration—neurons possibly destined for the SOC that never arrived and therefore fail to participate in auditory circuits. Recently, we constructed 3D volumetric models of the human SOC nuclei from young neurotypical subjects and subjects with ASD (Mansour and Kulesza, 2020). Consistent with our previous studies, we found that in ASD, all of the SOC nuclei except the VNTB occupy smaller volumes and this was not related to overall brain size. Our findings of severe dysmorphology and neuronal loss in the MSO of subjects as young as 2 years old and the observation of Purkinje cell loss with an intact inferior olive are consistent with developmental dysfunction before 28–30 weeks of gestation (Bauman and Kemper, 2005). Further, we propose that deficits in higher degree auditory function result from abnormal coding of temporal and spectral features by the cochlear nuclei (CN) and SOC. Based on our consistent observations of dysmorphology, we propose the MSO be added to the claustrum and cerebellar Purkinje cells as neuropathological hallmarks of ASD (Wegiel et al., 2014).

Modified Auditory Brainstem Circuitry in ASD

It is important to note that ASD is a spectrum disorder and not all individuals are affected to the same degree. Indeed, our morphological studies show not all subjects have the same degree of hypoplasia, the number of ectopic neurons,

or gliosis. We attribute hyposensitivity to sound to result from fewer neurons, smaller axons, and abnormal ascending projections to the CNIC. These changes undoubtedly contribute to changes in the ABR and ASR, problems with vocalizations and localization of sound sources and likely contribute extensively to dysfunction of the auditory forebrain. We believe that hypersensitivity and difficulty listening in background noise likely result from changes in the number of SOC or facial nucleus neurons, and/or their connectivity or alterations in the organ of Corti.

We have recently demonstrated that human MSO neurons form symmetric medial and lateral dendrites, that glycinergic inputs are segregated to the cell body and proximal dendrites while excitatory inputs are arranged further distally (Mansour and Kulesza, 2021). These features are crucial for normal MSO function. In subjects with ASD, not only are there fewer MSO neurons but these neurons are smaller, their dendrites are significantly shorter and issued in almost random directions (**Figure 3**). We believe that in ASD, the reduction in the size of dendrites results in less area for collecting and integrating inputs from the ipsilateral and contralateral ears, and the random arrangement likely results in a poorly organized tonotopic map in the MSO (**Figure 3**). As a result, MSO neurons are not able to precisely extract timing and spectral information from their binaural inputs. Furthermore, there is a significant reduction in the number of MSO neurons and likely reduced projection from the MSO and SOC. Together, these findings suggest that not only is there a significant reduction in the MSO and SOC projection to the CNIC, but also this input is not carrying the same type/quality of information about the auditory environment. We proposed that the changes observed by many researchers in ABRs can be attributed to the reduced number of brainstem neurons, smaller, poorly myelinated axons, and/or abnormal patterns of activation in the auditory nerve (AN), Tz, LL. Accordingly, we believe that subjects with ASD fail to encode many complex features of vocalizations and may miss subtle features and auditory cues.

The VNTB functions in multiple aspects of hearing including descending modulation of the cochlea and fine-tuning local and ascending circuits. In subjects with ASD, we have found no changes in size or number of VNTB neurons or volume occupied by this nucleus. The descending projection from the VNTB to the cochlea has an identified role in filtering sound necessary for listening in background noise. However, subjects with ASD have difficulties listening to background noise. We have yet to assess the connectivity of the VNTB in human subjects. But we have examined projections of the VNTB in an animal model of ASD and found no differences from control animals (this issue, Mansour and Kulesza, 2021). However, in human subjects, it is unclear if VNTB projections are intact and/or have normal function. A recent study showed abnormal OAEs in subjects with ASD (Bennetto et al., 2017) implicating dysfunction of the organ of Corti. Morphological studies of the cochlea, including afferent and efferent innervation, from subjects with ASD, will clarify the structural and functional roles of the sensory receptors in this condition.

Vestibular and Cerebellar Issues in ASD

A number of early morphological studies of subjects with ASD suggested the brainstem as the origin of dysfunction (Ornitz, 1969; Ogawa, 1989). Some of the first support for this hypothesis was provided by imaging studies revealing changes in the cerebellum (Bauman and Kemper, 1985; Courchesne et al., 1987, 1988, 1994a,b; Scott et al., 2009). Specifically, these studies found hypoplasia of the cerebellar vermis involving lobules VI and VII and more widespread involvement of the vermis including lobules I-V and VIII-X (Courchesne et al., 1994a,b; Levitt et al., 1999). Consistent with these imaging studies, microscopic

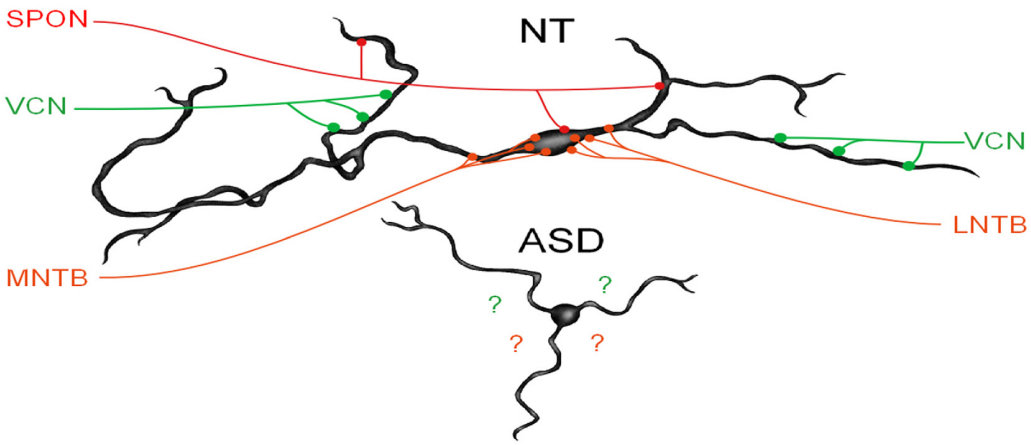

FIGURE 3 | MSO dysmorphology in ASD. The top image shows a reconstruction of a human MSO neuron (Mansour and Kulesza, 2021). Human MSO neurons have slender cell bodies that form symmetric dendrites on both the medial and lateral sides of the MSO cell column. MSO neurons receive symmetric glutamatergic input from both ipsilateral and contralateral VCN and these are distributed symmetrically on distal dendrites, glycinergic inputs are distributed primarily on the cell body and proximal dendrites and originate from the medial and lateral nuclei of the trapezoid body (MNTB and LNTB, respectively). Additionally, there are GABAergic inputs from the superior paraolivary nucleus (SPON). MSO neurons integrate these precisely arranged and timed inputs to extract spectral and temporal features of sound. MSO neurons in subjects with ASD lack the same morphology and distribution and the arrangement of these inputs are unknown.

studies of the cerebellum revealed variable changes in the size of cerebellar Purkinje cells, with fewer Purkinje cells in the posterior cerebellum and occasionally the vermis and fewer neurons in the deep cerebellar nuclei in ASD (Bauman et al., 1995; Bauman, 1996). However, other studies have shown no difference in cerebellum size/volume between subjects with ASD and NT subjects (Scott et al., 2009). These conflicting results in cerebellum morphology might be attributed to variations amongst study subjects, ASD severity, or diagnoses. Indeed, detailed and systematic studies of the cerebellum and brainstem are needed to fully appreciate how these brain regions are impacted in ASD.

While motor signs and symptoms are not diagnostic features of ASD, deficits in motor skills and coordination are receiving more attention (Gernsbacher et al., 2008; Bhat et al., 2012; Lai et al., 2014; Sacrey et al., 2014). Further, several studies have demonstrated dysfunction of the vestibular system and/or vestibular circuits in the cerebellum. A number of early studies indicated that subjects with ASD have postural issues, problems with balance (Ritvo et al., 1969; Ornitz, 1970; Molloy et al., 2003; Smoot Reinert et al., 2015), and abnormal responses to vestibular stimulation (Slavik et al., 1984). Specifically, after rotational stimulation subjects with ASD had a slower onset of the primary nystagmus response and fewer beats during the secondary response (Ornitz et al., 1985). Subjects with ASD have irregular patterns of horizontal gaze, abnormal rotation-induced vestibulo-ocular reflexes (VOR), and VOR-based tasks that were attributed to abnormal cerebellum and brainstem circuitry (Carson et al., 2017; Caldani et al., 2020). VOR has been proposed to serve some diagnostic value in ASD (Thabet, 2014). Young subjects with ASD have longer latency saccades compared to age-matched neurotypical controls (Furman et al., 2015). In a recent population-based study of over 10 million neurotypical and 61,000 children with ASD, it was found that ophthalmic dysfunction was far more common in children with ASD (Chang et al., 2021). Specifically, ophthalmic dysfunction was present in ∼14% of children with ASD, that strabismus was four times more common, and nystagmus was nearly 10 times more common in ASD. Interestingly, in a study of 62 subjects with ASD, end-stage nystagmus was associated with better performance on language, cognitive and motor screens (Pineda et al., 2015). Vestibular involvement in ASD is not as clear as auditory issues—in a study of 79 subjects with ASD ranging in age from 5–52 years of age there was no difference in responses to rotational stimulation (Furman et al., 2015) and in a study of 13 children with ASD there was no difference in post-rotary nystagmus (Goldberg et al., 2000). But, children with ASD have abnormal postural responses after vestibular stimulation (Smoot Reinert et al., 2015). Vestibular issues are likely under-reported in children with ASD and may go unrecognized. This is significant as unidentified, or untreated vestibular issues in childhood can have a number of poor outcomes. In particular, normal vestibular function is required for normal posture and gaze, development of fine motor skills, proper cognitive development and educational performance, and emotional and social behavior (reviewed in Van Hecke et al., 2019). The cerebellum also receives input from a number of non-motor/somatosensory sources and projects widely over the neuroaxis. Consistent with these projections, there is evidence that the cerebellum is involved in multiple functions beyond motor coordination via projections to the hippocampus, amygdala, and septal nuclei (Heath, 1973; Heath and Harper, 1974).

SUMMARY AND CONCLUSIONS

The literature provides abundant evidence for both structural and functional hearing deficits in ASD. These findings are consistent with key signs and symptoms, specifically that individuals with ASD appear unaware when people talk to them, but respond to non-verbal sounds, repeat words or phrases in place of normal speech and have abnormal reactions to sensory stimulation (CDC.gov, 2021). Importantly, both functional and anatomical investigations indicate these auditory problems are present at birth. Consistent with these findings, we propose that qualitative ABRs or ASRs be used to screen for ASD risk (Lukose et al., 2013; Mansour and Kulesza, 2020; in accordance with other researchers: Grewe et al., 1994). Observations of spontaneous nystagmus and testing of VORs are also simple and non-invasive. The literature also provides evidence for vestibular dysfunction in children diagnosed with ASD. Similarly, if these vestibular issues can be identified in the early postnatal period, they could lead to early diagnosis of ASD and/or raise suspicion for other neurodevelopmental conditions. The addition of vestibular assessment to a neonatal auditory testing panel, we believe, would only improve the diagnostic power of early screening. Accordingly, future research in this area should be centered on determining the predictive value of combined auditory and vestibular testing on newborns for diagnosis of ASD and/or other neurodevelopmental disorders. Currently, almost all US states require newborn hearing screening[1], although these tests are considered only on a pass/fail basis. We propose these initial screenings be evaluated on a quantitative basis to better stratify the risk of an ASD diagnosis. The addition of simple, noninvasive vestibular screening will only increase the value of auditory and vestibular assessment. Of course, the goal of early detection and diagnosis of ASD is early intervention to improve the quality of life and ensure the best possible outcomes and social/academic integration. There is evidence that early intervention for children with ASD focusing on eye contact, gesturing, and vocalizations results in significant improvements in the child's language and social interactions (Wong and Kwan, 2010).

AUTHOR CONTRIBUTIONS

YM: literature review, made figures, and revised the manuscript. AB: literature review and revised manuscript. RK: literature review, wrote draft, made figures, and revised the manuscript. All authors contributed to the article and approved the submitted version.

[1]CDC.gov/ncbddd/hearingloss/screening.html

REFERENCES

Alcántara, J. I., Weisblatt, E. J., Moore, B. C., and Bolton, P. F. (2004). Speech-in noise perception in high-functioning individuals with autism or Asperger's syndrome. *J. Child Psychol. Psychiatry* 45, 1107–1114. doi: 10.1111/j.1469-7610.2004.t01-1-00303.x

Arin, D. M., Bauman, M. L., and Kemper, T. L. (1991). The distribution of Purkinje cell loss in the cerebellum in autism. *Neurology* 41:307.

Azouz, H. G., Kozou, H., Khalil, M., Abdou, R. M., and Sakr, M. (2014). The correlation between central auditory processing in autistic children and their language processing abilities. *Int. J. Pediatr. Otorhinolaryngol.* 78, 2297–2300. doi: 10.1016/j.ijporl.2014.10.039

Bailey, A., Luthert, P., Dean, A., Harding, B., Janota, I., Montgomery, M., et al. (1998). A clinicopathological study of autism. *Brain* 121, 889–905. doi: 10.1093/brain/121.5.889

Baranek, G. T. (1999). Autism during infancy: a retrospective video analysis of sensory-motor and social behaviors at 9–12 months of age. *J. Autism Dev. Disord.* 29, 213–224. doi: 10.1023/a:1023080005650

Bauman, M. L. (1991). Microscopic neuroanatomic abnormalities in autism. *Pediatrics* 87, 791–796.

Bauman, M. L. (1996). Brief report: neuroanatomic observations of the brain in pervasive developmental disorders. *J. Autism Dev. Disord.* 26, 199–203. doi: 10.1007/BF02172012

Bauman, M., and Kemper, T. L. (1985). Histoanatomic observations of the brain in early infantile autism. *Neurology* 35, 866–874. doi: 10.1212/wnl.35.6.866

Bauman, M. L., and Kemper, T. L. (2005). Neuroanatomic observations of the brain in autism: a review and future directions. *Int. J. Dev. Neurosci.* 23, 183–187. doi: 10.1016/j.ijdevneu.2004.09.006

Bauman, M. L., Kemper, T. L., and Arin, D. M. (1995). Microscopic observations of the brain in Rett syndrome. *Neuropediatrics* 26, 105–108. doi: 10.1055/s-2007-979737

Bennetto, L., Keith, J. M., Allen, P. D., and Luebke, A. E. (2017). Children with autism spectrum disorder have reduced otoacoustic emissions at the 1 kHz mid-frequency region. *Autism Res.* 10, 337–345. doi: 10.1002/aur.1663

Bhat, A. N., Galloway, J. C., and Landa, R. J. (2012). Relation between early motor delay and later communication delay in infants at risk for autism. *Infant Behav. Dev.* 35, 838–846. doi: 10.1016/j.infbeh.2012.07.019

Bhatara, A., Babikian, T., Laugeson, E., Tachdjian, R., and Sininger, Y. S. (2013). Impaired timing and frequency discrimination in high-functioning autism spectrum disorders. *J. Autism Dev. Disord.* 43, 2312–2328. doi: 10.1007/s10803-013-1778-y

Bidet-Caulet, A., Latinus, M., Roux, S., Malvy, J., Bonnet-Brilhault, F., and Bruneau, N. (2017). Atypical sound discrimination in children with ASD as indicated by cortical ERPs. *J. Neurodev. Disord.* 9:13. doi: 10.1186/s11689-017-9194-9

Bolton, P. F., Golding, J., Emond, A., and Steer, C. D. (2012). Autism spectrum disorder and autistic traits in the Avon Longitudinal Study of Parents and Children: precursors and early signs. *J. Am. Acad. Child Adolesc. Psychiatry* 51, 249–260. doi: 10.1016/j.jaac.2011.12.009

Caldani, S., Baghdadi, M., Moscoso, A., Acquaviva, E., Gerard, C. L., Marcelli, V., et al. (2020). Vestibular functioning in children with neurodevelopmental disorders using the functional head impulse test. *Brain Sci.* 10:887. doi: 10.3390/brainsci10110887

Carson, T. B., Wilkes, B. J., Patel, K., Pineda, J. L., Ko, J. H., Newell, K. M., et al. (2017). Vestibulo-ocular reflex function in children with high-functioning autism spectrum disorders. *Autism Res.* 10, 251–266. doi: 10.1002/aur.1642

CDC.gov. (2021). Autism Spectrum Disorder (ASD). Available online at: http://www.cdc.gov/ncbddd/autism/index.html. Accessed November 19, 2017.

Ceponiene, R., Lepistö, T., Shestakova, A., Vanhala, R., Alku, P., Näätänen, R., et al. (2003). Speech-sound-selective auditory impairment in children with autism: they can perceive but do not attend. *Proc. Natl. Acad. Sci. U S A* 100, 5567–5572. doi: 10.1073/pnas.0835631100

Chang, M. Y., Doppee, D., Yu, F., Perez, C., Coleman, A. L., and Pineles, S. L. (2021). Prevalence of ophthalmologic diagnoses in children with autism spectrum disorder using the optum dataset: APopulation-based study. *Am. J. Ophthalmol.* 221, 147–153. doi: 10.1016/j.ajo.2020.08.048

Chen, J., Liang, C., Wei, Z., Cui, Z., Kong, X., Dong, C. J., et al. (2019). Atypical longitudinal development of speech-evoked auditory brainstem response in preschool children with autism spectrum disorders. *Autism Res.* 12, 1022–1031. doi: 10.1002/aur.2110

Ciesielski, K. T., Courchesne, E., and Elmasian, R. (1990). Effects of focused selective attention tasks on event-related potentials in autistic and normal individuals. *Electroencephalogr. Clin. Neurophysiol.* 75, 207–220. doi: 10.1016/0013-4694(90)90174-i

Collet, L., Roge, B., Descouens, D., Moron, P., Duverdy, F., and Urgell, H. (1993). Objective auditory dysfunction in infantile autism. *Lancet* 342, 923–924. doi: 10.1016/0140-6736(93)91969-s

Courchesne, E., Hesselink, J. R., Jernigan, T. L., and Yeung-Courchesne, R. (1987). Abnormal neuroanatomy in a nonretarded person with autism. Unusual findings with magnetic resonance imaging. *Arch. Neurol.* 44, 335–341. doi: 10.1001/archneur.1987.00520150073028

Courchesne, E., Saitoh, O., Townsend, J. P., Yeung-Courchesne, R., Press, G. A., Lincoln, A. J., et al. (1994a). Cerebellar hypoplasia and hyperplasia in infantile autism. *Lancet* 343, 63–64. doi: 10.1016/s0140-6736(94)90923-7

Courchesne, E., Townsend, J., and Saitoh, O. (1994b). The brain in infantile autism: posterior fossa structures are abnormal. *Neurology* 44, 214–223. doi: 10.1212/wnl.44.2.214

Courchesne, E., Yeung-Courchesne, R., Press, G. A., Hesselink, J. R., and Jernigan, T. L. (1988). Hypoplasia of cerebellar vermal lobules VI and VII in autism. *N. Engl. J. Med.* 318, 1349–1354. doi: 10.1056/NEJM198805263182102

Danesh, A. A., and Kaf, W. A. (2012). DPOAEs and contralateral acoustic stimulation and their link to sound hypersensitivity in children with autism. *Int. J. Audiol.* 51, 345–352. doi: 10.3109/14992027.2011.626202

Dawson, G., Toth, K., Abbott, R., Osterling, J., Munson, J., Estes, A., et al. (2004). Early social attention impairments in autism: social orienting, joint attention and attention to distress. *Dev. Psychol.* 40, 271–283. doi: 10.1037/0012-1649.40.2.271

Delgado, C. F., Simpson, E. A., Zeng, G., Delgado, R. E., and Miron, O. (2021). Newborn auditory brainstem responses in children with developmental disabilities. *J. Autism Dev. Disord.* doi: 10.1007/s10803-021-05126-1. [Online ahead of print].

Demopoulos, C., and Lewine, J. D. (2016). Audiometric profiles in autism spectrum disorders: does subclinical hearing loss impact communication? *Autism Res.* 9, 107–120. doi: 10.1002/aur.1495

ElMoazen, D., Sobhy, O., Abdou, R., and AbdelMotaleb, H. (2020). Binaural interaction component of the auditory brainstem response in children with autism spectrum disorder. *Int. J. Pediatr. Otorhinolaryngol.* 131:109850. doi: 10.1016/j.ijporl.2019.109850

Foss-Feig, J. H., Schauder, K. B., Key, A. P., Wallace, M. T., and Stone, W. L. (2017). Audition-specific temporal processing deficits associated with language function in children with autism spectrum disorder. *Autism Res.* 10, 1845–1856. doi: 10.1002/aur.1820

Furman, J. M., Osorio, M. J., and Minshew, N. J. (2015). Visual and vestibular induced eye movements in verbal children and adults with autism. *Autism Res.* 8, 658–667. doi: 10.1002/aur.1481

Gaffney, G. R., Kuperman, S., Tsai, L. Y., and Minchin, S. (1988). Morphological evidence of brainstem involvement in infantile autism. *Biol. Psychiatry* 24, 578–586. doi: 10.1016/0006-3223(88)90168-0

Gernsbacher, M. A., Sauer, E. A., Geye, H. M., Schweigert, E. K., and Goldsmith, H. (2008). Infant and toddler oral- and manual-motor skills predict later speech fluency in autism. *J. Child Psychol. Psychiatry* 49, 43–50. doi: 10.1111/j.1469-7610.2007.01820.x

Gillberg, C., Rosenhall, U., and Johansson, E. (1983). Auditory brainstem responses in childhood psychosis. *J. Autism Dev. Dis.* 13, 181–195. doi: 10.1007/BF01531818

Goldberg, M. C., Landa, R., Lasker, A., Cooper, L., and Zee, D. S. (2000). Evidence of normal cerebellar control of the vestibuloocular reflex (VOR) in children with high-functioning autism. *J. Autism Dev. Disord.* 30, 519–524. doi: 10.1023/a:1005631225367

Gomes, E., Pedroso, F. S., and Wagner, M. B. (2008). Auditory hypersensitivity in the autistic spectrum disorder. *Pro Fono* 20, 279–284. doi: 10.1590/s0104-56872008000400013

Gravel, J. S., Dunn, M., Lee, W. W., and Ellis, M. A. (2006). Peripheral audition of children on the autistic spectrum. *Ear Hear.* 27, 299–312. doi: 10.1097/01.aud.0000215979.65645.22

Greenspan, S. I., and Wieder, S. (1997). Developmental patterns and outcomes in infants and children with disorders in relating and communicating: a chart review of 200 cases of children with autistic spectrum diagnoses. *J. Dev. Learn. Dis.* 1, 87–141.

Grewe, T. S., Danhauer, J. L., Danhauer, K. J., and Thornton, A. R. (1994). Clinical use of otoacoustic emissions in children with autism. *Int. J. Pediatr. Otorhinolaryngol.* 30,123–132. doi: 10.1016/0165-5876(94)90195-3

Hashimoto, T., Tayama, M., Miyazaki, M., Murakawa, K., Shimakawa, S., Yoneda, Y., et al. (1993). Brainstem involvement in high functioning autistic children. *Acta Neurol Scand.* 88, 123–128. doi: 10.1111/j.1600-0404.1993.tb04203.x

Hashimoto, T., Tayama, M., Miyazaki, M., Sakurama, N., Yoshimoto, T., Murakawa, K., et al. (1992). Reduced brainstem size in children with autism. *Brain Dev.* 14, 94–97. doi: 10.1016/s0387-7604(12)80093-3

Hashimoto, T., Tayama, M., Murakawa, K., Yoshimoto, T., Miyazaki, M., Harada, M., et al. (1995). Development of the brainstem and cerebellum in autistic patients. *J. Autism Dev. Disord.* 25, 1–18. doi: 10.1007/BF02178163

Hayes, R. W., and Gordon, A. G. (1977). Auditory abnormalities in autistic children. *Lancet* 2:767. doi: 10.1016/s0140-6736(77)90278-1

Heath, R. G. (1973). Fastigial nucleus connections to the septal region in monkey and cat: a demonstration with evoked potentials of a bilateral pathway. *Biol. Psychiatry* 6, 193–196.

Heath, R. G., and Harper, J. W. (1974). Ascending projections of the cerebellar fastigial nucleus to the hippocampus, amygdala and other temporal lobe sites: evoked potential and histological studies in monkeys and cats. *Exp. Neurol.* 45, 268–287. doi: 10.1016/0014-4886(74)90118-6

Hermelin, B., and Frith, U. (1971). Psychological studies of childhood autism: can autistic children make sense of what they see and hear?. *J. Special Edu.* 5, 107–117.

Jayanath, S., and Ozonoff, S. (2020). First parental concerns and age at diagnosis of autism spectrum disorder: a retrospective review from malaysia. *Malays. J. Med. Sci.* 27, 78–89. doi: 10.21315/mjms2020.27.5.8

Jeste, S. S., and Nelson, C. A., 3rd (2009). Event related potentials in the understanding of autism spectrum disorders: an analytical review. *J. Autism Dev. Disord.* 39, 495–510. doi: 10.1007/s10803-008-0652-9

Källstrand, J., Olsson, O., Nehlstedt, S. F., Sköld, M. L., and Nielzén, S. (2010). Abnormal auditory forward masking pattern in the brainstem response of individuals with Asperger syndrome. *Neuropsychiatr. Dis. Treat.* 6, 289–296. doi: 10.2147/ndt.s10593

Kanner, L. (1943). Autistic disturbances of affective contact. *Nervous Child* 2, 217–250.

Khalfa, S., Bruneau, N., Rogé, B., Georgieff, N., Veuillet, E., Adrien, J. L., et al. (2001). Peripheral auditory asymmetry in infantile autism. *Eur. J. Neurosci.* 13, 628–632. doi: 10.1046/j.1460-9568.2001.01423.x

Khalfa, S., Bruneau, N., Rogé, B., Georgieff, N., Veuillet, E., Adrien, J. L., et al. (2004). Increased perception of loudness in autism. *Hear Res.* 198, 87–92. doi: 10.1016/j.heares.2004.07.006

Kleiman, M. D., Neff, S., and Rosman, N. P. (1992). The brain in infantile autism: are posterior fossa structures abnormal? *Neurology* 42, 753–760. doi: 10.1212/wnl.42.4.753

Klin, A. (1991). Young autistic children's listening preferences in regard to speech: a possible characterization of the symptom of social withdrawal. *J. Autism Dev. Disord.* 21, 29–42. doi: 10.1007/BF02206995

Klin, A. (1993). Auditory brainstem responses in autism: brainstem dysfunction or peripheral hearing loss? *J. Autism Dev. Disord.* 23, 15–35. doi: 10.1007/BF01066416

Koegel, R. L., and Schreibman, L. (1976). Identification of consistent responding to auditory stimuli by a functionally "deaf" autistic child. *J. Autism Child. Schizophr.* 6, 147–156. doi: 10.1007/BF01538058

Kulesza, R. J., Jr (2007). Cytoarchitecture of the human superior olivary complex: medial and lateral superior olive. *Hear Res.* 225, 80–90. doi: 10.1016/j.heares.2006.12.006

Kulesza, R. J., Jr, Lukose, R., and Stevens, L. V. (2011). Malformation of the human superior olive in autistic spectrum disorders. *Brain Res.* 1367, 360–371. doi: 10.1016/j.brainres.2010.10.015

Kulesza, R. J., and Mangunay, K. (2008). Morphological features of the medial superior olive in autism. *Brain Res.* 1200, 132–137. doi: 10.1016/j.brainres.2008.01.009

Kwon, S., Kim, J., Choe, B. H., Ko, C., and Park, S. (2007). Electrophysiologic assessment of central auditory processing by auditory brainstem responses in children with autism spectrum disorders. *J. Korean Med. Sci.* 22, 656–659. doi: 10.3346/jkms.2007.22.4.656

Lai, M.-C., Lombardo, M. V., and Baron-Cohen, S. (2014). Autism. *Lancet* 383, 896–910. doi: 10.1016/S0140-6736(13)61539-1

Levitt, J. G., Blanton, R., Capetillo-Cunliffe, L., Guthrie, D., Toga, A., and McCracken, J. T. (1999). Cerebellar vermis lobules VIII-X in autism. *Prog. Neuropsychopharmacol. Biol. Psychiatry* 23, 625–633. doi: 10.1016/s0278-5846(99)00021-4

Li, B., Bos, M. G., Stockmann, L., and Rieffe, C. (2020). Emotional functioning and the development of internalizing and externalizing problems in young boys with and without autism spectrum disorder. *Autism* 24, 200–210. doi: 10.1177/1362361319874644

Linke, A. C., Jao Keehn, R. J., Pueschel, E. B., Fishman, I., and Müller, R. A. (2018). Children with ASD show links between aberrant sound processing, social symptoms and atypical auditory interhemispheric and thalamocortical functional connectivity. *Dev. Cogn. Neurosci.* 29, 117–126. doi: 10.1016/j.dcn.2017.01.007

Lodhia, V., Brock, J., Johnson, B. W., and Hautus, M. J. (2014). Reduced object related negativity response indicates impaired auditory scene analysis in adults with autistic spectrum disorder. *PeerJ.* 2:e261. doi: 10.7717/peerj.261

Lodhia, V., Hautus, M. J., Johnson, B. W., and Brock, J. (2018). Atypical brain responses to auditory spatial cues in adults with autism spectrum disorder. *Eur. J. Neurosci.* 47, 682–689. doi: 10.1111/ejn.13694

Lukose, R., Beebe, K., and Kulesza, R. J. (2015). Organization of the human superior olivary complex in 15q duplication syndromes and autism spectrum disorders. *Neuroscience* 286, 216–230. doi: 10.1016/j.neuroscience.2014.11.033

Lukose, R., Brown, K., Barber, C. M., and Kulesza, R. J. (2013). Quantification of the stapedial reflex reveals delayed responses in autism. *Autism Res.* 6, 344–353. doi: 10.1002/aur.1297

Lukose, R., Schmidt, E., Wolski, T. P., Jr, Murawski, N. J., and Kulesza, R. J., Jr (2011). Malformation of the superior olivary complex in an animal model of autism. *Brain Res.* 1398, 102–112. doi: 10.1016/j.brainres.2011.05.013

Lysakowski, A., and Goldeberg, J. M. (2004). "Morphophysiology of theh vestibular periphery," in *The Vestibular System*, eds S. M. Highstein, R. R. Fay and A. N. Popper (New York: Springer).

Mansour, Y., and Kulesza, R. (2020). Three dimensional reconstructions of the superior olivary complex from children with autism spectrum disorder. *Hear Res.* 393:107974. doi: 10.1016/j.heares.2020.107974

Mansour, Y., and Kulesza, R. (2021). Distribution of glutamatergic and glycinergic inputs onto human auditory coincidence detector neurons. *Neuroscience* 468, 75–87. doi: 10.1016/j.neuroscience.2021.06.004

Martineau, J., Garreau, B., Roux, S., and Lelord, G. (1987). Auditory evoked responses and their modifications during conditioning paradigm in autistic children. *J. Autism Dev. Disord.* 17, 525–539. doi: 10.1007/BF01486968

Martineau, J., Roux, S., Adrien, J. L., Garreau, B., Barthélémy, C., and Lelord, G. (1992). Electrophysiological evidence of different abilities to form cross-modal associations in children with autistic behavior. *Electroencephalogr. Clin. Neurophysiol.* 82, 60–66. doi: 10.1016/0013-4694(92)90183-i

Maziade, M., Mérette, C., Cayer, M., Roy, M. A., Szatmari, P., Côté, R., et al. (2000). Prolongation of brainstem auditory-evoked responses in autistic probands and their unaffected relatives. *Arch. Gen. Psychiatry* 57, 1077–1083. doi: 10.1001/archpsyc.57.11.1077

Miron, O., Ari-Even Roth, D., Gabis, L. V., Henkin, Y., Shefer, S., Dinstein, I., et al. (2016). Prolonged auditory brainstem responses in infants with autism. *Autism Res.* 9, 689–695. doi: 10.1002/aur.1561

Miron, O., Beam, A. L., and Kohane, I. S. (2018). Auditory brainstem response in infants and children with autism spectrum disorder: a meta-analysis of wave, V. *Autism Res.* 11, 355–363. doi: 10.1002/aur.1886

Miron, O., Delgado, R. E., Delgado, C. F., Simpson, E. A., Yu, K. H., Gutierrez, A., et al. (2021). Prolonged auditory brainstem response in universal hearing screening of newborns with autism spectrum disorder. *Autism Res.* 14, 46–52. doi: 10.1002/aur.2422

Molloy, C. A., Dietrich, K. N., and Bhattacharya, A. (2003). Postural stability in children with autism spectrum disorder. *J. Autism Dev. Disord.* 33, 643–652. doi: 10.1023/b:jadd.0000006001.00667.4c

Murakami, J. W., Courchesne, E., Press, G. A., Yeung-Courchesne, R., and Hesselink, J. R. (1989). Reduced cerebellar hemisphere size and its relationship to vermal hypoplasia in autism. *Arch. Neurol.* 46, 689–694. doi: 10.1001/archneur.1989.00520420111032

O'Connor, K. (2012). Auditory processing in autism spectrum disorder: a review. *Neurosci. Biobehav. Rev.* 36, 836–854. doi: 10.1016/j.neubiorev.2011.11.008

Ogawa, T. (1989). [Neurophysiological study of autistic children]. *No To Hattatsu* 21, 163–169.

Orekhova, E. V., Tsetlin, M. M., Butorina, A. V., Novikova, S. I., Gratchev, V. V., Sokolov, P. A., et al. (2012). Auditory cortex responses to clicks and sensory modulation difficulties in children with autism spectrum disorders (ASD). *PLoS One* 7:e39906. doi: 10.1371/journal.pone.0039906

Ornitz, E. M. (1969). Disorders of perception common to early infantile autism and schizophrenia. *Compr. Psychiatry* 10, 259–274. doi: 10.1016/0010-440x(69)90002-9

Ornitz, E. M. (1970). Vestibular dysfunction in schizophrenia and childhood autism. *Compr. Psychiatry* 11, 159–173. doi: 10.1016/0010-440x(70)90157-4

Ornitz, E. M., Atwell, C. W., Kaplan, A. R., and Westlake, J. R. (1985). Brain-stem dysfunction in autism. Results of vestibular stimulation. *Arch. Gen. Psychiatry* 42, 1018–1025. doi: 10.1001/archpsyc.1985.01790330102012

Ornitz, E. M., Ritvo, E. R., Panman, L. M., Lee, Y. H., Carr, E. M., and Walter, R. D. (1968). The auditory evoked response in normal and autistic children during sleep. *Electroencephalogr. Clin. Neurophysiol.* 25, 221–230. doi: 10.1016/0013-4694(68)90019-9

Ornitz, E. M., Tanguay, P. E., Lee, J. C., Ritvo, E. R., Sivertsen, B., and Wilson, C. (1972). The effect of stimulus interval on the auditory evoked response during sleep in autistic children. *J. Autism Child. Schizophr.* 2, 140–150. doi: 10.1007/BF01537567

Osterling, J., and Dawson, G. J. (1994). Early recognition of children with autism: a study of first birthday home videotapes. *Autism Dev. Disord.* 24, 247–257. doi: 10.1007/BF02172225

Pineda, R., Melchior, K., Oberle, S., Inder, T., and Rogers, C. (2015). Assessment of autism symptoms during the neonatal period: is there early evidence of autism risk?. *Am. J. Occup. Ther.* 69, 6904220010p1–6904220010p11. doi: 10.5014/ajot.2015.015925

Piven, J., Nehme, E., Simon, J., Barta, P., Pearlson, G., and Folstein, S. E. (1992). Magnetic resonance imaging in autism: measurement of the cerebellum, pons and fourth ventricle. *Biol. Psychiatry* 31, 491–504. doi: 10.1016/0006-3223(92)90260-7

Ramezani, M., Lotfi, Y., Moossavi, A., and Bakhshi, E. (2019). Auditory brainstem response to speech in children with high functional autism spectrum disorder. *Neurol. Sci.* 40, 121–125. doi: 10.1007/s10072-018-3594-9

Reynolds, B. S., Newsom, C. D., and Lovaas, O. I. (1974). Auditory overselectivity in autistic children. *J. Abnorm. Child Psychol.* 2, 253–263. doi: 10.1007/BF00919253

Ritvo, E. R., Freeman, B. J., Scheibel, A. B., Duong, T., Robinson, H., Guthrie, D., et al. (1986). Lower purkinje cell counts in the cerebella of four autistic subjects: initial findings of the UCLA-NSAC autopsy research report. *Am. J. Psychiatry* 143, 862–866. doi: 10.1176/ajp.143.7.862

Ritvo, E. R., Ornitz, E. M., Eviatar, A., Markham, C. H., Brown, M. B., and Mason, A. (1969). Decreased postrotatory nystagmus in early infantile autism. *Neurology* 19, 653–658. doi: 10.1212/wnl.19.7.653

Rodier, P. M., Ingram, J. L., Tisdale, B., Nelson, S., and Romano, J. (1996). Embryological origin for autism: developmental anomalies of the cranial nerve motor nuclei. *J. Comp. Neurol.* 370, 247–261. doi: 10.1002/(SICI)1096-9861(19960624)370:2<247::AID-CNE8>3.0.CO;2-2

Roper, L., Arnold, P., and Monteiro, B. (2003). Co-occurrence of autism and deafness: diagnostic considerations. *Autism* 7, 245–253. doi: 10.1177/1362361303007003002

Rosenblum, S. M., Arick, J. R., Krug, D. A., Stubbs, E. G., Young, N. B., and Pelson, R. O. (1980). Auditory brainstem evoked responses in autistic children. *J. Autism Dev. Disord.* 10, 215–225. doi: 10.1186/s13195-020-00654-x.

Rosenhall, U., Nordin, V., Sandström, M., Ahlsén, G., and Gillberg, C. (1999). Autism and hearing loss. *J. Autism Dev. Disord.* 29, 349–357. doi: 10.1023/a:1023022709710

Roth, D. A., Muchnik, C., Shabtai, E., Hildesheimer, M., and Henkin, Y. (2012). Evidence for atypical auditory brainstem responses in young children with suspected autism spectrum disorders. *Dev. Med. Child Neurol.* 54, 23–29. doi: 10.1111/j.1469-8749.2011.04149.x

Russo, N., Nicol, T., Trommer, B., Zecker, S., and Kraus, N. (2009). Brainstem transcription of speech is disrupted in children with autism spectrum disorders. *Dev. Sci.* 12, 557–567. doi: 10.1111/j.1467-7687.2008.00790.x

Russo, N. M., Skoe, E., Trommer, B., Nicol, T., Zecker, S., Bradlow, A., et al. (2008). Deficient brainstem encoding of pitch in children with Autism Spectrum Disorders. *Clin. Neurophysiol.* 119, 1720–1731. doi: 10.1016/j.clinph.2008.01.108

Sacrey, L.-A. R., Germani, T., Bryson, S. E., and Zwaigenbaum, L. (2014). Reaching and grasping in autism spectrum disorder: a review of recent literature. *Front. Neurol.* 5:6. doi: 10.3389/fneur.2014.00006

Schofield, B. R. (2010). "Structural organization of the descending auditory pathway," in *The Oxford Handbook of Auditory Science: Auditory Brain.*, eds A. Rees and A. R. Palmer (New York, NY: Oxford University Press), 42–64.

Scott, J. A., Schumann, C. M., Goodlin-Jones, B. L., and Amaral, D. G. (2009). A comprehensive volumetric analysis of the cerebellum in children and adolescents with autism spectrum disorder. *Autism Res.* 2, 246–257. doi: 10.1002/aur.97

Sersen, E. A., Heaney, G., Clausen, J., Belser, R., and Rainbow, S. (1990). Brainstem auditory-evoked responses with and without sedation in autism and Down's syndrome. *Biol. Psychiatry* 27, 834–840. doi: 10.1016/0006-3223(90)90464-d

Slavik, B., Kitsuwa-Lowe, J., Danner, P., Green, J., and Ayres, A. (1984). Vestibular stimulation and eye contact in autistic children. *Neuropediatrics* 15, 33–36. doi: 10.1055/s-2008-1052337

Smith, D. E., Miller, S. D., Stewart, M., Walter, T. L., and McConnell, J. V. (1988). Conductive hearing loss in autistic, learning-disabled and normal children. *J. Autism Dev. Disord.* 18, 53–65. doi: 10.1007/BF02211818

Smoot Reinert, S., Jackson, K., and Bigelow, K. (2015). Using posturography to examine the immediate effects of vestibular therapy for children with autism spectrum disorders: a feasibility study. *Phys. Occup. Ther. Pediatr.* 35, 365–380. doi: 10.3109/01942638.2014.975313

Sohmer, H. (1982). Auditory nerve-brain stem responses (ABR) in children with developmental brain disorders and in high risk neonates. *Electroencephalogr. Clin. Neurophysiol. Suppl.* 36, 315–327.

Student, M., and Sohmer, H. (1978). Evidence from auditory nerve and brainstem evoked responses for an organic brain lesion in children with autistic traits. *J. Autism Child. Schizophr.* 8, 13–20. doi: 10.1007/BF01550274

Szelag, E., Kowalska, J., Galkowski, T., and Pöppel, E. (2004). Temporal processing deficits in high-functioning children with autism. *Br. J. Psychol.* 95, 269–282. doi: 10.1348/0007126041528167

Talge, N. M., Tudor, B. M., and Kileny, P. R. (2018). Click-evoked auditory brainstem responses and autism spectrum disorder: a meta-analytic review. *Autism Res.* 11, 916–927. doi: 10.1002/aur.1946

Tanguay, P. E., Edwards, R. M., Buchwald, J., Schwafel, J., and Allen, V. (1982). Auditory brainstem evoked responses in autistic children. *Arch. Gen. Psychiatry* 39, 174–180. doi: 10.1001/archpsyc.1982.04290020040008

Taş , M., Yilmaz, Ş., Bulut, E., Polat, Z., and Taş , A. (2017). Otoacoustic emissions in young children with autism. *J. Int. Adv. Otol.* 13, 327–332. doi: 10.5152/iao.2017.3105

Taylor, M. J., Rosenblatt, B., and Linschoten, L. (1982). Auditory brainstem response abnormalities in autistic children. *Can. J. Neurol. Sci.* 9, 429–433. doi: 10.1017/s0317167100044346

Teder-Sälejärvi, W. A., Pierce, K. L., Courchesne, E., and Hillyard, S. A. (2005). Auditory spatial localization and attention deficits in autistic adults. *Brain Res. Cogn. Brain Res.* 23, 221–234. doi: 10.1016/j.cogbrainres.2004.10.021

Thabet, E. M. (2014). Ocular vestibular evoked myogenic potentials n10 response in autism spectrum disorders children with auditory hypersensitivity: an indicator of semicircular canal dehiscence. *Eur. Arch. Otorhinolaryngol.* 271, 1283–1288. doi: 10.1007/s00405-013-2736-1

Tharpe, A. M., Bess, F. H., Sladen, D. P., Schissel, H., Couch, S., and Schery, T. (2006). Auditory characteristics of children with autism. *Ear Hear.* 27, 430–441. doi: 10.1097/01.aud.0000224981.60575.d8

Thivierge, J., Bédard, C., Côté, R., and Maziade, M. (1990). Brainstem auditory evoked response and subcortical abnormalities in autism. *Am. J. Psychiatry* 147, 1609–1613. doi: 10.1176/ajp.147.12.1609

Tomchek, S. D., and Dunn, W. (2007). Sensory processing in children with and without autism: a comparative study using the short sensory profile. *Am. J. Occup. Ther.* 61, 190–200. doi: 10.5014/ajot.61.2.190

Tu, S., Mason, C., Rooks-Ellis, D. L., and Lech, P. (2020). Odds of autism at 5 to 10 years of age for children who did not pass their automated auditory brainstem response newborn hearing screen, but were diagnosed with normal hearing. *J. Early Hear. Detect. Interv.* 5, 1–12. doi: 10.26077/cp8w-9r69

Van Hecke, R., Danneels, M., Dhooge, I., Van Waelvelde, H., Wiersema, J. R., Deconinck, F. J. A., et al. (2019). Vestibular function in children with neurodevelopmental disorders: a systematic review. *J. Autism Dev. Disord.* 49, 3328–3350. doi: 10.1007/s10803-019-04059-0

Warr, W. B. (1975). Olivocochlear and vestibular efferent neurons of the feline brain stem: their location, morphology and number determined by retrograde axonal transport and acetylcholinesterase histochemistry. *J. Comp. Neurol.* 161, 159–181. doi: 10.1002/cne.901610203

Wegiel, J., Flory, M., Kuchna, I., Nowicki, K., Ma, S. Y., Imaki, H., et al. (2014). Brainregion-specific alterations of the trajectories of neuronal volume growth throughout the lifespan in autism. *Acta Neuropathol. Commun.* 2:28. doi: 10.1186/2051-5960-2-28

Wegiel, J., Kuchna, I., Nowicki, K., Imaki, H., Wegiel, J., Marchi, E., et al. (2010). The neuropathology of autism: defects of neurogenesis and neuronal migration and dysplastic changes. *Acta Neuropathol.* 119, 755–770. doi: 10.1007/s00401-010-0655-4

Werner, E., Dawson, G., Osterling, J., and Dinno, N. (2000). Brief report: recognition of autism spectrum disorder before one year of age: a retrospective study based on home videotapes. *J. Autism Dev. Disord.* 30, 157–162. doi: 10.1023/a:1005463707029

Williams, R. S., Hauser, S. L., Purpura, D. P., DeLong, G. R., and Swisher, C. N. (1980). Autism and mental retardation: neuropathologic studies performed in four retarded persons with autistic behavior. *Arch. Neurol.* 37, 749–753. doi: 10.1001/archneur.1980.00500610029003

Wong, V. C., and Kwan, Q. K. (2010). Randomized controlled trial for early intervention for autism: a pilot study of the Autism 1–2–3 Project. *J. Autism Dev. Disord.* 40, 677–688. doi: 10.1007/s10803-009-0916-z

Wong, V., and Wong, S. N. (1991). Brainstem auditory evoked potential study in children with autistic disorder. *J. Autism Dev. Disord.* 21, 329–340. doi: 10.1007/BF02207329

Conflict of Interest: The authors declare that the research was conducted in the absence of any commercial or financial relationships that could be construed as a potential conflict of interest.

Publisher's Note: All claims expressed in this article are solely those of the authors and do not necessarily represent those of their affiliated organizations, or those of the publisher, the editors and the reviewers. Any product that may be evaluated in this article, or claim that may be made by its manufacturer, is not guaranteed or endorsed by the publisher.

frontiers in Integrative Neuroscience

ORIGINAL RESEARCH
published: 20 October 2021
doi: 10.3389/fnint.2021.748977

Functional and Neuropathological Evidence for a Role of the Brainstem in Autism

*Joan S. Baizer**

Department of Physiology and Biophysics, Jacobs School of Medicine and Biomedical Sciences, University at Buffalo, Buffalo, NY, United States

The brainstem includes many nuclei and fiber tracts that mediate a wide range of functions. Data from two parallel approaches to the study of autistic spectrum disorder (ASD) implicate many brainstem structures. The first approach is to identify the functions affected in ASD and then trace the neural systems mediating those functions. While not included as core symptoms, three areas of function are frequently impaired in ASD: (1) Motor control both of the limbs and body and the control of eye movements; (2) Sensory information processing in vestibular and auditory systems; (3) Control of affect. There are critical brainstem nuclei mediating each of those functions. There are many nuclei critical for eye movement control including the superior colliculus. Vestibular information is first processed in the four nuclei of the vestibular nuclear complex. Auditory information is relayed to the dorsal and ventral cochlear nuclei and subsequently processed in multiple other brainstem nuclei. Critical structures in affect regulation are the brainstem sources of serotonin and norepinephrine, the raphe nuclei and the locus ceruleus. The second approach is the analysis of abnormalities from direct study of ASD brains. The structure most commonly identified as abnormal in neuropathological studies is the cerebellum. It is classically a major component of the motor system, critical for coordination. It has also been implicated in cognitive and language functions, among the core symptoms of ASD. This structure works very closely with the cerebral cortex; the cortex and the cerebellum show parallel enlargement over evolution. The cerebellum receives input from cortex via relays in the pontine nuclei. In addition, climbing fiber input to cerebellum comes from the inferior olive of the medulla. Mossy fiber input comes from the arcuate nucleus of the medulla as well as the pontine nuclei. The cerebellum projects to several brainstem nuclei including the vestibular nuclear complex and the red nucleus. There are thus multiple brainstem nuclei distributed at all levels of the brainstem, medulla, pons, and midbrain, that participate in functions affected in ASD. There is direct evidence that the cerebellum may be abnormal in ASD. The evidence strongly indicates that analysis of these structures could add to our understanding of the neural basis of ASD.

Keywords: inferior olive, arcuate nucleus of the medulla, pontine nuclei, cerebellum, vestibular nuclear complex, cochlear nuclear complex

OPEN ACCESS

Edited by:
Eric London,
Institute for Basic Research in Developmental Disabilities (IBR), United States

Reviewed by:
Chin-An Josh Wang,
National Central University, Taiwan
Adrian Rodriguez-Contreras,
City College of New York (CUNY), United States
Brittany Travers,
University of Wisconsin-Madison, United States

***Correspondence:**
Joan S. Baizer
baizer@buffalo.edu

Received: *28 July 2021*
Accepted: *21 September 2021*
Published: *20 October 2021*

Citation:
Baizer JS (2021) Functional and Neuropathological Evidence for a Role of the Brainstem in Autism. Front. Integr. Neurosci. 15:748977. doi: 10.3389/fnint.2021.748977

INTRODUCTION

The goal of this review is to consider a possible role of the brainstem in autism or autistic spectrum disorder (ASD). The question of brainstem involvement is complex; the "brainstem" includes many structures and fiber tracts mediating a wide range of functions including sensory, motor, and affective. To develop hypotheses about the possible involvement of brainstem structures in ASD, we will first consider the implications of data from two complementary experimental approaches. The first approach has been to describe the functions are impaired in ASD; the next step then is to look at the neural systems mediating those functions, focusing on the brainstem components. The second approach has been to directly identify brain structures that affected in ASD brains, the next step from those data is to consider the afferent and efferent connections of those structures, again with a focus on brainstem relays. The perspective here is on the participation of the brainstem in circuitry in the adult brain. Another, complementary, perspective is discussed extensively by Dadalko and Travers (2018) who consider the role of brainstem structures in the development of the brain.

The First Question Is What Is ASD?

ASD is a neurodevelopmental disorder, thought to reflect abnormal brain development (DiCicco-Bloom et al., 2006; Geschwind, 2011). Symptoms are not usually apparent at birth, but emerge by about the age of 2–3 years old (Filipek et al., 1999; DiCicco-Bloom et al., 2006). There are some studies that argue for subtle earlier manifestations (Zwaigenbaum et al., 2005, 2013). ASD is a complicated diagnosis with much individual variability (this has been discussed by many authors, some examples: Ciaranello and Ciaranello, 1995; Filipek et al., 1999; DiCicco-Bloom et al., 2006; Grzadzinski et al., 2013; Zwaigenbaum et al., 2013; Lai et al., 2014; CDC, 2021). The diagnosis is based on behavioral analysis and not on genetics or biomarkers (discussion in Geschwind, 2011). At present, the causes of ASD are not understood; there is clearly a genetic component, but the genetics are complex (Folstein and Rutter, 1977a,b; Folstein and Rosen-Sheidley, 2001; Geschwind, 2011; Huguet et al., 2016). Patients with known genetic syndromes can meet the criteria for an ASD diagnosis, these syndromes include Down Syndrome, (DS; trisomy 21, Hepburn et al., 2008), Fragile X syndrome (FXS; Hoeft et al., 2011), Timothy Syndrome (Bett et al., 2013), Tuberous Sclerosis (Smalley, 1998), and Rett syndrome (Percy, 2011). In addition, there are many other genes with mutations associated with a risk of ASD (Campbell et al., 2007; Geschwind, 2011; Jiang et al., 2013; Pinto et al., 2014; Myers et al., 2020; Chawner et al., 2021). Data from twin studies suggest that there are non-genetic in addition to genetic factors determining the emergence of ASD (Kates et al., 2004). ASD is also associated with other neurological conditions like seizure disorders (about 39%) and intellectual disability (ID, about 45% Wegiel et al., 2012). Finally, ASD is a sexually dimorphic disorder, affecting more males than females (about 4:1, Folstein and Rosen-Sheidley, 2001; Yamasue et al., 2009), raising the possibility of sexually dimorphic effects in the brain. Thus the ASD population is medically, behaviorally, and genetically very heterogeneous.

Functions Affected in ASD

The criteria for the diagnosis of autism have changed over the years. The most recent criteria for Autism Spectrum Disorder are deficits in two areas (1) Social communication and interaction across multiple contexts and (2) Restricted and repetitive behaviors (DSM-5, 2013; see also Lai et al., 2014). However, there are many additional functional deficits that have been described in subsets of ASD patients. We will focus on three aspects of function whose neural substrates include brainstem nuclei: (1) Motor control both of the limbs and body and of the eyes. (2) Auditory and vestibular information processing. (3) Control of affect.

Motor Symptoms in ASD: Limbs and Body

While not a core deficit of ASD, problems with different aspects of motor control have been reported in many studies. Symptoms described include abnormal development of motor milestones, difficulties in postural control and gait, toe-walking, difficulty in learning to ride a bicycle, poor motor coordination and "clumsiness," dystonia or hypotonia, difficulties with motor learning, rigidity and repetitive and stereotyped motor behaviors like hand-flapping and rocking, and motor memory (Kohenraz et al., 1992; Ciaranello and Ciaranello, 1995; Teitelbaum et al., 1998; Dawson et al., 2000; Ming et al., 2007; Albinali et al., 2009; Boyd et al., 2012; MacDonald et al., 2012; Marko et al., 2015; Hannant et al., 2016; Eggleston et al., 2017; Bruchage et al., 2018; Bell et al., 2019; Neely et al., 2019; Bojanek et al., 2020). Motor symptoms are prevalent enough that some authors have proposed that motor deficits should be considered among the core symptoms of ASD (Mosconi and Sweeney, 2015). The severity of motor symptoms may correlate with impairments in cognitive and language domains (Bhat, 2021), suggesting that they reflect the overall atypical brain development. The wide range of motor symptoms again reflects the heterogeneity of ASD.

Motor Symptoms in ASD: Control of Eye Movements

There are many reports of eye movement abnormalities in ASD (reviews in Sweeney et al., 2004; Mosconi and Sweeney, 2015). Deficits have been reported in all types of voluntary eye movements: saccades, smooth pursuit and maintenance of fixation, but the exact nature of the deficits varies among studies. For saccadic eye movements, Rosenhall et al. (1988) tested saccades to targets and found hypometric saccades and reduced saccade velocity in ASD subjects. Takarae et al. (2004b) measured the accuracy of visually guided saccades and found greater variability in saccadic accuracy in ASD but no effects of saccade latency or velocity. Zalla et al. (2018) used a complex test of saccadic eye movement accuracy and found reduced saccadic gain and reduced peak saccade velocity in ASD. For smooth pursuit, Takarae et al. (2004a, 2008) found deficits in accurate tracking of moving targets and found longer latency and more "catch-up" saccades in ASD subjects. Deficits were also found in "saccadic adaptation" in a task in which the saccade target is moved before the target is acquired, a task eliciting learning in typical subjects (Mosconi et al., 2013). Nowinski et al. (2005) studied the ability to maintain fixation on visual targets and found more "intrusive saccades" in a task requiring subjects to

maintain fixation on a "remembered" (no longer visible) target. Wegiel et al. (2013) reported poor or no eye contact in ASD subjects. Overall the data support the hypothesis that control of eye movements is affected in ASD.

Sensory Processing: Auditory and Vestibular Systems

Sensory processing deficits, specifically of auditory and vestibular information, are also characteristic of ASD (discussion and additional references in Baranek et al., 2006; Lane et al., 2010; Mansour and Kulesza, 2020). While peripheral hearing loss is not found (Beers et al., 2014), there are many studies showing auditory dysfunction in children with ASD (references in Rimland and Edelson, 1995; Lukose et al., 2013; Kozou et al., 2018; Smith et al., 2019). Lukose et al. (2013) studied the acoustic stapedial reflex (ASR: contraction of the stapedius muscle of the middle ear in response to loud sounds) and found lower thresholds and longer latencies in ASD subjects. A number of auditory training schemes have been proposed to improve auditory processing (Rimland and Edelson, 1995; Russo et al., 2010; Gopal et al., 2020).

Several observations also suggest differences in processing vestibular stimuli (Kern et al., 2007). Some ASD behaviors like rocking (Dawson et al., 2000; Albinali et al., 2009) would increase vestibular input. Vestibular input is also critical for several motor functions including postural stability, another function affected in ASD (Molloy et al., 2003; Bojanek et al., 2020). Vestibular therapy is often proposed for children with ASD (Smoot Reinert et al., 2015).

Regulation of Affect

Atypical regulation of affect and attention are well-documented ASD symptoms (Harris et al., 1999; Konstantareas and Stewart, 2006; Mazefsky et al., 2013; Mazefsky and White, 2014).

We will return to a consideration of the circuitry underlying these functions after looking at what is known about changes in the brain in ASD.

The Brain in ASD

Many hypotheses about the neural basis of ASD postulate that the diverse symptoms reflect dysfunction in multiple (but, importantly, not all) brain regions and/or systems. Such dysfunction could have multiple manifestations: (1) Macroscopic structural differences in specific brain regions, including differences in axon tracts (numbers or diameters of axons). (2) Microscopic differences in neuronal structure. (3) Physiological differences affecting the action of critical circuits; such could arise from abnormalities in transmitters, receptors, and/or transporters. This perspective differentiates ASD from other genetically determined neurological diseases, e.g., Krabbe disease (Hunter'sHope, 2021) or FXS (Hagerman et al., 2017) where a single gene mutation affecting a single protein results in global effects on most or all neurons across multiple systems and structures.

There are many constraints in studying the human brain; invasive physiological and neuroanatomical (especially tract-tracing) techniques so extensively used in animal studies cannot be used in humans. The two major approaches for studying the human brain are (1) Postmortem examination of brains using histological techniques and (2) Analysis of brains in living subjects using imaging techniques.

Neuropathological Studies

Postmortem study of individual brains allows direct histological examination of the brain at the cellular/neurochemical level. The limitations of these studies are that only a few brains have been available for study, and the information about the range of ASD symptoms in any individual may be limited. The diversity of ASD symptoms and causes is mirrored by a diversity of neuropathological reports (summary in Palmen et al., 2004).

Imaging Studies in ASD

Imaging techniques include MRI to show structure, fMRI to show functional activation and DT-MRI to show connections. These studies can include relatively large numbers of ASD subjects and usually also include equivalent numbers of control subjects (review and references in Ecker, 2017; Dadalko and Travers, 2018).

Limitations: Subject selection

Integrating data from the many imaging, behavioral, and neuroanatomical studies of ASD is complicated by the fact that different studies use very different criteria for selection of subjects and of controls. Some studies include subjects with syndromes associated with ASD like DS or FXS (e.g., Kaufmann et al., 2003). Other studies explicitly exclude such subjects (for example Müller et al., 2001; Nowinski et al., 2005; Neely et al., 2019; Unruh et al., 2019). The neuroanatomical substrates for ASD in genetically different populations may be different. Hoeft et al. (2011) found differences between FXS and idiopathic ASD boys in the volume of cerebral gray matter and white matter in different cortical regions. Many behavioral and imaging studies are limited to subjects who are "high-functioning autistic"/Asperger's Syndrome (examples include Nowinski et al., 2005; Langen et al., 2007; Takarae et al., 2007; Catani et al., 2008). Some include only people with normal IQs (e.g., Hua et al., 2013; Oldehinkel et al., 2019). "Lower-functioning" individuals may have had behavior incompatible with the demands of behavioral or imaging studies, and in fact some studies have used sedation for structural imaging of ASD subjects (Sparks et al., 2002; Carper and Courchesne, 2005; Schumann et al., 2009; Zielinski et al., 2014; Lange et al., 2015); the necessity for sedation could further limit subject selection. The problems with the selection of appropriate controls have been thoughtfully discussed by Jarrold and Brock (2004). Therefore, there may be a population of lower IQ/behaviorally challenging ASD individuals excluded from many studies, especially imaging studies with behavioral demands. Post-mortem brain analyses probably include a higher percentage of ASD with Intellectual Disability (ID, for example Bailey et al., 1998) and/or behavioral challenges than do imaging studies. These issues complicate the efforts of trying to understand the biological basis of ASD in light of the heterogeneity in ASD characteristics and correlates.

Another concern with subject selection is that many studies use only male subjects (some examples: Müller et al., 2001; Schumann et al., 2004; Catani et al., 2008; Zielinski et al., 2014; Igelstrom et al., 2017), potentially missing sexually dimorphic anomalies. That such may exist is suggested by Libero et al. (2016) who found differences in "disproportionate megalencephaly" between girls and boys, with the boys affected and the girls not. A related problem concerns the variability in criteria that have been used for establishing an ASD diagnosis; issues of diagnosis and subject selection are summarized by Simmons et al. (2009).

WHAT DO WE KNOW ABOUT THE BRAIN IN ASD: CANDIDATE STRUCTURES AND THEIR CONNECTIONS

The Cerebellum in ASD

Many studies have found abnormalities of the cerebellum in ASD; data come from both neuropathological and imaging studies (Ritvo et al., 1986; Murakami et al., 1989; Bauman, 1991; Courchesne et al., 1994, 2011; Ciesielski et al., 1997; Bailey et al., 1998; Levitt et al., 1999; Purcell et al., 2001; Fatemi et al., 2002, 2012; Kaufmann et al., 2003; Allen et al., 2004; Palmen et al., 2004; Allen, 2005; Catani et al., 2008; Whitney et al., 2009; Yip et al., 2009; Wegiel et al., 2010, 2012, 2014; Donovan and Basson, 2017; Bruchage et al., 2018). However, different studies report different cerebellar abnormalities. The most common deficits seen in microscopic analysis of the cerebellum are loss of Purkinje cells and granule cells in cerebellar cortex, loss or abnormal appearance of neurons in the deep cerebellar nuclei and differences in the size of vermal lobules (Bauman, 1991; Kemper and Bauman, 2002; Whitney et al., 2009; Wegiel et al., 2014). Wegiel et al. (2013) reported dysplasia of the flocculus, a part of the cerebellum involved in eye movement control (Zee et al., 1981).

Structural imaging studies likewise have found differences in the size of parts of the vermis, but which lobules were affected and in which direction (bigger vs. smaller than in controls) varies among studies (Courchesne et al., 1994; Harris et al., 1999; Levitt et al., 1999; Kaufmann et al., 2003; Kates et al., 2004; Marko et al., 2015). Cerebellar hemispheres, as well as the vermis, may be smaller (Murakami et al., 1989). Catani et al. (2008) reported that the efferent pathway from the cerebellum, the superior cerebellar peduncle, is smaller in ASD. Hanaie et al. (2013) using DTI found structural differences in the superior cerebellar peduncles between ASD and control subjects; differences correlated with deficits in motor skills. Functional imaging data also confirm differences in cerebellar involvement between control and ASD subjects in a simple motor task (Allen et al., 2004).

Connections of the Cerebellum: The Brainstem

There is thus strong and consistent evidence that the cerebellum is affected in ASD. What is the significance of this result? The classical role of the cerebellum is in motor control (Evarts and Thach, 1969), including the control of eye movements (Robinson and Fuchs, 2001; Blazquez and Pastor, 2013). More recently, a role of the cerebellum in language and cognition has been proposed on the basis of anatomical and clinical studies (Strick et al., 2009; Buckner, 2013). Cerebellar dysfunction in ASD could therefore contribute to cognitive/language as well as motor deficits (Allen, 2005).

The findings of cerebellar abnormalities in ASD dictate consideration of its connections, and these connections make a compelling argument for the role of the brainstem in ASD. The cerebellum is connected to the brain by relays in brainstem and diencephalon. The cerebellum receives information from several "precerebellar" brainstem relays; the output of the cerebellum is via the neurons of the cerebellar deep nuclei that project to multiple brainstem structures (Asanuma et al., 1983a). Thus the neuroanatomical data suggest that both precerebellar brainstem structures as well as the brainstem targets of cerebellar outflow might be affected in ASD brains. What are these structures? **Figure 1** summarizes the critical connections of the cerebellum.

Precerebellar Brainstem Structures: Inferior Olive, Pontine Nuclei, and the Arcuate Nucleus

The cerebellum receives two kinds of afferent fibers, mossy fibers and climbing fibers (Eccles, 1967). The inferior olive is the sole source of climbing fibers that innervate the cerebellum and is also the recipient of feedback projections from the cerebellum. There is evidence for IO abnormalities in ASD in a few neuropathological cases (Bailey et al., 1998; Kemper and Bauman, 2002). However, interpretation of the results for the IO is complex. We found individual variability in the appearance of neurons and in the expression of calcium-binding proteins in normal subjects (Baizer et al., 2011b, 2018b). The age-pigment lipofuscin is especially prominent in IO neurons, and may correlate with age-related degenerative changes in IO neurons affecting protein expression (Mann and Yates, 1974;

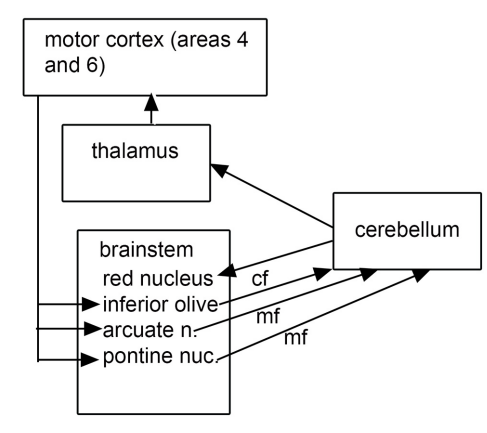

FIGURE 1 | The brainstem inputs and outputs of the cerebellum. cf, climbing fibers; mf, mossy fibers.

Mann et al., 1978). **Figure 2** illustrates the variability in shape and neurochemical properties of the IOpr in humans.

The Pontine Nuclei and the Cerebral Cortex

The pontine nuclei are a critical relay between the cerebral cortex and the cerebellum. The input to the pontine nuclei is from layer 5 pyramidal cells of various regions of the cerebral cortex (Brodal, 1968a,b,c, 1972a,b,c, 1978a,b; Glickstein et al., 1972, 1985; Gibson et al., 1977; Bjaalie, 1986; Legg et al., 1989; Bjaalie and Brodal, 1997; Bjaalie et al., 1997; Brodal and Bjaalie, 1992, 1997; Leergaard and Bjaalie, 2007). The pontine nuclei then project to the cerebellum. The pontine nuclei are implicated in ASD for two reasons, first the documented involvement of their target structure, the cerebellum, and second, the fact that many studies that have found involvement of their input structure, the cerebral cortex. We will therefore briefly review the role of the cerebral cortex in ASD.

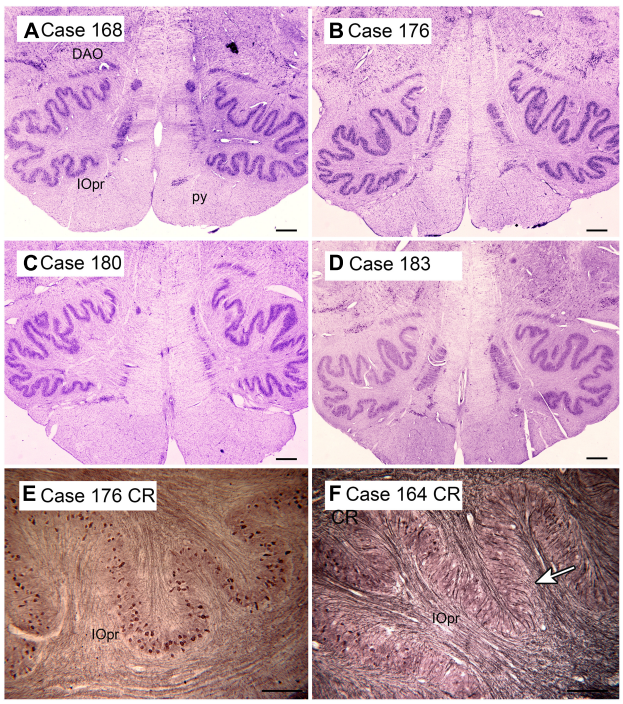

FIGURE 2 | Variability in the shape of the IOpr in humans. **(A–D)** The IOpr in cresyl violet stained transverse sections of the brainstem in four cases. Note the differences in the folding pattern among cases and the left-right asymmetry in each case. Scale bars = 1 mm. **(E,F)** Variability in the density of neurons expressing the calcium-binding protein calretinin (CR) illustrated in two cases. The arrow in **(F)** shows a region with few immunostained neurons. Scale bars = 250 μm. CR, calretinin; DAO, dorsal accessory olive; IOpr, principal nucleus of the inferior olive. **Figures 2**, **3**, **6**, and **8** show photomicrographs of sections that were prepared for several different projects on the human brainstem. Details of the methods are given in earlier publications (Baizer and Broussard, 2010; Baizer et al., 2011a,b, 2014, 2018a,b, 2021).

The Cerebellum, the Cerebral Cortex, and ASD

Different studies have found different cortical abnormalities in ASD. One finding has been brain overgrowth in some, but not all, very young ASD children that resolves at later ages (Courchesne et al., 2007, 2011; Libero et al., 2016). Overgrowth of specific regions (especially dorsolateral prefrontal cortex, DLPFC) of the cerebral cortex is a major contributor to differences in overall brain size (Carper and Courchesne, 2005; Courchesne and Pierce, 2005). Projections from the DLPFC to the pontine nuclei have been demonstrated in the monkey (Schmahmann and Pandya, 1997). Other investigators focused on the functional organization of the temporoparietal junction, and suggested differences in connectivity of this region with the cerebellum (Igelstrom et al., 2017). Alterations in cortical circuitry and the structure of cortical columns have also been reported (Casanova et al., 2003). These cortical differences might be reflected in corticopontine projections in the numbers or diameters of axons, or the distribution of projections.

The Cerebral Cortex and the Corpus Callosum

We have already considered one major efferent pathway from the cerebral cortex, the corticospinal/pontine tract. Another efferent pathway is the corpus callosum (CC). It interconnects the two cerebral hemispheres; neurons of origin are pyramidal cells found primarily in layers 3 and 5 (Jacobson and Trojanowski, 1974). Several studies have noted abnormalities in the CC in ASD, (additional references in Fingher et al., 2017) further evidence that the projections from cortex may be affected.

The Arcuate Nucleus

Another source of mossy fiber input to the cerebellum is from a structure unique to the human brain, the arcuate nucleus of the medulla (Essick, 1912; Baizer and Broussard, 2010; Baizer, 2014; Baizer et al., 2021). The arcuate has classically been considered a precerebellar structure (Essick, 1912). We have shown its size and shape to be very variable among normal human cases, again a complicating factor in interpreting data from ASD brains. **Figure 3** illustrates the variability of the size and shape of the arcuate nucleus in humans. In one report (Bailey et al., 1998) the arcuate was described as "larger than usual" but it was unclear what it was compared to. It too could be added to the list of structures to be analyzed in future postmortem or imaging brain studies.

Projection Targets of the Cerebellum

Targets of cerebellar outflow include thalamic nuclei and several brainstem structures including the red nucleus, the vestibular nuclear complex (VNC), the IO (Asanuma et al., 1983a,b; Hazrati and Parent, 1992) and the superior colliculus (Roldan and Reinoso-Suarez, 1981). The VNC will be considered in the context of vestibular information processing and the control of

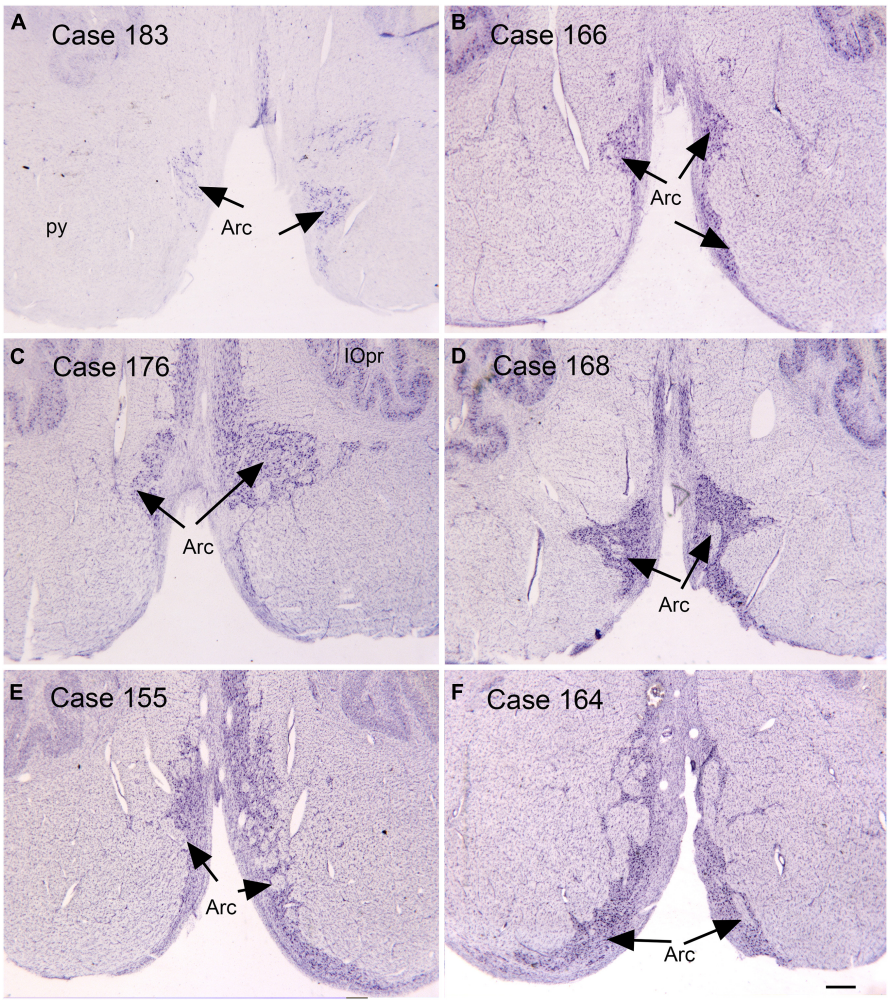

FIGURE 3 | Variability in the arcuate nucleus. **(A–F)** The arcuate nucleus (Arc, arrows) on cresyl violet stained transverse sections of the human brainstem. Note the differences in size and shape among cases, and the left-right asymmetry within cases. Scale bar = 0.5 mm. Arc, arcuate nucleus; IOpr, principal nucleus of the inferior olive; py, pyramidal tract.

eye movements, the IO was discussed above as it is also an input structure.

Red Nucleus

The red nucleus is a midbrain structure with a role in reaching and grasping (van Kan and McCurdy, 2001, 2002a,b). The red nucleus has two components, a parvocellular and a magnocellular division; the relative sizes of the two components has changed over evolution and the magnocellular component is much smaller in humans than in other mammals (Massion, 1967; Hicks and Onodera, 2012). It has not been specifically mentioned in the neuropathology of ASD, and may not have been examined.

We will now return to the question of possible brainstem involvement in the other functional deficits in autism: control of eye movements, sensory processing of auditory and vestibular information, and control of affect.

The Brainstem and the Control of Eye Movements

As discussed earlier, abnormal control of eye movements is often mentioned as an ASD symptom. The control of eye movements is mediated by many complexly interconnected brain structures (summary in **Figure 4**). Key regions include cortical frontal and supplemental eye fields (Robinson and Fuchs, 1969; Schiller et al., 1987; Fukushima et al., 2004; Roesch and Olson, 2005), the flocculus and vermis of the cerebellum (Lisberger and Fuchs, 1974; Kojima et al., 2010a,b,c, 2011), the superior colliculus of the midbrain (Wurtz and Goldberg, 1971, 1972; Stryker and Schiller, 1975), the substantia nigra pars reticulata (SNr; Hikosaka and Wurtz, 1983a,b, 1985) and the four nuclei of the vestibular nuclear complex, the VNC (Chubb and Fuchs, 1982; Chubb et al., 1984; Waespe and Henn, 1977, 1979, 1985). While abnormalities have been described of the cerebellum in ASD, the superior colliculus, the substantia nigra and the VNC

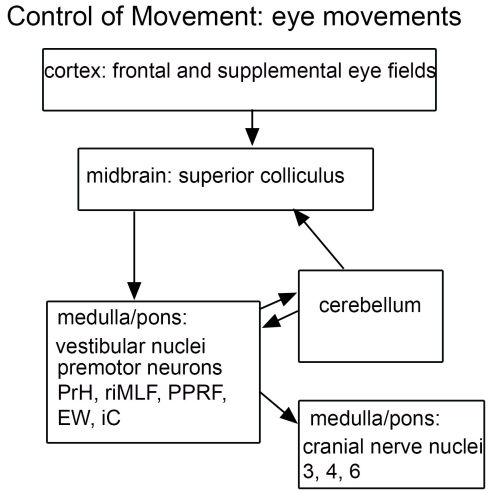

FIGURE 4 | Schematic of brainstem nuclei critical for eye movement control. Cranial nerve nuclei 3-oculomotor, 4-trochlear, 6-abducens; EW, Edinger-Westphal nucleus; iC, interstitial nucleus of Cajal; PrH, nucleus prepositus hypoglossi; PPRF, paramedian pontine reticular formation; riMLF, rostral interstitial nucleus of the medial longitudinal fasciculus; SNr, substantia nigra, pars reticulata.

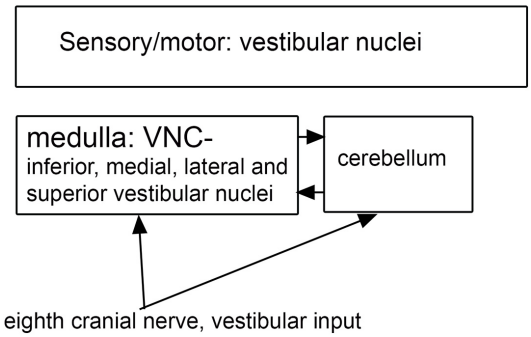

FIGURE 5 | Vestibular input to the vestibular nuclei of the brainstem.

have not been implicated in neuropathological studies (Bauman, 1991; Bauman et al., 1995; Bailey et al., 1998; Palmen et al., 2004). There are many other brainstem structures critical in eye movement control include cranial nerve nuclei 3, 4, and 6, (Fuchs and Luschei, 1970, 1971), premotor neurons in midbrain, pons, and medulla (Horn and Büttner-Ennever, 1998), the paramedian pontine reticular formation, (PPRF; Keller, 1974); the nucleus prepositus hypoglossi (PrH; Kaneko, 1992, 1997, 1999); the rostral interstitial nucleus of the medial longitudinal fasciculus (riMLF; Wang and Spencer, 1996; Sparks, 2002) and the Edinger-Westphal nucleus (EW; May et al., 2008). Many of the studies of these nuclei establishing their participation eye movement control have been electrophysiological. It is possible that differences in these structures in ASD brains might be detectable only physiologically, as altered functional circuitry, but not anatomically.

Vestibular Nuclear Complex

Both functional and anatomical evidence suggest that the vestibular nuclear complex (VNC) may be involved in ASD: (1) The disruptions of vestibular function, (2) The deficits in eye movement control, and (3) Connections with the cerebellum. The eighth cranial nerve distributes vestibular information to the four nuclei of the vestibular nuclear complex (VNC; **Figure 5**) and to the cerebellum (Barmack, 2003). The nuclei of the VNC are critical for the analysis of vestibular input and are also involved in the generation of vestibular-triggered eye movements like vestibular nystagmus and the vestibulo-ocular reflex, (VOR; Szentagothai, 1950). The VNC also receive projections from the flocculus (Balaban et al., 1981), an eye-movement related part of the cerebellum (Zee et al., 1981). The vestibular nuclei are relatively small structures and could be examined in future neuropathological analysis of ASD brains. We have studied the organization and neurochemical composition of the vestibular nuclear complex in several species including humans, and those data could be used for comparison with VNC organization in ASD brains (Baizer and Broussard, 2010; Baizer et al., 2011a; Baizer, 2014). **Figure 6** illustrates neurochemically defined subdivisions in the human VNC.

The Brainstem and Auditory Processing

There are multiple brainstem nuclei critical for the processing of auditory information including the cochlear nuclei, the nucleus of the trapezoid body, superior olivary complex, nuclei of the lateral lemniscus, and the inferior colliculus (schematic in **Figure 7**; Pickles, 2015; Smith et al., 2019). There are electrophysiological data (measurement of ABR, auditory brainstem response) suggesting that the brainstem structures may be affected in ASD (Rosenhall et al., 1988; Kwon et al., 2007). An early report found severe brainstem abnormalities in a single case, including aplasia of the superior olivary complex (SOC) and the seventh nerve nucleus (Rodier et al., 1996). Subsequent studies of the medial superior olive (MSO) have found more subtle differences at a cellular level in ASD brains. Quantitative analysis of the MSO showed hypoplasia with fewer, smaller and atypically shaped and oriented neurons (Kulesza and Mangunay, 2008; Smith et al., 2019; Mansour and Kulesza, 2020). Examination of the other components of the SOC also showed abnormalities in neuron numbers and shape (Kulesza et al., 2011; Lukose et al., 2015; Mansour and Kulesza, 2020). Those studies suggest that a similar cellular analysis of the other main brainstem auditory nuclei that interconnect with the SOC (cochlear nuclei, inferior colliculus) might also reveal abnormalities. We have studied the neurochemical organization of the dorsal and ventral cochlear nuclei in humans (Baizer et al., 2014, 2018a); these brain sections are available for comparison with sections from ASD brains. **Figures 8A,B** shows the dorsal and ventral cochlear nuclei in humans.

The Brainstem and Neural Substrates of Affect

Several studies have found abnormalities in the amygdala and hippocampus, structures involved in affect and memory

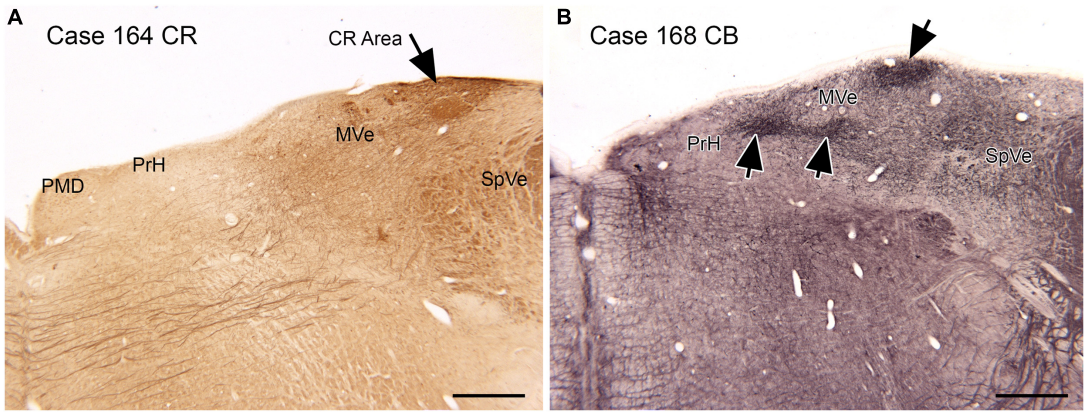

FIGURE 6 | Compartments in the medial vestibular nucleus (MVe) marked by immunoreactivity to calretinin (CR, **A**, arrow) and calbindin (CB, **B**, arrows). Scale bars = 1 mm. PrH, nucleus prepositus hypoglossi; PMD, nucleus paramedianus dorsalis; SpVe, spinal or inferior vestibular nucleus.

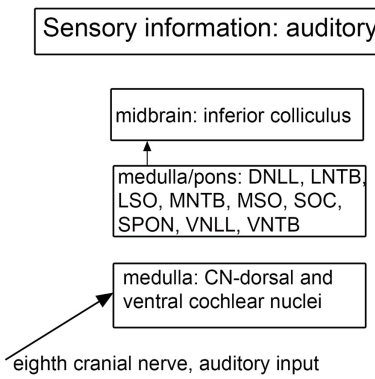

FIGURE 7 | Schematic showing the main brainstem nuclei of the auditory system. CN, cochlear nuclei; DNLL, dorsal nucleus of the lateral lemniscus; MNTB, medial nucleus of the trapezoid body; MSO, medial superior olive; SOC, superior olivary complex; SPON, superior paraolivary nucleus; VNLL ventral nucleus of the lateral lemniscus; VNTB, ventral nucleus of the trapezoid body.

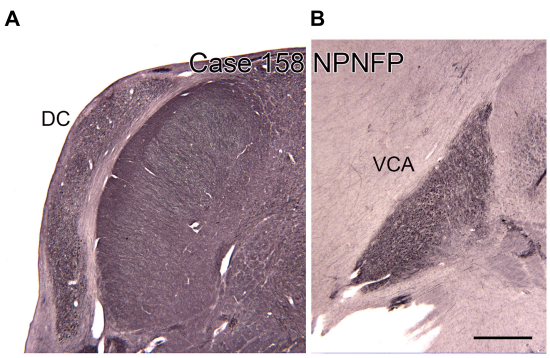

FIGURE 8 | The dorsal (DC, **A**) and ventral (VCA, **B**) cochlear nuclei in the human brain shown on transverse sections immunostained for non-phosphorylated neurofilament protein (NPNFP). Scale bar = 1 mm.

(Schumann et al., 2004). However, the regulation of affect also depends on monoaminergic input to the brain. There are two critical brainstem nuclei: the raphe nuclei (cells groups along midline of the brainstem that provide serotonergic input; Hornung, 2003) and the nucleus called the locus coeruleus (in the rostral pons, noradrenergic input; Schwarz and Luo, 2015). Drug therapies for mood disorders in ASD have included SSRIs and SNRIs (selective serotonin or norepinephrine reuptake inhibitors) (Henry et al., 2009; Nanjappa et al., 2020). Amitriptyline, which also affects norepinephrine reuptake, has been used to treat hyperactivity and impulsivity in ASD (Bhatti et al., 2013). One possible interpretation is inadequate production of serotonin and/or norepinephrine in ASD, or abnormalities in the receptors for those transmitters. Several studies provide anatomical and functional evidence for abnormalities in serotonergic function in ASD. Azmitia et al. (2011) found larger numbers of serotonergic fibers in one tract, the medial forebrain bundle, innervating the amygdala, as well as dystrophic (abnormally large diameter) serotonergic fibers in ASD brains. Beversdorf et al. (2012) reported a decrease in serotonin receptor-binding in the thalamus for high-functioning ASD subjects. Wong et al. (2020) showed that drug-manipulated serotonin levels affected levels of limbic system activation of ASD but not control subjects (assessed by fMRI) performing a face-matching task.

Summary and Future Studies

We have thus identified a large set of brainstem structures that may be implicated in ASD. How might those structures be affected? There could be structural differences, at a macroscopic (size, shape, or organization of a nucleus) or microscopic (differences in cellular characteristics, e.g., neuron size, dendritic tree spread, etc.) level. There could also be functional differences, e.g., in the efficacy of a transmitter, that would be seen at a physiological but not at a structural level. How can we investigate these possibilities? Imaging studies may be able to show abnormalities in the size and shape of larger brain

structures, but at present cannot reveal subtle differences in organization or neurochemical changes of smaller ones. Studies of the relatively small brainstem structures are possible through studies of individual brains, optimally from patients whose symptoms and history have been very well-characterized. Ideally, the brains would be from as uniform as possible a population; at minimum details like IQ, and the presence or absence of a seizure disorder would be available. Brains would then be studied by standard histological techniques, including cell, fiber, and immunohistochemical staining.

Immunohistochemistry (IHC) would be essential for studying the serotonergic and noradrenergic transmitter systems. IHC might be useful at looking at aspects of other transmitter systems as well, the density and distribution of receptors or transporters could be examined. Another set of antibodies that might be useful is those to calcium-binding proteins calbindin, calretinin and parvalbumin as their levels may reflect the underlying physiological states of neurons (Blumcke et al., 1990; Celio, 1990; Arai et al., 1991; Baimbridge et al., 1992; Conde et al., 1994; Baurle et al., 1997). The level of the analysis of ASD brains could range from simple examination of cell, fiber, or immunostained sections at the light microscopic level to more quantitative stereological analysis (numbers or packing density of neurons in a structure; for example see Whitney et al., 2009).

However, the analysis needs to be considered carefully. The basic question is simple: do ASD brain structures differ from those in "normal" brains, but the analysis is far from simple. The critical question is how do we define a "normal" brain? There is much variability among human brains in the location, size, shape, and sometimes neurochemical properties of neurons in different brainstem structures (see the data on the IOpr in Baizer et al., 2011b). There are two approaches to selecting comparison data. One is to attempt to obtain and process brains in the same laboratories using the same techniques from controls that are matched for gender, age, IQ, presence of a seizure disorder, etc. The second approach is to compare ASD brain sections with images of "normal" brains as shown either in atlases (Olszewski and Baxter, 1982; Paxinos and Huang, 1995) or in publications (for example Baizer and Broussard, 2010; Baizer et al., 2011b).

It also may be useful to narrow the study population by using a subset of ASD symptoms, e.g., studying only those with particular motor symptoms or eye movement deficits. The problem then is acquiring enough brains to get meaningful results. Another approach is to study a biologically defined population. One example is Fragile X (FXS) syndrome (Garber et al., 2008; Berry-Kravis et al., 2018) which has been used as an animal model of ASD (for example He et al., 2017). However, such studies, in humans or animals, have major limitations in contributing to an understanding of the neuroanatomy of ASD. First, the symptoms of FXS can vary widely, not everyone with FXS is diagnosed as ASD (Garber et al., 2008; Hagerman et al., 2017). Second, FXS causes deficits in a single protein (Fragile X mental retardation protein 1, FMRP, Hagerman et al., 2017). This protein does not have a neuroanatomically limited distribution (Hagerman et al., 2017; Telias, 2019). The mutation is likely to cause widespread functional disruption at the circuit level but it is unlikely that there would be localized structural differences in the brainstem, cerebellum or elsewhere in the brain that could be visualized by neuropathological analysis.

CONCLUSION

The topic of this review is the possible role of the brainstem in autism. We have summarized literature on the functions affected in ASD and the brain structures and circuits that mediate those functions. Many of these circuits have brainstem components, and we suggest candidate brainstem nuclei and tracts that may be functionally altered in ASD. However, because of the heterogeneity of possible causes and symptoms of ASD, proving the involvement of these structures may be a very difficult task. It may be that the concept of an autism "spectrum" is useful clinically but misleading in trying to understand the biological basis of ASD. The ASD "spectrum" may not in fact reflect a continuum but instead consist of many separate and independent biological disorders with overlapping manifestations at the behavioral level but diverse neuroanatomic and genetic underpinnings. Progress in genetic analysis is likely to clarify the biological understanding of ASD.

DATA AVAILABILITY STATEMENT

The raw data supporting the conclusions of this article will be made available by the authors, without undue reservation.

ETHICS STATEMENT

The studies involving human participants were reviewed and approved by the Hamilton Integrated Research Ethics Board (HiREB), McMaster University. The patients/participants provided their written informed consent to participate in this study.

AUTHOR CONTRIBUTIONS

JSB read the papers discussed in the literature review, processed the sections shown in the Figures, composed the schematic diagrams, and wrote the manuscript.

REFERENCES

Albinali, F., Goodwin, M. S., and Intille, S. S. (2009). "Recognizing stereotypical motor movements in the laboratory and classroom: a case study with children on the autism spectrum," in *Proceedings of the Ubicomp'09: Proceedings of the 11th Acm International Conference on Ubiquitous Computing*, (Orlando, FL).

Allen, G. (2005). The cerebellum in autism. *Clin. Neuropsychiatry* 2:16.

Allen, G., Muller, R. A., and Courchesne, E. (2004). Cerebellar function in autism: functional magnetic resonance image activation during a simple motor task. *Biol. Psychiatry* 56, 269–278. doi: 10.1016/j.biopsych.2004.06.005

Arai, R., Winsky, L., Arai, M., and Jacobowitz, D. M. (1991). Immunohistochemical localization of calretinin in the rat hindbrain. *J. Comp. Neurol.* 310, 21–44.

Asanuma, C., Thach, W. T., and Jones, E. G. (1983a). Brainstem and spinal projections of the deep cerebellar nuclei in the monkey, with observations on the brainstem projections of the dorsal column nuclei. *Brain Res.* 286, 299–322. doi: 10.1016/0165-0173(83)90017-6

Asanuma, C., Thach, W. T., and Jones, E. G. (1983b). Distribution of cerebellar terminations and their relation to other afferent terminations in the ventral lateral thalamic region of the monkey. *Brain Res.* 286, 237–265. doi: 10.1016/0165-0173(83)90015-2

Azmitia, E. C., Singh, J. S., Hou, X. P., and Wegiel, J. (2011). Dystrophic serotonin axons in postmortem brains from young autism patients. *Anat. Rec. (Hoboken)* 294, 1653–1662. doi: 10.1002/ar.21243

Bailey, A., Luthert, P., Dean, A., Harding, B., Janota, I., Montgomery, M., et al. (1998). A clinicopathological study of autism. *Brain* 121(Pt 5), 889–905. doi: 10.1093/brain/121.5.889

Baimbridge, K. G., Celio, M. R., and Rogers, J. H. (1992). Calcium-binding proteins in the nervous system. *Trends Neurosci.* 15, 303–308.

Baizer, J. S. (2014). Unique features of the human brainstem and cerebellum. *Front. Hum. Neurosci.* 8:202. doi: 10.3389/fnhum.2014.00202

Baizer, J. S., and Broussard, D. M. (2010). Expression of calcium-binding proteins and nNOS in the human vestibular and precerebellar brainstem. *J. Comp. Neurol.* 518, 872–895. doi: 10.1002/cne.22250

Baizer, J. S., Paolone, N. A., and Witelson, S. F. (2011a). Nonphosphorylated neurofilament protein is expressed by scattered neurons in the human vestibular brainstem. *Brain Res.* 1382, 45–56.

Baizer, J. S., Sherwood, C. C., Hof, P. R., Witelson, S. F., and Sultan, F. (2011b). Neurochemical and structural organization of the principal nucleus of the inferior olive in the human. *Anat. Rec. (Hoboken)* 294, 1198–1216. doi: 10.1002/ar.21400

Baizer, J. S., Wong, K. M., Paolone, N. A., Weinstock, N., Salvi, R. J., Manohar, S., et al. (2014). Laminar and neurochemical organization of the dorsal cochlear nucleus of the human, monkey, cat, and rodents. *Anat. Rec. (Hoboken)* 297, 1865–1884. doi: 10.1002/ar.23000

Baizer, J. S., Wong, K. M., Salvi, R. J., Manohar, S., Sherwood, C. C., Hof, P. R., et al. (2018a). Species differences in the organization of the ventral cochlear nucleus. *Anat. Rec. (Hoboken)* 301, 862–886. doi: 10.1002/ar.23751

Baizer, J. S., Wong, K. M., Sherwood, C. C., Hof, P. R., and Witelson, S. F. (2018b). Individual variability in the structural properties of neurons in the human inferior olive. *Brain Struct. Funct.* 223, 1667–1681. doi: 10.1007/s00429-017-1580-2

Baizer, J., Webster, C., and Witelson, S. F. (2021). Individual variability in the size and organization of the human arcuate nucleus. *Brain Struct. Funct.*

Balaban, C. D., Ito, M., and Watanabe, E. (1981). Demonstration of zonal projections from the cerebellar flocculus to vestibular nuclei in monkeys (*Macaca fuscata*). *Neurosci. Lett.* 27, 101–105. doi: 10.1016/0304-3940(81)90251-2

Baranek, G. T., David, F. J., Poe, M. D., Stone, W. L., and Watson, L. R. (2006). Sensory experiences questionnaire: discriminating sensory features in young children with autism, developmental delays, and typical development. *J. Child Psychol. Psychiatry* 47, 591–601. doi: 10.1111/j.1469-7610.2005.01546.x

Barmack, N. H. (2003). Central vestibular system: vestibular nuclei and posterior cerebellum. *Brain Res. Bull.* 60, 511–541. doi: 10.1016/s0361-9230(03)00055-8

Bauman, M. L. (1991). Microscopic neuroanatomic abnormalities in autism. *Pediatrics* 87(5 Pt 2), 791–796.

Bauman, M. L., Kemper, T. L., and Arin, D. M. (1995). Pervasive neuroanatomic abnormalities of the brain in three cases of Rett's syndrome. *Neurology* 45, 1581–1586. doi: 10.1212/wnl.45.8.1581

Baurle, J., Kleine, J., Grusser, O. J., and Guldin, W. (1997). Co-localization of glycine and calbindin D-28k in the vestibular ganglion of the rat. *Neuroreport* 8, 2443–2447.

Beers, A. N., McBoyle, M., Kakande, E., Dar Santos, R. C., and Kozak, F. K. (2014). Autism and peripheral hearing loss: a systematic review. *Int. J. Pediatr. Otorhinolaryngol.* 78, 96–101. doi: 10.1016/j.ijporl.2013.10.063

Bell, L., Wittkowski, A., and Hare, D. J. (2019). Movement disorders and syndromic autism: a systematic review. *J. Autism. Dev. Disord.* 49, 54–67. doi: 10.1007/s10803-018-3658-y

Berry-Kravis, E. M., Lindemann, L., Jonch, A. E., Apostol, G., Bear, M. F., Carpenter, R. L., et al. (2018). Drug development for neurodevelopmental disorders: lessons learned from fragile X syndrome. *Nat. Rev. Drug Discov.* 17, 280–299. doi: 10.1038/nrd.2017.221

Bett, G. C., Llis, A., Wersinger, S., Baizer, J., Duffey, M., and Rasmusson, R. L. (2013). A mouse model of timothy syndrome: a complex autistic disorder resulting from a point mutation in Cav1.2. *North Am. J. Med. Sci.* 5, 135–140.

Beversdorf, D. Q., Nordgren, R. E., Bonab, A. A., Fischman, A. J., Weise, S. B., Dougherty, D. D., et al. (2012). 5-HT2 receptor distribution shown by [18F] setoperone PET in high-functioning autistic adults. *J. Neuropsychiatry Clin. Neurosci.* 24, 191–197. doi: 10.1176/appi.neuropsych.11080202

Bhat, A. N. (2021). Motor impairment increases in children with autism spectrum disorder as a function of social communication, cognitive and functional impairment, repetitive behavior severity, and comorbid diagnoses: a SPARK study report. *Autism Res.* 14, 202–219. doi: 10.1002/aur.2453

Bhatti, I., Thome, A., Smith, P. O., Cook-Wiens, G., Yeh, H. W., Gaffney, G. R., et al. (2013). A retrospective study of amitriptyline in youth with autism spectrum disorders. *J. Autism. Dev. Disord.* 43, 1017–1027. doi: 10.1007/s10803-012-1647-0

Bjaalie, J. G. (1986). Distribution of corticopontine neurons in visual areas of the middle suprasylvian sulcus: quantitative studies in the cat. *Neuroscience* 18, 1013–1033. doi: 10.1016/0306-4522(86)90114-4

Bjaalie, J. G., and Brodal, P. (1997). Cat pontocerebellar network: numerical capacity and axonal collateral branching of neurones in the pontine nuclei projecting to individual parafloccular folia. *Neurosci. Res.* 27, 199–210. doi: 10.1016/s0168-0102(96)01149-2

Bjaalie, J. G., Sudbo, J., and Brodal, P. (1997). Corticopontine terminal fibres form small scale clusters and large scale lamellae in the cat. *Neuroreport* 8, 1651–1655. doi: 10.1097/00001756-199705060-00019

Blazquez, P., and Pastor, A. (2013). "Cerebellar control of eye movements," in *Handbook of the Cerebellum and Cerebellar Disorders*, eds M. Manto, D. Gruol, J. Schmahmann, N. Koibuchi, and F. Rossi (Berlin: Springer).

Blumcke, I., Hof, P. R., Morrison, J. H., and Celio, M. R. (1990). Distribution of parvalbumin immunoreactivity in the visual cortex of old world monkeys and humans. *J. Comp. Neurol.* 301, 417–432.

Bojanek, E. K., Wang, Z., White, S. P., and Mosconi, M. W. (2020). Postural control processes during standing and step initiation in autism spectrum disorder. *J. Neurodev. Disord* 12:1. doi: 10.1186/s11689-019-9305-x

Boyd, B. A., McDonough, S. G., and Bodfish, J. W. (2012). Evidence-based behavioral interventions for repetitive behaviors in autism. *J. Autism. Dev. Disord.* 42, 1236–1248. doi: 10.1007/s10803-011-1284-z

Brodal, P. (1968a). Demonstration of a somatotopically organized projection from the primary sensorimotor cortex to the pontine nuclei in the cat. *Folia Morphol. (Praha)* 16, 105–107.

Brodal, P. (1968b). The corticopontine projection in the cat. I. Demonstration of a somatotopically organized projection from the primary sensorimotor cortex. *Exp. Brain Res.* 5, 210–234.

Brodal, P. (1968c). The corticopontine projection in the cat. demonstration of a somatotopically organized projection from the second somatosensory cortex. *Arch. Ital. Biol.* 106, 310–312.

Brodal, P. (1972a). The corticopontine projection from the visual cortex in the cat. I. the total projection and the projection from area 17. *Brain Res.* 39, 297–317. doi: 10.1016/0006-8993(72)90438-6

Brodal, P. (1972b). The corticopontine projection from the visual cortex in the cat. II. the projection from areas 18 and 19. *Brain Res.* 39, 319–335. doi: 10.1016/0006-8993(72)90439-8

Brodal, P. (1972c). The corticopontine projection in the cat. the projection from the auditory cortex. *Arch. Ital. Biol.* 110, 119–144.

Brodal, P. (1978a). Principles of organization of the monkey corticopontine projection. *Brain Res.* 148, 214–218. doi: 10.1016/0006-8993(78)90392-x

Brodal, P. (1978b). The corticopontine projection in the rhesus monkey. *Origin Principles Organ.* 101, 251–283. doi: 10.1093/brain/101.2.251

Brodal, P., and Bjaalie, J. G. (1992). Organization of the pontine nuclei. *Neurosci. Res.* 13, 83–118. doi: 10.1016/0168-0102(92)90092-q

Brodal, P., and Bjaalie, J. G. (1997). Salient anatomic features of the cortico-ponto-cerebellar pathway. *Prog. Brain Res.* 114, 227–249. doi: 10.1016/s0079-6123(08)63367-1

Bruchage, M. M. K., Bucci, M.-P., and Becker, E. B. E. (2018). Cerebellar involvement in autism and ADHD. *Handb. Clin. Neurol.* 155, 61–72.

Buckner, R. L. (2013). The cerebellum and cognitive function: 25 years of insight from anatomy and neuroimaging. *Neuron* 80, 807–815. doi: 10.1016/j.neuron.2013.10.044

Campbell, D. B., D'Oronzio, R., Garbett, K., Ebert, P. J., Mirnics, K., Levitt, P., et al. (2007). Disruption of cerebral cortex MET signaling in autism spectrum disorder. *Ann. Neurol.* 62, 243–250. doi: 10.1002/ana.21180

Carper, R. A., and Courchesne, E. (2005). Localized enlargement of the frontal cortex in early autism. *Biol. Psychiatry* 57, 126–133. doi: 10.1016/j.biopsych.2004.11.005

Casanova, M. F., Buxhoeveden, D., and Gomez, J. (2003). Disruption in the inhibitory architecture of the cell minicolumn: implications for autism. *Neuroscientist* 9, 496–507. doi: 10.1177/1073858403253552

Catani, M., Jones, D. K., Daly, E., Embiricos, N., Deeley, Q., Pugliese, L., et al. (2008). Altered cerebellar feedback projections in Asperger syndrome. *Neuroimage* 41, 1184–1191. doi: 10.1016/j.neuroimage.2008.03.041

CDC (2021). *Austism Spectrum Disorder (ASD)*. Atlanta: CDC.

Celio, M. R. (1990). Calbindin D-28k and parvalbumin in the rat nervous system. *Neuroscience* 35, 375–475.

Chawner, S., Doherty, J. L., Anney, R. J. L., Antshel, K. M., Bearden, C. E., Bernier, R., et al. (2021). A genetics-first approach to dissecting the heterogeneity of autism: phenotypic comparison of autism risk copy number variants. *Am. J. Psychiatry* 178, 77–86. doi: 10.1176/appi.ajp.2020.20010015

Chubb, M. C., and Fuchs, A. F. (1982). Contribution of y group of vestibular nuclei and dentate nucleus of cerebellum to generation of vertical smooth eye movements. *J. Neurophysiol.* 48, 75–99. doi: 10.1152/jn.1982.48.1.75

Chubb, M. C., Fuchs, A. F., and Scudder, C. A. (1984). Neuron activity in monkey vestibular nuclei during vertical vestibular stimulation and eye movements. *J. Neurophysiol.* 52, 724–742. doi: 10.1152/jn.1984.52.4.724

Ciaranello, A. L., and Ciaranello, R. D. (1995). The neurobiology of infantile autism. *Annu. Rev. Neurosci.* 18, 101–128. doi: 10.1146/annurev.ne.18.030195.000533

Ciesielski, K. T., Harris, R. J., Hart, B. L., and Pabst, H. F. (1997). Cerebellar hypoplasia and frontal lobe cognitive deficits in disorders of early childhood. *Neuropsychologia* 35, 643–655. doi: 10.1016/s0028-3932(96)00119-4

Conde, F., Lund, J. S., Jacobowitz, D. M., Baimbridge, K. G., and Lewis, D. A. (1994). Local circuit neurons immunoreactive for calretinin, calbindin D-28k or parvalbumin in monkey prefrontal cortex: distribution and morphology. *J. Comp. Neurol.* 341, 95–116. doi: 10.1002/cne.903410109

Courchesne, E., Mouton, P. R., Calhoun, M. E., Semendeferi, K., Ahrens-Barbeau, C., Hallet, M. J., et al. (2011). Neuron number and size in prefrontal cortex of children with autism. *JAMA* 306, 2001–2010. doi: 10.1001/jama.2011.1638

Courchesne, E., and Pierce, K. (2005). Why the frontal cortex in autism might be talking only to itself: local over-connectivity but long-distance disconnection. *Curr. Opin. Neurobiol.* 15, 225–230. doi: 10.1016/j.conb.2005.03.001

Courchesne, E., Pierce, K., Schumann, C. M., Redcay, E., Buckwalter, J. A., Kennedy, D. P., et al. (2007). Mapping early brain development in autism. *Neuron* 56, 399–413. doi: 10.1016/j.neuron.2007.10.016

Courchesne, E., Saitoh, O., Yeung-Courchesne, R., Press, G. A., Lincoln, A. J., Haas, R. H., et al. (1994). Abnormality of cerebellar vermian lobules VI and VII in patients with infantile autism: identification of hypoplastic and hyperplastic subgroups with MR imaging. *AJR Am. J. Roentgenol.* 162, 123–130. doi: 10.2214/ajr.162.1.8273650

Dadalko, O. I., and Travers, B. G. (2018). Evidence for brainstem contributions to autism spectrum disorders. *Front. Integr. Neurosci.* 12:47. doi: 10.3389/fnint.2018.00047

Dawson, G., Osterling, J., Meltzoff, A. N., and Kuhl, P. (2000). Case study of the development of an infant with autism from birth to two years of age. *J. Appl. Dev. Psychol.* 21, 299–313. doi: 10.1016/S0193-3973(99)00042-8

DiCicco-Bloom, E., Lord, C., Zwaigenbaum, L., Courchesne, E., Dager, S. R., Schmitz, C., et al. (2006). The developmental neurobiology of autism spectrum disorder. *J. Neurosci.* 26, 6897–6906. doi: 10.1523/JNEUROSCI.1712-06.2006

Donovan, A. P., and Basson, M. A. (2017). The neuroanatomy of autism - a developmental perspective. *J. Anat.* 230, 4–15. doi: 10.1111/joa.12542

DSM-5 (2013). *Diagnostic and Statistical Manual of Mental Disorders*, 5th Edn. Virginia, VA: American Psychiatric Association.

Eccles, J. C. (1967). Circuits in the cerebellar control of movement. *Proc. Natl. Acad. Sci. U S A.* 58, 336–343. doi: 10.1073/pnas.58.1.336

Ecker, C. (2017). The neuroanatomy of autism spectrum disorder: an overview of structural neuroimaging findings and their translatability to the clinical setting. *Autism* 21, 18–28. doi: 10.1177/1362361315627136

Eggleston, J. D., Harry, J. R., Hickman, R. A., and Dufek, J. S. (2017). Analysis of gait symmetry during over-ground walking in children with autism spectrum disorder. *Gait Posture* 55, 162–166. doi: 10.1016/j.gaitpost.2017.04.026

Essick, C. R. (1912). The development of the nuclei pontis and the nucleus arcuatus in man. *Am. J. Anatomy* 13, 25–54.

Evarts, E. V., and Thach, W. T. (1969). Motor mechanisms of the CNS: cerebrocerebellar interrelations. *Annu. Rev. Physiol.* 31, 451–498. doi: 10.1146/annurev.ph.31.030169.002315

Fatemi, S. H., Aldinger, K. A., Ashwood, P., Bauman, M. L., Blaha, C. D., Blatt, G. J., et al. (2012). Consensus paper: pathological role of the cerebellum in autism. *Cerebellum* 11, 777–807. doi: 10.1007/s12311-012-0355-9

Fatemi, S. H., Halt, A. R., Realmuto, G., Earle, J., Kist, D. A., Thuras, P., et al. (2002). Purkinje cell size is reduced in cerebellum of patients with autism. *Cell Mol. Neurobiol.* 22, 171–175. doi: 10.1023/a:1019861721160

Filipek, P. A., Accardo, P. J., Baranek, G. T., Cook, E. H. Jr., Dawson, G., Gordon, B., et al. (1999). The screening and diagnosis of autistic spectrum disorders. *J. Autism. Dev. Disord.* 29, 439–484. doi: 10.1023/a:1021943802493

Fingher, N., Dinstein, I., Ben-Shachar, M., Haar, S., Dale, A. M., Eyler, L., et al. (2017). Toddlers later diagnosed with autism exhibit multiple structural abnormalities in temporal corpus callosum fibers. *Cortex* 97, 291–305. doi: 10.1016/j.cortex.2016.12.024

Folstein, S., and Rutter, M. (1977a). Genetic influences and infantile autism. *Nature* 265, 726–728. doi: 10.1038/265726a0

Folstein, S., and Rutter, M. (1977b). Infantile autism: a genetic study of 21 twin pairs. *J. Child Psychol. Psychiatry* 18, 297–321. doi: 10.1111/j.1469-7610.1977.tb00443.x

Folstein, S. E., and Rosen-Sheidley, B. (2001). Genetics of autism: complex aetiology for a heterogeneous disorder. *Nat. Rev. Genet.* 2, 943–955. doi: 10.1038/35103559

Fuchs, A. F., and Luschei, E. S. (1970). Firing patterns of abducens neurons of alert monkeys in relationship to horizontal eye movement. *J. Neurophysiol.* 33, 382–392. doi: 10.1152/jn.1970.33.3.382

Fuchs, A. F., and Luschei, E. S. (1971). The activity of single trochlear nerve fibers during eye movements in the alert monkey. *Exp. Brain Res.* 13, 78–89. doi: 10.1007/BF00236431

Fukushima, J., Akao, T., Takeichi, N., Kurkin, S., Kaneko, C. R., and Fukushima, K. (2004). Pursuit-related neurons in the supplementary eye fields: discharge during pursuit and passive whole body rotation. *J. Neurophysiol.* 91, 2809–2825. doi: 10.1152/jn.01128.2003

Garber, K. B., Visootsak, J., and Warren, S. T. (2008). Fragile X syndrome. *Eur. J. Hum. Genet.* 16, 666–672. doi: 10.1038/ejhg.2008.61

Geschwind, D. H. (2011). Genetics of autism spectrum disorders. *Trends Cogn. Sci.* 15, 409–416. doi: 10.1016/j.tics.2011.07.003

Gibson, A., Glickstein, M., and Stein, J. F. (1977). The projection from visual pontine nucleus neurones to the cerebellum in cats [proceedings]. *J. Physiol.* 272:88.

Glickstein, M., May, J. G. III, and Mercier, B. E. (1985). Corticopontine projection in the macaque: the distribution of labelled cortical cells after large injections of horseradish peroxidase in the pontine nuclei. *J. Comp. Neurol.* 235, 343–359. doi: 10.1002/cne.902350306

Glickstein, M., Stein, J., and King, R. A. (1972). Visual input to the pontine nuclei. *Science* 178, 1110–1111. doi: 10.1126/science.178.4065.1110

Gopal, K. V., Schafer, E. C., Mathews, L., Nandy, R., Beaudoin, D., Schadt, L., et al. (2020). Effects of auditory training on electrophysiological measures in individuals with autism spectrum disorder. *J. Am. Acad. Audiol.* 31, 96–104. doi: 10.3766/jaaa.18063

Grzadzinski, R., Huerta, M., and Lord, C. (2013). DSM-5 and autism spectrum disorders (ASDs): an opportunity for identifying ASD subtypes. *Mol. Autism* 4:12. doi: 10.1186/2040-2392-4-12

Hagerman, R. J., Berry-Kravis, E., Hazlett, H. C., Bailey, D. B. Jr., Moine, H., Kooy, R. F., et al. (2017). Fragile X syndrome. *Nat. Rev. Dis. Primers* 3:17065. doi: 10.1038/nrdp.2017.65

Hanaie, R., Mohri, I., Kagitani-Shimono, K., Tachibana, M., Azuma, J., Matsuzaki, J., et al. (2013). Altered microstructural connectivity of the

superior cerebellar peduncle is related to motor dysfunction in children with autistic spectrum disorders. *Cerebellum* 12, 645–656. doi: 10.1007/s12311-013-0475-x

Hannant, P., Cassidy, S., Tavassoli, T., and Mann, F. (2016). Sensorimotor difficulties are associated with the severity of autism spectrum conditions. *Front. Integr. Neurosci.* 10:28. doi: 10.3389/fnint.2016.00028

Harris, N. S., Courchesne, E., Townsend, J., Carper, R. A., and Lord, C. (1999). Neuroanatomic contributions to slowed orienting of attention in children with autism. *Brain Res. Cogn. Brain Res.* 8, 61–71. doi: 10.1016/s0926-6410(99)00006-3

Hazrati, L. N., and Parent, A. (1992). Projection from the deep cerebellar nuclei to the pedunculopontine nucleus in the squirrel monkey. *Brain Res.* 585, 267–271. doi: 10.1016/0006-8993(92)91216-2

He, C. X., Cantu, D. A., Mantri, S. S., Zeiger, W. A., Goel, A., and Portera-Cailliau, C. (2017). Tactile defensiveness and impaired adaptation of neuronal activity in the Fmr1 knock-out mouse model of autism. *J. Neurosci.* 37, 6475–6487. doi: 10.1523/JNEUROSCI.0651-17.2017

Henry, C. A., Shervin, D., Neumeyer, A., Steingard, R., Spybrook, J., Choueiri, R., et al. (2009). Retrial of selective serotonin reuptake inhibitors in children with pervasive developmental disorders: a retrospective chart review. *J. Child Adolesc. Psychopharmacol.* 19, 111–117. doi: 10.1089/cap.2008.037

Hepburn, S., Philofsky, A., Fidler, D. J., and Rogers, S. (2008). Autism symptoms in toddlers with down syndrome: a descriptive study. *J. Appl. Res. Intell. Disabil.* 21, 48–57. doi: 10.1111/j.1468-3148.2007.00368.x

Hicks, T. P., and Onodera, S. (2012). The mammalian red nucleus and its role in motor systems, including the emergence of bipedalism and language. *Prog. Neurobiol.* 96, 165–175. doi: 10.1016/j.pneurobio.2011.12.002

Hikosaka, O., and Wurtz, R. H. (1983a). Visual and oculomotor functions of monkey substantia nigra pars reticulata. III. memory-contingent visual and saccade responses. *J. Neurophysiol.* 49, 1268–1284. doi: 10.1152/jn.1983.49.5.1268

Hikosaka, O., and Wurtz, R. H. (1983b). Visual and oculomotor functions of monkey substantia nigra pars reticulata. IV. Relation of substantia nigra to superior colliculus. *J. Neurophysiol.* 49, 1285–1301. doi: 10.1152/jn.1983.49.5.1285

Hikosaka, O., and Wurtz, R. H. (1985). Modification of saccadic eye movements by GABA-related substances. II. effects of muscimol in monkey substantia nigra pars reticulata. *J. Neurophysiol.* 53, 292–308. doi: 10.1152/jn.1985.53.1.292

Hoeft, F., Walter, E., Lightbody, A. A., Hazlett, H. C., Chang, C., Piven, J., et al. (2011). Neuroanatomical differences in toddler boys with fragile x syndrome and idiopathic autism. *Arch. Gen. Psychiatry* 68, 295–305. doi: 10.1001/archgenpsychiatry.2010.153

Horn, A. K., and Büttner-Ennever, J. A. (1998). Premotor neurons for vertical eye movements in the rostral mesencephalon of monkey and human: histologic identification by parvalbumin immunostaining. *J. Comp. Neurol.* 392, 413–427.

Hornung, J. P. (2003). The human raphe nuclei and the serotonergic system. *J. Chem. Neuroanat.* 26, 331–343. doi: 10.1016/j.jchemneu.2003.10.002

Hua, X., Thompson, P. M., Leow, A. D., Madsen, S. K., Caplan, R., Alger, J. R., et al. (2013). Brain growth rate abnormalities visualized in adolescents with autism. *Hum. Brain Mapp.* 34, 425–436. doi: 10.1002/hbm.21441

Huguet, G., Benabou, M., and Bourgeron, T. (2016). "The genetics of autism spectrum disorders," in *A Time for Metabolism and Hormones*, eds P. Sassone-Corsi and Y. Christen (Cham (CH): Springer), doi: 10.1007/978-3-319-27069-2_11

Hunter'sHope (2021). *Krabbe Disease*. Available online at: https://www.huntershope.org/family-care/leukodystrophies/krabbe-disease/ (accessed June 21, 2021)

Igelstrom, K. M., Webb, T. W., and Graziano, M. S. A. (2017). Functional connectivity between the temporoparietal cortex and cerebellum in autism spectrum disorder. *Cereb. Cortex* 27, 2617–2627. doi: 10.1093/cercor/bhw079

Jacobson, S., and Trojanowski, J. Q. (1974). The cells of origin of the corpus callosum in rat, cat and rhesus monkey. *Brain Res.* 74, 149–155. doi: 10.1016/0006-8993(74)90118-8

Jarrold, C., and Brock, J. (2004). To match or not to match? methodological issues in autism-related research. *J. Autism. Dev. Disord.* 34, 81–86. doi: 10.1023/b:jadd.0000018078.82542.ab

Jiang, Y. H., Yuen, R. K., Jin, X., Wang, M., Chen, N., Wu, X., et al. (2013). Detection of clinically relevant genetic variants in autism spectrum disorder by whole-genome sequencing. *Am. J. Hum. Genet.* 93, 249–263. doi: 10.1016/j.ajhg.2013.06.012

Kaneko, C. R. (1992). Effects of ibotenic acid lesions of nucleus prepositus hypoglossi on optokinetic and vestibular eye movements in the alert, trained monkey. *Ann. N. Y. Acad. Sci.* 656, 408–427. doi: 10.1111/j.1749-6632.1992.tb25225.x

Kaneko, C. R. (1997). Eye movement deficits after ibotenic acid lesions of the nucleus prepositus hypoglossi in monkeys. I. saccades and fixation. *J. Neurophysiol.* 78, 1753–1768. doi: 10.1152/jn.1997.78.4.1753

Kaneko, C. R. (1999). Eye movement deficits following ibotenic acid lesions of the nucleus prepositus hypoglossi in monkeys II. pursuit, vestibular, and optokinetic responses. *J. Neurophysiol.* 81, 668–681. doi: 10.1152/jn.1999.81.2.668

Kates, W. R., Burnette, C. P., Eliez, S., Strunge, L. A., Kaplan, D., Landa, R., et al. (2004). Neuroanatomic variation in monozygotic twin pairs discordant for the narrow phenotype for autism. *Am. J. Psychiatry* 161, 539–546. doi: 10.1176/appi.ajp.161.3.539

Kaufmann, W. E., Cooper, K. L., Mostofsky, S. H., Capone, G. T., Kates, W. R., Newschaffer, C. J., et al. (2003). Specificity of cerebellar vermian abnormalities in autism: a quantitative magnetic resonance imaging study. *J. Child Neurol.* 18, 463–470. doi: 10.1177/08830738030180070501

Keller, E. L. (1974). Participation of medial pontine reticular formation in eye movement generation in monkey. *J. Neurophysiol.* 37, 316–332. doi: 10.1152/jn.1974.37.2.316

Kemper, T. L., and Bauman, M. L. (2002). Neuropathology of infantile autism. *Mol. Psychiatry* 7(Suppl. 2), S12–S13. doi: 10.1038/sj.mp.4001165

Kern, J. K., Garver, C. R., Grannemann, B. D., Trivedi, M. H., Carmody, T., Andrews, A. A., et al. (2007). Response to vestibular sensory events in autism. *Res. Autism Spect. Dis.* 1, 67–74. doi: 10.1016/j.rasd.2006.07.006

Kohenraz, R., Volkmar, F. R., and Cohen, D. J. (1992). Postural control in children with autism. *J. Autism. Dev. Disord.* 22, 419–432. doi: 10.1007/Bf01048244

Kojima, Y., Soetedjo, R., and Fuchs, A. F. (2010a). Behavior of the oculomotor vermis for five different types of saccade. *J. Neurophysiol.* 104, 3667–3676. doi: 10.1152/jn.00558.2010

Kojima, Y., Soetedjo, R., and Fuchs, A. F. (2010b). Changes in simple spike activity of some Purkinje cells in the oculomotor vermis during saccade adaptation are appropriate to participate in motor learning. *J. Neurosci.* 30, 3715–3727. doi: 10.1523/JNEUROSCI.4953-09.2010

Kojima, Y., Soetedjo, R., and Fuchs, A. F. (2010c). Effects of GABA agonist and antagonist injections into the oculomotor vermis on horizontal saccades. *Brain Res.* 1366, 93–100. doi: 10.1016/j.brainres.2010.10.027

Kojima, Y., Soetedjo, R., and Fuchs, A. F. (2011). Effect of inactivation and disinhibition of the oculomotor vermis on saccade adaptation. *Brain Res.* 1401, 30–39. doi: 10.1016/j.brainres.2011.05.027

Konstantareas, M. M., and Stewart, K. (2006). affect regulation and temperament in children with autism spectrum disorder. *J. Autism. Dev. Disord.* 36, 143–154. doi: 10.1007/s10803-005-0051-4

Kozou, H., Azouz, H. G., Abdou, R. M., and Shaltout, A. (2018). Evaluation and remediation of central auditory processing disorders in children with autism spectrum disorders. *Int. J. Pediatr. Otorhinolaryngol.* 104, 36–42. doi: 10.1016/j.ijporl.2017.10.039

Kulesza, R. J. Jr., Lukose, R., and Stevens, L. V. (2011). Malformation of the human superior olive in autistic spectrum disorders. *Brain Res.* 1367, 360–371. doi: 10.1016/j.brainres.2010.10.015

Kulesza, R. J., and Mangunay, K. (2008). Morphological features of the medial superior olive in autism. *Brain Res.* 1200, 132–137. doi: 10.1016/j.brainres.2008.01.009

Kwon, S., Kim, J., Choe, B. H., Ko, C., and Park, S. (2007). Electrophysiologic assessment of central auditory processing by auditory brainstem responses in children with autism spectrum disorders. *J. Korean Med. Sci.* 22, 656–659. doi: 10.3346/jkms.2007.22.4.656

Lai, M. C., Lombardo, M. V., and Baron-Cohen, S. (2014). Autism. *Lancet* 383, 896–910. doi: 10.1016/S0140-6736(13)61539-1

Lane, A. E., Young, R. L., Baker, A. E., and Angley, M. T. (2010). Sensory processing subtypes in autism: association with adaptive behavior. *J. Autism. Dev. Disord.* 40, 112–122. doi: 10.1007/s10803-009-0840-2

Lange, N., Travers, B. G., Bigler, Prigge, M. B., Froehlich, A. L., Nielsen, J. A., et al. (2015). Longitudinal volumetric brain changes in autism spectrum disorder ages 6-35 years. *Autism Res.* 8, 82–93. doi: 10.1002/aur.1427

Langen, M., Durston, S., Staal, W. G., Palmen, S. J., and van Engeland, H. (2007). Caudate nucleus is enlarged in high-functioning medication-naive subjects with autism. *Biol. Psychiatry* 62, 262–266. doi: 10.1016/j.biopsych.2006.09.040

Leergaard, T. B., and Bjaalie, J. G. (2007). Topography of the complete corticopontine projection: from experiments to principal Maps. *Front. Neurosci.* 1:211–223. doi: 10.3389/neuro.01.1.1.016.2007

Legg, C. R., Mercier, B., and Glickstein, M. (1989). Corticopontine projection in the rat: the distribution of labelled cortical cells after large injections of horseradish peroxidase in the pontine nuclei. *J. Comp. Neurol.* 286, 427–441. doi: 10.1002/cne.902860403

Levitt, J. G., Blanton, R., Capetillo-Cunliffe, L., Guthrie, D., Toga, A., and McCracken, J. T. (1999). Cerebellar vermis lobules VIII-X in autism. *Prog. Neuropsychopharmacol. Biol. Psychiatry* 23, 625–633. doi: 10.1016/s0278-5846(99)00021-4

Libero, L. E., Nordahl, C. W., Li, D. D., Ferrer, E., Rogers, S. J., and Amaral, D. G. (2016). Persistence of megalencephaly in a subgroup of young boys with autism spectrum disorder. *Autism Res.* 9, 1169–1182. doi: 10.1002/aur.1643

Lisberger, S. G., and Fuchs, A. F. (1974). Response of flocculus Purkinje cells to adequate vestibular stimulation in the alert monkey: fixation vs. compensatory eye movements. *Brain Res.* 69, 347–353.

Lukose, R., Beebe, K., and Kulesza, R. J. Jr. (2015). Organization of the human superior olivary complex in 15q duplication syndromes and autism spectrum disorders. *Neuroscience* 286, 216–230. doi: 10.1016/j.neuroscience.2014.11.033

Lukose, R., Brown, K., Barber, C. M., and Kulesza, R. J. Jr. (2013). Quantification of the stapedial reflex reveals delayed responses in autism. *Autism Res.* 6, 344–353. doi: 10.1002/aur.1297

MacDonald, M., Esposito, P., Hauck, J., Jeong, I., Hornyak, J., Argento, A., et al. (2012). Bicycle training for youth with down syndrome and autism spectrum disorders. *Focus Autism Dev. Dis.* 27, 12–21. doi: 10.1177/1088357611428333

Mann, D. M., and Yates, P. O. (1974). Lipoprotein pigments–their relationship to ageing in the human nervous system. I. the lipofuscin content of nerve cells. *Brain* 97, 481–488.

Mann, D. M., Yates, P. O., and Stamp, J. E. (1978). The relationship between lipofuscin pigment and ageing in the human nervous system. *J. Neurol. Sci.* 37, 83–93.

Mansour, Y., and Kulesza, R. (2020). Three dimensional reconstructions of the superior olivary complex from children with autism spectrum disorder. *Hear. Res.* 393:107974. doi: 10.1016/j.heares.2020.107974

Marko, M. K., Crocetti, D., Hulst, T., Donchin, O., Shadmehr, R., and Mostofsky, S. H. (2015). Behavioural and neural basis of anomalous motor learning in children with autism. *Brain* 138(Pt 3), 784–797. doi: 10.1093/brain/awu394

Massion, J. (1967). The mammalian red nucleus. *Physiol. Rev.* 47, 383–436. doi: 10.1152/physrev.1967.47.3.383

May, P. J., Reiner, A. J., and Ryabinin, A. E. (2008). Comparison of the distributions of urocortin-containing and cholinergic neurons in the perioculomotor midbrain of the cat and macaque. *J. Comp. Neurol.* 507, 1300–1316. doi: 10.1002/cne.21514

Mazefsky, C. A., Herrington, J., Siegel, M., Scarpa, A., Maddox, B. B., Scahill, L., et al. (2013). The role of emotion regulation in autism spectrum disorder. *J. Am. Acad. Child Adolesc. Psychiatry* 52, 679–688. doi: 10.1016/j.jaac.2013.05.006

Mazefsky, C. A., and White, S. W. (2014). Emotion regulation: concepts & practice in autism spectrum disorder. *Child Adolesc. Psychiatr. Clin. N. Am.* 23, 15–24. doi: 10.1016/j.chc.2013.07.002

Ming, X., Brimacombe, M., and Wagner, G. C. (2007). Prevalence of motor impairment in autism spectrum disorders. *Brain Dev.* 29, 565–570. doi: 10.1016/j.braindev.2007.03.002

Molloy, C. A., Dietrich, K. N., and Bhattacharya, A. (2003). Postural stability in children with autism spectrum disorder. *J. Autism. Dev. Disord.* 33, 643–652. doi: 10.1023/b:jadd.0000006001.00667.4c

Mosconi, M. W., Luna, B., Kay-Stacey, M., Nowinski, C. V., Rubin, L. H., Scudder, C., et al. (2013). Saccade adaptation abnormalities implicate dysfunction of cerebellar-dependent learning mechanisms in Autism Spectrum Disorders (ASD). *PLoS One* 8:e63709. doi: 10.1371/journal.pone.0063709

Mosconi, M. W., and Sweeney, J. A. (2015). Sensorimotor dysfunctions as primary features of autism spectrum disorders. *Sci. China Life Sci.* 58, 1016–1023. doi: 10.1007/s11427-015-4894-4

Müller, R. A., Pierce, K., Ambrose, J. B., Allen, G., and Courchesne, E. (2001). Atypical patterns of cerebral motor activation in autism: a functional magnetic resonance study. *Biol. Psychiatry* 49, 665–676. doi: 10.1016/s0006-3223(00)01004-0

Murakami, J. W., Courchesne, E., Press, G. A., Yeung-Courchesne, R., and Hesselink, J. R. (1989). Reduced cerebellar hemisphere size and its relationship to vermal hypoplasia in autism. *Arch. Neurol.* 46, 689–694. doi: 10.1001/archneur.1989.00520420111032

Myers, S. M., Challman, T. D., Bernier, R., Bourgeron, T., Chung, W. K., Constantino, J. N., et al. (2020). Insufficient evidence for "Autism-Specific". *Genes. Am. J. Hum. Genet.* 106, 587–595. doi: 10.1016/j.ajhg.2020.04.004

Nanjappa, M., Voyiaziakis, E., Pradhan, B., and Mannekote Thippaiah, S. (2020). Use of selective serotonin and norepinephrine reuptake inhibitors (SNRIs) in the treatment of autism spectrum disorder (ASD), comorbid psychiatric disorders and ASD-associated symptoms: A clinical review. *CNS Spectrums* doi: 10.1017/S109285292000214X Online ahead of print.

Neely, K. A., Mohanty, S., Schmitt, L. M., Wang, Z., Sweeney, J. A., and Mosconi, M. W. (2019). Motor memory deficits contribute to motor impairments in autism spectrum disorder. *J. Autism. Dev. Disord.* 49, 2675–2684. doi: 10.1007/s10803-016-2806-5

Nowinski, C. V., Minshew, N. J., Luna, B., Takarae, Y., and Sweeney, J. A. (2005). Oculomotor studies of cerebellar function in autism. *Psychiatry Res.* 137, 11–19. doi: 10.1016/j.psychres.2005.07.005

Oldehinkel, M., Mennes, M., Marquand, A., Charman, T., Tillmann, J., Ecker, C., et al. (2019). Altered connectivity between cerebellum, visual, and sensory-motor networks in autism spectrum disorder: results from the EU-AIMS longitudinal european autism project. *Biol. Psychiatry Cogn. Neurosci. Neuroimag.* 4, 260–270. doi: 10.1016/j.bpsc.2018.11.010

Olszewski, J., and Baxter, D. (1982). *Cytoarchitecture of the Human Brain Stem*, 2nd edn. Basel: Karger.

Palmen, S. J., van Engeland, H., Hof, P. R., and Schmitz, C. (2004). Neuropathological findings in autism. *Brain* 127(Pt 12), 2572–2583. doi: 10.1093/brain/awh287

Paxinos, G., and Huang, X. F. (1995). *Atlas of the Human Brainstem*. San Diego, CA: Academic Press.

Percy, A. K. (2011). Rett syndrome: exploring the autism link. *Arch. Neurol.* 68, 985–989. doi: 10.1001/archneurol.2011.149

Pickles, J. (2015). "Auditory pathways: anatomy and physiology," in *Handbok of Clinical Neurology*, eds G. Celesia and G. Hickok (Amsterdam: Elsevier).

Pinto, D., Delaby, E., Merico, D., Barbosa, M., Merikangas, A., Klei, L., et al. (2014). Convergence of genes and cellular pathways dysregulated in autism spectrum disorders. *Am. J. Hum. Genet.* 94, 677–694. doi: 10.1016/j.ajhg.2014.03.018

Purcell, A. E., Jeon, O. H., Zimmerman, A. W., Blue, M. E., and Pevsner, J. (2001). Postmortem brain abnormalities of the glutamate neurotransmitter system in autism. *Neurology* 57, 1618–1628. doi: 10.1212/wnl.57.9.1618

Rimland, B., and Edelson, S. M. (1995). Brief report: a pilot study of auditory integration training in autism. *J. Autism. Dev. Disord.* 25, 61–70. doi: 10.1007/BF02178168

Ritvo, E. R., Freeman, B. J., Scheibel, A. B., Duong, T., Robinson, H., Guthrie, D., et al. (1986). Lower Purkinje cell counts in the cerebella of four autistic subjects: initial findings of the UCLA-NSAC autopsy research report. *Am. J. Psychiatry* 143, 862–866. doi: 10.1176/ajp.143.7.862

Robinson, D. A., and Fuchs, A. F. (1969). Eye movements evoked by stimulation of frontal eye fields. *J. Neurophysiol.* 32, 637–648. doi: 10.1152/jn.1969.32.5.637

Robinson, F. R., and Fuchs, A. F. (2001). The role of the cerebellum in voluntary eye movements. *Annu. Rev. Neurosci.* 24, 981–1004. doi: 10.1146/annurev.neuro.24.1.981

Rodier, P. M., Ingram, J. L., Tisdale, B., Nelson, S., and Romano, J. (1996). Embryological origin for autism: developmental anomalies of the cranial nerve motor nuclei. *J. Comp. Neurol.* 370, 247–261.

Roesch, M. R., and Olson, C. R. (2005). Neuronal activity dependent on anticipated and elapsed delay in macaque prefrontal cortex, frontal and supplementary eye

fields, and premotor cortex. *J. Neurophysiol.* 94, 1469–1497. doi: 10.1152/jn.00064.2005

Roldan, M., and Reinoso-Suarez, F. (1981). Cerebellar projections to the superior colliculus in the cat. *J. Neurosci.* 1, 827–834. doi: 10.1523/JNEUROSCI.01-08-00827.1981

Rosenhall, U., Johansson, E., and Gillberg, C. (1988). Oculomotor findings in autistic children. *J. Laryngol. Otol.* 102, 435–439. doi: 10.1017/s0022215100105286

Russo, N. M., Hornickel, J., Nicol, T., Zecker, S., and Kraus, N. (2010). Biological changes in auditory function following training in children with autism spectrum disorders. *Behav. Brain Funct.* 6:60. doi: 10.1186/1744-9081-6-60

Schiller, P. H., Sandell, J. H., and Maunsell, J. H. (1987). The effect of frontal eye field and superior colliculus lesions on saccadic latencies in the rhesus monkey. *J. Neurophysiol.* 57, 1033–1049. doi: 10.1152/jn.1987.57.4.1033

Schmahmann, J. D., and Pandya, D. N. (1997). Anatomic organization of the basilar pontine projections from prefrontal cortices in rhesus monkey. *J. Neurosci.* 17, 438–458.

Schumann, C. M., Barnes, C. C., Lord, C., and Courchesne, E. (2009). Amygdala enlargement in toddlers with autism related to severity of social and communication impairments. *Biol. Psychiatry* 66, 942–949. doi: 10.1016/j.biopsych.2009.07.007

Schumann, C. M., Hamstra, J., Goodlin-Jones, B. L., Lotspeich, L. J., Kwon, H., Buonocore, M. H., et al. (2004). The amygdala is enlarged in children but not adolescents with autism; the hippocampus is enlarged at all ages. *J. Neurosci.* 24, 6392–6401. doi: 10.1523/JNEUROSCI.1297-04.2004

Schwarz, L. A., and Luo, L. (2015). Organization of the locus coeruleus-norepinephrine system. *Curr. Biol.* 25, R1051–R1056. doi: 10.1016/j.cub.2015.09.039

Simmons, D. R., Robertson, A. E., McKay, L. S., Toal, E., McAleer, P., and Pollick, F. E. (2009). Vision in autism spectrum disorders. *Vis. Res.* 49, 2705–2739. doi: 10.1016/j.visres.2009.08.005

Smalley, S. L. (1998). Autism and tuberous sclerosis. *J. Autism. Dev. Disord.* 28, 407–414. doi: 10.1023/a:1026052421693

Smith, A., Storti, S., Lukose, R., and Kulesza, R. J. Jr. (2019). Structural and functional aberrations of the auditory brainstem in autism spectrum disorder. *J. Am. Osteopath. Assoc.* 119, 41–50. doi: 10.7556/jaoa.2019.007

Smoot Reinert, S., Jackson, K., and Bigelow, K. (2015). Using posturography to examine the immediate effects of vestibular therapy for children with autism spectrum disorders: a feasibility study. *Phys. Occup. Ther. Pediatr.* 35, 365–380. doi: 10.3109/01942638.2014.975313

Sparks, B. F., Friedman, S. D., Shaw, D. W., Aylward, E. H., Echelard, D., Artru, A. A., et al. (2002). Brain structural abnormalities in young children with autism spectrum disorder. *Neurology* 59, 184–192. doi: 10.1212/wnl.59.2.184

Sparks, D. L. (2002). The brainstem control of saccadic eye movements. *Nat. Rev. Neurosci.* 3, 952–964. doi: 10.1038/nrn986

Strick, P. L., Dum, R. P., and Fiez, J. A. (2009). Cerebellum and nonmotor function. *Annu. Rev. Neurosci.* 32, 413–434. doi: 10.1146/annurev.neuro.31.060407.125606

Stryker, M. P., and Schiller, P. H. (1975). Eye and head movements evoked by electrical stimulation of monkey superior colliculus. *Exp. Brain Res.* 23, 103–112. doi: 10.1007/BF00238733

Sweeney, J. A., Takarae, Y., Macmillan, C., Luna, B., and Minshew, N. J. (2004). Eye movements in neurodevelopmental disorders. *Curr. Opin. Neurol.* 17, 37–42. doi: 10.1097/00019052-200402000-00007

Szentagothai, J. (1950). The elementary vestibulo-ocular reflex arc. *J. Neurophysiol.* 13, 395–407. doi: 10.1152/jn.1950.13.6.395

Takarae, Y., Luna, B., Minshew, N. J., and Sweeney, J. A. (2008). Patterns of visual sensory and sensorimotor abnormalities in autism vary in relation to history of early language delay. *J. Int. Neuropsychol. Soc.* 14, 980–989. doi: 10.1017/S1355617708081277

Takarae, Y., Minshew, N. J., Luna, B., Krisky, C. M., and Sweeney, J. A. (2004a). Pursuit eye movement deficits in autism. *Brain* 127(Pt 12), 2584–2594. doi: 10.1093/brain/awh307

Takarae, Y., Minshew, N. J., Luna, B., and Sweeney, J. A. (2004b). Oculomotor abnormalities parallel cerebellar histopathology in autism. *J. Neurol. Neurosur.* 75, 1359–1361. doi: 10.1136/jnnp.2003.022491

Takarae, Y., Minshew, N. J., Luna, B., and Sweeney, J. A. (2007). Atypical involvement of frontostriatal systems during sensorimotor control in autism. *Psychiatry Res.* 156, 117–127. doi: 10.1016/j.pscychresns.2007.03.008

Teitelbaum, P., Teitelbaum, O., Nye, J., Fryman, J., and Maurer, R. G. (1998). Movement analysis in infancy may be useful for early diagnosis of autism. *Proc. Natl. Acad. Sci. U S A.* 95, 13982–13987. doi: 10.1073/pnas.95.23.13982

Telias, M. (2019). Molecular mechanisms of synaptic dysregulation in fragile X syndrome and autism spectrum disorders. *Front. Mol. Neurosci.* 12:51. doi: 10.3389/fnmol.2019.00051

Unruh, K. E., Martin, L. E., Magnon, G., Vaillancourt, D. E., Sweeney, J. A., and Mosconi, M. W. (2019). Cortical and subcortical alterations associated with precision visuomotor behavior in individuals with autism spectrum disorder. *J. Neurophysiol.* 122, 1330–1341. doi: 10.1152/jn.00286.2019

van Kan, P. L., and McCurdy, M. L. (2001). Role of primate magnocellular red nucleus neurons in controlling hand preshaping during reaching to grasp. *J. Neurophysiol.* 85, 1461–1478. doi: 10.1152/jn.2001.85.4.1461

van Kan, P. L., and McCurdy, M. L. (2002a). Contribution of primate magnocellular red nucleus to timing of hand preshaping during reaching to grasp. *J. Neurophysiol.* 87, 1473–1487. doi: 10.1152/jn.00038.2001

van Kan, P. L., and McCurdy, M. L. (2002b). Discharge of primate magnocellular red nucleus neurons during reaching to grasp in different spatial locations. *Exp. Brain Res.* 142, 151–157. doi: 10.1007/s00221-001-0924-5

Waespe, W., and Henn, V. (1977). Vestibular nuclei activity during optokinetic after-nystagmus (OKAN) in the alert monkey. *Exp. Brain Res.* 30, 323–330. doi: 10.1007/BF00237259

Waespe, W., and Henn, V. (1979). Motion information in the vestibular nuclei of alert monkeys: visual and vestibular input vs. optomotor output. *Prog. Brain Res.* 50, 683–693. doi: 10.1016/S0079-6123(08)60865-1

Waespe, W., and Henn, V. (1985). Cooperative functions of vestibular nuclei neurons and floccular Purkinje cells in the control of nystagmus slow phase velocity: single cell recordings and lesion studies in the monkey. *Rev. Oculomot Res.* 1, 233–250.

Wang, S. F., and Spencer, R. F. (1996). Spatial organization of premotor neurons related to vertical upward and downward saccadic eye movements in the rostral interstitial nucleus of the medial longitudinal fasciculus (riMLF) in the cat. *J. Comp. Neurol.* 366, 163–180.

Wegiel, J., Flory, M., Kuchna, I., Nowicki, K., Ma, S. Y., Imaki, H., et al. (2014). Stereological study of the neuronal number and volume of 38 brain subdivisions of subjects diagnosed with autism reveals significant alterations restricted to the striatum, amygdala and cerebellum. *Acta Neuropathol. Commun.* 2:141. doi: 10.1186/s40478-014-0141-7

Wegiel, J., Kuchna, I., Nowicki, K., Imaki, H., Wegiel, J., Ma, S. Y., et al. (2013). Contribution of olivofloccular circuitry developmental defects to atypical gaze in autism. *Brain Res.* 1512, 106–122. doi: 10.1016/j.brainres.2013.03.037

Wegiel, J., Kuchna, I., Nowicki, K., Imaki, H., Wegiel, J., Marchi, E., et al. (2010). The neuropathology of autism: defects of neurogenesis and neuronal migration, and dysplastic changes. *Acta Neuropathol.* 119, 755–770. doi: 10.1007/s00401-010-0655-4

Wegiel, J., Schanen, N. C., Cook, E. H., Sigman, M., Brown, W. T., Kuchna, I., et al. (2012). Differences between the pattern of developmental abnormalities in autism associated with duplications 15q11.2-q13 and idiopathic autism. *J. Neuropathol. Exp. Neurol.* 71, 382–397. doi: 10.1097/NEN.0b013e318251f537

Whitney, E. R., Kemper, T. L., Rosene, D. L., Bauman, M. L., and Blatt, G. J. (2009). Density of cerebellar basket and stellate cells in autism: evidence for a late developmental loss of Purkinje cells. *J. Neurosci. Res.* 87, 2245–2254. doi: 10.1002/jnr.22056

Wong, N. M. L., Findon, J. L., Wichers, R. H., Giampietro, V., Stoencheva, V., Murphy, C. M., et al. (2020). Serotonin differentially modulates the temporal dynamics of the limbic response to facial emotions in male adults with and without autism spectrum disorder (ASD): a randomised placebo-controlled single-dose crossover trial. *Neuropsychopharmacology* 45, 2248–2256. doi: 10.1038/s41386-020-0693-0

Wurtz, R. H., and Goldberg, M. E. (1971). Superior colliculus cell responses related to eye movements in awake monkeys. *Science* 171, 82–84. doi: 10.1126/science.171.3966.82

Wurtz, R. H., and Goldberg, M. E. (1972). The role of the superior colliculus in visually-evoked eye movements. *Bibl. Ophthalmol.* 82, 149–158.

Yamasue, H., Kuwabara, H., Kawakubo, Y., and Kasai, K. (2009). Oxytocin, sexually dimorphic features of the social brain, and autism. *Psychiatry Clin. Neurosci.* 63, 129–140. doi: 10.1111/j.1440-1819.2009.01944.x

Yip, J., Soghomonian, J. J., and Blatt, G. J. (2009). Decreased GAD65 mRNA levels in select subpopulations of neurons in the cerebellar dentate nuclei in autism: an in situ hybridization study. *Autism Res.* 2, 50–59. doi: 10.1002/aur.62

Zalla, T., Seassau, M., Cazalis, F., Gras, D., and Leboyer, M. (2018). Saccadic eye movements in adults with high-functioning autism spectrum disorder. *Autism* 22, 195–204. doi: 10.1177/1362361316667057

Zee, D. S., Yamazaki, A., Butler, P. H., and Gucer, G. (1981). Effects of ablation of flocculus and paraflocculus of eye movements in primate. *J. Neurophysiol.* 46, 878–899. doi: 10.1152/jn.1981.46.4.878

Zielinski, B. A., Prigge, M. B., Nielsen, J. A., Froehlich, A. L., Abildskov, T. J., Anderson, J. S., et al. (2014). Longitudinal changes in cortical thickness in autism and typical development. *Brain* 137(Pt 6), 1799–1812. doi: 10.1093/brain/awu083

Zwaigenbaum, L., Bryson, S., and Garon, N. (2013). Early identification of autism spectrum disorders. *Behav. Brain Res.* 251, 133–146. doi: 10.1016/j.bbr.2013.04.004

Zwaigenbaum, L., Bryson, S., Rogers, T., Roberts, W., Brian, J., and Szatmari, P. (2005). Behavioral manifestations of autism in the first year of life. *Int. J. Dev. Neurosci.* 23, 143–152. doi: 10.1016/j.ijdevneu.2004.05.001

Conflict of Interest: The author declares that the research was conducted in the absence of any commercial or financial relationships that could be construed as a potential conflict of interest.

frontiers in Integrative Neuroscience

SYSTEMATIC REVIEW
published: 01 November 2021
doi: 10.3389/fnint.2021.760116

A Systematic Review of Brainstem Contributions to Autism Spectrum Disorder

Ala Seif[1,2,3], *Carly Shea*[1,3], *Susanne Schmid*[1,2,3]* *and Ryan A. Stevenson*[1,3]

[1] Brain and Mind Institute, University of Western Ontario, London, ON, Canada, [2] Department of Anatomy and Cell Biology, Schulich School of Medicine and Dentistry, University of Western Ontario, London, ON, Canada, [3] Department of Psychology, University of Western Ontario, London, ON, Canada

Autism spectrum disorder (ASD) is a neurodevelopmental disorder that affects one in 66 children in Canada. The contributions of changes in the cortex and cerebellum to autism have been studied for decades. However, our understanding of brainstem contributions has only started to emerge more recently. Disruptions of sensory processing, startle response, sensory filtering, sensorimotor gating, multisensory integration and sleep are all features of ASD and are processes in which the brainstem is involved. In addition, preliminary research into brainstem contribution emphasizes the importance of the developmental timeline rather than just the mature brainstem. Therefore, the purpose of this systematic review is to compile histological, behavioral, neuroimaging, and electrophysiological evidence from human and animal studies about brainstem contributions and their functional implications in autism. Moreover, due to the developmental nature of autism, the review pays attention to the atypical brainstem development and compares findings based on age. Overall, there is evidence of an important role of brainstem disruptions in ASD, but there is still the need to examine the brainstem across the life span, from infancy to adulthood which could lead the way for early diagnosis and possibly treatment of ASD.

Keywords: autism spectrum disorder, brainstem, development, sensory, olivary complex, auditory, systematic review

OPEN ACCESS

Edited by:
Randy J. Kulesza, Lake Erie College of Osteopathic Medicine, United States

Reviewed by:
Milica Pejovic-Milovancevic, Institute of Mental Health (Belgrade), Serbia
Miguel Ángel García-Cabezas, Universidad Autónoma de Madrid y Consejo Superior de Investigaciones Científicas, Spain

***Correspondence:**
Susanne Schmid
susanne.schmid@schulich.uwo.ca

Received: *17 August 2021*
Accepted: *30 September 2021*
Published: *01 November 2021*

Citation:
Seif A, Shea C, Schmid S and Stevenson RA (2021) A Systematic Review of Brainstem Contributions to Autism Spectrum Disorder. Front. Integr. Neurosci. 15:760116. doi: 10.3389/fnint.2021.760116

INTRODUCTION

Autism spectrum disorder (ASD) is a neurodevelopmental disorder with a high prevalence of 1 in 66 in Canada and it disproportionately affects male with prevalence of 1 in 42 (Ofner et al., 2018). A range of core ASD symptoms, such as impairments in social communication skills combined with restricted and repeated behaviors and interests, as well as motor stereotypies, could be related to sensory disruptions (Sinclair et al., 2017). Autistic individuals also avoid sensory stimuli and/or display sensory seeking behavior (Sinclair et al., 2017). Moreover, disruptions of sensory processing, startle response, sensory filtering, sensorimotor gating, multisensory integration, and sleep are all features of ASD and are processes that the brainstem is crucially involved in.

The brainstem is the structure that connects the cerebrum to the spinal cord and cerebellum. It consists of three main components in ascending order: medulla oblongata, pons, and the midbrain (Moller, 2006). It is a conduit for the ascending and descending pathways between the cerebellum and spinal cord, and it houses the cranial nerves and integrated vital systems. Autistic individuals

often experience symptoms associated with auditory brainstem abnormalities such as difficulty with auditory temporal processing while having normal hearing threshold, impaired sound localization, poor speech recognition in noise and abnormal sound sensitivity (Pillion et al., 2018). The auditory brainstem pathway includes the cochlear nucleus (CN), superior olivary complex (SOC), and inferior colliculus which are in pairs on either side of the brainstem and connected by afferent relay pathways, including the lateral lemniscus. The CN receives input from the peripheral auditory system and is located at the connection between the medulla and the pons. The CN's main function is to maintain the frequency information extracted by the cochlea in the inner ear. It then projects bilaterally to the SOC, where binaural sound cues are processed for sound localization. The olivocochlear bundle, which projects from the SOC, serves to protect the inner ear from loud sounds and high levels of background noise (Moller, 2006).

The pathogenesis of ASD has long been studied, but no definitive conclusion has been reached. The alterations of cortex and cerebellum are investigated regularly due to their more obvious involvement in the cognitive symptoms of autism such as social difficulties and language delay. What is more often overlooked is the cascading effect of abnormal brainstem development and/or delays in brainstem processing on higher brain centers. Studying the potential origin of autism symptoms in the brainstem is important for early diagnosis and intervention.

Our understanding of brainstem contributions to autism has only started to emerge. Research involving the brainstem has been relatively slow due to technological difficulties. Its small size, functional diversity, and anatomy makes the brainstem less accessible for studying than the cortex. There is, however, a growing body of evidence regarding its contributions to autism. Therefore, this systematic review compiles research investigating the involvement of the brainstem in the pathogenesis of ASD. This paper includes studies examining histological, neuroimaging, and electrophysiological evidence from human and animal studies about brainstem contributions and their functional implications in autism. Moreover, we compared papers with distinct age ranges for an understanding of developmental delay implication on ASD. This is especially important due to the developmental nature of ASD.

METHODS

Study Design

A systematic review was chosen due to its systematic approach in identifying and summarizing all the work in this field. This review follows the guidelines set by the Joanna Briggs Institute, according to the Manual for Evidence Synthesis (Aromataris and Munn, 2020), the Peer Review of Electronic Search Strategies Guidelines (McGowan et al., 2016), and the Preferred Reporting Items for Systematic Reviews and Meta-Analysis (Shamseer et al., 2015). This project was pre-registered with the Open Science Foundation (osf.io/2hd6m).

Eligibility Criteria

The eligibility criteria for the included work is based on the population, exposure, comparison and outcome (PICO) framework (Aromataris and Munn, 2020). The population is defined as anyone with a clinical diagnosis of ASD including autism, Asperger syndrome, Atypical autism and the equivalents in Diagnostic and Statistical Manual of Mental Disorders (DSM-III; American Psychiatric Association, 1980), DSM-IV (American Psychiatric Association, 1994), and DSM-V (American Psychiatric Association, 2013) classification systems and/or with confirmation of diagnosis using Autism Diagnostic Interview-Revised (ADI-R; Rutter et al., 2003) or Autism Diagnostic Observation Schedule (ADOS; Lord et al., 1999). Moreover, participants with comorbidities are also included due to their high prevalence in autism. The study population also included animal models of autism. The intervention/methodologies are the application of histological, neuroimaging, or electrophysiological experiments designed to study the involvement of brainstem in autism. The comparison is to healthy controls and the outcome is the experimental results. Case studies and case series were excluded, and all studies had to be controlled. Finally, we did not limit the search by a start date to ensure the comprehensiveness of this review. We restricted the review to English, peer-reviewed and primary research publications.

Search Strategy

Information Sources

The search strategy was reviewed by a library scientist (Meagan Stanley) and reviewed by two independent researchers (R.S, S.S). Initial search terms were piloted in two databases, MEDLINE and EMBASE, and titles and abstracts were screened for additional search terms. We applied our search within MEDLINE, EMBASE, and PsychInfo through the Ovid interface, as well as CINAHL via the EBSCO interface, SCOPUS, and Cochrane library. We used appropriate subject headings for each database and all key words synonymous with "autism spectrum disorder" and "brainstem." The search strategy is in **Table 1**. The preliminary search was conducted on October 25th, 2020 and the final search was conducted on October 28th, 2020.

Selection and Sources of Evidence

Two independent reviewers (A.S and C.S or R.S) screened the titles and abstracts of every unique article for inclusion eligibility through the Covidence software. Subsequently, one reviewer conducted the full-text screening to ensure eligibility criteria is met. Extraction was completed by one reviewer (A.S).

Quality Assessment

The quality assessment of the publications included was made based on guidelines set by the Joanna Briggs Institute, according to the Manual for Evidence Synthesis (Aromataris and Munn, 2020). The checklist for each study was as below.

1. Were the groups comparable other than the presence of disease in cases or the absence of disease in controls?
2. Were cases and controls matched appropriately?

3. Were the same criteria used for identification of cases and controls?
4. Was exposure measured in a standard, valid and reliable way?
5. Was exposure measured in the same way for cases and controls?
6. Were confounding factors identified?
7. Were strategies to deal with confounding factors stated?
8. Were outcomes assessed in a standard, valid and reliable way for cases and controls?
9. Was the exposure period of interest long enough to be meaningful?
10. Was appropriate statistical analysis used?

TABLE 1 | Search strategy used to search on all databases.

	Concept 1	Concept 2
Key concepts	Autism	Brainstem
Free text terms/natural language terms (synonyms, UK/US terminology, medical/laymen's terms, acronyms/ abbreviations, more narrow search terms)	• autism • autistic • asperger* • PDD-NOS • Kanner syndrome • Kanner's syndrome • Kanner's syndrome • pervasive developmental • PDD-NOS	• brain stem • brain stems • brainstem • brainstems • pons • pon • ponte • pontes • pontine • pontis • Olivary • Olive brain • oliva brain • olivae • olivaris • olive nucleus • midbrain • mid brain • midbrains • mesencephalon • mesencephalons • mesencephalic • mesencephali • colliculus • colliculi • quadrageminal • quadrigeminal • thalamencephalon • thalamencephalons • thalamus • thalamic • neothalamus • thalami • cuneiform nucleus • formatio reticulari • formatio reticularis • reticular formation • reticular formations • reticular substance • reticular system • substantia reticulari
Controlled vocabulary terms/Subject terms (MeSH terms, Emtree terms) *Consider: explode, major headings, subheadings*	• Child Development Disorders, Pervasive • Asperger Syndrome • Autistic Disorder • Autism Spectrum Disorder • autism	• Reticular Formation • Midbrain Reticular Formation • Thalamus • thalamus reticular nucleus • Thalamic Nuclei • Superior Colliculi • Inferior Colliculi • Mesencephalon • Pons • pontine tegmentum • ventral pons • pons reticular formation • pons angle • olivary nucleus • olivary body • Brain Stem

RESULTS

The search identified 4,565 references, of which 1,678 were duplicates. The 2,887 unique studies were screened based on their title and abstract which narrowed them down to 225 papers for full text review. Afterwards 94 studies were accepted to be included of which 58 are human studies and 36 are animal studies (**Figure 1**: PRISMA Diagram). All included studies fulfilled at least 6 of the quality assessment criteria. **Supplementary Table 1** summarizes all human studies and **Supplementary Table 2** summarizes all animal studies and includes their quality scores.

Brainstem Morphology Studies

Post-mortem

The morphological studies based on the post-mortem brain are relatively few, possibly due to the difficulty in obtaining brain tissue. Most of the studies in this are led by Kulesza et al. using brain tissue specimens obtained from the Autism Brain Net previously known as Autism Tissue program (Kulesza

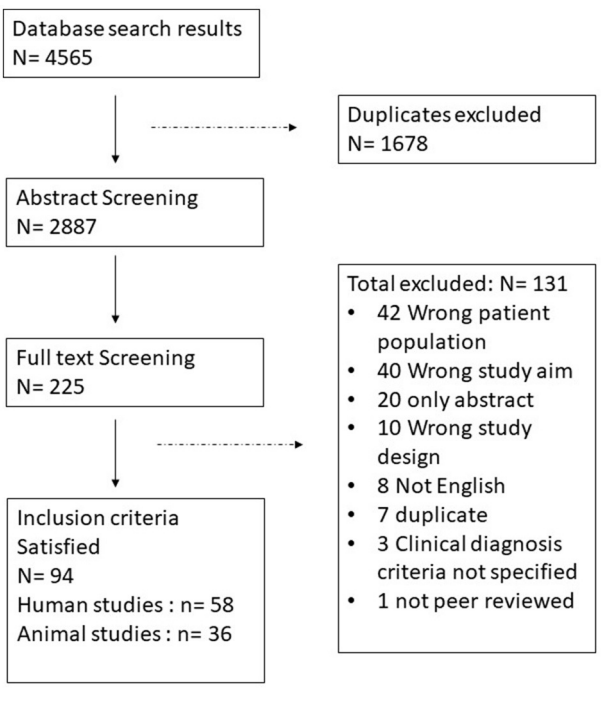

FIGURE 1 | PRISMA diagram, identification and selection process of the papers.

and Mangunay, 2008; Kulesza et al., 2011; Mansour and Kulesza, 2020). Kulesza et al., investigated the disruption of the cytoarchitecture in the lower auditory brainstem, which is the superior olivary complex (SOC) and cochlear nucleus (CN). The SOC neurons have altered cell body morphology and reduced neuronal numbers in the autistic brains (Kulesza et al., 2011). Moreover, in a three dimensional reconstruction of SOC made using Amira software, the overall volume of SOC nuclei of autistic individuals were significantly smaller than controls (Mansour and Kulesza, 2020).

The medial superior olive (MSO) nuclei were the most constantly and severely malformed nuclei (Kulesza and Mangunay, 2008; Kulesza et al., 2011). They also occupied significantly smaller volumes in autistic brains compared to controls, as seen in a three-dimensional reconstruction of the SOC. MSO nuclei were significantly smaller than the control in terms of cell body area, perimeter and major axis (Kulesza and Mangunay, 2008). In addition, the neurons were significantly rounder (Kulesza and Mangunay, 2008). However, there was a significant variance in the angle measurements indicating that the orientation of MSO in the autistic group was more heterogenous than the control.

The number of lateral superior olive (LSO) cell nuclei are significantly less in autistic brains compared to control. The LSO neurons occupy significantly smaller volume (Mansour and Kulesza, 2020) and are also significantly smaller in area and more round in autistic brains (Kulesza et al., 2011). There are differences in ratio of the oval to the fusiform to the stellate medial nuclei of the trapezoid body (MNTB) neurons in autism. The number of MNTB neurons is significantly less and the neurons have a trend of being smaller (Kulesza et al., 2011) a finding corroborated via three-dimensional reconstruction (Mansour and Kulesza, 2020). Moreover, they are less round and of different orientation (Kulesza et al., 2011). The superior paraolivary nucleus (SPON) neurons occupy a significantly smaller volume, are less in number, and rounder in autistic brains (Kulesza et al., 2011). Ventral nucleus of the trapezoid body (VNTB) neurons are rounder in ASD (Kulesza et al., 2011). Lateral nucleus of the trapezoid body neurons are significantly fewer (Kulesza et al., 2011), smaller (Kulesza et al., 2011; Mansour and Kulesza, 2020), and rounder in the autistic brain (Kulesza et al., 2011). Finally, the overall volume of the SOC is consistent across brain weights and changes in the size of the SOC, and its constituent nuclei in ASD are not likely due to changes in total brain weight (Mansour and Kulesza, 2020). SOC nuclei have a role in sound localization and coding of sound temporal features (Mansour and Kulesza, 2020), therefore those alterations could have a role in the auditory dysfunction experienced in ASD.

Wegiel et al. (2014) examined the percentage of nucleus volume in a neuronal cell in different brain regions including inferior olive and substantia nigra in a post-mortem study. They divided the participants into 3 different groups based on age, 4–8, 11–23, and 29–64 years. Deficits in volume of neuronal nucleus were significant only for the age group 4–8 years (Wegiel et al., 2014). The deficit was moderate (<20%) in the inferior olive and mild (<10%) in substantia nigra. The neuronal cytoplasm volume was measured as total neuron volume minus neuronal nucleus volume. In ASD, there is a deficit of 4% of neuronal cytoplasm volume in the substantia nigra (Wegiel et al., 2014). In addition, the trajectory of neuronal nucleus volume in ASD was opposite to the control trajectory. The autistic cohort had a significant increase in at least one of the older groups while a distinctive feature of control was a decrease in neuronal nucleus volumes in both older groups (Wegiel et al., 2014). A different study quantified the oxytocin receptor and the structurally related vasopressin 1a receptor in the superior colliculi in post-mortem specimens of autistic and neurotypical individuals and found no difference (Freeman et al., 2018).

A study used immunocytochemistry to compare angiogenesis in post-mortem brains of 10 autistic young adults and their age matched controls. It reported increased and prolonged neural development in the brainstem including midbrain and pons (Azmitia et al., 2016).

The takeaway of post-mortem studies is that there is an age dependent (Wegiel et al., 2014) malformation in the shapes of the different olivary complex cells (Kulesza and Mangunay, 2008; Kulesza et al., 2011; Wegiel et al., 2014; Mansour and Kulesza, 2020) and substantia nigra (Wegiel et al., 2014). However, it is important to keep in mind that all post-mortem studies are based on small samples.

Neuroimaging

Analysis of brainstem size and its components (pons, medulla, midbrain) using MRI scans has mixed results. The most common result is a reduction in brainstem size. One of the earliest studies suggested a trend in brainstem area reduction (Hashimoto et al., 1989). Another early study, found that the brainstem and pons of autistic individuals was significantly smaller than in controls (Gaffney et al., 1988). Recent studies confirmed these results. A significant reduction in total brainstem size has been consistently observed (Gaffney et al., 1988; Hashimoto et al., 1995; Herbert et al., 2003; Fredo et al., 2014). In one study of 20 adult autistic men and their age, gender and IQ matched controls, total brainstem volume was reduced, however, it was proportional to total brain volume and volume of other regional areas (Herbert et al., 2003). Two studies reported a reduction in brainstem gray matter (Jou et al., 2009; Toal et al., 2010). The first, a study of 22 autistic male children, showed significant reduction in gray matter before and after controlling for total brain volume (Jou et al., 2009) while the second, a study of 39 adults males diagnosed with Asperger's syndrome (Toal et al., 2010), also showed gray matter reduction when compared with age and gender matched controls. A study using PET scans to examine serotonin transporter availability in the gray matter of 15 autistic adults and their matched controls (age, gender, IQ) exhibited significant reduction in serotonin transporter availability in brainstem gray matter (Andersson et al., 2020). Three studies that used voxel based morphometry to investigate white matter reported brainstem white matter reduction (Craig et al., 2007; Toal et al., 2010; Hanaie et al., 2016). One of the studies investigated the white matter in autistic women and concluded that they had a smaller density of white matter in pons (Craig et al., 2007). While another study reported that white matter in the regions corresponding to parts of the central tegmental

tract/medial lemniscus (CTT/ML) were significantly smaller in ASD group (Hanaie et al., 2016).

Hashimoto et al. conducted 8 studies investigating the brainstem structures by analyzing MRI scans. One of the biggest studies was with a sample of 102 ASD participants in the age range of 3 months to 20 years along with 112 age- and gender-matched controls (Hashimoto et al., 1995). The results reported that the brainstem size and the size of its three components (pons, midbrain, and medulla oblongata) increased with development and revealed a statistically significant correlation coefficient with age for both groups but the area of the brainstem in the autistic group was significantly smaller than those in the control group across all ages (Hashimoto et al., 1995). A study reported a significantly smaller midbrain, pons and medulla oblongata for the autistic group (Hashimoto et al., 1993b) while another study reported the significance for smaller size only in the midbrain and medulla oblongata when the groups were IQ matched (Hashimoto et al., 1993a). In a study in which autistic participants with intellectual disability were compared to non-autistic participants with intellectual disability, there was no absolute difference in brainstem area but there was a significant reduction in ratio of midbrain and medulla to posterior fossa (Hashimoto et al., 1992a). Moreover, when autistic participants were grouped into either a heterogenous IQ group, low IQ group ($IQ < 80$) or high IQ group ($IQ > 80$), all groups indicated that MRI brainstem width in autistic children differs from that in the control group. Brainstem width of the ASD group was smaller than the control and this difference tends to be exacerbated in the low IQ group (Hashimoto et al., 1992b). The maximum width in the middle portion of the pons was significantly smaller for the autistic heterogenous IQ group and autistic low IQ group compared to the controls (Hashimoto et al., 1992b).

However, another study with a much smaller sample size compared to previous studies had an opposing outcome of increased brainstem volume in autism when comparing 6 autistic children with mean age 53 ± 16 months to 38 controls with matching age, gender, and intellectual functioning (Bosco et al., 2019). A study that compared the pons size of 14 autistic participants to 2 control groups either age, sex and IQ matched or age, sex and socioeconomic status matched found no group difference after correcting for mid-sagittal brain area (Piven et al., 1992). Two other studies investigating the brainstem area reported no significant difference between autistic participants and healthy controls (Garber and Ritvo, 1992; Hardan et al., 2001).

Another group used high angular resolution diffusion-weighted imaging and functional MRI data to examine structural and functional connectivity of the mesolimbic reward pathway (Supekar et al., 2018). They identified the nucleus accumbens and the ventral tegmental area (VTA) white matter tract and found structural aberrations in these tracts in two cohorts of autistic children (Supekar et al., 2018). Moreover, they showed that structural aberrations are accompanied by aberrant functional interactions between nucleus accumbens and VTA in response to social stimuli (Supekar et al., 2018).

Two studies aimed to study textural features of the brainstem, which provide a complementary basis for volumetric morphometric analysis by summarizing distributions of localized image measurements (Chaddad et al., 2017). One study observed that the mean entropy values, which is the distribution of pixels values over intensity levels of a MRI scan, obtained from the subcortical regions are significantly higher in 30 autistic subjects (Jac Fredo et al., 2015) while the second study with 575 ASD participants concluded no significant textural feature differences in the brainstem (Chaddad et al., 2017).

In summary the brainstem of autistic individuals is likely smaller in size than healthy controls as concluded by most studies (Gaffney et al., 1988; Hashimoto et al., 1989, 1992a,b, 1993a,b, 1995; Herbert et al., 2003; Craig et al., 2007; Jou et al., 2009; Toal et al., 2010; Fredo et al., 2014; Hanaie et al., 2016; Andersson et al., 2020). The reduction is also observed in the brainstem white matter (Craig et al., 2007; Toal et al., 2010; Hanaie et al., 2016) and gray matter (Jou et al., 2009; Toal et al., 2010). In studies that investigated specific brainstem components, a reduction is seen in the medulla (Hashimoto et al., 1992a,b, 1993a,b, 1995), the midbrain (Hashimoto et al., 1992a,b, 1993a,b, 1995) and the pons (Hashimoto et al., 1992b, 1993b, 1995). These results go hand in hand with post-mortem studies indicating abnormalities in the overall size of brainstem and malformation of component nuclei of it.

Neuroimaging Relating to Behavior

The relationship between brainstem anatomy and sensory-motor function has also been evaluated in autism. A group investigated the relationship between brainstem gray matter volume and sensory sensitivity as measured by the Sensory Profile Questionnaire (SPQ) and it observed a significant positive correlation between oral sensory sensitivity factor and brainstem gray matter (Jou et al., 2009). Another group investigated if atypical white matter microstructure in the brain mediated the relationship between motor skills and ASD symptom severity. Fractional anisotropy of the brainstem corticospinal tract predicted both grip strength and autism symptom severity and mediated the relationship between the two (Travers et al., 2015). It suggested that brainstem white matter might contribute to autism symptoms and grip strength in ASD (Travers et al., 2015). Another group aimed to relate brainstem white matter to motor performance in autism using Movement Assessment Battery for Children 2 (M-ABC 2) in which higher scores are indicative of better motor performance (Hanaie et al., 2016). The study reported a significant positive correlation between the total test score on the M-ABC 2 and the volume of brainstem white matter (Hanaie et al., 2016).

A study investigated the correlation between language development and neuroanatomy of ASD participants with and without a language delay and neurotypicals (Lai et al., 2014). Neuroanatomy was assessed by MRI images and language development was measured by verbal IQ through a word generativity test using the F-A-S task and a phonological memory test using the non-word repetition task (Lai et al., 2014). Language delay was associated with larger total gray matter volume and larger relative volume of the pons and medulla oblongata in adulthood (Lai et al., 2014).

Another study utilized fMRI to examine the effect of constraining gaze in the eye-region on activation of the subcortical system, specifically the superior colliculus in the brainstem. Participants looked at facial emotional stimuli by either free-viewing or by being restricted to eye-region conditions (Hadjikhani et al., 2017). ASD and controls had similar activation patterns in free viewing but the ASD group had higher superior colliculus activation in the constrained to look in the eyes condition (Hadjikhani et al., 2017). Additionally, there was a positive correlation between autism symptom severity and subcortical system activation for stimuli of fear and neutral faces, in the free viewing condition (Hadjikhani et al., 2017).

Finally, a study used imaging-genetics data from a discovery sample of 27,034 individuals and identified 45 brainstem-associated genetic loci, including the first linked to midbrain, pons, and medulla oblongata volumes, and mapped them to 305 genes (Elvsåshagen et al., 2020). Of those genetic loci, 9 were jointly associated with the brainstem volumes and autism (Elvsåshagen et al., 2020). Notably, the shared genetic loci exhibited a mixed pattern of allelic effect directions such as associations with both larger and smaller brainstem volumes (Elvsåshagen et al., 2020).

Functional Studies

Auditory Brainstem Response (ABR)

ABRs are auditory evoked potentials measured at the scalp that are used clinically to assess the functional integrity of the auditory pathway. ABRs consist of five distinct positive peaks during the first 10 ms following the presentation of a sound (Moller, 2006). Peak I and peak II are generated by the auditory nerve while the other peaks are generated by the contributions of different anatomical structures (Moller, 2006). Peak III is generated by the CN. The SOC is suggested to be the generator of peak IV (Moller, 2006). The peak V tip is generated by the lateral lemniscus (LL) and it terminates on the inferior colliculus (IC) (**Figure 2A**; Moller, 2006).

The most studied aspects of ABR waveforms are the absolute latencies of the peaks and the interpeak latencies, while few papers examine peak amplitudes. Peak I latency is found to be prolonged in ASD (Tanguay et al., 1982; Rosenhall et al., 2003; Magliaro et al., 2010; Azouz et al., 2014; Ververi et al., 2015) when compared to controls. This suggests the presence of very early differences in auditory processing in autism, even as early as the auditory nerve (**Figure 2B**). Peak III latency is also found to be delayed (Magliaro et al., 2010) and prolonged (Tanguay et al., 1982) as well as peak I- III inter peak latency (Maziade et al., 2000; Magliaro et al., 2010) possibly due to alterations at the CN (**Figure 2B**). In addition, peak I-III IPL is found to be prolonged in autistic probands and their first-degree relatives (Maziade et al., 2000). Peak V is also found to be prolonged in ASD groups when compared to healthy controls (Rosenhall et al., 2003; Russo et al., 2008; Azouz et al., 2014; Ververi et al., 2015) which is generated by LL and IC (**Figure 2B**), but could potentially be due to the cascading effect of previous locations along the primary auditory pathway such as SOC. As previously discussed, the morphology of SOC is found to be altered in the post-mortem brains of autistic individuals (Kulesza and Mangunay, 2008; Kulesza et al., 2011; Wegiel et al., 2014; Mansour and Kulesza, 2020). Moreover, abnormalities in peak III-V IPL (**Figure 2B**) are found (Rosenhall et al., 2003; Tas et al., 2007; Azouz et al., 2014; Jones et al., 2020; Kamita et al., 2020). The most common ABR finding is that the wave is prolonged in

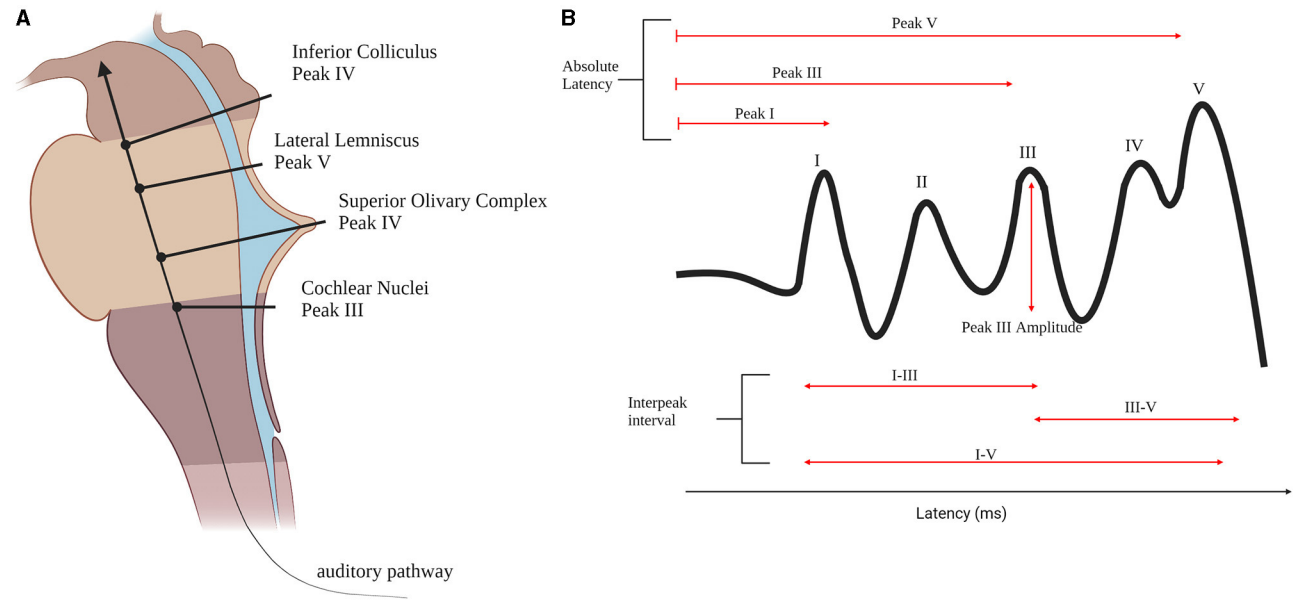

FIGURE 2 | Brainstem auditory pathway. **(A)** The brainstem auditory pathway and the corresponding ABR peaks generators in the brainstem. **(B)** An ABR wave and the measures found to be different between autistic individuals and controls. Created with bioRender.com.

ASD (Rosenhall et al., 2003; Tas et al., 2007; Azouz et al., 2014; Kamita et al., 2020). IPL of peak I-V differences are found as well (**Figure 2B**; Ververi et al., 2015; Jones et al., 2020).

Amplitudes are not commonly examined, and results are inconsistent. A group found peak III amplitude to be lower for ASD when a forward masking condition was applied (**Figure 2B**; Källstrand et al., 2010) while two others found it to be higher (Ververi et al., 2015; Claesdotter-Knutsson et al., 2019). Another study found that the ASD group had higher correlation between right and left ears compared to the typically developing participants (Claesdotter-Knutsson et al., 2019) which could be related to difficulties in the processing of everyday sounds.

ABRs are also used as a conventional hearing test for newborns. Some studies have found abnormalities in click evoked ABR of newborns that were later diagnosed with autism (Cohen et al., 2013; Miron et al., 2016, 2021). They had significant prolongations of their ABR phase and V-negative latency compared to the newborns that weren't diagnosed with ASD (Miron et al., 2021). A longitudinal study with a year time difference found typically developed toddlers did not have a change in their ABR while autistic toddlers had a shortening in peak V latency and peaks I-V IPL at T2 (Li et al., 2020). Regardless of the change within the two timepoints, autistic toddlers still had longer latencies of peak III and peak V, and longer IPL of peaks I-III and peaks I-V at both timepoints (Li et al., 2020). Nonetheless a study examining the differences between ASD and typically developing controls found no differences (Tharpe et al., 2006).

Speech evoked ABR abnormalities were also identified. Autistic children exhibited deficits in both the neural synchrony (timing; Russo et al., 2009) and phase locking (frequency encoding) of speech sounds (Russo et al., 2008, 2009). They also exhibited reduced magnitude and fidelity of speech evoked ABR and excessive degradation of responses by background noise in comparison to typically developing controls (Russo et al., 2009). A study examined speech evoked ABR at two different timepoints with an average 10 months between them for preschool children. At T1, the wave V and A latencies were prolonged, whereas the wave E amplitude was decreased and the wave F latency prolonged at T2 (Chen et al., 2019). Between the two recordings, the wave V latency was shortened, and amplitudes of wave A and C increased (Chen et al., 2019). Whereas, another study found longer wave V for school aged ASD children (Kamita et al., 2020). A study concluded that latencies of all speech-evoked ABR waves and V-A complex duration are longer in the ASD group compared to healthy controls (Ramezani et al., 2019). Other studies found differences in specific waves such as latencies in waves C, D, E, F (El Shennawy et al., 2014), and wave O (El Shennawy et al., 2014; Jones et al., 2020). Moreover, a difference in amplitude between the ASD and the control groups is observed in waves C, D, E, F, and O (El Shennawy et al., 2014).

The results of ABR are less consistent in terms of how the waves of autistic individuals are different than control but the general trend indicates some form of abnormality (Tanguay et al., 1982; Maziade et al., 2000; Rosenhall et al., 2003; Tas et al., 2007; Russo et al., 2008, 2009; Källstrand et al., 2010; Magliaro et al., 2010; Azouz et al., 2014; El Shennawy et al., 2014; Wegiel et al., 2014; Ververi et al., 2015; Miron et al., 2016, 2021; Chen et al., 2019; Claesdotter-Knutsson et al., 2019; Ramezani et al., 2019; Jones et al., 2020; Kamita et al., 2020; Li et al., 2020).

Pupillometry and Eye Tracking

A study utilized changes in pupil size to examine whether autistic individuals exhibit differences in phasic locus coeruleus (LC) activity compared with typically developing controls under different attentional demands. The phasic pupillary response is an indication of LC activity because it is specifically associated with LC-mediated processing and allows for between group comparisons not confounded by unrelated individual differences in pupil size oydistractor tones. The results indicated that under tightly controlled conditions, task-evoked pupil responses are lower in ASD group than in controls, but only in the presence of task-irrelevant stimuli (Granovetter et al., 2019). This suggests that autistic individuals experience atypical modulation of LC activity in accordance with changes in attentional demands, offering a mechanistic account for attentional atypicality in ASD (Granovetter et al., 2019).

A study that utilized eye control to study attentional demands had participants make saccades to peripheral targets while recording their eye movement using EOG (Schmitt et al., 2014). The recordings of the autistic participants had reduced accuracy, elevated variability in accuracy across trials, and reduced peak velocity and prolonged duration (Schmitt et al., 2014). The saccades took longer to reach peak velocity but had no change in the duration of saccade deceleration (Schmitt et al., 2014). Defined brainstem circuits are implicated in the control of saccadic eye movement, therefore this suggested reduced excitatory activity in the burst cells of the pons (Schmitt et al., 2014).

Cardiovascular Autonomic Monitoring System

One study aimed to measure baseline cardiovascular autonomic function in autistic children using the NeuroScope, a device that can measure this brainstem function in real-time. They measured resting cardiac vagal tone (CVT), cardiac sensitivity to baroreflex (CSB), mean arterial blood pressure (MAP), diastolic blood pressure (DBP), systolic blood pressure (SBP) and heart rate (HR) for three groups of children (Ming et al., 2005). The groups consisted of autistic children without autonomic abnormality symptoms, autistic children with autonomic abnormalities and age matched healthy controls. The CVT and CSB were significantly lower in association with a significant elevation in HR, MAP and DBP in all autistic children compared with the healthy controls (Ming et al., 2005). Moreover, the levels of CVT and CSB were lower in the symptomatic than in the asymptomatic group. These results suggest that there is low baseline cardiac parasympathetic activity with evidence of elevated sympathetic tone in autistic children regardless of having symptoms or signs of autonomic abnormalities (Ming et al., 2005).

Animal Studies

Autism is a complicated condition diagnosed on a series of behavioral characteristics that are, in some cases, uniquely

human. Due to this complicated nature of autism, there is no single animal model that can represent the diagnosis in its entirety. Instead, different animal models of autism reflect particular symptoms associated with autism. Therefore, there are not animal models that are more or less valid representations of autism as a whole, but rather the choice of animal model used should reflect its ability to mirror the particular symptom or set of symptoms being studied (Möhrle et al., 2020). The animal models included in this review either genetically or environmentally induce such autism core symptoms and are all validated in this respect.

Fmr1 Knockout Model

Fragile X syndrome (FXS) is caused by loss of functional expression of Fmr1 gene and it is the most prevalent single-gene cause of ASD (Ascano et al., 2012). It results from an expansion of the CGG repeats in the promoter region of the *FMR1* gene, which reduces the amount of fragile X mental retardation protein (FMRP) produced (Ascano et al., 2012). FMRP acts as a modulator of mRNA translation and has numerous target genes (Ascano et al., 2012). A study investigated the molecular role of FMRP in the avian nucleus laminaris (NL) which is a brainstem nucleus necessary for binaural processing by performing proteomic analysis of NL (Sakano et al., 2017). They identified 94 proteins that are a potential FMRP target (Sakano et al., 2017). These proteins are enriched in pathways involved in cellular growth, cellular trafficking, and transmembrane transport (Sakano et al., 2017). They also confirmed the direct interaction between FMRP and Rhoc (Sakano et al., 2017). Another study investigated the role of FMRP in axonal development of the auditory brainstem by inducing FMRP downregulation in avian embryos using CRISPR/Cas9 and shRNA techniques. It resulted in perturbed axonal pathfinding, delay in midline crossing, excess branching of neurites, and axonal targeting errors during the period of circuit development (Wang et al., 2020).

A single study used *Fmr1* knock-out (KO) zebrafish to model the alterations of sensory networks at a cellular level using calcium imaging (Constantin et al., 2020). They identified that the KO larvae had more auditory responsive neurons in the primary auditory regions including the hindbrain and thalamus that were more caudally distributed (Constantin et al., 2020).

Most studies based their work on rodent KO models. The cell size of the KO mice ventral cochlear nucleus (VCN) and the medial nucleus of the trapezoid body (MNTB) was smaller and vesicular GABA transporter protein (VGAT) expression in MNTB was significantly greater than in wild-type (WT) animals (Rotschafer et al., 2015). The same group investigated the developmental phenotypes of *Fmr1* KO mice in the VCN, MNTB, and the lateral superior olive (LSO, Rotschafer and Cramer, 2017). They found that VCN cell size is normal until after hearing onset, while MNTB and LSO show cell size decreases earlier (Rotschafer and Cramer, 2017). VGAT (inhibitory synapse marker) expression was elevated relative to VGLUT (excitatory synapse marker) in KO MNTB before hearing onset (postnatal day 6, Rotschafer and Cramer, 2017). In addition, astrocyte numbers were elevated in KO in VCN and LSO after hearing onset (postnatal day 14, Rotschafer and Cramer, 2017). This means that some phenotypes are observed before auditory activity, while others emerge later, suggesting that FMRP acts at multiple sites and timepoints in auditory system development.

Another study demonstrated the effect of FMRP loss on synaptic rearrangement and function of LSO neurons in adult animals using whole-cell current- and voltage-clamp recordings (Garcia-Pino et al., 2017). KO mice showed a greatly enhanced excitatory synaptic input strength in neurons of LSO, which integrates ipsilateral excitation and contralateral inhibition to compute interaural level differences (Garcia-Pino et al., 2017). In contrast, inhibitory input properties remained unaffected (Garcia-Pino et al., 2017). Moreover, there is an increased number of cochlear nucleus fibers converging onto one LSO neuron. Without any change to individual synapse properties, the immunolabeling of excitatory ending markers revealed an increase in the immunolabeled area, supporting abnormally elevated excitatory input numbers (Garcia-Pino et al., 2017). Due to disturbed development of LSO circuitry, auditory processing was also affected in adult KO mice as shown with single-unit recordings of LSO neurons (Garcia-Pino et al., 2017). Immunofluorescence was used to map the expression of FMRP in the SOC (Ruby et al., 2015). At postnatal day 50, FMRP was widely expressed in neurons of SOC of control rats but not KO. In addition, KO rats had many SOC neurons with a smaller soma and rounder MSO neurons when compared to controls, indicating abnormal neuronal morphology (Ruby et al., 2015), which is similar to what is seen in human post-mortem analysis studies (Kulesza and Mangunay, 2008; Kulesza et al., 2011; Mansour and Kulesza, 2020). There was also a reduction in the expression of glutamic acid decarboxylase (GAD67), a GABA marker, in neurons of the superior paraolivary complex (SPON) and a reduction in the number of calyx terminals associated with neurons of the MNTB (Ruby et al., 2015).

Neural correlates of auditory hypersensitivity in the developing inferior colliculus (IC) in KO mouse were examined using c-Fos immunolabeling and *in vivo* single unit recordings (Nguyen et al., 2020). There was an increase in density of c-Fos neurons in the IC, but not auditory cortex, of KO mice at postnatal day 21 and postnatal day 34 following sound presentation. In addition, *in vivo* single-unit recordings showed that IC neurons of KO mice are hyper responsive to amplitude-modulated tones and tone bursts during development and showed broader frequency tuning curves (Nguyen et al., 2020). KO mice were also used to examine ABRs and quantify excitatory and inhibitory inputs to auditory brainstem nuclei (Rotschafer et al., 2015). The KO showed elevated response thresholds to both click and tone stimuli, ABR amplitudes for early peaks were reduced and the growth of the peak I response with sound intensity was less steep compared with WT (Rotschafer et al., 2015). A study used conditional deletion or expression of *Fmr1* in different cell populations to determine whether *Fmr1* deletion in those cells was sufficient or necessary, respectively, for the audiogenic seizures (AGS) phenotype in male mice. It indicated that *Fmr1* deletion in subcortical glutamatergic neurons that express vesicular glutamate transporter 2 (VGlut2) underlies AGSs (Gonzalez et al., 2019). *Fmr1* deletion in glutamatergic

neurons in the IC is necessary for the phenotype, which represents the most precise genetic localization to date for causing AGSs in mice (Gonzalez et al., 2019). It also showed that selective *Fmr1* expression in glutamatergic neurons in an otherwise *Fmr1* KO mouse eliminates AGSs (Gonzalez et al., 2019).

All studies concluded that there were profound differences in *Fmr1* KO auditory brainstem compared to WT. In addition, the studies that focused on the developmental trajectory emphasized its importance (Garcia-Pino et al., 2017; Rotschafer and Cramer, 2017). Identified FMRP target proteins are involved in cellular growth, cellular trafficking, and transmembrane transport (Sakano et al., 2017) and FMRP downregulation resulted in perturbation and errors during the period of circuit development (Wang et al., 2020). Moreover, KO mice had abnormalities in different SOC components (Ruby et al., 2015; Garcia-Pino et al., 2017; Rotschafer and Cramer, 2017). Finally, there's a relationship between KO IC, sound hypersensitivity (Nguyen et al., 2020) and abnormal ABR (Rotschafer et al., 2015).

Shank3 Knockout Model

SHANK3 is a gene that encodes the excitatory synapse scaffolding protein SHANK3, and mutations of it have been identified in gene-linkage studies to be associated with ASD (Oberman et al., 2015). Disruptions in SHANK3 domains in mutant mice are associated with behavioral phenotypes and social deficits, but the specific neuronal circuit alterations for the behavioral deficits have not been fully understood (Bariselli et al., 2016). To test whether optogenetic activation of neurons in the dorsal raphe nucleus (DRN) or dopamine neurons in the ventral tegmental area (VTA) may be effective in rescuing the autistic-like social deficits in Shank3 mutant autism mouse model, social training coupled with optogenetic activation of DRN or VTA was performed in KO and WT animals (Luo et al., 2017). The autistic-like social deficits of KO were rescued by social training coupled with optogenetic activation of neurons in the DRN, but not by stimulating dopamine neurons in the VTA, which is a classical reward center (Luo et al., 2017). Another study used shRNA to model Shank3 insufficiency in the VTA of mice (Bariselli et al., 2016). In contrast to the previous study, optogenetic stimulation of the DA neuron in VTA was sufficient to enhance social preference (Bariselli et al., 2016). Additionally, they found that Shank3 downregulation impairs postnatal maturation of metabotropic glutamate receptor 1 (mGluR1) leading to abnormalities in the maturation of excitatory synapses in VTA, driving lifelong synaptic, circuit and behavioral deficits. Systemic treatment with a positive allosteric modulator of mGluR1 during the postnatal period rescued synapse maturation and normalized social deficits in adulthood (Bariselli et al., 2016). The difference in results of DA VTA optogenetic stimulation between the two studies could be due to the mice's age during stimulation and social training. In the second study, mice were between 6 and 7 weeks old when the social preference test was made (Bariselli et al., 2016), whereas age was unfortunately not clearly stated in the first study. However, it is quite possible that there is a critical age period for reversing behavioral impairments.

Transgenic (ChR2)-C128S Mutant Mice

To investigate whether the activation of the striatonigral direct pathways is sufficient to induce repetitive behaviors, a study applied optogenetics to activate the substantia nigra pars reticulata (SNr) of a transgenic (ChR2)-C128S mutant mice, which resulted in sustained and chronic repetitive behaviors (Bouchekioua et al., 2018).

Ube3a Model

A common and highly penetrant genetic form of ASD results from maternally inherited 15q11-13 triplications that triple the neuron-expressed gene dosage of *UBE3A* (Krishnan et al., 2017). This study showed that increasing *Ube3a* dose in the cell nucleus downregulates the glutamatergic synapse organizer *Cbln1*, which is needed for sociability in mice (Krishnan et al., 2017). It also used a viral vector to activate *Cbln1* in VTA glutamatergic neurons and to reverse the sociability deficits induced by *Ube3a* (Krishnan et al., 2017). Another study examined monoamine levels in *Ube3a* duplicate mice and found that compared to controls, dopamine levels were elevated in *Ube3a* duplicate mice and 5HT levels were decreased in paternal *Ube3a* duplicate mice (Farook et al., 2012).

α_7-nAChR Knockout Model

The encoding gene for the α7-subunit of nicotinic acetylcholine receptor (α7-nAChR) has been associated with ASD (Felix et al., 2019). Using ABRs, a study investigated if α7-nAChR loss of function is associated with abnormal auditory temporal processing (Felix et al., 2019). The KO animals displayed delayed responses with degraded spiking precision. There was a similar delay in responses of neurons in the SPON and ventral nucleus of the lateral lemniscus both of which are thought to shape temporal precision in the midbrain (Felix et al., 2019). The delay in ABR peaks is also found in other animal models (Strata et al., 2005; Scott et al., 2018) and in autistic individuals (Tanguay et al., 1982; Maziade et al., 2000; Rosenhall et al., 2003; Russo et al., 2008; Magliaro et al., 2010; Azouz et al., 2014; Ververi et al., 2015). Moreover, forward masking and gap detection are impaired in KO (Felix et al., 2019), reflecting the forward masking impairment observed in autistic individuals (Källstrand et al., 2010).

VPA-Exposed Model

Gestational exposure to valproic acid (VPA), a commonly used anticonvulsant, antiepileptic and mood stabilizer, results in deficits of social behavior in the offspring, modeling ASD symptoms (Dubiel and Kulesza, 2016; Ágota et al., 2020). A study compared developmental neurotoxicity when rats are exposed to VPA at E9 or E11 (Kuwagata et al., 2009). VPA-exposed rats at E11 had abnormal migration of TH-positive and 5-HT neurons, possibly due to the appearance of an abnormally running nerve tract in the pons (Kuwagata et al., 2009). Those observations were more prominent in rats that were shipped pregnant rather than in house bred, which could be due to increased stress (Kuwagata et al., 2009).

Autism is sometimes associated with facial palsy, therefore a study investigated the development of facial nuclei using

the VPA-exposed model (Oyabu et al., 2013a). Embryos were exposed to VPA at E9.5 and facial nuclei were analyzed by *in situ* hybridization at E13.5, E14.5, and E15.5 (Oyabu et al., 2013a). The pattern of development was similar between VPA-exposed rats and controls, but the caudal migration of neurons was hindered, and the facial nuclei were smaller in VPA-exposed rats (Oyabu et al., 2013a).

Neuromorphological changes of the dopamine system were studied using the iDISCO method for 3D imaging (Ágota et al., 2020). There was a reduction of mesotelencephalic (MT) axonal fascicles and widening of the MT tract (Ágota et al., 2020). Moreover, there is a reduction of dopaminergic VTA neurons, and tissue level of DA in ventrobasal telencephalic regions but an increase in neuron number in SN (Ágota et al., 2020).

The rostral raphe nucleus (RRN) of E11.5 VPA-exposed rats had narrower neuronal distribution and the whole-embryo had reduced sonic hedgehog expression (Oyabu et al., 2013b). Additionally, another study demonstrated that VPA exposed rats have abnormal 5-HT neuronal differentiation and migration possibly due to distorted patterning of the dorsal raphe nucleus (DRN) and perturbed 5-HT levels postnatally (Miyazaki et al., 2005). Electrical activity of DRN neurons recorded *in vitro* resulted in an increase for VPA-exposed rats (Wang et al., 2018). When examining the mechanism behind the increased excitation/inhibition ratio in synapses, it was found that there was a reduced paired-pulse ratio (PPR) of evoked excitatory postsynaptic currents and increased frequency but unaltered PPR of evoked inhibitory postsynaptic currents (Wang et al., 2018). Therefore, it was concluded that there is an enhanced glutamate but not GABA release (Wang et al., 2018). Moreover, the glutamatergic synaptic transmission was maximized due to occluded spike timing dependent long-term potentiation at the glutamatergic synapses. The intrinsic membrane properties of DRN 5-HT neurons were not altered (Wang et al., 2018).

Neuronal activity in the brainstem circuits was examined using tonotopic maps in VPA-exposed rats via c-Fos expression induced through prolonged auditory stimulation (Dubiel and Kulesza, 2016). More c-Fos neurons were identified with larger dispersion and shifted tonotopic bands in the VPA- exposed rats (Dubiel and Kulesza, 2016). The same group examined the key components of the auditory hindbrain, the ventral cochlear nucleus (VCN) and the SOC of the VPA-exposed rats (Zimmerman et al., 2018). There were significantly fewer and irregularly shaped neurons in both the VCN and the SOC (Zimmerman et al., 2018). Additionally, there was a reduced calbindin and calretinin immunoreactivity and a lower density of dopaminergic terminals (Zimmerman et al., 2018). However, there was no difference in the structure of calyx terminals in the MNTB (Zimmerman et al., 2018). A detailed morphometric analysis of the VPA-exposed SOC concluded MSO and VNTB neurons were smaller and rounder and SPON neurons were smaller, with a different orientation compared to the controls (Lukose et al., 2011). Both MNTB and LSO neurons were larger in VPA-exposed rats and MNTB neurons were generally rounder, while LSO were rounder only in the medial and central limbs (Lukose et al., 2011). Another study examined LL and IC in VPA-exposed rats and found that neurons in the central nucleus of the IC and the dorsal nucleus of the LL were larger than the controls (Mansour et al., 2019). In addition, there were significantly fewer calbindin-immunopositive neurons in the dorsal nucleus of the LL (Mansour et al., 2019). Moreover, VPA exposure resulted in fewer dopaminergic terminals in the central nucleus of the IC (Mansour et al., 2019). Finally, this group examined the proportions of retrogradely labeled neurons in the nuclei of the LL, SOC and CN using stereotaxic injections of the retrograde tracer *Fast Blue* into the central nucleus of the IC (Zimmerman et al., 2020). There were fewer neurons in the auditory brainstem after VPA exposure and fewer neurons that were retrogradely labeled from the central nucleus of the IC (Zimmerman et al., 2020). This indicates altered patterns of input to the auditory midbrain of VPA-exposed rats. Taken together, these results indicate extensive structural and functional abnormalities throughout the auditory brainstem. It is suggested that VPA exposure causes abnormal ascending projections to the IC from both the CN and SOC. Those abnormalities result in difficulties in localization of sound sources and abnormal temporal processing of complex sounds such as vocalizations (Zimmerman et al., 2020).

Thalidomide Exposed Model

Exposure to thalidomide (THAL) during the first trimester has been verified as related to the risk of autism in epidemiological studies (Matsuzaki et al., 2012). THAL-exposed rats had a decreased SOC immunoreactivity and smaller MNTB compared to control (Ida-Eto et al., 2017). Another study exposed rats to 16-kHz pure tone auditory stimulus and c-Fos immunostaining (Tsugiyama et al., 2020). THAL rats had an increased number of c-Fos-positive neurons in MNTB compared to the control (Tsugiyama et al., 2020).

A study replicated the results obtained in VPA- exposed rats in THAL-exposed rats, which were a caudal shift of the 5-HT positive neuronal population in the DRN and a decrease in Shh mRNA expression (Miyazaki et al., 2005). Both THAL and VPA had an irreversible effect on the 5-HT neuronal differentiation and migration (Miyazaki et al., 2005). The same model had a decreased SOC immunoreactivity and smaller MNTB compared to control.

Cntnap2 Knockout

A loss-of-function mutation in the *CNTNAP2* gene is strongly associated with ASD and language processing deficits therefore one study examined the impact of *Cntnap2* loss on auditory processing, filtering, and reactivity throughout development and young adulthood of rats (Scott et al., 2018). Similar to the atypical ABR responses in autistic individuals mentioned above (Tanguay et al., 1982; Maziade et al., 2000; Rosenhall et al., 2003; Tas et al., 2007; Russo et al., 2008; Magliaro et al., 2010; Azouz et al., 2014; Ververi et al., 2015; Jones et al., 2020; Kamita et al., 2020), hearing thresholds were not altered in KO rats, but there was a reduction in response amplitudes and a delay in response latency of the ABR for juvenile KO animals compared to WT (Scott et al., 2018). The alterations in ABR normalized in adult KO rats indicating a delay in auditory brainstem development (Scott et al., 2018). However, adolescent KO rats displayed deficits

in sensory filtering and sensorimotor gating accompanied by increased startle reactivity that persisted into adulthood (Scott et al., 2018).

Black and Tan BRachyury T+ Itpr3tf/J (BTBR) Model

The BTBR strain is a phenotypic ASD model which displays behaviors associated with ASD in humans (Chao et al., 2020). BTBR mice have impaired sociability, altered ultrasonic vocalization, and increased self-grooming behaviors which are indicators of impaired sociability, and restricted and repeated behaviors (Chao et al., 2020).

A reduction in TH immunostaining of dopaminergic neurons is observed in the substantia nigra of BTBR mice compared to WT (Chao et al., 2020). They also exhibited decreased expression of striatal dopamine transporter (DAT) and increased spatial coupling between VGLUT1 and TH signals, while no difference is seen in GAD67 (Chao et al., 2020). Additionally, intranasal administration of DA alleviated impairments in non-selective attention, object-based attention, and social approaching (Chao et al., 2020). Taken together, the results indicate a hypofunction of the DA system.

Integrin β3 (ITGβ3) Knockout

The *ITGβ3* gene is associated with both autism and the serotonin system (Ellegood et al., 2012). Volumetric differences between *ITGβ3* KO and WT mice were examined using high resolution magnetic resonance imaging (Ellegood et al., 2012). There was an 11% reduction in total KO brain volume and a decrease in the lateral wings of the DRN indicating the connection between the *ITGβ3* gene and the development of the serotonin system (Ellegood et al., 2012).

Perinatal Anoxia (PA)

ABRs of rats that underwent PA, an epigenetic factor to autism, and control rats, revealed that PA rats had a delay in all peaks after peak I (Strata et al., 2005). Moreover, interpeak intervals were longer in PA compared to control (Strata et al., 2005). Similar to the ABR alterations in autistic individuals (Tanguay et al., 1982; Maziade et al., 2000; Rosenhall et al., 2003; Tas et al., 2007; Russo et al., 2008; Magliaro et al., 2010; Azouz et al., 2014; Ververi et al., 2015; Jones et al., 2020; Kamita et al., 2020).

Radiation Exposure

Prenatal perturbation such as exposure to ionizing radiation or viral infection during early gestation has been linked to neuropsychiatric illnesses including autism. Rhesus macaque monkeys were exposed *in utero* to x-irradiation and allowed to mature to full adulthood (Selemon and Begovic, 2020). Stereological cell counts and soma size measurements of neurons in the SN and VTA revealed a 33% reduction in mean total neuron number in the irradiated monkeys but no difference in soma size between both groups (Selemon and Begovic, 2020).

Neuroligin 3 (Nlgn3) Knockout

Nlgn3 is an ASD-associated synaptic adhesion molecule (Bariselli et al., 2018). VTA DA neuron-specific down-regulation of *Nlgn3* induced aberrant exploration of non-familiar conspecifics as well as deficit in habituation processing (Bariselli et al., 2018). Exploration of a not familiar stimuli is linked with glutamatergic inputs onto VTA DA neurons and an impairment of this novelty-induced synaptic plasticity is seen in in *Nlgn3* KO and *Nlgn3* VTA DA knockdown mice (Bariselli et al., 2018).

BALB/c Mice

BALB/c mice express dysregulation in the serotonergic system, therefore two studies examined the role of the serotonergic system in social behaviors that are relevant for ASD (Payet et al., 2018; Russo et al., 2019). In the first study, mice were treated with fluoxetine, a selective serotonin reuptake inhibitor (SSRIs), either acutely or chronically and exposed to the three-chambered social approach test (Payet et al., 2018). Social behavior was decreased by acute fluoxetine, but it increased by chronic fluoxetine compared to controls (Payet et al., 2018). TPH2 enzyme activity was not impacted by SSRI administration, but serotonergic neurons were differentially affected (Payet et al., 2018). The second study showed that BALB/c mice displayed reduced social behavior in three-chamber sociability test and increased anxious behavior in the elevated plus-maze, in combination with decreased 5-HTP accumulation in the rostral and mid-rostrocaudal DRN (Russo et al., 2019).

DISCUSSION

A final consensus on the morphometric brainstem differences associated with ASD has not been reached, but the most common observation is an alteration in the brainstem size. Studies that observed reduction in either total brainstem volume or at least one of its components (Gaffney et al., 1988; Hashimoto et al., 1989, 1992a,b, 1993a,b, 1995; Herbert et al., 2003; Craig et al., 2007; Jou et al., 2009; Toal et al., 2010; Fredo et al., 2014; Hanaie et al., 2016; Andersson et al., 2020) are more common than studies with any other outcome. Moreover, post-mortem analysis of autistic brains showcased malformation in cells of the olivary complex (Kulesza and Mangunay, 2008; Kulesza et al., 2011; Wegiel et al., 2014).

In accordance with human studies, animal studies also found extensive structural abnormalities throughout the auditory brainstem. VPA-exposed animals have fewer and more dysmorphic VCN (Zimmerman et al., 2018) and SOC (Lukose et al., 2011; Zimmerman et al., 2018) neurons. SOC abnormalities are also seen in the Fmr1 KO model (Ruby et al., 2015; Garcia-Pino et al., 2017; Rotschafer and Cramer, 2017) and THAL-exposed rats (Ida-Eto et al., 2017; Tsugiyama et al., 2020). The morphometric malformation of SOC components in VPA-exposed rats (Lukose et al., 2011) were consistent with malformation in SOC of autistic brains (Kulesza et al., 2011). There are also fewer neurons retrogradely labeled from the central nucleus of the IC (Zimmerman et al., 2020). All this indicates a dysfunction in the ascending projections from the CN and SOC to the IC.

Moreover, the LC is another pons nucleus that is suggested to be atypical in ASD (Granovetter et al., 2019). Autistic individuals experience atypical modulation of LC activity in accordance with changes in attentional demands (Granovetter et al., 2019). Abnormalities in autonomic functioning such as

low baseline cardiac parasympathetic activity with evidence of elevated sympathetic tone are seen even in asymptotic autistic individuals (Ming et al., 2005) indicating possible alteration in the brainstem structure that is central in ASD. In addition, studies found a link between brainstem structure and sensory sensitivity (Jou et al., 2009) or motor performance (Travers et al., 2015; Hanaie et al., 2016) in ASD. Taken together, these results suggest that structural aspects of the brainstem, specifically the pons may be related to ASD pathogenies.

The differences of functional measures of the brainstem such as ABR indicate some form of abnormality. A common ABR abnormality is in the peak III amplitude and/or latency (Tanguay et al., 1982; Källstrand et al., 2010; Magliaro et al., 2010; Dabbous, 2012; Ververi et al., 2015; Claesdotter-Knutsson et al., 2019) which is suggested to be an indicator of SOC (Moller, 2006) activity. Additionally, ABR abnormalities are also seen in animal models such as Fmr1 KO mice (Rotschafer et al., 2015), α7-nAChR KO mice (Felix et al., 2019), Cntnap2 KO rats (Scott et al., 2018) and PA (Strata et al., 2005). However, the abnormalities within the animal models are not consistent across different models. Peak I abnormalities are seen in Fmr1 KO mice (Rotschafer et al., 2015) but not observed in Cntnap2 KO rats (Scott et al., 2018) α7-nAChR KO mice (Felix et al., 2019), and PA (Strata et al., 2005). Moreover, animal studies investigating activation of brainstem neurons found a more widespread activation in VPA-exposed rats in response to Dubiel and Kulesza (2016) compared to controls, which suggests that abnormal activation patterns result in altered processing of auditory stimuli.

Brainstem serotonergic system alterations are observed in animal studies using VPA-exposed models (Miyazaki et al., 2005; Kuwagata et al., 2009; Oyabu et al., 2013b; Wang et al., 2018), Thal-exposed model (Miyazaki et al., 2005), ITGβ3 KO (Ellegood et al., 2012) and BALB/c mice (Payet et al., 2018; Russo et al., 2019). Dopaminergic system alterations such as cell morphology and cell count in the SN (Chao et al., 2020; Selemon and Begovic, 2020) or impairment in synaptic plasticity (Bariselli et al., 2018) has been noticed in different animal models including Nlgn3 VTA DA knockdown mice (Bariselli et al., 2018), *in utero* radiation exposed monkeys (Selemon and Begovic, 2020) and BTBR mice (Chao et al., 2020).

To see the effect of age on the brainstem development, we analyzed the age ranges of participants in the studies that reported a negative outcome, meaning no difference between the ASD population and controls. No animal studies reported a negative outcome. However, six human studies showed no differences between the ASD participants and controls (Garber and Ritvo, 1992; Piven et al., 1992; Hardan et al., 2001; Tharpe et al., 2006; Chaddad et al., 2017; Freeman et al., 2018), five of them included adult participants. The total number of studies with only children participants is 31, the number of studies with only adults is 7, the number of studies that included both children and adults is 18, and the remaining studies did not specify age. Four of the negative outcome studies had vast age ranges of 4.45–67.33 years (Freeman et al., 2018), 12.2–51.8 years (Hardan et al., 2001), 8–38 years (Piven et al., 1992), and 18–38 years of age (Garber and Ritvo, 1992), but the means for all of them fell within the adult age range with means m = 19.89 ± 15.34 years, m = 27.7 ± 10.7 years, m = 22.4 ±10.1 years and m = 27.2 ± 5.3 years, respectively. The fifth study included only the mean m=17.01 ± 8.36 years (Chaddad et al., 2017). The sixth study was the only one with only children participants aged 3–10 years (Tharpe et al., 2006). 33.3% of studies with an age mean greater than 18 ($n = 12$) reported a negative outcome while only 5% of studies with an age mean <18 ($n = 40$) reported a negative outcome. Moreover, a post-mortem study that divided the participants into three different groups based on age, 4–8, 11–23, and 29–64 years reported deficits in volume of neuronal nucleus was significant only for the age group 4–8 years (Wegiel et al., 2014).

An animal study that investigated developmental implications using Fmr1 KO showed different abnormalities in SOC morphologies before and after hearing onset (Rotschafer and Cramer, 2017). Moreover, a study using the Cntnap2 KO model observed ABR alterations in juvenile KO rats that normalizes in adulthood, but the deficits in sensory filtering and sensorimotor gating accompanied by increased startle reactivity persisted into adulthood (Scott et al., 2018).

Two longitudinal studies found a difference in the development between autistic and typically developing toddlers. The difference in development between both groups was reduced after a year (Chen et al., 2019; Li et al., 2020). Differences in ABRs (Li et al., 2020) and speech-ABRs (Chen et al., 2019) of autistic and typically developing children were reduced between the two recording sessions that were months apart. This is similar to what is observed in Cntnap2 rat models in which ABR alterations in juvenile KO rats don't persist into adulthood (Scott et al., 2018). Additionally, retrospective studies reported that this delay is observed in newborns that are later diagnosed with ASD (Cohen et al., 2013; Miron et al., 2016).

The results highlight the age effect in autism because of unequal studies with negative outcome in adult populations compared to children populations, and longitudinal studies showing a reduced difference between the ASD and controls as they develop. This warrants both studies with strictly defined and small age ranges for comparison and longitudinal studies that follow up with the same individuals as they develop because a component of the pathogenesis of autism could be a delay in brainstem development. The brainstem holds within it the ascending sensory pathways and a delay in its development could have a cascading effect on the cortex.

CONCLUSION

Morphological and structural changes in brainstem size and shape of key brainstem nuclei are observed in both autistic humans (Gaffney et al., 1988; Hashimoto et al., 1989, 1992a,b, 1993a,b, 1995; Herbert et al., 2003; Craig et al., 2007; Kulesza and Mangunay, 2008; Jou et al., 2009; Toal et al., 2010; Kulesza et al., 2011; Fredo et al., 2014; Wegiel et al., 2014; Hanaie et al., 2016; Andersson et al., 2020) and in rodent models of autism (Lukose et al., 2011; Ruby et al., 2015; Garcia-Pino et al., 2017;

Ida-Eto et al., 2017; Rotschafer and Cramer, 2017; Zimmerman et al., 2018, 2020; Tsugiyama et al., 2020). Moreover, functional abnormalities are also observed in autistic humans (Tanguay et al., 1982; Ming et al., 2005; Jou et al., 2009; Källstrand et al., 2010; Magliaro et al., 2010; Dabbous, 2012; Travers et al., 2015; Ververi et al., 2015; Hanaie et al., 2016; Claesdotter-Knutsson et al., 2019; Granovetter et al., 2019) and rodent models of autism (Strata et al., 2005; Rotschafer et al., 2015; Scott et al., 2018; Felix et al., 2019). Some studies leveraged the animal models of autism for deeper explorations of serotonergic (Miyazaki et al., 2005; Kuwagata et al., 2009; Ellegood et al., 2012; Oyabu et al., 2013b; Payet et al., 2018; Wang et al., 2018; Russo et al., 2019) and dopaminergic neurotransmitter systems (Chao et al., 2020; Selemon and Begovic, 2020) of which alterations are found in both.

The differences between humans and other species lie in the degree of higher-order cognitive processes, top-down feedback and modulation which consequently gives rise to more complex behaviors in humans compared to other species (Scott et al., 2021). However, the brainstem presents a unique translational opportunity to study the potential mechanisms of disruption in autism since it is highly conserved across species. This translational approach should be exploited using more invasive explorations in animal models to provide answers into the pathogensis of autism. Future studies should aim to investigate the alterations in cellular mechanism that could be the cause of morphological and functional differences seen across species, coupled with human studies on the role of the brainstem in clinical symptomatology of autism that is uniquely human.

AUTHOR'S NOTE

This protocol was registered with the Open Science Framework (osf.io/2hd6m).

DATA AVAILABILITY STATEMENT

The original contributions presented in the study are included in the article/**Supplementary Material**, further inquiries can be directed to the corresponding author/s.

AUTHOR CONTRIBUTIONS

AS was responsible for the conception, the acquisition, and analysis and interpretation of data for the work. CS and RS were second reviewers for the screening of papers. RS and SS were involved in revising the review paper critically and to ultimately provide approval for publication of the content. All authors contributed to the article and approved the submitted version.

FUNDING

AS is funded by Ontario Graduate Scholarship 2021-2022. RS is funded by an NSERC Discovery Grant (RGPIN-2017-04656), a SSHRC Insight Grant (435-2017-0936), the University of Western Ontario Faculty Development Research Fund, the province of Ontario Early Researcher Award, and a Canadian Foundation for Innovation John R. Evans Leaders Fund (37497). Thanks also to the contributions of Western's Brain and Mind Institute and Western's BrainsCAN grant funded by CFREF. We would also like to thank all the quarantining and lock-downs that made this work possible.

SUPPLEMENTARY MATERIAL

The Supplementary Material for this article can be found online at: https://www.frontiersin.org/articles/10.3389/fnint.2021.760116/full#supplementary-material

Supplementary Table 1 | Summary of all human studies.

Supplementary Table 2 | Summary of all animal studies.

REFERENCES

Ágota, Á., Kemecsei, R., Company, V., Murcia-Ramón, R., Juarez, I., Gerecsei, L. I., et al. (2020). Gestational exposure to sodium valproate disrupts fasciculation of the mesotelencephalic dopaminergic tract, with a selective reduction of dopaminergic output from the ventral tegmental area. *Front. Neuroanat.* 14, 1–19. doi: 10.3389/fnana.2020.00029

American Psychiatric Association (1980). *Diagnostic and Statistical Manual of Mental Disorders,* 3rd Edn.

American Psychiatric Association (1994). *DSM-IV: Diagnostic and Statistical Manual of Mental Disorders*.

American Psychiatric Association (2013). *Diagnostic and Statistical Manual of Mental Disorders,* 5th Edn. doi: 10.1176/appi.books.9780890425596

Andersson, M., Tangen, Ä., Farde, L., Bölte, S., Halldin, C., Borg, J., et al. (2020). Serotonin transporter availability in adults with autism—a positron emission tomography study. *Mol. Psychiatry*. 26, 1647–1658.

Aromataris, E., and Munn, Z. (eds.). (2020). *JBI Manual for Evidence Synthesis*. JBI. doi: 10.46658/JBIMES-20-01

Ascano, M., Mukherjee, N., Bandaru, P., Miller, J. B., Nusbaum, J. D., Corcoran, D. L., et al. (2012). FMRP targets distinct mRNA sequence elements to regulate protein expression. *Nature* 492, 382–386. doi: 10.1038/nature11737

Azmitia, E. C., Saccomano, Z. T., Alzoobaee, M. F., Boldrini, M., and Whitaker-Azmitia, P. M. (2016). Persistent angiogenesis in the autism brain: an immunocytochemical study of postmortem cortex, brainstem and cerebellum. *J. Autism Dev. Disord.* 46, 1307–1318. doi: 10.1007/s10803-015-2672-6

Azouz, H. G., kozou, H., Khalil, M., Abdou, R. M., and Sakr, M. (2014). The correlation between central auditory processing in autistic children and their language processing abilities. *Int. J. Pediatr. Otorhinolaryngol.* 78, 2297–2300. doi: 10.1016/j.ijporl.2014.10.039

Bariselli, S., Hörnberg, H., Prévost-Solié, C., Musardo, S., Hatstatt-Burklé, L., Scheiffele, P., et al. (2018). Role of VTA dopamine neurons and neuroligin 3 in sociability traits related to nonfamiliar conspecific interaction. *Nat. Commun.* 9:3173. doi: 10.1038/s41467-018-05382-3

Bariselli, S., Tzanoulinou, S., Glangetas, C., Prévost-Solié, C., Pucci, L., Viguié, J., et al. (2016). SHANK3 controls maturation of social reward circuits in the VTA. *Nat. Neurosci.* 19, 926–934. doi: 10.1038/nn.4319

Bosco, P., Giuliano, A., Delafield-Butt, J., Muratori, F., Calderoni, S., and Retico, A. (2019). Brainstem enlargement in preschool children with autism: results from an intermethod agreement study of segmentation algorithms. *Hum. Brain Mapp.* 40, 7–19. doi: 10.1002/hbm.24351

Bouchekioua, Y., Tsutsui-Kimura, I., Sano, H., Koizumi, M., Tanaka, K. F., Yoshida, K., et al. (2018). Striatonigral direct pathway activation is sufficient to induce repetitive behaviors. *Neurosci. Res.* 132, 53–57. doi: 10.1016/j.neures.2017.09.007

Chaddad, A., Desrosiers, C., and Toews, M. (2017). Multi-scale radiomic analysis of sub-cortical regions in MRI related to autism, gender and age. *Sci. Rep.* 7, 1–17. doi: 10.1038/srep45639

Chao, O. Y., Pathak, S. S., Zhang, H., Dunaway, N., Li, J. S., Mattern, C., et al. (2020). Altered dopaminergic pathways and therapeutic effects of intranasal dopamine in two distinct mouse models of autism. *Mol. Brain* 13, 1–16. doi: 10.1186/s13041-020-00649-7

Chen, J., Liang, C., Wei, Z., Cui, Z., Kong, X., Dong, C. jian, Lai, Y., et al. (2019). Atypical longitudinal development of speech-evoked auditory brainstem response in preschool children with autism spectrum disorders. *Autism Res.* 12, 1022–1031. doi: 10.1002/aur.2110

Claesdotter-Knutsson, E., Åkerlund, S., Cervin, M., Råstam, M., and Lindvall, M. (2019). Abnormal auditory brainstem response in the pons region in youth with autism. *Neurol. Psychiatry Brain Res.* 32, 122–125. doi: 10.1016/j.npbr.2019.03.009

Cohen, I. L., Gardner, J. M., Karmel, B. Z., Phan, H. T. T., Kittler, P., Gomez, T. R., et al. (2013). Neonatal brainstem function and 4-month arousal-modulated attention are jointly associated with autism. *Autism Res.* 6, 11–22. doi: 10.1002/aur.1259

Constantin, L., Poulsen, R. E., Scholz, L. A., Favre-Bulle, I. A., Taylor, M. A., Sun, B., et al. (2020). Altered brain-wide auditory networks in a zebrafish model of fragile X syndrome. *BMC Biol.* 18, 1–17. doi: 10.1186/s12915-020-00857-6

Craig, M. C., Zaman, S. H., Daly, E. M., Cutter, W. J., Robertson, D. M. W., Hallahan, B., et al. (2007). Women with autistic-spectrum disorder: magnetic resonance imaging study of brain anatomy. *Br. J. Psychiatry* 191, 224–228. doi: 10.1192/bjp.bp.106.034603

Dabbous, A. O. (2012). Characteristics of auditory brainstem response latencies in children with autism spectrum disorders. *Audiol. Med.* 10, 122–131. doi: 10.3109/1651386X.2012.708986

Dubiel, A., and Kulesza, R. J. (2016). Prenatal valproic acid exposure disrupts tonotopic c-Fos expression in the rat brainstem. *Neuroscience* 324, 511–523. doi: 10.1016/j.neuroscience.2016.01.030

El Shennawy, A. M., El Khosht, M., Ghannoum, H., and El Meguid, N. A. (2014). Electrophysiologic assessment of auditory function in children with autism and attention-deficit and hyperactivity disorder. *Ocena Elektrofizjologiczna Funkcji Słuchowych U Dzieci Z Autyzmem Oraz Zespołem Nadpobudliwości Psychoruchowej.* 4, 26–34. doi: 10.17430/891185

Ellegood, J., Henkelman, R. M., and Lerch, J. P. (2012). Neuroanatomical assessment of the integrin β3 mouse model related to autism and the serotonin system using high resolution MRI. *Front. Psychiatry.* 3:37. doi: 10.3389/fpsyt.2012.00037

Elvsåshagen, T., Bahrami, S., van der Meer, D., Agartz, I., Alnæs, D., Barch, D. M., et al. (2020). The genetic architecture of human brainstem structures and their involvement in common brain disorders. *Nat. Commun.* 11:4016. doi: 10.1038/s41467-020-17376-1

Farook, M. F., DeCuypere, M., Hyland, K., Takumi, T., LeDoux, M. S., and Reiter, L. T. (2012). Altered serotonin, dopamine and norepinepherine levels in 15q duplication and Angelman syndrome mouse models. *PLoS ONE* 7:e43030. doi: 10.1371/journal.pone.0043030

Felix, R. A., Chavez, V. A., Novicio, D. M., Morley, B. J., and Portfors, C. V. (2019). Nicotinic acetylcholine receptor subunit α7-knockout mice exhibit degraded auditory temporal processing. *J. Neurophysiol.* 122, 451–465. doi: 10.1152/jn.00170.2019

Fredo, A. R. J., Kavitha, G., and Ramakrishnan, S. (2014). Segmentation and morphometric analysis of subcortical regions in autistic MR brain images using fuzzy Gaussian distribution model-based distance regularised multi-phase level set. *Int. J. Biomed. Eng. Technol.* 15, 211–223. doi: 10.1504/IJBET.2014.064647

Freeman, S. M., Palumbo, M. C., Lawrence, R. H., Smith, A. L., Goodman, M. M., and Bales, K. L. (2018). Effect of age and autism spectrum disorder on oxytocin receptor density in the human basal forebrain and midbrain. *Transl. Psychiatry* 8:257. doi: 10.1038/s41398-018-0315-3

Gaffney, G. R., Kuperman, S., Tsai, L. Y., and Minchin, S. (1988). Morphological evidence for brainstem involvement in infantile autism. *Biol. Psychiatry* 24, 578–586. doi: 10.1016/0006-3223(88)90168-0

Garber, H. J., and Ritvo, E. R. (1992). Magnetic resonance imaging of the posterior fossa in autistic adults. *Clin. Res. Rep.* 149, 245–247. doi: 10.1176/ajp.149.2.245

Garcia-Pino, E., Gessele, N., and Koch, U. (2017). Enhanced excitatory connectivity and disturbed sound processing in the auditory brainstem of fragile X mice. *J. Neurosci.* 37, 7403–7419. doi: 10.1523/JNEUROSCI.2310-16.2017

Gonzalez, D., Tomasek, M., Hays, S., Sridhar, V., Ammanuel, S., Chang, C. W., et al. (2019). Audiogenic seizures in the Fmr1 knock-out mouse are induced by Fmr1 deletion in subcortical, VGlut2-expressing excitatory neurons and require deletion in the inferior colliculus. *J. Neurosci.* 39, 9852–9863. doi: 10.1523/JNEUROSCI.0886-19.2019

Granovetter, M., Burlingham, C., Blauch, N., Minshew, N., Heeger, D., and Behrmann, M. (2019). Uncharacteristic task-evoked pupillary responses implicate atypical locus coeruleus activity in autism. *J. Neurosci.* 40, 3815–3826. doi: 10.1523/JNEUROSCI.2680-19.2020

Hadjikhani, N., Åsberg Johnels, J., Zürcher, N. R., Lassalle, A., Guillon, Q., Hippolyte, L., et al. (2017). Look me in the eyes: constraining gaze in the eye-region provokes abnormally high subcortical activation in autism. *Sci. Rep.* 7:3163. doi: 10.1038/s41598-017-03378-5

Hanaie, R., Mohri, I., Kagitani-Shimono, K., Tachibana, M., Matsuzaki, J., Hirata, I., et al. (2016). White matter volume in the brainstem and inferior parietal lobule is related to motor performance in children with autism spectrum disorder: a voxel-based morphometry study. *Autism Res.* 9, 981–992. doi: 10.1002/aur.1605

Hardan, A. Y., Minshew, N. J., Harenski, K., and Keshavan, M. S. (2001). Posterior fossa magnetic resonance imaging in autism. *J. Am. Acad. Child Adolesc. Psychiatry* 40, 666–672. doi: 10.1097/00004583-200106000-00011

Hashimoto, T., Murakawa, K., Miyazaki, M., Tayama, M., and Kuroda, Y. (1992a). Magnetic resonance imaging of the brain structures in the posterior fossa in retarded autistic children. *Acta Paediatr.* 81, 1030–1034. doi: 10.1111/j.1651-2227.1992.tb12169.x

Hashimoto, T., Tayama, M., Miyazaki, M., Murakawa, K., and Kuroda, Y. (1993a). Brainstem and cerebellar vermis involvement in autistic children. *J. Child Neurol.* 8, 149–153. doi: 10.1177/088307389300800207

Hashimoto, T., Tayama, M., Miyazaki, M., Murakawa, K., Shimakawa, S., Yoneda, Y., et al. (1993b). Brainstem involvement in high functioning autistic children. *Acta Neurol. Scand.* 88, 123–128. doi: 10.1111/j.1600-0404.1993.tb04203.x

Hashimoto, T., Tayama, M., Miyazaki, M., Sakurama, N., Yoshimoto, T., Murakawa, K., et al. (1992b). Reduced brainstem size in children with autism. *Brain Dev.* 14, 94–97. doi: 10.1016/S0387-7604(12)80093-3

Hashimoto, T., Tayama, M., Mori, K., Fujino, K., Miyazaki, M., and Kuroda, Y. (1989). Magnetic resonance imaging in autism: preliminary report. *Neuropediatrics* 20, 142–146. doi: 10.1055/s-2008-1071280

Hashimoto, T., Tayama, M., Murakawa, K., Yoshimoto, T., Miyazaki, M., Harada, M., et al. (1995). Development of the brainstem and cerebellum in autistic patients. *J. Autism Dev. Disord.* 25, 1–18. doi: 10.1007/BF02178163

Herbert, M. R., Ziegler, D. A., Deutsch, C. K., O'Brien, L. M., Lange, N., Bakardjiev, A., et al. (2003). Dissociations of cerebral cortex, subcortical and cerebral white matter volumes in autistic boys. *Brain* 126, 1182–1192. doi: 10.1093/brain/awg110

Ida-Eto, M., Hara, N., Ohkawara, T., and Narita, M. (2017). Mechanism of auditory hypersensitivity in human autism using autism model rats. *Pediatr. Int.* 59, 404–407. doi: 10.1111/ped,.13186

Jac Fredo, A. R., Kavitha, G., and Ramakrishnan, S. (2015). "Subcortical region segmentation using fuzzy based augmented lagrangian multiphase level sets method in autistic mr brain images," in *52nd Annual Rocky Mountain Bioengineering Symposium and 52nd International ISA Biomedical Sciences Instrumentation Symposium 2015*, (Chennai, India) *April*, 326–334.

Jones, M. K., Kraus, N., Bonacina, S., Nicol, T., Otto-Meyer, S., and Roberts, M. Y. (2020). Auditory processing differences in toddlers with autism spectrum disorder. *J. Speech Lang. Hear. Res.* 63, 1608–1617. doi: 10.1044/2020_JSLHR-19-00061

Jou, R. J., Minshew, N. J., Melhem, N. M., Keshavan, M. S., and Hardan, A. Y. (2009). Brainstem volumetric alterations in children with autism. *Psychol. Med.* 39, 1347–1354. doi: 10.1017/S0033291708004376

Källstrand, J., Olsson, O., Nehlstedt, S. F., Sköld, M. L., and Nielzén2, S. (2010). Abnormal auditory forward masking pattern in the brainstem response of individuals with Asperger syndrome. *Neuropsychiatr. Dis. Treat.* 6, 289–296. doi: 10.2147/ndt.s10593

Kamita, M. K., Silva, L. A. F., Magliaro, F. C. L., Kawai, R. Y. C., Fernandes, F. D. M., and Matas, C. G. (2020). Brainstem auditory evoked potentials in children with autism spectrum disorder. *J. Pediatr.* 96, 386–392. doi: 10.1016/j.jped.2018.12.010

Krishnan, V., Stoppel, D. C., Nong, Y., Johnson, M. A., Nadler, M. J. S., Ozkaynak, E., et al. (2017). Autism gene Ube3a and seizures impair sociability by repressing VTA Cbln1. *Nature* 543, 507–512. doi: 10.1038/nature21678

Kulesza, R. J., Lukose, R., and Stevens, L. V. (2011). Malformation of the human superior olive in autistic spectrum disorders. *Brain Res.* 1367, 360–371. doi: 10.1016/j.brainres.2010.10.015

Kulesza, R. J., and Mangunay, K. (2008). Morphological features of the medial superior olive in autism. *Brain Res.* 1200, 132–137. doi: 10.1016/j.brainres.2008.01.009

Kuwagata, M., Ogawa, T., Shioda, S., and Nagata, T. (2009). Observation of fetal brain in a rat valproate-induced autism model: a developmental neurotoxicity study. *Int. J. Dev. Neurosci.* 27, 399–405. doi: 10.1016/j.ijdevneu.2009.01.006

Lai, M. C., Lombardo, M. V., Ecker, C., Chakrabarti, B., Suckling, J., Bullmore, E. T., et al. (2014). Neuroanatomy of individual differences in language in adult males with autism. *Cereb. Cortex* 25, 3613–3628. doi: 10.1093/cercor/bhu211

Li, A., Gao, G., Fu, T., Pang, W., Zhang, X., Qin, Z., et al. (2020). Continued development of auditory ability in autism spectrum disorder children: a clinical study on click-evoked auditory brainstem response. *Int. J. Pediatr. Otorhinolaryngol.* 138:110305. doi: 10.1016/j.ijporl.2020.110305

Lord, C., Rutter, M., DiLavore, P., and Risi, S. (1999). *ADOS. Autism Diagnostic Observation Schedule. Manual.* Los Angeles, CA: WPS.

Lukose, R., Schmidt, E., Wolski, T. P., Murawski, N. J., and Kulesza, R. J. (2011). Malformation of the superior olivary complex in an animal model of autism. *Brain Res.* 1398, 102–112. doi: 10.1016/j.brainres.2011.05.013

Luo, J., Feng, Q., Wei, L., and Luo, M. (2017). Optogenetic activation of dorsal raphe neurons rescues the autistic-like social deficits in Shank3 knockout mice. *Cell Res.* 27, 950–953. doi: 10.1038/cr.2017.52

Magliaro, F. C. L., Scheuer, C. I., Júnior, F. B. A., and Matas, C. G. (2010). Estudo dos potenciais evocados auditivos em autismo. *Pro-Fono* 22, 31–36. doi: 10.1590/S0104-56872010000100007

Mansour, Y., and Kulesza, R. (2020). Three dimensional reconstructions of the superior olivary complex from children with autism spectrum disorder. *Hear. Res.* 393:107974. doi: 10.1016/j.heares.2020.107974

Mansour, Y., Mangold, S., Chosky, D., and Kulesza, R. J. (2019). Auditory midbrain hypoplasia and dysmorphology after prenatal valproic acid exposure. *Neuroscience* 396, 79–93. doi: 10.1016/j.neuroscience.2018.11.016

Matsuzaki, H., Iwata, K., Manabe, T., and Mori, N. (2012). Triggers for autism: genetic and environmental factors. *J. Cent. Nerv. Syst. Dis.* 4:JCNSD.S9058. doi: 10.4137/JCNSD.S9058

Maziade, M., Merette, C., Cayer, M., Roy, M. A., Szatmari, P., Cote, R., et al. (2000). Prolongation of brainstem auditory-evoked responses in autistic probands and their unaffected relatives. *Arch. Gen. Psychiatry* 57, 1077–1083. doi: 10.1001/archpsyc.57.11.1077

McGowan, J., Sampson, M., Salzwedel, D. M., Cogo, E., Foerster, V., and Lefebvre, C. (2016). PRESS peer review of electronic search strategies: 2015 guideline statement. *J. Clin. Epidemiol.* 75, 40–46. doi: 10.1016/j.jclinepi.2016.01.021

Ming, X., Julu, P. O. O., Brimacombe, M., Connor, S., and Daniels, M. L. (2005). Reduced cardiac parasympathetic activity in children with autism. *Brain Dev.* 27, 509–516. doi: 10.1016/j.braindev.2005.01.003

Miron, O., Ari-Even Roth, D., Gabis, L. V., Henkin, Y., Shefer, S., Dinstein, I., et al. (2016). Prolonged auditory brainstem responses in infants with autism. *Autism Res.* 9, 689–695. doi: 10.1002/aur.1561

Miron, O., Delgado, R. E., Delgado, C. F., Simpson, E. A., Yu, K. H., Gutierrez, A., et al. (2021). Prolonged auditory brainstem response in universal hearing screening of newborns with autism spectrum disorder. *Autism Res.* 14, 46–52. doi: 10.1002/aur.2422

Miyazaki, K., Narita, N., and Narita, M. (2005). Maternal administration of thalidomide or valproic acid causes abnormal serotonergic neurons in the offspring: Implication for pathogenesis of autism. *Int. J. Dev. Neurosci.* 23, 287–297. doi: 10.1016/j.ijdevneu.2004.05.004

Möhrle, D., Fernández, M., Peñagarikano, O., Frick, A., Allman, B., and Schmid, S. (2020). What we can learn from a genetic rodent model about autism. *Neurosci. Biobehav. Rev.* 109, 29–53. doi: 10.1016/j.neubiorev.2019.12.015

Moller, A. R. (2006). "Hearing," in *Anatomy, Physiology, and Disorders of the Auditory System*, 2nd Edn. Elsevier Science and Technology.

Nguyen, A. O., Binder, D. K., Ethell, I. M., and Razak, K. A. (2020). Abnormal development of auditory responses in the inferior colliculus of a mouse model of Fragile X Syndrome. *J. Neurophysiol.* 123, 2101–2121. doi: 10.1152/jn.00706.2019

Oberman, L. M., Boccuto, L., Cascio, L., Sarasua, S., and Kaufmann, W. E. (2015). Autism spectrum disorder in Phelan-McDermid syndrome: initial characterization and genotype-phenotype correlations. *Orphanet J. Rare Dis.* 10, 1–9. doi: 10.1186/s13023-015-0323-9

Ofner, M., Coles, A., Decou, M., Lou, D.o, M. T., Bienek, A., Snider, J., and Ugnat, A.-M. (2018). *Autism Spectrum Disorder Among Children And Youth In Canada 2018*. Public Health Agency of Canada.

Oyabu, A., Narita, M., and Tashiro, Y. (2013a). The effects of prenatal exposure to valproic acid on the initial development of serotonergic neurons. *Int. J. Dev. Neurosci.* 31, 202–208. doi: 10.1016/j.ijdevneu.2013.01.006

Oyabu, A., Tashiro, Y., Oyama, T., Ujihara, K., Ohkawara, T., Ida-Eto, M., et al. (2013b). Morphology of the facial motor nuclei in a rat model of autism during early development. *Int. J. Dev. Neurosci.* 31, 138–144. doi: 10.1016/j.ijdevneu.2012.12.002

Payet, J. M., Burnie, E., Sathananthan, N. J., Russo, A. M., Lawther, A. J., Kent, S., et al. (2018). Exposure to acute and chronic fluoxetine has differential effects on sociability and activity of serotonergic neurons in the dorsal raphe nucleus of juvenile male BALB/c mice. *Neuroscience* 386, 1–15. doi: 10.1016/j.neuroscience.2018.06.022

Pillion, J. P., Boatman-Reich, D., and Gordon, B. (2018). Auditory brainstem pathology in autism spectrum disorder: a review. *Cogn. Behav. Neurol.* 31, 53–78. doi: 10.1097/WNN.0000000000000154

Piven, J., Nehme, E., Simon, J., Barta, P., Pearlson, G., and Folstein, S. E. (1992). Magnetic resonance imaging in autism: measurement of the cerebellum, pons, and fourth ventricle. *Biol. Psychiatry* 31, 491–504. doi: 10.1016/0006-3223(92)90260-7

Ramezani, M., Lotfi, Y., Moossavi, A., and Bakhshi, E. (2019). Auditory brainstem response to speech in children with high functional autism spectrum disorder. *Neurol. Sci.* 40, 121–125. doi: 10.1007/s10072-018-3594-9

Rosenhall, U., Nordin, V., Brantberg, K., and Gillberg, C. (2003). Autism and auditory brain stem responses. *Ear Hear.* 24, 206–214. doi: 10.1097/01.AUD.0000069326.11466.7E

Rotschafer, S. E., and Cramer, K. S. (2017). Developmental emergence of phenotypes in the auditory brainstem nuclei of Fmr1 knockout mice. *ENeuro.* 4. doi: 10.1523/ENEURO.0264-17.2017

Rotschafer, S. E., Marshak, S., and Cramer, K. S. (2015). Deletion of Fmr1 alters function and synaptic inputs in the auditory brainstem. *PLoS ONE.* 10:e0117266. doi: 10.1371/journal.pone.0117266

Ruby, K., Falvey, K., and Kulesza, R. J. (2015). Abnormal neuronal morphology and neurochemistry in the auditory brainstem of Fmr1 knockout rats. *Neuroscience* 303, 285–298. doi: 10.1016/j.neuroscience.2015.06.061

Russo, A. M., Lawther, A. J., Prior, B. M., Isbel, L., Somers, W. G., Lesku, J. A., et al. (2019). Social approach, anxiety, and altered tryptophan hydroxylase 2 activity in juvenile BALB/c and C57BL/6J mice. *Behav. Brain Res.* 359, 918–926. doi: 10.1016/j.bbr.2018.06.019

Russo, N., Nicol, T., Trommer, B., Zecker, S., and Kraus, N. (2009). Brainstem transcription of speech is disrupted in children with autism spectrum disorders. *Dev. Sci.* 12, 557–567. doi: 10.1111/j.1467-7687.2008.00790.x

Russo, N., Skoe, E., Trommer, B., Nicol, T., Zecker, S., Bradlow, A., et al. (2008). Deficient brainstem encoding of pitch in children with Autism Spectrum Disorders. *Clin. Neurophysiol.* 119, 1720–1731. doi: 10.1016/j.clinph.2008.01.108

Rutter, M., Le Couteur, A., and Lord, C. (2003). *ADI-R. Autism Diagnostic Interview Revised. Manual*. Los Angeles, CA: Western Psychological Services.

Sakano, H., Zorio, D. A. R., Wang, X., Ting, Y. S., Noble, W. S., MacCoss, M. J., et al. (2017). Proteomic analyses of nucleus laminaris identified candidate targets of the fragile X mental retardation protein. *J. Comp. Neurol.* 525, 3341–3359. doi: 10.1002/cne.24281

Schmitt, L. M., Cook, E. H., Sweeney, J. A., and Mosconi, M. W. (2014). Saccadic eye movement abnormalities in autism spectrum disorder indicate dysfunctions in cerebellum and brainstem. *Mol. Autism* 5, 1–13. doi: 10.1186/2040-2392-5-47

Scott, K. E., Schormans, A. L., Pacoli, K. Y., De Oliveira, C., Allman, B. L., and Schmid, S. (2018). Altered auditory processing, filtering, and reactivity in the cntnap2 knock-out rat model for neurodevelopmental disorders. *J. Neurosci.* 38, 8588–8604. doi: 10.1523/JNEUROSCI.0759-18.2018

Scott, K. E., Schulz, S. E., Moehrle, D., Allman, B. L., Oram Cardy, J. E., Stevenson, R. A., et al. (2021). Closing the species gap: translational approaches to studying sensory processing differences relevant for autism spectrum disorder. *Autism Res.* 14, 1322–1331. doi: 10.1002/aur.2533

Selemon, L. D., and Begovic, A. (2020). Reduced midbrain dopamine neuron number in the adult non-human primate brain after fetal radiation exposure. *Neuroscience* 442, 193–201. doi: 10.1016/j.neuroscience.2020.07.005

Shamseer, L., Moher, D., Clarke, M., Ghersi, D., Liberati, A., Petticrew, M., et al. (2015). Preferred reporting items for systematic review and meta-analysis protocols (PRISMA-P) 2015: elaboration and explanation. *BMJ* 349:g7647. doi: 10.1136/bmj.g7647

Sinclair, D., Oranje, B., Razak, K. A., Siegel, S. J., and Schmid, S. (2017). Sensory processing in autism spectrum disorders and Fragile X syndrome—From the clinic to animal models. *Neurosci. Biobehav. Rev.* 76, 235–253. doi: 10.1016/j.neubiorev.2016.05.029

Strata, F., Delpolyi, A. R., Bonham, B. H., Chang, E. F., Liu, R. C., Nakahara, H., et al. (2005). Perinatal anoxia degrades auditory system function in rats. *Proc. Natl. Acad. Sci. U.S.A.* 102, 19156–19161. doi: 10.1073/pnas.0509520102

Supekar, K., Kochalka, J., Schaer, M., Wakeman, H., Qin, S., Padmanabhan, A., et al. (2018). Deficits in mesolimbic reward pathway underlie social interaction impairments in children with autism. *Brain* 141, 2795–2805. doi: 10.1093/brain/awy191

Tanguay, P., Edwards, R., Buchwald, J., Schwafel, J., and Allen, V. (1982). Auditory brainstem evoked responses in autistic children. *Arch. Gen. Psychiatry* 39, 174–180. doi: 10.1001/archpsyc.1982.04290020040008

Tas, A., Yagiz, R., Tas, M., Esme, M., Uzun, C., and Karasalihoglu, R. A. (2007). Evaluation of hearing in children with autism by using TEOAE and ABR. *Autism* 11, 73–79. doi: 10.1177/1362361307070908

Tharpe, A. M., Bess, F. H., Sladen, D. P., Schissel, H., Couch, S., and Schery, T. (2006). Auditory characteristics of children with autism. *Ear Hear.* 27, 430–441. doi: 10.1097/01.aud.0000224981.60575.d8

Toal, F., Daly, E. M., Page, L., Deeley, Q., Hallahan, B., Bloemen, O., et al. (2010). Clinical and anatomical heterogeneity in autistic spectrum disorder: a structural MRI study. *Psychol. Med.* 40, 1171–1181. doi: 10.1017/S0033291709991541

Travers, B. G., Bigler, E. D., Tromp, D. P. M., Adluru, N., Destiche, D., Samsin, D., et al. (2015). Brainstem white matter predicts individual differences in manual motor difficulties and symptom severity in autism. *J. Autism Dev. Disord.* 45, 3030–3040. doi: 10.1007/s10803-015-2467-9

Tsugiyama, L. E., Ida-Eto, M., Ohkawara, T., Noro, Y., and Narita, M. (2020). Altered neuronal activity in the auditory brainstem following sound stimulation in thalidomide-induced autism model rats. *Congenit. Anom.* 60, 82–86. doi: 10.1111/cga.12353

Ververi, A., Vargiami, E., Papadopoulou, V., Tryfonas, D., and Zafeiriou, D. I. (2015). Brainstem auditory evoked potentials in boys with autism: Still searching for the hidden truth. *Iranian J. Child Neurol.* 9, 21–28.

Wang, R., Hausknecht, K., Shen, R. Y., and Haj-Dahmane, S. (2018). Potentiation of glutamatergic synaptic transmission onto dorsal raphe serotonergic neurons in the valproic acid model of autism. *Front. Pharmacol.* 9:1185. doi: 10.3389/fphar.2018.01185

Wang, X., Kohl, A., Yu, X., Zorio, D. A. R., Klar, A., Sela-Donenfeld, D., et al. (2020). Temporal-specific roles of fragile X mental retardation protein in the development of the hindbrain auditory circuit. *Development* 147:dev188797. doi: 10.1242/dev.188797

Wegiel, J., Flory, M., Kuchna, I., Nowicki, K., Ma, S. Y., Imaki, H., et al. (2014). Brain-region-specific alterations of the trajectories of neuronal volume growth throughout the lifespan in autism. *Acta Neuropathol. Commun.* 2, 1–18. doi: 10.1186/2051-5960-2-28

Zimmerman, R., Patel, R., Smith, A., Pasos, J., and Kulesza, R. J. (2018). Repeated prenatal exposure to valproic acid results in auditory brainstem hypoplasia and reduced calcium binding protein immunolabeling. *Neuroscience* 377, 53–68. doi: 10.1016/j.neuroscience.2018.02.030

Zimmerman, R., Smith, A., Fech, T., Mansour, Y., and Kulesza, R. J. (2020). *In utero* exposure to valproic acid disrupts ascending projections to the central nucleus of the inferior colliculus from the auditory brainstem. *Exp. Brain Res.* 238, 551–563. doi: 10.1007/s00221-020-05729-7

Conflict of Interest: The authors declare that the research was conducted in the absence of any commercial or financial relationships that could be construed as a potential conflict of interest.

Publisher's Note: All claims expressed in this article are solely those of the authors and do not necessarily represent those of their affiliated organizations, or those of the publisher, the editors and the reviewers. Any product that may be evaluated in this article, or claim that may be made by its manufacturer, is not guaranteed or endorsed by the publisher.

frontiers in Integrative Neuroscience

PERSPECTIVE
published: 10 November 2021
doi: 10.3389/fnint.2021.759614

The Brainstem-Informed Autism Framework: Early Life Neurobehavioral Markers

Or Burstein[1†] *and Ronny Geva*[1,2*†]

[1] Department of Psychology, Bar-Ilan University, Ramat Gan, Israel, [2] Gonda Multidisciplinary Brain Research Center, Bar-Ilan University, Ramat Gan, Israel

Autism spectrum disorders (ASD) have long-term implications on functioning at multiple levels. In this perspective, we offer a brainstem-informed autism framework (BIAF) that traces the protracted neurobehavioral manifestations of ASD to early life brainstem dysfunctions. Early life brainstem-mediated markers involving functions of autonomic/arousal regulation, sleep-wake homeostasis, and sensorimotor integration are delineated. Their possible contributions to the early identification of susceptible infants are discussed. We suggest that the BIAF expands our multidimensional understanding of ASD by focusing on the early involvement of brainstem systems. Importantly, we propose an integrated BIAF screener that brings about the prospect of a sensitive and reliable early life diagnostic scheme for weighing the risk for ASD. The BIAF screener could provide clinicians substantial gains in the future and may carve customized interventions long before the current DSM ASD phenotype is manifested using dyadic co-regulation of brainstem-informed autism markers.

Keywords: autism spectrum disorders (ASD), brainstem, auditory brainstem evoked response (ABR), respiratory sinus arrhythmia (RSA), sleep, sensory processing, arousal, neonates

OPEN ACCESS

Edited by:
Eric London,
Institute for Basic Research in Developmental Disabilities (IBR), United States

Reviewed by:
Miguel Ángel García-Cabezas, Universidad Autónoma de Madrid y Consejo Superior de Investigaciones Científicas, Spain
Martha Welch, Columbia University, United States

***Correspondence:**
Ronny Geva
Ronny.Geva@biu.ac.il

[†] *These authors have contributed equally to this work*

Received: *16 August 2021*
Accepted: *18 October 2021*
Published: *10 November 2021*

Citation:
Burstein O and Geva R (2021) The Brainstem-Informed Autism Framework: Early Life Neurobehavioral Markers. Front. Integr. Neurosci. 15:759614. doi: 10.3389/fnint.2021.759614

INTRODUCTION

The brainstem and its rostral networks underlie a wide array of operations, ranging from autonomic functions such as respiration (Bianchi and Gestreau, 2009), cardiovascular activity (Dampney, 2016), and sleep-wake regulation (Scammell et al., 2017), through sensorimotor reactivity (Kobayashi and Isa, 2002), and even involvement in consciousness and self-awareness (Parvizi and Damasio, 2001).

Autism spectrum disorders (ASD) are a set of neurodevelopmental disorders manifested in deficits in social-communication abilities and restrictive and repetitive behaviors (American Psychiatric Association [APA], 2013). Despite the DSM nosology that classifies ASD as a unified construct, various findings suggest a high degree of heterogeneity in ASD phenomenological manifestation and genetic basis that nevertheless share common cellular and molecular features, including alterations in neurogenesis, synaptogenesis, and structural formation (Gilbert and Man, 2017). Recent accounts, some from our lab, emphasize the role of early brainstem functions in the epiphenomena of ASD (Dadalko and Travers, 2018; Delafield-Butt and Trevarthen, 2018); namely, in social attention (Geva et al., 2017), communication (Geva et al., 2013, 2014), and repetitive behaviors (Cohen et al., 2013; Gandhi and Lee, 2021)– all key features of ASD.

Social attention, communication, and adaptation of behavior have primary roles in the human core being already at birth. Hence, we suggest that brainstem circuits that mature in very early life and even during fetal stages to regulate vital autonomic functions (Zec and Kinney, 2003), have a central role in shaping social communication and adaptation of behavior. We suggest that given the early maturation of brainstem pathways, their pervasive role in functioning at multiple levels, and their specific involvement in social-communication deficits, brainstem functions enable a valuable window into the pathophysiology of ASD. Its neurobehavioral manifestations are already evident in the first phases of postnatal life.

Research thus far suggests brainstem involvement in ASD by typically denoting a unitary brainstem marker. Building upon an integration of the literature, in the current perspective, we propose a brainstem-informed autism framework (BIAF) that zooms in on the distinct paths by which compromised brainstem functions possibly stir development and increase the susceptibility for ASD-related symptomatology. We then suggest that zooming out to look at the full battery of brainstem-related expressions, rather than individual markers, may enable constructing a highly sensitive early risk neurobehavioral screening tool of ASD.

THE FORMATION OF BRAINSTEM NETWORKS

Principal morphological changes in the embryonic brainstem in multiple organisms buds during the first trimester of pregnancy (ten Donkelaar et al., 2014). Animal models indicate that the genesis of motoneurons in rhombomeres 7 and 8 commence approximately at the fourth week of fetal life; these neurons subsequently migrate and form the vagal nerve nuclei, including the dorsal motor nucleus, nucleus ambiguus, solitary tract nucleus, and spinal trigeminal nucleus (ten Donkelaar et al., 2014; Watson et al., 2019). The neural functionality of brainstem pathways is noted from early gestational stages (Glover et al., 2008; Marrs and Spirou, 2012). A post-mortem specimens study of the medulla in human fetuses indicated that a neural branching from and into the solitary tract nucleus is established and expedites cardiorespiratory control around gestational age (GA) of 20 weeks (Zec and Kinney, 2003). The development of vital parasympathetic functions is further secured from mid-gestation to parturition as myelination of the vagal nerve roots progresses (Tanaka et al., 1995). Importantly, myelination of efferent fibers from the nucleus ambiguus to the sinus nodes that regulate cardiac pace is accelerated (Porges, 2011) and stabilizes the parasympathetic activity when reaching term age as manifested by increased heart rate variability at the higher (*i.e.*, above 0.2 Hz) frequencies (Longin et al., 2006). Similar neuro-maturational processes involving the birth of neurons in hindbrain rhombomeres and mesencephalic neuromeres, neurons migration, and axonal navigation contribute to the formation of the cranial nerves sensorimotor nuclei in the brainstem from Carnegie stage 12 (O'Rahilly and Müller, 2006; ten Donkelaar et al., 2014). These structures support auditory, ocular, tactile, gustatory, and olfaction development and shape motor reactivity in a progressive fashion. As such, early postnatal myelination of axons radically increases the rate and synchronicity of transmission through the auditory pathway, emanating from the cochlear nuclei, superior olive, lateral lemniscus, and inferior colliculus (Sano et al., 2007), alongside other sensorimotor paths that evolve in tight temporospatial constraints.

Optimal structuring of the brainstem has vast implications on neurocognitive sequelae, as the early structural building blocks of these early maturing networks influence the emerging operations of higher-order top-down limbic and neocortical systems. Eventually, brainstem networks affect functions from basic reception through multisensory and motor integration (Geva and Feldman, 2008), in ways that affect behavioral inhibition (Geva et al., 2014), higher-order social engagement (Geva et al., 2017), and social communication capacities (Geva et al., 2013). As such, evaluation of brainstem integrity offers multiple candidate markers for ASD. These markers are potentially diagnosable at term age and soon thereafter.

To date, the research has mostly treated each BIAF factor as a single primary marker. We review each one shortly and suggest that their integration presents a strong case for a cohesive BIAF. We shall focus on the hallmarks of brainstem functions: cardiac, respiratory, and arousal regulation; sleep-wake homeostasis; and primary sensorimotor operations. Following the exploration of their main effects and interactions, we will delineate a BIAF, focusing on how it first unfolds in gestation and the post-birth period.

CONTROL OF AROUSAL: CARDIOVASCULAR AND RESPIRATORY DEVELOPMENT

The vertical hierarchical framework was formulated in our lab to delineate the development of self-regulation and positioned brainstem functions at the crux of the model (Geva and Feldman, 2008). According to this model, brainstem networks serve pivotal roles in regulating the young infant's arousal responses to sensations. Recent notions accentuate that nascent autonomic conditioning of socioemotional reflexes and arousal responses occur at the brainstem and peripheral levels and prior to the top-down cortical navigation of arousal (Ludwig and Welch, 2020). Poor arousal regulation is one of the key features of ASD (Prince et al., 2017; Cuve et al., 2018; Corbett et al., 2019; de Vries et al., 2021), evident by hyper- or hypo-arousal reactivity of the autonomic system in response to sensory stimulation. Particularly in infants who are siblings of children with ASD (Zivan et al., 2021). The functional implications of autonomic dysfunctions in individuals with ASD are vividly apparent in an array of markers, including pupil diameter (Zivan et al., 2021), electrodermal activity (Prince et al., 2017), and the coordination of heart rate and breathing (Corbett et al., 2019). These autonomic functions are by and large regulated at first by brainstem networks that mature in late-term stages and have been suggested to serve social engagement purposes (Porges, 2001).

The inner workings of the mechanisms involved in this interplay are now under investigation using different models and an array of techniques. Here we note some of the literature that exemplifies the richness of data and intricate set of interlinked neurophysiological processes currently explored.

Possible causes for the abnormalities in autonomic functions in ASD are aberrations in cerebellar-brainstem white matter tracts, involving insufficient glial maturation and axonal growth differences noted in infancy and early childhood (Shukla et al., 2010; Yu et al., 2020), altered white matter connectivity of brainstem tracts found in tractography machine learning analysis (Zhang et al., 2018), and atypical structuring of the medullary arcuate nucleus which is involved in cardiorespiratory regulation (Bailey et al., 1998). The exact trajectory and localization of histogenesis and primal autonomic circuitries development in ASD remain to be further elucidated. Hopefully, future studies will clarify whether abnormal patterns of myelination, axonal navigation, and circuits formation of vagal nerve nuclei during embryonic and neonatal development are implicated in the autonomic sequelae of individuals with ASD. Even though the developmental pathophysiological course is not yet fully established, several cardiorespiratory indices were utilized to weigh the involvement of vagal functions in ASD research. We shall focus on respiratory sinus arrhythmia (RSA).

Respiratory sinus arrhythmia measures the variations in heart rate as a function of the respiration cycle and is regarded as an applicable index of the vagal tone and its coordination by the nucleus ambiguus (Berntson et al., 1993). Porges' polyvagal theory proposes that inner physiological experiences are innervated by socio-emotional sensations right from birth and that this interplay underlies the nascent steps of social development (Porges, 1995, 2011, 2021).

A recent comprehensive meta-analysis (Cheng et al., 2020) involving participants with ages spanning the first three decades of life revealed that diagnosis of ASD was associated with diminished baseline RSA and diminished RSA reactivity during social experiences. A previous prospective study including a cohort of very preterm children has shown that neonatal RSA indices predicted social competence at the age of three (Doussard-Roosevelt et al., 1997) and then at school age (Doussard-Roosevelt et al., 2001). Further, infants diagnosed with ASD in late childhood showed a blunted pattern of RSA development from the age of 18 months (Sheinkopf et al., 2019). The RSA findings imply that the alignment of vagal resources with the social environment, mostly those involving the adaptive switching between tranquil/non-engaged and charged/engaged states, scaffolds the building blocks of social development from birth. It further accentuates that cardiovascular hypo- and hyper-arousal reactivity might affect vigilance and impede the prospect of a durable engagement with parents, peers, and significant others in ASD.

Vigilance models have been proposed to explain a range of psychopathological processes from mania to attention deficits (Hegerl and Hensch, 2014). These models have noted links between poor arousal regulation, unstable vigilance, and sleep deficits. We suggest that these notions are highly relevant to the BIAF.

SLEEP AS A SOCIAL AWAKENER

Primal sleep-wake substrates in the brainstem promote sleep rhythms long before the anterior limbic circuits gain dominance (Villablanca et al., 2001). Given the primary involvement of brainstem networks in sleep regulation, the BIAF suggests that congenital compromised brainstem functions could instigate sleep-wake dysregulations from the neonatal period. Then, it might perturb the brainstem-limbo-cortical connectivity and lead to long-term sleep deficits (Geva and Feldman, 2010; Blumberg et al., 2014).

The primal sleep-wake system consists of wake-promoting loci in the reticular formation along the brainstem, including the monoaminergic locus coeruleus (LC) and dorsal raphe nucleus (DRN), and the cholinergic laterodorsal tegmental nucleus and parabrachial nuclei; the primal GABAergic sleep-promoting structures include the nucleus pontis oralis, nucleus subcoeruleus and the Purkinje cells in the cerebellum (Phillips and Robinson, 2007; Blumberg et al., 2014; Sokoloff et al., 2015). These brainstem-cerebellar hubs are highly implicated in the ultradian cyclicity of sleep-wake bouts during the first weeks of extrauterine life (Geva and Feldman, 2010). Infant sleep is marked by high rates of REM sleep that have a vital neuroprotective role and is guided by the aforementioned brainstem loci (Heraghty et al., 2008). Accordingly, lesions and morphological abnormalities in both gray and white matter in pontine and adjacent regions are associated with reduced REM sleep in human adults (Landau et al., 2005; Scherfler et al., 2011). Further, sleep organization and a smooth transition between sleep stages seem important. Fragmented neonatal sleep has been noted to impede infant attention orienting at 18 months of age (Geva et al., 2016). One should keep in mind these phenomena when considering the trajectories of sleep integrity in populations with ASD.

Children, adolescents, and adults with ASD display various sleep abnormalities, including decreased sleeping time, delayed sleep latency, and less efficient sleep (Elrod and Hood, 2015; Lugo et al., 2020; Chen et al., 2021), and show a strikingly elevated risk for sleep disorders (Lai et al., 2019; Lugo et al., 2020). These findings suggest that sleep deficits and ASD possibly stem from a similar neuropathological disrupted circuitry that involves the brainstem in a major way.

Studies have illustrated several influences of the brainstem in sleep-wake dysregulation in ASD populations. Vis-à-vis inhibitory pathways, genetic findings suggest that ASD is associated with microduplications copy-number variations in the chromosome 15q11–q13 region responsible for coding the $GABA_A$ receptor's subunits (Sebat et al., 2007; Meguro-Horike et al., 2011; Sanders et al., 2012). Accordingly, post-mortem studies found a decrease in GABAergic Purkinje neurons in cerebellum specimens of deceased ASD patients (Bailey et al., 1998; Palmen et al., 2004). Functional alterations in the activity of excitatory networks involving the LC are found in children with ASD (Bast et al., 2018; Huang et al., 2021). Taken together, these suggest that an imbalance between the primary excitatory (*e.g.*, the monoaminergic LC and DRN) and inhibitory (*e.g.*, the GABAergic Purkinje cells) circuits (Coghlan et al., 2012) of the

brainstem is involved in the pathogenesis of sleep disturbances in ASD patients, as well as affecting other arousal-related domains (Wintler et al., 2020).

The extent of sleep deficits could also be viewed as a distinct factor that affects social development. Several findings support this latter notion. First, abnormal sleep patterns in early life are associated with subsequent ASD diagnosis and symptoms (Humphreys et al., 2014; Saenz et al., 2015; Miike et al., 2020). Further, in children with ASD, shorter sleep duration exacerbates the severity of both repetitive behaviors and social-communication deficits (Schreck et al., 2004; Tudor et al., 2012; Veatch et al., 2017). The hazards posed by sleep disruptions in children with ASD urged clinicians to recommend that sleep-wake homeostasis issues be assessed and managed as a central feature in the therapeutic plan of ASD patients (Cohen et al., 2014; Abel et al., 2017; Souders et al., 2017). This agenda accentuates the primary role sleep possibly serves in the evolution of ASD and the neuroprotective role of sleep in its containment (Wintler et al., 2020).

The findings suggest that sleep and arousal play a major role in ASD. Sleep disturbances are plausibly a result of fetal, genetic, and epigenetic brainstem-mediated antecedents. At the same time, they stand by themselves as factors that might exacerbate the risk for ASD or lead to more severe symptoms by impeding brain development and its regulated reactivity to stimulation through the various senses.

THE STEM OF THE SENSES

Atypical behavioral responses to sensory stimulation are a ubiquitous characteristic of ASD (Marco et al., 2011). Research on unimodal sensory processing and multisensory integration using various neuroimaging techniques demonstrated significant alterations in sensory processing neural substrates (Marco et al., 2011). Here we briefly review some of the unimodal and multisensory processing findings that pertain to the BIAF.

Auditory Processing

A feasible aperture into neonatal brainstem auditory functions involves the highly utilized auditory brainstem evoked response (ABR) test. The ABR is broadly implemented across the globe as a screener for hearing deficits in newborns (Morton and Nance, 2006; Levit et al., 2015). Diving into its characteristics enables uncovering its germaneness to autism. In the ABR procedure, newborns are exposed to auditory stimulations (*i.e.*, click or speech sounds in standardized dB levels) while an electrode attached to the scalp measures the electrophysiological activity. The latencies of neuro-electrical fluctuations following the auditory stimuli are typically manifested in five major wave peaks in neuro-typical adults; waves I and II originate from the auditory vestibular nerve, while wave peaks III–V putatively reflect the reaction of deeper structures including the cochlear nuclei (wave III), superior olive (wave IV) and lateral lemniscus and inferior colliculus (wave V; Wilkinson and Jiang, 2006). Apart from its conventional role for detecting hearing deficits, the ABR presents intriguing information on deficient brainstem maturation, detectable already in the late-term period in ways pertaining to ASD risk detection.

Both functional and structural brainstem auditory path alterations are noted in individuals with ASD. Changes in neural transmission rates through the brainstem (most prominently a delayed V peak latency) that appear already at birth have been associated with increased risk for subsequent diagnosis of ASD (Cohen et al., 2013; Miron et al., 2016, 2021; Tu et al., 2020). This association persists throughout infancy, toddlerhood, and childhood (Miron et al., 2018; Talge et al., 2018). Along with the functional differences in brainstem auditory structures, morphological studies have demonstrated durable alterations in size, volume, and neuronal density in the superior olive (Kulesza et al., 2011; Mansour and Kulesza, 2020), as well as abnormal geometric arrangements of cells body shape and orientation (Kulesza and Mangunay, 2008). Taken together, abnormalities in brainstem auditory centers may be a relatively stable marker of ASD, which stands so a long way before autism symptoms onset.

What does a deficient ABR at birth imply concerning the mechanisms driving ASD? Two non-mutually exclusive options come to mind: First, a deficit in reception, filtering, and processing of auditory signals (Morton and Nance, 2006; Levit et al., 2015). A deficit in auditory processing may account for persistent disruptions in neuro-cognitive development. Inability to perceive vocal cues and produce them well has a profound effect on social and communication capacities (Del Zoppo et al., 2015; Petersen and Hurley, 2017). Accordingly, an auditory processing deficit is highly prevalent in populations diagnosed with ASD (O'Connor, 2012; Williams et al., 2020). Impairments such as auditory hypersensitivity (Williams et al., 2021) and diminished background noise filtering (Park et al., 2017) can obstruct the ability to prepare ahead of time and might lead to intensified anxiety, repetitive behaviors, and a strong need to keep routines and rigidly anticipated schedules (Schaaf et al., 2011; Kargas et al., 2015; Kanakri et al., 2017; Park et al., 2017; Ahmmed and Mukherjee, 2021). As such, the auditory path alone already accounts well for a large portion of ASD phenomenology.

Alternatively, even when the infant's hearing threshold is preserved, an asynchronous auditory nerve firing or delayed processing evident in the ABR may signal altered neural programming that operates in a pervasive manner. These alterations affect a widely distributed network that goes beyond the direct effect of disrupted auditory functions, on to language and communication development (Miron et al., 2016; Geva et al., 2017; Chen et al., 2019). Notably, individuals diagnosed with ASD display increased susceptibility not only to auditory processing deficits but to difficulties in other sensorial modalities, such as vision.

Visual Processing and Gaze

The optic tract develops *via* a genetically driven regulation of axonal growth, navigation, and neuronal migration in the retinogeniculate pathway. The tract's development also depends on endogenous and exogenous stimulation during the first years of life to secure and strengthen the synapses that refine the topographic map in the thalamic lateral geniculate nucleus and primary visual cortex (Graven, 2004). The more primal

and fast to react dorsal visual stream is highly operational during the first months of life, relaying low-resolution data from the rods with increased sensitivity to changes in the exterior scenery (Hammarrenger et al., 2003; Bridge et al., 2016). The role of the superior colliculus (SC) in the dorsal stream has been recently highlighted, suggesting that in the neonatal period, this midbrain structure is pertinent for exercising focal oculomotor operations, receiving and integrating multimodal sensory inputs, and communicating with higher-order visual-neural configurations (Pitti et al., 2013; Jure, 2019). The SC is, thus, highly involved in rudimentary social behaviors, including the preference to fixate on human faces and the ability to detect and imitate emotion-resonating facial expressions (Jure, 2019). Neonatal experiences drive the SC to refine its ability to integrate inputs from diverse sensorial modalities in ways that expand social capabilities (Stein et al., 2014). Impairments in SC-contingent functions are found in populations with ASD.

An important line of evidence accentuating the major role of visual refinement through the SC for social-communication development is that congenital blindness is a significant risk factor for ASD, affecting approximately 50% of infants born without the ability to see (Jure et al., 2016). Ample evidence for the apparent vulnerability of the dorsal stream network is noted in a wide range of both genetic and acquired developmental disorders (Grinter et al., 2010; Braddick et al., 2011). With specific regard to ASD (Grinter et al., 2010), deficits in stabilizing visual fixation at 6–9 months were shown to predict social-communication problems at 36 months (Wass et al., 2015). These data suggest that deficits in apprehending the spatial grid and dynamic movements of objects (abilities rooted in the dorsal stream) have a major effect on the ability to execute contingent motor actions with social agents.

Notably, during the first year of life, the "fine-tuning" of the visual system for processing complex and socially charged stimuli is impaired in infants who are siblings of children with ASD (Zivan et al., 2021) and in those who are subsequently diagnosed with ASD (Zwaigenbaum et al., 2005; Elsabbagh et al., 2012; Jones and Klin, 2013). Later in development, abnormalities in social gaze patterns (Wegiel et al., 2013; Frazier et al., 2017) and other oculomotor functions (Johnson et al., 2016) are significantly associated with ASD. We suggest that the association between newborns' visual processing indices, particularly the reactivity to highly salient, social, and moving stimuli, could serve as possible markers for a dorsal-colliculi deficiency in the BIAF and should be further investigated. Similar somatosensory processing dysfunctions should be further addressed.

Gustatory and Olfaction Processing

Individuals diagnosed with ASD are more likely to have odors and tastes identification impairments (Bennetto et al., 2007; Boudjarane et al., 2017). Of specific interest to the BIAF is the trigeminal bottom-up olfactory pathway that innervates the nasal mucosa to execute protective respiratory reflexes in the presence of noxious odorants (Pérez de los Cobos Pallares et al., 2016). Operations of this pathway can be observed in newborns' behavioral responses of disgust following exposure to unpleasant odors (Soussignan et al., 1997) and their autonomic regulation of breathing (Marlier et al., 2005). One of the primary odors for newborns is maternal odors during feeding. A meta-analysis found a negative association between maternal breastfeeding and ASD (Tseng et al., 2019); the authors interpreted the results by suggesting that breastfeeding has a moderating effect, but the involved mechanism is yet to be determined. Apart from the acknowledged importance of touch and emotional investment associated with breastfeeding, congenital deficits in olfactory, gustatory, and motor functions could add significantly to the accounts of both phenomena and to difficulties in the initiation of breastfeeding (Suberi et al., 2018). Taken together, these data suggest that impaired trigeminal reflexes in the newborn could be an additional BIAF early marker.

Tactile-Motor Integration

Changes in responses to tactile stimulation have been acknowledged as a distinguishable feature of people with ASD (Wiggins et al., 2009; Foss-Feig et al., 2012; Balasco et al., 2020). Importantly, this network is rooted in the brainstem. The inferior olivary nucleus (ION) is an axial brainstem hub that receives multimodal sensory inputs, including tactile sensations. Through climbing excitatory fibers to the Purkinje cells, the ION enables the execution of coordinated motor actions (Wu et al., 2010; Ju et al., 2019).

Aberrant structuring of the ION, as found in populations with ASD (Rodier et al., 1996; Bailey et al., 1998), might restrain the valence of early life experiences, and the latency and proclivity to react *via* oscillations of efferent motor fibers (Arndt et al., 2005). Indeed, reduced tactile-motor reactivity at 12 months in the context of parent-child interaction was shown to be a risk factor for a subsequent diagnosis of ASD (Baranek, 1999). Given that collecting tactile information depends on perception and execution of movement, the findings suggest that the difficulties in tactile processing in children with ASD are intertwined with motor development. This notion is corroborated by the increased risk for impairments in motor functioning found in infants and toddlers who later develop autism (West, 2019). Taken together, these suggest that a deficit in ION-mediated tactile-motor rhythmicity might progress into a broader difficulty in the timing of communication and compromise social-communication efficacy in ASD.

Sensorimotor Exchanges

A shortfall in synchronous sensorimotor communications with the world is almost intrinsic to the experience of children with ASD and their caregivers. It has profound implications on developmental outcomes in isolating the self from the social sphere, restricting exposure to familiar sensations, and limiting the sense of communicative agency (Delafield-Butt and Trevarthen, 2018).

Rhythmic communications, in which our senses swiftly grasp the exterior surrounding and contribute to it with our actions, are essential for building our sense of relatedness with the world and the people around us (Keller et al., 2014). The reviewed early life indices of sensorimotor integration suggest that early dysfunctions in brainstem systems impede the typical progression of the embodiment of social exchanges *via* alterations

of the valence of sensorial inputs and the latency, vitality, and congruency of sensorimotor reactions. Importantly, several markers that could trace the full-blown ASD phenotype to brainstem-mediated abnormalities in newborns and infants were pinpointed. Their integration enables the development of an integrated BIAF.

INTEGRATING INDIVIDUAL MARKERS INTO A COHESIVE BRAINSTEM-INFORMED AUTISM FRAMEWORK

It has been shown that the ABR alone has a noteworthy sensitivity for detecting infants who later develop ASD, with 70% accuracy (Miron et al., 2016). We suggest that integrating the individual markers points to the importance of a cohesive early life BIAF. The advent of such a framework offers advancements in our multidimensional understanding of autism. First, the BIAF proposes that the susceptibility to ASD develops during gestation and marks the neural networks that account for its early presentations, those that precede DSM symptoms oftentimes. Secondly, given the richness of the pathways traversing through the brainstem, the BIAF accounts for the heterogeneity in autism. Thirdly, the integrated BIAF may inform and promote the establishment of a clinical screener that will build upon prominent indices of brainstem functions to reach high sensitivity and reliability for weighing the risk for social development deficits. Such a screener could also ascertain the domain-specific impairments for each infant and reveal in which functions auxiliary support is necessitated (*e.g.*, auditory or tactile processing, autonomic-arousal reactivity, sleep hygiene, etc.). Accordingly, an early life BIAF screener could provide clinicians substantial gains vis-à-vis early detection of susceptible populations using electrophysiological indices (**Figure 1**, depicted on the right) along with behavioral ones (**Figure 1**, depicted on the left). The BIAF screener may carve new opportunities for customized interventions for the specific infant's needs.

Theoretical and Clinical Applications of the Brainstem-Informed Autism Framework

The BIAF has impactful applications for the scientific and clinical fields in the following key areas: (a) diagnostics, (b) prevention and moderation of symptoms, and (c) applicability. We suggest that these domains should be advanced in the following directions:

a. Diagnostics: An early life screener for detecting compromised brainstem functions should be implemented by assembling pertinent brainstem-mediated indices. A possible screener could consist of cardiorespiratory (*e.g.*, RSA), sleep-related (*e.g.*, actigraphy), and behavioral (*e.g.*, facial-emotional reactivity) indices. We suggest that such a screener should be further evaluated and could bring about remarkable prospects for early detection of susceptibility to ASD.

   While detection of some of the proposed BIAF markers requires further research, the use of brainstem-mediated indices in the neonatal period can already enable pinpointing susceptible populations, as ABR protocols for the detection of early risk for autism are available (Miron et al., 2016). However, we suggest that adding additional BIAF indices may improve the sensitivity of early ASD detection compared to relying only on the ABR.

b. Prevention: Early detection of risk for ASD may enable referral to follow-up assessments and interventions at a sensitive period when the brain plasticity is exceptionally high. The opportunity of amending the pervasive changes in neural architecture has a high potential in moderating the protracted disturbances in brainstem functions, including cardiorespiratory reactivity, sleep-wake homeostasis, and sensorimotor development (Welch et al., 2015, 2020; Beebe et al., 2018).

c. Support, Intervention, and Vital Care: Recent notions highlight the pivotal role of calming regulatory interaction cycles between the child and the environment in shaping autonomic and social development (Ludwig and Welch, 2020), thus, expanding the role of parent-child interaction that is also central to our vertical hierarchical model (Geva and Feldman, 2008). These weighty notions of the *calming cycle theory* suggest that brainstem-mediated symptoms often associated with ASD should be viewed as treatable traits shaped in a dyadic context at sensitive stages of development. Assimilation of these ideas urges clinicians and scientists to conceptualize physio-emotional development as an open *co*-regulatory feedback system, including infants (and even fetuses) and their caregivers, rather than a process of a singular entity working in solitude (Ludwig and Welch, 2019). Such an approach suggests that the infant's ability to regulate the autonomic activity for homeostasis, socioemotional and learning purposes is materialized in concert with the caregiver, as a dyad. We embrace this approach and suggest that aiding infant-caregiver dyads in preventing hyperexcitation and promoting tranquil dyadic experiences could be vital for moderating the risks posed by brainstem dysfunctions in susceptible infants. We further suggest that nurturing parents' ability to mind and accurately attend to susceptible infants' autonomic and sensorimotor cues is highly promising and calls for further evaluations in future BIAF interventions studies.

d. Applicability: Implementation of an early life BIAF screener for identifying infants with an increased risk for ASD could prove to be highly applicable and, in the long term, may aid in diminishing to some extent the related economic burden in several ways:

   i. The ABR is a cost-effective test and is already administered to millions of newborns worldwide. It could be easily recalibrated using specifically tailored protocols (Miron et al., 2016) to detect early

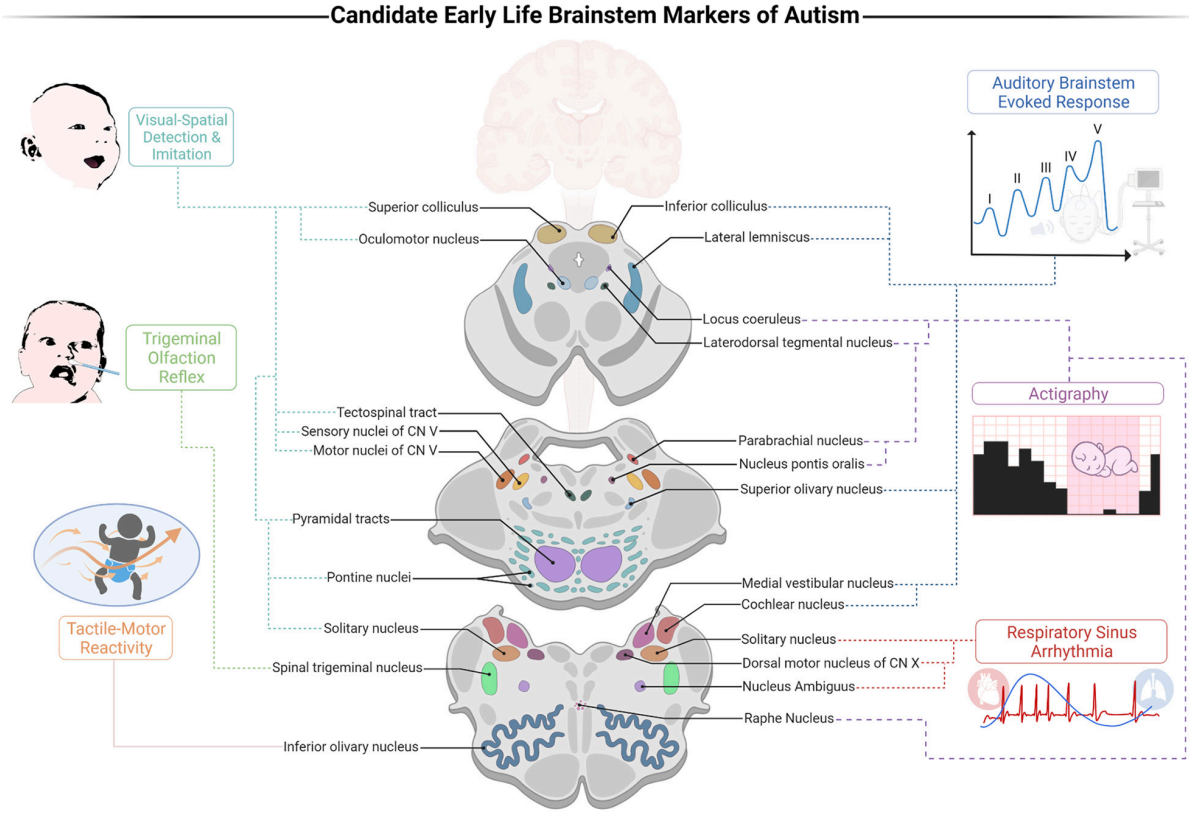

FIGURE 1 | A proposed brainstem-informed autism framework (BIAF) screener for identification of early risk for autism spectrum disorders (ASD). Illustration of the links between the suggested markers and their brainstem substrates. Auditory processing is weighed by the auditory brainstem evoked response (ABR) test (specifically, a delayed V peak latency); DSW: near birth. Control of arousal is weighed by the cardiorespiratory index of respiratory sinus arrhythmia (RSA); developmental screening window (DSW): 0–12 months. Olfaction processing is weighed by the trigeminal olfaction reflex (disgust response following exposure to noxious odorants); DSW: 0–2 months. Sleep-wake regulation is weighed by actigraphy indices (*e.g.*, sleeping duration and sleep efficiency); DSW: 1–4 months. Visual processing and gaze are weighed by the abilities to detect and imitate emotional resonating facial expressions; DSW: 1–6 months. Tactile-motor integration is weighed by indices of response thresholds following tactile stimulation; DSW: 1–12 months. Created with BioRender.com.

risk for long-term social-communication deficits on large scales.

ii. Developing a cohesive BIAF screener could reinforce the sensitivity of the ABR with additional brainstem-mediated behavioral, cardiorespiratory, arousal, and sleep-wake indices, hence, possibly transforming the prospect of early detection of ASD from theoretical to applicable. As time is of the essence, early identification of susceptible infants could provide us with better opportunities to amend the long-term developmental outcomes by referring them and their families to early interventions when brain plasticity is most receptive to modification– targeting primary brainstem-mediated neurobehavioral symptoms that are often associated with ASD.

iii. Offering treatments compatible with the BIAF early in development is highly promising. Treatments that employ co-regulatory processes targeting brainstem-informed domains by fostering calming cycles carry the prospect of ameliorating to some extent the pervasiveness and suffering attributed to social-communication deficits throughout life (Geva and Feldman, 2008; Welch et al., 2015, 2020).

DATA AVAILABILITY STATEMENT

The original contributions presented in the study are included in the article/supplementary material, further inquiries can be directed to the corresponding author.

AUTHOR CONTRIBUTIONS

Both authors wrote the manuscript together and contributed equally to this article, and approved the submitted version.

FUNDING

This article was funded by the Neurodevelopmental Psychology Cathedra (NPC). The NPC had no involvement in the writing of the manuscript and in its implications.

REFERENCES

Abel, E., Kim, S. Y., Kellerman, A. M., and Brodhead, M. T. (2017). Recommendations for Identifying Sleep Problems and Treatment Resources for Children with Autism Spectrum Disorder. *Behav. Anal. Pract.* 10, 261–269. doi: 10.1007/s40617-016-0158-4

Ahmmed, A. U., and Mukherjee, D. (2021). Auditory processing and non-auditory factors associated with hyperacusis in children with auditory processing disorder (APD). *Hear. Balanc. Commun.* 19, 4–15. doi: 10.1080/21695717.2020.1727216

American Psychiatric Association [APA] (2013). *Diagnostic and Statistical Manual of Mental Disorders, Fifth Edition*. Virginia: American Psychiatric Association.

Arndt, T. L., Stodgell, C. J., and Rodier, P. M. (2005). The teratology of autism. *Int. J. Dev. Neurosci.* 23, 189–199. doi: 10.1016/j.ijdevneu.2004.11.001

Bailey, A., Luthert, P., Dean, A., Harding, B., Janota, I., Montgomery, M., et al. (1998). A clinicopathological study of autism. *Brain* 121, 889–905. doi: 10.1093/brain/121.5.889

Balasco, L., Provenzano, G., and Bozzi, Y. (2020). Sensory Abnormalities in Autism spectrum disorders: a focus on the Tactile Domain, from genetic mouse models to the clinic. *Front. Psychiatry* 10:1016. doi: 10.3389/fpsyt.2019.01016

Baranek, G. T. (1999). Autism during infancy: a retrospective video analysis of sensory-motor and social behaviors at 9–12 months of age. *J. Autism Dev. Disord.* 29, 213–224. doi: 10.1023/A:1023080005650

Bast, N., Poustka, L., and Freitag, C. M. (2018). The locus coeruleus–norepinephrine system as pacemaker of attention – a developmental mechanism of derailed attentional function in autism spectrum disorder. *Eur. J. Neurosci.* 47, 115–125. doi: 10.1111/ejn.13795

Beebe, B., Myers, M. M., Lee, S. H., Lange, A., Ewing, J., Rubinchik, N., et al. (2018). Family nurture intervention for preterm infants facilitates positive mother–infant face-to-face engagement at 4 months. *Dev. Psychol.* 54, 2016–2031. doi: 10.1037/dev0000557

Bennetto, L., Kuschner, E. S., and Hyman, S. L. (2007). Olfaction and Taste Processing in Autism. *Biol. Psychiatry* 62, 1015–1021. doi: 10.1016/J.BIOPSYCH.2007.04.019

Berntson, G. G., Cacioppo, J. T., and Quigley, K. S. (1993). Respiratory sinus arrhythmia: autonomic origins, physiological mechanisms, and psychophysiological implications. *Psychophysiology* 30, 183–196. doi: 10.1111/J.1469-8986.1993.TB01731.X

Bianchi, A. L., and Gestreau, C. (2009). The brainstem respiratory network: an overview of a half century of research. *Respir. Physiol. Neurobiol.* 168, 4–12. doi: 10.1016/j.resp.2009.04.019

Blumberg, M. S., Gall, A. J., and Todd, W. D. (2014). The development of sleep–wake rhythms and the search for elemental circuits in the infant brain. *Behav. Neurosci.* 128, 250–263. doi: 10.1037/a0035891

Boudjarane, M. A., Grandgeorge, M., Marianowski, R., Misery, L., and Lemonnier, É (2017). Perception of odors and tastes in autism spectrum disorders: a systematic review of assessments. *Autism Res.* 10, 1045–1057. doi: 10.1002/AUR.1760

Braddick, O., Atkinson, J., and Wattam-Bell, J. (2011). "VERP and brain imaging for identifying levels of visual dorsal and ventral stream function in typical and preterm infants," in *Gene Expression to Neurobiology and Behavior: Human Brain Development and Developmental Disorders*, Chap. 6, eds O. Braddick, J. Atkinson, and G. Innocenti (Armsterdam: Elsevier), 95–111.

Bridge, H., Leopold, D. A., and Bourne, J. A. (2016). Adaptive Pulvinar Circuitry Supports Visual Cognition. *Trends Cogn. Sci.* 20, 146–157. doi: 10.1016/j.tics.2015.10.003

Chen, J., Liang, C., Wei, Z., Cui, Z., Kong, X., Dong, C., et al. (2019). Atypical longitudinal development of speech−evoked auditory brainstem response in preschool children with autism spectrum disorders. *Autism Res.* 12, 1022–1031. doi: 10.1002/aur.2110

Chen, X., Liu, H., Wu, Y., Xuan, K., Zhao, T., and Sun, Y. (2021). Characteristics of sleep architecture in autism spectrum disorders: a meta-analysis based on polysomnographic research. *Psychiatry Res.* 296:113677. doi: 10.1016/j.psychres.2020.113677

Cheng, Y.-C., Huang, Y.-C., and Huang, W.-L. (2020). Heart rate variability in individuals with autism spectrum disorders: a meta-analysis. *Neurosci. Biobehav. Rev.* 118, 463–471. doi: 10.1016/j.neubiorev.2020.08.007

Coghlan, S., Horder, J., Inkster, B., Mendez, M. A., Murphy, D. G., and Nutt, D. J. (2012). GABA system dysfunction in autism and related disorders: from synapse to symptoms. *Neurosci. Biobehav. Rev.* 36, 2044–2055. doi: 10.1016/j.neubiorev.2012.07.005

Cohen, I. L., Gardner, J. M., Karmel, B. Z., Phan, H. T. T., Kittler, P., Gomez, T. R., et al. (2013). Neonatal Brainstem Function and 4-Month Arousal-Modulated Attention Are Jointly Associated With Autism. *Autism Res.* 6, 11–22. doi: 10.1002/AUR.1259

Cohen, S., Conduit, R., Lockley, S. W., Rajaratnam, S. M., and Cornish, K. M. (2014). The relationship between sleep and behavior in autism spectrum disorder (ASD): a review. *J. Neurodev. Disord.* 6:44. doi: 10.1186/1866-1955-6-44

Corbett, B. A., Muscatello, R. A., and Baldinger, C. (2019). Comparing stress and arousal systems in response to different social contexts in children with ASD. *Biol. Psychol.* 140, 119–130. doi: 10.1016/j.biopsycho.2018.12.010

Cuve, H. C., Gao, Y., and Fuse, A. (2018). Is it avoidance or hypoarousal? A systematic review of emotion recognition, eye-tracking, and psychophysiological studies in young adults with autism spectrum conditions. *Res. Autism Spectr. Disord.* 55, 1–13. doi: 10.1016/j.rasd.2018.07.002

Dadalko, O. I., and Travers, B. G. (2018). Evidence for brainstem contributions to autism spectrum disorders. *Front. Integr. Neurosci.* 12:47. doi: 10.3389/fnint.2018.00047

Dampney, R. A. L. (2016). Central neural control of the cardiovascular system: current perspectives. *Adv. Physiol. Educ.* 40, 283–296. doi: 10.1152/advan.00027.2016

de Vries, L., Fouquaet, I., Boets, B., Naulaers, G., and Steyaert, J. (2021). Autism spectrum disorder and pupillometry: a systematic review and meta-analysis. *Neurosci. Biobehav. Rev.* 120, 479–508. doi: 10.1016/j.neubiorev.2020.09.032

Del Zoppo, C., Sanchez, L., and Lind, C. (2015). A long-term follow-up of children and adolescents referred for assessment of auditory processing disorder. *Int. J. Audiol.* 54, 368–375. doi: 10.3109/14992027.2014.972523

Delafield-Butt, J., and Trevarthen, C. (2018). "On the brainstem origin of autism: disruption to movements of the primary self," in *Autism: The Movement-Sensing Perspective*, eds E. Torres and C. Whyatt (Boca Raton: CRC Press), 119–137.

Doussard-Roosevelt, J. A., McClenny, B. D., and Porges, S. W. (2001). Neonatal cardiac vagal tone and school-age developmental outcome in very low birth weight infants. *Dev. Psychobiol.* 38, 56–66.

Doussard-Roosevelt, J. A., Porges, S. W., Scanlon, J. W., Alemi, B., and Scanlon, K. B. (1997). Vagal Regulation of Heart Rate in the Prediction of Developmental Outcome for Very Low Birth Weight Preterm Infants. *Child Dev.* 68, 173–186. doi: 10.1111/j.1467-8624.1997.tb01934.x

Elrod, M. G., and Hood, B. S. (2015). Sleep Differences Among Children With Autism Spectrum Disorders and Typically Developing Peers. *J. Dev. Behav. Pediatr.* 36, 166–177. doi: 10.1097/DBP.0000000000000140

Elsabbagh, M., Mercure, E., Hudry, K., Chandler, S., Pasco, G., Charman, T., et al. (2012). Infant neural sensitivity to dynamic eye gaze is associated with later emerging autism. *Curr. Biol.* 22, 338–342. doi: 10.1016/j.cub.2011.12.056

Foss-Feig, J. H., Heacock, J. L., and Cascio, C. J. (2012). Tactile responsiveness patterns and their association with core features in autism spectrum disorders. *Res. Autism Spectr. Disord.* 6, 337–344. doi: 10.1016/j.rasd.2011.06.007

Frazier, T. W., Strauss, M., Klingemier, E. W., Zetzer, E. E., Hardan, A. Y., Eng, C., et al. (2017). A Meta-analysis of gaze differences to social and nonsocial information between individuals with and without autism. *J. Am. Acad. Child Adolesc. Psychiatry* 56, 546–555. doi: 10.1016/j.jaac.2017.05.005

Gandhi, T., and Lee, C. C. (2021). Neural mechanisms underlying repetitive behaviors in rodent models of autism spectrum disorders. *Front. Cell. Neurosci.* 14:592710. doi: 10.3389/fncel.2020.592710

Geva, R., and Feldman, R. (2008). A neurobiological model for the effects of early brainstem functioning on the development of behavior and emotion regulation in infants: implications for prenatal and perinatal risk. *J. Child Psychol. Psychiatry* 49, 1031–1041. doi: 10.1111/j.1469-7610.2008.01918.x

Geva, R., and Feldman, R. (2010). "Circadian sleep-wake rhythms in preterm infants," in *Biological Clocks: Effects on Behavior, Health and Outlook*, eds O. Salvenmoser, and B. Meklau (New York: NOVA Science Publishers Inc), 101–120.

Geva, R., Dital, A., Ramon, D., Yarmolovsky, J., Gidron, M., and Kuint, J. (2017). Brainstem as a developmental gateway to social attention. *J. Child Psychol. Psychiatry* 58, 1351–1359. doi: 10.1111/jcpp.12746

Geva, R., Schreiber, J., Segal-Caspi, L., and Markus-Shiffman, M. (2014). Neonatal brainstem dysfunction after preterm birth predicts behavioral inhibition. *J. Child Psychol. Psychiatry* 55, 802–810. doi: 10.1111/jcpp.12188

Geva, R., Sopher, K., Kurtzman, L., Galili, G., Feldman, R., and Kuint, J. (2013). Neonatal brainstem dysfunction risks infant social engagement. *Soc. Cogn. Affect. Neurosci.* 8, 158–164. doi: 10.1093/scan/nsr082

Geva, R., Yaron, H., and Kuint, J. (2016). Neonatal Sleep Predicts Attention Orienting and Distractibility. *J. Atten. Disord.* 20, 138–150. doi: 10.1177/1087054713491493

Gilbert, J., and Man, H.-Y. (2017). Fundamental elements in Autism: from neurogenesis and neurite growth to synaptic plasticity. *Front. Cell. Neurosci.* 11:359. doi: 10.3389/fncel.2017.00359

Glover, J. C., Sato, K., and Sato, Y.-M. (2008). Using voltage-sensitive dye recording to image the functional development of neuronal circuits in vertebrate embryos. *Dev. Neurobiol.* 68, 804–816. doi: 10.1002/dneu.20629

Graven, S. N. (2004). Early neurosensory visual development of the fetus and newborn. *Clin. Perinatol.* 31, 199–216. doi: 10.1016/j.clp.2004.04.010

Grinter, E. J., Maybery, M. T., and Badcock, D. R. (2010). Vision in developmental disorders: is there a dorsal stream deficit? *Brain Res. Bull.* 82, 147–160. doi: 10.1016/j.brainresbull.2010.02.016

Hammarrenger, B., Hammarrenger, B., Leporé, F., Lippé, S., Lippé, S., Labrosse, M., et al. (2003). Magnocellular and parvocellular developmental course in infants during the first year of life. *Doc. Ophthalmol.* 107, 225–233. doi: 10.1023/B:DOOP.0000005331.66114.05

Hegerl, U., and Hensch, T. (2014). The vigilance regulation model of affective disorders and ADHD. *Neurosci. Biobehav. Rev.* 44, 45–57. doi: 10.1016/j.neubiorev.2012.10.008

Heraghty, J. L., Hilliard, T. N., Henderson, A. J., and Fleming, P. J. (2008). The physiology of sleep in infants. *Arch. Dis. Child.* 93, 982–985. doi: 10.1136/adc.2006.113290

Huang, Y., Yu, S., Wilson, G., Park, J., Cheng, M., Kong, X., et al. (2021). Altered extended locus coeruleus and ventral tegmental area networks in boys with autism spectrum disorders: a resting-state functional connectivity study. *Neuropsychiatr. Dis. Treat.* 17, 1207–1216. doi: 10.2147/NDT.S301106

Humphreys, J. S., Gringras, P., Blair, P. S., Scott, N., Henderson, J., Fleming, P. J., et al. (2014). Sleep patterns in children with autistic spectrum disorders: a prospective cohort study. *Arch. Dis. Child.* 99, 114–118. doi: 10.1136/archdischild-2013-304083

Johnson, B. P., Lum, J. A. G., Rinehart, N. J., and Fielding, J. (2016). Ocular motor disturbances in autism spectrum disorders: systematic review and comprehensive meta-analysis. *Neurosci. Biobehav. Rev.* 69, 260–279. doi: 10.1016/j.neubiorev.2016.08.007

Jones, W., and Klin, A. (2013). Attention to eyes is present but in decline in 2–6-month-old infants later diagnosed with autism. *Nature* 504, 427–431. doi: 10.1038/nature12715

Ju, C., Bosman, L. W. J., Hoogland, T. M., Velauthapillai, A., Murugesan, P., Warnaar, P., et al. (2019). Neurons of the inferior olive respond to broad classes of sensory input while subject to homeostatic control. *J. Physiol.* 597, 2483–2514. doi: 10.1113/JP277413

Jure, R. (2019). Autism Pathogenesis: the Superior Colliculus. *Front. Neurosci.* 12:1029. doi: 10.3389/fnins.2018.01029

Jure, R., Pogonza, R., and Rapin, I. (2016). Autism Spectrum Disorders (ASD) in blind children: very high prevalence, potentially better outlook. *J. Autism Dev. Disord.* 46, 749–759. doi: 10.1007/s10803-015-2612-5

Kanakri, S. M., Shepley, M., Tassinary, L. G., Varni, J. W., and Fawaz, H. M. (2017). An Observational study of classroom acoustical design and repetitive behaviors in children with Autism. *Environ. Behav.* 49, 847–873. doi: 10.1177/0013916516669389

Kargas, N., López, B., Reddy, V., and Morris, P. (2015). The relationship between auditory processing and restricted, repetitive behaviors in adults with autism spectrum disorders. *J. Autism Dev. Disord.* 45, 658–668. doi: 10.1007/s10803-014-2219-2

Keller, P. E., Novembre, G., and Hove, M. J. (2014). Rhythm in joint action: psychological and neurophysiological mechanisms for real-time interpersonal coordination. *Philos. Trans. R. Soc. B Biol. Sci.* 369:20130394. doi: 10.1098/rstb.2013.0394

Kobayashi, Y., and Isa, T. (2002). Sensory-motor gating and cognitive control by the brainstem cholinergic system. *Neural Networks* 15, 731–741. doi: 10.1016/S0893-6080(02)00059-X

Kulesza, R. J., and Mangunay, K. (2008). Morphological features of the medial superior olive in autism. *Brain Res.* 1200, 132–137. doi: 10.1016/j.brainres.2008.01.009

Kulesza, R. J., Lukose, R., and Stevens, L. V. (2011). Malformation of the human superior olive in autistic spectrum disorders. *Brain Res.* 1367, 360–371. doi: 10.1016/j.brainres.2010.10.015

Lai, M.-C., Kassee, C., Besney, R., Bonato, S., Hull, L., Mandy, W., et al. (2019). Prevalence of co-occurring mental health diagnoses in the autism population: a systematic review and meta-analysis. *Lancet Psychiatry* 6, 819–829. doi: 10.1016/S2215-0366(19)30289-5

Landau, M. E., Maldonado, J. Y., and Jabbari, B. (2005). The effects of isolated brainstem lesions on human REM sleep. *Sleep Med.* 6, 37–40. doi: 10.1016/j.sleep.2004.08.007

Levit, Y., Himmelfarb, M., and Dollberg, S. (2015). Sensitivity of the automated auditory brainstem response in neonatal hearing screening. *Pediatrics* 136, e641–7. doi: 10.1542/peds.2014-3784

Longin, E., Gerstner, T., Schaible, T., Lenz, T., and König, S. (2006). Maturation of the autonomic nervous system: differences in heart rate variability in premature vs. term infants. *J. Perinat. Med.* 34, 303–308. doi: 10.1515/JPM.2006.058

Ludwig, R. J., and Welch, M. G. (2019). Darwin's Other Dilemmas and the Theoretical Roots of Emotional Connection. *Front. Psychol.* 10:683. doi: 10.3389/fpsyg.2019.00683

Ludwig, R. J., and Welch, M. G. (2020). How babies learn: the autonomic socioemotional reflex. *Early Hum. Dev.* 151:105183. doi: 10.1016/j.earlhumdev.2020.105183

Lugo, J., Fadeuilhe, C., Gisbert, L., Setien, I., Delgado, M., Corrales, M., et al. (2020). Sleep in adults with autism spectrum disorder and attention deficit/hyperactivity disorder: a systematic review and meta-analysis. *Eur. Neuropsychopharmacol.* 38, 1–24. doi: 10.1016/j.euroneuro.2020.07.004

Mansour, Y., and Kulesza, R. (2020). Three dimensional reconstructions of the superior olivary complex from children with autism spectrum disorder. *Hear. Res.* 393:107974. doi: 10.1016/j.heares.2020.107974

Marco, E. J., Hinkley, L. B. N., Hill, S. S., and Nagarajan, S. S. (2011). Sensory Processing in Autism: a review of neurophysiologic findings. *Pediatr. Res.* 69, 48R–54R. doi: 10.1203/PDR.0b013e3182130c54

Marlier, L., Gaugler, C., and Messer, J. (2005). Olfactory stimulation prevents apnea in premature newborns. *Pediatrics* 115, 83–88. doi: 10.1542/peds.2004-0865

Marrs, G. S., and Spirou, G. A. (2012). Embryonic assembly of auditory circuits: spiral ganglion and brainstem. *J. Physiol.* 590, 2391–2408. doi: 10.1113/jphysiol.2011.226886

Meguro-Horike, M., Yasui, D. H., Powell, W., Schroeder, D. I., Oshimura, M., LaSalle, J. M., et al. (2011). Neuron-specific impairment of inter-chromosomal pairing and transcription in a novel model of human 15q-duplication syndrome. *Hum. Mol. Genet.* 20, 3798–3810. doi: 10.1093/hmg/ddr298

Miike, T., Toyoura, M., Tonooka, S., Konishi, Y., Oniki, K., Saruwatari, J., et al. (2020). Neonatal irritable sleep-wake rhythm as a predictor of autism spectrum disorders. *Neurobiol. Sleep Circadian Rhythm.* 9:100053. doi: 10.1016/j.nbscr.2020.100053

Miron, O., Ari—Even Roth, D., Gabis, L. V., Henkin, Y., Shefer, S., Dinstein, I., et al. (2016). Prolonged auditory brainstem responses in infants with autism. *Autism Res.* 9, 689–695. doi: 10.1002/aur.1561

Miron, O., Beam, A. L., and Kohane, I. S. (2018). Auditory brainstem response in infants and children with autism spectrum disorder: a meta-analysis of wave V. *Autism Res.* 11, 355–363. doi: 10.1002/AUR.1886

Miron, O., Delgado, R. E., Delgado, C. F., Simpson, E. A., Yu, K.-H. K., Gutierrez, A., et al. (2021). Prolonged auditory brainstem response in universal hearing screening of newborns with autism spectrum disorder. *Autism Res.* 14, 46–52. doi: 10.1002/aur.2422

Morton, C. C., and Nance, W. E. (2006). Newborn hearing screening — a silent revolution. *N. Engl. J. Med.* 354, 2151–2164. doi: 10.1056/NEJMra050700

O'Connor, K. (2012). Auditory processing in autism spectrum disorder: a review. *Neurosci. Biobehav. Rev.* 36, 836–854. doi: 10.1016/J.NEUBIOREV.2011.11.008

O'Rahilly, R., and Müller, F. (2006). *The Embryonic Human Brain*. Hoboken: John Wiley & Sons, Inc.

Palmen, S. J. M. C., van Engeland, H., Hof, P. R., and Schmitz, C. (2004). Neuropathological findings in autism. *Brain* 127, 2572–2583. doi: 10.1093/brain/awh287

Park, W. J., Schauder, K. B., Zhang, R., Bennetto, L., and Tadin, D. (2017). High internal noise and poor external noise filtering characterize perception

in autism spectrum disorder. *Sci. Rep.* 7:17584. doi: 10.1038/s41598-017-17676-5

Parvizi, J., and Damasio, A. (2001). Consciousness and the brainstem. *Cognition* 79, 135–160. doi: 10.1016/S0010-0277(00)00127-X

Pérez de los Cobos Pallares, F., Bautista, T. G., Stanić, D., Egger, V., and Dutschmann, M. (2016). Brainstem-mediated sniffing and respiratory modulation during odor stimulation. *Respir. Physiol. Neurobiol.* 233, 17–24. doi: 10.1016/j.resp.2016.07.008

Petersen, C. L., and Hurley, L. M. (2017). Putting it in Context: linking Auditory processing with social behavior circuits in the vertebrate brain. *Integr. Comp. Biol.* 57, 865–877. doi: 10.1093/ICB/ICX055

Phillips, A. J. K., and Robinson, P. A. (2007). A quantitative model of sleep-wake dynamics based on the physiology of the brainstem ascending arousal system. *J. Biol. Rhythms* 22, 167–179. doi: 10.1177/0748730406297512

Pitti, A., Kuniyoshi, Y., Quoy, M., and Gaussier, P. (2013). Modeling the minimal newborn's intersubjective mind: the visuotopic-somatotopic alignment hypothesis in the superior colliculus. *PLoS One* 8:e69474. doi: 10.1371/journal.pone.0069474

Porges, S. W. (1995). Orienting in a defensive world: mammalian modifications of our evolutionary heritage. A Polyvagal Theory. *Psychophysiology* 32, 301–318. doi: 10.1111/j.1469-8986.1995.tb01213.x

Porges, S. W. (2001). The polyvagal theory: phylogenetic substrates of a social nervous system. *Int. J. Psychophysiol.* 42, 123–146. doi: 10.1016/S0167-8760(01)00162-3

Porges, S. W. (2011). *The Polyvagal Theory: Neurophysiological Foundations Of Emotions, Attachment, Communication, And Self-Regulation*. New York: W. W. Norton & Company.

Porges, S. W. (2021). Polyvagal theory: a biobehavioral journey to sociality. *Compr. Psychoneuroendocrinol.* 7:100069. doi: 10.1016/j.cpnec.2021.100069

Prince, E. B., Kim, E. S., Wall, C. A., Gisin, E., Goodwin, M. S., Simmons, E. S., et al. (2017). The relationship between autism symptoms and arousal level in toddlers with autism spectrum disorder, as measured by electrodermal activity. *Autism* 21, 504–508. doi: 10.1177/1362361316648816

Rodier, P. M., Ingram, J. L., Tisdale, B., Nelson, S., and Romano, J. (1996). Embryological origin for autism: developmental anomalies of the cranial nerve motor nuclei. *J. Comp. Neurol.* 370, 247–261.

Saenz, J., Yaugher, A., and Alexander, G. M. (2015). Sleep in Infancy Predicts Gender Specific Social-Emotional Problems in Toddlers. *Front. Pediatr.* 3:42. doi: 10.3389/fped.2015.00042

Sanders, S. J., Murtha, M. T., Gupta, A. R., Murdoch, J. D., Raubeson, M. J., Willsey, A. J., et al. (2012). De novo mutations revealed by whole-exome sequencing are strongly associated with autism. *Nature* 485, 237–241. doi: 10.1038/nature10945

Sano, M., Kaga, K., Kuan, C. C., Ino, K., and Mima, K. (2007). Early myelination patterns in the brainstem auditory nuclei and pathway: MRI evaluation study. *Int. J. Pediatr. Otorhinolaryngol.* 71, 1105–1115. doi: 10.1016/j.ijporl.2007.04.002

Scammell, T. E., Arrigoni, E., and Lipton, J. O. (2017). Neural Circuitry of Wakefulness and Sleep. *Neuron* 93, 747–765. doi: 10.1016/j.neuron.2017.01.014

Schaaf, R. C., Toth-Cohen, S., Johnson, S. L., Outten, G., and Benevides, T. W. (2011). The everyday routines of families of children with autism. *Autism* 15, 373–389. doi: 10.1177/1362361310386505

Scherfler, C., Frauscher, B., Schocke, M., Iranzo, A., Gschliesser, V., Seppi, K., et al. (2011). White and gray matter abnormalities in idiopathic rapid eye movement sleep behavior disorder: a diffusion-tensor imaging and voxel-based morphometry study. *Ann. Neurol.* 69, 400–407. doi: 10.1002/ana.22245

Schreck, K. A., Mulick, J. A., and Smith, A. F. (2004). Sleep problems as possible predictors of intensified symptoms of autism. *Res. Dev. Disabil.* 25, 57–66. doi: 10.1016/j.ridd.2003.04.007

Sebat, J., Lakshmi, B., Malhotra, D., Troge, J., Lese-Martin, C., Walsh, T., et al. (2007). Strong Association of De Novo Copy Number Mutations with Autism. *Science* 316, 445–449. doi: 10.1126/science.1138659

Sheinkopf, S. J., Levine, T. P., McCormick, C. E. B., Puggioni, G., Conradt, E., Lagasse, L. L., et al. (2019). Developmental trajectories of autonomic functioning in autism from birth to early childhood. *Biol. Psychol.* 142, 13–18. doi: 10.1016/j.biopsycho.2019.01.003

Shukla, D. K., Keehn, B., Lincoln, A. J., and Müller, R.-A. (2010). White matter compromise of callosal and subcortical fiber tracts in children with autism spectrum disorder: a diffusion tensor imaging study. *J. Am. Acad. Child Adolesc. Psychiatry* 49, 1269–1278. doi: 10.1016/j.jaac.2010.08.018

Sokoloff, G., Uitermarkt, B. D., and Blumberg, M. S. (2015). REM sleep twitches rouse nascent cerebellar circuits: implications for sensorimotor development. *Dev. Neurobiol.* 75, 1140–1153. doi: 10.1002/dneu.22177

Souders, M. C., Zavodny, S., Eriksen, W., Sinko, R., Connell, J., Kerns, C., et al. (2017). Sleep in Children with Autism Spectrum Disorder. *Curr. Psychiatry Rep.* 19:34. doi: 10.1007/s11920-017-0782-x

Soussignan, R., Schaal, B., Marlier, L., and Jiang, T. (1997). Facial and Autonomic Responses to Biological and Artificial Olfactory Stimuli in Human Neonates. *Physiol. Behav.* 62, 745–758. doi: 10.1016/S0031-9384(97)00187-X

Stein, B. E., Stanford, T. R., and Rowland, B. A. (2014). Development of multisensory integration from the perspective of the individual neuron. *Nat. Rev. Neurosci.* 15, 520–535. doi: 10.1038/nrn3742

Suberi, M., Morag, I., Strauss, T., and Geva, R. (2018). Feeding Imprinting: the extreme test case of premature infants born with very low birth weight. *Child Dev.* 89, 1553–1566. doi: 10.1111/cdev.12923

Talge, N. M., Tudor, B. M., and Kileny, P. R. (2018). Click-evoked auditory brainstem responses and autism spectrum disorder: a meta-analytic review. *Autism Res.* 11, 916–927. doi: 10.1002/AUR.1946

Tanaka, S., Mito, T., and Takashima, S. (1995). Progress of myelination in the human fetal spinal nerve roots, spinal cord and brainstem with myelin basic protein immunohistochemistry. *Early Hum. Dev.* 41, 49–59. doi: 10.1016/0378-3782(94)01608-R

ten Donkelaar, H. J., Cruysberg, J. R. M., Pennings, R., and Lammens, M. (2014). "Development and Developmental Disorders of the Brain Stem," in *Clinical Neuroembryology*, eds H. J. ten Donkelaar, M. Lammens, and A. Hori (Berlin: Springer), 321–370.

Tseng, P.-T., Chen, Y.-W., Stubbs, B., Carvalho, A. F., Whiteley, P., Tang, C.-H., et al. (2019). Maternal breastfeeding and autism spectrum disorder in children: a systematic review and meta-analysis. *Nutr. Neurosci.* 22, 354–362. doi: 10.1080/1028415X.2017.1388598

Tu, S., Mason, C., Rooks-Ellis, D., and Lech, P. (2020). Odds of Autism at 5 to 10 Years of age for children who did not pass their AABR newborn hearing screen, but were diagnosed with normal hearing. *J. Early Hear. Detect. Interv.* 5, 1–12. doi: 10.26077/cp8w-9r69

Tudor, M. E., Hoffman, C. D., and Sweeney, D. P. (2012). Children With Autism: sleep problems and symptom severity. *Focus Autism Other Dev. Disabl.* 27, 254–262. doi: 10.1177/1088357612457989

Veatch, O. J., Sutcliffe, J. S., Warren, Z. E., Keenan, B. T., Potter, M. H., and Malow, B. A. (2017). Shorter sleep duration is associated with social impairment and comorbidities in ASD. *Autism Res.* 10, 1221–1238. doi: 10.1002/aur.1765

Villablanca, J., de Andrés, I., and Olmstead, C. (2001). Sleep–waking states develop independently in the isolated forebrain and brain stem following early postnatal midbrain transection in cats. *Neuroscience* 106, 717–731. doi: 10.1016/S0306-4522(01)00329-3

Wass, S. V., Jones, E. J. H., Gliga, T., Smith, T. J., Charman, T., and Johnson, M. H. (2015). Shorter spontaneous fixation durations in infants with later emerging autism. *Sci. Rep.* 5:8284. doi: 10.1038/srep08284

Watson, C., Bartholomaeus, C., and Puelles, L. (2019). Time for Radical Changes in Brain Stem Nomenclature—Applying the Lessons From Developmental Gene Patterns. *Front. Neuroanat.* 13:10. doi: 10.3389/fnana.2019.00010

Wegiel, J., Kuchna, I., Nowicki, K., Imaki, H., Wegiel, J., Yong Ma, S., et al. (2013). Contribution of olivofloccular circuitry developmental defects to atypical gaze in autism. *Brain Res.* 1512, 106–122. doi: 10.1016/j.brainres.2013.03.037

Welch, M. G., Barone, J. L., Porges, S. W., Hane, A. A., Kwon, K. Y., Ludwig, R. J., et al. (2020). Family nurture intervention in the NICU increases autonomic regulation in mothers and children at 4-5 years of age: follow-up results from a randomized controlled trial. *PLoS One* 15:e0236930. doi: 10.1371/journal.pone.0236930

Welch, M. G., Firestein, M. R., Austin, J., Hane, A. A., Stark, R. I., Hofer, M. A., et al. (2015). Family nurture intervention in the neonatal intensive care unit improves social−relatedness, attention, and neurodevelopment of preterm infants at 18 months in a randomized controlled trial. *J. Child Psychol. Psychiatry* 56, 1202–1211. doi: 10.1111/jcpp.12405

West, K. L. (2019). Infant motor development in Autism spectrum disorder: a synthesis and Meta−analysis. *Child Dev.* 90, 2053–2070. doi: 10.1111/cdev.13086

Wiggins, L. D., Robins, D. L., Bakeman, R., and Adamson, L. B. (2009). Breif Report: sensory abnormalities as distinguishing symptoms of autism spectrum disorders in young children. *J. Autism Dev. Disord.* 39, 1087–1091. doi: 10.1007/s10803-009-0711-x

Wilkinson, A. R., and Jiang, Z. D. (2006). Brainstem auditory evoked response in neonatal neurology. *Semin. Fetal Neonatal Med.* 11, 444–451. doi: 10.1016/j.siny.2006.07.005

Williams, Z. J., Abdelmessih, P. G., Key, A. P., and Woynaroski, T. G. (2020). Cortical auditory processing of simple stimuli is altered in Autism: a Meta-analysis of auditory evoked responses. *Biol. Psychiatry Cogn. Neurosci. Neuroimaging* 6, 767–781. doi: 10.1016/J.BPSC.2020.09.011

Williams, Z. J., He, J. L., Cascio, C. J., and Woynaroski, T. G. (2021). A review of decreased sound tolerance in autism: definitions, phenomenology, and potential mechanisms. *Neurosci. Biobehav. Rev.* 121, 1–17. doi: 10.1016/j.neubiorev.2020.11.030

Wintler, T., Schoch, H., Frank, M. G., and Peixoto, L. (2020). Sleep, brain development, and autism spectrum disorders: insights from animal models. *J. Neurosci. Res.* 98, 1137–1149. doi: 10.1002/jnr.24619

Wu, X., Nestrasil, I., Ashe, J., Tuite, P., and Bushara, K. (2010). Inferior olive response to passive tactile and visual stimulation with variable interstimulus intervals. *Cerebellum* 9, 598–602. doi: 10.1007/s12311-010-0203-8

Yu, Q., Peng, Y., Kang, H., Peng, Q., Ouyang, M., Slinger, M., et al. (2020). Differential White Matter Maturation from Birth to 8 Years of Age. *Cereb. Cortex* 30, 2674–2690. doi: 10.1093/cercor/bhz268

Zec, N., and Kinney, H. C. (2003). Anatomic relationships of the human nucleus of the solitary tract in the medulla oblongata: a DiI labeling study. *Auton. Neurosci. Basic Clin.* 105, 131–144. doi: 10.1016/S1566-0702(03)00027-4

Zhang, F., Savadjiev, P., Cai, W., Song, Y., Rathi, Y., Tunç, B., et al. (2018). Whole brain white matter connectivity analysis using machine learning: an application to autism. *Neuroimage* 172, 826–837. doi: 10.1016/j.neuroimage.2017.10.029

Zivan, M., Morag, I., Yarmolovsky, J., and Geva, R. (2021). Hyper-Reactivity to salience limits social interaction among infants born pre-term and infant siblings of children With ASD. *Front. Psychiatry* 12:646838. doi: 10.3389/fpsyt.2021.646838

Zwaigenbaum, L., Bryson, S., Rogers, T., Roberts, W., Brian, J., and Szatmari, P. (2005). Behavioral manifestations of autism in the first year of life. *Int. J. Dev. Neurosci.* 23, 143–152. doi: 10.1016/j.ijdevneu.2004.05.001

Conflict of Interest: The authors declare that the research was conducted in the absence of any commercial or financial relationships that could be construed as a potential conflict of interest.

Publisher's Note: All claims expressed in this article are solely those of the authors and do not necessarily represent those of their affiliated organizations, or those of the publisher, the editors and the reviewers. Any product that may be evaluated in this article, or claim that may be made by its manufacturer, is not guaranteed or endorsed by the publisher.

frontiers in Integrative Neuroscience

ORIGINAL RESEARCH
published: 17 January 2022
doi: 10.3389/fnint.2021.803483

Auditory Brain Stem Responses in the C57BL/6J Fragile X Syndrome-Knockout Mouse Model

*Amita Chawla and Elizabeth A. McCullagh**

Department of Integrative Biology, Oklahoma State University, Stillwater, OK, United States

Sensory hypersensitivity, especially in the auditory system, is a common symptom in Fragile X syndrome (FXS), the most common monogenic form of intellectual disability. However, linking phenotypes across genetic background strains of mouse models has been a challenge and could underly some of the issues with translatability of drug studies to the human condition. This study is the first to characterize the auditory brain stem response (ABR), a minimally invasive physiological readout of early auditory processing that is also used in humans, in a commonly used mouse background strain model of FXS, C57BL/6J. We measured morphological features of pinna and head and used ABR to measure the hearing range, and monaural and binaural auditory responses in hemizygous males, homozygous females, and heterozygous females compared with those in wild-type mice. Consistent with previous study, we showed no difference in morphological parameters across genotypes or sexes. There was no significant difference in hearing range between the sexes or genotypes, however there was a trend towards high frequency hearing loss in male FXS mice. In contrast, female mice with homozygous FXS had a decreased amplitude of wave IV of the monaural ABR, while there was no difference in males for amplitudes and no change in latency of ABR waveforms across sexes and genotypes. Finally, males with FXS had an increased latency of the binaural interaction component (BIC) at 0 interaural timing difference compared with that in wild-type males. These findings further clarify auditory brain stem processing in FXS by adding more information across genetic background strains allowing for a better understanding of shared phenotypes.

Keywords: auditory brainstem response (ABR), Fragile X Syndrome, binaural hearing, sex differences, mouse model

OPEN ACCESS

Edited by:
Randy J. Kulesza, Lake Erie College of Osteopathic Medicine, United States

Reviewed by:
Charles H. Large, Autifony Therapeutics Ltd., United Kingdom
Adrian Rodriguez-Contreras, City College of New York (CUNY), United States

***Correspondence:**
Elizabeth A. McCullagh
elizabeth.mccullagh@okstate.edu

Received: *28 October 2021*
Accepted: *14 December 2021*
Published: *17 January 2022*

Citation:
Chawla A and McCullagh EA (2022) Auditory Brain Stem Responses in the C57BL/6J Fragile X Syndrome-Knockout Mouse Model. Front. Integr. Neurosci. 15:803483. doi: 10.3389/fnint.2021.803483

INTRODUCTION

Fragile X syndrome (FXS) is the most common monogenic form of autism spectrum disorder (ASD) and shares many attributes of ASDs, including auditory hypersensitivity and other sensory disruptions (Abbeduto and Hagerman, 1997; Chen and Toth, 2001; Hagerman and Hagerman, 2002; Arnett et al., 2014). FXS is a tractable genetic model for ASD with several commercially available models, including the rat and mouse (The Dutch-Belgian Fragile X Consorthium et al., 1994; Till et al., 2015; Tian et al., 2017). Despite the common use of these models to study the FXS, phenotypes are not always shared between species and background strains, particularly for sensory processing. As a result, drug therapies have struggled to rescue the human disorder (Dahlhaus, 2018). One of the most common symptoms described in people with FXS and autism spectrum disorder (ASD) is auditory hypersensitivity (Ethridge et al., 2017; Stefanelli et al., 2020).

Clinically, auditory phenotypes present as reduced auditory attention, impaired habituation to auditory stimuli, reduced prepulse inhibition of acoustic startle, and overall hypersensitivity to auditory conditions (reviewed in Sinclair et al., 2017; Rais et al., 2018; Razak et al., 2021) that have likely both cortical and subcortical origins. Indeed, much of the research in this area has focused on cortical measures of auditory phenotypes, which receive inputs from lower auditory regions that may also be disrupted but less likely to be measured clinically. The mechanisms that underly auditory alterations are unknown, but likely involve the entirety of the ascending pathway from the periphery to the cortex (reviewed in McCullagh et al., 2020b). A complete characterization of auditory processing from the periphery to cortex across sexes, background strains, and models is needed to fully understand shared phenotypes and circuitry involved in this common symptom.

The auditory brain stem is one brain region in the ascending auditory pathway that has been shown to have anatomical, physiological, and behavioral alterations in mouse models with FXS (Brown et al., 2010; Beebe et al., 2014; Wang et al., 2014, 2015; Rotschafer et al., 2015; Garcia-Pino et al., 2017; McCullagh et al., 2017, 2020a; Rotschafer and Cramer, 2017; Curry et al., 2018; El-Hassar et al., 2019; Lu, 2019) that likely underly or contribute to the overall auditory phenotypes exhibited in both humans and animal models. Much like auditory hypersensitivity in humans, mice exhibit changes to the prepulse inhibition to the acoustic startle response, abnormal EEG activity, and, in the most extreme form, audiogenic seizures when presented with loud sounds (Chen and Toth, 2001; Lovelace et al., 2018, 2020; McCullagh et al., 2020a), making them a potentially suitable model for this sensory phenotype. The auditory brain stem is the first site of binaural processing of sound location in the brain using interaural timing and level differences (i.e., ITD and ILD, respectively) to compute sound source locations (Grothe et al., 2010). This brain area is also involved in separating spatial channels allowing for complex listening environments. Disruptions in this spatial separation and binaural processing could lead to auditory hypersensitivity due to the inability to separate sound sources (Bronkhorst, 2015). One measure of auditory brain stem physiology, and binaural hearing, that can be directly translated between animal models and humans is the auditory brain stem response (ABR) (Laumen et al., 2016).

The ABR is a minimally invasive physiological measure that allows for a simultaneous assessment of sound processing across multiple brain stem nuclei, as each wave of the ABR directly corresponds to distinct areas of the ascending auditory brain stem pathway. These features make the ABR an attractive translational tool. Indeed, recent evidence suggests that ABR measurements are an early indicator of auditory dysfunction in ASD (Santos et al., 2017). ABRs can also be used to assess binaural hearing, which is essential for sound localization and hearing in noisy environments and often impaired in ASD (Visser et al., 2013). Monoaural ABRs can be recorded by stimulating each ear separately, and binaural responses can be generated by stimulating both ears simultaneously. The sum of the two monaural (i.e., left and right) responses should equal the binaural (i.e., both ear) responses since the recruited neural activity from each ear should be double when stimulated simultaneously. However, this is not the case, there is a difference that arises when the summed monoaural responses are subtracted from the binaural response, called the binaural interaction component (BIC). The BIC is thought to be a direct measure of binaural processing ability in humans and animals that requires the precise balance of excitatory and inhibitory drive in brain stem sound localization circuits (Laumen et al., 2016).

In this study, we reported on the hearing ability, using the ABR and morphological craniofacial and pinna features, of the most common mouse model with FXS, C57BL/6J across the sexes and females heterozygous for the Fmr1 mutation. We hypothesized that there may be sex differences in ABRs independent of the FXS genotype, but that in addition, FXS animals are likely to have alterations in peak amplitude or latency of ABRs and impaired high-frequency hearing compared with wild-type consistent with work in other mouse strains with FXS (Kim et al., 2013; Rotschafer et al., 2015; El-Hassar et al., 2019). Establishing core auditory phenotypes across the sexes and different mouse strains is key to creating a toolbox of techniques that may translate to human FXS both to validate the utility of animal models to human conditions but also add to potential measures for the efficacy of the drug or other treatment options.

MATERIALS AND METHODS

All experiments complied with all applicable laws, National Institutes of Health guidelines, and were approved by the Oklahoma State University IACUC.

Animals

Experiments were conducted in C57BL/6J (stock #000664, B6) wild-type background, hemizygous male, homozygous male and female, or heterozygous female *Fmr1* mutant mice (B6.129P2-*Fmr1*^{TM1Cgr}/J stock #003025, Fmr1 or Fmr1 het, respectively) obtained from the Jackson Laboratory and bred at Oklahoma State University (Bar Harbor, ME, United States) (The Dutch-Belgian Fragile X Consorthium et al., 1994). Animals were generated for these experiments from stocks by both mixed and single genotype mating allowing for the creation of heterozygotes and some littermate controls, as well as maintenance of breeding lines. There was no significant main effect of litter (i.e., mixed or single genotype) for any of the experiments. Sex was treated as a biological variable, and differences between the sexes, when present, are noted in the results. The numbers of animals for each experiment used are listed in the figure legends and range from 6–10 animals per sex and genotype. Animals ranged in age from 62–120 days (i.e., average ages per genotype 89 $\pm$ 4 days B6, 101 $\pm$ 3 days Fmr1, and 97 $\pm$ 4 days Fmr1 het).

Morphological Measures

Features of animal's head, pinna, and body mass (weight) were measured for each genotype using 6 Inch Stainless Steel Electronic Vernier Calipers (DIGI-Science Accumatic digital caliper Gyros Precision Tools Monsey, NY, United States) and an electronic scale. The distance between the two pinnae (i.e.,

interpinna distance), distance from the nose to the middle of the pinna (i.e., nose to pinna distance), and pinna width and length were measured (**Figure 1A**). The effective diameter was calculated as the square root of pinna length times pinna width (Anbuhl et al., 2017).

Auditory Brain Stem Responses

Auditory brain stem response recordings were performed using similar methods from previously published study (Benichoux et al., 2018; McCullagh et al., 2020a; New et al., 2021). Animals were anesthetized using two mixtures of ketamine-xylazine 60 mg/kg ketamine and 10 mg/kg xylazine for initial induction followed by maintenance doses of 25 mg/kg ketamine and 12 mg/kg xylazine. Once anesthesia was confirmed by lack of a toe-pinch reflex, animals were transferred to a small sound attenuating chamber (Noise Barriers Lake Forest, IL, United States), and the body temperature was maintained using a water-pump heating pad. Subdermal needle electrodes were placed under the skin between the ears (i.e., apex), directly behind the apex in the nape (i.e., reference), and in the back leg for ground. This montage has been shown to be particularly effective in generating the BIC (Levine, 1981; Laumen et al., 2016). Evoked potentials from subdermal needle electrodes were acquired and amplified using Tucker-Davis Technologies (TDT, Alachua, FL, United States) RA4LI head stage and a TDT RA16PA preamplifier. Further amplification was provided by a TDT Multi I/O processor RZ5 connected to a PC with custom Python software for data recording. Data

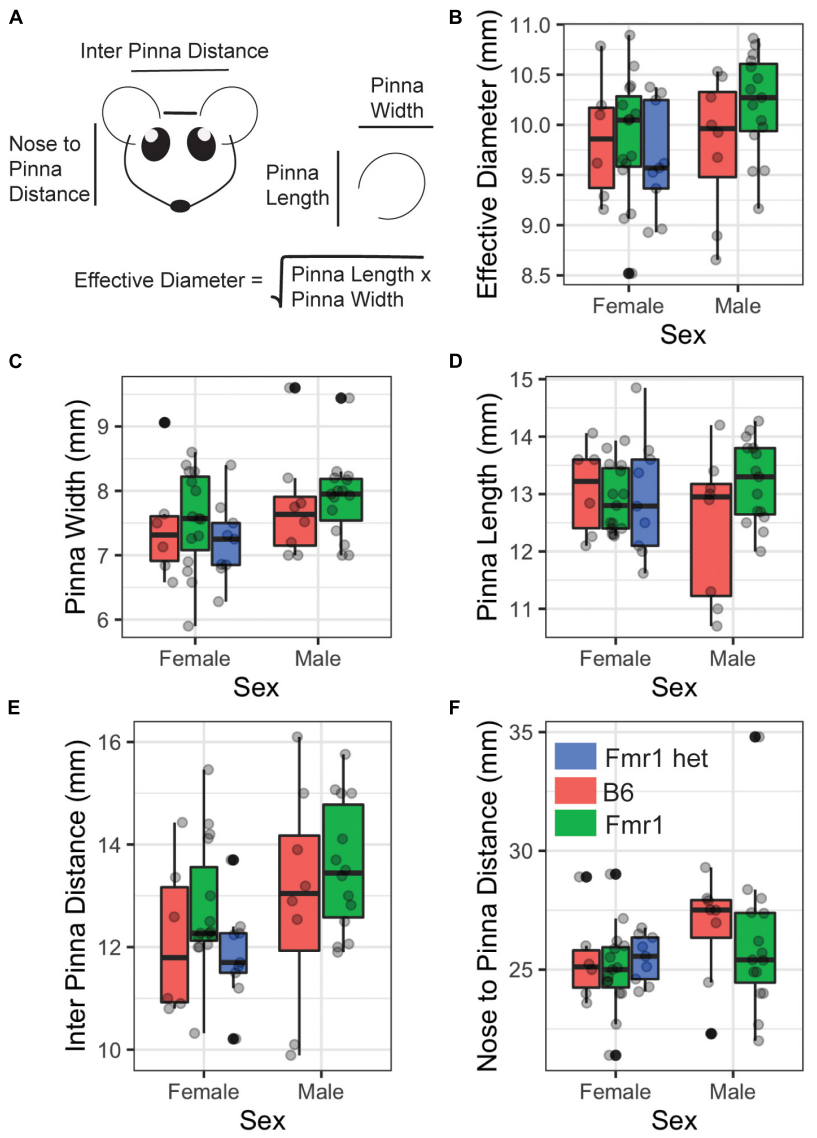

FIGURE 1 | Morphological features of Fragile X syndrome (FXS) mice. Pinna and head features **(A)** were measured between the sexes (*x*-axis) and genotypes (purple = B6, teal = Fmr1, and yellow = Fmr1 het). There was no difference between the sexes or genotypes for any of the measures [effective diameter **(B)**, pinna width **(C)**, pinna length **(D)**, interpinna length **(E)**, or nose to pinna length **(F)**]. Data represent 6 B6, 15 Fmr1, and 9 Fmr1 het females and 8 B6 and 15 Fmr1 males.

were averaged across 500–1,000 repetitions per condition and processed using a second-order 50–3,000 Hz filter over 12 ms of recording time.

Sound stimuli (refer below for varying types) were presented to the animal through TDT EC-1 electrostatic speakers (frequencies 32–46 kHz) or TDT MF-1 multifield speakers (frequencies 1–24 kHz and broadband clicks) coupled through custom earpieces fitted with Etymotic ER-7C probe microphones (Etymotic Research Inc., Elk Grove Village, IL, United States) for the in-ear calibration (Beutelmann et al., 2015). Sounds were generated using a TDT RP2.1 Real-Time processor controlled by the custom Python code at a sampling rate of 97656.25 Hz. Sounds were presented at an interstimulus interval of 30 ms with a standard deviation of 5 ms (Laumen et al., 2016). An additional rejection threshold was set to eliminate high-amplitude heart rate responses from average traces and improve the signal-to-noise ratio.

Audiogram

The hearing range of animals was tested using the threshold for hearing across different frequencies (i.e., 1, 2, 4, 8, 16, 24, 32, 46 kHz) of sound. Threshold was determined using a visual detection method (Brittan-Powell and Dooling, 2004), or the lowest level (dB SPL) a response could be detected. Audiogram stimuli consisted of tone bursts (2 ms ± 1 ms on/off ramps) of varying frequency and intensity.

Monaural Auditory Brain Stem Responses

Broadband click stimuli (i.e., 0.1 ms transient) were presented to each ear independently to generate monaural evoked potentials. Peak amplitude (i.e., the voltage from peak to trough) and latency (i.e., time to peak amplitude) were measured across the four peaks of the ABR waveform at 90 dB SPL (**Figure 2A**). The trough was considered the lowest point for that wave. Monaural data from the two ears were averaged to determine the monaural amplitude and latency for each animal. Similar to hearing thresholds across frequency, click threshold was determined for each genotype and sex. Click threshold is determined by decreasing the intensity of sound in 5–10 dB SPL steps until ABR waveforms disappear.

Binaural Auditory Brain Stem Responses

Broadband click stimuli at 90 dB SPL were also presented to both ears simultaneously to generate a binaural evoked potential. The BIC of the ABR was calculated by subtracting the sum of the two monaural ABRs from the binaural ABR (Laumen et al., 2016; Benichoux et al., 2018) (**Figures 2B,C**). BIC amplitude and latency were then measured using the custom Python software, with amplitude being relative to the zero baselines of the measurement (**Figure 2C**, gray area with line). BIC was characterized as the prominent negative DN1 wave corresponding to the fourth wave of the binaural and summed ABR (**Figure 2B**). To measure ITD computation using the BIC, animals were presented with stimuli that had varying ITDs of ± 2 ms in 0.5 ms steps, and corresponding BIC amplitudes and latencies were calculated like above. This ITD range was chosen to be comparable to other studies in small rodents (Benichoux et al., 2018).

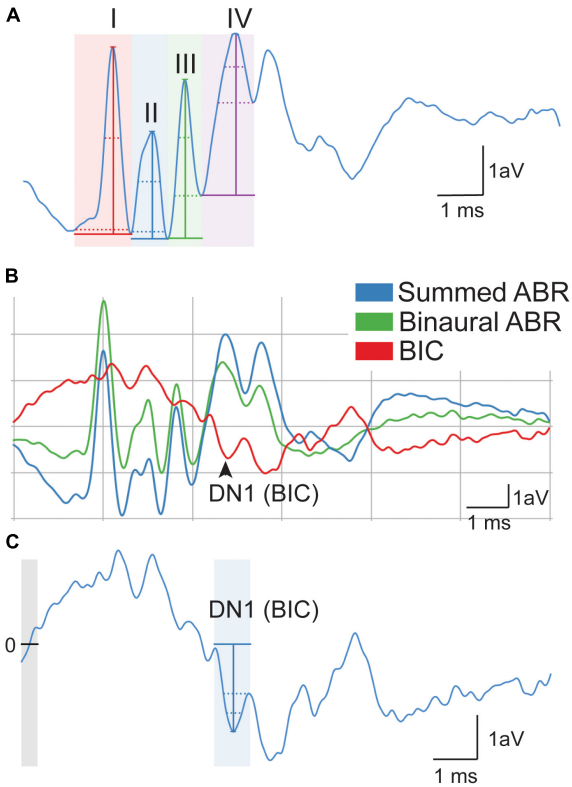

FIGURE 2 | Quantification of auditory brain stem response (ABR) signals. Monaural ABR amplitudes were quantified for each ear as the voltage between the peak of the ABR and trough of the waveform for waves I–IV **(A)**. Latency was calculated as the time when the height of the peak occurred. DN1 or binaural interaction component (BIC) (i.e., red) was calculated as the prominent negative peak corresponding with wave IV of the summed (blue) and binaural (green) **(B)**. BIC is calculated as the summed ABR subtracted from the binaural ABR. The BIC amplitude was calculated as the voltage at the peak of the DN1 waveform to the baseline (0, line, and gray area) of the measurement **(C)**. The scale represents 1 arbitrary voltage (aV) unit (Y) during 1 ms (X).

Analysis of Auditory Brain Stem Response Waveforms

The custom python software was used to analyze evoked potentials for monaural and binaural stimuli (New et al., 2021). To account for fluctuation in the baseline signal of the ABR, raw traces were zeroed to establish a baseline across traces. The software included automatic peak detection with the capability of manual correction or deselection upon visual confirmation.

Statistical Analyses

Figures were generated using R Studio (R Core Team, 2013), ggplot2 (Wickham, 2016), and Adobe Illustrator (Adobe, San Jose, CA, United States) software. Data points in **Figures 3**, **4**, and **5** represent means, error bars reflect standard error, boxplots in **Figure 1** display the median and 25–75th percentiles (or 1st

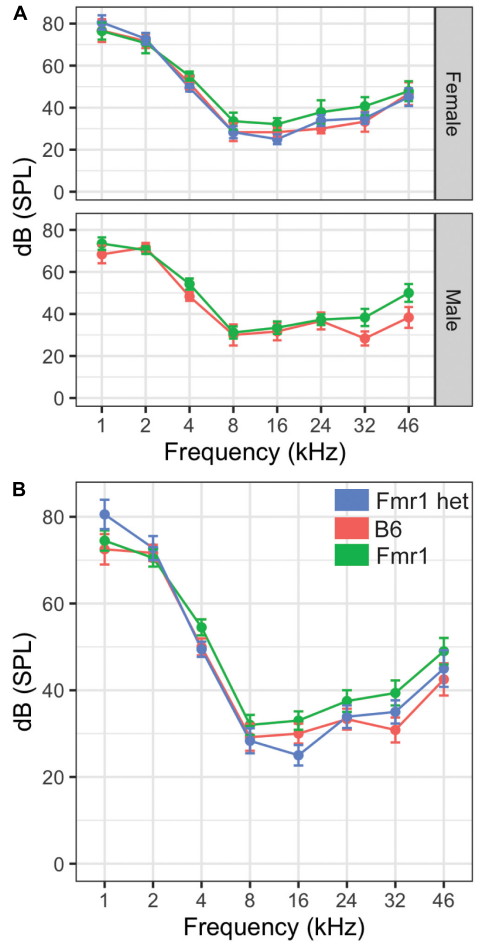

FIGURE 3 | Hearing threshold (dB SPL) was measured across frequencies (1–46 kHz) in male and female mice of all genotypes **(A)**. There were no differences in the hearing range between Fmr1 (green), B6 (red), and Fmr1 het (blue) mice of either sex (top panel **A**). When sexes were combined, there was no significant difference in hearing across frequencies **(B)**. Data represent 6 B6, 7 Fmr1, 9 Fmr1 het females and 6 B6, 11 Fmr1 males.

and 3rd quartiles, respectively), the whiskers represent ± 1.5 times the interquartile range. The data that falls outside the range are plotted as individual points. Multivariate data (i.e., monaural peak amplitude and latency, audiogram, and BIC amplitude and latency across ITD) were analyzed using linear mixed effects (lme4) models (Bates et al., 2015) with sex, genotype, litter, and condition (i.e., ITD, frequency, peak) as fixed effects and animal as a random effect. It was expected that there may be differences between the sexes and genotypes; therefore, *a priori*, it was determined that estimated marginal means [emmeans; (Lenth, 2019)] would be used for pairwise comparisons between sexes and genotype. Two-way ANOVAs were performed to compare relationships between morphological features, sex, and genotype with the adjusted Tukey *post hoc* analysis to compare groups. Where values are indicated as statistically significant between the two genotypes, * indicated a p-value of <0.05, ** $p < 0.01$, and *** $p < 0.0001$.

RESULTS

We used both morphological and physiological features to examine hearing differences in a commonly used mouse model with FXS, C57BL/6J across genotypes and sexes. Hearing measurements included the frequency hearing range, monaural hearing ability, and binaural processing using the ABR, while morphological features included pinna and head measurements.

Morphological Features

People with FXS have altered craniofacial features, including large ears (Loesch et al., 1988). Consistent with our previous work (McCullagh et al., 2020a), we saw no difference between B6, Fmr1, or Fmr1 het animals for pinna attributes (**Figure 1C** pinna width, **Figure 1D** pinna length, **Figure 1B** effective diameter). In addition, pinna characteristics were the same between the sexes independent of genotype (p = 0.175 pinna width, p = 0.96 pinna length, p = 0.267 effective diameter **Figures 1B–D**). When genotypes were compared within the same sex, there were no differences in weight, but sexes were significantly different independent of genotype (p = 0.0023) with females weighing significantly less than males. Similar to the pinna morphology, there was no significant difference in either distance between pinna or distance from the nose to pinna between the genotypes or sexes (**Figures 1E,F**). These data suggest that mice do not share the same craniofacial changes, at least in the measurements described here, as people with FXS.

Hearing Range

Our previous study showed that Fmr1 mice have increased thresholds for high-frequency hearing compared with those in B6 at 16 kHz (McCullagh et al., 2020a). However, that study was limited by measuring only three frequencies (i.e., 4, 8, and 16 kHz) and seven mice of each genotype (i.e., combined sexes). Mice hear much higher frequencies than humans (Radziwon et al., 2009); therefore, we wanted to measure whether this high-frequency hearing loss exists across the frequencies in which mice hear in Fmr1 mutants and with a more in-depth sex-specific analysis. Interestingly, there were no differences between genotypes across the frequencies tested (**Figure 3**). There were no significant differences in hearing range between the sexes. Best frequencies for both genotypes, as indicated by lower threshold, of mice were between 8–46 kHz consistent with specialized high frequency hearing.

Monaural Hearing

Amplitude and latency of monaural ABRs correspond with the neural activity across the ascending auditory pathway, with each wave representing different brain areas involved in the auditory processing (Alvarado et al., 2012). Other studies have shown both latency and amplitude alterations in the FVB mouse strain of Fmr1 mutation (Kim et al., 2013; Rotschafer et al., 2015; El-Hassar et al., 2019). We measured ABR responses of Fmr1 mutants to monaural click stimuli compared with B6 mutant mice to determine if they have a similar ABR phenotype to the

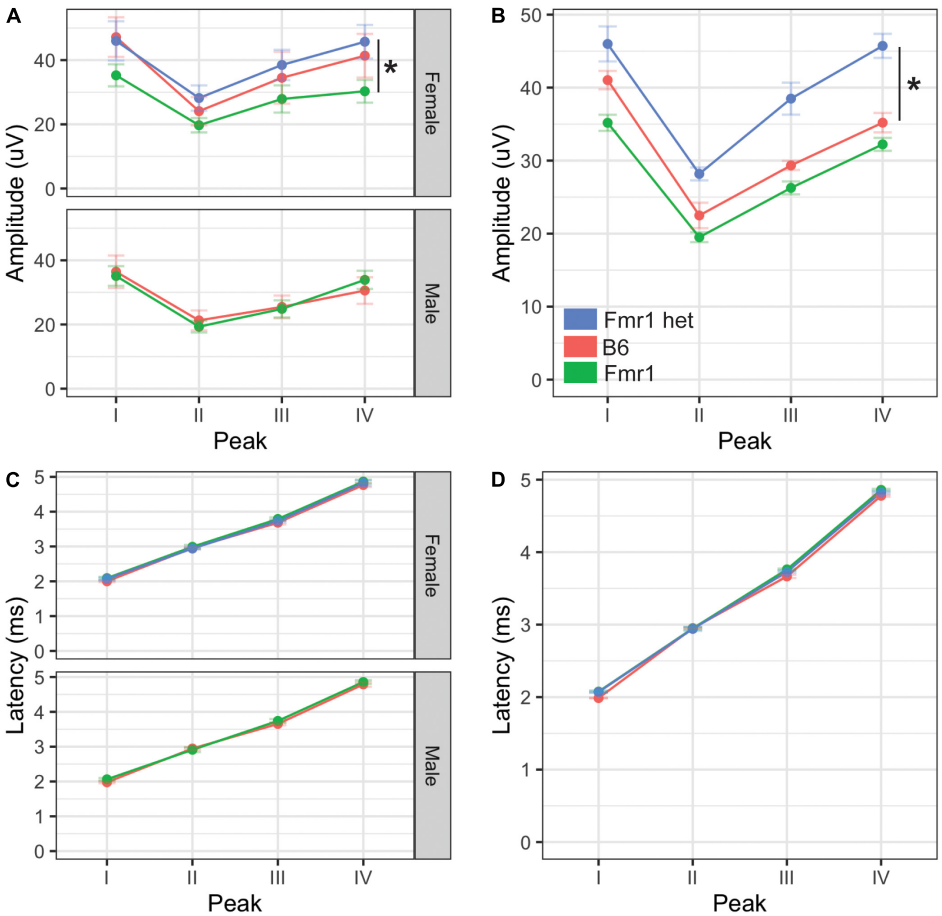

FIGURE 4 | Monaural hearing in mice with FXS. Monaural amplitudes and latencies for peaks I–IV of the ABR were recorded for Fmr1, Fmr1 het, and B6 animals. Peak IV amplitude was significantly lower in Fmr1 mice females compared with Fmr1 het females (**A**, upper). There were no significant differences in amplitudes for males (**A**, lower). When combined, there was a significant difference in Fmr1 het animals compared with Fmr1 **(B)**. There was no difference in latency of peaks I–IV between sexes **(C)** or genotypes **(D)**. *$p < 0.05$. Data represent 6 B6, 12 Fmr1, and 9 Fmr1 het females and 8 B6 and 14 Fmr1 males.

FVB strain. We saw no differences in overall click threshold for either genotype or sex ($p = 0.102$ genotype and $p = 0.47$ for sex). The amplitude of monaural responses was significantly lower for wave IV of the ABR in Fmr1 females compared with Fmr1 het females (**Figure 4A** upper). Indeed, Fmr1 het female amplitudes were closer to B6 than Fmr1 females, though Fmr1 females were not significantly different from B6. In contrast, Fmr1 male amplitudes for waves I–IV were not different from B6 (**Figure 4A** lower). When sexes were combined, Fmr1 het females had significantly higher amplitudes than B6 and were close to being significantly higher than Fmr1 mice ($p = 0.0593$). Consistent with sex driving the differences in genotype, peak amplitudes varied between the sexes. Female B6 mice had significantly higher amplitude peaks I and IV compared with B6 males ($p = 0.0295$ peak I and $p = 0.0289$ peak IV). In contrast, there were no sex differences between male and female Fmr1 mice, suggesting a more male-like phenotype (i.e., independent of genotype) in homozygous Fmr1 females. There were no differences between the sexes or genotypes in latency of monaural peaks (**Figures 4C,D**).

Binaural Hearing

While the monaural ABR provides information about binaural areas of the brain stem (i.e., potentially peaks III and IV), since they are elicited by either sound played directly to one ear (closed field) or equally to both ears (open field), little information can be gained about binaural integration of sound information. We used the BIC of the ABR to measure the ability of the binaural processing of the brain stem as the BIC varies with ITDs played to both ears. We saw no differences in amplitude of the BIC at any ITD between the two genotypes ($p = 0.809$) or with sex ($p = 0.6904$, **Figures 5A,B**), although there was a significant difference between Fmr1 male and female mouse BIC amplitudes at 1.5 ms ITD. There were no differences between the sexes for B6 mice for any ITD amplitude. Latency of the BIC was significantly slower in male Fmr1 compared with that in B6 males (**Figure 5C**, lower panel) only at 0 ITD, with no difference in genotype for female mice (**Figure 5C**, upper panel). When data were combined for sexes across genotypes, there was no significant difference in the latency of the BIC at any ITD (**Figure 5D**). There were differences in latency of the BIC between B6 (-1.5 ms) and Fmr1

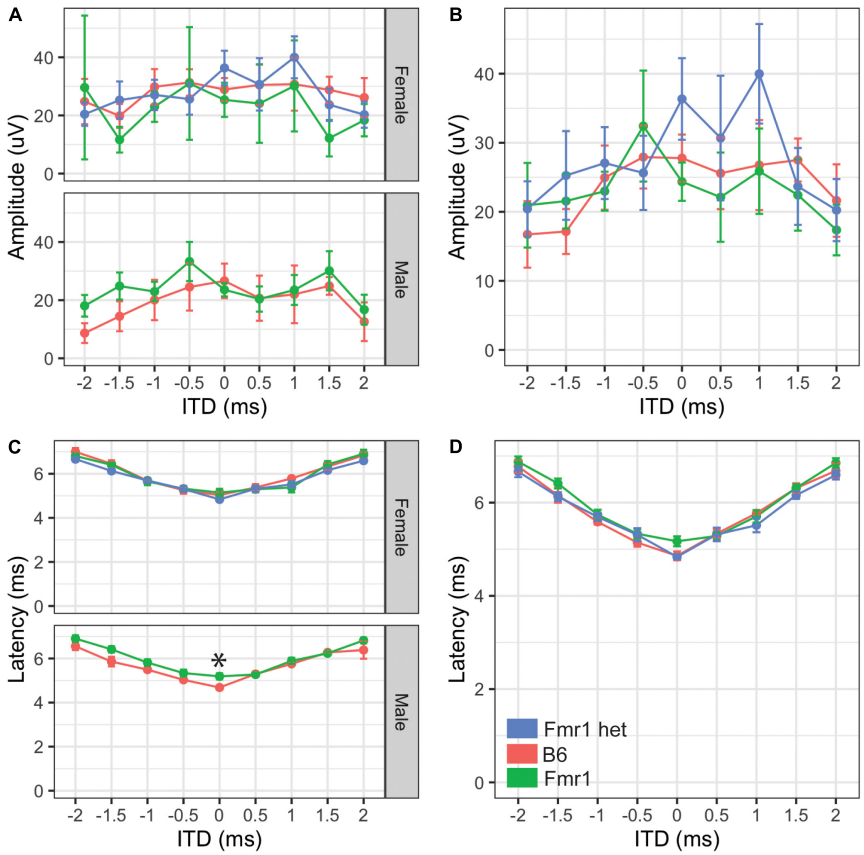

FIGURE 5 | Binaural hearing in Fragile X syndrome (FXS) mice. Binaural amplitudes and latencies for the BIC at ITDs between –2 to + 2 ms in 0.5 ms steps were recorded for Fmr1 (green), Fmr1 het (blue), and B6 (red) animals. No differences in amplitude of the BIC with ITD for females (**A**, upper) or males (**A**, lower). When the sexes were combined, there was no significant difference in amplitude of the BIC with ITD **(B)**. Fmr1 males had significantly longer latency of the BIC at 0 ITD compared with B6 males (C, lower), while there was no difference in latency of female responses (**C**, upper). When the sexes were combined, there was no difference in the BIC latency across ITDs between the genotypes **(D)**. *$p < 0.05$. Data represent 6 B6, 7 Fmr1, and 9 Fmr1 het females and 6 B6 and 9 Fmr1 males.

(1 ms) males and females although there was no overall main effect of sex ($p = 0.3367$).

DISCUSSION

This is the first study to characterize the ABR in the C57BL/6J Fmr1 mutant mouse and, in particular, highlights morphological characteristics, hearing range, monaural ABRs, and binaural integration across sexes and in heterozygote females. Consistent with previous study, we saw an increase in the hearing threshold at high frequencies in Fmr1 mice, although this phenotype is male specific and no change in morphology (pinna or facial characteristics) (McCullagh et al., 2020a). Female Fmr1 mice have reduced wave IV amplitudes of the monaural ABR, and wild-type females have increased wave I and IV amplitudes compared with B6 males, suggesting that female Fmr1 mice have a more male-like phenotype for monaural ABR amplitude. Finally, we showed that male Fmr1 mice have increased latency of the BIC at 0 ITD but not other ITDs or changes in amplitude of the BIC across ITD compared with B6 animals, suggesting changes in the timing of the processing of binaural information that does not change overall ITD following ability.

The pinnae size and shape are the first two features available to determine sound localization ability in animals with external ears (Butler, 1975; Musicant and Butler, 1984). Craniofacial alterations including prominent ears and elongated face are hallmark features of humans with FXS (Loesch et al., 1988; Heulens et al., 2013) and indeed may be a factor in auditory hypersensitivity that has been underexplored. Consistent with our previous study, we saw no alterations in the pinna or facial characteristics in the C57BL/6J mouse model with FXS (McCullagh et al., 2020a) using calipers as a measurement tool. Others have explored differences in the morphological skull in mice with FXS using different tools, such as CT/MRI (Ellegood et al., 2010) and micro-CT (Heulens et al., 2013) with mixed results. Heulens et al., 2013 showed alterations in skull and jaw characteristics that had not been characterized previously with a similar technique (Ellegood et al., 2010) although differences may be due to how features were measured. We also saw no difference in weight of Fmr1 animals compared with the wild-type, which is in contrast to our previous study where we noted that Fmr1 animals weighed less than wild-type (McCullagh et al., 2020a) and others that showed an increase in male Fmr1 mouse weight compared with the wild-type (Leboucher et al., 2019). Differences in weight may be due to the inclusion of female

animals (McCullagh et al., 2020a) and older animals (Leboucher et al., 2019). Overall changes in pinna morphology may still be an important factor in sound localization ability in Fmr1 animals and should be explored with more detailed techniques to determine if increased pinna measures in both humans and animal models may underly some aspect of auditory hypersensitivity symptomology.

Our previous results showed increased hearing thresholds at high frequencies (16 kHz) measured by ABR in the C57BL/6J Fmr1 strain with data combined for the sexes (McCullagh et al., 2020a). In the current study, we do not see increased thresholds at 16 kHz but do see a trend towards increased thresholds at higher frequencies in male Fmr1 mice specifically, though not significant. These data are consistent with the increased thresholds across frequencies seen in adult male FVB Fmr1 mice (Rotschafer et al., 2015), though note that there was no change in threshold across frequencies in males of the same FVB strain at younger ages (Kim et al., 2013; El-Hassar et al., 2019). Additional studies should examine the hearing range across development and sexes in both strains to further show whether loss of high-frequency hearing is a conserved feature in FXS.

Previous studies in the FVB Fmr1 mouse line show a robust wave I amplitude decrease in males across ages (Rotschafer et al., 2015; El-Hassar et al., 2019), although see Kim et al. (2013). We did not see any change in wave I amplitude in the C57BL/6J Fmr1 line in adult animals of either sex. These conflicting results may be in part due to the earlier onset age-related hearing loss, which can be seen as decreases in early waves of the ABR, that occurs in the B6 background (Hunter and Willott, 1987). Changes in wave I amplitude specific to FXS may be masked by overall decreases in wave I amplitude across genotypes in this background. Interestingly, data in male FVB Fmr1 mice show no differences (adults, Kim et al., 2013; Rotschafer et al., 2015) or increased amplitudes in wave IV of the ABR (young, El-Hassar et al., 2019), whereas our data show a decreased wave IV amplitude in Fmr1 females on the B6 background. These differences again may be due to differences in sexes and ages of animals tested. Finally, our finding of no difference in latency of monaural waves is consistent with the majority of the work in FVB mice (Rotschafer et al., 2015; El-Hassar et al., 2019), although note that Kim et al., 2013 showed shorter latency for wave I. Our data further add to the knowledge of ABR phenotypes that might be consistent across genotypes.

While ours is the first study to characterize the BIC in an FXS-mutant mouse strain, our data are consistent with the BIC as it varies with ITD in mice (Benichoux et al., 2018). Namely, mice have a small range of ITD cues available due to their small head size, and therefore, the BIC amplitude decreases with increasing ITD between the ears, but this overall amplitude change is smaller than animals with more dominant ITD hearing ability (such as chinchilla or cats)(Benichoux et al., 2018). Additionally, consistent with previous study, the BIC latency gets longer with increasing ITD (Ferber et al., 2016; Laumen et al., 2016; Benichoux et al., 2018). Interestingly, our work in mice with FXS is consistent with an increased latency of the BIC seen in a study in autistic people (ElMoazen et al., 2019), although they also see a decrease in the amplitude of the BIC. Our findings that the BIC latency is only significant in males at 0 ITD potentially suggest that there is overall slowing of binaural processing in the brain stem, which may ultimately impact binaural hearing, but that it is not dependent on ITD, which would be consistent with mice that do not rely as predominantly on ITD cues compared with other species. In addition, while these results do not directly measure auditory hypersensitivity, underlying alterations to the timing of brain stem or amplitude of brain stem regions will impact later processing of this information as it moves through the ascending auditory pathway to other subcortical and cortical areas.

The subject of sex differences in animal models is important for fully understanding the complexities of disorders such as ASD or FXS, which seem to impact females differently than males (Werling and Geschwind, 2013; Nolan et al., 2017). In FXS, due to it being an X-linked disorder, there is a higher prevalence in males than females, which can undergo X-inactivation on the effected X chromosome (i.e., genetic mosaicism) (Kirchgessner et al., 1995). However, mice offer a unique opportunity to measure both heterozygote and homozygous females giving insight into potential sex differences related to loss of Fmr1 on one or both X chromosomes. Our data suggest that there are indeed differences in auditory phenotypes between heterozygous and homozygous females (wave IV amplitude) in addition to differences between males and females. These and future data comparing female Fmr1 subtypes may give insight into the role of X-inactivation in phenotypes of auditory brain stem processing.

CONCLUSION

This study offers important insight into auditory phenotypes that may be shared or differ between background strains of mice with FXS. In addition, while subtle, we showed sex-specific and full or heterozygote mutation-specific differences in the auditory brain stem function for both monaural and binaural hearing in B6 background mice. Further studies measuring auditory phenotypes for B6 mice in earlier ages across the sexes would be useful to further characterize potential similarities compared with the FVB Fmr1 strain. In addition, characterizing the BIC in the FVB strain would be useful to elucidate if latency phenotypes are consistent across backgrounds.

DATA AVAILABILITY STATEMENT

The raw data supporting the conclusions of this article will be made available by the authors, without undue reservation.

ETHICS STATEMENT

The animal study was reviewed and approved by Oklahoma State University IACUC.

AUTHOR CONTRIBUTIONS

EM and AC collected the data for the manuscript. EM performed the statistical analyses, created the figures for the manuscript, and

developed the ideas and methods. Both authors helped write and revise the manuscript.

FUNDING

Supported by NIH 1R15HD105231-01. Preliminary work was also funded by a FRAXA research grant and NIH 3T32DC012280-05S1.

ACKNOWLEDGMENTS

We would like to thank members of the McCullagh lab and team mouse, including Ishani Ray and Sabiha Alam, which assisted with ABRs. Furthermore, we would like to acknowledge Shani Poleg and Daniel Tollin for helping us set up these experiments in Colorado and continue them in Oklahoma.

REFERENCES

Abbeduto, L., and Hagerman, R. J. (1997). Language and communication in fragile X syndrome. *Ment. Retard. Dev. Disabil. Res. Rev.* 3, 313–322. doi: 10.1002/(SICI)1098-277919973:4<313::AID-MRDD6<3.0.CO;2-O

Alvarado, J. C., Fuentes-Santamaría, V., Jareño-Flores, T., Blanco, J. L., and Juiz, J. M. (2012). Normal variations in the morphology of auditory brainstem response (ABR) waveforms: a study in Wistar rats. *Neurosci. Res.* 73, 302–311. doi: 10.1016/j.neures.2012.05.001

Anbuhl, K. L., Benichoux, V., Greene, N. T., Brown, A. D., and Tollin, D. J. (2017). Development of the head, pinnae, and acoustical cues to sound location in a precocial species, the guinea pig (*Cavia porcellus*). *Hear Res.* 356, 35–50. doi: 10.1016/j.heares.2017.10.015

Arnett, M. T., Herman, D. H., and McGee, A. W. (2014). Deficits in tactile learning in a mouse model of fragile X syndrome. *PLoS One* 9:e109116. doi: 10.1371/journal.pone.0109116

Bates, D., Mächler, M., Bolker, B., and Walker, S. (2015). Fitting linear mixed-effects models using lme4. *J. Statist. Softw.* 67, 1–48. doi: 10.18637/jss.v067.i01

Beebe, K., Wang, Y., and Kulesza, R. (2014). Distribution of fragile X mental retardation protein in the human auditory brainstem. *Neuroscience* 273, 79–91. doi: 10.1016/j.neuroscience.2014.05.006

Benichoux, V., Ferber, A., Hunt, S., Hughes, E., and Tollin, D. (2018). Across species "natural ablation" reveals the brainstem source of a noninvasive biomarker of binaural hearing. *J. Neurosci.* 38, 8563–8573. doi: 10.1523/JNEUROSCI.1211-18.2018

Beutelmann, R., Laumen, G., Tollin, D., and Klump, G. M. (2015). Amplitude and phase equalization of stimuli for click evoked auditory brainstem responses. *J. Acoust. Soc. Am.* 137, EL71–EL77. doi: 10.1121/1.4903921

Brittan-Powell, E. F., and Dooling, R. J. (2004). Development of auditory sensitivity in budgerigars (*Melopsittacus undulatus*). *J. Acoust. Soc. Am.* 115, 3092–3102. doi: 10.1121/1.1739479

Bronkhorst, A. W. (2015). The cocktail-party problem revisited: early processing and selection of multi-talker speech. *Atten. Percept. Psychophys.* 77, 1465–1487. doi: 10.3758/s13414-015-0882-9

Brown, M. R., Kronengold, J., Gazula, V.-R., Chen, Y., Strumbos, J. G., Sigworth, F. J., et al. (2010). Fragile X mental retardation protein controls gating of the sodium-activated potassium channel Slack. *Nat. Neurosci.* 13, 819–821. doi: 10.1038/nn.2563

Butler, R. A. (1975). "The influence of the external and middle ear on auditory discriminations," in *Auditory System: Physiology (CNS) Behavioral Studies Psychoacoustics Handbook of Sensory Physiology*, eds M. Abeles, R. A. Bredberg, J. Butler, H. Casseday, J. E. Desmedt, I. T. Diamond, et al. (Berlin: Springer), 247–260. doi: 10.1007/978-3-642-65995-9_6

Chen, L., and Toth, M. (2001). Fragile X mice develop sensory hyperreactivity to auditory stimuli. *Neuroscience* 103, 1043–1050. doi: 10.1016/s0306-4522(01)00036-7

Curry, R. J., Peng, K., and Lu, Y. (2018). Neurotransmitter- and release-mode-specific modulation of inhibitory transmission by group I metabotropic glutamate receptors in central auditory neurons of the mouse. *J. Neurosci.* 38, 8187–8199. doi: 10.1523/JNEUROSCI.0603-18.2018

Dahlhaus, R. (2018). Of men and mice: modeling the fragile X syndrome. *Front. Mol. Neurosci.* 11:41. doi: 10.3389/fnmol.2018.00041

El-Hassar, L., Song, L., Tan, W. J. T., Large, C. H., Alvaro, G., Santos-Sacchi, J., et al. (2019). Modulators of Kv3 potassium channels rescue the auditory function of fragile X mice. *J. Neurosci.* 39, 4797–4813. doi: 10.1523/JNEUROSCI.0839-18.2019

Ellegood, J., Pacey, L. K., Hampson, D. R., Lerch, J. P., and Henkelman, R. M. (2010). Anatomical phenotyping in a mouse model of fragile X syndrome with magnetic resonance imaging. *Neuroimage* 53, 1023–1029. doi: 10.1016/j.neuroimage.2010.03.038

ElMoazen, D., Sobhy, O., Abdou, R., and Ismail, H. (2019). Binaural interaction component of the auditory brainstem response in children with autism spectrum disorder. *Int. J. Pediat. Otorhinolaryngol.* 19:109850. doi: 10.1016/j.ijporl.2019.109850

Ethridge, L. E., White, S. P., Mosconi, M. W., Wang, J., Pedapati, E. V., Erickson, C. A., et al. (2017). Neural synchronization deficits linked to cortical hyper-excitability and auditory hypersensitivity in fragile X syndrome. *Mol. Autism* 8:140. doi: 10.1186/s13229-017-0140-1

Ferber, A. T., Benichoux, V., and Tollin, D. J. (2016). Test-retest reliability of the binaural interaction component of the auditory brainstem response. *Ear Hear* 37, e291–e301. doi: 10.1097/AUD.0000000000000315

Garcia-Pino, E., Gessele, N., and Koch, U. (2017). Enhanced excitatory connectivity and disturbed sound processing in the auditory brainstem of fragile X mice. *J. Neurosci.* 37, 7403–7419. doi: 10.1523/JNEUROSCI.2310-16.2017

Grothe, B., Pecka, M., and McAlpine, D. (2010). Mechanisms of sound localization in mammals. *Physiol. Rev.* 90, 983–1012. doi: 10.1152/physrev.00026.2009

Hagerman, R. J., and Hagerman, P. J. (2002). *Fragile X Syndrome: Diagnosis, Treatment and Research*. Baltimore, MY: Johns Hopkins University Press.

Heulens, I., Suttie, M., Postnov, A., De Clerck, N., Perrotta, C. S., Mattina, T., et al. (2013). Craniofacial characteristics of fragile X syndrome in mouse and man. *Eur. J. Hum. Genet.* 21, 816–823. doi: 10.1038/ejhg.2012.265

Hunter, K. P., and Willott, J. F. (1987). Aging and the auditory brainstem response in mice with severe or minimal presbycusis. *Hear Res.* 30, 207–218. doi: 10.1016/0378-5955(87)90137-7

Kim, H., Gibboni, R., Kirkhart, C., and Bao, S. (2013). Impaired critical period plasticity in primary auditory cortex of fragile X model mice. *J. Neurosci.* 33, 15686–15692. doi: 10.1523/JNEUROSCI.3246-12.2013

Kirchgessner, C. U., Warren, S. T., and Willard, H. F. (1995). X inactivation of the FMR1 fragile X mental retardation gene. *J. Med. Genet.* 32, 925–929. doi: 10.1136/jmg.32.12.925

Laumen, G., Ferber, A. T., Klump, G. M., and Tollin, D. J. (2016). The physiological basis and clinical use of the binaural interaction component of the auditory brainstem response. *Ear Hear* 37, e276–e290. doi: 10.1097/AUD.0000000000000301

Leboucher, A., Bermudez-Martin, P., Mouska, X., Amri, E.-Z., Pisani, D. F., and Davidovic, L. (2019). Fmr1-deficiency impacts body composition, skeleton, and bone microstructure in a mouse model of fragile X syndrome. *Front. Endocrinol. (Lausanne)* 10:678. doi: 10.3389/fendo.2019.00678

Lenth, R. (2019). *emmeans: Estimated Marginal Means, aka Least-Squares Means.* Available online at: https://CRAN.R-project.org/package=emmeans

Levine, R. A. (1981). Binaural interaction in brainstem potentials of human subjects. *Ann. Neurol.* 9, 384–393. doi: 10.1002/ana.410090412

Loesch, D. Z., Lafranchi, M., and Scott, D. (1988). Anthropometry in martin-bell syndrome. *Am. J. Med. Genet.* 30, 149–164. doi: 10.1002/ajmg.1320300113

Lovelace, J. W., Ethell, I. M., Binder, D. K., and Razak, K. A. (2018). Translation-relevant EEG phenotypes in a mouse model of Fragile X Syndrome. *Neurobiol. Dis.* 115, 39–48. doi: 10.1016/j.nbd.2018.03.012

Lovelace, J. W., Rais, M., Palacios, A. R., Shuai, X., Bishay, S., Popa, O., et al. (2020). Deletion of Fmr1 from forebrain excitatory neurons triggers abnormal cellular,

EEG and behavioral phenotypes in the auditory cortex of a mouse model of Fragile X Syndrome. *Cereb. Cortex* 30, 969–988. doi: 10.1093/cercor/bhz141

Lu, Y. (2019). Subtle differences in synaptic transmission in medial nucleus of trapezoid body neurons between wild-type and Fmr1 knockout mice. *Brain Res.* 1717, 95–103. doi: 10.1016/j.brainres.2019.04.006

McCullagh, E. A., Poleg, S., Greene, N. T., Huntsman, M. M., Tollin, D. J., and Klug, A. (2020a). Characterization of auditory and binaural spatial hearing in a fragile X syndrome mouse model. *eNeuro* 7:ENEURO.0300–19.2019. doi: 10.1523/ENEURO.0300-19.2019

McCullagh, E. A., Rotschafer, S. E., Auerbach, B. D., Klug, A., Kaczmarek, L. K., Cramer, K. S., et al. (2020b). Mechanisms underlying auditory processing deficits in fragile X syndrome. *FASEB J.* 34, 3501–3518. doi: 10.1096/fj.201902435R

McCullagh, E. A., Salcedo, E., Huntsman, M. M., and Klug, A. (2017). Tonotopic alterations in inhibitory input to the medial nucleus of the trapezoid body in a mouse model of Fragile X syndrome. *J. Comparat. Neurol.* 262:375. doi: 10.1002/cne.24290

Musicant, A. D., and Butler, R. A. (1984). The influence of pinnae-based spectral cues on sound localization. *J. Acoust. Soc. Am.* 75, 1195–1200. doi: 10.1121/1.390770

New, E. M., Li, B.-Z., Lei, T., and McCullagh, E. A. (2021). *Hearing Ability of Prairie Voles (Microtus ochrogaster)*. **. doi: 10.1101/2021.10.07.463519

Nolan, S. O., Reynolds, C. D., Smith, G. D., Holley, A. J., Escobar, B., Chandler, M. A., et al. (2017). Deletion of Fmr1 results in sex-specific changes in behavior. *Brain Behavior* 7:e00800. doi: 10.1002/brb3.800

R Core Team (2013). *R: A Language and Environment for Statistical Computing*. Vienna: R Foundation for Statistical Computing.

Radziwon, K. E., June, K. M., Stolzberg, D. J., Xu-Friedman, M. A., Salvi, R. J., and Dent, M. L. (2009). Behaviorally measured audiograms and gap detection thresholds in CBA/CaJ mice. *J. Comp. Physiol. A Neuroethol. Sens. Neural Behav. Physiol.* 195, 961–969. doi: 10.1007/s00359-009-0472-1

Rais, M., Binder, D. K., Razak, K. A., and Ethell, I. M. (2018). Sensory processing phenotypes in fragile X syndrome. *ASN Neuro* 10, 1–19. doi: 10.1177/1759091418801092

Razak, K. A., Binder, D. K., and Ethell, I. M. (2021). Neural correlates of auditory hypersensitivity in fragile X syndrome. *Front. Psychiatry* 12:1544. doi: 10.3389/fpsyt.2021.720752

Rotschafer, S. E., and Cramer, K. S. (2017). Developmental emergence of phenotypes in the auditory brainstem nuclei of Fmr1Knockout mice. *eNeuro* 4, 1–21. doi: 10.1523/ENEURO.0264-17.2017

Rotschafer, S. E., Marshak, S., and Cramer, K. S. (2015). Deletion of Fmr1 alters function and synaptic inputs in the auditory brainstem. *PLoS One* 10:e0117266. doi: 10.1371/journal.pone.0117266

Santos, M., Marques, C., Nóbrega Pinto, A., Fernandes, R., Coutinho, M. B., Almeida, E., et al. (2017). Autism spectrum disorders and the amplitude of auditory brainstem response wave I. *Autism. Res.* 10, 1300–1305. doi: 10.1002/aur.1771

Sinclair, D., Oranje, B., Razak, K. A., Siegel, S. J., and Schmid, S. (2017). Sensory processing in autism spectrum disorders and Fragile X syndrome—From the clinic to animal models. *Neurosci. Biobehav. Rev.* 76, 235–253. doi: 10.1016/j.neubiorev.2016.05.029

Stefanelli, A. C. G. F., Zanchetta, S., Furtado, E. F., Stefanelli, A. C. G. F., Zanchetta, S., and Furtado, E. F. (2020). Auditory hyper-responsiveness in autism spectrum disorder, terminologies and physiological mechanisms involved: systematic review. *CoDAS* 32:287. doi: 10.1590/2317-1782/20192018287

The Dutch-Belgian Fragile X Consorthium, Bakker, C. E., Verheij, C., Willemsen, R., van der Helm, R., Oerlemans, F., et al. (1994). Fmr1 knockout mice: a model to study fragile X mental retardation. *Cell* 78, 23–33. doi: 10.1016/0092-8674(94)90569-X

Tian, Y., Yang, C., Shang, S., Cai, Y., Deng, X., Zhang, J., et al. (2017). Loss of FMRP impaired hippocampal long-term plasticity and spatial learning in rats. *Front. Mol. Neurosci.* 10:269. doi: 10.3389/fnmol.2017.00269

Till, S. M., Asiminas, A., Jackson, A. D., Katsanevaki, D., Barnes, S. A., Osterweil, E. K., et al. (2015). Conserved hippocampal cellular pathophysiology but distinct behavioural deficits in a new rat model of FXS. *Hum. Mol. Genet.* 24, 5977–5984. doi: 10.1093/hmg/ddv299

Visser, E., Zwiers, M. P., Kan, C. C., Hoekstra, L., van Opstal, A. J., and Buitelaar, J. K. (2013). Atypical vertical sound localization and sound-onset sensitivity in people with autism spectrum disorders. *J. Psychiatry Neurosci.* 38, 398–406. doi: 10.1503/jpn.120177

Wang, T., de Kok, L., Willemsen, R., Elgersma, Y., and Borst, J. G. G. (2015). In vivo synaptic transmission and morphology in mouse models of Tuberous sclerosis, Fragile X syndrome, Neurofibromatosis type 1, and Costello syndrome. *Front. Cell Neurosci.* 9:234. doi: 10.3389/fncel.2015.00234

Wang, Y., Sakano, H., Beebe, K., Brown, M. R., de Laat, R., Bothwell, M., et al. (2014). Intense and specialized dendritic localization of the fragile X mental retardation protein in binaural brainstem neurons: a comparative study in the alligator, chicken, gerbil, and human: FMRP localization in NL/MSO dendrites. *J. Comparat. Neurol.* 522, 2107–2128. doi: 10.1002/cne.23520

Werling, D. M., and Geschwind, D. H. (2013). Sex differences in autism spectrum disorders. *Curr. Opin. Neurol.* 26, 146–153. doi: 10.1097/WCO.0b013e32835ee548

Wickham, H. (2016). *ggplot2: Elegant Graphics for Data Analysis*. New York, NY: Springer-Verlag.

Conflict of Interest: The authors declare that the research was conducted in the absence of any commercial or financial relationships that could be construed as a potential conflict of interest.

The handling editor declared a past co-authorship with one of the authors EM.

frontiers in Integrative Neuroscience

MINI REVIEW
published: 28 January 2022
doi: 10.3389/fnint.2022.810425

Cerebellar Contributions to Social Cognition in ASD: A Predictive Processing Framework

Isabelle R. Frosch[1], *Vijay A. Mittal*[1,2,3,4,5] *and Anila M. D'Mello*[6]*

[1]Department of Psychology, Northwestern University, Evanston, IL, United States, [2]Institute for Innovations in Developmental Sciences, Northwestern University, Evanston and Chicago, IL, United States, [3]Department of Psychiatry, Northwestern University, Chicago, IL, United States, [4]Department of Medical Social Sciences, Northwestern University, Chicago, IL, United States, [5]Institute for Policy Research, Northwestern University, Chicago, IL, United States, [6]McGovern Institute for Brain Research, Massachusetts Institute of Technology, Cambridge, MA, United States

Functional, structural, and cytoarchitectural differences in the cerebellum are consistently reported in Autism Spectrum Disorders (ASD). Despite this, the mechanisms governing cerebellar contributions to ASD, particularly within the sociocognitive domain, are not well understood. Recently, it has been suggested that several core features of ASD may be associated with challenges creating and using prior expectations or predictions to rapidly adapt to changing stimuli or situations, also known as adaptive prediction. Importantly, neuroimaging, clinical, and animal work find that the cerebellum supports adaptive prediction in both motor and non-motor domains. Perturbations to the cerebellum *via* injury or neuromodulation have been associated with impairments in predictive skills. Here, we review evidence for a cerebellar role in social cognition and adaptive prediction across individuals with and without ASD.

Keywords: autism spectrum disorder (ASD), cerebellum, adaptive prediction, predictive processing, neuroimaging, social cognition, language, action perception

OPEN ACCESS

Edited by:
Eric London, Institute for Basic Research in Developmental Disabilities (IBR), United States

Reviewed by:
Aleksandra Badura, Erasmus Medical Center, Netherlands

***Correspondence:**
Anila M. D'Mello
admello@mit.edu

Received: *06 November 2021*
Accepted: *04 January 2022*
Published: *28 January 2022*

Citation:
Frosch IR, Mittal VA and D'Mello AM (2022) Cerebellar Contributions to Social Cognition in ASD: A Predictive Processing Framework. Front. Integr. Neurosci. 16:810425. doi: 10.3389/fnint.2022.810425

INTRODUCTION

Differences in social cognition, including interpreting socio-communicative intent from gestures and adapting behaviors to different social contexts are characteristic of Autism Spectrum Disorders (ASD; American Psychiatric Association, 2013). Although many brain regions support social cognition, over the past decades, there has been a growing recognition of the sociocognitive role of the cerebellum in both typical and atypical development (Fatemi et al., 2012; D'Mello and Stoodley, 2015; Stoodley and Tsai, 2021). The importance of the cerebellum to social cognition is particularly evidenced by its involvement in this capacity in ASD: the cerebellum is the most consistently implicated structure in ASD and neuroimaging, clinical, and preclinical studies in ASD consistently report associations between the cerebellum and social behaviors (Steadman et al., 2014, D'Mello and Stoodley, 2015; Ellegood et al., 2015). Moreover, neuromodulation of the cerebellum in ASD mouse models can ameliorate social symptoms (Stoodley et al., 2017). What remains lacking are mechanistic frameworks designed to integrate this wealth of empirical and conceptual work. In the motor realm, the cerebellum is well established as a core structure in adaptive prediction—or the process by which we make and update models of our world to optimize behavior (Ito, 2006). More recently, the field has begun to understand that the cerebellum also

contributes to adaptive prediction in social cognition, which requires us to interpret the actions of others, anticipate what they might say and when they might say it, and infer mental states from their actions and words (Koster-Hale and Saxe, 2013; Stoodley and Tsai, 2021). Here, we review the existing evidence for a cerebellar role in adaptive prediction and explore whether differences in cerebellar adaptive prediction may contribute to both strengths and challenges in social cognition in ASD. This review begins by discussing the importance of adaptive prediction for social cognition and then moves to a discussion of the basic organization of the cerebellum as well as empirical evidence for cerebellar contributions to adaptive prediction in social cognition. Next, it turns to examining the literature on differences in adaptive prediction for social cognition in autism, specifically focusing on cerebellar findings. We conclude with directions for future research on cerebellar adaptive prediction and ASD.

LINKING ADAPTIVE PREDICTION AND SOCIAL COGNITION IN ASD

Adaptive prediction facilitates the integration of proximal and distal experiences (Friston, 2005) to render social information processing efficient in the moment. This involves using past experiences to: (1) derive intent from the actions of others; (2) anticipate what they may say; and (3) infer their mental states (i.e., theory of mind or mentalizing) to enable rapid online correction of our own behaviors in response (Koster-Hale and Saxe, 2013). Consider a conversational partner who repeatedly clears their throat. We may infer that they want to interject and respond by pausing. If they do not interject, or if they mention recovering from a cold, we adapt our future behavior accordingly (e.g., pause less or speak louder in response to this behavior). Updating socio-cognitive models with novel information thereby impacts thoughts and actions.

A consistent observation is that some autistic individuals[1] do not rely on past information to flexibly adjust their behavior and adapt to changing situations (Cannon et al., 2021). This observation has shaped predictive coding theoretical frameworks of ASD and may explain challenges (Pellicano and Burr, 2012; Lawson et al., 2014; Sinha et al., 2014; Van de Cruys et al., 2014) and strengths characteristics of ASD (Rozenkrantz et al., 2021). Autistic self-reports also describe social cognition as an explicit process. In relaying her experience of social cognition to Oliver Sacks, Temple Grandin—a prominent autistic scientist—describes that she had not accumulated the implicit knowledge of social conventions that many non-autistic individuals build up over a lifetime (Sacks, 1993). Rather, her understanding of the intentions, actions, and mental states of others was a logical, computed process, based largely on explicit recall of former experiences and overt associations. She refers to these former experiences as "videos" in her internal "library of experiences", and describes explicitly coupling these "videos" with extensive research to predict what someone in a certain context might think or do.

[1]Throughout the manuscript, we use identify-first language ("autistic individuals") rather than person-first language ("individuals with autism"), and use the terms "neurotypical(s)" and "non-autistic(s)" interchangeably, to reflect the preferences of many in the autistic community (Vivanti, 2020; Bottema-Beutel et al., 2021).

ADAPTIVE PREDICTION IN THE CEREBELLUM: FROM NEURONS TO NETWORKS

The cerebellum contains over 50% of the neurons in the central nervous system and plays an important role in modulating motor and cognitive functions. Specific cerebellar subregions are linked to discrete supratentorial regions *via* a series of reciprocal, closed-loop circuits. Cerebellar outputs reach the cortex *via* the thalamus, and input to the cerebellum arrives from the cortex *via* the pons. These loops provide the putative circuitry by which the cerebellum can modulate cortical processes, and also underpin regional specificity in cerebellar topography. For instance, the anterior cerebellum is reciprocally connected to sensorimotor cerebral cortices and is involved in motor behaviors, while the posterolateral cerebellum is connected to non-motor association cortices and is involved in cognitive behaviors (Buckner et al., 2011; Bernard et al., 2012; **Figure 1A**). Importantly, our understanding of cerebellar functional topography is evolving, and newer studies have shown that the cerebellum houses representations of many discrete cognitive behaviors (D'Mello et al., 2020a) and tasks (King et al., 2019). Unlike the cerebral cortex, cytoarchitecture is consistent throughout the cerebellum. Therefore, it is suggested that the cerebellum conducts one fundamental operation on any input it receives (Schmahmann, 2004; Diedrichsen et al., 2019). In the motor realm, one hypothesis is that this operation involves adaptive prediction, and the underlying mechanics have been studied in detail. Traditional models of cerebellar adaptive prediction hold that copies of motor commands from the motor cortex ("efference copy") are used to create predictions of the sensory consequences of actions, enabling the cerebellum to optimize actions without needing to wait for sensory feedback which is, by definition, delayed. The cerebellum can adjust these predictions based on sensory feedback. Mismatches between actual and predicted sensory feedback result in sensory prediction errors and updates to the original prediction. Cerebellar predictions and internal models can be refined over time, allowing for rapid, online adaptation of motor behaviors and long-term corrections (Ito, 2006; Shadmehr et al., 2010). At the cellular level, this process is supported in part by granule cells that carry contextual information from the rest of the brain (for example, efference copies, or other learned representations), and synapse onto Purkinje cells (the sole output of the cerebellar cortex) *via* parallel fibers. In addition, climbing fibers from the inferior olive provide prediction error signals to Purkinje cells, which distinguish which granule cell inputs are most informative. These prediction errors can be signed or unsigned, signaling exactly *how* cerebellar Purkinje cells should respond to alter behavior (see Corlett et al., 2022 for evidence of prediction error in human cerebellum). Inputs from climbing fibers can cause long-term depression (LTD) at parallel fiber-Purkinje cell synapses—potentially serving to inhibit actions

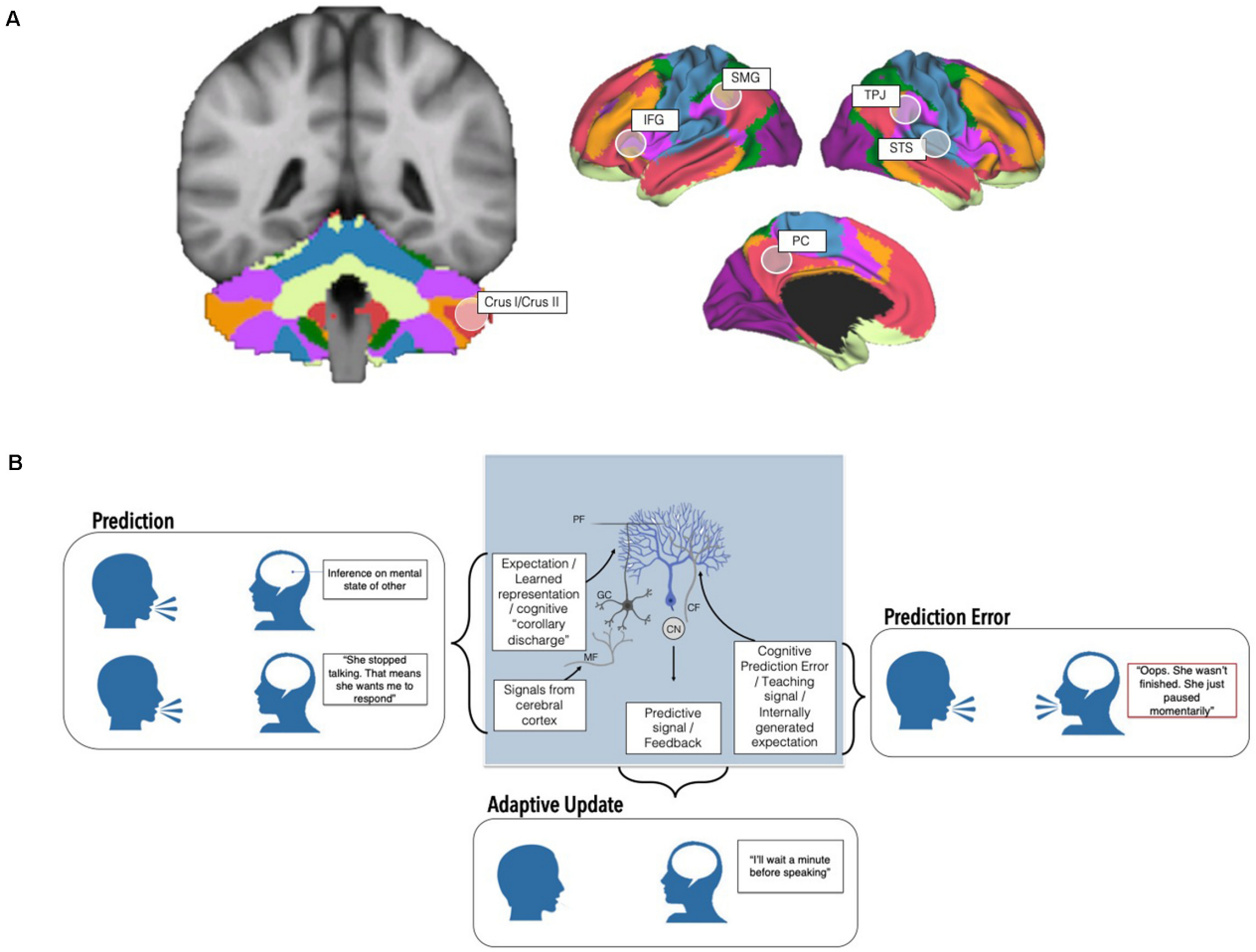

FIGURE 1 | Cerebellar contributions to adaptive prediction in social cognition from neurons to networks. **(A)** The posterolateral cerebellum, particularly Crus I/II, is a node of whole-brain cognitive resting state networks including the Default Mode (red) and Frontoparietal networks (orange; Buckner et al., 2011; Yeo et al., 2011; other networks visualized include dorsal (green) and ventral attention (violet), somatomotor (blue), visual (purple), and limbic (cream)). In addition to resting state networks, several task-based neuroimaging studies find that discrete regions of the cerebellum are maximally engaged by specific tasks (e.g., Stoodley and Schmahmann, 2009; Guell et al., 2018; King et al., 2019). This cerebellar region is also functionally connected with and consistently activated alongside regions implicated in theory of mind (right temporoparietal junction, TPJ, right superior temporal sulcus, STS, and the precuneus, PC) and language processing (left inferior frontal gyrus, IFG, left supramarginal gyrus, SMG). **(B)** At the cellular level, Granule cells (GC) receive input from the rest of the brain and spinal cord *via* mossy fibers (MF) and may transmit expectation-related information *via* their parallel fiber (PF) axons to Purkinje cells, the principal neurons of the cerebellum. On the other hand, prediction errors are carried by climbing fibers (CF) originating in the inferior olive, which also synapse onto Purkinje cells (blue). Climbing fiber input to Purkinje cells is thought to signal which granule cell signals are most important in a given context (Wagner and Luo, 2020 for review). Predictive signals and feedback are ultimately relayed to the rest of the brain *via* output from the cerebellar nuclei (CN). These circuits, and interactions between the cerebellum and the rest of the brain, ultimately enable the creation and deployment of predictions, prediction errors, and adaptive changes to behavior. Altered cerebellar cytoarchitecture, circuitry, and connections with the cerebrum may affect different aspects of adaptive predictions with relevance for sociocognitive challenges in autism.

that resulted in sensory prediction errors (Wagner and Luo, 2020 for review; **Figure 1B**). Notably, the circuitry underlying cerebellar sensorimotor adaptive prediction is complex, and our understanding of the contributions of specific neuronal subtypes is rapidly evolving (Hull, 2020). For example, there is evidence that cerebellar neurons both scaffold learning how to perform an action, and also learning which action is the correct one to perform in a given context (Medina, 2019). In addition, teaching signals hypothesized to be carried by climbing fibers can be modulated by experience, suggesting that the cerebellum may play a role beyond simple error-based learning (see Hull, 2020 for discussion).

This emerging evidence, coupled with the strikingly uniform cytoarchitecture within the cerebellum, has been used to propose that similar adaptive predictive computations are performed in the posterior cerebellum on sociolinguistic inputs from non-motor regions (Sokolov et al., 2017; though see Diedrichsen et al., 2019 for a discussion on how uniform circuits may not be directly related to uniform function, and evidence for multiple functionalities in the cerebellum). These inputs, coupled with unique regional specialization of cell types, electrophysiological properties, and expression patterns of Purkinje cells in the posterior lobe, likely support more complex sociolinguistic adaptive prediction (Kozareva et al., 2021). In this view, instead of

motor efference copies, the posterior cerebellum uses "cognitive" efference copies to form sociocognitive predictions which allow us to anticipate what a social partner is likely to think or say (Van Overwalle et al., 2014). These efference copies may include inferences of another's mental states arising from theory of mind regions or semantic information from language-relevant regions (**Figure 1A**). Supporting this, several neuroimaging studies find that the posterolateral cerebellum, particularly lobules VI-VIII, represents sociolinguistic predictions and prediction errors (Moberget and Ivry, 2016; Ernst et al., 2019; Van Overwalle et al., 2019; Corlett et al., 2022). Neuromodulation of these regions perturbs predictive language behaviors and social sequencing (Lesage et al., 2012, 2017; D'Mello et al., 2017; Van Overwalle et al., 2020). Strikingly, cognitive predictions and even violations of cognitive predictions, not just motor predictions (i.e., reward prediction error, reward expectation, reward delivery) can be carried by cerebellar granule cells (**Figure 1B**). For example, an elegant study in mice found that the cerebellum is monosynaptically connected to the ventral tegmental area (VTA), a key region in reward processing, and that cerebellar neurons that projected to the VTA were preferentially activated when mice engaged in social approach behaviors (Carta et al., 2019). These findings have expanded traditional views of cerebellar circuitry, to incorporate non-motor signals that could influence cognitive behaviors (Wagner and Luo, 2020).

CEREBELLAR ADAPTIVE PREDICTION AND SOCIAL COGNITION: RELEVANCE TO AUTISM SPECTRUM DISORDERS

There is a large literature characterizing cerebellar contributions to autism (see Fatemi et al., 2012; D'Mello and Stoodley, 2015 for review). For instance, the most consistent findings in neuroimaging studies of ASD include reduced volume in cerebellar Crus I and II. These regions are thought to be particularly implicated in ASD given their connections with contralateral cerebral sociolinguistic regions, as well as with the default mode and frontoparietal networks (**Figure 1A**). Postmortem studies in autistic individuals find that Purkinje cell reductions are greatest in Crus I/II (Fatemi et al., 2002; Skefos et al., 2014), and modulation of these regions in animal models of ASD can both cause and rescue social challenges as well as other behaviors characteristic of ASD (Tsai et al., 2012; Stoodley et al., 2017; Badura et al., 2018). Lesions to the posterolateral cerebellum in premature infants, children, and even in adulthood can result in mutism, expressive and receptive language difficulty, and sociocognitive and executive function challenges (e.g., Schmahmann and Sherman, 1998; Limperopoulos et al., 2007; Gudrunardottir et al., 2011; and many others) . Despite existing literatures on the cerebellum and adaptive prediction, the compelling links between the cerebellum and autism, and the interest in adaptive prediction frameworks in autism, few theoretical or empirical studies have explicitly linked these fields. We bridge existing literature across these domains to describe how cerebellar adaptive prediction may contribute to cognitive strengths and challenges in ASD.

Interpreting the Actions of Others

Human actions are relatively standard, enabling us to form expectations about what movements someone might make next, and use these to understand what goals they are trying to achieve. Action perception—inferring goals from action, and understanding why actions are being performed—relies on sensory inputs, but is largely a cognitive process and scaffolds higher-order inferences necessary for theory of mind. Several empirical studies report that autistic individuals show difficulty inferring goals from others' actions (Zalla et al., 2010; Schuwerk et al., 2016), using contextual priors to facilitate action prediction (Amoruso et al., 2019) and internally representing the observed actions of others (Cattaneo et al., 2007).

In non-autistic individuals, these inferences engage lobules VI, Crus I/II (Sokolov et al., 2012, 2014; Abdelgabar et al., 2019; Van Overwalle et al., 2020). For example, when shown point-light displays or moving shapes, non-autistics quickly infer biological motion, or even emotionality and intent (Jack and Pelphrey, 2015, Jack et al., 2017). Stronger Crus I/II activation, and increased connectivity between these regions and the posterior superior temporal sulcus (pSTS)—a region implicated in action inference—is associated with increased likelihood of describing motion in social-affective, vs. motor terms. Activation in lobule VI and Crus I/II also reflect imitation and mirroring (inferring the goals of another's actions by matching them to representations of our own actions; Jack et al., 2011; Van Overwalle et al., 2014). Damage, degeneration, and disruption of the cerebellum can affect action perception (Sokolov et al., 2010). For example, transcranial magnetic stimulation (TMS) to the posterior cerebellum impairs action perception, and the ability to distinguish biological motion from random motion (Ferrari et al., 2019). In addition, cerebellar degeneration in spinocerebellar ataxias is associated with worse action perception ability (Abdelgabar et al., 2019). Children with cerebellar tumors show difficulty using others' actions to predict and infer outcomes and, unlike typically-developing peers and peers with supratentorial tumors, show no contextual facilitation of action interpretation (Butti et al., 2020). This suggests that cerebellar disruption may uniquely affect the use of contextual priors to predict likely action outcomes.

Few studies have explicitly examined cerebellar contributions to action perception and inference in ASD. One study found reduced activation in the posterior cerebellum of autistic individuals (bilateral Crus I) during action imitation compared to non-autistic participants (Jack and Morris, 2014). Reduced activation in Crus I/II in ASD during biological motion processing was associated with greater parent-reported social challenges (Jack et al., 2017). Moreover, reduced connectivity between right Crus I/II and the contralateral pSTS was associated with parent-reported mentalizing skills in autistic children (Jack and Morris, 2014). Interestingly, atypical connection patterns within this circuit (e.g., increased connectivity in ipsilateral, non-canonical Crus I/II-pSTS circuits)

were also associated with self-reported social difficulties (Jack et al., 2017).

Anticipating the Words of Others

Language comprehension is fundamentally predictive, and prior linguistic knowledge and context help to resolve ambiguity when linguistic input is noisy. Several studies have reported that predictive linguistic processing is altered in ASD and that autistic individuals rely less on context to resolve ambiguous words (though see Hahn et al., 2015). For example, when reading ambiguous words aloud (e.g., "read"), autistic children were less likely to vary their pronunciation as a function of changes in surrounding words (Hala et al., 2007; Wagley et al., 2020). Some studies find that autistic children also do not show neural signatures of faciliatory language processing (e.g., reduced engagement of language regions over several repetitions of surprising linguistic input; fewer changes in linguistic brain regions with increased exposure to speech; Scott-Van Zeeland et al., 2010; Wagley et al., 2020).

Neuroimaging and clinical evidence support a role for the posterior cerebellum in linguistic prediction (see Argyropoulos, 2016 for review). Crus I/II activation increases during the formation of a semantic prediction (Moberget et al., 2014; D'Mello et al., 2017; Lesage et al., 2017), and engagement of these lobules is highest when decisions about semantic plausibility must be made quickly (D'Mello et al., 2020b). Cerebellar activation also represents violations of linguistic predictions, and subsequent adjustments to internal models (Sheu and Desmond, 2021). One study found that improvements in the perception of previously ambiguous words were associated with increased right Crus I activation (Guediche et al., 2014). Cerebellar neuromodulation and damage alter word and phrase-level priming (Argyropoulos, 2011; Gilligan and Rafal, 2019), verb generation, predictive sentence processing, and internal monitoring of speech errors (Gebhart et al., 2002; Stoodley and Schmahmann, 2009; Runnqvist et al., 2016).

Cerebellar contributions to language prediction in ASD have not been directly investigated. However, many studies find reduced cerebellar activation during language processing and decreased connectivity between the cerebellum and cortical language networks in autistic children and adults compared to non-autistic individuals (Verly et al., 2014; D'Mello and Stoodley, 2015). Further, structural and functional differences in the posterior cerebellum have been associated with early language delay and ability in ASD (Verly et al., 2014; D'Mello et al., 2016; Hegarty et al., 2018).

Inferring the Mental States of Others

Theory of Mind (TOM), or mentalizing, refers to the ability to infer the beliefs, thoughts, and goals of others. This process engages regions across the cerebral cortex including prefrontal areas, the temporo-parietal junction, and the precuneus (see Adolphs, 2009 for review of the TOM network). TOM is perhaps one of the most studied aspects of ASD. Studies find that autistic individuals showed reduced reliance on prior expectations when attempting to infer the intentions of others and that these reductions were associated with higher self-reported social difficulties (Chambon et al., 2017).

Mentalizing reliably engages the posterior cerebellum in non-autistic individuals (Van Overwalle et al., 2014; Nguyen et al., 2017). The cerebellum contains representations of the DMN, a network that overlaps with the TOM network, and contains a fine-grained representation of the temporoparietal junction (TPJ)—a core node of the TOM network (Igelström et al., 2017). Cerebellar damage can result in difficulty with mentalizing, interpreting the emotions of others, and even interpreting social scenes (Van Overwalle et al., 2020; Clausi et al., 2021a). As in the case of predictive language processing, few studies have explicitly linked the cerebellum to mentalizing abilities in ASD and those that do often focus on biological motion and action perception (see section above). However, the putative substrates for cerebellar contributions to mentalizing challenges in ASD exist (Leggio and Olivito, 2018). For instance, autistic individuals show similar TOM profiles to cerebellar lesion patients (e.g., lower scores on Reading the Mind in the Eyes and Faux Pas Tasks) and have overlapping reductions in gray matter (though this study did not find associations between cerebellar volume and TOM scores in either group; Clausi et al., 2021b). Additionally, reduced connectivity between the cerebellum and regions implicated in TOM have been reported in ASD (Khan et al., 2015). One such study reported that while the functional organization of the temporo-parietal junction (TPJ) was intact, there was reduced connectivity between the TPJ and Crus I/II of the cerebellum in autistic individuals (Igelström et al., 2017).

Altered Cerebellar Adaptive Prediction and Strengths in ASD

The majority of studies examining social cognition, the cerebellum, and adaptive prediction abilities in ASD focus on deficits or challenges in these domains. However, reduced reliance on predictions and past experience can be a strength in ASD, for example in the domains of reasoning, decision making, and cognitive biases (see Rozenkrantz et al., 2021). Despite this, few studies have taken strengths-based approaches when assessing how cerebellar contributions to adaptive prediction may play a role in the heterogeneous profile of strengths and challenges in ASD. One such study demonstrated that Purkinje-cell specific mouse models of ASD (e.g., L7-Tsc1) show *both* sensory deficits and sensory learning strengths (i.e., outperform wildtype mice on a sensory-accumulation learning task; Oostland et al., 2021). One interpretation of this is that reduced predictive capacity as a result of cerebellar impairment can result in an increased focus on recent or incoming sensory information and allow for stronger learning.

DISCUSSION

Adaptive prediction frameworks have been useful in organizing our understanding of social cognition in ASD and developing hypotheses for future research. The cerebellum, a structure known for its role in adaptive prediction, is often excluded

from empirical neuroimaging studies and theoretical discussions of neural substrates of social cognition in ASD. This renders disentangling the lack of cerebellar findings from the lack of cerebellar involvement in these domains difficult. Future research should take a whole-brain approach and strive to interpret cerebellar results within the context of the existing literature when possible. Moreover, some studies report that autistic individuals do not show difficulty using past experience to adapt behavior at lower levels of processing (e.g., visual, motion perception; Sandhu et al., 2019), and that these differences only emerge for higher-order stimuli or demands. Future research should look across levels of processing to determine which aspects of ASD may be best explained by cerebellar-specific adaptive prediction mechanisms. Future studies should also take care to assess whether cerebellar contributions to adaptive prediction can explain the heterogeneous profile of strengths and challenges in ASD. Notably, early injury to the cerebellum can result in the development of ASD-relevant behaviors which persist into adulthood (Wang et al., 2014). Understanding how cerebellar adaptive prediction contributes to socio-cognitive development is especially relevant for ASD—a neurodevelopmental disorder. Lastly, cerebellar differences and atypical adaptive prediction are found in multiple psychiatric and neurodevelopmental disorders. This suggests that the cerebellum might be a domain-general predictive processor across cognitive domains and categorical diagnoses (Sokolov et al., 2010; Diedrichsen et al., 2019; D'Mello and Rozenkrantz, 2020). A transdiagnostic approach to adaptive prediction differences may reveal shared neurobiological mechanisms across neurodevelopmental and psychiatric conditions.

AUTHOR CONTRIBUTIONS

IF and AD conceptualized and wrote the initial draft. VM provided feedback and contributed to the final draft. All authors contributed to the article and approved the submitted version.

FUNDING

This work was supported by the National Institute of Mental Health (F32 MH117933 to AD).

ACKNOWLEDGMENTS

We acknowledge helpful feedback and discussion on the manuscript from Amanda O'Brien as well as their funding sources.

REFERENCES

Abdelgabar, A. R., Suttrup, J., Broersen, R., Bhandari, R., Picard, S., Keysers, C., et al. (2019). Action perception recruits the cerebellum and is impaired in patients with spinocerebellar ataxia. *Brain* 142, 3791–3805. doi: 10.1093/brain/awz337

Adolphs, R. (2009). The social brain: neural basis of social knowledge. *Annu. Rev. Psychol.* 60, 693–716. doi: 10.1146/annurev.psych.60.110707.163514

American Psychiatric Association. (2013). Diagnostic and statistical manual of mental disorders (5th ed.) Arlington, VA: American Psychiatric Association.

Amoruso, L., Narzisi, A., Pinzino, M., Finisguerra, A., Billeci, L., Calderoni, S., et al. (2019). Contextual priors do not modulate action prediction in children with autism. *Proc. R. Soc. B Biol. Sci.* 286:20191319. doi: 10.1098/rspb.2019.1319

Argyropoulos, G. P. (2011). Cerebellar theta-burst stimulation selectively enhances lexical associative priming. *Cerebellum* 10, 540–550. doi: 10.1007/s12311-011-0269-y

Argyropoulos, G. P. D. (2016). The cerebellum, internal models and prediction in ''non-motor'' aspects of language: a critical review. *Brain Lang.* 161, 4–17. doi: 10.1016/j.bandl.2015.08.003

Badura, A., Verpeut, J. L., Metzger, J. W., Pereira, T. D., Pisano, T. J., Deverett, B., et al. (2018). Normal cognitive and social development require posterior cerebellar activity. *eLife* 7:e36401. doi: 10.7554/eLife.36401

Bernard, J. A., Seidler, R. D., Hassevoort, K. M., Benson, B. L., Welsh, R. C., Wiggins, J. L., et al. (2012). Resting state cortico-cerebellar functional connectivity networks: A comparison of anatomical and self-organizing map approaches. *Front. Neuroanat.* 6:31. doi: 10.3389/fnana.2012.00031

Bottema-Beutel, K., Kapp, S. K., Lester, J. N., Sasson, N. J., and Hand, B. N. (2021). Avoiding ableist language: suggestions for autism researchers. *Autism Adulthood* 3, 18–29. doi: 10.1089/aut.2020.0014

Buckner, R. L., Krienen, F. M., Castellanos, A., Diaz, J. C., and Yeo, B. T. T. (2011). The organization of the human cerebellum estimated by intrinsic functional connectivity. *J. Neurophysiol.* 106, 2322–2345. doi: 10.1152/jn.00339.2011

Butti, N., Corti, C., Finisguerra, A., Bardoni, A., Borgatti, R., Poggi, G., et al. (2020). Cerebellar damage affects contextual priors for action prediction in patients with childhood brain tumor. *Cerebellum* 19, 799–811. doi: 10.1007/s12311-020-01168-w

Cannon, J., O'Brien, A. M., Bungert, L., and Sinha, P. (2021). Prediction in autism spectrum disorder: a systematic review of empirical evidence. *Autism Res.* 14, 604–630. doi: 10.1002/aur.2482

Carta, I., Chen, C. H., Schott, A. L., Dorizan, S., and Khodakhah, K. (2019). Cerebellar modulation of the reward circuitry and social behavior. *Science* 363:eaav0581. doi: 10.1126/science.aav0581

Cattaneo, L., Fabbri-Destro, M., Boria, S., Pieraccini, C., Monti, A., Cossu, G., et al. (2007). Impairment of actions chains in autism and its possible role in intention understanding. *Proc. Natl. Acad. Sci. U S A* 104, 17825–17830. doi: 10.1073/pnas.0706273104

Chambon, V., Farrer, C., Pacherie, E., Jacquet, P. O., Leboyer, M., and Zalla, T. (2017). Reduced sensitivity to social priors during action prediction in adults with autism spectrum disorders. *Cognition* 160, 17–26. doi: 10.1016/j.cognition.2016.12.005

Clausi, S., Olivito, G., Siciliano, L., Lupo, M., Bozzali, M., Masciullo, M., et al. (2021a). The neurobiological underpinning of the social cognition impairments in patients with spinocerebellar ataxia type 2. *Cortex* 138, 101–112. doi: 10.1016/j.cortex.2020.12.027

Clausi, S., Olivito, G., Siciliano, L., Lupo, M., Laghi, F., Baiocco, R., et al. (2021b). The cerebellum is linked to theory of mind alterations in autism. A direct clinical and MRI comparison between individuals with autism and cerebellar neurodegenerative pathologies. *Autism Res.* 14, 2300–2313. doi: 10.1002/aur.2593

Corlett, P. R., Mollick, J. A., and Kober, H. (2022). Meta-analysis of human prediction error for incentives, perception, cognition, and action. *Neuropsychopharmacology* doi: 10.1038/s41386-021-01264-3

D'Mello, A. M., Centanni, T. M., Gabrieli, J. D. E., and Christodoulou, J. A. (2020a). Cerebellar contributions to rapid semantic processing in reading. *Brain Lang.* 208:104828. doi: 10.1016/j.bandl.2020.104828

D'Mello, A. M., Gabrieli, J. D. E., and Nee, D. E. (2020b). Evidence for hierarchical cognitive control in the human cerebellum. *Curr. Biol.* 30, 1881–1892.e3. doi: 10.1016/j.cub.2020.03.028

D'Mello, A. M., Moore, D. M., Crocetti, D., Mostofsky, S. H., and Stoodley, C. J. (2016). Cerebellar gray matter differentiates children with early language delay in autism. *Autism Res.* 9, 1191–1204. doi: 10.1002/aur.1622

D'Mello, A. M., and Rozenkrantz, L. (2020). Neural mechanisms for prediction: from action to higher-order cognition. *J. Neurosci.* 40, 5158–5160. doi: 10.1523/JNEUROSCI.0732-20.2020

D'Mello, A. M., and Stoodley, C. J. (2015). Cerebro-cerebellar circuits in autism spectrum disorder. *Front. Neurosci.* 9:408. doi: 10.3389/fnins.2015.00408

D'Mello, A. M., Turkeltaub, P. E., and Stoodley, C. J. (2017). Cerebellar tDCS modulates neural circuits during semantic prediction: a combined tDCS-fMRI study. *J. Neurosci.* 37, 1604–1613. doi: 10.1523/JNEUROSCI.2818-16.2017

Diedrichsen, J., King, M., Hernandez-Castillo, C., Sereno, M., and Ivry, R. B. (2019). Universal transform or multiple functionality? Understanding the contribution of the human cerebellum across task domains. *Neuron* 102, 918–928. doi: 10.1016/j.neuron.2019.04.021

Ellegood, J., Anagnostou, E., Babineau, B. A., Crawley, J. N., Lin, L., Genestine, M., et al. (2015). Clustering autism: using neuroanatomical differences in 26 mouse models to gain insight into the heterogeneity. *Mol. Psychiatry* 20, 118–125. doi: 10.1038/mp.2014.98

Ernst, T. M., Brol, A. E., Gratz, M., Ritter, C., Bingel, U., Schlamann, M., et al. (2019). The cerebellum is involved in processing of predictions and prediction errors in a fear conditioning paradigm. *eLife* 8:e46831. doi: 10.7554/eLife.46831

Fatemi, S. H., Aldinger, K. A., Ashwood, P., Bauman, M. L., Blaha, C. D., Blatt, G. J., et al. (2012). Consensus paper: pathological role of the cerebellum in autism. *Cerebellum* 11, 777–807. doi: 10.1007/s12311-012-0355-9

Fatemi, S. H., Halt, A. R., Realmuto, G., Earle, J., Kist, D. A., Thuras, P., et al. (2002). Purkinje cell size is reduced in cerebellum of patients with autism. *Cell. Mol. Neurobiol.* 22, 171–175. doi: 10.1023/a:1019861721160

Ferrari, C., Ciricugno, A., Battelli, L., Grossman, E. D., and Cattaneo, Z. (2019). Distinct cerebellar regions for body motion discrimination. *Soc. Cogn. Affect. Neurosci.* 10:nsz088. doi: 10.1093/scan/nsz088

Friston, K. (2005). A theory of cortical responses. *Philos. Trans. R. Soc. B Biol. Sci.* 360, 815–836. doi: 10.1098/rstb.2005.1622

Gebhart, A. L., Petersen, S. E., and Thach, W. T. (2002). Role of the posterolateral cerebellum in language. *Ann. N Y Acad. Sci.* 978, 318–333. doi: 10.1111/j.1749-6632.2002.tb07577.x

Gilligan, T. M., and Rafal, R. D. (2019). An opponent process cerebellar asymmetry for regulating word association priming. *Cerebellum* 18, 47–55. doi: 10.1007/s12311-018-0949-y

Gudrunardottir, T., Sehested, A., Juhler, M., and Schmiegelow, K. (2011). Cerebellar mutism: review of the literature. *Childs Nerv. Syst.* 27, 355–363. doi: 10.1007/s00381-010-1328-2

Guediche, S., Holt, L. L., Laurent, P., Lim, S.-J., and Fiez, J. A. (2014). Evidence for cerebellar contributions to adaptive plasticity in speech perception. *Cereb. Cortex* 25, 1867–1877. doi: 10.1093/cercor/bht428

Guell, X., Gabrieli, J. D. E., and Schmahmann, J. D. (2018). Triple representation of language, working memory, social and emotion processing in the cerebellum: convergent evidence from task and seed-based resting-state fMRI analyses in a single large cohort. *Neuroimage* 172, 437–449. doi: 10.1016/j.neuroimage.2018.01.082

Hahn, N., Snedeker, J., and Rabagliati, H. (2015). Rapid linguistic ambiguity resolution in young children with autism spectrum disorder: eye tracking evidence for the limits of weak central coherence. *Autism Res.* 8, 717–726. doi: 10.1002/aur.1487

Hala, S., Pexman, P. M., and Glenwright, M. (2007). Priming the meaning of homographs in typically developing children and children with autism. *J. Autism Dev. Disord.* 37, 329–340. doi: 10.1007/s10803-006-0162-6

Hegarty, J. P., 2nd, Weber, D. J., Cirstea, C. M., and Beversdorf, D. Q. (2018). Cerebro-cerebellar functional connectivity is associated with cerebellar excitation-inhibition balance in autism spectrum disorder. *J. Autism Dev. Disord.* 48, 3460–3473. doi: 10.1007/s10803-018-3613-y

Hull, C. (2020). Prediction signals in the cerebellum: beyond supervised motor learning. *ELife* 9:e54073. doi: 10.7554/eLife.54073

Igelström, K. M., Webb, T. W., and Graziano, M. S. A. (2017). Functional connectivity between the temporoparietal cortex and cerebellum in autism spectrum disorder. *Cereb. Cortex* 27, 2617–2627. doi: 10.1093/cercor/bhw079

Ito, M. (2006). Cerebellar circuitry as a neuronal machine. *Prog. Neurobiol.* 78, 272–303. doi: 10.1016/j.pneurobio.2006.02.006

Jack, A., Englander, Z. A., and Morris, J. P. (2011). Subcortical contributions to effective connectivity in brain networks supporting imitation. *Neuropsychologia* 49, 3689–3698. doi: 10.1016/j.neuropsychologia.2011.09.024

Jack, A., Keifer, C. M., and Pelphrey, K. A. (2017). Cerebellar contributions to biological motion perception in autism and typical development. *Hum. Brain Mapp.* 38, 1914–1932. doi: 10.1002/hbm.23493

Jack, A., and Morris, J. P. (2014). Neocerebellar contributions to social perception in adolescents with autism spectrum disorder. *Dev. Cogn. Neurosci.* 10, 77–92. doi: 10.1016/j.dcn.2014.08.001

Jack, A., and Pelphrey, K. A. (2015). Neural correlates of animacy attribution include neocerebellum in healthy adults. *Cereb. Cortex* 25, 4240–4247. doi: 10.1093/cercor/bhu146

Khan, A. J., Nair, A., Keown, C. L., Datko, M. C., Lincoln, A. J., and Müller, R.-A. (2015). Cerebro-cerebellar resting state functional connectivity in children and adolescents with autism spectrum disorder. *Biol. Psychiatry* 78, 625–634. doi: 10.1016/j.biopsych.2015.03.024

King, M., Hernandez-Castillo, C. R., Poldrack, R. A., Ivry, R. B., and Diedrichsen, J. (2019). Functional boundaries in the human cerebellum revealed by a multi-domain task battery. *Nat. Neurosci.* 22, 1371–1378. doi: 10.1038/s41593-019-0436-x

Koster-Hale, J., and Saxe, R. (2013). Theory of mind: a neural prediction problem. *Neuron* 79, 836–848. doi: 10.1016/j.neuron.2013.08.020

Kozareva, V., Martin, C., Osorno, T., Rudolph, S., Guo, C., Vanderburg, C., et al. (2021). A transcriptomic atlas of mouse cerebellar cortex comprehensively defines cell types. *Nature* 598, 214–219. doi: 10.1038/s41586-021-03220-z

Lawson, R. P., Rees, G., and Friston, K. J. (2014). An aberrant precision account of autism. *Front. Hum. Neurosci.* 8:302. doi: 10.3389/fnhum.2014.00302

Leggio, M., and Olivito, G. (2018). Topography of the cerebellum in relation to social brain regions and emotions. *Handb. Clin. Neurol.* 154, 71–84. doi: 10.1016/B978-0-444-63956-1.00005-9

Lesage, E., Hansen, P. C., and Miall, R. C. (2017). Right lateral cerebellum represents linguistic predictability. *J. Neurosci.* 37, 6231–6241. doi: 10.1523/JNEUROSCI.3203-16.2017

Lesage, E., Morgan, B. E., Olson, A. C., Meyer, A. S., and Miall, R. C. (2012). Cerebellar rTMS disrupts predictive language processing. *Curr. Biol.* 22, R794–R795. doi: 10.1016/j.cub.2012.07.006

Limperopoulos, C., Bassan, H., Gauvreau, K., Robertson, R. L., Sullivan, N. R., Benson, C. B., et al. (2007). Does cerebellar injury in premature infants contribute to the high prevalence of long-term cognitive, learning and behavioral disability in survivors? *Pediatrics* 120, 584–593. doi: 10.1542/peds.2007-1041

Medina, J. F. (2019). Teaching the cerebellum about reward. *Nat. Neurosci.* 22, 846–848. doi: 10.1038/s41593-019-0409-0

Moberget, T., Gullesen, E. H., Andersson, S., Ivry, R. B., and Endestad, T. (2014). Generalized role for the cerebellum in encoding internal models: evidence from semantic processing. *J. Neurosci.* 34, 2871–2878. doi: 10.1523/JNEUROSCI.2264-13.2014

Moberget, T., and Ivry, R. B. (2016). Cerebellar contributions to motor control and language comprehension: searching for common computational principles. *Ann. NY Acad. Sci.* 1369, 154–171. doi: 10.1111/nyas.13094

Nguyen, V. T., Sonkusare, S., Stadler, J., Hu, X., Breakspear, M., and Guo, C. C. (2017). Distinct cerebellar contributions to cognitive-perceptual dynamics during natural viewing. *Cereb. Cortex* 27, 5652–5662. doi: 10.1093/cercor/bhw334

Oostland, M., Kislin, M., Chen, Y., Chen, T., Venditto, S. J., Deverett, B., et al. (2021). Enhanced learning and sensory salience in a cerebellar mouse autism model. *boiRxiv* [Preprint]. 2021.12.23.474034. doi: 10.1101/2021.12.23.474034

Pellicano, E., and Burr, D. (2012). When the world becomes "too real": a Bayesian explanation of autistic perception. *Trends Cogn. Sci.* 16, 504–510. doi: 10.1016/j.tics.2012.08.009

Rozenkrantz, L., D'Mello, A. M., and Gabrieli, J. D. E. (2021). Enhanced rationality in autism spectrum disorder. *Trends Cogn. Sci.* 25, 685–696. doi: 10.1016/j.tics.2021.05.004

Runnqvist, E., Bonnard, M., Gauvin, H. S., Attarian, S., Trébuchon, A., Hartsuiker, R. J., et al. (2016). Internal modeling of upcoming speech: a causal role of the right posterior cerebellum in non-motor aspects of language production. *Cortex* 81, 203–214. doi: 10.1016/j.cortex.2016.05.008

Sacks, O. (1993). An anthropologist on mars. *The New Yorker* Available online at: http://www.newyorker.com/magazine/1993/12/27/anthropologist-mars.

Sandhu, T. R., Rees, G., and Lawson, R. P. (2019). Preserved low-level visual gain control in autistic adults [version 1; peer review: 2 approved with reservations]. *Wellcome Open Res.* 4:208. doi: 10.12688/wellcomeopenres.15615.1

Schmahmann, J. D. (2004). Disorders of the cerebellum: ataxia, dysmetria of thought and the cerebellar cognitive affective syndrome. *J. Neuropsychiatry Clin. Neurosci.* 16, 367–378. doi: 10.1176/jnp.16.3.367

Schmahmann, J. D., and Sherman, J. C. (1998). The cerebellar cognitive affective syndrome. *Brain* 121, 561–579. doi: 10.1093/brain/121.4.561

Schuwerk, T., Sodian, B., and Paulus, M. (2016). Cognitive mechanisms underlying action prediction in children and adults with autism spectrum condition. *J. Autism Dev. Disord.* 46, 3623–3639. doi: 10.1007/s10803-016-2899-x

Scott-Van Zeeland, A. A., McNealy, K., Wang, A. T., Sigman, M., Bookheimer, S. Y., and Dapretto, M. (2010). No neural evidence of statistical learning during exposure to artificial languages in children with autism spectrum disorders. *Biol. Psychiatry* 68, 345–351. doi: 10.1016/j.biopsych.2010.01.011

Shadmehr, R., Smith, M. A., and Krakauer, J. W. (2010). Error correction, sensory prediction and adaptation in motor control. *Annu. Rev. Neurosci.* 33, 89–108. doi: 10.1146/annurev-neuro-060909-153135

Sheu, Y.-S., and Desmond, J. E. (2021). Cerebro-cerebellar response to sequence violation in a cognitive task: an fMRI study. *Cerebellum* doi: 10.1007/s12311-021-01279-y. [Online ahead of print].

Sinha, P., Kjelgaard, M. M., Gandhi, T. K., Tsourides, K., Cardinaux, A. L., Pantazis, D., et al. (2014). Autism as a disorder of prediction. *Proc. Natl. Acad. Sci. U S A* 111, 15220–15225. doi: 10.1073/pnas.1416797111

Skefos, J., Cummings, C., Enzer, K., Holiday, J., Weed, K., Levy, E., et al. (2014). Regional alterations in purkinje cell density in patients with autism. *PloS One* 9:e81255. doi: 10.1371/journal.pone.0081255

Sokolov, A. A., Erb, M., Gharabaghi, A., Grodd, W., Tatagiba, M. S., and Pavlova, M. A. (2012). Biological motion processing: the left cerebellum communicates with the right superior temporal sulcus. *Neuroimage* 59, 2824–2830. doi: 10.1016/j.neuroimage.2011.08.039

Sokolov, A. A., Erb, M., Grodd, W., and Pavlova, M. A. (2014). Structural loop between the cerebellum and the superior temporal sulcus: evidence from diffusion tensor imaging. *Cereb. Cortex* 24, 626–632. doi: 10.1093/cercor/bhs346

Sokolov, A. A., Gharabaghi, A., Tatagiba, M. S., and Pavlova, M. (2010). Cerebellar engagement in an action observation network. *Cereb. Cortex* 20, 486–491. doi: 10.1093/cercor/bhp117

Sokolov, A. A., Miall, R. C., and Ivry, R. B. (2017). The cerebellum: adaptive prediction for movement and cognition. *Trends Cogn. Sci.* 21, 313–332. doi: 10.1016/j.tics.2017.02.005

Steadman, P. E., Ellegood, J., Szulc, K. U., Turnbull, D. H., Joyner, A. L., Henkelman, R. M., et al. (2014). Genetic effects on cerebellar structure across mouse models of autism using a magnetic resonance imaging atlas. *Autism Res.* 7, 124–137. doi: 10.1002/aur.1344

Stoodley, C. J., D'Mello, A. M., Ellegood, J., Jakkamsetti, V., Liu, P., Nebel, M. B., et al. (2017). Altered cerebellar connectivity in autism and cerebellar-mediated rescue of autism-related behaviors in mice. *Nat. Neurosci.* 20, 1744–1751. doi: 10.1038/s41593-017-0004-1

Stoodley, C. J., and Schmahmann, J. D. (2009). Functional topography in the human cerebellum: a meta-analysis of neuroimaging studies. *Neuroimage* 44, 489–501. doi: 10.1016/j.neuroimage.2008.08.039

Stoodley, C. J., and Tsai, P. T. (2021). Adaptive prediction for social contexts: the cerebellar contribution to typical and atypical social behaviors. *Annu. Rev. Neurosci.* 44, 475–493. doi: 10.1146/annurev-neuro-100120-092143

Tsai, P. T., Hull, C., Chu, Y., Greene-Colozzi, E., Sadowski, A. R., Leech, J. M., et al. (2012). Autistic-like behaviour and cerebellar dysfunction in Purkinje cell Tsc1 mutant mice. *Nature* 488, 647–651. doi: 10.1038/nature11310

Van de Cruys, S., Evers, K., Van der Hallen, R., Van Eylen, L., Boets, B., de-Wit, L., et al. (2014). Precise minds in uncertain worlds: predictive coding in autism. *Psychol. Rev.* 121, 649–675. doi: 10.1037/a0037665

Van Overwalle, F., Baetens, K., Mariën, P., and Vandekerckhove, M. (2014). Social cognition and the cerebellum: a meta-analysis of over 350 fMRI studies. *Neuroimage* 86, 554–572. doi: 10.1016/j.neuroimage.2013.09.033

Van Overwalle, F., De Coninck, S., Heleven, E., Perrotta, G., Taib, N. O. B., Manto, M., et al. (2019). The role of the cerebellum in reconstructing social action sequences: a pilot study. *Soc. Cogn. Affect. Neurosci.* 14, 549–558. doi: 10.1093/scan/nsz032

Van Overwalle, F., Manto, M., Cattaneo, Z., Clausi, S., Ferrari, C., Gabrieli, J. D. E., et al. (2020). Consensus paper: cerebellum and social cognition. *Cerebellum* 19, 833–868. doi: 10.1007/s12311-020-01155-1

Verly, M., Verhoeven, J., Zink, I., Mantini, D., Peeters, R., Deprez, S., et al. (2014). Altered functional connectivity of the language network in ASD: role of classical language areas and cerebellum. *Neuroimage Clin.* 4, 374–382. doi: 10.1016/j.nicl.2014.01.008

Vivanti, G. (2020). Ask the editor: what is the most appropriate way to talk about individuals with a diagnosis of autism? *J. Autism Dev. Disord.* 50, 691–693. doi: 10.1007/s10803-019-04280-x

Wagley, N., Lajiness-O'Neill, R., Hay, J. S. F., Ugolini, M., Bowyer, S. M., Kovelman, I., et al. (2020). Predictive processing during a naturalistic statistical learning task in ASD. *eNeuro* 7:ENEURO.0069-19.2020. doi: 10.1523/ENEURO.0069-19.2020

Wagner, M. J., and Luo, L. (2020). Neocortex-cerebellum circuits for cognitive processing. *Trends Neurosci.* 43, 42–54. doi: 10.1016/j.tins.2019.11.002

Wang, S. S.-H., Kloth, A. D., and Badura, A. (2014). The cerebellum, sensitive periods and autism. *Neuron* 83, 518–532. doi: 10.1016/j.neuron.2014.07.016

Yeo, B. T., Krienen, F. M., Sepulcre, J., Sabuncu, M. R., Lashkari, D., Hollinshead, M., et al. (2011). The organization of the human cerebral cortex estimated by intrinsic functional connectivity. *J. Neurophysiol.* 106, 1125–1165. doi: 10.1152/jn.00338.2011

Zalla, T., Labruyère, N., Clément, A., and Georgieff, N. (2010). Predicting ensuing actions in children and adolescents with autism spectrum disorders. *Exp. Brain Res.* 201, 809–819. doi: 10.1007/s00221-009-2096-7

Conflict of Interest: The authors declare that the research was conducted in the absence of any commercial or financial relationships that could be construed as a potential conflict of interest.

Publisher's Note: All claims expressed in this article are solely those of the authors and do not necessarily represent those of their affiliated organizations, or those of the publisher, the editors and the reviewers. Any product that may be evaluated in this article, or claim that may be made by its manufacturer, is not guaranteed or endorsed by the publisher.

frontiers in Integrative Neuroscience

MINI REVIEW
published: 09 February 2022
doi: 10.3389/fnint.2022.804221

Synapse Maturation and Developmental Impairment in the Medial Nucleus of the Trapezoid Body

*Sima M. Chokr, Giedre Milinkeviciute and Karina S. Cramer**

Department of Neurobiology and Behavior, University of California, Irvine, Irvine, CA, United States

Sound localization requires rapid interpretation of signal speed, intensity, and frequency. Precise neurotransmission of auditory signals relies on specialized auditory brainstem synapses including the calyx of Held, the large encapsulating input to principal neurons in the medial nucleus of the trapezoid body (MNTB). During development, synapses in the MNTB are established, eliminated, and strengthened, thereby forming an excitatory/inhibitory (E/I) synapse profile. However, in neurodevelopmental disorders such as autism spectrum disorder (ASD), E/I neurotransmission is altered, and auditory phenotypes emerge anatomically, molecularly, and functionally. Here we review factors required for normal synapse development in this auditory brainstem pathway and discuss how it is affected by mutations in ASD-linked genes.

Keywords: cochlear nucleus, medial nucleus of the trapezoid body, tonotopy, synaptic pruning, calyx of Held

OPEN ACCESS

Edited by:
Patricia Gaspar, Institut National de la Santé et de la Recherche Médicale (INSERM), France

Reviewed by:
Maria Eulalia Rubio, University of Pittsburgh, United States
Jean Livet, Institut National de la Santé et de la Recherche Médicale (INSERM), France

***Correspondence:**
Karina S. Cramer
cramerk@uci.edu

Received: *29 October 2021*
Accepted: *17 January 2022*
Published: *09 February 2022*

Citation:
Chokr SM, Milinkeviciute G and Cramer KS (2022) Synapse Maturation and Developmental Impairment in the Medial Nucleus of the Trapezoid Body. Front. Integr. Neurosci. 16:804221. doi: 10.3389/fnint.2022.804221

INTRODUCTION

Neurodevelopmental disorders with auditory phenotypes, such as autism spectrum disorder (ASD) and schizophrenia (SZ), display altered balance of excitatory and inhibitory (E/I) neurotransmission throughout the brain. Sound localization depends on the E/I ratio in auditory brainstem nuclei and higher auditory structures. Errors in neurotransmission lead to altered signal speed, strength, duration, and ultimately signal interpretation. A consequence of these E/I neurotransmission errors can be observed in ASD, which is often accompanied by sensory symptoms including sound hyper- or hyposensitivity (Van der Molen et al., 2012; Knoth et al., 2014). The establishment of normal E/I ratios in auditory brainstem nuclei begins during embryonic and postnatal development, with additional refinement after hearing onset. Impairments in sound localization have been reported in patients with ASD and SZ (Matthews et al., 2007; Perrin et al., 2010; Visser et al., 2013; Smith et al., 2019), and studies of young and adult brains showed abnormalities in brainstem sizes (Hashimoto et al., 1992; Nopoulos et al., 2001; Claesdotter-Hybbinette et al., 2015). Epidemiological data have highlighted a potential for ASD susceptibility during a gestational period of brainstem development (reviewed in Dadalko and Travers, 2018). Studies using animal models of autism have shown alterations in the E/I ratio and signal strength in the sound localization pathway during postnatal development (Rotschafer et al., 2015; Ruby et al., 2015; Garcia-Pino et al., 2017; Smith et al., 2019). However, physiological differences of auditory brainstem development in sound processing disorders require further investigation. Notably, brainstem alterations in SZ and attention deficit hyperactivity disorder (ADHD) are poorly understood. Here, we discuss factors required for normal development of the E/I ratio in the sound localization circuit and summarize signaling pathways that are altered in models of ASD.

MEDIAL NUCLEUS OF THE TRAPEZOID BODY: DEVELOPMENT AND EFFECTS OF NEURODEVELOPMENTAL DISORDERS

Auditory stimuli are detected by cochlear hair cells that transmit signals centrally through peripheral processes of spiral ganglion neurons (SGN). Central processes of SGNs bifurcate upon entering the brainstem to innervate the ventral and dorsal parts of the cochlear nucleus (CN) (Fekete et al., 1984). SGNs directly connect the hair cell in the periphery to its neuronal target in the CN, which then relays excitatory glutamatergic signals to auditory brainstem nuclei and higher auditory structures. Globular bushy cells (GBCs) receive endbulb inputs from SGNs and project to the contralateral medial nucleus of the trapezoid body (MNTB) through a specialized central synapse, the calyx of Held (**Figure 1A**; Harrison and Irving, 1966; Spirou et al., 2005). MNTB neurons provide inhibitory glycinergic input to the lateral superior olive (LSO), medial superior olive (MSO), ventral nucleus of the lateral lemniscus, and superior periolivary nucleus (SPON) (Liu et al., 2014; Kulesza and Grothe, 2015; Kopp-Scheinpflug et al., 2018; Torres Cadenas et al., 2020). The MNTB is a main contributor of inhibition within the sound localization pathway through its termination onto MSO and LSO neurons and provides monaural temporal information via its connection to the SPON (Zarbin et al., 1981; Moore and Caspary, 1983; Kuwabara and Zook, 1992; Sommer et al., 1993; Behrend et al., 2002; Dehmel et al., 2002; Kulesza, 2007). LSO simultaneously receives excitatory projections from spherical bushy cells in the ipsilateral ventral cochlear nucleus (VCN) and inhibitory input from ipsilateral MNTB (**Figure 1A**). The balance of excitation and inhibition in LSO allows for computation of interaural level differences used in sound localization. Tonotopy is conserved across the central auditory pathway, which in turn allows the listener to localize sounds based on signal speed, intensity, and frequency within the brainstem and higher auditory regions.

The precision of the sound localization pathway requires orchestrated maturation of cell number, synapse number and strength, and neurotransmitter phenotypes (Kotak et al., 1998; Nabekura et al., 2004; Gillespie et al., 2005; Lee et al., 2016). In the VCN, the endbulb of Held expands and develops elaborate branches (Cant and Morest, 1979; Ryugo and Sento, 1991; Nicol and Walmsley, 2002). The establishment of the mature calyx of Held in MNTB requires the elimination of multiple small inputs until exactly one calyx remains, strengthens, and forms a highly reticulated encapsulation of a principal cell soma by the onset of hearing at about P12 (Held, 1893; Kuwabara and Zook, 1991; Kuwabara et al., 1991; Hoffpauir et al., 2006; Holcomb et al., 2013). As calyces mature, MNTB neurons exhibit faster IPSC depression following hearing onset (Rajaram et al., 2020). MNTB-LSO connections also strengthen as they decrease in IPSC amplitude leading up to hearing onset while MNTB-MSO synapse amplitudes continue to decrease following hearing onset (Kim and Kandler, 2003; Magnusson et al., 2005; Walcher et al., 2011; Pilati et al., 2016; Rajaram et al., 2020). In the gerbil, MNTB-LSO synapse strengthening is largely completed by the third postnatal week, and studies using cochlear ablations suggest that synaptic pruning and topographic establishment during the postnatal period are activity-dependent (Sanes et al., 1992; Sanes and Takács, 1993; Kandler and Gillespie, 2005).

Factors Required for Proper MNTB Development

The MNTB forms by E17 (Morest, 1969; Kandler and Friauf, 1993; Hoffpauir et al., 2010), and proto-calyceal inputs can be seen before birth (Hoffpauir et al., 2010; Borst and Soria van Hoeve, 2012). Axon guidance molecules such as ephrin-B2, Netrin-1, DCC, and Robo3 guide GBC axons across the midline toward contralateral MNTB (Howell et al., 2007; Hsieh et al., 2010; Yu and Goodrich, 2014). Bone morphogenic protein (BMP)-receptor signaling early in development is required for correct GBC axonal targeting, pruning, and calyceal growth (Kolson et al., 2016b; Kronander et al., 2019). BMP signaling is altered in autism model organisms, and in humans, several signaling pathways associated with BMP are disrupted in ASD (Kumar et al., 2019). For instance, in the rodent, silencing *Fmr1*, a gene linked to fragile X syndrome, which is often correlated with autism, leads to an upregulation in BMP type II receptor and its signaling kinase (Kashima et al., 2016). In the brainstem, *Fmr1* deletion leads to stunted SOC nuclei development, reduced pruning of inhibitory synapses in the MNTB and CN, and delays in auditory brainstem signal propagation (Rotschafer et al., 2015; Ruby et al., 2015; McCullagh et al., 2020). In the LSO, *Fmr1* KO mice showed higher levels of excitatory input strength while inhibitory synapses were not affected (Garcia-Pino et al., 2017). Recent studies have noted hypoplasia in autistic brains, with significant reductions in SOC nuclei size, and cell volume and shape in the MNTB (Kulesza et al., 2011; Lukose et al., 2015). It is thus clear that within the MNTB there are anatomical and molecular abnormalities, impairments in synapse development and elimination, and functional deficits which result from genetic manipulation of an ASD-linked gene.

SYNAPSE ORGANIZATION AND STRENGTHENING

Proper synapse development in the MNTB requires spontaneous firing patterns, which aid in the establishment of topographic arrangements of cell structure and function along the MNTB mediolateral axis (Hoffpauir et al., 2006; Rodriguez-Contreras et al., 2008; Holcomb et al., 2013; Xiao et al., 2013). In newborn prehearing rodents, spatially restricted and synchronous spontaneous activity in inner hair cells propagates along the developing auditory brainstem and refines the tonotopic maps (Friauf et al., 1999; Kandler et al., 2009; Sonntag et al., 2009; Tritsch et al., 2010; Crins et al., 2011; Leighton and Lohmann, 2016; Sun et al., 2018; Di Guilmi and Rodríguez-Contreras, 2021). Prior to P4, MNTB axons are abundant yet topographically imprecise (Sanes and Siverls, 1991). By P9, MNTB-LSO connections are refined, topographic precision is increased, and synapses are strengthened following activity-dependent pruning (Sanes and Friauf, 2000;

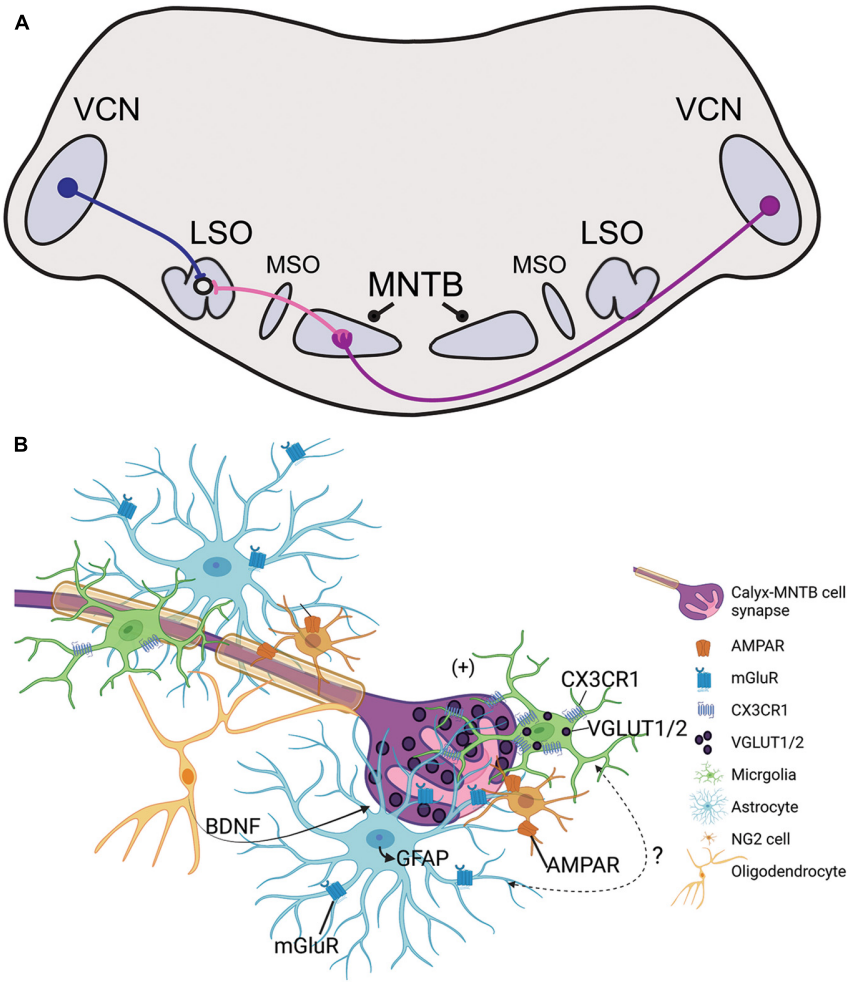

FIGURE 1 | (A) Illustration of the sound localization pathway in the auditory brainstem. Globular bushy cells (purple) cross the midline and terminate onto the contralateral medial nucleus of the trapezoid body (MNTB) through the calyx of Held. MNTB neurons provide inhibitory input to cells in the medial superior olive (MSO) and lateral superior olive (LSO; projections shown in pink). LSO neurons simultaneously receive excitatory input from the ipsilateral ventral cochlear nucleus (VCN) via spherical bushy cells (blue). The excitatory/inhibitory ratio in the LSO is used in interaural level difference computation to facilitate sound source localization. **(B)** Schematic representation of glial signaling at the calyx of Held during development. The GBC axon is highly myelinated and terminates in the calyx of Held (purple), which is surrounded by microglia (green), astrocytes (light blue), NG2 cells (orange), and oligodendrocytes (yellow). Glutamatergic vesicles (dark purple) are released from the calyx and dominantly modulate the MNTB neuron (pink). Synapse development and strengthening depend on oligodendrocyte secretion of BDNF, and receptors such as NG2-AMPAR and astrocyte-mGluR which respond to calyceal glutamatergic release. Microglia contain VGLUT1/2 puncta and express CX3CR1, a receptor that modulates inhibitory pruning in the MNTB during circuit formation. Microglia elimination reduces GFAP expression in the MNTB but the signaling mechanism involving microglia-astrocyte communication has not been identified.

Kim and Kandler, 2003; Müller et al., 2009, 2019; Hirtz et al., 2012; Clause et al., 2014). Genetic removal of the α9 subunit of nicotinic acetylcholine receptors (α9 KO) affects spontaneous firing patterns without altering overall activity levels and prohibits functional and structural sharpening of the inhibitory tonotopic map in the projection from MNTB to LSO (Clause et al., 2014), demonstrating that temporal patterns of spontaneous activity are important in development.

The mature MNTB contains a cell size gradient, which increases from the most medial (high frequency) to the most lateral (low frequency) regions (Weatherstone et al., 2017; Milinkeviciute et al., 2021a). *Fmr1* KO mice have a delay in the establishment of the cell size gradient across the MNTB mediolateral axis (Rotschafer et al., 2015). Calyces also increase in size along the tonotopic axis (Milinkeviciute et al., 2021a). Membrane capacitance is correlated with larger synaptic input across the tonotopic axis and time constants are faster in the medial neurons compared to the lateral neurons (Weatherstone et al., 2017). These tonotopic variations reflect the optimization of MNTB cells for function at a wide range of frequencies.

Ion channels are tonotopically distributed in the MNTB, and this gradient can be disrupted with hearing impairment (von Hehn et al., 2004). Kv3.1 tonotopic distribution is lost in mice lacking *Fmr1* (Strumbos et al., 2010). Congenital removal of *Pak1*, an autism-linked gene which normally regulates the development and maintenance of hair cell stereocilia, results in

profound hearing loss and a reduction in synapse density in the cochleae, which may disable the establishment of topography (Cheng et al., 2021).

Inhibitory Synapse Distribution

Synaptic puncta are also distributed in a gradient across the MNTB mediolateral axis. Glycine transporter 2 (GLYT2) positive puncta can be detected in the MNTB prior to hearing onset and increase in expression across the mediolateral axis in the adult mouse (Friauf et al., 1999; Altieri et al., 2014; Milinkeviciute et al., 2021a). Loss of the microglial fractalkine receptor *Cx3cr1*, an ASD and SZ-linked gene (Ishizuka et al., 2017), disrupts the topographic distribution of GLYT2 in the MNTB, leads to a loss of MNTB neural size gradients and faster signal transmission, as measured by the auditory brainstem response (ABR) (Ishizuka et al., 2017; Milinkeviciute et al., 2021a). The MNTB in *Fmr1* KO mice shows elevated levels of GABA/glycinergic marker vesicular GABA transporter (VGAT) (Rotschafer et al., 2015; Ruby et al., 2015). Functionally *Fmr1* KO mice have diminished peak amplitudes as measured by the ABR, and fewer all-or-none EPSCs in the MNTB (Rotschafer et al., 2015; Lu, 2019). Together, these studies show that autism-linked genes appear to influence distributions of ion channels and levels of inhibitory synapses, potentially altering balance in E/I neurotransmission.

GLIAL MECHANISMS IN SYNAPTIC PRUNING

Synaptic development, elimination, and maintenance are also mediated by glial cells. *Post-mortem* examinations of ASD or SZ brains have shown increased glial cell number and activation levels, and models of these neurodevelopmental disorders display altered glial pathology (Rodriguez and Kern, 2011; Laskaris et al., 2016). Glia contact and modulate synapses both during development and in the mature brain. Developmental fate-mapping studies show that glial cell expansion during development coincides with the formation of neural circuits in the auditory brainstem; SOC cell-type specific markers co-labeled with glial cell markers in the MNTB (Brandebura et al., 2018). At P0, glia, including microglia, astrocytes, and oligodendrocytes, sparsely occupy lateral regions of the brainstem including the CN and over the first two postnatal weeks can be detected in more medial regions (Dinh et al., 2014; Saliu et al., 2014). In the MNTB, neuron-enriched genes decrease across the first two postnatal weeks, while glia-enriched genes increase within the same time frame (Kolson et al., 2016a). Glial cells interact with calyces and MNTB principal cells in an orchestrated manner both during development and adulthood (Dinh et al., 2014; Kolson et al., 2016a).

Astrocytes Contact and Modulate MNTB Synapses

Astrocytes contact pre- and postsynaptic membranes in MNTB (Elezgarai et al., 2001) and these contacts elicit slow inward currents through gliotransmisson in the mature MNTB (Reyes-Haro et al., 2010). Astrocytes lie in close apposition to the developing calyx of Held (**Figure 1B**; Dinh et al., 2014). In the MNTB astrocytes are coupled via gap junctions, and a single astrocyte can contact multiple MNTB principal cells and directly contact calyceal membranes in the active zones of the synapse (Müller et al., 2009; Reyes-Haro et al., 2010). Astrocytes express glutamate transporters and receptors, but calyceal activity does not trigger glutamate uptake currents in astrocytes (Bergles and Jahr, 1997; Renden et al., 2005; Reyes-Haro et al., 2010). The vellous processes of astrocytes contain metabotropic glutamate receptors in mice, reported at P6-18, which allows for uptake of excess glutamate from calyces and prevention of glutamate receptor saturation in the immature calyx (**Figure 1B**; Elezgarai et al., 2001; Sätzler et al., 2002; Renden et al., 2005; Uwechue et al., 2012).

Pharmacological ablation of microglia during development decreases expression of glial fibrillary acidic protein (GFAP), a marker for mature astrocytes, in the MNTB (Milinkeviciute et al., 2019). When microglia return to control levels following the cessation of treatment, GFAP expression is restored to that of age-matched control mice (Milinkeviciute et al., 2021b). Deletion of Cx3cr1, expressed primarily on microglia, leads to an increase in GFAP expression in the MNTB (**Figure 1B**; Milinkeviciute et al., 2021a). Mice lacking *Fmr1* have significantly more astrocytes in the VCN and LSO at P14, but there were no differences in the MNTB at this age, despite the abnormal cell numbers and sizes found in the MNTB at that age (Rotschafer et al., 2015). Studies of astrocytes in the auditory brainstem of SZ or ADHD are lacking, despite the evidence of reactive astrogliosis found in SZ or abnormal astrocytosis in ADHD models (Lim and Mah, 2015; Tarasov et al., 2020).

Oligodendrocytes Regulate Calyx Function

Non-calyceal spaces surrounding MNTB principal cells are filled with microglia, astrocytes, and/or oligodendrocytes (**Figure 1B**;

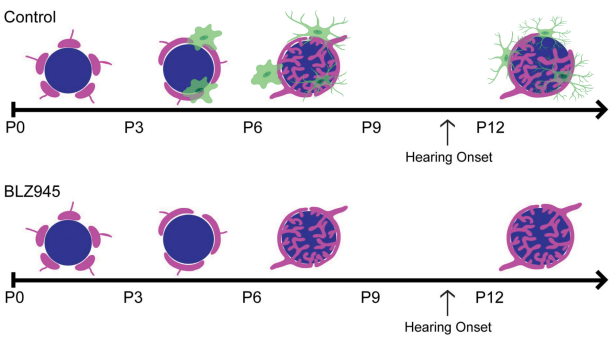

FIGURE 2 | (Top) Schematic representation of calyceal pruning during the first two postnatal weeks. Proto-calyces (magenta) innervate MNTB cells (blue) and are eliminated until a single dominant input remains. Microglia (green) are seen near calyces and display mature morphology after hearing onset. **(Bottom)** Microglia elimination with BLZ945 impairs calyceal pruning and leads to higher levels of polyinnervated MNTB neurons. Adapted from Milinkeviciute et al. (2019).

Elezgarai et al., 2001; Reyes-Haro et al., 2010; Holcomb et al., 2013; Dinh et al., 2014). Firing patterns of GBCs can influence axon diameter and myelin thickness, suggesting that GBCs may regulate their own myelination (Sinclair et al., 2017). Neuron/glia antigen 2 (NG2)-glia, typically regarded as oligodendrocyte progenitor cells (Eugenín-von Bernhardi and Dimou, 2016), also interact with the calyx of Held and receive excitatory input from calyces through AMPA-receptor mediated "synapse-like" inputs (**Figure 1B**; Müller et al., 2009). NG2 cells are involved in fast signaling with synapses in the mature and developing CNS (Bergles et al., 2000). In the brainstem, oligodendrocytes release BDNF to modulate the glutamate vesicle pool at the nerve terminal, thereby mediating calyx strength and synaptic plasticity in an activity-dependent manner (Berret et al., 2017; Jang et al., 2019). BDNF has been detected at abnormal levels in ASD and SZ patients (Bryn et al., 2015; Gören, 2016; Saghazadeh and Rezaei, 2017; Peng et al., 2018). The development of oligodendrocytes and NG2 cells are dependent on postnatal microglia (Hagemeyer et al., 2017). Although auditory brainstem functions of BDNF in ASD or SZ models are unknown, this signaling pathway could be a regulatory mechanism for E/I balance at the level of the MNTB.

Microglia Regulate Synapse Elimination and Brainstem Function

Microglia have increasingly become regarded as circuit sculptors in that they shape axonal projections, eliminate excess synapses, and strengthen intact connections (Paolicelli et al., 2011; Kettenmann et al., 2013). *Post-mortem* examinations of ASD brains showed higher microglial densities in the cerebral cortex (Tetreault et al., 2012) and abnormal microglial-neural spatial organization in the prefrontal cortex (Morgan et al., 2012). Further, inhibition of microglial activation is a potential therapeutic strategy for SZ, and microglial modulation may be a strategy to induce synaptic pruning in ASD (Monji et al., 2009; Andoh et al., 2019). Thus, it is interesting to identify the roles of microglia in auditory circuit development. Microglia can be sparsely detected in the VCN as early as P0, with expression patterns in the MNTB appearing by P6 (Dinh et al., 2014). Microglia in the early postnatal period first appear to have an amoeboid shape and later show a ramified morphology with more extended processes, indicating microglial maturation. In the mouse MNTB, microglial numbers peak by P14, an age after hearing onset. Microglia are in close apposition with the calyx of Held, with their processes interposed between calyces and MNTB principal cells, and peak in number at a time when excess synaptic contacts are pruned (**Figure 2**; Holcomb et al., 2013; Dinh et al., 2014). Loss of microglia during development impairs calyceal pruning after hearing onset (**Figure 2**; Milinkeviciute et al., 2019). VGLUT1/2 puncta were observed within microglia, possibly indicating that microglia engulf glutamatergic terminals during pruning. After cessation of the microglial-inhibiting drug BLZ945, microglia gradually returned from lateral to medial regions of the brainstem, recapitulating the pattern seen in normal development. The return of microglia was associated with recovery of auditory brainstem maturation and partial recovery of deficits in the auditory brainstem response (Dinh et al., 2014; Milinkeviciute et al., 2021b). Microglia may also influence the pruning of inhibitory synapses in the auditory system, as deletion of microglial *Cx3cr1* was associated with impaired pruning of inhibitory synapses in MNTB (Milinkeviciute et al., 2021a).

In animals deafened after the first postnatal week, microglia in VCN have more active morphology compared to the control group, which showed more ramified processes (Noda et al., 2019). In mice with cochlear removals activated microglia in the VCN were in close apposition to glutamatergic but not GABAergic synapses (Janz and Illing, 2014). Further, deafening led to an upregulation of phagocytic and anti-inflammatory markers in the VCN (Noda et al., 2019). From these studies, it appears that microglia regulate the elimination of synapses during auditory circuit development. Whether similar findings would be detected in a model of sensory processing disorders is not known. A potential clue is that mice that lack certain autism-linked genes, such as *Fmr1* and *Cx3cr1*, show impaired pruning and that ASD and SZ are linked with abnormal microglia.

CONCLUDING REMARKS

In this review, we discussed factors that are required for normal MNTB development as well as ASD-related models that impair auditory development. The establishment of the MNTB requires factors that regulate axon guidance, development of synapses as well as topographic gradients, synapse elimination, and synapse strengthening. In models of ASD, loss of *Fmr1*, *Pak1*, or *Cx3cr1* results in structural and functional alterations of synapses and an altered glial cell profile. These factors may similarly alter synaptic balance in SZ, ADHD, or other neurodevelopmental disorders.

AUTHOR CONTRIBUTIONS

SC, GM, and KC wrote and edited the manuscript. All authors contributed to the article and approved the submitted version.

FUNDING

This work was supported by NIH NIDCD DC010796 and NIH T32 DC010775.

REFERENCES

Altieri, S. C., Zhao, T., Jalabi, W., and Maricich, S. M. (2014). Development of glycinergic innervation to the murine LSO and SPN in the presence and absence of the MNTB. *Front. Neural. Circuits* 8:109. doi: 10.3389/fncir.2014.00109

Andoh, M., Ikegaya, Y., and Koyama, R. (2019). Microglia as possible therapeutic targets for autism spectrum disorders. *Prog. Mol. Biol. Transl. Sci.* 167, 223–245. doi: 10.1016/bs.pmbts.2019.06.012

Behrend, O., Brand, A., Kapfer, C., and Grothe, B. (2002). Auditory response properties in the superior paraolivary nucleus of the gerbil. *J. Neurophysiol.* 87, 2915–2928. doi: 10.1152/jn.2002.87.6.2915

Bergles, D. E., and Jahr, C. E. (1997). Synaptic activation of glutamate transporters in hippocampal astrocytes. *Neuron* 19, 1297–1308. doi: 10.1016/S0896-6273(00)80420-1

Bergles, D. E., Roberts, J. D., Somogyi, P., and Jahr, C. E. (2000). Glutamatergic synapses on oligodendrocyte precursor cells in the hippocampus. *Nature* 405, 187–191. doi: 10.1038/35012083

Berret, E., Barron, T., Xu, J., Debner, E., Kim, E. J., and Kim, J. H. (2017). Oligodendroglial excitability mediated by glutamatergic inputs and Nav1.2 activation. *Nat. Commun.* 8:557. doi: 10.1038/s41467-017-00688-0

Borst, J. G., and Soria van Hoeve, J. (2012). The calyx of Held synapse: from model synapse to auditory relay. *Annu. Rev. Physiol.* 74, 199–224. doi: 10.1146/annurev-physiol-020911-153236

Brandebura, A. N., Morehead, M., Heller, D. T., Holcomb, P., Kolson, D. R., Jones, G., et al. (2018). Glial Cell Expansion Coincides with Neural Circuit Formation in the Developing Auditory Brainstem. *Dev. Neurobiol.* 78, 1097–1116. doi: 10.1002/dneu.22633

Bryn, V., Halvorsen, B., Ueland, T., Isaksen, J., Kolkova, K., Ravn, K., et al. (2015). Brain derived neurotrophic factor (BDNF) and autism spectrum disorders (ASD) in childhood. *Eur. J. Paediatr. Neurol.* 19, 411–414. doi: 10.1016/j.ejpn.2015.03.005

Cant, N. B., and Morest, D. K. (1979). The bushy cells in the anteroventral cochlear nucleus of the cat. *Neuroscience* 4, 1925–1945. doi: 10.1016/0306-4522(79)90066-6

Cheng, C., Hou, Y., Zhang, Z., Wang, Y., Lu, L., Zhang, L., et al. (2021). Disruption of the autism-related gene Pak1 causes stereocilia disorganization, hair cell loss, and deafness in mice. *J. Genet. Genom.* 48, 324–332. doi: 10.1016/j.jgg.2021.03.010

Claesdotter-Hybbinette, E., Safdarzadeh-Haghighi, M., Råstam, M., and Lindvall, M. (2015). Abnormal brainstem auditory response in young females with ADHD. *Psychiatry Res.* 229, 750–754. doi: 10.1016/j.psychres.2015.08.007

Clause, A., Kim, G., Sonntag, M., Weisz, C. J., Vetter, D. E., Rûbsamen, R., et al. (2014). The precise temporal pattern of prehearing spontaneous activity is necessary for tonotopic map refinement. *Neuron* 82, 822–835. doi: 10.1016/j.neuron.2014.04.001

Crins, T. T., Rusu, S. I., Rodríguez-Contreras, A., and Borst, J. G. (2011). Developmental changes in short-term plasticity at the rat calyx of Held synapse. *J. Neurosci.* 31, 11706–11717. doi: 10.1523/JNEUROSCI.1995-11.2011

Dadalko, O. I., and Travers, B. G. (2018). Evidence for Brainstem Contributions to Autism Spectrum Disorders. *Front. Integr. Neurosci.* 12:47. doi: 10.3389/fnint.2018.00047

Dehmel, S., Kopp-Scheinpflug, C., Dörrscheidt, G. J., and Rübsamen, R. (2002). Electrophysiological characterization of the superior paraolivary nucleus in the Mongolian gerbil. *Hear Res.* 172, 18–36. doi: 10.1016/S0378-5955(02)00353-2

Di Guilmi, M. N., and Rodríguez-Contreras, A. (2021). Characterization of Developmental Changes in Spontaneous Electrical Activity of Medial Superior Olivary Neurons Before Hearing Onset With a Combination of Injectable and Volatile Anesthesia. *Front. Neurosci.* 15:654479. doi: 10.3389/fnins.2021.654479

Dinh, M. L., Koppel, S. J., Korn, M. J., and Cramer, K. S. (2014). Distribution of glial cells in the auditory brainstem: normal development and effects of unilateral lesion. *Neuroscience* 278, 237–252. doi: 10.1016/j.neuroscience.2014.08.016

Elezgarai, I., Bilbao, A., Mateos, J. M., Azkue, J. J., Benítez, R., Osorio, A., et al. (2001). Group II metabotropic glutamate receptors are differentially expressed in the medial nucleus of the trapezoid body in the developing and adult rat. *Neuroscience* 104, 487–498. doi: 10.1016/S0306-4522(01)00080-X

Eugenín-von Bernhardi, J., and Dimou, L. (2016). NG2-glia. *Adv. Exp. Med. Biol.* 949, 27–45. doi: 10.1007/978-3-319-40764-7_2

Fekete, D. M., Rouiller, E. M., Liberman, M. C., and Ryugo, D. K. (1984). The central projections of intracellularly labeled auditory nerve fibers in cats. *J. Comp. Neurol.* 229, 432–450. doi: 10.1002/cne.902290311

Friauf, E., Aragón, C., Löhrke, S., Westenfelder, B., and Zafra, F. (1999). Developmental expression of the glycine transporter GLYT2 in the auditory system of rats suggests involvement in synapse maturation. *J. Comp. Neurol.* 412, 17–37. doi: 10.1002/(SICI)1096-9861(19990913)412:1<17::AID-CNE2>3.0.CO;2-E

Garcia-Pino, E., Gessele, N., and Koch, U. (2017). Enhanced Excitatory Connectivity and Disturbed Sound Processing in the Auditory Brainstem of Fragile X Mice. *J. Neurosci.* 37, 7403–7419. doi: 10.1523/JNEUROSCI.2310-16.2017

Gillespie, D. C., Kim, G., and Kandler, K. (2005). Inhibitory synapses in the developing auditory system are glutamatergic. *Nat. Neurosci.* 8, 332–338. doi: 10.1038/nn1397

Gören, J. L. (2016). Brain-derived neurotrophic factor and schizophrenia. *Ment. Health Clin.* 6, 285–288. doi: 10.9740/mhc.2016.11.285

Hagemeyer, N., Hanft, K. M., Akriditou, M. A., Unger, N., Park, E. S., Stanley, E. R., et al. (2017). Microglia contribute to normal myelinogenesis and to oligodendrocyte progenitor maintenance during adulthood. *Acta. Neuropathol.* 134, 441–458. doi: 10.1007/s00401-017-1747-1

Harrison, J. M., and Irving, R. (1966). Ascending connections of the anterior ventral cochlear nucleus in the rat. *J. Comp. Neurol.* 126, 51–63. doi: 10.1002/cne.901260105

Hashimoto, T., Tayama, M., Miyazaki, M., Sakurama, N., Yoshimoto, T., Murakawa, K., et al. (1992). Reduced brainstem size in children with autism. *Brain Dev.* 14, 94–97. doi: 10.1016/S0387-7604(12)80093-3

Held, H. (1893). Die zentrale Gehörleitung. *Arch. Anat. Physiol. Anat. Abtheil.* 17, 201–248.

Hirtz, J. J., Braun, N., Griesemer, D., Hannes, C., Janz, K., Löhrke, S., et al. (2012). Synaptic refinement of an inhibitory topographic map in the auditory brainstem requires functional Cav1.3 calcium channels. *J. Neurosci.* 32, 14602–14616. doi: 10.1523/JNEUROSCI.0765-12.2012

Hoffpauir, B. K., Grimes, J. L., Mathers, P. H., and Spirou, G. A. (2006). Synaptogenesis of the calyx of Held: rapid onset of function and one-to-one morphological innervation. *J. Neurosci.* 26, 5511–5523. doi: 10.1523/JNEUROSCI.5525-05.2006

Hoffpauir, B. K., Kolson, D. R., Mathers, P. H., and Spirou, G. A. (2010). Maturation of synaptic partners: functional phenotype and synaptic organization tuned in synchrony. *J. Physiol.* 588, 4365–4385. doi: 10.1113/jphysiol.2010.198564

Holcomb, P. S., Hoffpauir, B. K., Hoyson, M. C., Jackson, D. R., Deerinck, T. J., Marrs, G. S., et al. (2013). Synaptic inputs compete during rapid formation of the calyx of Held: a new model system for neural development. *J. Neurosci.* 33, 12954–12969. doi: 10.1523/JNEUROSCI.1087-13.2013

Howell, D. M., Morgan, W. J., Jarjour, A. A., Spirou, G. A., Berrebi, A. S., Kennedy, T. E., et al. (2007). Molecular guidance cues necessary for axon pathfinding from the ventral cochlear nucleus. *J. Comp. Neurol.* 504, 533–549. doi: 10.1002/cne.21443

Hsieh, C. Y., Nakamura, P. A., Luk, S. O., Miko, I. J., Henkemeyer, M., and Cramer, K. S. (2010). Ephrin-B Reverse Signaling Is Required for Formation of Strictly Contralateral Auditory Brainstem Pathways. *J. Neurosci.* 30, 9840–9849. doi: 10.1523/JNEUROSCI.0386-10.2010

Ishizuka, K., Fujita, Y., Kawabata, T., Kimura, H., Iwayama, Y., Inada, T., et al. (2017). Rare genetic variants in CX3CR1 and their contribution to the increased risk of schizophrenia and autism spectrum disorders. *Trans. Psychiatry* 7, e1184–e1184. doi: 10.1038/tp.2017.173

Jang, M., Gould, E., Xu, J., Kim, E. J., and Kim, J. H. (2019). Oligodendrocytes regulate presynaptic properties and neurotransmission through BDNF signaling in the mouse brainstem. *Elife* 8:e42156. doi: 10.7554/eLife.42156

Janz, P., and Illing, R.-B. (2014). A role for microglial cells in reshaping neuronal circuitry of the adult rat auditory brainstem after its sensory deafferentation. *J. Neurosci. Res.* 92, 432–445. doi: 10.1002/jnr.23334

Kandler, K., Clause, A., and Noh, J. (2009). Tonotopic reorganization of developing auditory brainstem circuits. *Nat. Neurosci.* 12, 711–717. doi: 10.1038/nn.2332

Kandler, K., and Friauf, E. (1993). Pre- and postnatal development of efferent connections of the cochlear nucleus in the rat. *J. Comp. Neurol.* 328, 161–184. doi: 10.1002/cne.903280202

Kandler, K., and Gillespie, D. C. (2005). Developmental refinement of inhibitory sound-localization circuits. *Trends Neurosci.* 28, 290–296. doi: 10.1016/j.tins.2005.04.007

Kashima, R., Roy, S., Ascano, M., Martinez-Cerdeno, V., Ariza-Torres, J., Kim, S., et al. (2016). Augmented noncanonical BMP type II receptor signaling

mediates the synaptic abnormality of fragile X syndrome. *Sci. Signal.* 9:ra58. doi: 10.1126/scisignal.aaf6060

Kettenmann, H., Kirchhoff, F., and Verkhratsky, A. (2013). Microglia: new roles for the synaptic stripper. *Neuron* 77, 10–18. doi: 10.1016/j.neuron.2012.12.023

Kim, G., and Kandler, K. (2003). Elimination and strengthening of glycinergic/GABAergic connections during tonotopic map formation. *Nat. Neurosci.* 6, 282–290. doi: 10.1038/nn1015

Knoth, I. S., Vannasing, P., Major, P., Michaud, J. L., and Lippé, S. (2014). Alterations of visual and auditory evoked potentials in fragile X syndrome. *Inter. J. Dev. Neurosci.* 36, 90–97. doi: 10.1016/j.ijdevneu.2014.05.003

Kolson, D. R., Wan, J., Wu, J., Dehoff, M., Brandebura, A. N., Qian, J., et al. (2016a). Temporal patterns of gene expression during calyx of held development. *Dev. Neurobiol.* 76, 166–189.

Kolson, D. R., Wan, J., Wu, J., Dehoff, M., Brandebura, A. N., Qian, J., et al. (2016b). Temporal patterns of gene expression during calyx of held development. *Dev. Neurobiol.* 76, 166–189. doi: 10.1002/dneu.22306

Kopp-Scheinpflug, C., Sinclair, J. L., and Linden, J. F. (2018). When Sound Stops:offset Responses in the Auditory System. *Trends Neurosci.* 41, 712–728. doi: 10.1016/j.tins.2018.08.009

Kotak, V. C., Korada, S., Schwartz, I. R., and Sanes, D. H. (1998). A developmental shift from GABAergic to glycinergic transmission in the central auditory system. *J. Neurosci.* 18, 4646–4655. doi: 10.1523/JNEUROSCI.18-12-04646.1998

Kronander, E., Clark, C., and Schneggenburger, R. (2019). Role of BMP Signaling for the Formation of Auditory Brainstem Nuclei and Large Auditory Relay Synapses. *Dev. Neurobiol.* 79, 155–174. doi: 10.1002/dneu.22661

Kulesza, R. J. Jr. (2007). Cytoarchitecture of the human superior olivary complex: medial and lateral superior olive. *Hear Res.* 225, 80–90. doi: 10.1016/j.heares.2006.12.006

Kulesza, R. J. Jr., and Grothe, B. (2015). Yes, there is a medial nucleus of the trapezoid body in humans. *Front. Neuroanat.* 9:35. doi: 10.3389/fnana.2015.00035

Kulesza, R. J. Jr., Lukose, R., and Stevens, L. V. (2011). Malformation of the human superior olive in autistic spectrum disorders. *Brain Res.* 1367, 360–371. doi: 10.1016/j.brainres.2010.10.015

Kumar, S., Reynolds, K., Ji, Y., Gu, R., Rai, S., and Zhou, C. J. (2019). Impaired neurodevelopmental pathways in autism spectrum disorder: a review of signaling mechanisms and crosstalk. *J. Neurodevelop. Disord.* 11:10. doi: 10.1186/s11689-019-9268-y

Kuwabara, N., DiCaprio, R. A., and Zook, J. M. (1991). Afferents to the medial nucleus of the trapezoid body and their collateral projections. *J. Comp. Neurol.* 314, 684–706. doi: 10.1002/cne.903140405

Kuwabara, N., and Zook, J. M. (1991). Classification of the principal cells of the medial nucleus of the trapezoid body. *J. Comp. Neurol.* 314, 707–720. doi: 10.1002/cne.903140406

Kuwabara, N., and Zook, J. M. (1992). Projections to the medial superior olive from the medial and lateral nuclei of the trapezoid body in rodents and bats. *J. Comp. Neurol.* 324, 522–538. doi: 10.1002/cne.903240406

Laskaris, L. E., Di Biase, M. A., Everall, I., Chana, G., Christopoulos, A., Skafidas, E., et al. (2016). Microglial activation and progressive brain changes in schizophrenia. *Br. J. Pharmacol.* 173, 666–680. doi: 10.1111/bph.13364

Lee, H., Bach, E., Noh, J., Delpire, E., and Kandler, K. (2016). Hyperpolarization-independent maturation and refinement of GABA/glycinergic connections in the auditory brain stem. *J. Neurophysiol.* 115, 1170–1182. doi: 10.1152/jn.00926.2015

Leighton, A. H., and Lohmann, C. (2016). The Wiring of Developing Sensory Circuits-From Patterned Spontaneous Activity to Synaptic Plasticity Mechanisms. *Front. Neural. Circuits* 10:71. doi: 10.3389/fncir.2016.00071

Lim, S.-Y., and Mah, W. (2015). Abnormal Astrocytosis in the Basal Ganglia Pathway of Git1(-/-) Mice. *Mol. Cells* 38, 540–547. doi: 10.14348/molcells.2015.0041

Liu, H. H., Huang, C. F., and Wang, X. (2014). Acoustic signal characteristic detection by neurons in ventral nucleus of the lateral lemniscus in mice. *Dongwuxue Yanjiu* 35, 500–509.

Lu, Y. (2019). Subtle differences in synaptic transmission in medial nucleus of trapezoid body neurons between wild-type and Fmr1 knockout mice. *Brain Res.* 1717, 95–103. doi: 10.1016/j.brainres.2019.04.006

Lukose, R., Beebe, K., and Kulesza, R. J. Jr. (2015). Organization of the human superior olivary complex in 15q duplication syndromes and autism spectrum disorders. *Neuroscience* 286, 216–230. doi: 10.1016/j.neuroscience.2014.11.033

Magnusson, A. K., Kapfer, C., Grothe, B., and Koch, U. (2005). Maturation of glycinergic inhibition in the gerbil medial superior olive after hearing onset. *J. Physiol.* 568, 497–512. doi: 10.1113/jphysiol.2005.094763

Matthews, N., Todd, J., Budd, T. W., Cooper, G., and Michie, P. T. (2007). Auditory lateralization in schizophrenia–mismatch negativity and behavioral evidence of a selective impairment in encoding interaural time cues. *Clin. Neurophysiol.* 118, 833–844. doi: 10.1016/j.clinph.2006.11.017

McCullagh, E. A., Rotschafer, S. E., Auerbach, B. D., Klug, A., Kaczmarek, L. K., Cramer, K. S., et al. (2020). Mechanisms underlying auditory processing deficits in Fragile X syndrome. *Faseb J.* 34, 3501–3518. doi: 10.1096/fj.201902435R

Milinkeviciute, G., Chokr, S. M., Castro, E. M., and Cramer, K. S. (2021a). CX3CR1 mutation alters synaptic and astrocytic protein expression, topographic gradients, and response latencies in the auditory brainstem. *J. Comp. Neurol.* 529, 3076–3097. doi: 10.1002/cne.25150

Milinkeviciute, G., Chokr, S. M., and Cramer, K. S. (2021b). Auditory Brainstem Deficits from Early Treatment with a CSF1R Inhibitor Largely Recover with Microglial Repopulation. *eNeuro* 8, ENEURO.318–ENEURO.320. doi: 10.1523/ENEURO.0318-20.2021

Milinkeviciute, G., Henningfield, C. M., Muniak, M. A., Chokr, S. M., Green, K. N., and Cramer, K. S. (2019). Microglia Regulate Pruning of Specialized Synapses in the Auditory Brainstem. *Front. Neural. Circuits* 13:55. doi: 10.3389/fncir.2019.00055

Monji, A., Kato, T., and Kanba, S. (2009). Cytokines and schizophrenia:microglia hypothesis of schizophrenia. *Psychiatry Clin. Neurosci.* 63, 257–265. doi: 10.1111/j.1440-1819.2009.01945.x

Moore, M. J., and Caspary, D. M. (1983). Strychnine blocks binaural inhibition in lateral superior olivary neurons. *J. Neurosci.* 3, 237–242. doi: 10.1523/JNEUROSCI.03-01-00237.1983

Morest, D. K. (1969). The differentiation of cerebral dendrites:a study of the post-migratory neuroblast in the medial nucleus of the trapezoid body. *Z Anat. Entwicklungsgesch* 128, 271–289. doi: 10.1007/BF00522528

Morgan, J. T., Chana, G., Abramson, I., Semendeferi, K., Courchesne, E., and Everall, I. P. (2012). Abnormal microglial-neuronal spatial organization in the dorsolateral prefrontal cortex in autism. *Brain Res.* 1456, 72–81. doi: 10.1016/j.brainres.2012.03.036

Müller, J., Reyes-Haro, D., Pivneva, T., Nolte, C., Schaette, R., Lübke, J., et al. (2009). The principal neurons of the medial nucleus of the trapezoid body and NG2(+) glial cells receive coordinated excitatory synaptic input. *J. Gen. Physiol.* 134, 115–127. doi: 10.1085/jgp.200910194

Müller, N. I. C., Sonntag, M., Maraslioglu, A., Hirtz, J. J., and Friauf, E. (2019). Topographic map refinement and synaptic strengthening of a sound localization circuit require spontaneous peripheral activity. *J. Physiol.* 597, 5469–5493. doi: 10.1113/JP277757

Nabekura, J., Katsurabayashi, S., Kakazu, Y., Shibata, S., Matsubara, A., Jinno, S., et al. (2004). Developmental switch from GABA to glycine release in single central synaptic terminals. *Nat. Neurosci.* 7, 17–23. doi: 10.1038/nn1170

Nicol, M. J., and Walmsley, B. (2002). Ultrastructural basis of synaptic transmission between endbulbs of Held and bushy cells in the rat cochlear nucleus. *J. Physiol.* 539, 713–723. doi: 10.1113/jphysiol.2001.012972

Noda, M., Hatano, M., Hattori, T., Takarada-Iemata, M., Shinozaki, T., Sugimoto, H., et al. (2019). Microglial activation in the cochlear nucleus after early hearing loss in rats. *Auris Nasus Larynx* 46, 716–723. doi: 10.1016/j.anl.2019.02.006

Nopoulos, P. C., Ceilley, J. W., Gailis, E. A., and Andreasen, N. C. (2001). An MRI study of midbrain morphology in patients with schizophrenia: relationship to psychosis, neuroleptics, and cerebellar neural circuitry. *Biol. Psychiatry* 49, 13–19. doi: 10.1016/S0006-3223(00)01059-3

Paolicelli, R. C., Bolasco, G., Pagani, F., Maggi, L., Scianni, M., Panzanelli, P., et al. (2011). Synaptic pruning by microglia is necessary for normal brain development. *Science* 333, 1456–1458. doi: 10.1126/science.1202529

Peng, S., Li, W., Lv, L., Zhang, Z., and Zhan, X. (2018). BDNF as a biomarker in diagnosis and evaluation of treatment for schizophrenia and depression. *Discov. Med.* 26, 127–136.

Perrin, M. A., Butler, P. D., DiCostanzo, J., Forchelli, G., Silipo, G., and Javitt, D. C. (2010). Spatial localization deficits and auditory cortical dysfunction in schizophrenia. *Schizophr Res.* 124, 161–168. doi: 10.1016/j.schres.2010.06.004

Pilati, N., Linley, D. M., Selvaskandan, H., Uchitel, O., Hennig, M. H., Kopp-Scheinpflug, C., et al. (2016). Acoustic trauma slows AMPA receptor-mediated EPSCs in the auditory brainstem, reducing GluA4 subunit expression as a mechanism to rescue binaural function. *J. Physiol.* 594, 3683–3703. doi: 10.1113/JP271929

Rajaram, E., Pagella, S., Grothe, B., and Kopp-Scheinpflug, C. (2020). Physiological and anatomical development of glycinergic inhibition in the mouse superior paraolivary nucleus following hearing onset. *J. Neurophysiol.* 124, 471–483. doi: 10.1152/jn.00053.2020

Renden, R., Taschenberger, H., Puente, N., Rusakov, D. A., Duvoisin, R., Wang, L. Y., et al. (2005). Glutamate transporter studies reveal the pruning of metabotropic glutamate receptors and absence of AMPA receptor desensitization at mature calyx of Held synapses. *J. Neurosci.* 25, 8482–8497. doi: 10.1523/JNEUROSCI.1848-05.2005

Reyes-Haro, D., Müller, J., Boresch, M., Pivneva, T., Benedetti, B., Scheller, A., et al. (2010). Neuron-astrocyte interactions in the medial nucleus of the trapezoid body. *J. Gen. Physiol.* 135, 583–594. doi: 10.1085/jgp.200910354

Rodriguez-Contreras, A., van Hoeve, J. S., Habets, R. L., Locher, H., and Borst, J. G. (2008). Dynamic development of the calyx of Held synapse. *Proc. Natl. Acad. Sci. U.S.A.* 105, 5603–5608. doi: 10.1073/pnas.0801395105

Rodriguez, J. I., and Kern, J. K. (2011). Evidence of microglial activation in autism and its possible role in brain underconnectivity. *Neuron Glia. Biol.* 7, 205–213. doi: 10.1017/S1740925X12000142

Rotschafer, S. E., Marshak, S., and Cramer, K. S. (2015). Deletion of Fmr1 alters function and synaptic inputs in the auditory brainstem. *PLoS One* 10:e0117266. doi: 10.1371/journal.pone.0117266

Ruby, K., Falvey, K., and Kulesza, R. J. (2015). Abnormal neuronal morphology and neurochemistry in the auditory brainstem of Fmr1 knockout rats. *Neuroscience* 303, 285–298. doi: 10.1016/j.neuroscience.2015.06.061

Ryugo, D. K., and Sento, S. (1991). Synaptic connections of the auditory nerve in cats: relationship between endbulbs of held and spherical bushy cells. *J. Comp. Neurol.* 305, 35–48. doi: 10.1002/cne.903050105

Saghazadeh, A., and Rezaei, N. (2017). Brain-Derived Neurotrophic Factor Levels in Autism:a Systematic Review and Meta-Analysis. *J. Autism Dev. Disord.* 47, 1018–1029. doi: 10.1007/s10803-016-3024-x

Saliu, A., Adise, S., Xian, S., Kudelska, K., and Rodríguez-Contreras, A. (2014). Natural and lesion-induced decrease in cell proliferation in the medial nucleus of the trapezoid body during hearing development. *J. Comp. Neurol.* 522, 971–985. doi: 10.1002/cne.23473

Sanes, D. H., and Friauf, E. (2000). Development and influence of inhibition in the lateral superior olivary nucleus. *Hear Res.* 147, 46–58. doi: 10.1016/S0378-5955(00)00119-2

Sanes, D. H., Markowitz, S., Bernstein, J., and Wardlow, J. (1992). The influence of inhibitory afferents on the development of postsynaptic dendritic arbors. *J. Comp. Neurol.* 321, 637–644. doi: 10.1002/cne.903210410

Sanes, D. H., and Siverls, V. (1991). Development and specificity of inhibitory terminal arborizations in the central nervous system. *J. Neurobiol.* 22, 837–854. doi: 10.1002/neu.480220805

Sanes, D. H., and Takács, C. (1993). Activity-dependent refinement of inhibitory connections. *Eur. J. Neurosci.* 5, 570–574. doi: 10.1111/j.1460-9568.1993.tb00522.x

Sätzler, K., Söhl, L. F., Bollmann, J. H., Borst, J. G. G., Frotscher, M., Sakmann, B., et al. (2002). Three-Dimensional Reconstruction of a Calyx of Held and Its Postsynaptic Principal Neuron in the Medial Nucleus of the Trapezoid Body. *J. Neurosci.* 22, 10567–10579. doi: 10.1523/JNEUROSCI.22-24-10567.2002

Sinclair, J. L., Fischl, M. J., Alexandrova, O., Heβ, M., Grothe, B., Leibold, C., et al. (2017). Sound-Evoked Activity Influences Myelination of Brainstem Axons in the Trapezoid Body. *J. Neurosci.* 37, 8239–8255. doi: 10.1523/JNEUROSCI.3728-16.2017

Smith, A., Storti, S., Lukose, R., and Kulesza, R. J. Jr. (2019). Structural and Functional Aberrations of the Auditory Brainstem in Autism Spectrum Disorder. *J. Am. Osteopath. Assoc.* 119, 41–50. doi: 10.7556/jaoa.2019.007

Sommer, I., Lingenhöhl, K., and Friauf, E. (1993). Principal cells of the rat medial nucleus of the trapezoid body: an intracellular in vivo study of their physiology and morphology. *Exp. Brain Res.* 95, 223–239. doi: 10.1007/BF00229781

Sonntag, M., Englitz, B., Kopp-Scheinpflug, C., and Rübsamen, R. (2009). Early postnatal development of spontaneous and acoustically evoked discharge activity of principal cells of the medial nucleus of the trapezoid body: an in vivo study in mice. *J. Neurosci.* 29, 9510–9520. doi: 10.1523/JNEUROSCI.1377-09.2009

Spirou, G. A., Rager, J., and Manis, P. B. (2005). Convergence of auditory-nerve fiber projections onto globular bushy cells. *Neuroscience* 136, 843–863. doi: 10.1016/j.neuroscience.2005.08.068

Strumbos, J. G., Brown, M. R., Kronengold, J., Polley, D. B., and Kaczmarek, L. K. (2010). Fragile X Mental Retardation Protein Is Required for Rapid Experience-Dependent Regulation of the Potassium Channel Kv3.1b. *J. Neurosci.* 30, 10263–10271. doi: 10.1523/JNEUROSCI.1125-10.2010

Sun, S., Babola, T., Pregernig, G., So, K. S., Nguyen, M., Su, S. M., et al. (2018). Hair Cell Mechanotransduction Regulates Spontaneous Activity and Spiral Ganglion Subtype Specification in the Auditory System. *Cell* 174, 1247–1263. doi: 10.1016/j.cell.2018.07.008

Tarasov, V. V., Svistunov, A. A., Chubarev, V. N., Sologova, S. S., Mukhortova, P., Levushkin, D., et al. (2020). Alterations of Astrocytes in the Context of Schizophrenic Dementia. *Front. Pharmacol.* 10:1612. doi: 10.3389/fphar.2019.01612

Tetreault, N. A., Hakeem, A. Y., Jiang, S., Williams, B. A., Allman, E., Wold, B. J., et al. (2012). Microglia in the cerebral cortex in autism. *J. Autism Dev. Disord.* 42, 2569–2584. doi: 10.1007/s10803-012-1513-0

Torres Cadenas, L., Fischl, M. J., and Weisz, C. J. C. (2020). Synaptic Inhibition of Medial Olivocochlear Efferent Neurons by Neurons of the Medial Nucleus of the Trapezoid Body. *J. Neurosci.* 40, 509–525. doi: 10.1523/JNEUROSCI.1288-19.2019

Tritsch, N. X., Rodriguez-Contreras, A., Crins, T. T., Wang, H. C., Borst, J. G., and Bergles, D. E. (2010). Calcium action potentials in hair cells pattern auditory neuron activity before hearing onset. *Nat. Neurosci.* 13, 1050–1052. doi: 10.1038/nn.2604

Uwechue, N. M., Marx, M.-C., Chevy, Q., and Billups, B. (2012). Activation of glutamate transport evokes rapid glutamine release from perisynaptic astrocytes. *J. Physiol.* 590, 2317–2331. doi: 10.1113/jphysiol.2011.226605

Van der Molen, M. J. W., Van der Molen, M. W., Ridderinkhof, K. R., Hamel, B. C. J., Curfs, L. M. G., and Ramakers, G. J. A. (2012). Auditory and visual cortical activity during selective attention in fragile X syndrome: A cascade of processing deficiencies. *Clin. Neurophysiol.* 123, 720–729. doi: 10.1016/j.clinph.2011.08.023

Visser, E., Zwiers, M. P., Kan, C. C., Hoekstra, L., van Opstal, A. J., and Buitelaar, J. K. (2013). Atypical vertical sound localization and sound-onset sensitivity in people with autism spectrum disorders. *J. Psychiatry Neurosci.* 38, 398–406. doi: 10.1503/jpn.120177

von Hehn, C. A., Bhattacharjee, A., and Kaczmarek, L. K. (2004). Loss of Kv3.1 tonotopicity and alterations in cAMP response element-binding protein signaling in central auditory neurons of hearing impaired mice. *J. Neurosci.* 24, 1936–1940. doi: 10.1523/JNEUROSCI.4554-03.2004

Walcher, J., Hassfurth, B., Grothe, B., and Koch, U. (2011). Comparative posthearing development of inhibitory inputs to the lateral superior olive in gerbils and mice. *J. Neurophysiol.* 106, 1443–1453. doi: 10.1152/jn.01087.2010

Weatherstone, J. H., Kopp-Scheinpflug, C., Pilati, N., Wang, Y., Forsythe, I. D., Rubel, E. W., et al. (2017). Maintenance of neuronal size gradient in MNTB requires sound-evoked activity. *J. Neurophysiol.* 117, 756–766. doi: 10.1152/jn.00528.2016

Xiao, L., Michalski, N., Kronander, E., Gjoni, E., Genoud, C., Knott, G., et al. (2013). BMP signaling specifies the development of a large and fast CNS synapse. *Nat. Neurosci.* 16, 856–864.

Yu, W. M., and Goodrich, L. V. (2014). Morphological and physiological development of auditory synapses. *Hear Res.* 311, 3–16.

Zarbin, M. A., Wamsley, J. K., and Kuhar, M. J. (1981). Glycine receptor: light microscopic autoradiographic localization with [3H]strychnine. *J. Neurosci.* 1, 532–547.

Conflict of Interest: The authors declare that the research was conducted in the absence of any commercial or financial relationships that could be construed as a potential conflict of interest.

Publisher's Note: All claims expressed in this article are solely those of the authors and do not necessarily represent those of their affiliated organizations, or those of the publisher, the editors and the reviewers. Any product that may be evaluated in this article, or claim that may be made by its manufacturer, is not guaranteed or endorsed by the publisher.

frontiers in Integrative Neuroscience

ORIGINAL RESEARCH
published: 03 March 2022
doi: 10.3389/fnint.2022.804743

Improving Imaging of the Brainstem and Cerebellum in Autistic Children: Transformation-Based High-Resolution Diffusion MRI (TiDi-Fused) in the Human Brainstem

*Jose Guerrero-Gonzalez[1,2†], Olivia Surgent[1,3†], Nagesh Adluru[1,4], Gregory R. Kirk[1], Douglas C. Dean III[1,2,5], Steven R. Kecskemeti[1], Andrew L. Alexander[1,2,6] and Brittany G. Travers[1,7]**

[1]Waisman Center, University of Wisconsin-Madison, Madison, WI, United States, [2]Department of Medical Physics, University of Wisconsin-Madison, Madison, WI, United States, [3]Neuroscience Training Program, University of Wisconsin-Madison, Madison, WI, United States, [4]Department of Radiology, University of Wisconsin-Madison, Madison, WI, United States, [5]Department of Pediatrics, University of Wisconsin-Madison, Madison, WI, United States, [6]Department of Psychiatry, University of Wisconsin-Madison, Madison, WI, United States, [7]Occupational Therapy Program in the Department of Kinesiology, University of Wisconsin-Madison, Madison, WI, United States

OPEN ACCESS

Edited by:
Randy J. Kulesza, Lake Erie College of Osteopathic Medicine, United States

Reviewed by:
Nataliia Maryenko, Kharkiv National Medical University, Ukraine
Nguyen Minh Duc, Pham Ngoc Thach University of Medicine, Vietnam

***Correspondence:**
Brittany G. Travers
btravers@wisc.edu

†These authors have contributed equally to this work and share first authorship

Received: *29 October 2021*
Accepted: *31 January 2022*
Published: *03 March 2022*

Citation:
Guerrero-Gonzalez J, Surgent O, Adluru N, Kirk GR, Dean DC III, Kecskemeti SR, Alexander AL and Travers BG (2022) Improving Imaging of the Brainstem and Cerebellum in Autistic Children: Transformation-Based High-Resolution Diffusion MRI (TiDi-Fused) in the Human Brainstem. Front. Integr. Neurosci. 16:804743. doi: 10.3389/fnint.2022.804743

Diffusion-weighted magnetic resonance imaging (dMRI) of the brainstem is technically challenging, especially in young autistic children as nearby tissue-air interfaces and motion (voluntary and physiological) can lead to artifacts. This limits the availability of high-resolution images, which are desirable for improving the ability to study brainstem structures. Furthermore, inherently low signal-to-noise ratios, geometric distortions, and sensitivity to motion not related to molecular diffusion have resulted in limited techniques for high-resolution data acquisition compared to other modalities such as T1-weighted imaging. Here, we implement a method for achieving increased apparent spatial resolution in pediatric dMRI that hinges on accurate geometric distortion correction and on high fidelity within subject image registration between dMRI and magnetization prepared rapid acquisition gradient echo (MPnRAGE) images. We call this post-processing pipeline T1 weighted-diffusion fused, or "TiDi-Fused". Data used in this work consists of dMRI data (2.4 mm resolution, corrected using FSL's Topup) and T1-weighted (T1w) MPnRAGE anatomical data (1 mm resolution) acquired from 128 autistic and non-autistic children (ages 6–10 years old). Accurate correction of geometric distortion permitted for a further increase in apparent resolution of the dMRI scan via boundary-based registration to the MPnRAGE T1w. Estimation of fiber orientation distributions and further analyses were carried out in the T1w space. Data processed with the TiDi-Fused method were qualitatively and quantitatively compared to data processed with conventional dMRI processing methods. Results show the advantages of the TiDi-Fused pipeline including sharper brainstem gray-white matter tissue contrast, improved inter-subject spatial alignment for group analyses of dMRI based measures, accurate spatial alignment with histology-based imaging of the brainstem, reduced variability in brainstem-cerebellar white matter tracts, and

more robust biologically plausible relationships between age and brainstem-cerebellar white matter tracts. Overall, this work identifies a promising pipeline for achieving high-resolution imaging of brainstem structures in pediatric and clinical populations who may not be able to endure long scan times. This pipeline may serve as a gateway for feasibly elucidating brainstem contributions to autism and other conditions.

Keywords: dMRI (diffusion magnetic resonance imaging), MPnRAGE, autism, brainstem, boundary-based registration

INTRODUCTION

Precise quantification of brainstem microstructure in autistic[1] children is important as cytoarchitectural properties of the brainstem may contribute to the etiology of autism spectrum disorder (ASD). Brainstem white matter in autistic youth has been associated with motor skills (Hanaie et al., 2013; Travers et al., 2015; Surgent et al., 2021), sensory features (Jou et al., 2009; Wolff et al., 2017), and core autism traits (Travers et al., 2015; Wolff et al., 2017). Further, epidemiological, behavioral, histological, and model organism-based studies have generated hypotheses regarding brainstem contributions to ASD [reviewed by Dadalko and Travers (2018)]. Intriguingly, the first biology-based theory of autism (Rimland, 1964) suggested that autism traits were associated with abnormalities in the reticular formation, a cluster of gray matter nuclei within the brainstem. However, direct testing of this hypothesis has been limited by technical challenges that have prevented high-resolution imaging capable of probing the detailed structures of the brainstem *in vivo*.

Traditional magnetic resonance imaging (MRI) has lacked sufficient quality to characterize the intricately interwoven white matter bundles that wrap around the non-uniformly shaped gray matter nuclei within the brainstem, which itself is a relatively small structure. Structural, T1-weighted (T1w) MRI can achieve high spatial resolution but demonstrates poor contrast between the gray and white matter in the brainstem. This poor contrast makes it challenging to distinguish specific brainstem white matter tracts and gray matter nuclei. In comparison, diffusion MRI (dMRI), a powerful neuroimaging modality for *in vivo* quantification of white matter microstructure, can distinguish between different tissue types and fiber orientations within the brainstem, thereby revealing distinctions among brainstem substructures. However, geometric distortions that impact the brainstem are common in dMRI (Jezzard and Balaban, 1995; Du et al., 2002; Irfanoglu et al., 2015) and can make brainstem white matter tracts appear spuriously intertwined (Irfanoglu et al., 2012). Additionally, higher dMRI spatial resolution is needed due to the small size of brainstem structures (Ford et al., 2013; Lützkendorf et al., 2018) but comes at the cost of a lower signal-to-noise ratio (SNR) at each voxel (Edelstein et al., 1986; Jones, 2012), much longer scan times, or amplified imaging artifacts due to bulk motion and magnetic field inhomogeneities (Holdsworth et al., 2019). Moreover, increased involuntary head motion in autistic children (Yendiki et al., 2014) as well as physiological motion related to cerebrospinal fluid (CSF) pulsation (Karampinos et al., 2009), is likely to exacerbate these limitations, making imaging of brainstem structures even more challenging in autistic individuals.

To address these dMRI challenges, we recently implemented a dMRI protocol that improves brainstem images by using multi-shell diffusion acquisition to adjudicate among crossing fibers (Pines et al., 2020) and by correcting for brainstem-impacting echo planar imaging (EPI) geometric distortions using multiple non-diffusion-weighted volumes with reverse phase-encoded directions (Andersson et al., 2003; Smith et al., 2004). Using these dMRI images and what we will here forth refer to as the "conventional" dMRI processing pipeline, we found improved delineations among the white matter tracts of the brainstem compared to previous dMRI processing pipelines (**Figure 1**). However, further improvements to the apparent spatial resolution of brainstem dMRI at the acquisition level would require increased scan time and/or decreased SNR, neither of which are viable options. Longer scan times would not be feasible for our sample of autistic children and decreased SNR would have negative cascading impacts on dMRI scan quality. Therefore, to address the need for higher apparent spatial resolution in these data, the present study tests a pipeline for combining (or fusing) T1w and dMRI scans [**T**1 weighted-diffusion **fused**, or "TiDi-Fused" for short (phonetically pronounced *tai-dee*)] that ameliorates common challenges in pediatric brainstem imaging and enables increased apparent resolution of the brainstem and cerebellar structures in autistic and non-autistic children. This technique combines the complementary strengths of both the T1w and dMRI scans to enhance tissue contrast and apparent spatial resolution in the brainstem and surrounding regions. To address the limitation of head motion in the TiDi-Fused processing, our T1w images were acquired with magnetization prepared rapid acquisition gradient echo (MPnRAGE; Kecskemeti et al., 2016, 2018; Kecskemeti and Alexander, 2020a). MPnRAGE retrospectively addresses head motion artifacts that are common in pediatric neuroimaging (Kecskemeti and Alexander, 2020b), provides more reproducible cortical region definitions (Kecskemeti et al., 2021), and produces sharper delineations of gray/white matter boundaries than standard T1w images (Kecskemeti et al., 2018). The anatomical accuracy of MPnRAGE allows for high fidelity dMRI-to-T1w boundary-based registration.

Therefore, the aim of the present study was to compare the quality of our TiDi Fused post-processing method with

[1]Identity-first language is used throughout the article to reflect the preference of those in the autism community (Kenny et al., 2016; Bottema-Beutel et al., 2021).

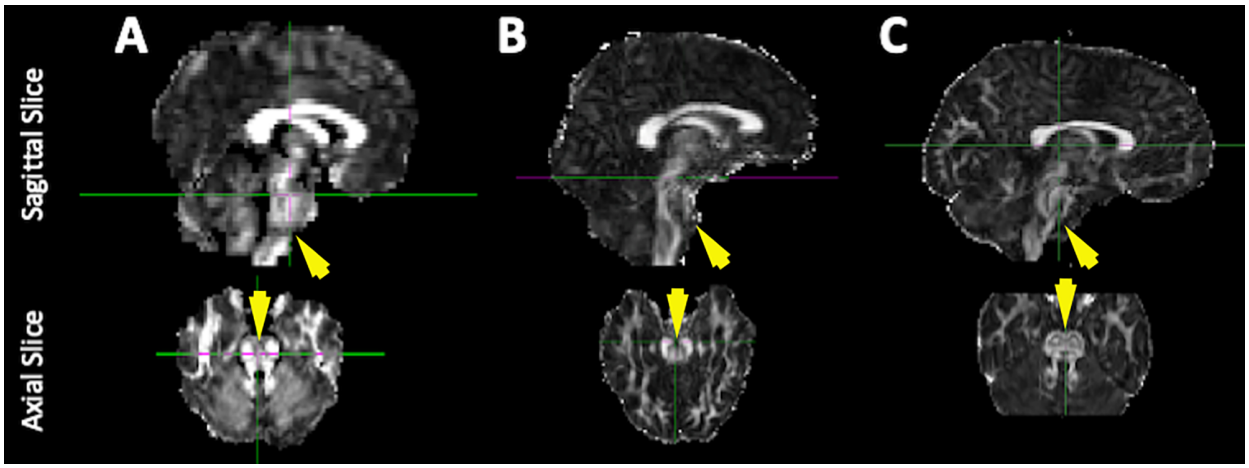

FIGURE 1 | Improvements to the quality of brainstem imaging through modifications to dMRI acquisition. Representative diffusion-weighted images from our previous work including the current conventional method. Example FA maps derived from dMRI scans **(A)** with low spatial resolution and no EPI distortion correction [used in Travers et al. (2015)], **(B)** with higher spatial resolution but no EPI distortion correction (collected between 2014 and 2016), and **(C)** with higher spatial resolution and EPI distortion correction (collected between 2016 and 2020, conventional processing pipeline).

our conventional dMRI method in autistic and non-autistic children (ages 6–10 years) using the following techniques: (1) visual comparison of image characteristics in relation to histology-based atlases (Sitek et al., 2019); (2) region-of-interest-based comparisons of coefficients of variation (CoV) in an atlas of brainstem-cerebellar white matter tracts (Tang et al., 2018); and (3) effect size comparisons of age predictions for the brainstem-cerebellar white matter tracts. We hypothesized that the TiDi-Fused brainstem images would show both visual and quantitative improvements over the conventional pipeline through the visibly clearer brainstem and cerebellar structural distinctions, improved registration with histologically derived brainstem atlases, lower CoVs (reduced variability) across brainstem tracts of interest, and stronger, positive relationships between age and apparent fiber density (AFD; Raffelt et al., 2012b).

MATERIALS AND METHODS

Participants

One-hundred and twenty-eight participants (ages 6.0–10.97, 37 female) were included in this study, with 56 in the autistic group (6.14–10.84 years, 12 females) and 72 in the non-autistic group (6.02–10.97 years, 25 females). No participants had a previous diagnosis of tuberous sclerosis, Down syndrome, fragile X, hypoxia-ischemia, notable and uncorrected hearing or vision loss, or a history of severe head injury. The institutional review board at the University of Wisconsin-Madison approved all procedures. In each case, the child participant provided assent, and a parent or guardian provided informed consent.

To confirm previous community diagnoses of ASD, participants in the autistic group were comprehensively evaluated and met cutoffs on either: (1) the Autism Diagnostic Observation Schedule, 2nd edition (ADOS-2; cutoff = 8; Lord et al., 2012) and the Autism Diagnostic Interview-Revised (ADI-R; Rutter et al., 2003b) or (2) the Social Responsiveness Scale, second edition (SRS-2; cutoff = 60; Constantino and Gruber, 2012) and the Social Communication Questionnaire (SCQ; cutoff = 15; Rutter et al., 2003a). Non-autistic participants were required to score less than eight on the SCQ (Rutter et al., 2003a). Additionally, participants were excluded from the non-autistic group if they had a previous diagnosis of another neurodevelopmental disorder, including ADD/ADHD, bipolar disorder, major depressive disorder, or if they had a first-degree relative with ASD. **Supplementary Table 1** summarizes participant details.

Image Acquisition

Imaging data were acquired on a 3T GE Discovery MR750 scanner (Waukesha, WI) at the Waisman Center at the University of Wisconsin–Madison. Diffusion-weighted images (DWIs) were obtained using a 32-channel phased array head coil (Nova Medical, Wilmington, MA) and a multi-shell spin-EPI pulse sequence [9 directions at b = 350 s · mm^{-2}, 18 directions at 800 s · mm^{-2}, and 36 directions at b = 2,000 s · mm^{-2}, and 6 non-diffusion-weighted (b = 0 s · mm^{-2}) volumes; TR/TE = 9,000/74.4 ms; FOV = 230 mm × 230 mm, in-plane resolution 2.4 mm × 2.4 mm, interpolated with zero-filling to 1.8 mm × 1.8 mm; 76 slices, slice thickness 3.6 mm, slice spacing 1.8 mm; ∼10 min]. An additional six non-diffusion-weighted volumes with reverse phase-encoded direction were collected for use in correcting susceptibility-induced artifacts, which tend to be severe around the brainstem in EPI acquisitions. Whole-brain structural imaging was done using a 3D T1w MPnRAGE sequence with 1 mm isotropic resolution (∼8 min). The MPnRAGE pulse sequence is a novel imaging method that combines magnetization preparation using inversion recovery with a rapid 3D radial

TABLE 1 | Comparison of conventional and TiDi-Fused processing pipelines.

	Conventional pipeline	TiDi-Fused pipeline
DWI Acquisition		
Pulse Sequence	Multi-shell spin EPI pulse sequence	Multi-shell spin EPI pulse sequence
Resolution	In-plane resolution 2.4 × 2.4 mm, interpolated to 1.8 × 1.8 mm	In-plane resolution 2.4 × 2.4 mm, interpolated to 1.8 × 1.8 mm.
Data Curation	Denoising, corrections for Gibbs Ringing, eddy currents, EPI distortion	Denoising, corrections for Gibbs Ringing, eddy currents, EPI distortion.
Apparent Resolution Enhancement*	Upsample DWI to achieve apparent resolution of 1.3 mm	Fuse T1-weighted and diffusion images with boundary-based registration (BBR) to achieve apparent resolution of 1.0 mm.
Diffusion Data Modeling	Estimate FOD and apparent fiber density (AFD)	Estimate FOD and apparent fiber density (AFD)
Population Template Construction*	Construct FOD population template using MRTrix3	Construct T1-weighted population template using ANTs.
Inter-Subject Spatial Normalization*	Diffeomorphically transform individual FOD maps to FOD template	(1) Diffeomorphically transform individual T1-weighted images to T1-weighted population template (2) Apply transformations to individual FOD maps.
Atlas Alignment*	Align FOD template to atlas (MNI) space using ANTs	Align T1-weighted template to atlas (MNI) space using ANTs.
Region of Interest Mapping to Individual Native Space	Transform data using warps generated from inter-subject spatial normalization	Transform data using warps generated from inter-subject spatial normalization.
Apparent Fiber Density (AFD) Value Extraction	Calculate the weighted median values from regions/tracts of interest in individual native space	Calculate the weighted median values from regions/tracts of interest in individual native space.

**Denotes steps in which the method pipelines differ.*

k-space readout (Kecskemeti et al., 2016). The MPnRAGE reconstruction enables retrospective head-motion correction (Kecskemeti et al., 2018), tissue-specific segmentation, and reliable quantitative T1 mapping (Kecskemeti et al., 2021).

Image Processing

Data Curation

A comparison of the conventional and TiDi-Fused pipelines are summarized in **Table 1**. In both pipelines, DWI data were processed to minimize noise (Veraart et al., 2016a,b), Gibbs ringing (Kellner et al., 2016), motion, eddy current (Andersson and Sotiropoulos, 2016; Andersson et al., 2016, 2017) and EPI distortion artifacts (Andersson et al., 2003).

Apparent Spatial Resolution Enhancement

In the conventional pipeline, a spatial resolution of dMRI data was up-sampled using MRtrix3's "mrgrid" (Tournier et al., 2019) with cubic interpolation to 1.3 mm isotropic voxels prior to estimating the fiber orientation distributions (FODs[2]).

In the TiDi-Fused pipeline, image-modality fusion was used to enhance the apparent spatial resolution. Image-modality fusion was conducted *via* spatial alignment of mean b0 volume to the T1w image derived from the MPnRAGE. The spatial alignment was done using rigid transformations (six degrees of freedom) implemented with the boundary-based registration (BBR; Greve and Fischl, 2009) routine in the FreeSurfer image analysis suite (Dale et al., 1999). With BBR, brain tissue boundaries estimated with FreeSurfer on the T1w image were maximally aligned with the expected image intensity gradients across those boundaries in the b0 image. The estimated transformation that resulted from the optimal alignment was then applied to the entire dMRI series with cubic B-spline interpolation up-sampled to the T1-w resolution (1 mm isotropic) using ANTs (Avants et al., 2011). Finally, the rotational component of the rigid body transformation was applied to the dMRI encoding directions. Subsequently, multiple operations on the diffusion scans, including estimation of fiber orientation distributions, were carried out in the up-sampled space.

Fiber Orientation Distribution

In the conventional and TiDi-Fused pipelines, dMRI data were spherically deconvolved with positivity constraints (Jeurissen et al., 2014) using an estimated shell and tissue specific response functions (Dhollander et al., 2016; averaged across the participants in the study) in order to estimate fiber orientation distributions (FODs) at each voxel in the brain as shown in **Table 1**.

Apparent Fiber Density

In both pipelines, following FOD estimation, apparent fiber density (AFD; Raffelt et al., 2012b) was calculated. AFD represents the sum of the amplitudes of the FOD lobes in each voxel and has been proposed as a measure of intracellular volume fraction from high angular resolution dMRI (Raffelt et al., 2012b). In order to generate AFD, global intensity normalization in the log-domain was first performed on the three different (WM, GM, CSF) FODs using the "mtnormalise" command in MRTrix3 (Dhollander et al., 2021). With normalized white matter FOD maps in hand, the apparent fiber density was computed as the first component ($l = 0$; typically referred to as DC term) of the white matter FOD series scaled by $2\sqrt{\pi}$.

[2]https://mrtrix.readthedocs.io/en/3.0.3/fixel_based_analysis/mt_fibre_density_crosssection.html

Inter-subject Image Alignment

In the conventional pipeline, an FOD template was created using the "population_template" routine in MRtrix3 with default settings (Tournier et al., 2019). This template was estimated from all 128 individuals, thus resulting in spatially aligned individual FOD maps to the template and corresponding diffeomorphic and affine transforms.

In the TiDi-fused pipeline, a study-specific T1-w template was first estimated using the "antsMultivariateTemplateConstruction" script in ANTs with four iterations (Avants et al., 2010, 2011; Klein et al., 2010). This template was also estimated from all participants. The resulting affine and local non-linear transformations were composed and then applied to the FOD maps with FOD reorientation using MRTrix3 (Raffelt et al., 2012a). An FOD template was then created from the aligned FOD maps by averaging them across subjects. This resulted in the T1w and FOD templates in the same spatial coordinate system.

Histological and Probabilistic Atlas Registration

Apparent fiber density was examined in 23 brainstem and cerebellar probabilistic white matter tracts defined in an atlas in which the tracts were identified by filtering whole brain tractography using regions manually defined by a neuroanatomist as described in more detail in Tang et al. (2018). The MNI152 template was aligned to the FOD templates created by the two processing pipelines. In the conventional pipeline, this was achieved by affine and diffeomorphic image alignment between the DC term of the template FOD and the MNI T1w image using "antsRegistration" (Avants et al., 2011) and mutual information as the cost function in the non-linear stage. In the TiDi-Fused pipeline, the MPnRAGE-T1w study-specific template was aligned with the MNI152 T1w image also using "antsRegistration" with affine and diffeomorphic transformations with correlation coefficient as the cost function in the non-linear stage. The probabilistic tract atlas was transformed to the FOD template space using the estimated warps and cubic interpolation. The tracts were then mapped to subject specific native space by applying the inverse transformations estimated during the template construction.

Additionally, histology-based data were aligned to the FOD templates created in each pipeline using the same procedure outlined above. The data consist of the BigBrain 3-D Volume Data Release 2015 (Amunts et al., 2013) 100 μm version with optimal alignment to ICBM152 2009b non-linear symmetric[3], 500 μm (Fonov et al., 2009) T1w template conducted by Sitek et al. (2019). The auditory brainstem nuclei also published in Sitek et al. (2019), were then mapped to each of the estimated FOD templates. A comparison of the histological data aligned to ICBM152 and the study specific template spaces is shown in **Supplementary Figure 1**.

Track Density Imaging

Track density imaging (TDI) is a post processing approach based on tractography that offers the ability to increase anatomical contrast in white mater (Calamante et al., 2010). To visually compare the resulting contrast in TDI in the brainstem with the BigBrain histology data, we produced TDI maps based on the FOD templates generated with each of the two pipelines. In each case, whole brain probabilistic tractography was performed using MRTrix3 using the white matter FODs seeded from a white matter mask that was generated by thresholding the DC term ($\geq$0.05) of the FOD (Tournier et al., 2010). Twenty million streamlines were generated and used to calculate TDI maps at an isotropic spatial resolution of 0.25 mm. To display directional information of fibers, TDI maps were represented as directionally encoded color maps. Histology overlaid on the TDI maps is shown in **Figure 2**.

Statistical Analysis

Weighted median values of the AFD in 23 brainstem tracts in native space were extracted for both the conventional dMRI and TiDi-Fused pipelines. Coefficients of variation (CoVs) across the subjects defined as the ratio of the standard deviation to the mean values of the weighted medians, were computed for each of the tracts. Statistical differences between the two pipelines were assessed using a Wilcoxon signed-rank test, in consideration that the data may not be normally distributed.

Pearson correlations between age and AFD in the conventional and TiDi-Fused pipelines were performed for each brainstem white matter region of interest. Model fit was tested through examination of R^2 values to represent explained variance. To directly test whether there were significant differences in the model fit between the conventional and TiDi-Fused pipelines, a mixed effects linear model was also conducted in each region of interest, predicting AFD as a function of age, pipeline (conventional vs. TiDi-Fused), and the age-by-pipeline interaction.

RESULTS

Enhanced Brainstem Visualization

TiDi-Fused processing of dMRI images resulted in enhanced visualization of gray and white matter structures within the brainstem and cerebellar areas compared to conventional dMRI processing. **Figure 2** visually shows the benefits of the TiDi-Fused pipeline in terms of spatial alignment of population-level data to a histologically derived atlas of the brainstem. Specifically, TiDi-Fused processed images show crisp alignment with histologically defined boundaries in the pontine region and strong registration of dorsal brainstem white matter tracts, demonstrating the effects of enhanced apparent resolution and improved tissue contrast in the TiDi-Fused images. At the single subject-level, dMRI images processed with the TiDi-Fused pipeline, demonstrate improved visibility of gray-white matter boundaries and sharpened patterns of cerebellar arborization (**Figure 3**).

Improved Precision in Estimates of White Matter Properties

Improvements to estimates of brainstem white matter microstructural properties were assessed through analysis of AFD CoV within 23 brainstem white matter tracts that were

[3]http://www.bic.mni.mcgill.ca/ServicesAtlases/ICBM152NLin2009

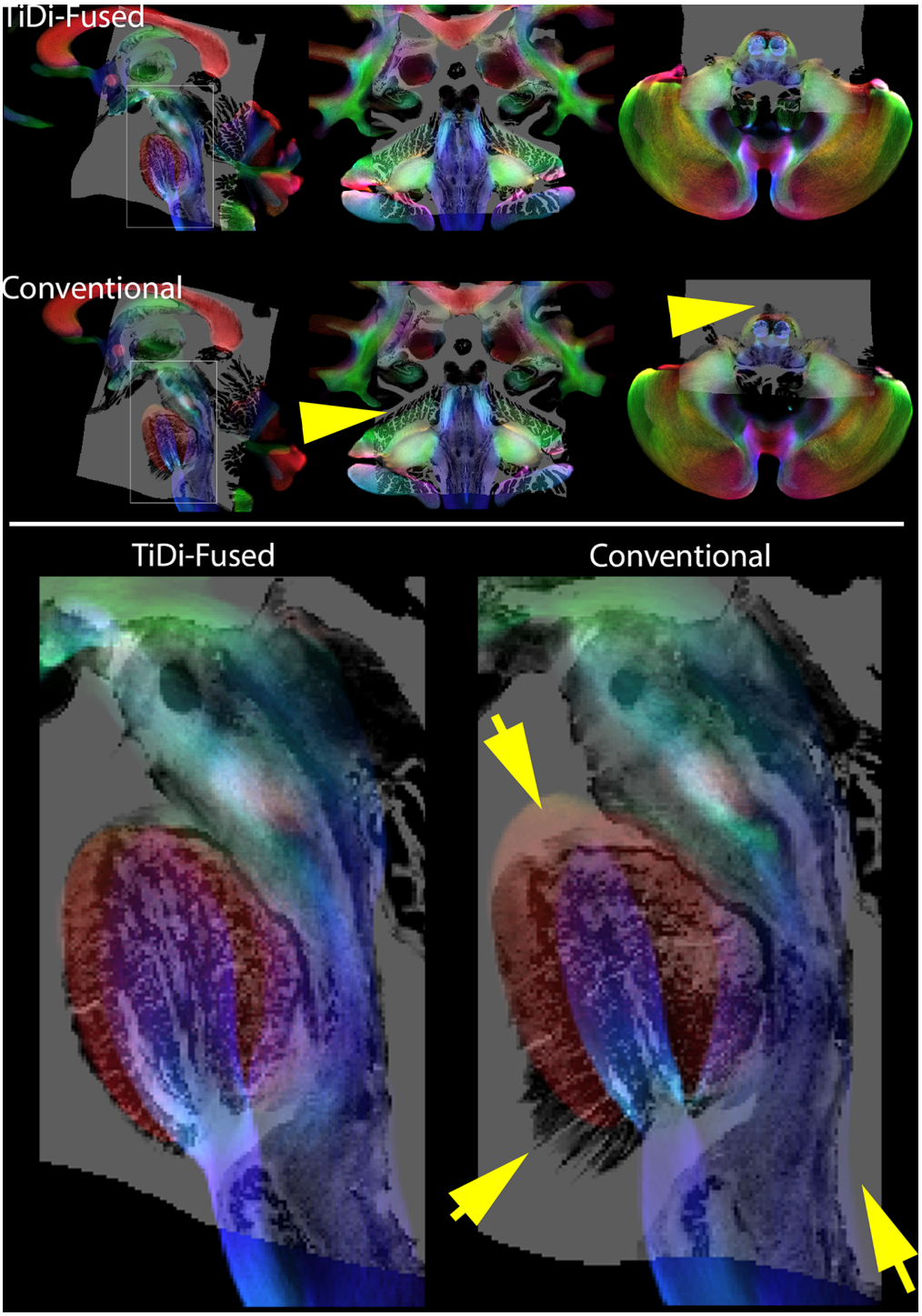

FIGURE 2 | Histology overlays on TDI. Top panel: Histology on Track Density Imaging maps resulting from each of the two pipelines—sagittal (right), coronal (middle), and axial (left). Bottom panel: Amplified sagittal view of histology on TDI in brainstem highlights the better spatial alignment resulting from TiDi-Fused. Note the arrows pointing to areas were the conventional pipeline leads to badly aligned regions with histology. In contrast, using TiDi-Fused leads to a mapping of histology that is much better supported by the underlying TDI contrast.

precisely delineated in dMRI data processed with conventional and with TiDi-Fused pipelines. All white matter regions of interest had lower CoV measurements in the tracts derived from the TiDi-Fused pipeline compared to those calculated from images processed with the conventional pipeline (**Figure 4A**). A Wilcoxon signed-rank exact test comparing the CoVs of

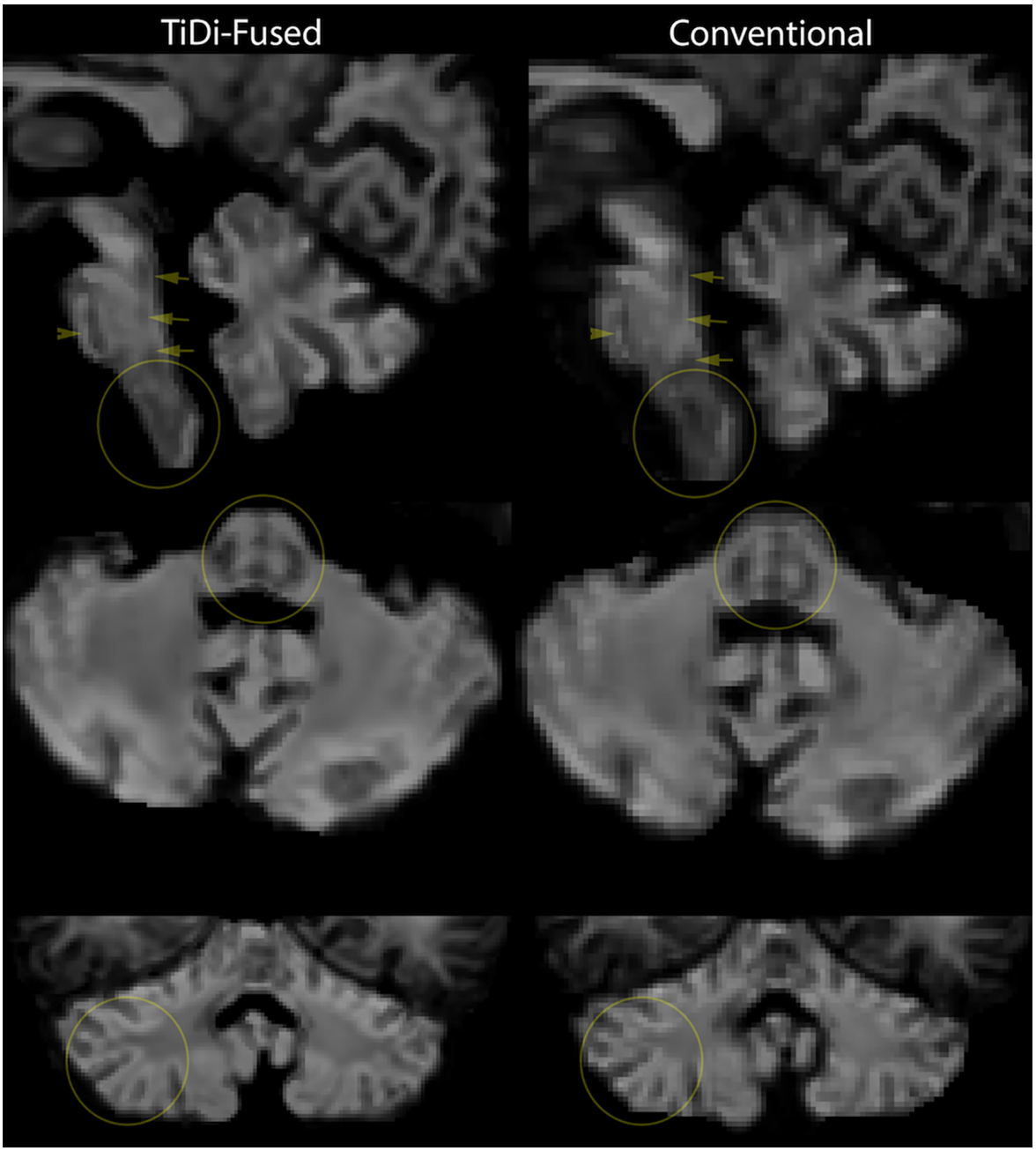

FIGURE 3 | Single-subject-level improvement (non-autistic 7-year-old) in gray-white matter contrast seen in apparent fiber density (AFD) in the brainstem and cerebellum. We chose the first scan of the study to demonstrate this, but this effect was representative of the dataset.

brainstem regions processed with the conventional (M = 9.3%, SD = 1.8%) and TiDi-Fused pipelines (M = 7.2%, SD = 1.6%) showed that CoV was significantly reduced in the TiDi-Fused pipeline, $z = -5.15$, $p <$ 2.4e-07. Across the regions, the reduction in CV was on average 2.1% (95% confidence interval: 1.7% to 2.5%).

In 21 of 23 white matter tracts, the AFD values extracted from TiDi-Fused processed data showed stronger correlations with age, as indexed by higher R^2, than those extracted from the conventional pipeline (**Figure 4B**, **Supplementary Table 1**). The only tracts that did not show improved linear fit were in the left inferior cerebellar peduncle (ICPMC and ICPVC). Further, a positive relationship between AFD and age was found in 23 of 23 tracts using the TiDi pipeline but only 12/23 tracts using the conventional pipeline (**Supplementary Table 2**).

Linear mixed effects models were used to determine whether the dMRI pipeline optimization significantly impacted estimates of the relationship between age and AFD. In 21 of 23 brainstem

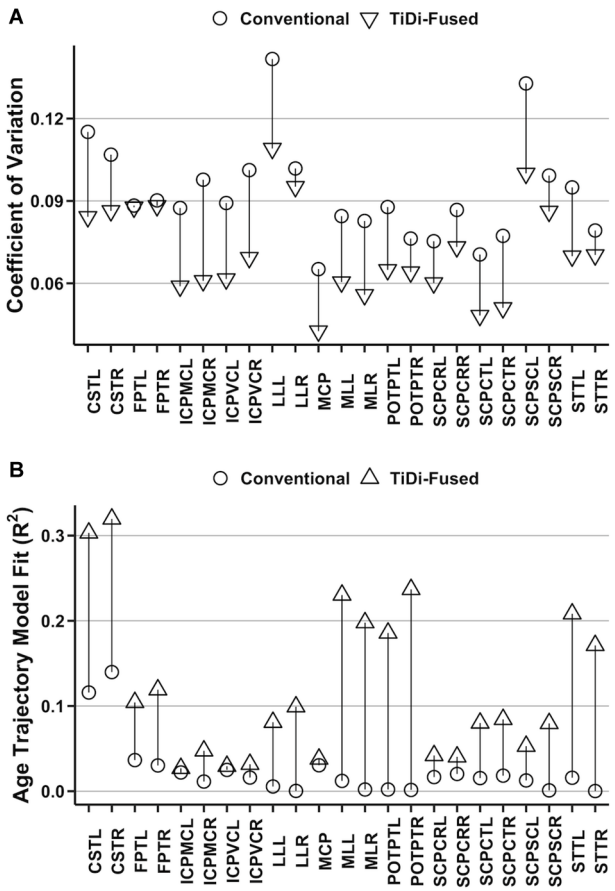

FIGURE 4 | Quantitative analysis of original and optimized pipelines using brainstem white matter regions of interest. **(A)** Comparison of coefficient of variation in the original and optimized pipelines. **(B)** Proportion of age trajectory variance (R^2) explained by apparent fiber density (AFD) in each white matter tract.

white matter tracts, significant age-by-pipeline interactions ($p < 0.05$) were found (**Supplementary Table 3**), indicating that the optimized dMRI pipeline statistically altered estimates of AFD-age relationships. The left SCPSC and left frontopontine tracts were the only white matter regions not to show statistically significant age-by-pipeline interactions.

DISCUSSION

To set the stage for *in vivo* testing of hypotheses regarding brainstem contributions to autism symptoms, this study set out to implement and test a T1w-dMRI fused (TiDi-Fused) processing pipeline that enhances resolution and accurate delineation of brainstem structures in autistic and non-autistic children. The TiDi-Fused pipeline harnesses the strengths of T1w and dMRI imaging techniques to generate high apparent resolution dMRI maps without sacrificing SNR or requiring long scan times. Previously, high brainstem anatomical clarity using dMRI has only been possible through the use of *ex vivo* imaging (Ford et al., 2013) or lengthy acquisition protocols (∼60 min) that are not suitable for a pediatric population (Shi and Toga, 2017), making the present application of TiDi-Fusion to a neurodiverse pediatric sample a critical advancement in pediatric neuroimaging. Through direct comparison of our TiDi-Fused pipeline and our conventional dMRI processing pipeline, we demonstrated substantial improvement in visualization, alignment, and quantification of brainstem structures in autistic and non-autistic youth.

TiDi-Fused processing greatly improved the ability to distinguish white matter tracts and gray matter nuclei in the anatomically complex brainstem, leading to high-resolution representations of brainstem structures in autistic children from data collected *in vivo*. TiDi-Fused processing enhanced visual assessment of brainstem white matter pathways and improved alignment with a histological atlas of precisely delineated gray matter nuclei. These high-resolution brainstem images and well-defined regions of interest generated from the TiDi-Fused processing pipeline provide the opportunity to test hypotheses regarding the contributions of the brainstem to autism that have been produced in other scientific fields [e.g., histology, cellular biology, model organisms; reviewed by Dadalko and Travers (2018)]. For example, TiDi-Fused processing offers the opportunity to delineate brainstem structures, like the reticular formation, which was at the heart of Rimland's (1964) hypothesis. In this way, TiDi-Fused processing may now enable examinations into the relatively unexplored territory of the brainstem in autism and in other difficult-to-image populations with conditions that may involve the brainstem (e.g., Alzheimer's or Parkinson's disease; Halliday et al., 1990; Simic et al., 2009; Arribarat et al., 2020). Moreover, while the TiDi-Fused pipeline involves registration with the T1w component of the MPnRAGE sequence, future work may benefit from fusing the dMRI with other quantitative structural MRI images or contrasts, which may provide additional information about brainstem composition.

Compared to the conventional pipeline, the TiDi-Fused pipeline not only enhanced the quality of brainstem visualization but also statistically improved the reliability of microstructural property measurements. This quantitative improvement of the TiDi-Fused pipeline over the conventional pipeline was demonstrated in two ways: (1) lower variability (CoV) across all measurements of AFD in brainstem white matter tracts; and (2) stronger relationships with age. The increased reliability of the TiDi-Fused data, as indexed by lower CoV across all brainstem white matter tracts, is especially critical in the brainstem, as the brainstem white matter bundles are smaller in size than most cerebral white matter structures and can be heavily impacted by spurious measurements. This notion is further supported by the improved estimates of AFD-age relationships in the data processed with the TiDi-Fused pipeline compared to the data processed with the conventional pipeline. AFD values from TiDi-Fused data also show more biologically plausible (positive) age trajectories that are corroborated by previous accounts of AFD development of large white matter tracts in non-autistic youth (Dimond et al., 2020) and align with previous work done to assess diagnostic differences in white matter development in various white matter tracts throughout the brain (Andrews et al., 2021). The TiDi-Fused processing pipeline, therefore, appears to

allow for more reliable estimates of white matter microstructure (less variability) and improved biological plausibility, which can, in turn, enhance the validity of *in vivo* assessments of brainstem-behavior relationships in autistic and non-autistic youth.

The present findings should be contextualized in light of limitations. One potential limitation was that we compared across different apparent resolutions: 1.3 mm^3 in the conventional scans compared to 1.0 mm^3 in the TiDi-Fused scans. While a more direct comparison would have been to compare 1 mm^3 to 1 mm^3, we opted to keep our conventional scan at the MRTrix3 recommended apparent resolution of 1.3 mm^3 (Fibre density and cross-section - Multi-tissue CSD) to maintain consistency with current best practices. Another limitation is that we did not have a measure of ground truth for brainstem neurobiology in our participants. To compensate, we opted for visual alignment with histology data and quantitative measures that examined reliability (CoV) and biological plausibility (age effects). However, future work should examine additional measures to validate this approach.

Overall, the TiDi-Fused processing pipeline demonstrated enhanced assessment of brainstem structures in autistic children, providing the opportunity to conduct feasible *in vivo* investigations of the brainstem that has not to date been possible. The TiDi-Fused processing pipeline increases apparent spatial resolution without compromising SNR or requiring long scan times, resulting in both visual and quantitative improvements to brainstem analysis in autistic and non-autistic children. Therefore, the present pipeline represents a critical advancement in our ability to use MRI to understand the role of the brainstem in autism.

DATA AVAILABILITY STATEMENT

The raw data supporting the conclusions of this article will be made available by the authors, without undue reservation.

ETHICS STATEMENT

The studies involving human participants were reviewed and approved by University of Wisconsin-Madison Health Sciences Institutional Review Board. Written informed consent to participate in this study was provided by the participants' legal guardian/next of kin.

AUTHOR CONTRIBUTIONS

JG-G, OS, NA, GK, DD, AA, and BT contributed to conception and design of the study. JG-G, OS, NA, DD, SK, and AA made contributions to image processing. NA and OS performed the statistical analysis. OS wrote the first draft of the manuscript. JG-G, NA, and BT wrote sections of the manuscript. All authors contributed to the article and approved the submitted version.

FUNDING

This work was supported by the Hartwell Foundation's Individual Biomedical Award (to BT) and the National Institutes of Health [P30 HD003352, U54 HD090256, and P50 HD105353 to the Waisman Center, R01 HD094715 to BT and AA, and T32 CA009206 to the University of Wisconsin Radiological Sciences Training Program]. NA was partially supported by NIH grants R01 NS111022, R01 NS117568, P01 AI132132, R01 AI138647, and R01 AG037639. DD was partially supported by NIH grant R00 MH11056. The content is solely the responsibility of the authors and does not necessarily represent the official views of the National Institutes of Health.

ACKNOWLEDGMENTS

We thank the participants and their families for their time and effort towards this research. We would like to thank Dr. Olga Dadalko for data processing and problem solving in earlier versions of this dataset. We would like to thank Laura Bradley, Katie Phillips, Desiree Taylor, and Kristine McLaughlin for their leadership in the logistics of data collection. We would like to thank all members of the Waisman Center's Motor and Brain Development Lab and the Brain Imaging Core for making the MRI an accessible and friendly environment for our participants.

SUPPLEMENTARY MATERIALS

The Supplementary Material for this article can be found online at: https://www.frontiersin.org/articles/10.3389/fnint.2022.804743/full#supplementary-material.

REFERENCES

Amunts, K., Lepage, C., Borgeat, L., Mohlberg, H., Dickscheid, T., Rousseau, M.-E., et al. (2013). Bigbrain: an ultrahigh-resolution 3D human brain model. *Science* 340, 1472–1475. doi: 10.1126/science.1235381

Andersson, J. L. R., Graham, M. S., Drobnjak, I., Zhang, H., Filippini, N., and Bastiani, M. (2017). Towards a comprehensive framework for movement and distortion correction of diffusion MR images: within volume movement. *Neuroimage* 152, 450–466. doi: 10.1016/j.neuroimage.2017.02.085

Andersson, J. L. R., Graham, M. S., Zsoldos, E., and Sotiropoulos, S. N. (2016). Incorporating outlier detection and replacement into a non-parametric framework for movement and distortion correction of diffusion MR images. *Neuroimage* 141, 556–572. doi: 10.1016/j.neuroimage.2016.06.058

Andersson, J. L. R., Skare, S., and Ashburner, J. (2003). How to correct susceptibility distortions in spin-echo echo-planar images: application to diffusion tensor imaging. *Neuroimage* 20, 870–888. doi: 10.1016/S1053-8119(03)00336-7

Andersson, J. L. R., and Sotiropoulos, S. N. (2016). An integrated approach to correction for off-resonance effects and subject movement in diffusion MR imaging. *Neuroimage* 125, 1063–1078. doi: 10.1016/j.neuroimage.2015.10.019

Andrews, D. S., Lee, J. K., Harvey, D. J., Waizbard-Bartov, E., Solomon, M., Rogers, S. J., et al. (2021). A longitudinal study of white matter development

in relation to changes in autism severity across early childhood. *Biol. Psychiatry* 89, 424–432. doi: 10.1016/j.biopsych.2020.10.013

Arribarat, G., De Barros, A., and Péran, P. (2020). Modern brainstem MRI techniques for the diagnosis of Parkinson's disease and Parkinsonisms. *Front. Neurol.* 11:791. doi: 10.3389/fneur.2020.00791

Avants, B. B., Tustison, N. J., Song, G., Cook, P. A., Klein, A., and Gee, J. C. (2011). A reproducible evaluation of ANTs similarity metric performance in brain image registration. *Neuroimage* 54, 2033–2044. doi: 10.1016/j.neuroimage.2010.09.025

Avants, B. B., Yushkevich, P., Pluta, J., Minkoff, D., Korczykowski, M., Detre, J., et al. (2010). The optimal template effect in hippocampus studies of diseased populations. *Neuroimage* 49, 2457–2466. doi: 10.1016/j.neuroimage.2009.09.062

Bottema-Beutel, K., Kapp, S. K., Lester, J. N., Sasson, N. J., and Hand, B. N. (2021). Avoiding ableist language: suggestions for autism researchers. *Autism Adulthood* 3, 18–29. doi: 10.1089/aut.2020.0014

Calamante, F., Tournier, J.-D., Jackson, G. D., and Connelly, A. (2010). Track-density imaging (TDI): super-resolution white matter imaging using whole-brain track-density mapping. *Neuroimage* 53, 1233–1243. doi: 10.1016/j.neuroimage.2010.07.024

Constantino, J., and Gruber, C. (2012). Social Responsiveness Scale-Second Edition (SRS-2). Torrance, CA: Western Psychological Services.

Dadalko, O. I., and Travers, B. G. (2018). Evidence for brainstem contributions to autism spectrum disorders. *Front. Integr. Neurosci.* 12:47. doi: 10.3389/fnint.2018.00047

Dale, A. M., Fischl, B., and Sereno, M. I. (1999). Cortical surface-based analysis. *Neuroimage* 9, 179–194. doi: 10.1006/nimg.1998.0395

Dhollander, T., Raffelt, D., and Connelly, A. (2016). "Unsupervised 3-tissue response function estimation from single-shell or multi-shell diffusion MR data without a co-registered T1 image," in *ISMRM Workshop on Breaking the Barriers of Diffusion MRI* (Lisbon, Portugal).

Dhollander, T., Tabbara, R., Rosnarho-Tornstrand, J., Tournier, J.-D., Raffelt, D., and Connelly, A. (2021). "Multi-tissue log-domain intensity and inhomogeneity normalisation for quantitative apparent fibre density," in *Proc. ISMRM, 2021*, 29, 2472.

Dimond, D., Rohr, C. S., Smith, R. E., Dhollander, T., Cho, I., Lebel, C., et al. (2020). Early childhood development of white matter fiber density and morphology. *Neuroimage* 210:116552. doi: 10.1016/j.neuroimage.2020.116552

Du, Y. P., Joe Zhou, X., and Bernstein, M. A. (2002). Correction of concomitant magnetic field-induced image artifacts in nonaxial echo-planar imaging. *Magn. Reson. Med.* 48, 509–515. doi: 10.1002/mrm.10249

Edelstein, W. A., Glover, G. H., Hardy, C. J., and Redington, R. W. (1986). The intrinsic signal-to-noise ratio in NMR imaging. *Magn. Reson. Med.* 3, 604–618. doi: 10.1002/mrm.1910030413

Fibre density and cross-section - Multi-tissue CSD. Available online at: https://mrtrix.readthedocs.io/en/3.0.3/fixel_based_analysis/mt_fibre_density_cross-section.html.

Fonov, V., Evans, A., McKinstry, R., Almli, C., and Collins, D. (2009). Unbiased nonlinear average age-appropriate brain templates from birth to adulthood. *Neuroimage* 47:S102. doi: 10.1016/S1053-8119(09)70884-5

Ford, A. A., Colon-Perez, L., Triplett, W. T., Gullett, J. M., Mareci, T. H., and FitzGerald, D. B. (2013). Imaging white matter in human brainstem. *Front. Hum. Neurosci.* 7:400. doi: 10.3389/fnhum.2013.00400

Greve, D. N., and Fischl, B. (2009). Accurate and robust brain image alignment using boundary-based registration. *Neuroimage* 48, 63–72. doi: 10.1016/j.neuroimage.2009.06.060

Halliday, G. M., Li, Y. W., Blumbergs, P. C., Joh, T. H., Cotton, R. G., Howe, P. R., et al. (1990). Neuropathology of immunohistochemically identified brainstem neurons in Parkinson's disease. *Ann. Neurol.* 27, 373–385. doi: 10.1002/ana.410270405

Hanaie, R., Mohri, I., Kagitani-Shimono, K., Tachibana, M., Azuma, J., Matsuzaki, J., et al. (2013). Altered microstructural connectivity of the superior serebellar peduncle is related to motor dysfunction in children with autistic spectrum disorders. *Cerebellum* 12, 645–656. doi: 10.1007/s12311-013-0475-x

Holdsworth, S. J., O'Halloran, R., and Setsompop, K. (2019). The quest for high spatial resolution diffusion-weighted imaging of the human brain *in vivo*. *NMR Biomed.* 32:e4056. doi: 10.1002/nbm.4056

Irfanoglu, M. O., Modi, P., Nayak, A., Hutchinson, E. B., Sarlls, J., and Pierpaoli, C. (2015). DR-BUDDI (Diffeomorphic registration for blip-Up blip-down diffusion imaging) method for correcting echo planar imaging distortions. *Neuroimage* 106, 284–299. doi: 10.1016/j.neuroimage.2014.11.042

Irfanoglu, M. O., Walker, L., Sarlls, J., Marenco, S., and Pierpaoli, C. (2012). Effects of image distortions originating from susceptibility variations and concomitant fields on diffusion MRI tractography results. *Neuroimage* 61, 275–288. doi: 10.1016/j.neuroimage.2012.02.054

Jeurissen, B., Tournier, J.-D., Dhollander, T., Connelly, A., and Sijbers, J. (2014). Multi-tissue constrained spherical deconvolution for improved analysis of multi-shell diffusion MRI data. *Neuroimage* 103, 411–426. doi: 10.1016/j.neuroimage.2014.07.061

Jezzard, P., and Balaban, R. S. (1995). Correction for geometric distortion in echo planar images from B0 field variations. *Magn. Reson. Med.* 34, 65–73. doi: 10.1002/mrm.1910340111

Jones, D. K. (2012). *Diffusion MRI*. Oxford University Press doi: 10.1093/med/9780195369779.001.0001

Jou, R. J., Minshew, N. J., Melhem, N. M., Keshavan, M. S., and Hardan, A. Y. (2009). Brainstem volumetric alterations in children with autism. *Psychol. Med.* 39, 1347–1354. doi: 10.1017/S0033291708004376

Karampinos, D. C., Van, A. T., Olivero, W. C., Georgiadis, J. G., and Sutton, B. P. (2009). High-resolution diffusion tensor imaging of the human pons with a reduced field-of-view, multishot, variable-density, spiral acquisition at 3 T: high-resolution DTI of the human pons. *Magn. Reson. Med.* 62, 1007–1016. doi: 10.1002/mrm.22105

Kecskemeti, S., and Alexander, A. L. (2020a). Three-dimensional motion-corrected T1 relaxometry with MPnRAGE. *Magn. Reson. Med.* 84, 2400–2411. doi: 10.1002/mrm.28283

Kecskemeti, S. R., and Alexander, A. L. (2020b). Test-retest of automated segmentation with different motion correction strategies: a comparison of prospective versus retrospective methods. *Neuroimage* 209:116494. doi: 10.1016/j.neuroimage.2019.116494

Kecskemeti, S., Freeman, A., Travers, B. G., and Alexander, A. L. (2021). FreeSurfer based cortical mapping and T1-relaxometry with MPnRAGE: test-retest reliability with and without retrospective motion correction. *Neuroimage* 242:118447. doi: 10.1016/j.neuroimage.2021.118447

Kecskemeti, S., Samsonov, A., Hurley, S. A., Dean, D. C., Field, A., and Alexander, A. L. (2016). MPnRAGE: A technique to simultaneously acquire hundreds of differently contrasted MPRAGE images with applications to quantitative T1 mapping. *Magn. Reson. Med.* 75, 1040–1053. doi: 10.1002/mrm.25674

Kecskemeti, S., Samsonov, A., Velikina, J., Field, A. S., Turski, P., Rowley, H., et al. (2018). Robust motion correction strategy for structural MRI in unsedated children demonstrated with three-dimensional radial MPnRAGE. *Radiology* 289, 509–516. doi: 10.1148/radiol.2018180180

Kellner, E., Dhital, B., Kiselev, V. G., and Reisert, M. (2016). Gibbs-ringing artifact removal based on local subvoxel-shifts: gibbs-ringing artifact removal. *Magn. Reson. Med.* 76, 1574–1581. doi: 10.1002/mrm.26054

Kenny, L., Hattersley, C., Molins, B., Buckley, C., Povey, C., and Pellicano, E. (2016). Which terms should be used to describe autism? Perspectives from the UK autism community. *Autism* 20, 442–462. doi: 10.1177/1362361315588200

Klein, A., Ghosh, S. S., Avants, B., Yeo, B. T. T., Fischl, B., Ardekani, B., et al. (2010). Evaluation of volume-based and surface-based brain image registration methods. *Neuroimage* 51, 214–220. doi: 10.1016/j.neuroimage.2010.01.091

Lord, C., Rutter, M., Risi, S., Gotham, K., and Bishop, S. (2012). *Autism Diagnostic Observation Schedule-2nd Edition (ADOS-2)*. Los Angeles, CA: Western Psychological Corporation.

Lützkendorf, R., Heidemann, R. M., Feiweier, T., Luchtmann, M., Baecke, S., Kaufmann, J., et al. (2018). Mapping fine-scale anatomy of gray matter, white matter and trigeminal-root region applying spherical deconvolution to high-resolution 7-T diffusion MRI. *MAGMA* 31, 701–713. doi: 10.1007/s10334-018-0705-9

Pines, A. R., Cieslak, M., Larsen, B., Baum, G. L., Cook, P. A., Adebimpe, A., et al. (2020). Leveraging multi-shell diffusion for studies of brain development in

youth and young adulthood. *Dev. Cogn. Neurosci.* 43:100788. doi: 10.1016/j.dcn.2020.100788

Raffelt, D., Tournier, J.-D., Crozier, S., Connelly, A., and Salvado, O. (2012a). Reorientation of fiber orientation distributions using apodized point spread functions. *Magn. Reson. Med.* 67, 844–855. doi: 10.1002/mrm.23058

Raffelt, D., Tournier, J.-D., Rose, S., Ridgway, G. R., Henderson, R., Crozier, S., et al. (2012b). Apparent fibre density: a novel measure for the analysis of diffusion-weighted magnetic resonance images. *Neuroimage* 59, 3976–3994. doi: 10.1016/j.neuroimage.2011.10.045

Rimland, B. (1964). *Infantile autism: The Syndrome And Its Implications for a Neural Theory of Behavior*. East Norwalk, CT: Appleton-Century -Crofts.

Rutter, M., Bailey, A. J., and Lord, C. (2003a). *The Social Communication Questionnaire: Manual*. Los Angeles, CA: Western Psychological Services.

Rutter, M., Le Couteur, A., and Lord, C. (2003b). *Autism Diagnostic Interview Revised*. Los Angeles, CA: Western Psychological Services.

Shi, Y., and Toga, A. W. (2017). Connectome imaging for mapping human brain pathways. *Mol. Psychiatry* 22, 1230–1240. doi: 10.1038/mp.2017.92

Simic, G., Stanic, G., Mladinov, M., Jovanov-Milosevic, N., Kostovic, I., and Hof, P. R. (2009). Does Alzheimer's disease begin in the brainstem? *Neuropathol. Appl. Neurobiol.* 35, 532–554. doi: 10.1111/j.1365-2990.2009.01038.x

Sitek, K. R., Gulban, O. F., Calabrese, E., Johnson, G. A., Lage-Castellanos, A., Moerel, M., et al. (2019). Mapping the human subcortical auditory system using histology, postmortem MRI and *in vivo* MRI at 7T. *eLife* 8:e48932. doi: 10.7554/eLife.48932

Smith, S. M., Jenkinson, M., Woolrich, M. W., Beckmann, C. F., Behrens, T. E. J., Johansen-Berg, H., et al. (2004). Advances in functional and structural MR image analysis and implementation as FSL. *Neuroimage* 23, S208–S219. doi: 10.1016/j.neuroimage.2004.07.051

Surgent, O., Dean, D. C., Alexander, A. L., Dadalko, O. I., Guerrero-Gonzalez, J., Taylor, D., et al. (2021). Neurobiological and behavioural outcomes of biofeedback-based training in autism: a randomized controlled trial. *Brain Commun.* 3:fcab112. doi: 10.1093/braincomms/fcab112

Tang, Y., Sun, W., Toga, A. W., Ringman, J. M., and Shi, Y. (2018). A probabilistic atlas of human brainstem pathways based on connectome imaging data. *Neuroimage* 169, 227–239. doi: 10.1016/j.neuroimage.2017.12.042

Tournier, J.-D., Calamante, F., and Connelly, A. (2010). "Improved probabilistic streamlines tractography by 2nd order integration over fibre orientation distributions," in *Proc. Intl. Soc. Mag. Reson. Med.*. 8, 1670. Available online at: https://archive.ismrm.org/2010/1670.html.

Tournier, J.-D., Smith, R., Raffelt, D., Tabbara, R., Dhollander, T., Pietsch, M., et al. (2019). MRtrix3: A fast, flexible and open software framework for medical image processing and visualisation. *Neuroimage* 202:116137. doi: 10.1016/j.neuroimage.2019.116137

Travers, B. G., Bigler, E. D., Tromp, D. P. M., Adluru, N., Destiche, D., Samsin, D., et al. (2015). Brainstem white matter predicts individual differences in manual motor difficulties and symptom severity in autism. *J. Autism Dev. Dis.* 45, 3030–3040. doi: 10.1007/s10803-015-2467-9

Veraart, J., Fieremans, E., and Novikov, D. S. (2016a). Diffusion MRI noise mapping using random matrix theory: diffusion MRI noise mapping. *Magn. Reson. Med.* 76, 1582–1593. doi: 10.1002/mrm.26059

Veraart, J., Novikov, D. S., Christiaens, D., Ades-aron, B., Sijbers, J., and Fieremans, E. (2016b). Denoising of diffusion MRI using random matrix theory. *Neuroimage* 142, 394–406. doi: 10.1016/j.neuroimage.2016.08.016

Wolff, J. J., Swanson, M. R., Elison, J. T., Gerig, G., Pruett, J. R., Styner, M. A., et al. (2017). Neural circuitry at age 6 months associated with later repetitive behavior and sensory responsiveness in autism. *Mol. Autism* 8:8. doi: 10.1186/s13229-017-0126-z

Yendiki, A., Koldewyn, K., Kakunoori, S., Kanwisher, N., and Fischl, B. (2014). Spurious group differences due to head motion in a diffusion MRI study. *Neuroimage* 88, 79–90. doi: 10.1016/j.neuroimage.2013.11.027

Conflict of Interest: AA is part owner of ImgGyd, LLC and inseRT MRI, Inc. (also listed as TherVoyant). While both companies are involved in developing MRI-based surgery techniques, neither are associated with any current areas of his research, including the present publication. All other authors report no biomedical financial interests of potential conflicts of interest.

The remaining authors declare that the research was conducted in the absence of any commercial or financial relationships that could be construed as a potential conflict of interest.

Publisher's Note: All claims expressed in this article are solely those of the authors and do not necessarily represent those of their affiliated organizations, or those of the publisher, the editors and the reviewers. Any product that may be evaluated in this article, or claim that may be made by its manufacturer, is not guaranteed or endorsed by the publisher.

frontiers in Integrative Neuroscience

ORIGINAL RESEARCH
published: 16 March 2022
doi: 10.3389/fnint.2022.804881

Embryonic Valproate Exposure Alters Mesencephalic Dopaminergic Neurons Distribution and Septal Dopaminergic Gene Expression in Domestic Chicks

Alice Adiletta[1†], *Alessandra Pross*[1,2†], *Nicolò Taricco*[1] *and Paola Sgadò*[1*]

[1] *Center for Mind/Brain Sciences, University of Trento, Rovereto, Italy,* [2] *Lleida's Institute for Biomedical Research Dr. Pifarre Foundation (IRBLleida), Lleida, Spain*

In recent years, the role of the dopaminergic system in the regulation of social behavior is being progressively outlined, and dysfunctions of the dopaminergic system are increasingly associated with neurodevelopmental disorders, including autism spectrum disorder (ASD). To study the role of the dopaminergic (DA) system in an animal model of ASD, we investigated the effects of embryonic exposure to valproic acid (VPA) on the postnatal development of the mesencephalic DA system in the domestic chick. We found that VPA affected the rostro-caudal distribution of DA neurons, without changing the expression levels of several dopaminergic markers in the mesencephalon. We also investigated a potential consequence of this altered DA neuronal distribution in the septum, a social brain area previously associated to social behavior in several vertebrate species, describing alterations in the expression of genes linked to DA neurotransmission. These findings support the emerging hypothesis of a role of DA dysfunction in ASD pathogenesis. Together with previous studies showing impairments of early social orienting behavior, these data also support the use of the domestic chick model to investigate the neurobiological mechanisms potentially involved in early ASD symptoms.

Keywords: autism spectrum disorder, valproic acid, brain development, dopamine, midbrain, septum, domestic chicks

OPEN ACCESS

Edited by:
Patricia Gaspar, Institut National de la Santé et de la Recherche Médicale (INSERM), France

Reviewed by:
Laurence Goutebroze, Institut National de la Santé et de la Recherche Médicale (INSERM), France
Lesley J. Rogers, University of New England, Australia
Melissa Martin, US Environmental Protection Agency (EPA), United States

***Correspondence:**
Paola Sgadò
paola.sgado@unitn.it

[†] *These authors have contributed equally to this work and share first authorship*

Received: *29 October 2021*
Accepted: *07 February 2022*
Published: *16 March 2022*

Citation:
Adiletta A, Pross A, Taricco N and Sgadò P (2022) Embryonic Valproate Exposure Alters Mesencephalic Dopaminergic Neurons Distribution and Septal Dopaminergic Gene Expression in Domestic Chicks. Front. Integr. Neurosci. 16:804881. doi: 10.3389/fnint.2022.804881

INTRODUCTION

Autism spectrum disorder (ASD) comprises a group of neurodevelopmental conditions strongly characterized by impairments in sociability and social communication. In recent years, the role of the dopaminergic (DA) system in the regulation of social behavior in animal models is being progressively outlined (Gunaydin and Deisseroth, 2014; Yamaguchi et al., 2017; Silva et al., 2020), often in association to motivational and reward mechanisms (Bariselli et al., 2018), while dysfunctions of the dopaminergic system in neurodevelopmental disorders and ASD are also emerging (Scott-Van Zeeland et al., 2010; Supekar et al., 2018; Zürcher et al., 2021).

Neuromodulatory systems, such as the those for the neurotransmitter dopamine, are evolutionarily very conserved (Yamamoto and Vernier, 2011), emerge in early embryonic development from ancient brain areas and are already mature at birth (Ferrari et al., 2012), innervating the neonatal brain. Thus, they represent an ideal target to modulate complex cognitive

abilities originating in early development, such as social orienting behavior. Approximately 75% of the total number of DA cells in the brain are located in the ventral part of the mesencephalon, giving rise to two major ascending DA systems that project to specific brain areas (Björklund and Dunnett, 2007). DA neurons in the mammalian ventral tegmental area (VTA) of the mesencephalon mainly project to the ventral striatum, the septum, the amygdala and the medial prefrontal cortex and constitute the mesocorticolimbic (or mesolimbic) pathway. Neurons of this pathway belong to the reward system and are thought to play a major role in controlling social reward, social learning and affiliative behavior. On the other hand, neurons originating in the mammalian substantia nigra (SN) and innervating the dorsal striatum, form the mesostriatal pathway and are mainly involved in motor control. Despite the distinct categorization, neurons of the SN and the VTA have a complex organization and are intertwined in the mesencephalon, having also partially overlapping projections and sharing similar functions (Wise, 2009; Ilango et al., 2014). Furthermore, both DA mesencephalic nuclei are also blended with other type of neurons, as for example GABA and glutamate releasing neurons (Morales and Margolis, 2017) that contribute to their functional features (Bourdy et al., 2014).

In humans, the activation of the mesocorticolimbic pathway has been associated to processing of social stimuli (Spreckelmeyer et al., 2009), while a reduced activation of the same pathway has been described in children and adults with ASD (Scott-Van Zeeland et al., 2010; Supekar et al., 2018). Pharmacological studies in mice have shown that administration of DA mimetic and antagonizing drugs can modulate social interaction bidirectionally. In a seminal work Gunaydin and coworkers (Gunaydin et al., 2014) demonstrated a causal link between activation of VTA DA neurons and social interaction in mice using optogenetic tools. In addition, chemogenetic inhibition of VTA neurons projecting to Nucleus Accumbens (NAc) in mice has been associated to reduced social novelty seeking (Bariselli et al., 2018) and the molecular bases of such mechanisms in neurodevelopmental disorders models are starting to be elucidated (Bariselli et al., 2016, 2018). Recent studies have also highlighted the role of the lateral septum, a limbic structure strongly innervated by the VTA DA neurons, in sociability and social novelty seeking in mice (Mesic et al., 2015), emphasizing the role of DA neurotransmission in the regulation of social behavior (Hostetler et al., 2017; Shin et al., 2018). Overall, it appears that activation of the mesolimbic system, connecting the VTA to the NAc and to the LS, have a prosocial effect on social stimuli processing as well as on social interaction.

In this study, we harnessed the evolutionary conserved nature of the DA neuromodulatory system to investigate the neurobiological mechanisms affected by valproic acid (VPA) treatment in domestic chicks and potentially linked to the social behavioral deficits underlying ASD. VPA is an anticonvulsant known to interfere with development of the social brain, whose prenatal exposure is associated in humans with neural tube malformations, reduced cognitive function, and an increased risk for developing ASD (Christensen et al., 2013). VPA embryonic exposure has been extensively used to model ASD core symptoms in diverse animal species (see for a review Bambini-Junior et al., 2014) including the domestic chick, where it induces alterations of several aspects of social behavior (Nishigori et al., 2013; Sgadò et al., 2018; Lorenzi et al., 2019; Zachar et al., 2019; Adiletta et al., 2021). Nishigori et al. (2013) investigated the effect of different doses and time of administration and found that 35 μmole/egg of VPA injected at E14 induced alterations in social aggregation without affecting filial imprinting. We have expanded this study confirming a detrimental effect of VPA on early emerging social responses to different type of visual stimuli, either stationary (the face-like configuration visible in a stuffed hen, Sgadò et al., 2018; or in a schematic representation Adiletta et al., 2021) or dynamic (speed changes Lorenzi et al., 2019). An additional study by Zachar et al. (2019) analyzed the effect of a different VPA dose (35 μM) on several aspects of social behavior, passive avoidance learning and anxiety. The authors found reduced social exploration and sociability deficits, appearing at the third postnatal week, while no alterations in avoidance learning or social communication was reported (Zachar et al., 2019).

Here we examined the anatomical and molecular layout of the mesencephalic DA system in domestic chicks exposed to VPA during embryonic development. We found that VPA affected the rostro-caudal distribution of DA neurons, without changing the expression levels of several dopaminergic markers in the mesencephalon. We also investigated a potential consequence of this altered DA neuronal distribution in the septum, a social brain area previously associated to social behavior in several vertebrate species (Lorenzi et al., 2017; Mayer et al., 2017; Clemens et al., 2020) and we observed alterations in the expression of genes linked to DA neurotransmission.

MATERIALS AND METHODS

Ethical Approval

All experiments were conducted according to the current Italian and European Community laws for the ethical treatment of animals. The experimental procedures were approved by the Ethical Committee of the University of Trento and licensed by the Italian Health Ministry (permit number 986/2016-PR).

Embryo Injections

Fertilized eggs of domestic chicks (*Gallus gallus*), of the Ross 308 (Aviagen) strain, were obtained from a local commercial hatchery [Agricola Berica, Montegalda (VI), Italy]. Upon arrival the eggs were incubated in the dark at 37.5°C and 60% relative humidity, with rocking. One week before the predicted date of hatching, on embryonic day 14 (E14), fertilized eggs were selected by a light test and injected. Chick embryo injection was performed according to previous reports (Nishigori et al., 2013; Sgadò et al., 2018). Briefly, a small hole was made on the flat end of the egg and either VPA (Sodium Valproate, Sigma Aldrich, 35 μmoles) or vehicle (double distilled injectable water; CTRL group) were administered by dropping 200 μl of solution into the air sac of each fertilized egg. Eggs were assigned to the treatment groups randomly. After sealing the hole with paper tape, eggs were placed back in the incubator until E18, when they were prepared for

hatching by incubation at 37.7°C, with 72% humidity, and in complete darkness. The day of hatching was considered post-hatching day 0 (P0).

Immunohistochemistry

After 2 days of dark incubation, P2 chicks were overdosed by an intramuscular injection of 0.05 ml per 10 g of body weight of Ketamine/Xylazine Solution (1:1 Ketamine 10 mg/ml + Xylazine 2 mg/ml). After 5 min chicks were transcardially perfused with phosphate-buffered saline (PBS) and ice-cold paraformaldehyde (4% PFA in PBS). Before removing the brain from the skulls, a coronal plane cut was performed using a stereotaxic apparatus (Kuenzel and Masson, 1988) to ensure correct orientation following the stereotaxic coordinates (45°) for coronal sectioning. Brains were then embedded in 7% bovine gelatine in PBS (4.2 g Bovine gelatine in 60 ml PBS at 40°C), using the plane cut to position the brain on the coronal plane. After cooling, the brains were post-fixed and cryopreserved in 4% PFA/PBS/20% sucrose for approximately 6 h at room temperature, and then transferred to 30% Sucrose/0.4%PFA/PBS for further 72 h. Brains were then frozen in dry ice for 30 min before sectioning the entire brain in 60 μm coronal serial sections. For free-floating immunostaining, sections were washed 3 times in PBST (0.005% Triton/PBS) between each of the following steps. After incubation in 0.3% H_2O_2/PBS for 20 min, the sections were treated for 30 min with blocking solution (3% normal goat serum in PBS). Primary antibody reaction was carried out for 10 days at 4°C in blocking solution (1:1000 mouse monoclonal Tyrosine Hydroxylase antibody; T2928, Sigma-Aldrich). Sections were then incubated in biotinylated goat-anti-mouse antibody for 24 h at 4°C in blocking solution (1:200, BA-1000, Vector Laboratories). Color reaction was performed using the Vectastain Elite ABC Kit (PK-6100, Vector Laboratories) and the DAB kit (SK-4600, Vector Laboratories) following the manufacturer instructions. Finally, sections were rinsed and mounted on gelatin-coated slides, dehydrated and coverslipped.

Cell Counts

Counts of Tyrosine Hydroxylase (TH) positive cells in the substantia nigra and VTA were performed on 8 sets of serial sections per animal, sampled at 300 μm intervals (n = 3 CTRL and 3 VPA chicks). Counting of TH immunoreactive cells was performed blind to the experimental condition using ZEN imaging software (Zeiss, Germany). All the sections were aligned on the rostral to caudal axis using Plate 34 of the chick brain atlas as reference (Puelles et al., 2007). A rectangle of 150 × 250 pixels (pixel size = 0.43 μm) was placed over the samples and TH-positive cells within this area were manually counted. Cell densities were separately counted in the SN and the VTA as number of cells/area. For each analyzed brain slice, the sampling field was moved randomly through the area of interest at least four times for each dopaminergic subgroup.

Tissue Dissection

For microdissection of the SN and the VTA neurons, P2 chicks reared in complete darkness were euthanized via carbon dioxide gaseous asphyxiation, their brain extracted and then fast-frozen in dry-ice-cold isopentane solution. 100 μm coronal sections were cut using a Leica CM1850 UV Cryostat at −15°C, and stored at −20°C. To better localize the targeted areas, sections were stained for 15 min with a 0.01% cresyl violet solution dissolved in 100% ethanol, and then progressively dehydrated in 75, 90, and 100% ethanol (1 min/each). All solutions were prepared fresh and filter-sterilized to avoid RNases contaminations. Substantia nigra and VTA regions were finally dissected out using a 20G needle and immediately processed for total RNA extraction. For dissections of the septum, P2 chicks reared in darkness were euthanized by carbon dioxide gaseous asphyxiation, the brain extracted, and the area of interest directly dissected. Briefly, two coronal cuts were performed approximately 2 and 4 mm anterior to the bregma to isolate the septum in the anterior-posterior axis according to Puelles et al. (2007) and the septum was carefully removed with forceps, fresh frozen in dry ice and immediately processed for total RNA extraction.

Total RNA Extraction

Total RNA extraction from the septum was performed using the RNeasy Mini Kit (QIAGEN), while RNA from SN and VTA samples was extracted using the PicoPure™ RNA Isolation Kit (Applied Biosystems™, Thermo Fisher Scientific). Both extractions were performed according to the manufacturers' instructions. Reverse transcription for both types of extracted materials was performed with the SuperScript™ VILO™ cDNA Synthesis Kit (Invitrogen, Thermo Fisher Scientific; Monza, Italy), following manufacturer's instructions.

Reverse Transcription-Quantitative Polymerase Chain Reaction

Reverse transcription-quantitative polymerase chain reaction (RT-qPCR) was carried out with PowerUp™ SYBR™ Green Master Mix (2x) (Thermo Fisher Scientific; Monza, Italy) for the septum and with SsoAdvanced™ Universal SYBR® Green Supermix (Bio-Rad, Milan, Italy) for mesencephalic samples. Both reactions were performed using a CFX96™ Real-Time System (Bio-Rad, Milan, Italy). Commercially synthesized primers (Merck Life Science Srl, Milan, Italy) used in this work are listed in **Table 1**. Quantitation cycles (Cq) values were calculated using the second derivative maximum method. Data were normalized on the expression of TBP (TATA-Box Binding Protein) and HMBS (Hydroxymethylbilane Synthase) reference genes using the DeltaCt (dCt) method (Pfaffl, 2001).

Statistical Analysis

Statistical evaluation of the effect of treatment on the distribution and number of DA neurons of the different subgroups and of the log2 gene expression levels (dCt) was assessed using mixed-effect models using the *nlme* package in *R*.[1] For Tukey pairwise comparison tests, we used the *emmeans* package in *R*.[2]

[1]https://cran.r-project.org/web/packages/nlme/index.html

[2]https://cran.r-project.org/web/packages/emmeans/index.html

TABLE 1 | Primers used for RT-qPCR.

Gene name		Primer sequence	Gene name		Primer sequence
DRD1	Forward	*CGTCTCATGTCTGCTATCTGTAAG*	5HTR2A	Forward	*ACCTCTGTGCCATCTCATTG*
	Reverse	*AAGAGTCCCTTTCCACAAGC*		Reverse	*CCAAAGACAGGGATAGGCATG*
DRD2	Forward	*GACAAATGCACTCATCCAGAAG*	TH	Forward	*CGAGACTTTGATCCTGATGCTG*
	Reverse	*ACACCATCTCCATTTCCATCTC*		Reverse	*GTATTTCACTGAGAAGGGCCTC*
GRIN2A	Forward	*ATACATCTTTGCCACTACGGG*	TPH2	Forward	*CAGTATGTACGACACGGCTC*
	Reverse	*AAATACCAGTCAGCCACAGG*		Reverse	*TTCGTCAGATGCTCCCAATG*
GRIN2B	Forward	*CTTCATGGGTGTCTGCTCTG*	GABRA1	Forward	*GAAGATGGCTCTCGACTGAAC*
	Reverse	*GGATGTTGGAATGGGTGTTG*		Reverse	*CCTCTTCAAGTGAAAATGTGTAGTC*
DARPP32	Forward	*AGATCCAATTCTCAGTGCCG*	GABBR2	Forward	*TTGGCTTGGGATTGTCTACG*
	Reverse	*ACTCGTCCTCTACATCTGGG*		Reverse	*CTCATTCCGATGTATTTGCTGTC*
5HTT	Forward	*GCTACTGCATAGGAACCTCTTC*	GAD1	Forward	*ATCCACCGCTAACACCAAC*
	Reverse	*TTCTGTGGCTGTTTCTGGAG*		Reverse	*CGCCATCTTTATTCGACCATCC*
CREB1	Forward	*CTCCAGACGTTGACTATGACC*	EN1	Forward	*CTCAACGAGTCCCAGATCAAG*
	Reverse	*AGGTCTGTACATCTCCTGAGG*		Reverse	*TCTTTGTCCTGCACCGTG*
OXTR	Forward	*TGTGCTGGACGCCCTTCT*	TBP	Forward	*CTTCGTGCCCGAAATGCT*
	Reverse	*TCCTGCGGAGCGTTGGT*		Reverse	*GCGCAGTAGTACGTGGTTCTCTT*
5HTR1A	Forward	*ATTATGGGCACCTTCATCCTC*	HMBS	Forward	*GGTTGAGATGCTCCGTGAGTTT*
	Reverse	*GCACTTACTGTCACAAAAGGG*		Reverse	*GGCTCTTCTCCCCAATCTTAGAA*

RESULTS

Previous studies demonstrated a remarkable effect of exposure to VPA during embryonic development on the dopaminergic system (Schiavi et al., 2019; Ádám et al., 2020; Messina et al., 2020; Román et al., 2021). To evaluate the effect of VPA on the dopaminergic system of domestic chicks, we performed immunohistochemical analysis and quantification of DA cell number in the SN and the VTA of VPA- and vehicle injected chicks, 48 h after hatching (P2). Brain sections from VPA- and vehicle-injected domestic chicks were immunolabeled for Tyrosine Hydroxylase (TH), the rate limiting enzyme for DA synthesis. Representative images of TH immunohistochemically labeled cells in the SN and VTA are shown in **Figure 1A** and **Supplementary Figure 1**. TH-positive cells where then counted and DA cell densities (cells/area, see section "Materials and Methods") were quantified in each of the serial sections encompassing the mesencephalon, separating neurons of the SN from those of the VTA, and outlining their respective rostro-caudal distribution. To assess the effect of treatment (VPA and CTRL), DA group (SN and VTA) and rostro-caudal distribution (a set of 8 sections, from the most rostral to the most caudal) on DA density, we used a linear mixed model (LMM), considering treatment, group and section as fixed factors. We compared a model with random-intercepts-only to one with random slope and intercepts, without covariance between intercepts and slope, and found that the second model fitted the data significantly better. We found that the overall density of DA cells was significantly different between the two DA groups [SN vs. VTA: $F_{(1,60)} = 40.2371$, $p < 0.0001$] and in the different rostro-caudal positions [sections: $F_{(7,60)} = 10.5726$, $p < 0.0001$] but no significant main effect of treatment was found in the overall number of DA cells (**Figure 1B**; mean cells/area in substantia nigra CTRL 5.574 [95% C.I. 4.232–6.915], VPA 5.574 [95% C.I. 2.451–8.696] in VTA CTRL 9.302 [95% C.I. 2.354–16.250], VPA 9.229 [95% C.I. 8.064–10.394; treatment: $F_{(1,4)} = 0.7096$, $p = 0.4470$]. We also observed a significant interaction between treatment and section [treatment*section: $F_{(7,60)} = 4.2912$, $p = 0.0007$], indicating an effect of treatment on the rostro-caudal distribution of DA neurons. More interestingly, a triple interaction between treatment, section and group was observed [treatment*section*group: $F_{(7,60)} = 2.2929$, $p = 0.0387$], suggesting that the effect of treatment on the rostro-caudal distribution was different in the two DA subgroups (**Figures 1C,D**). No other significant interactions were found between the other factors [treatment*group: $F_{(1,60)} = 0.0039$, $p = 0.9503$; section*group: $F_{(7,60)} = 2.1493$, $p = 0.0518$]. Given the differences on the overall density of DA cells in the subgroups, we analyzed VTA and SN distribution separately. The pairwise comparison of the cell densities in VPA and vehicle-treated domestic chicks in each section of the separate groups (**Figures 1C,D**) revealed a change in the distribution of the DA cell densities toward the posterior part of the mesencephalon, and thus a caudal shift in the distribution of DA neurons in VPA-injected chick compared to controls, more prominent in the substantia nigra [**Figure 1C**; CTRL vs. VPA, section1 $t_{(4)} = 8.7974$, $p = 0.0009$; section 2 $t_{(4)} = 3.1817$, $p = 0.0335$; section 3 $t_{(4)} = 2.4302$, $p = 0.0720$; section 4 $t_{(4)} = 1.9438$, $p = 0.1238$; section 5 $t_{(4)} = 0.5757$, $p = 0.5957$; section 6 $t_{(4)} = -3.5038$, $p = 0.0248$, section 7 $t_{(4)} = -3.7756$, $p = 0.0195$; section 8 $t_{(4)} = -5.0059$, $p = 0.0075$] than in the VTA [**Figure 1D**; CTRL vs. VPA, section1 $t_{(4)} = 3.3448$, $p = 0.0287$; section 2 $t_{(4)} = 1.0207$, $p = 0.3651$; section 3 $t_{(4)} = 1.0597$, $p = 0.3490$; section 4 $t_{(4)} = -1.6494$, $p = 0.1744$; section 5 $t_{(4)} = -1.0495$ $p = 0.3532$; section 6 $t_{(4)} = 0.4148$, $p = 0.6996$, section 7 $t_{(4)} = -0.2410$ $p = 0.8214$; section 8 $t_{(4)} = -3.8945$ $p = 0.0176$]. Overall, our statistical analysis indicated a significant effect of VPA injection in the second embryonic week on the development

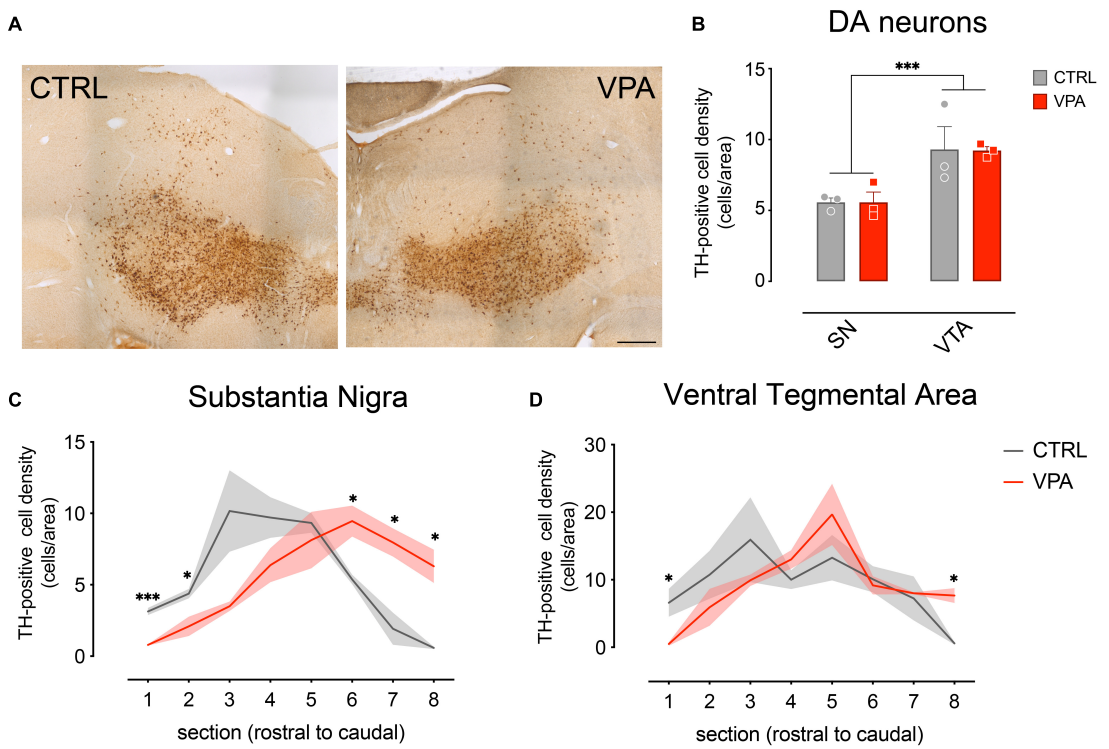

FIGURE 1 | Immunohistochemical analysis and quantification of cell densities. **(A)** Brain sections from CTRL and VPA chicks immunolabeled for Tyrosine Hydroxylase (TH). **(B)** Number of TH-positive DA neurons in both SN and VTA. TH-positive cells count was performed on 8 sets of serial sections per animal, sampled at 300 μm intervals. Rostro-caudal alignment of the brain sections was based on atlas reference (Plate 34 from Puelles et al., 2007). **(C)** Substantia Nigra DA cell density measured in its rostro-caudal distribution. **(D)** Ventral Tegmental Area DA cell density measured in its rostro-caudal distribution. Scale bar 500 μm. $^{*}p < 0.05$, $^{***}p < 0.001$.

of the mesencephalic dopaminergic neurons detectable at P2 as an alteration of the rostro-caudal distribution of DA cells.

To assess the molecular changes induced by VPA on the dopaminergic system at P2, we micro-dissected DA neurons of the SN and VTA (**Figure 2A**; $n = 6$ animal per treatment group, two independent experiments) of the entire rostro-caudal distribution, and measured the expression levels of genes involved in development (En1, TH, TPH2, Gad1) and neurotransmission (DRD1, DRD2, 5HTR1A, 5HTR2A, GABRA1, GABBR2). To assess the effect of treatment, DA group and transcripts, we used a linear mixed model, considering treatment, group and transcript as fixed factors and the experimental unit (experiment) as random factor. We compared a model with random-intercepts-only to one with random slopes and intercepts and found that the random slopes and intercepts model fitted the data significantly better. The statistical analysis indicated a significant difference in the expression levels between the transcripts analyzed in the two dopaminergic subgroups [transcripts: $F_{(8,152)} = 406.6968$, $p < 0.0001$; group: $F_{(1,152)} = 3.7786$, $p = 0.0538$; gene*group: $F_{(8,152)} = 42.0532$, $p < 0.0001$], however we could not detect any significant effect of VPA exposure at E14 on the expression of the genes at P2 [treatment: $F_{(1,10)} = 0.0372$, $p = 0.8509$; treatment*gene: $F_{(8,152)} = 0.2526$, $p = 0.9795$; treatment*group: $F_{(1,152)} = 0.1096$, $p = 0.7410$; treatment*gene*group: $F_{(8,152)} = 0.7626$, $p = 0.6362$]. Independent on the treatment, some of the genes showed differences in expression levels between the two dopaminergic subgroups as indicated by the Tukey pairwise comparison for the transcripts in each DA subgroup (**Figure 2B**; SN vs. VTA). DRD2 [$t_{(152)} = 4.8848$, $p < 0.0001$], TH [$t_{(152)} = 6.2522$, $p < 0.0001$], GAD1 [$t_{(152)} = 4.4819$, $p < 0.0001$] and GABRA1 [$t_{(152)} = 2.8885$, $p = 0.0044$] show increased levels in the SN compared to the VTA, while TPH2 [$t_{(152)} = -15.5918$, $p < 0.0001$] was expressed at higher levels in the VTA.

We then examined gene expression changes in the septum, a brain area highly innervated by dopaminergic input coming from the SN and the VTA (Montagnese et al., 2008) and involved in social behavior (Hostetler et al., 2017; Shin et al., 2018), that has been shown to activate in domestic chicks in response to exposure to conspecifics (Lorenzi et al., 2017; Mayer et al., 2017). We assessed the expression of genes involved in neurotransmission (**Figure 3**; $n = 8$ animals per group, four independent experiments), such as the dopamine receptors (DRD1 and DRD2) and the DA responsive protein DARPP32, the serotonin receptors (5HTR1A and 5HTR2A) and the serotonin transporter 5HTT, and genes involved in synaptic plasticity coding for the NMDA subunits (GRIN2A and GRIN2B), and CREB1. We also measured the expression

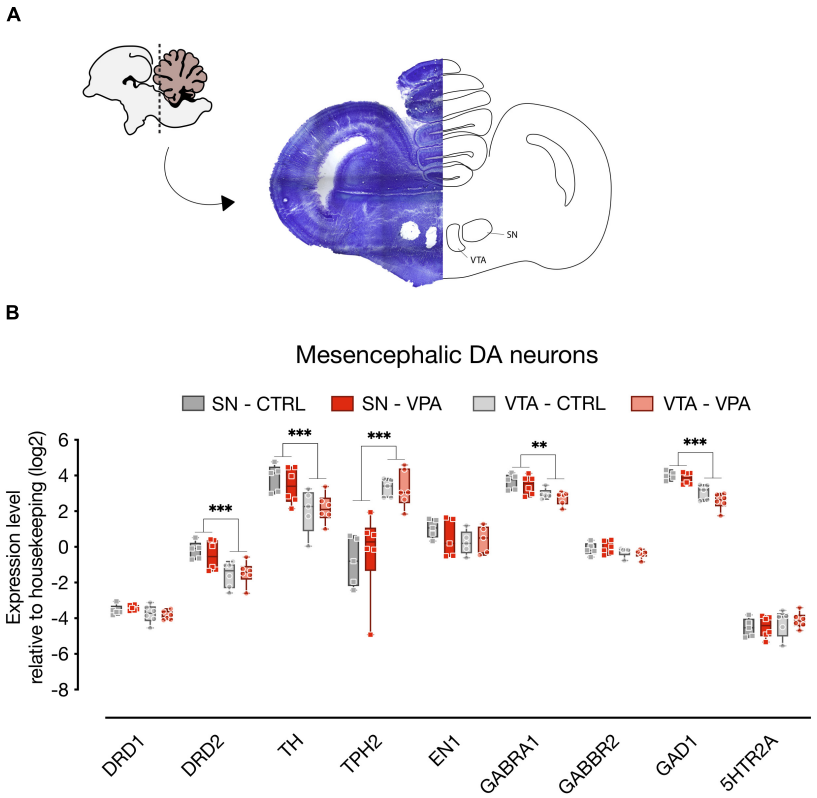

FIGURE 2 | Gene expression levels in the SN and VTA. **(A)** Schematic representation of the microdissected areas of interest (SN, Substantia Nigra; VTA, Ventral Tegmental Area) from coronal sections (adapted from Plate 33 in Puelles et al., 2007). **(B)** Box and whisker plot (median, min to max) of relative expression (dCt, log2) values for each group. Changes in expression of DRD1, DRD2, TH, TPH2, EN1, GABRA1, GABBR2, GAD1, and 5HTR2A in both SN and VTA of VPA- and vehicle-injected chicks were analyzed at P2. $^{**}p < 0.01$, $^{***}p < 0.0001$.

levels of the mesotocin receptor (OXTR), the avian homolog of oxytocin, since the lateral part of the septum is known to receive consistent oxytocinergic innervation (Loveland et al., 2019; Horiai et al., 2020). We again used linear mixed models to evaluate the effect of treatment (CTRL vs. VPA) and transcripts, and found that the best fitting model was a random slopes and intercepts model with the same parameters used for analysis of gene expression in the mesencephalon. We found a significant main effect of treatment [$F_{(1,138)} = 7.7599$, $p = 0.0061$] and a significant differences in the levels of expression of the transcripts [$F_{(9,138)} = 39.1627$, $p < 0.0001$]. We also observed a significant interaction between treatment and transcript [$F_{(9,138)} = 5.1513$, $p < 0.0001$], indicating an effect of treatment on some of the transcripts. The Tukey pairwise comparison indicated that expression of DRD1 [$t_{(138)} = 2.0741$, $p = 0.0399$], DARPP32 [$t_{(138)} = 5.6749$, $p < 0.0001$], and GRIN2A [$t_{(138)} = 2.9705$, $p = 0.0035$] was decreased in VPA-injected chicks (**Figure 3**), while 5HTT [$t_{(138)} = -2.0297$, $p = 0.0443$] expression was increased by the treatment, and expression of the other transcripts did not change [5HTR1A: $t_{(138)} = 1.4917$, $p = 0.1381$; 5HTR2A: $t_{(138)} = -0.5621$, $p = 0.5749$; CREB1: $t_{(138)} = 0.7844$, $p = 0.4342$; DRD2: $t_{(138)} = 1.5030$, $p = 0.1351$; GRIN2B: $t_{(138)} = 1.6429$, $p = 0.1027$; OXTR: $t_{(138)} = -0.2558$, $p = 0.7985$].

DISCUSSION

The dopaminergic system has been shown to influence key aspects of social and affiliative behavior in humans and other vertebrates (Opendak et al., 2021; Solié et al., 2022), and to cooperate in modulating key components of the social brain network (Gunaydin and Deisseroth, 2014). In addition, accumulating evidence point to an involvement of DA neurotransmission in atypical social development in children with ASD (Scott-Van Zeeland et al., 2010; Supekar et al., 2018; Zürcher et al., 2021).

In the present study, we investigated developmental dysregulations of the DA system in a VPA model of ASD implemented in domestic chicks, that could potentially contribute to the behavioral deficits observed in the chicks' spontaneous responses to social stimuli, including altered response to faces (Adiletta et al., 2021). More specifically, we analyzed the number, distribution, and the developmental gene expression of DA neurons in the postnatal mesencephalon of domestic chicks embryonically exposed to VPA, and then assessed gene expression changes in the septum, a region of the social brain network highly innervated by DA terminals (Lindvall and Stenevi, 1978; Gaspar et al., 1985) and involved in sociability and social novelty seeking (Mesic et al., 2015).

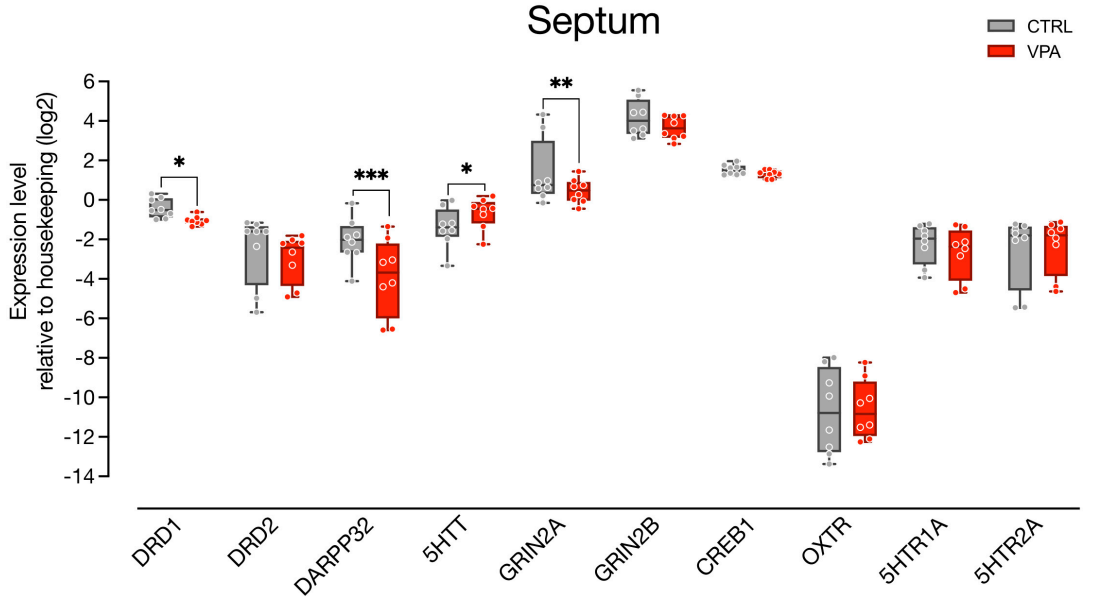

FIGURE 3 | Gene expression levels in the septum. Box and whisker plot (median, min to max) of relative expression (dCt, log2) values for each group. Changes in expression of DRD1, DRD2, DARPP32, 5HTT, GRIN2A, GRIN2B, CREB1, OXTR, 5HTR1A, and 5HTR2A in septum samples collected from P2 chicks embryonically exposed to VPA. *$p < 0.05$, **$p < 0.001$, ***$p < 0.0001$.

Consistent with our hypothesis of an effect of VPA on the DA system, when analyzing the rostro-caudal portions of the mesencephalon, we observed a caudal shift in the distribution of mesencephalic DA population at P2, 9 days after embryonic exposure to VPA. Neuroanatomical alterations of mesencephalic TH population was already described in mice exposed to VPA by Ádám et al. (2020), however, without analyses on the distribution of the DA population. Moreover, differently from the work of Ádám et al. (2020), here we found no difference in the density of DA neurons (measured as number of cells/area) between the two treatments groups, suggesting the preservation of the overall profile of the DA population in our model, as indicated also by our gene expression analysis in the mesencephalon. Interestingly, VPA exposure was performed at E14, long after embryonic dopaminergic proliferation and differentiation events have terminated (Andersson et al., 2006), deeming unlikely a direct influence of VPA on neurogenesis or differentiation of DA neurons. A recent report by Huang et al. (2019) has described developmental expansion in the DA and serotonin neurons in chicken mid-late embryogenesis, revealing an increase in TH expression in the mesencephalon between E12 and E14 and later, between E16 and E19, accompanied by increased levels of DA in the brainstem. Thus, waves of DA neuron expansions may also occur in mid-late embryogenesis. In the light of these data, VPA treatment could impinge on this naturally occurring late expansion of the DA population and then affect the distribution/migration of the newly born DA neurons, causing a shift in their rostro-caudal positioning. Our data on the expression of TH suggest that VPA does not regulate proliferation of the DA population, nor does it affect the number of DA neurons, as confirmed by the cell counts and by the expression of both TH and En1, that did not change upon treatment with VPA. The observed changes in DA neurons distribution may occur through different mechanisms. One possibility is through regulation of genes affecting migration, as for example the CXC motif chemokine receptor 4 (Cxcr4), a G-protein coupled receptor binding to the chemokine Cxcl12, and involved in cell migration (Li and Ransohoff, 2008). Cxcr4 controls the migration of hippocampal neurons and interneurons (Wang et al., 2011), and its expression is regulated by VPA prenatal administration in mice (Sakai et al., 2018). Embryonic exposure with VPA in mice induces a downregulation of Cxcr4 and an increase in the density of hippocampal granule cells that are aberrantly positioned, this phenotype is reversed by postnatal overexpression of Cxcr4 (Sakai et al., 2018). The mechanisms through which VPA acts on Cxcr4 in murine hippocampal granule cells is still not entirely clear. VPA could directly affect Cxcr4 expression or it could affect cell migration through its well-known effect on GABA, since GABA agonists have been shown to activate Cxcr4 (Guyon et al., 2013). Interestingly, CxCl12/Cxcr4 signaling also regulates the migration and orientation of DA neurons during development in mice (Yang et al., 2013). Future studies will clarify the mechanisms through which VPA exerts its effect on DA neurons and whether other brainstem populations, as for example the serotonergic neurons of the raphe nuclei, are also affected by VPA treatment.

To investigate the potential consequences of the observed rostro-caudal shift in the distribution of the mesencephalic DA neurons, we have also assessed changes in the expression of genes involved in DA neurotransmission in one of the target regions of the mesocorticolimbic pathway, the septum,

known to modulate different aspects of social behavior in mice (see for a review Menon et al., 2022) as well as in domestic chicks (Lorenzi et al., 2017; Mayer et al., 2017). We found that DRD1, DARPP32 and GRIN2A were downregulated upon VPA exposure, suggesting deficits in dopaminergic signaling in this brain region. Previous studies have investigated the role of dopaminergic signaling in social behavior, demonstrating increased DARPP32 phophorylation mediated by DRD1 signaling in the nucleus accumbens of rats subjected to same-sex social interactions (Scheggi et al., 2020). Direct stimulation of DRD1 in the nucleus accumbens has also been shown to produce significant increase in same-sex social interaction in mice (Gunaydin et al., 2014). Interestingly, VPA embryonic exposure in rats abolishes the DRD1-mediated phosphorylation of DARPP32 (Scheggi et al., 2020) suggesting that a decrease in the DRD1-mediated signaling could produce detrimental effects on social behavior. It remains to be established how exactly VPA may act on DRD1 expression and whether a similar mechanism is also in place in the septum of domestic chicks in association to exposure to social partners.

We also found that expression of the serotonin transporter (5HTT) was increased in the septum, suggestive of alterations also in serotonergic neurotransmission. Several studies and meta-analysis have confirmed an increase in 5HT in the blood (hyperserotonemia) of autistic individuals, such that hyperserotonemia has become a reliable biomarker for these disorders (see for a review Lam et al., 2006; Gabriele et al., 2014). Epidemiological and animal model studies have suggested that perinatal alterations in 5HT, either above or below typical levels, may cause social behavioral deficits resembling ASD (Garbarino et al., 2019).

Previous studies have reported alterations in the number of DA neurons or in DA neurotransmission in several animal models of ASD (see for a recent review Kosillo and Bateup, 2021). A reduction in the number of DA neurons in the SN (but not the VTA) was found in adult mice lacking the Fmr1 gene (Fish et al., 2013). Further studies demonstrated reduced striatal DA transmission and striatal DA re-uptake without significant changes in the striatal tissue DA content in Fmr1 mutant mice (Fulks et al., 2010; Sørensen et al., 2015). Alterations in DA-mediated responses have also been reported in the BTBR mice (Squillace et al., 2014), a model for idiopathic autism, accompanied by decreased TH expression in several DA innervated brain regions (Chao et al., 2020). Interestingly, intranasal dopamine administration efficiently rescued the cognitive and social deficits of both BTBR and Fmr1 mutant ASD models (Chao et al., 2020), suggesting a causal role of DA deficiency in the behavioral phenotype of the mice.

Notably, in our study, we investigated for the first time DA-related deficits on an ASD model implemented in the domestic chicks. Differently from other common animal models, chicks are precocial species able to independently behave soon after hatching (Versace and Vallortigara, 2015), displaying remarkable early and spontaneous social responses, already shown to have similar features to the social orienting behavior observed in human newborns (Di Giorgio et al., 2017). Domestic chicks also enable researchers to study early neurodevelopmental mechanisms, without the interference of sophisticated, divergent, strategies of adaptive learning that emerge later. We thus believe that the domestic chick represents an ideal candidate model to study the causal relationship between social orienting behavior, emerging at early postnatal stages, and any underlying neurobiological alterations mediated by VPA or any other genetic manipulation associated to ASD. Further studies should thus investigate the potential causal relationship between DA signaling alterations and the early social orienting deficits observed in VPA exposed chicks, including impairments in face processing and affiliative behavior.

DATA AVAILABILITY STATEMENT

The original contributions presented in the study are included in the article/**Supplementary Material**, further inquiries can be directed to the corresponding author.

ETHICS STATEMENT

The animal study was reviewed and approved by the Ethical Committee of the University of Trento and the Italian Health Ministry (permit number 986/2016-PR).

AUTHOR CONTRIBUTIONS

PS conceived and designed the experiments. AA and AP conducted the experiments. NT provided technical support. PS and AA analyzed the data and wrote the manuscript. All authors read and approved the final manuscript.

FUNDING

This work was supported by the University of Trento (intramural funds to AA, NT, and PS).

ACKNOWLEDGMENTS

We thank Giorgio Vallortigara and Andrea Messina for their support. Dr. Tommaso Pecchia for help with the experimental apparatus, Grazia Gambardella and Roberta Guidolin for administrative help and Ciro Petrone for animal facility management.

SUPPLEMENTARY MATERIAL

The Supplementary Material for this article can be found online at: https://www.frontiersin.org/articles/10.3389/fnint.2022.804881/full#supplementary-material

REFERENCES

Ádám, Á, Kemecsei, R., Company, V., Murcia-Ramón, R., Juarez, I., Gerecsei, L., et al. (2020). Gestational exposure to sodium valproate disrupts fasciculation of the mesotelencephalic dopaminergic tract, with a selective reduction of dopaminergic output from the ventral tegmental area. *Front. Neuroanat.* 14:29. doi: 10.3389/fnana.2020.00029

Adiletta, A., Pedrana, S., Rosa-Salva, O., and Sgadò, P. (2021). Spontaneous visual preference for face-like stimuli is impaired in newly-hatched domestic chicks exposed to valproic acid during embryogenesis. *Front. Behav. Neurosci.* 15:733140. doi: 10.3389/fnbeh.2021.733140

Andersson, E., Tryggvason, U., Deng, Q., Friling, S., Alekseenko, Z., Robert, B., et al. (2006). Identification of intrinsic determinants of midbrain dopamine neurons. *Cell* 124, 393–405. doi: 10.1016/j.cell.2005.10.037

Bambini-Junior, V., Baronio, D., MacKenzie, J., Zanatta, G., Riesgo, R., dos, S., et al. (2014). "Prenatal exposure to valproate in animals and autism," in *Comprehensive Guide to Autism*, eds V. Patel, V. Preedy, and C. Martin (New York, NY: Springer), 1779–1793.

Bariselli, S., Hörnberg, H., Prévost-Solié, C., Musardo, S., Hatstatt-Burklé, L., Scheiffele, P., et al. (2018). Role of VTA dopamine neurons and neuroligin 3 in sociability traits related to nonfamiliar conspecific interaction. *Nat. Commun.* 9:3173. doi: 10.1038/s41467-018-05382-3

Bariselli, S., Tzanoulinou, S., Glangetas, C., Prévost-Solié, C., Pucci, L., Viguié, J., et al. (2016). SHANK3 controls maturation of social reward circuits in the VTA. *Nat. Neurosci.* 19, 926–934. doi: 10.1038/nn.4319

Björklund, A., and Dunnett, S. (2007). Dopamine neuron systems in the brain: an update. *Trends Neurosci.* 30, 194–202. doi: 10.1016/j.tins.2007.03.006

Bourdy, R., Sánchez-Catalán, M.-J., Kaufling, J., Balcita-Pedicino, J. J., Freund-Mercier, M.-J., Veinante, P., et al. (2014). Control of the nigrostriatal dopamine neuron activity and motor function by the tail of the ventral tegmental area. *Neuropsychopharmacology* 39, 2788–2798. doi: 10.1038/npp.2014.129

Chao, O. Y., Pathak, S. S., Zhang, H., Dunaway, N., Li, J.-S., Mattern, C., et al. (2020). Altered dopaminergic pathways and therapeutic effects of intranasal dopamine in two distinct mouse models of autism. *Mol. Brain* 13:111. doi: 10.1186/s13041-020-00649-7

Christensen, J., Grønborg, T., Sørensen, M., Schendel, D., Parner, E., Pedersen, L., et al. (2013). Prenatal valproate exposure and risk of autism spectrum disorders and childhood autism. *JAMA* 309, 1696–1703.

Clemens, A. M., Wang, H., and Brecht, M. (2020). The lateral septum mediates kinship behavior in the rat. *Nat. Commun.* 11:3161. doi: 10.1038/s41467-020-16489-x

Di Giorgio, E., Loveland, J. L., Mayer, U., Rosa-Salva, O., Versace, E., and Vallortigara, G. (2017). Filial responses as predisposed and learned preferences: early attachment in chicks and babies. *Behav. Brain Res.* 325, 90–104. doi: 10.1016/j.bbr.2016.09.018

Ferrari, D., Mdzomba, B., Dehorter, N., Lopez, C., Michel, F., Libersat, F., et al. (2012). Midbrain dopaminergic neurons generate calcium and sodium currents and release dopamine in the striatum of pups. *Front. Cell Neurosci.* 6:7. doi: 10.3389/fncel.2012.00007

Fish, E. W., Krouse, M. C., Stringfield, S. J., Diberto, J. F., Robinson, J. E., and Malanga, C. J. (2013). Changes in sensitivity of reward and motor behavior to dopaminergic, glutamatergic, and cholinergic drugs in a mouse model of fragile X syndrome. *PLoS One* 8:e77896. doi: 10.1371/journal.pone.0077896

Fulks, J. L., O'Bryhim, B. E., Wenzel, S. K., Fowler, S. C., Vorontsova, E., Pinkston, J. W., et al. (2010). Dopamine release and uptake impairments and behavioral alterations observed in mice that model fragile x mental retardation syndrome. *ACS Chem. Neurosci.* 1, 679–690. doi: 10.1021/cn100032f

Gabriele, S., Sacco, R., and Persico, A. M. (2014). Blood serotonin levels in autism spectrum disorder: a systematic review and meta-analysis. *Eur. Neuropsychopharmacol.* 24, 919–929. doi: 10.1016/j.euroneuro.2014.02.004

Garbarino, V. R., Gilman, T. L., Daws, L. C., and Gould, G. G. (2019). Extreme enhancement or depletion of serotonin transporter function and serotonin availability in autism spectrum disorder. *Pharmacol. Res.* 140, 85–99. doi: 10.1016/j.phrs.2018.07.010

Gaspar, P., Berger, B., Alvarez, C., Vigny, A., and Henry, J. P. (1985). Catecholaminergic innervation of the septal area in man: immunocytochemical study using TH and DBH antibodies. *J. Comp. Neurol.* 241, 12–33. doi: 10.1002/cne.902410103

Gunaydin, L., Grosenick, L., Finkelstein, J., Kauvar, I., Fenno, L., Adhikari, A., et al. (2014). Natural neural projection dynamics underlying social behavior. *Cell* 157, 1535–1551. doi: 10.1016/j.cell.2014.05.017

Gunaydin, L. A., and Deisseroth, K. (2014). Dopaminergic dynamics contributing to social behavior. *Cold Spring Harb. Symp. Quant. Biol.* 79, 221–227. doi: 10.1101/SQB.2014.79.024711

Guyon, A., Kussrow, A., Olmsted, I., Sandoz, G., Bornhop, D., and Nahon, J. (2013). Baclofen and other GABAB receptor agents are allosteric modulators of the CXCL12 chemokine receptor CXCR4. *J. Neurosci.* 33, 11643–11654.

Horiai, M., Otsuka, A., Hidema, S., Hiraoka, Y., Hayashi, R., Miyazaki, S., et al. (2020). Targeting oxytocin receptor (Oxtr)-expressing neurons in the lateral septum to restore social novelty in autism spectrum disorder mouse models. *Sci. Rep.* 10:22173. doi: 10.1038/s41598-020-79109-0

Hostetler, C. M., Hinde, K., Maninger, N., Mendoza, S. P., Mason, W. A., Rowland, D. J., et al. (2017). Effects of pair bonding on dopamine D1 receptors in monogamous male titi monkeys (Callicebus cupreus). *Am. J. Primatol.* 79, 1–9. doi: 10.1002/ajp.22612

Huang, X., Kuang, S., Applegate, T., Lin, T., and Cheng, H. (2019). The development of the serotonergic and dopaminergic systems during chicken mid-late embryogenesis. *Mol. Cell Endocrinol.* 493:110472. doi: 10.1016/j.mce.2019.110472

Ilango, A., Kesner, A. J., Keller, K. L., Stuber, G. D., Bonci, A., and Ikemoto, S. (2014). Similar roles of substantia nigra and ventral tegmental dopamine neurons in reward and aversion. *J. Neurosci.* 34, 817–822. doi: 10.1523/JNEUROSCI.1703-13.2014

Kosillo, P., and Bateup, H. (2021). Dopaminergic dysregulation in syndromic autism spectrum disorders: insights from genetic mouse models. *Front. Neural Circuits* 15:700968. doi: 10.3389/fncir.2021.700968

Kuenzel, W. J., and Masson, M. (1988). *A Stereotaxic Atlas of the Brain of the Chick (Gallus Domesticus)*. Baltimore, MD: Johns Hopkins University Press.

Lam, K. S. L., Aman, M. G., and Arnold, L. E. (2006). Neurochemical correlates of autistic disorder: a review of the literature. *Res. Dev. Disabil.* 27, 254–289. doi: 10.1016/j.ridd.2005.03.003

Li, M., and Ransohoff, R. (2008). Multiple roles of chemokine CXCL12 in the central nervous system: a migration from immunology to neurobiology. *Prog. Neurobiol.* 84, 116–131. doi: 10.1016/j.pneurobio.2007.11.003

Lindvall, O., and Stenevi, U. (1978). Dopamine and noradrenaline neurons projecting to the septal area in the rat. *Cell Tissue Res.* 190, 383–407. doi: 10.1007/BF00219554

Lorenzi, E., Mayer, U., Rosa-Salva, O., and Vallortigara, G. (2017). Dynamic features of animate motion activate septal and preoptic areas in visually naïve chicks (*Gallus gallus*). *Neuroscience* 354, 54–68. doi: 10.1016/j.neuroscience.2017.04.022

Lorenzi, E., Pross, A., Rosa-Salva, O., Versace, E., Sgadò, P., and Vallortigara, G. (2019). Embryonic exposure to valproic acid affects social predispositions for dynamic cues of animate motion in newly-hatched chicks. *Front. Physiol.* 10:501. doi: 10.3389/fphys.2019.00501

Loveland, J. L., Stewart, M. G., and Vallortigara, G. (2019). Effects of oxytocin-family peptides and substance P on locomotor activity and filial preferences in visually naïve chicks. *Eur. J. Neurosci.* 50, 3674–3687. doi: 10.1111/ejn.14520

Mayer, U., Rosa-Salva, O., and Vallortigara, G. (2017). First exposure to an alive conspecific activates septal and amygdaloid nuclei in visually-naïve domestic chicks (*Gallus gallus*). *Behav. Brain Res.* 317, 71–81. doi: 10.1016/j.bbr.2016.09.031

Menon, R., Süß, T., Oliveira, V., Neumann, I., and Bludau, A. (2022). Neurobiology of the lateral septum: regulation of social behavior. *Trends Neurosci.* 45, 27–40. doi: 10.1016/j.tins.2021.10.010

Mesic, I., Guzman, Y. F., Guedea, A. L., Jovasevic, V., Corcoran, K. A., Leaderbrand, K., et al. (2015). Double dissociation of the roles of metabotropic glutamate receptor 5 and oxytocin receptor in discrete social behaviors. *Neuropsychopharmacology* 40, 2337–2346. doi: 10.1038/npp.2015.81

Messina, A., Boiti, A., Sovrano, V., and Sgadò, P. (2020). Micromolar valproic acid doses preserve survival and induce molecular alterations in neurodevelopmental genes in two strains of zebrafish larvae. *Biomolecules* 10:1364. doi: 10.3390/biom10101364

Montagnese, C., Zachar, G., Bálint, E., and Csillag, A. (2008). Afferent connections of septal nuclei of the domestic chick (*Gallus domesticus*): a retrograde pathway tracing study. *J. Comp. Neurol.* 511, 109–150. doi: 10.1002/cne.21837

Morales, M., and Margolis, E. (2017). Ventral tegmental area: cellular heterogeneity, connectivity and behaviour. *Nat. Rev. Neurosci.* 18, 73–85. doi: 10.1038/nrn.2016.165

Nishigori, H., Kagami, K., Takahashi, A., Tezuka, Y., Sanbe, A., and Nishigori, H. (2013). Impaired social behavior in chicks exposed to sodium valproate during the last week of embryogenesis. *Psychopharmacology* 227, 393–402. doi: 10.1007/s00213-013-2979-y

Opendak, M., Raineki, C., Perry, R., Rincón-Cortés, M., Song, S., Zanca, R., et al. (2021). Bidirectional control of infant rat social behavior via dopaminergic innervation of the basolateral amygdala. *Neuron* 109, 4018–4035.e7. doi: 10.1016/j.neuron.2021.09.041

Pfaffl, M. W. (2001). A new mathematical model for relative quantification in real-time RT-PCR. *Nucleic Acids Res.* 29:e45. doi: 10.1093/nar/29.9.e45

Puelles, L., Martinez-de-la-Torre, M., Martinez, S., Watson, C., and Paxinos, G. (2007). *The Chick Brain in Stereotaxic Coordinates: An Atlas featuring Neuromeric Subdivisions and Mammalian Homologies*. Amsterdam: Elsevier Science.

Román, V., Adham, N., Foley, A., Hanratty, L., Farkas, B., Lendvai, B., et al. (2021). Cariprazine alleviates core behavioral deficits in the prenatal valproic acid exposure model of autism spectrum disorder. *Psychopharmacology* 238, 2381–2392. doi: 10.1007/s00213-021-05851-6

Sakai, A., Matsuda, T., Doi, H., Nagaishi, Y., Kato, K., and Nakashima, K. (2018). Ectopic neurogenesis induced by prenatal antiepileptic drug exposure augments seizure susceptibility in adult mice. *Proc. Natl. Acad. Sci. U. S. A.* 115, 4270–4275.

Scheggi, S., Guzzi, F., Braccagni, G., De Montis, M., Parenti, M., and Gambarana, C. (2020). Targeting PPARα in the rat valproic acid model of autism: focus on social motivational impairment and sex-related differences. *Mol. Autism* 11:62. doi: 10.1186/s13229-020-00358-x

Schiavi, S., Iezzi, D., Manduca, A., Leone, S., Melancia, F., Carbone, C., et al. (2019). Reward-related behavioral, neurochemical and electrophysiological changes in a rat model of autism based on prenatal exposure to valproic acid. *Front. Cell Neurosci.* 13:479. doi: 10.3389/fncel.2019.00479

Scott-Van Zeeland, A., Dapretto, M., Ghahremani, D., Poldrack, R., and Bookheimer, S. (2010). Reward processing in autism. *Autism Res.* 3, 53–67.

Sgadò, P., Rosa-Salva, O., Versace, E., and Vallortigara, G. (2018). Embryonic exposure to valproic acid impairs social predispositions of newly-hatched chicks. *Sci. Rep.* 8:5919. doi: 10.1038/s41598-018-24202-8

Shin, S., Pribiag, H., Lilascharoen, V., Knowland, D., Wang, X.-Y., and Lim, B. K. (2018). Drd3 signaling in the lateral septum mediates early life stress-induced social dysfunction. *Neuron* 97, 195–208.e6. doi: 10.1016/j.neuron.2017.11.040

Silva, P. A., Trigo, S., Marques, C. I., Cardoso, G. C., and Soares, M. C. (2020). Experimental evidence for a role of dopamine in avian personality traits. *J. Exp. Biol.* 223:jeb216499. doi: 10.1242/JEB.216499

Solié, C., Girard, B., Righetti, B., Tapparel, M., and Bellone, C. (2022). VTA dopamine neuron activity encodes social interaction and promotes reinforcement learning through social prediction error. *Nat. Neurosci.* 25, 86–97. doi: 10.1038/s41593-021-00972-9

Sørensen, E. M., Bertelsen, F., Weikop, P., Skovborg, M. M., Banke, T., Drasbek, K. R., et al. (2015). Hyperactivity and lack of social discrimination in the adolescent Fmr1 knockout mouse. *Behav. Pharmacol.* 26, 733–740. doi: 10.1097/FBP.0000000000000152

Spreckelmeyer, K., Krach, S., Kohls, G., Rademacher, L., Irmak, A., Konrad, K., et al. (2009). Anticipation of monetary and social reward differently activates mesolimbic brain structures in men and women. *Soc. Cogn. Affect Neurosci.* 4, 158–165. doi: 10.1093/scan/nsn051

Squillace, M., Dodero, L., Federici, M., Migliarini, S., Errico, F., Napolitano, F., et al. (2014). Dysfunctional dopaminergic neurotransmission in asocial BTBR mice. *Transl. Psychiatry* 4:e427. doi: 10.1038/tp.2014.69

Supekar, K., Kochalka, J., Schaer, M., Wakeman, H., Qin, S., Padmanabhan, A., et al. (2018). Deficits in mesolimbic reward pathway underlie social interaction impairments in children with autism. *Brain* 141, 2795–2805. doi: 10.1093/brain/awy191

Versace, E., and Vallortigara, G. (2015). Origins of knowledge: insights from precocial species. *Front. Behav. Neurosci.* 9:338. doi: 10.3389/fnbeh.2015.00338

Wang, Y., Li, G., Stanco, A., Long, J., Crawford, D., Potter, G., et al. (2011). CXCR4 and CXCR7 have distinct functions in regulating interneuron migration. *Neuron* 69, 61–76. doi: 10.1016/j.neuron.2010.12.005

Wise, R. (2009). Roles for nigrostriatal–not just mesocorticolimbic–dopamine in reward and addiction. *Trends Neurosci.* 32, 517–524. doi: 10.1016/j.tins.2009.06.004

Yamaguchi, Y., Lee, Y.-A., Kato, A., Jas, E., and Goto, Y. (2017). The roles of dopamine D2 receptor in the social hierarchy of rodents and primates. *Sci. Rep.* 7:43348. doi: 10.1038/srep43348

Yamamoto, K., and Vernier, P. (2011). The evolution of dopamine systems in chordates. *Front. Neuroanat.* 5:21. doi: 10.3389/fnana.2011.00021

Yang, S., Edman, L., Sánchez-Alcañiz, J., Fritz, N., Bonilla, S., Hecht, J., et al. (2013). Cxcl12/Cxcr4 signaling controls the migration and process orientation of A9-A10 dopaminergic neurons. *Development* 140, 4554–4564. doi: 10.1242/dev.098145

Zachar, G., Tóth, A., Gerecsei, L., Zsebõk, S., Ádám, Á, and Csillag, A. (2019). Valproate exposure in ovo attenuates the acquisition of social preferences of young post-hatch domestic chicks. *Front. Physiol.* 10:881. doi: 10.3389/fphys.2019.00881

Zürcher, N. R., Walsh, E. C., Phillips, R. D., Cernasov, P. M., Tseng, C.-E. J., Dharanikota, A., et al. (2021). A simultaneous [11C]raclopride positron emission tomography and functional magnetic resonance imaging investigation of striatal dopamine binding in autism. *Transl. Psychiatry* 11:33. doi: 10.1038/s41398-020-01170-0

Conflict of Interest: The authors declare that the research was conducted in the absence of any commercial or financial relationships that could be construed as a potential conflict of interest.

Publisher's Note: All claims expressed in this article are solely those of the authors and do not necessarily represent those of their affiliated organizations, or those of the publisher, the editors and the reviewers. Any product that may be evaluated in this article, or claim that may be made by its manufacturer, is not guaranteed or endorsed by the publisher.

frontiers | Frontiers in Integrative Neuroscience

ORIGINAL RESEARCH
published: 03 May 2022
doi: 10.3389/fnint.2022.821109

Cerebellar Volumes and Sensorimotor Behavior in Autism Spectrum Disorder

*Walker S. McKinney[1,2], Shannon E. Kelly[1,3], Kathryn E. Unruh[1], Robin L. Shafer[1], John A. Sweeney[4], Martin Styner[5] and Matthew W. Mosconi[1,2,3]**

[1] Schiefelbusch Institute for Life Span Studies and Kansas Center for Autism Research and Training (K-CART), University of Kansas, Lawrence, KS, United States, [2] Clinical Child Psychology Program, University of Kansas, Lawrence, KS, United States, [3] Department of Psychology, University of Kansas, Lawrence, KS, United States, [4] Department of Psychiatry and Behavioral Neuroscience, University of Cincinnati College of Medicine, Cincinnati, OH, United States, [5] Department of Psychiatry and Computer Science, University of North Carolina at Chapel Hill, Chapel Hill, NC, United States

Background: Sensorimotor issues are common in autism spectrum disorder (ASD), though their neural bases are not well understood. The cerebellum is vital to sensorimotor control and reduced cerebellar volumes in ASD have been documented. Our study examined the extent to which cerebellar volumes are associated with multiple sensorimotor behaviors in ASD.

Materials and Methods: Fifty-eight participants with ASD and 34 typically developing (TD) controls (8–30 years) completed a structural MRI scan and precision grip testing, oculomotor testing, or both. Force variability during precision gripping as well as absolute error and trial-to-trial error variability of visually guided saccades were examined. Volumes of cerebellar lobules, vermis, and white matter were quantified. The relationships between each cerebellar region of interest (ROI) and force variability, saccade error, and saccade error variability were examined.

Results: Relative to TD controls, individuals with ASD showed increased force variability. Individuals with ASD showed a reduced volume of cerebellar vermis VI-VII relative to TD controls. Relative to TD females, females with ASD showed a reduced volume of bilateral cerebellar Crus II/lobule VIIB. Increased volume of Crus I was associated with increased force variability. Increased volume of vermal lobules VI-VII was associated with reduced saccade error for TD controls but not individuals with ASD. Increased right lobule VIII and cerebellar white matter volumes as well as reduced right lobule VI and right lobule X volumes were associated with greater ASD symptom severity. Reduced volumes of right Crus II/lobule VIIB were associated with greater ASD symptom severity in only males, while reduced volumes of right Crus I were associated with more severe restricted and repetitive behaviors only in females.

Conclusion: Our finding that increased force variability in ASD is associated with greater cerebellar Crus I volumes indicates that disruption of sensory feedback processing supported by Crus I may contribute to skeletomotor differences in ASD. Results showing that volumes of vermal lobules VI-VII are associated with saccade precision in TD but

OPEN ACCESS

Edited by:
Eric London, Institute for Basic Research in Developmental Disabilities (IBR), United States

Reviewed by:
Anila Maria D'Mello, Massachusetts Institute of Technology, United States
Lana Vasung, Harvard Medical School, United States

***Correspondence:**
Matthew W. Mosconi
mosconi@ku.edu

Received: *23 November 2021*
Accepted: *31 March 2022*
Published: *03 May 2022*

Citation:
McKinney WS, Kelly SE, Unruh KE, Shafer RL, Sweeney JA, Styner M and Mosconi MW (2022) Cerebellar Volumes and Sensorimotor Behavior in Autism Spectrum Disorder. Front. Integr. Neurosci. 16:821109. doi: 10.3389/fnint.2022.821109

not ASD implicates atypical organization of the brain systems supporting oculomotor control in ASD. Associations between volumes of cerebellar subregions and ASD symptom severity suggest cerebellar pathological processes may contribute to multiple developmental challenges in ASD.

Keywords: cerebellum, volumetry, autism spectrum disorder (ASD), sensorimotor, oculomotor, MRI, structure, Crus I

INTRODUCTION

Autism spectrum disorder (ASD) is a neurodevelopmental disability for which brain mechanisms are not well understood. Sensorimotor difficulties are present in 70–80% of individuals with ASD (Dewey et al., 2007; Green et al., 2009) and are predictive of functional outcomes, including daily living skills (Travers et al., 2017). They also represent promising targets for advancing understanding of the underlying brain mechanisms of ASD because they are: (1) supported by cortical-cerebellar networks that are well-defined through animal and human lesion studies (Smith et al., 1981; Molinari et al., 1997; Hilber et al., 1998; Brochier et al., 1999; Kelly and Strick, 2003) and consistently implicated in ASD [for reviews, see Fatemi et al. (2012) and Mosconi et al. (2015b)]; (2) familial, suggesting that they may serve as endophenotypes representing polygenic risk (Mosconi et al., 2010; Mous et al., 2017), and; (3) associated with core features of ASD (Murray et al., 2006; LeBarton and Iverson, 2016; Travers et al., 2017; Iverson et al., 2019). Clarifying neuroanatomical substrates associated with sensorimotor differences in ASD is therefore important for understanding the pathophysiological mechanisms associated with the disorder(s).

Individuals with ASD show sensorimotor differences across effector systems, including skeletomotor and oculomotor systems. Multiple studies have documented reduced control of skeletomotor behavior in ASD including increased variability of both upper (Mosconi et al., 2015a; Wang et al., 2015; Unruh et al., 2021) and lower limb behavior (Glazebrook et al., 2006; Marko et al., 2015). Atypical oculomotor function in ASD has also been documented, including reduced accuracy and increased amplitude variability of saccades (Takarae et al., 2004; Stanley-Cary et al., 2011; Schmitt et al., 2014). These findings converge to suggest that individuals with ASD demonstrate alterations in sensorimotor processes spanning multiple effector systems and multiple types of behavior, including both sustained actions and rapid, ballistic movements.

Both sustained and rapid sensorimotor behaviors are supported by well-defined cortical, subcortical, and cerebellar systems. Cerebellum is particularly important for refining motor output through the comparison of internal predictive models of initial motor plans (i.e., "feedforward models") and sensory feedback error information (Bastian, 2006; Shadmehr and Krakauer, 2008). During skeletomotor control, the lateral cerebellum (Crus I) integrates sensory feedback with feedforward models to refine motor output *via* anterior cerebellum (lobules I-V), lobule VI, and afferent relays to the primary motor cortex (M1) *via* the thalamus (Stein, 1986; Stein and Glickstein, 1992; Glickstein, 2000; Vaillancourt et al., 2006). Crus I plays a role in multiple motor and non-motor functions (Stoodley and Schmahmann, 2009; Stoodley et al., 2012), suggesting that it supports internal model representations and refinements across multiple neural systems (Kelly and Strick, 2003; Ito, 2008). Within the motor domain, reciprocal connections between cerebellar Crus I and M1 form a closed-loop circuit that supports the online refinement of endpoint target selection during movement (Proville et al., 2014). Reciprocal connections between M1 and cerebellar lobule VIII, which houses a secondary somatotopic representation, also support the refinement of motor output, largely as a supplement to anterior cerebellum and Crus I during the early stages of sensorimotor learning due to enhanced task demands (Steele and Penhune, 2010; Kuper et al., 2014; Bonzano et al., 2015).

Discrete oculomotor cerebellar networks support accurate eye movements generated in response to visual stimuli. Visually guided saccadic and smooth pursuit eye movements are generated through projections from the posterior vermal lobules VI-VII to caudal fastigial nuclei and subsequent execution by abducens motoneurons innervating the lateral rectus muscles (Ohtsuka and Noda, 1992; Scudder et al., 2002). Across skeletomotor and oculomotor cerebellar networks, white matter tracts support the integration of motor and sensory information *via* intracerebellar, afferent (through middle cerebellar peduncles), and efferent (through superior cerebellar peduncles) pathways (Salmi et al., 2010; Roberts et al., 2013; Koppelmans et al., 2015).

Structural MRI studies in ASD implicate multiple cerebellar subregions important for skeletomotor and oculomotor control. Within cerebellar Crus I, both increased (Stoodley, 2014; D'Mello et al., 2016) and decreased volumes have been reported (Yu et al., 2011; Duerden et al., 2012), though separate studies have not shown differences between individuals with ASD and TD controls (Nickl-Jockschat et al., 2012; DeRamus and Kana, 2015). Cerebellar lobules I-V show decreased volumes in individuals with ASD relative to typically developing (TD) controls (Allen et al., 2004; Duerden et al., 2012; Marko et al., 2015), and hemispheric lobule VI shows increased volumes in ASD relative to TD controls (Nickl-Jockschat et al., 2012). Structural differences in vermal lobules associated with oculomotor control also have been documented in ASD, including reduced volumes of vermal lobules VI-VII (Courchesne et al., 2001; Kaufmann et al., 2003; Stanfield et al., 2008; Webb et al., 2009; Crucitti et al., 2020), though others have suggested that vermal hypoplasia may be specific to individuals with (Stanfield et al., 2008) or

without (Scott et al., 2009) comorbid intellectual/developmental disability. These structural MRI findings not only implicate dysmorphology of cerebellar lobules important for skeletomotor and oculomotor control in ASD, but also suggest patterns of cerebellar structural variation differ across separate lobules and as a function of clinical or behavioral characteristics (e.g., intellectual/developmental disability).

While several studies have examined the associations between cerebral regional volumes and sensorimotor abilities in ASD (Mostofsky et al., 2007; Mahajan et al., 2016; Lin et al., 2019), only one known study has assessed the covariation of cerebellar morphometry and skeletomotor behavior in ASD, and no known studies have examined the relationships between volumetrics of different cerebellar subregions and multiple separate sensorimotor behaviors in ASD (e.g., skeletomotor and oculomotor). During a reaching test, Marko et al. (2015) demonstrated that children with ASD show a reduced ability to adapt to visual perturbations and that these difficulties are associated with reduced volumes of bilateral cerebellar lobules I-V, VI, and VIII. These findings suggest that alterations in the cerebellar structure in ASD are associated with a reduced ability to integrate online visual feedback information to rapidly update internal action representations that are used to guide initial motor output.

In the present study, we examined the relationships between the volumes of multiple cerebellar subregions and both skeletomotor and oculomotor behaviors in ASD. Regarding skeletomotor control, consistent with our prior behavioral studies (Mosconi et al., 2015a; Wang et al., 2015; Unruh et al., 2021), we predicted that individuals with ASD would show increased force variability. Consistent with the role of cerebellar Crus I in skeletomotor control (Vaillancourt et al., 2006; Proville et al., 2014) and differences between individuals with ASD and TD controls in Crus I function (Unruh et al., 2019; Wang et al., 2019; Lepping et al., 2021), we predicted that force variability increases in ASD would be associated with cerebellar Crus I volumes. Regarding oculomotor control, consistent with previous behavioral studies (Takarae et al., 2004; Stanley-Cary et al., 2011; Schmitt et al., 2014; Unruh et al., 2021), we expected individuals with ASD would show increased saccade error and trial-to-trial error variability. Consistent with previous structural MRI studies (Courchesne et al., 2001; Kaufmann et al., 2003; Stanfield et al., 2008; Webb et al., 2009; Crucitti et al., 2020), we predicted that individuals with ASD would show reduced volume of vermal lobules VI/VII compared to TD controls who would be associated with more severe saccade dysmetria in ASD. Exploratory analyses of separate cerebellar subregions and white matter and their associations with precision gripping variability and saccade error and error variability were also conducted. Based on the findings that cerebellar structural variation may be associated with core ASD symptoms, we also examined the relationships between cerebellar lobular, vermis, and white matter volumes with clinically rated social-communication abnormalities and restricted, repetitive behaviors.

MATERIALS AND METHODS

Participants

Fifty-eight participants with ASD and 34 TD controls matched on age (8–30 years), sex, and handedness completed a structural MRI scan and either precision grip testing, oculomotor testing, or both (**Table 1**). Due to scheduling constraints and pauses in testing related to COVID-19, not all participants completed all three components of testing. Forty-four participants with ASD and 29 TD controls completed both the MRI scan and precision grip testing. Forty-two participants with ASD and 25 TD controls completed both the MRI scan and oculomotor testing. Participants with ASD were recruited through outpatient clinics. Participants from both groups were recruited through community advertisements and our research registries.

All participants with ASD met DSM-5 criteria as determined by the Autism Diagnostic Observation Schedule—Second Edition (ADOS-2; Lord et al., 2012), Autism Diagnostic Interview—Revised (ADI-R; Lord et al., 1994), and expert clinical opinion according to DSM 5 criteria (American Psychiatric Association [APA], 2013). All participants with ASD either had a previous diagnosis of ASD or were strongly suspected to meet the diagnostic criteria for ASD by their medical provider. General cognitive abilities (IQ) were assessed using the Wechsler Abbreviated Scale of Intelligence—Second Edition (WASI-II; Wechsler, 2011). Due to restrictions regarding in-person testing during the COVID-19 pandemic, 20 participants completed a

TABLE 1 | Participant characteristics.

	TD Controls	ASD
N	34 (18 F)	58 (21 F)
Age	17.1 (5.6)	15.7 (4.9)
% right-handed	91.20%	79.30%
Race		
% White	76.5%	82.8%
% Black	5.9%	–
% American Indian or Alaska Native	–	1.7%
% Asian American/Pacific Islander	2.9%	1.7%
% More than one race	11.8%	12.1%
% Not specified or unknown	2.9%	1.7%
Ethnicity		
% Hispanic/Latinx	20.6%	13.8%
Weight in kg	58.2 (20.1)	63.1 (21.8)
Height in cm	161.3 (12.7)	164.5 (13.9)
VIQ	110 (10)	99 (17)
PIQ	114 (10)	100 (17)
Left hand MVC	71.3 (26.8)	57.8 (22.0)
Right hand MVC	70.8 (27.4)	55.0 (20.7)
ADOS CSS	-	5.9 (2.3)
RBS-R Total Score	-	29.5 (19.0)

ASD, autism spectrum disorder; F, female; VIQ, verbal IQ; PIQ, performance IQ; ADOS CSS, Autism Diagnostic Observation Schedule Calculated Severity Score; RBS-R, Repetitive Behaviors Scale—Revised; Values reported as M (SD).

remote administration of the two-subtest version of the WASI-II based on the publisher's recommendations. Exclusionary criteria for participants with ASD included full-scale IQ less than 60 or a known genetic or metabolic disorder associated with ASD (e.g., fragile X syndrome, tuberous sclerosis complex). Exclusionary criteria for TD controls included the presence of any lifetime psychiatric or neurodevelopmental disorder, or a family history of neurodevelopmental disorders in the first- or second-degree relatives. Exclusionary criteria for both groups included a history of a significant psychiatric disorder (e.g., schizophrenia, bipolar disorder, and personality disorder), meningitis, encephalitis, seizure disorder, or head trauma with loss of consciousness, current use of medications known to affect sensorimotor functioning (e.g., stimulants, benzodiazepines, and anticonvulsants; Reilly et al., 2008), and significant complications during pregnancy, labor, or delivery. All participants refrained from caffeine, nicotine, alcohol, and recreational drug use on the day of testing.

Precision Grip Testing

During precision grip testing, participants were seated 52 cm away from a 69 cm LCD monitor (resolution = 1,366 × 768; refresh rate = 120 Hz). Their hands were pronated and lay flat with digits comfortably extended while gripping two opposing precision ELFF-B4-100N load cells of 1.27 cm in diameter (Measurement Specialties, Hampton, VA, United States) with their thumb and forefinger (**Figure 1A**). Load cells were secured to custom-made forearm rests mounted to a table (75 cm in height). Electrical resistance changes from the load cells were amplified by four individual resistive bridge strain amplifiers (V72-25; Coulbourn Instruments, Allentown, PA, United States). Amplifier output was sampled continuously at 200 Hz by an analog-to-digital converter (National Instruments, Austin, TX, United States) at 16-bit resolution and converted to Newtons (N) of force using a calibration factor derived from known weights before the study. The system can detect forces down to 0.0016 N.

Before testing, each participant's maximum voluntary contraction (MVC) was calculated separately for each hand using the average of the maximum force output from three trials in which participants pressed as hard as they could for three seconds (s). MVC trials alternated between hands and were separated by 30 s of rest.

During testing, participants gripped the opposing load cells while viewing two horizontal bars: a horizontal white "force" bar that moved upward with increased force and downward with decreased force and a static target bar that was red during rest (**Figure 1B**) and turned green to cue the participant to begin pressing at the start of each trial (**Figure 1C**). Participants received two instructions: (1) to press the load cells as quickly as possible when the red target bar turns green, and (2) to keep pressing so that the force bar stays as steady as possible at the level of the green target bar. The target bar was set at 15% of each participant's MVC and the visual angle was set at 0.623°. Participants completed the precision grip testing with their left and right hands separately. For each hand, participants completed three 15 s trials separated by 15 s rest periods. The order of hand tested was counterbalanced across participants.

Oculomotor Testing

Oculomotor testing was administered in a darkened black room using a chinrest positioned 61 cm from a 27-inch BenQ monitor (refresh rate: 144 Hz; resolution: 2,560 × 1,440). Visual stimuli were presented using SR Research Experiment Builder (SR Research Ltd., Ontario, CA, United States), and participants' eye movements were recorded using an EyeLink 1000 Plus infrared, binocular camera (sampling rate: 500 Hz; accuracy: 0.25–0.5°; SR Research Ltd., Ontario, CA, United States). Participants performed a five-point calibration prior to each block of trials.

Participants completed 60 trials of a visually guided saccade task, separated into two blocks (30 trials per block). During this task, participants fixed their gaze on a centrally located crosshair for 1.5–2 s at the start of each trial (**Figure 1D**), then were presented peripheral targets (**Figure 1E**) (i.e., white circles, 0.3° in diameter) at ± 12° or 24° of visual angle for 1.5 ss.

MRI Data Acquisition

Participants completed a structural MRI scan with a 3T whole-body scanner (Siemens Skyra) and a 32-channel head coil. Participants lay supine with their head stabilized using adjustable padding. A whole-brain T1-weighted (MPRAGE) anatomical scan was acquired across 176 contiguous sagittal slices at 1.200 × 1.055 × 1.055 mm^3 (FOV 176 × 240 × 256 mm^3; matrix 176 × 240 × 256 mm^3; TR = 2.3 s; TE = 2.95 ms; inversion delay to the center k-line 900 ms; flip angle = 9°; pixel bandwidth = 240 Hz; duration 5:12).

Data Processing

Precision Grip Data Processing

Force data were analyzed using custom MATLAB scripts previously developed by our lab (Wang et al., 2015). The force time series was digitally filtered using a fourth-order Butterworth filter and a 15 Hz low-pass cutoff. To assess precision grip performance, the sustained portion of the force timeseries was examined, defined as the 12 s period preceding the appearance of the stop cue (target bar turned from green to red). Portions of the sustained force output in which participants released the force transducers and force output was reduced to zero for greater than 1 s were excluded from analyses. Trials were excluded if they contained less than 8 s of sustained force output following the offset of the initial increase in force, defined as the time-point when the rate of force increase fell below 5% of the peak rate of force increase and the force level was within 90–110% of the mean force of the sustained phase. The peak rate of force increase was defined as the maximum value of the first derivative of the force trace. To assess force variability, the coefficient of variation (CoV) was derived by dividing the standard deviation (SD) of the sustained force time series by the mean of the sustained force time series for each trial.

Oculomotor Data Processing

Oculomotor data was filtered prior to scoring using digital finite impulse response filters with non-linear transition bands. Visual inspection of eye movement data was conducted to detect and correct or exclude data confounded by blinks or head movements. The accuracy of the primary saccade was measured

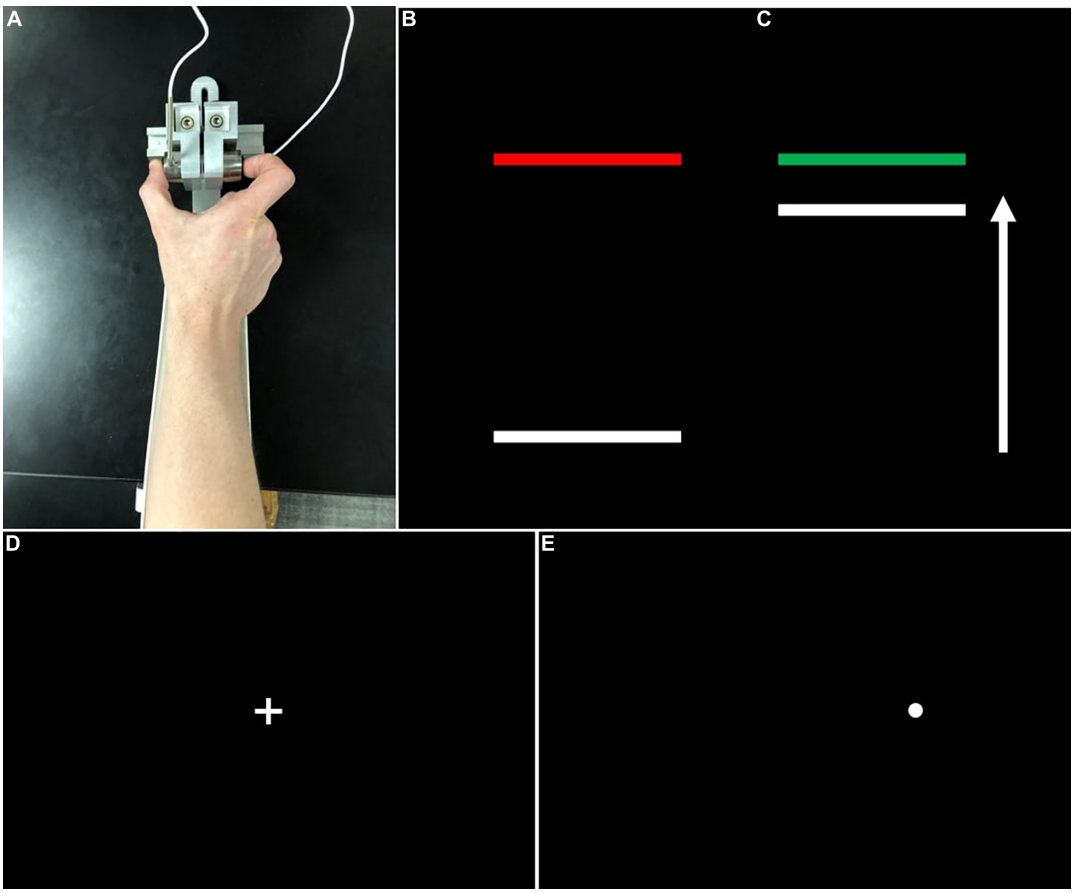

FIGURE 1 | (A) Grip configuration and load cells for precision grip testing. Participants pressed with their thumb and forefinger against two precision load cells. Participants pressed the load cells as quickly as possible when the red target bar **(B)** turned green **(C)** and continued pressing to maintain the force bar steady at the level of the green target bar. **(D)** During visually guided saccade testing, participants fixed their gaze on a centrally located crosshair at the start of each trial, then looked quickly toward **(E)** peripheral targets (i.e., white circles) which appeared pseudorandomly at ± 12° or 24° of visual angle.

as the absolute value of the horizontal distance in degrees of visual angle between the eye location at saccade offset and the target location. The primary saccade was defined as the first saccade that moved at least 20% of the distance to the target. Saccade offset was defined as the timepoint at which the eye velocity fell below 30°/s. Saccades with latencies $\leq$ 70 ms were considered anticipatory and excluded from analyses. Saccade error variability was calculated as the SD of saccade accuracy across trials.

MRI Data Processing

Cerebellar lobules were automatically segmented using the Automatic Cerebellum Anatomical Parcelation using U-Net with Locally Constrained Optimization (ACAPULCO; version 0.2.2) pipeline (Han et al., 2020) and accompanying pediatric template (Carass et al., 2018). Image inhomogeneities were corrected using N4 (Tustison et al., 2010). The 1 mm isotropic ICBM 2009c template was used to register the corrected image to MNI space (Fonov et al., 2011). A bounding box was drawn around the cerebellum, and a modified U-Net was used to segment individual lobules. The parcelated image was transformed back to the original image space and the volume of each region of interest (ROI) was calculated.

Following automated segmentation, cerebellar parcelations were visually inspected by two separate raters. Discrepancies were discussed and resolved *via* consensus. Extensions of the parcelation into non-cerebellum (e.g., meninges, 4th ventricle) were manually corrected using ITK-SNAP (Yushkevich et al., 2006). Volumes of 18 ROIs were extracted (**Figure 2**), including separate left and right cerebellar lobules I-V, lobule VI, Crus I, Crus II/lobule VIIB, lobule VIII, lobule IX, and lobule X, as well as vermal lobules I-V, VI-VII, VIII-X, and cerebellar white matter. Raw cerebellar volumes were examined without controlling for total tissue volume since our primary focus was on associations between volumes of individual cerebellar subregions and sensorimotor/clinical behaviors as opposed to the relationships between cerebellar and more diffuse cortical and subcortical structural variations, including regions not thought to be strongly associated with sensorimotor outcomes of interest. Further, given the differences in total tissue volume in ASD (Lange et al., 2015) and distinct scaling factors across the cerebrum and cerebellum (de Jong et al., 2017), normalization to

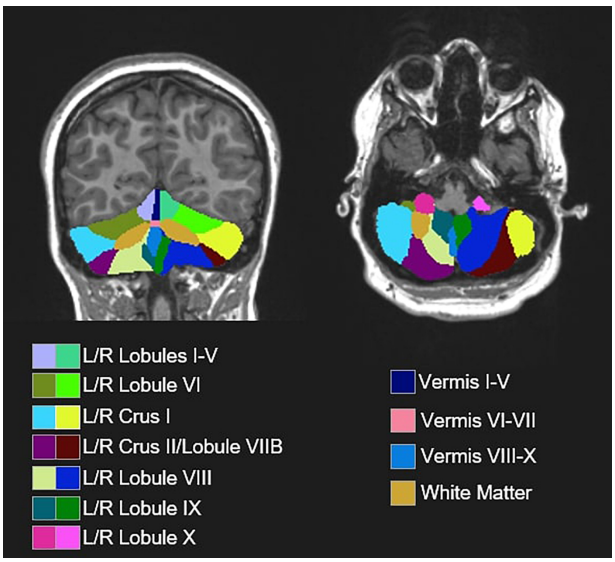

FIGURE 2 | Representative segmentation from a single subject depicting 18 cerebellar ROIs obtained from automated segmentation procedures (ACAPULCO; Han et al., 2020) and an accompanying pediatric template (Carass et al., 2018).

outcomes, such as intracranial volume (ICV) risks incorporating substantial variance unrelated to group differences in the cerebellar volume. Other measures (e.g., body size) possibly affecting the brain size were similar across groups (**Table 1**).

Clinical Measures

To assess ASD symptom severity, the calibrated severity score (CSS) from the ADOS-2 was examined. The CSS is an aggregate score ranging from 1 to 10 that allows for the comparison of symptom severity across different ADOS-2 modules. Higher CSS scores reflect more severe ASD symptoms. Caregivers of participants with ASD also completed the repetitive behavior scale-revised (RBS-R; Bodfish et al., 2000; Lam and Aman, 2007), a caregiver-report questionnaire assessing restricted and repetitive behaviors common in ASD. We examined the RBS-R total score. Due to scheduling issues related to the COVID-19 pandemic, not all participants with ASD completed the ADOS-2 and RBS-R. Forty-nine participants with ASD completed the ADOS-2 and 51 completed the RBS-R.

Statistical Analyses

Linear mixed effects models were used to examine group differences in force variability. Hand (left vs. right) was included as a level one predictor (within-subjects), while group (TD vs. ASD), sex, and age at task administration were included as level two predictors (between-subjects). The group × hand, group × sex, and group × age interaction terms also were examined. Similar linear mixed effects models were used to examine group differences in saccade error and saccade error variability, where target step amplitude (12° vs. 24°) and direction (left vs. right) were included as level one predictors, and group, sex, and age at task administration were included as level two predictors. Associated two- and three-way interaction terms (i.e., group × direction, group × amplitude, group × direction × amplitude) were also examined.

Separate linear mixed effects models were used to examine group differences in the cerebellar volume. For cerebellar hemisphere ROIs (14 ROIs: separate left and right cerebellar lobules I-V, lobule VI, Crus I, Crus II/lobule VIIB, lobule VIII, lobule IX, and lobule X), models included hemisphere (left vs. right) as a level one predictor. Group, sex, and age at MRI administration were included as level two predictors. Associated two- and three-way interaction terms were also examined. Identical models without a hemisphere predictor were used to examine group differences in the cerebellar vermis ROIs and the cerebellar white matter.

Linear mixed effects models were also used to examine group differences in the association between cerebellar volumes and grip and saccade behavior. For force variability, the primary ROIs examined were cerebellar lobules I-V, lobule VI, and Crus I based on prior functional studies documenting the involvement of these subregions in manual motor behavior (Vaillancourt et al., 2006; Stoodley et al., 2012). For absolute error of visually guided saccades, the primary ROI examined was vermal lobules VI-VII based on the known functional role of posterior vermis in the oculomotor control (Ohtsuka and Noda, 1992; Scudder et al., 2002). The Benjamini–Hochberg procedure was used to control the number of models examined at a false-discovery rate of 5% and alpha level of 0.05. We also conducted separate exploratory analyses of associations between behavioral outcomes and the volume of all other cerebellar ROIs. These analyses were considered exploratory and hypothesis-generating, so no Type I error correction was applied. For force variability, behavior-cerebellar volume models included hand as a level one predictor. For saccade error and saccade error variability, amplitude and direction were included as level one predictors. For both sets of models, group, brain volume, and age at MRI administration were included as level two predictors. Sex was included as a covariate of no interest. Three-way interactions (grip: group × hand × volume; oculomotor: group × direction × volume, group × amplitude × volume) and nested two-way interactions were also examined.

For participants with ASD, similar linear mixed effects models were used to examine the associations between cerebellar ROI volumes and ASD severity measured using the ADOS CSS and RBS-R total score. Models included separate hemispheric predictors for the seven homologous ROIs. Separate regression models were used to examine the linear associations between clinical outcomes and the four non-lateralized ROIs. Given distinct patterns of cerebellar development across males and females in TD (Tiemeier et al., 2010) and previously reported sex-specific associations between the cerebellar volume and clinical symptoms (Supekar and Menon, 2015), two-way interaction terms of sex × volume were also examined. These analyses were considered exploratory and hypothesis-generating, so no Type I error correction was applied.

For all analyses, interaction terms were iteratively removed if their inclusion did not improve the model fit, consistent

with the best-practice recommendations in maintaining model parsimony (Matuschek et al., 2017). Force variability was log-transformed for all analyses due to its non-normal distribution. All other outcomes were normally distributed. Age was group-mean centered. R version 4.1.0 ("Camp Pontanezen") was used for all analyses. Mixed effects models were constructed using the *lme4* package (Bates et al., 2015). Simple slopes estimates used to probe interaction effects were obtained using the *interactions* package (Long, 2019).

RESULTS

Precision Grip Force

Relative to TD controls, individuals with ASD showed reduced left- [$t(49.73) = -2.223$, $p = 0.031$] and right-hand MVC [$t(48.57) = -2.639$, $p = 0.011$].

Individuals with ASD showed elevated force variability compared to TD controls [$F_{(1,64.75)} = 17.01$, $p < 0.001$]. Increased age was associated with lower force variability [$F_{(1,65.08)} = 34.040$, $p < 0.001$]. Force variability was similar across hands [$F_{(1,67.62)} = 0.636$, $p = 0.428$] and sexes [$F_{(1,64.71)} = 0.218$, $p = 0.642$].

Saccade Precision

Saccade error was similar for individuals with ASD and TD controls [$F_{(1,59)} = 0.056$, $p = 0.815$]. Increased age was associated with reduced saccade error, though this relationship was at a trend level [$F_{(1,59)} = 2.819$, $p = 0.098$]. Saccade error was the greatest for leftward 24° saccades [amplitude × direction: $F_{(1,192)} = 21.262$, $p < 0.001$]. Saccade error was similar across males and females [$F_{(1,59)} = 0.234$, $p = 0.631$].

Saccade error variability was similar between individuals with ASD and TD controls [$F_{(1,59)} = 1.739$, $p = 0.192$]. Increased age was associated with reduced saccade error variability [$F_{(1,59)} = 5.393$, $p = 0.024$]. Saccade error variability was the greatest for leftward 24° saccades [amplitude × direction: $F_{(1,192)} = 18.348$, $p < 0.001$]. Saccade error variability was similar between males and females [$F_{(1,59)} = 0.299$, $p = 0.586$].

Cerebellar Volumetrics

Cerebellar Hemisphere Lobules

Individuals with ASD and TD controls showed no differences in volumes of cerebellar lobules I-V [**Table 2**; $F_{(1,87)} = 1.585$, $p = 0.211$]. Males showed greater volumes of cerebellar lobules I-V than females [$F_{(1,87)} = 17.840$, $p < 0.001$]. Volumes of cerebellar lobules I-V were greater for the left compared to the right hemispheres [$F_{(1,90)} = 4.038$, $p = 0.047$], though this difference did not survive correction for multiple comparisons ($p_{crit} = 0.029$).

Individuals with ASD and TD controls showed no differences in volumes of cerebellar lobule VI [$F_{(1,86)} = 0.003$, $p = 0.958$]. Group differences in the volume of cerebellar lobule VI varied across sexes [group × sex: $F_{(1,86)} = 5.610$, $p = 0.020$], but this finding did not survive the correction for multiple comparisons ($p_{crit} = 0.014$). Specifically, males with ASD showed reduced volumes relative to TD males [$t(86) = -1.686$, $p = 0.337$], while females with ASD showed greater volumes relative to TD females [$t(86) = 1.676$, $p = 0.343$]. Volumes of lobule VI were greater for the left compared to the right hemisphere [$F_{(1,90)} = 4.953$, $p = 0.029$], but this difference did not survive the correction for multiple comparisons ($p_{crit} = 0.021$).

Individuals with ASD and TD controls showed no differences in volumes of cerebellar Crus I [$F_{(1,87)} = 0.117$, $p = 0.733$]. Males showed greater volumes of cerebellar Crus I than females [$F_{(1,87)} = 15.276$, $p < 0.001$].

Group differences in the volume of cerebellar Crus II/lobule VIIB varied across sexes [**Figure 3**; group × sex: $F_{(1,86)} = 7.570$, $p = 0.007$]. Specifically, females with ASD showed reduced volumes of Crus II/lobule VIIB relative to TD females [$t(86) = -2.625$, $p = 0.049$], while males with ASD and TD showed similar volumes [$t(86) = 1.245$, $p = 0.600$]. Volumes of Crus II/lobule VIIB were greater for the left compared to the right hemisphere [$F_{(1,90)} = 84.119$, $p < 0.001$].

Males showed greater volumes of lobule VIII than females [$F_{(1,87)} = 45.560$, $p < 0.001$]. Individuals with ASD showed differences in the volumes of lobule VIII that varied as a function of hemisphere [group × hemisphere: $F_{(1,89)} = 4.890$, $p = 0.030$], though this finding did not survive the correction for multiple comparisons ($p_{crit} = 0.007$). Specifically, relative to TD controls, individuals with ASD showed smaller volumes of left lobule VIII [$t(110) = -0.858$, $p = 0.827$], but greater volumes of right lobule VIII [$t(110) = 0.657$, $p = 0.913$].

Individuals with ASD and TD controls showed no differences in volumes of cerebellar lobule IX [$F_{(1,87)} = 0.124$, $p = 0.726$]. Males showed greater volumes of lobule IX than females [$F_{(1,87)} = 16.841$, $p < 0.001$].

Individuals with ASD and TD controls showed no differences in volumes of cerebellar lobule X [$F_{(1,87)} = 0.068$, $p = 0.795$].

TABLE 2 | Volume of lateralized regions of interest (ROIs).

	Lobules I-V	Lobule VI	Crus I	Crus II/Lobule VIIB	Lobule VIII	Lobule IX	Lobule X
Controls							
Left	6.57 (0.93)	10.85 (1.44)	15.53 (1.96)	15.45 (2.18)	12.32 (1.74)	3.72 (0.67)	0.61 (0.11)
Right	6.47 (0.98)	10.45 (1.48)	15.95 (2.04)	14.35 (2.07)	12.70 (1.63)	3.64 (0.67)	0.60 (0.09)
ASD							
Left	6.48 (0.99)	10.82 (1.18)	15.85 (2.05)	15.34 (2.03)	12.38 (1.51)	3.71 (0.66)	0.59 (0.10)
Right	6.33 (0.93)	10.68 (1.20)	15.92 (2.34)	14.02 (2.34)	13.21 (1.94)	3.68 (0.66)	0.62 (0.09)

Values reported as M (SD); Volume is reported as cm^3.

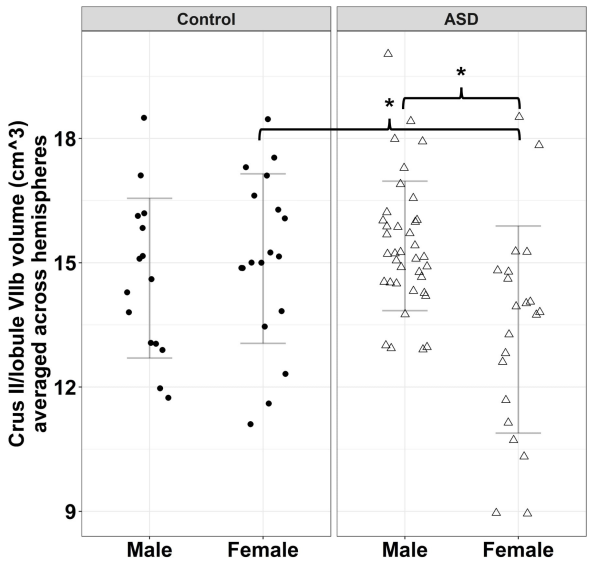

FIGURE 3 | Sex-dependent group differences in Crus II/lobule VIIB volume. Error bars reflect mean ± 1 SD. * denotes $p < 0.05$.

Males showed greater volumes of lobule X than females [$F_{(1,87)} = 20.908$, $p < 0.001$].

Cerebellar Vermis and White Matter

Individuals with ASD showed reduced volumes of cerebellar vermal lobules I-V relative to TD controls, though this effect was at a trend level [$F_{(1,87)} = 3.718$, $p = 0.057$]. Males showed greater volumes of vermal lobules I-V than females [$F_{(1,87)} = 19.252$, $p < 0.001$].

Relative to TD controls, individuals with ASD showed reduced volumes of cerebellar vermal lobules VI-VII [**Figure 4** and **Table 3**; $F_{(1,87)} = 8.119$, $p = 0.005$]. Males showed greater volumes of vermal lobules VI-VII than females [$F_{(1,87)} = 4.708$, $p = 0.033$].

Individuals with ASD and TD controls showed similar volumes of vermal lobules VIII-X [$F_{(1,87)} = 0.960$, $p = 0.330$]. Males showed greater volumes of vermal lobules VIII-X than females [$F_{(1,87)} = 8.118$, $p = 0.005$].

Individuals with ASD and TD controls showed similar volumes of cerebellar white matter [$F_{(1,86)} = 0.892$, $p = 0.348$]. Males showed greater volumes of cerebellar white matter than females [$F_{(1,86)} = 24.919$, $p < 0.001$]. Increased age was associated with greater volume of cerebellar white matter for TD controls ($\beta = 0.129$, $p < 0.001$), but not individuals with ASD ($\beta = 0.035$, $p = 0.268$), though this finding did not survive the correction for multiple comparisons [group × age: $F_{(1,86)} = 3.971$, $p = 0.049$; $p_{crit} = 0.013$].

Cerebellar Volume and Sensorimotor Behavior

Cerebellar Associations With Precision Grip Force Variability

Force variability was not associated with volumes of right lobules I-V [$F_{(1,66.57)} = 0.461$, $p = 0.500$], right lobule VI [$F_{(1,66.62)} = 0.013$, $p = 0.910$], left lobules I-V [$F_{(1,66.50)} = 0.431$, $p = 0.514$], or left lobule VI [$F_{(1,66.52)} = 0.373$, $p = 0.544$]. Increased force variability was associated with increased volume of both right Crus I [$F_{(1,68.73)} = 7.737$, $p = 0.007$] and left Crus I [$F_{(1,69.78)} = 8.312$, $p = 0.005$].

Exploratory analyses of associations between non-skeletomotor cerebellar ROIs and precision grip behavior indicated that the relationship between the volume of right lobule VIII and force variability varied across hands [hand × volume: $F_{(1,67.27)} = 5.278$, $p = 0.025$], reflecting the finding that increased volume of right lobule VIII was associated with reduced left- ($\beta = -0.097$, $p = 0.026$) but not right-hand force variability ($\beta = -0.035$, $p = 0.409$). Similarly, the relationship between volume of left lobule VIII and force variability varied across hands hand × volume: $F_{(1,67.14)} = 4.943$, $p = 0.030$], such that increased volume of left lobule VIII was associated with reduced left- ($\beta = -0.074$, $p = 0.121$) but not right-hand force variability ($\beta = -0.007$, $p = 0.876$). Increased right lobule IX [$F_{(1,69.86)} = 2.875$, $p = 0.094$] and left lobule IX [$F_{(1,70.39)} = 3.221$, $p = 0.077$] volumes were associated with increased force variability, though these relationships were at a trend level. Increased cerebellar white matter volume was associated with reduced force variability [$F_{(1,66.67)} = 6.212$, $p = 0.015$]. No other associations between cerebellar volume and force variability were significant, and all associations between force variability and cerebellar volume were similar across groups.

Cerebellar Associations With Saccade Error

Associations between the volumes of vermal lobules VI-VII and saccade error varied across groups, though this interaction was at a trend level [**Figure 5**; group × volume: $F_{(1,60)} = 3.896$, $p = 0.053$]; greater volumes of vermal lobules VI-VII were associated with reduced saccade error in TD controls ($\beta = -1.022$, $p = 0.007$), but not individuals with ASD ($\beta = -0.124$, $p = 0.671$).

Exploratory analyses indicated that the relationships between saccade error and volume of right Crus II/lobule VIIB varied as a function of group and target step amplitude [group × amplitude × volume: $F_{(1,189)} = 6.781$, $p = 0.010$]. At 24° only, increased volume of right Crus II/lobule VIIB was associated with lower saccade error for TD controls ($\beta = -0.129$, $p < 0.001$), while greater volume was associated with more severe saccade error for individuals with ASD ($\beta = 0.065$, $p = 0.021$). The relationships between saccade error and volume of left Crus II/lobule VIIB also varied as a function of group and target step amplitude [group × amplitude × volume: $F_{(1,189)} = 9.662$, $p = 0.002$]. At 24° only, increased left Crus II/lobule VIIB volume was associated with lower saccade error for TD controls ($\beta = -0.117$, $p = 0.002$), while increased volume was associated with greater error for individuals with ASD ($\beta = 0.092$, $p = 0.003$).

Increased volume of right lobule VIII was associated with lower saccade error for TD controls ($\beta = -0.107$, $p = 0.008$) but not for individuals with ASD [$\beta = -0.016$, $p = 0.590$; group × volume: $F_{(1,60)} = 4.151$, $p = 0.046$]. The relationships between saccade error and volume of left lobule VIII varied as a function of group and target step amplitude [group × amplitude × volume: $F_{(1,189)} = 9.213$, $p = 0.003$]. Increased volume of left lobule VIII was associated with lower

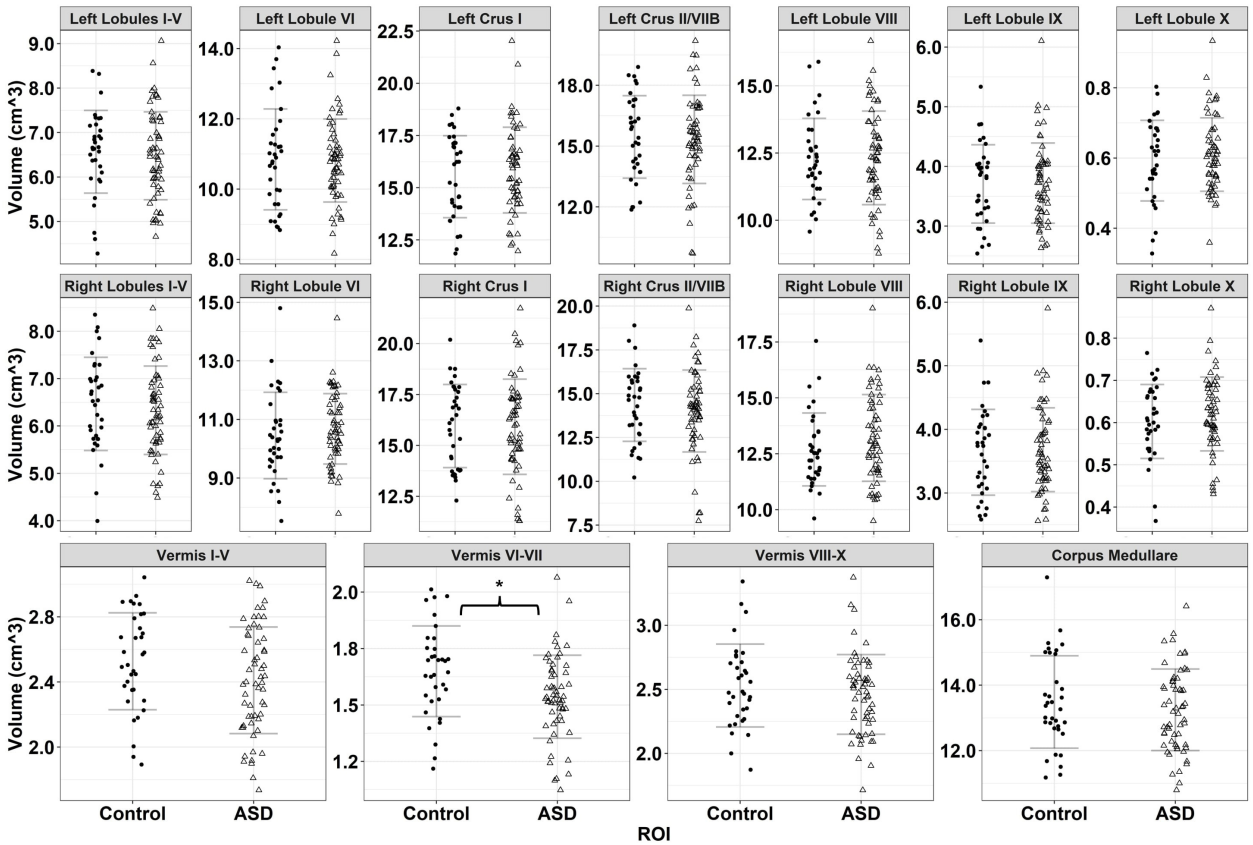

FIGURE 4 | Volumes for 18 cerebellar ROIs for typically developing controls (black circles) and individuals with ASD (empty triangles). Error bars reflect mean ± 1 SD. * denotes $p < 0.05$.

TABLE 3 | Volume of vermal and white matter ROIs.

	Vermal lobules I-V	Vermal lobules VI-VII	Vermal lobules VIII-X	White matter
Controls	2.53 (0.30)	1.65 (0.20)	2.53 (0.32)	13.49 (1.41)
ASD	2.41 (0.33)	1.54 (0.18)	2.46 (0.31)	13.25 (1.25)

Values reported as M (SD); Volume is reported as cm^3.

saccade error for TD controls across 12° (β = −0.113, $p = 0.018$) and 24° (β = −0.239, $p < 0.001$), while increased volume was only related to saccade error for individuals with ASD at 12° (β = −0.077, $p = 0.038$) but not 24° (β = 0.011, $p = 0.758$).

The relationships between saccade error and volume of right lobule X also varied as a function of group and target step amplitude [group × amplitude × volume: $F_{(1,189)} = 6.285$, $p = 0.013$]. At 24° only, the increased volume of right lobule X was associated with lower saccade error for TD controls (β = −3.178, $p = 0.016$), while increased volume was not related to saccade error for individuals with ASD (β = −0.095, $p = 0.912$).

The relationships between saccade error and volume of vermal lobules I-V varied as a function of group and target step amplitude [group × amplitude × volume: $F_{(1,189)} = 6.298$, $p = 0.013$]. At 24° only, increased volume of vermal lobules I-V was associated with lower saccade error for TD controls (β = −0.641, $p = 0.026$), while increased volume was not related to saccade error for individuals with ASD (β = 0.252, $p = 0.255$).

Increased cerebellar white matter volume was associated with lower saccade error, though this relationship was at a trend level [$F_{(1,61)} = 2.799$, $p = 0.099$].

Cerebellar Associations With Saccade Error Variability

The relationships between saccade error variability and volumes of vermal lobules VI-VII varied as a function of group and target direction [group × direction × volume: $F_{(1,189)} = 4.111$, $p = 0.044$]. Greater volumes of vermal lobules VI-VII were associated with reduced *leftward* saccade error variability for TD controls (β = −0.137, $p = 0.609$) and individuals with ASD (β = −0.185, $p = 0.385$), while greater volume was associated with lower *rightward* saccade error variability for TD controls (β = −0.416, $p = 0.123$) but not individuals with ASD (β = 0.256, $p = 0.231$).

Exploratory analyses indicated that increased volume of right Crus II/lobule VIIB was associated with lower saccade error variability for TD controls (β = −0.043, $p = 0.017$) but not for individuals with ASD [β = 0.005, $p = 0.722$; group × volume: $F_{(1,60)} = 4.488$, $p = 0.038$].

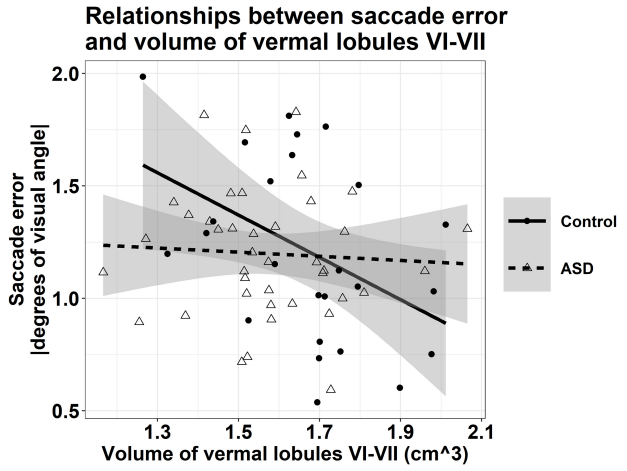

FIGURE 5 | Relationship between the volume of vermal lobules VI-VII and saccade error, averaged across target direction and amplitude. Greater volumes of vermal lobules VI-VII were associated with reduced saccade error in TD controls (r = –0.438, p = 0.007), but not individuals with ASD (r = –0.060, p = 0.671). Shaded regions reflect the 95% confidence interval of a group-level linear fit.

Increased right [$F_{(1,61)}$ = 5.647, p = 0.021] and left lobule VIII volumes [$F_{(1,61)}$ = 15.050, $p < 0.001$] were associated with lower saccade error variability.

The relationships between saccade error variability and volume of right lobule X varied as a function of group and target step amplitude [group × amplitude × volume: $F_{(1,187)}$ = 4.214, p = 0.041]. For TD controls, increased volume of right lobule X was associated with greater saccade error variability at 12° (β = 0.665, p = 0.380) but lower saccade error variability at 24° (β = −0.519, p = 0.493). For individuals with ASD, increased volume of right lobule X was associated with lower saccade error variability at 12° (β = −0.522, p = 0.294) but greater saccade error variability at 24° (β = 0.208, p = 0.675).

Increased volume of cerebellar white matter was associated with lower saccade error variability, though this relationship was at a trend level [$F_{(1,61)}$ = 3.965, p = 0.051].

Cerebellar Associations With Autism Spectrum Disorder Severity

Increased volumes of cerebellar white matter [**Figure 6A**; $F_{(1,42)}$ = 6.331, p = 0.016] and right lobule VIII [**Figure 6B**; $F_{(1,41)}$ = 6.044, p = 0.018] were associated with more severe clinically rated ASD symptoms (ADOS-CSS). Smaller volumes of right lobule X were associated with more severe ASD symptoms [**Figure 6C**; $F_{(1,41)}$ = 9.887, p = 0.003]. The relationship between right Crus II/lobule VIIB volume and ASD symptom severity varied across males and females with ASD; smaller volumes were associated with more severe ASD symptoms in males (β = −0.688, p = 0.033), but not females [**Figure 7A**; β = −0.023, p = 0.935; sex × volume: $F_{(1,40)}$ = 4.381, p = 0.043].

Increased volume of right lobule VI was associated with reduced clinically rated RRB severity as measured by the RBS-R [**Figure 6D**; $F_{(1,44)}$ = 5.484, p = 0.024]. The relationship between volume of right Crus I and severity of RRBs varied across males and females with ASD; increased volume of right Crus I was associated with reduced severity of RRBs in females (β = −6.488, p = 0.048), but not males [**Figure 7B**; β = −1.077, p = 0.675; sex × volume: $F_{(1,43)}$ = 4.210, p = 0.046].

DISCUSSION

We found that associations between cerebellar structure and sensorimotor behaviors vary across effector systems and are different in ASD and TD controls, suggesting atypical cerebellar development is associated with multiple sensorimotor difficulties in ASD. We also document differences in cerebellar volumes in individuals with ASD relative to TD controls which varied across subregions and between males and females. Specifically, we found that cerebellar volumetric reductions in ASD compared to TD controls were specific to vermal lobules VI-VII, consistent with prior studies (Stanfield et al., 2008; Crucitti et al., 2020). We also found that females with ASD showed reduced volumes of bilateral cerebellar Crus II/lobule VIIB relative to TD females, while TD males and males with ASD showed similar volumes, indicating females with ASD may show distinct patterns of neuropathology relative to males with ASD. We also show that volumes of cerebellar white matter and right lobules VI, VIII, and X each are associated with clinically rated ASD symptoms, suggesting that cerebellar structural differences may play a role in core features of the disorder(s). Last, we show that reduced volume of right Crus I was associated with more severe restricted and repetitive behaviors females only, while reduced volume of right Crus II was associated with greater ASD symptom severity in males only, suggesting that cerebellar correlates of clinical symptoms may be sex-specific.

Volumetrics of Discrete Cerebellar Subregions in Autism Spectrum Disorder

We found that individuals with ASD show reduced volume of vermal lobules VI-VII relative to TD controls, consistent with multiple prior studies and meta-analyses (Townsend et al., 1999; Kaufmann et al., 2003; Stanfield et al., 2008; Stoodley, 2014; Crucitti et al., 2020). Vermal lobules VI-VII ("oculomotor vermis") Purkinje cells innervate caudal fastigial nuclei cerebellar output to brainstem movement cells that initiate eye movements (Ohtsuka and Noda, 1992; Scudder et al., 2002). Ablation of oculomotor vermis in non-human primates increases saccade error and saccade error variability independent of damage to cerebellar nuclei, highlighting the role of oculomotor vermis in encoding amplitude information to maximize saccade accuracy (Takagi et al., 1998). Our findings converge with previous reports of reduced activation of oculomotor vermis and cerebellar hemispheres during visually guided saccades in ASD relative to TD controls to implicate abnormal structural development of oculomotor vermis in ASD (Takarae et al., 2007). Histopathological findings suggest that vermal hypoplasia in ASD may reflect perinatal loss of Purkinje cells postmigration (Whitney et al., 2009) or postnatal disruptions in granular cell migration (Courchesne et al., 1988)

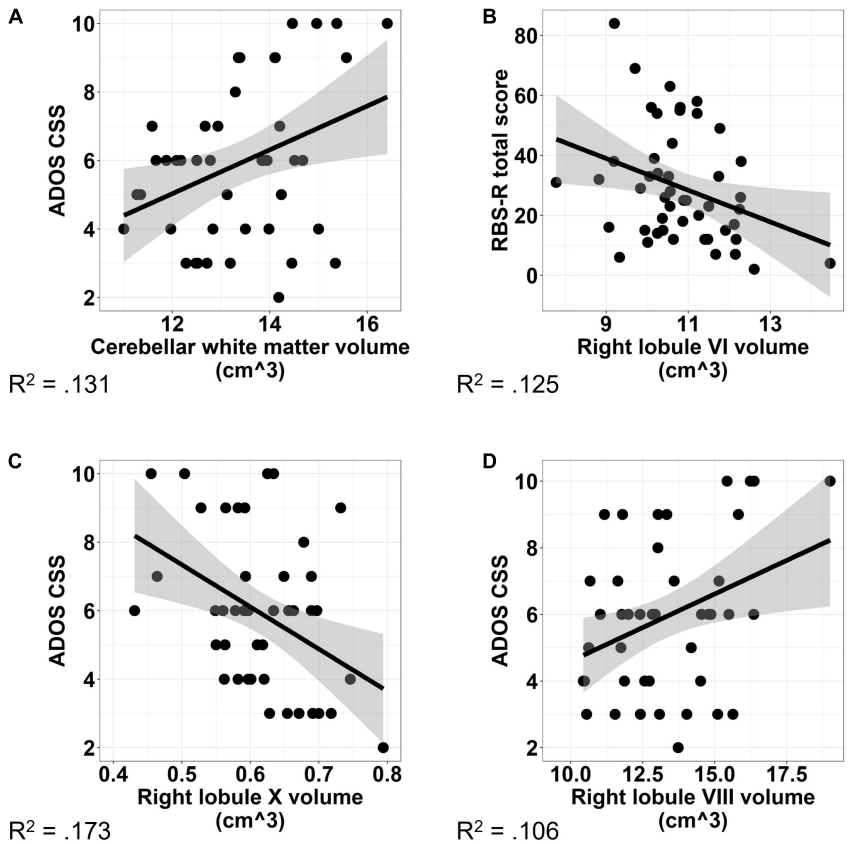

FIGURE 6 | Associations between cerebellar volume and ASD symptom severity. Increased volume of cerebellar white matter **(A)** and right lobule VIII **(B)** were associated with increased ASD symptom severity as measured using the ADOS-2 Calibrated Severity Score. Increased volume of right lobule X **(C)** was associated with reduced ASD symptom severity. Increased volume of right lobule VI **(D)** was associated with reduced severity of RRBs as measured using the Repetitive Behaviors Scale—Revised. The shaded region reflects the 95% confidence interval of a linear fit. R^2 values reflect the proportion of variance in clinical symptoms accounted for by the cerebellar volume in a one-term model. ADOS CSS, Autism Diagnostic Observation Schedule Calibrated Severity Score; RBS-R, Repetitive Behaviors Scale—Revised.

suggesting neurodevelopmental processes contributing to cerebellar pathology and risk of ASD begins early in ontogeny.

We also found that females with ASD show reduced volume of bilateral cerebellar Crus II/lobule VIIB relative to males with ASD and TD females. Reduced volume of cerebellar Crus II has been reported in school-aged children (8–13 years) with ASD across sexes (D'Mello et al., 2016), though studies of younger children (2–7 years) have indicated right Crus II volumes are selectively *increased* in females with ASD (Retico et al., 2016). While we did not examine group by sex by age interactions for structural outcomes due to the relatively small number of females with ASD at younger ages in our sample, these findings together implicate the early overgrowth of Crus II in female patients may be followed by a period of attenuated growth relative to TD during middle childhood and into adulthood. This neurodevelopmental pattern would be consistent with trajectories of total brain volumes in ASD that appear to be characterized by early overgrowth in the first years of life followed by slowed growth and reduced volumes in adulthood (Courchesne et al., 2011). Given the dense connectivity between Crus II and prefrontal cortex (PFC) *via* dentate nuclei and thalamus (O'Reilly et al., 2010; Stoodley et al., 2012), these results are also consistent with a prior study showing that early cortical overgrowth in ASD may be more severe in PFC networks (Carper et al., 2002).

Associations Between Cerebellar Structure and Sensorimotor Behaviors in Autism Spectrum Disorder

We replicate our prior findings that individuals with ASD show increased force variability during precision gripping (Mosconi et al., 2015a; Wang et al., 2015) and extend these results by demonstrating that increases in force variability are associated with increased bilateral Crus I and reduced cerebellar white matter volumes. Along with lobules V/VI, cerebellar Crus I shows selective involvement in the control of hand movements and increased activation during precision gripping (Vaillancourt et al., 2006; Neely et al., 2013). These prior results highlight functional gradients that cut across anatomically defined cerebellar subregions (Guell et al., 2018) but, combined with our results, these indicate structural variations associated

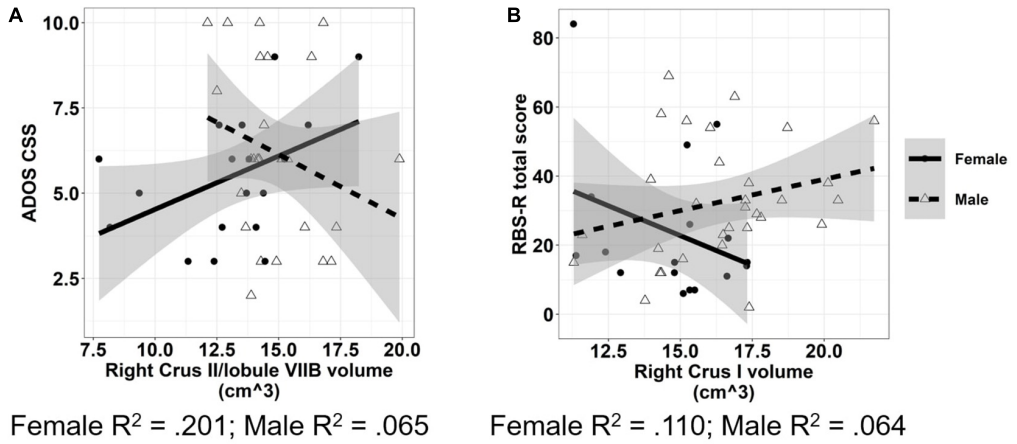

FIGURE 7 | Associations between cerebellar volumes and ASD symptom severity which vary across males and females. Increased volume of cerebellar right Crus II/lobule VIIB **(A)** was associated with reduced ASD symptom severity in males, but not females. Increased volume of cerebellar right Crus I **(B)** was associated with reduced severity of RRBs in females, but not males. The shaded region reflects the 95% confidence interval of a linear fit. R^2 values reflect the proportion of variance in clinical symptoms accounted for by cerebellar ROI volume in a one-term model. ADOS CSS, Autism Diagnostic Observation Schedule Calibrated Severity Score; RBS-R, Repetitive Behaviors Scale—Revised.

with atypical skeletomotor behavior in ASD are relatively circumscribed to posterior-lateral cerebellum. Innervation of Crus I from sensory cortices *via* pontine nuclei supports reactive adjustments of motor output translated to motor cortex through thalamus (Proville et al., 2014). Alterations of Crus I anatomy may disrupt the integration of sensory feedback during sustained motor actions as during our test of continuous precision grip force. Consistent with this hypothesis, we have found abnormal Crus I functional connectivity with visuomotor cortical targets, including posterior parietal and frontal/prefrontal cortices, associated with increased force variability in ASD during rest (Wang et al., 2019) and precision gripping (Lepping et al., 2021). Altered Crus I functional connectivity with medial PFC and inferior parietal cortex also appears to be strongly associated with separate clinical dimensions of ASD including both social-communication challenges and increased severity of repetitive behaviors as demonstrated by both patient and mouse genetic model studies (Stoodley et al., 2017; Tsai et al., 2018; Kelly et al., 2020). These results suggest a critical role of Crus I in the development of multiple clinical traits associated with ASD and implicate posterior-lateral cerebellar networks as strong candidates for targeted therapeutics aimed at improving sensorimotor and associated developmental outcomes.

Consistent with previously reported associations between increased cerebellar white matter and greater finger tapping speed and manual dexterity in TD (Koppelmans et al., 2015), our study indicates that white matter volume is associated with precision motor performance in ASD. Diffusion tensor imaging (DTI) studies of individuals with ASD have shown reduced microstructural integrity of cerebellar white matter, including increased mean diffusivity of middle cerebellar peduncles, the primary cortical-brainstem afferent pathway to cerebellum (Groen et al., 2011), and reduced fractional anisotropy and increased mean diffusivity of superior cerebellar peduncles, the primary efferent pathway to cerebral cortex from cerebellum (Catani et al., 2008; Sivaswamy et al., 2010). Our findings add to this literature by demonstrating that dysmaturation of cerebellar white matter is associated with reduced fine motor precision and suggest that intracerebellar structural connectivity alterations in ASD may contribute to difficulties with sensorimotor control.

Our finding that greater volumes of vermal lobules VI-VII were associated with reduced saccade error and rightward saccade error variability in TD controls is consistent with prior human and non-human primate studies demonstrating the selective involvement of posterior vermis in modulating the precision of saccadic eye movements (Vahedi et al., 1995; Takagi et al., 1998; Golla et al., 2008). In contrast, volumes of vermal lobules VI-VII were not associated with saccade accuracy in ASD, suggesting that cerebellar correlates of saccade amplitude precision are different in ASD. The limited association of volumes of vermal lobules VI-VII and oculomotor control in ASD may reflect increased involvement of separate cortical or subcortical systems in supporting eye movement precision in patients as suggested by a prior functional MRI study of saccades (Takarae et al., 2007). Specifically, studying visually guided saccades in adults with ASD, Takarae et al. (2007) showed reduced activation of cerebellar vermis and hemispheres in ASD relative to TD controls, but increased activation of the dorsolateral PFC, caudate, thalamus, and the anterior cingulate cortex in patients suggesting frontostriatal networks may compensate for atypical function in cerebellar motor systems in ASD. Combined with our findings of reduced volume of vermal lobules VI-VII in ASD and similar oculomotor performance across ASD and TD, as well as evidence that alterations in posterior vermis likely emerge early in neurodevelopment in ASD (Courchesne et al., 1988; Whitney et al., 2009; Crucitti et al., 2020), these prior functional MRI findings combine with our structural MRI-sensorimotor results to suggest reorganization of cortical and subcortical systems in ASD may compensate for early emerging pathology of the oculomotor vermis in ASD to support the control of saccadic eye movements. It is also possible that the differential associations

between volumes of oculomotor vermis and saccade precision in ASD and TD reflect unique features of our ASD sample. Specifically, we did not see oculomotor differences in our ASD sample, in contrast to multiple prior studies from our group and others (Takarae et al., 2004; Luna et al., 2007; Johnson et al., 2012; Schmitt et al., 2014; Unruh et al., 2021). These differences may reflect a limited range of cognitive abilities in our sample that only included individuals who could complete both eye movement and MRI procedures. Differences in saccade accuracy may also vary across other demographic or clinical characteristics; for example, we studied a greater proportion of females with ASD relative to previous studies (Johnson et al., 2012; Unruh et al., 2021).

Associations With Clinical Symptoms

Our findings of associations between clinically rated ASD symptom severity and volumes of multiple cerebellar subregions, including right cerebellar lobules VI, VIII, and X, as well as cerebellar white matter are consistent with the known role of cerebellum in the modulation of cognitive and social-communicative functions (Schmahmann et al., 2007). Through reciprocal cerebellar-cortical circuits, the cerebellum serves to modify skilled sensorimotor actions (Stein and Glickstein, 1992), emotional expression (Aarsen et al., 2004), and social behaviors (Kelly et al., 2020) affected in ASD. Differences across these areas may reflect difficulties integrating cortical feedback with internal models and prior expectations to refine output. As multiple networks (e.g., cognitive control, default mode network, and sensorimotor) are represented within individual cerebellar lobules (Buckner et al., 2011; Guell et al., 2018), even circumscribed cerebellar pathology may have downstream effects on the developing brain by impacting multiple cortical networks and developmental abilities (for review, see Stoodley and Limperopoulos, 2016). Our findings highlight a key relationship between cerebellar structural integrity and neurodevelopmental outcomes while adding to a growing body of literature documenting associations between cerebellar anatomy and core features of ASD (Rojas et al., 2006; Riva et al., 2013; D'Mello et al., 2015). Further, and consistent with previous studies, we also demonstrate that associations between cerebellar structure and core ASD symptoms may vary across males and females (Supekar and Menon, 2015), implicating sex-specific clinical correlates of cerebellar pathology.

Limitations and Future Directions

Our study has several limitations that should be addressed in future studies. First, inclusion of a greater number of females will be important given sex-specific patterns of cerebellar development in TD (Tiemeier et al., 2010) and our findings that sensorimotor and clinical associations vary as a function of sex in ASD. Second, while we examined the functional correlates of cerebellar structural variation across a relatively wide age range, longitudinal studies are needed to clarify the patterns of cerebellar subregions over development and their associations with sensorimotor and clinical outcomes. Previous research suggests cerebellar volumetric differences and their association with clinical symptoms vary across development in ASD (D'Mello et al., 2016; Retico et al., 2016). For example, while vermal hypoplasia is present early in development and persists into adolescence in ASD, associations with clinical symptoms appear to be more readily detectable in older children (Webb et al., 2009; Riva et al., 2013; D'Mello et al., 2015). While we did not examine age-associated variations in brain-behavior associations due to our limited power to detect higher order age-associated interactions, the mean age of participants in our sample was in adolescence and therefore may have amplified associations between the structural variation and clinical symptoms.

Conclusion

Studying relationships between multiple cerebellar subregions and both skeletomotor and oculomotor behavior in individuals with ASD, we found that increased force variability is associated with increased volume of bilateral Crus I, whereas reduced saccade error is associated with increased volume of vermal lobules VI/VII in TD controls but not individuals with ASD. These findings suggest associations between sensorimotor behavior and cerebellar structure vary across subregions and effector systems in ASD. We also document associations between core clinical symptoms of ASD and volumes of multiple cerebellar subregions, several of which are sex-specific, suggesting that cerebellar pathology may have wide ranging impacts on development in ASD that need to be understood in the context of significant heterogeneity across the autism spectrum.

DATA AVAILABILITY STATEMENT

The raw behavioral data supporting the conclusions of this manuscript will be made available by the authors, without undue reservation, to any qualified researcher. Structural MRI and clinical data are publicly available through the National Database for Autism Research (NDAR; https://nda.nih.gov/edit_collection.html?id=2711).

ETHICS STATEMENT

This study was carried out in accordance with the recommendations of the University of Kansas Medical Center Institutional Review Board with written informed consent from all subjects. Caregivers of minor participants gave written informed consent, minor participants gave written assent, and adult participants gave written informed consent in accordance with the Declaration of Helsinki.

AUTHOR CONTRIBUTIONS

MM was responsible for the conception and design of the study. WM and SK performed the clinical evaluations under the supervision of MM. WM and SK collected the behavioral and MRI data and scored the raw data. WM, SK, and MM performed the statistical analyses. WM, SK, KU, RS, JS, MS, and MM drafted and edited the manuscript. All authors interpreted the results and approved the final version of the manuscript.

FUNDING

This study was funded by R01 MH112734 (PI: MM), F31 MH126572 (PI: WM), and U54 HD090216 (PI: Colombo).

ACKNOWLEDGMENTS

We would like to thank the participants for their time and effort in participating in the study. We would also like to thank Dr. Kandace Fleming at the Life Span Institute, University of Kansas for her assistance and consultation in the construction of the statistical models, Ms. Shelby Parmer at the University of Kansas for her assistance in the review of structural MRI data, Ms. Erin Bojanek at the University of Kansas for her assistance in the scoring of the raw behavioral data, and Dr. Zheng Wang at the University of Florida for her assistance in the writing of the MATLAB scoring programs for the data analyses.

REFERENCES

Aarsen, F. K., Van Dongen, H. R., Paquier, P. F., Van Mourik, M., and Catsman-Berrevoets, C. E. (2004). Long-term sequelae in children after cerebellar astrocytoma surgery. *Neurology* 62, 1311–1316. doi: 10.1212/01.wnl.0000120549.77188.36

Allen, G., Muller, R. A., and Courchesne, E. (2004). Cerebellar function in autism: functional magnetic resonance image activation during a simple motor task. *Biol. Psychiatry* 56, 269–278. doi: 10.1016/j.biopsych.2004.06.005

American Psychiatric Association [APA] (2013). *Diagnostic and Statistical Manual of Mental Disorders*. Washington, DC: APA.

Bastian, A. J. (2006). Learning to predict the future: the cerebellum adapts feedforward movement control. *Curr. Opin. Neurobiol.* 16, 645–649. doi: 10.1016/j.conb.2006.08.016

Bates, D., Machler, M., Bolker, B. M., and Walker, S. C. (2015). Fitting linear mixed-effects models using lme4. *J. Stat. Softw.* 67, 1–48.

Bodfish, J. W., Symons, F. J., Parker, D. E., and Lewis, M. H. (2000). Varieties of repetitive behavior in autism: comparisons to mental retardation. *J. Autism Dev. Disord.* 30, 237–243. doi: 10.1023/a:1005596502855

Bonzano, L., Palmaro, E., Teodorescu, R., Fleysher, L., Inglese, M., and Bove, M. (2015). Functional connectivity in the resting-state motor networks influences the kinematic processes during motor sequence learning. *Eur. J. Neurosci.* 41, 243–253. doi: 10.1111/ejn.12755

Brochier, T., Boudreau, M. J., Pare, M., and Smith, A. M. (1999). The effects of muscimol inactivation of small regions of motor and somatosensory cortex on independent finger movements and force control in the precision grip. *Exp. Brain Res.* 128, 31–40. doi: 10.1007/s002210050814

Buckner, R. L., Krienen, F. M., Castellanos, A., Diaz, J. C., and Yeo, B. T. (2011). The organization of the human cerebellum estimated by intrinsic functional connectivity. *J. Neurophysiol.* 106, 2322–2345. doi: 10.1152/jn.00339.2011

Carass, A., Cuzzocreo, J. L., Han, S., Hernandez-Castillo, C. R., Rasser, P. E., Ganz, M., et al. (2018). Comparing fully automated state-of-the-art cerebellum parcellation from magnetic resonance images. *Neuroimage* 183, 150–172. doi: 10.1016/j.neuroimage.2018.08.003

Carper, R. A., Moses, P., Tigue, Z. D., and Courchesne, E. (2002). Cerebral lobes in autism: early hyperplasia and abnormal age effects. *Neuroimage* 16, 1038–1051. doi: 10.1006/nimg.2002.1099

Catani, M., Jones, D. K., Daly, E., Embiricos, N., Deeley, Q., Pugliese, L., et al. (2008). Altered cerebellar feedback projections in Asperger syndrome. *Neuroimage* 41, 1184–1191. doi: 10.1016/j.neuroimage.2008.03.041

Courchesne, E., Campbell, K., and Solso, S. (2011). Brain growth across the life span in autism: age-specific changes in anatomical pathology. *Brain Res.* 1380, 138–145. doi: 10.1016/j.brainres.2010.09.101

Courchesne, E., Karns, C. M., Davis, H. R., Ziccardi, R., Carper, R. A., Tigue, Z. D., et al. (2001). Unusual brain growth patterns in early life in patients with autistic disorder: an MRI study. *Neurology* 57, 245–254. doi: 10.1212/wnl.57.2.245

Courchesne, E., Yeung-Courchesne, R., Press, G. A., Hesselink, J. R., and Jernigan, T. L. (1988). Hypoplasia of cerebellar vermal lobules VI and VII in autism. *N. Engl. J. Med.* 318, 1349–1354. doi: 10.1056/NEJM198805263182102

Crucitti, J., Hyde, C., Enticott, P. G., and Stokes, M. A. (2020). Are vermal lobules VI-VII smaller in autism spectrum disorder? *Cerebellum* 19, 617–628. doi: 10.1007/s12311-020-01143-5

D'Mello, A. M., Crocetti, D., Mostofsky, S. H., and Stoodley, C. J. (2015). Cerebellar gray matter and lobular volumes correlate with core autism symptoms. *Neuroimage Clin.* 7, 631–639. doi: 10.1016/j.nicl.2015.02.007

D'Mello, A. M., Moore, D. M., Crocetti, D., Mostofsky, S. H., and Stoodley, C. J. (2016). Cerebellar gray matter differentiates children with early language delay in autism. *Autism Res.* 9, 1191–1204. doi: 10.1002/aur.1622

de Jong, L. W., Vidal, J. S., Forsberg, L. E., Zijdenbos, A. P., Haight, T., Alzheimer's Disease Neuroimaging Initiative, et al. (2017). Allometric scaling of brain regions to intra-cranial volume: an epidemiological MRI study. *Hum. Brain Mapp.* 38, 151–164. doi: 10.1002/hbm.23351

DeRamus, T. P., and Kana, R. K. (2015). Anatomical likelihood estimation meta-analysis of grey and white matter anomalies in autism spectrum disorders. *Neuroimage Clin.* 7, 525–536. doi: 10.1016/j.nicl.2014.11.004

Dewey, D., Cantell, M., and Crawford, S. G. (2007). Motor and gestural performance in children with autism spectrum disorders, developmental coordination disorder, and/or attention deficit hyperactivity disorder. *J. Int. Neuropsychol. Soc.* 13, 246–256. doi: 10.1017/S1355617707070270

Duerden, E. G., Mak-Fan, K. M., Taylor, M. J., and Roberts, S. W. (2012). Regional differences in grey and white matter in children and adults with autism spectrum disorders: an activation likelihood estimate (ALE) meta-analysis. *Autism Res.* 5, 49–66. doi: 10.1002/aur.235

Fatemi, S. H., Aldinger, K. A., Ashwood, P., Bauman, M. L., Blaha, C. D., Blatt, G. J., et al. (2012). Consensus paper: pathological role of the cerebellum in autism. *Cerebellum* 11, 777–807. doi: 10.1007/s12311-012-0355-9

Fonov, V., Evans, A. C., Botteron, K., Almli, C. R., McKinstry, R. C., and Collins, D. L. (2011). Unbiased average age-appropriate atlases for pediatric studies. *Neuroimage* 54, 313–327. doi: 10.1016/j.neuroimage.2010.07.033

Glazebrook, C. M., Elliott, D., and Lyons, J. (2006). A kinematic analysis of how young adults with and without autism plan and control goal-directed movements. *Motor Control* 10, 244–264. doi: 10.1123/mcj.10.3.244

Glickstein, M. (2000). How are visual areas of the brain connected to motor areas for the sensory guidance of movement? *Trends Neurosci.* 23, 613–617. doi: 10.1016/s0166-2236(00)01681-7

Golla, H., Tziridis, K., Haarmeier, T., Catz, N., Barash, S., and Thier, P. (2008). Reduced saccadic resilience and impaired saccadic adaptation due to cerebellar disease. *Eur. J. Neurosci.* 27, 132–144. doi: 10.1111/j.1460-9568.2007.05996.x

Green, D., Charman, T., Pickles, A., Chandler, S., Loucas, T., Simonoff, E., et al. (2009). Impairment in movement skills of children with autistic spectrum disorders. *Dev. Med. Child Neurol.* 51, 311–316. doi: 10.1111/j.1469-8749.2008.03242.x

Groen, W. B., Buitelaar, J. K., van der Gaag, R. J., and Zwiers, M. P. (2011). Pervasive microstructural abnormalities in autism: a DTI study. *J. Psychiatry Neurosci.* 36, 32–40. doi: 10.1503/jpn.090100

Guell, X., Schmahmann, J. D., Gabrieli, J., and Ghosh, S. S. (2018). Functional gradients of the cerebellum. *Elife* 7:e36652. doi: 10.7554/eLife.36652

Han, S., Carass, A., He, Y., and Prince, J. L. (2020). Automatic cerebellum anatomical parcellation using U-Net with locally constrained optimization. *Neuroimage* 218:116819. doi: 10.1016/j.neuroimage.2020.116819

Hilber, P., Jouen, F., Delhaye-Bouchaud, N., Mariani, J., and Caston, J. (1998). Differential roles of cerebellar cortex and deep cerebellar nuclei in learning and retention of a spatial task: studies in intact and cerebellectomized lurcher mutant mice. *Behav. Genet.* 28, 299–308. doi: 10.1023/a:1021675514883

Ito, M. (2008). Opinion - Control of mental activities by internal models in the cerebellum. *Nat. Rev. Neurosci.* 9, 304–313. doi: 10.1038/nrn2332

Iverson, J. M., Shic, F., Wall, C. A., Chawarska, K., Curtin, S., Estes, A., et al. (2019). Early motor abilities in infants at heightened versus low risk for ASD: a baby siblings research consortium (BSRC) study. *J. Abnorm. Psychol.* 128, 69–80. doi: 10.1037/abn0000390

Johnson, B., Rinehart, N., Papadopoulos, N., Tonge, B., Millist, L., White, O., et al. (2012). A closer look at visually guided saccades in autism and Asperger's disorder. *Front. Integr. Neurosci.* 6:99. doi: 10.3389/fnint.2012.00099

Kaufmann, W. E., Cooper, K. L., Mostofsky, S. H., Capone, G. T., Kates, W. R., Newschaffer, C. J., et al. (2003). Specificity of cerebellar vermian abnormalities in autism: a quantitative magnetic resonance imaging study. *J. Child Neurol.* 18, 463–470. doi: 10.1177/08830738030180070501

Kelly, E., Meng, F., Fujita, H., Morgado, F., Kazemi, Y., Rice, L. C., et al. (2020). Regulation of autism-relevant behaviors by cerebellar-prefrontal cortical circuits. *Nat. Neurosci.* 23, 1102–1110. doi: 10.1038/s41593-020-0665-z

Kelly, R. M., and Strick, P. L. (2003). Cerebellar loops with motor cortex and prefrontal cortex of a nonhuman primate. *J. Neurosci.* 23, 8432–8444. doi: 10.1523/JNEUROSCI.23-23-08432.2003

Koppelmans, V., Hirsiger, S., Mérillat, S., Jäncke, L., and Seidler, R. D. (2015). Cerebellar gray and white matter volume and their relation with age and manual motor performance in healthy older adults. *Hum. Brain Mapp.* 36, 2352–2363. doi: 10.1002/hbm.22775

Kuper, M., Wunnemann, M. J., Thurling, M., Stefanescu, R. M., Maderwald, S., Elles, H. G., et al. (2014). Activation of the cerebellar cortex and the dentate nucleus in a prism adaptation fMRI study. *Hum. Brain Mapp.* 35, 1574–1586. doi: 10.1002/hbm.22274

Lam, K. S., and Aman, M. G. (2007). The repetitive behavior scale-revised: independent validation in individuals with autism spectrum disorders. *J. Autism Dev. Disord.* 37, 855–866. doi: 10.1007/s10803-006-0213-z

Lange, N., Travers, B. G., Bigler, E. D., Prigge, M. B., Froehlich, A. L., Nielsen, J. A., et al. (2015). Longitudinal volumetric brain changes in autism spectrum disorder ages 6-35 years. *Autism Res.* 8, 82–93. doi: 10.1002/aur.1427

LeBarton, E. S., and Iverson, J. M. (2016). Associations between gross motor and communicative development in at-risk infants. *Infant Behav. Dev.* 44, 59–67. doi: 10.1016/j.infbeh.2016.05.003

Lepping, R. J., McKinney, W. S., Magnon, G. C., Keedy, S. K., Wang, Z., Coombes, S. A., et al. (2021). Visuomotor brain network activation and functional connectivity among individuals with autism spectrum disorder. *Hum. Brain Mapp.* n/a(n/a), doi: 10.1002/hbm.25692

Lin, C. W., Lin, H. Y., Lo, Y. C., Chen, Y. J., Hsu, Y. C., Chen, Y. L., et al. (2019). Alterations in white matter microstructure and regional volume are related to motor functions in boys with autism spectrum disorder. *Prog. Neuropsychopharmacol. Biol. Psychiatry* 90, 76–83. doi: 10.1016/j.pnpbp.2018.11.008

Long, J. A. (2019). Interactions: Comprehensive, User-Friendly Toolkit for Probing Interactions" R Package Version 1.1.0.

Lord, C., Rutter, M., and Le Couteur, A. (1994). Autism diagnostic interview-revised: a revised version of a diagnostic interview for caregivers of individuals with possible pervasive developmental disorders. *J. Autism Dev. Disord.* 24, 659–685. doi: 10.1007/BF02172145

Lord, C., Rutter, M., DiLavore, P., Risi, S., Gotham, K., and Bishop, S. (2012). *Autism Diagnostic Observation Schedule (ADOS-2): Modules 1-4*. Los Angeles, CA: Western Psychological Services.

Luna, B., Doll, S. K., Hegedus, S. J., Minshew, N. J., and Sweeney, J. A. (2007). Maturation of executive function in autism. *Biol. Psychiatry* 61, 474–481. doi: 10.1016/j.biopsych.2006.02.030

Mahajan, R., Dirlikov, B., Crocetti, D., and Mostofsky, S. H. (2016). Motor circuit anatomy in children with autism spectrum disorder with or without attention deficit hyperactivity disorder. *Autism Res.* 9, 67–81. doi: 10.1002/aur.1497

Marko, M. K., Crocetti, D., Hulst, T., Donchin, O., Shadmehr, R., and Mostofsky, S. H. (2015). Behavioural and neural basis of anomalous motor learning in children with autism. *Brain* 138(Pt. 3), 784–797. doi: 10.1093/brain/awu394

Matuschek, H., Kliegl, R., Vasishth, S., Baayen, H., and Bates, D. (2017). Balancing Type I error and power in linear mixed models. *J. Mem. Lang.* 94, 305–315. doi: 10.1016/j.jml.2017.01.001

Molinari, M., Leggio, M. G., Solida, A., Ciorra, R., Misciagna, S., Silveri, M. C., et al. (1997). Cerebellum and procedural learning: evidence from focal cerebellar lesions. *Brain* 120(Pt. 10), 1753–1762. doi: 10.1093/brain/120.10.1753

Mosconi, M. W., Kay, M., D'Cruz, A. M., Guter, S., Kapur, K., Macmillan, C., et al. (2010). Neurobehavioral abnormalities in first-degree relatives of individuals with autism. *Arch. Gen. Psychiatry* 67, 830–840. doi: 10.1001/archgenpsychiatry.2010.87

Mosconi, M. W., Mohanty, S., Greene, R. K., Cook, E. H., Vaillancourt, D. E., and Sweeney, J. A. (2015a). Feedforward and feedback motor control abnormalities implicate cerebellar dysfunctions in autism spectrum disorder. *J. Neurosci.* 35, 2015–2025. doi: 10.1523/JNEUROSCI.2731-14.2015

Mosconi, M. W., Wang, Z., Schmitt, L. M., Tsai, P., and Sweeney, J. A. (2015b). The role of cerebellar circuitry alterations in the pathophysiology of autism spectrum disorders. *Front. Neurosci.* 9:296. doi: 10.3389/fnins.2015.00296

Mostofsky, S. H., Burgess, M. P., and Gidley Larson, J. C. (2007). Increased motor cortex white matter volume predicts motor impairment in autism. *Brain* 130(Pt. 8), 2117–2122. doi: 10.1093/brain/awm129

Mous, S. E., Jiang, A., Agrawal, A., and Constantino, J. N. (2017). Attention and motor deficits index non-specific background liabilities that predict autism recurrence in siblings. *J. Neurodev. Disord.* 9:32. doi: 10.1186/s11689-017-9212-y

Murray, G. K., Veijola, J., Moilanen, K., Miettunen, J., Glahn, D. C., Cannon, T. D., et al. (2006). Infant motor development is associated with adult cognitive categorisation in a longitudinal birth cohort study. *J. Child Psychol. Psychiatry* 47, 25–29. doi: 10.1111/j.1469-7610.2005.01450.x

Neely, K. A., Coombes, S. A., Planetta, P. J., and Vaillancourt, D. E. (2013). Segregated and overlapping neural circuits exist for the production of static and dynamic precision grip force. *Hum. Brain Mapp.* 34, 698–712. doi: 10.1002/hbm.21467

Nickl-Jockschat, T., Habel, U., Michel, T. M., Manning, J., Laird, A. R., Fox, P. T., et al. (2012). Brain structure anomalies in autism spectrum disorder–a meta-analysis of VBM studies using anatomic likelihood estimation. *Hum. Brain Mapp.* 33, 1470–1489. doi: 10.1002/hbm.21299

O'Reilly, J. X., Beckmann, C. F., Tomassini, V., Ramnani, N., and Johansen-Berg, H. (2010). Distinct and overlapping functional zones in the cerebellum defined by resting state functional connectivity. *Cereb. Cortex* 20, 953–965. doi: 10.1093/cercor/bhp157

Ohtsuka, K., and Noda, H. (1992). Burst discharges of mossy fibers in the oculomotor vermis of macaque monkeys during saccadic eye movements. *Neurosci. Res.* 15, 102–114. doi: 10.1016/0168-0102(92)90023-6

Proville, R. D., Spolidoro, M., Guyon, N., Dugue, G. P., Selimi, F., Isope, P., et al. (2014). Cerebellum involvement in cortical sensorimotor circuits for the control of voluntary movements. *Nat. Neurosci.* 17, 1233–1239. doi: 10.1038/nn.3773

Reilly, J. L., Lencer, R., Bishop, J. R., Keedy, S., and Sweeney, J. A. (2008). Pharmacological treatment effects on eye movement control. *Brain Cogn.* 68, 415–435. doi: 10.1016/j.bandc.2008.08.026

Retico, A., Giuliano, A., Tancredi, R., Cosenza, A., Apicella, F., Narzisi, A., et al. (2016). The effect of gender on the neuroanatomy of children with autism spectrum disorders: a support vector machine case-control study. *Mol. Autism* 7:5. doi: 10.1186/s13229-015-0067-3

Riva, D., Annunziata, S., Contarino, V., Erbetta, A., Aquino, D., and Bulgheroni, S. (2013). Gray matter reduction in the vermis and CRUS-II is associated with social and interaction deficits in low-functioning children with autistic spectrum disorders: a VBM-DARTEL Study. *Cerebellum* 12, 676–685. doi: 10.1007/s12311-013-0469-8

Roberts, R. E., Bain, P. G., Day, B. L., and Husain, M. (2013). Individual differences in expert motor coordination associated with white matter microstructure in the cerebellum. *Cereb. Cortex* 23, 2282–2292. doi: 10.1093/cercor/bhs219

Rojas, D. C., Peterson, E., Winterrowd, E., Reite, M. L., Rogers, S. J., and Tregellas, J. R. (2006). Regional gray matter volumetric changes in autism associated with social and repetitive behavior symptoms. *BMC Psychiatry* 6:56. doi: 10.1186/1471-244x-6-56

Salmi, J., Pallesen, K. J., Neuvonen, T., Brattico, E., Korvenoja, A., Salonen, O., et al. (2010). Cognitive and motor loops of the human cerebro-cerebellar system. *J. Cogn. Neurosci.* 22, 2663–2676. doi: 10.1162/jocn.2009.21382

Schmahmann, J. D., Weilburg, J. B., and Sherman, J. C. (2007). The neuropsychiatry of the cerebellum - insights from the clinic. *Cerebellum* 6, 254–267. doi: 10.1080/14734220701490995

Schmitt, L. M., Cook, E. H., Sweeney, J. A., and Mosconi, M. W. (2014). Saccadic eye movement abnormalities in autism spectrum disorder indicate dysfunctions in cerebellum and brainstem. *Mol. Autism* 5:47. doi: 10.1186/2040-2392-5-47

Scott, J. A., Schumann, C. M., Goodlin-Jones, B. L., and Amaral, D. G. (2009). A comprehensive volumetric analysis of the cerebellum in children and adolescents with autism spectrum disorder. *Autism Res.* 2, 246–257. doi: 10.1002/aur.97

Scudder, C. A., Kaneko, C. S., and Fuchs, A. F. (2002). The brainstem burst generator for saccadic eye movements: a modern synthesis. *Exp. Brain Res.* 142, 439–462. doi: 10.1007/s00221-001-0912-9

Shadmehr, R., and Krakauer, J. W. (2008). A computational neuroanatomy for motor control. *Exp. Brain Res.* 185, 359–381. doi: 10.1007/s00221-008-1280-5

Sivaswamy, L., Kumar, A., Rajan, D., Behen, M., Muzik, O., Chugani, D., et al. (2010). A diffusion tensor imaging study of the cerebellar pathways in children with autism spectrum disorder. *J. Child Neurol.* 25, 1223–1231. doi: 10.1177/0883073809358765

Smith, A. M., Bourbonnais, D., and Blanchette, G. (1981). Interaction between forced grasping and a learned precision grip after ablation of the supplementary motor area. *Brain Res.* 222, 395–400. doi: 10.1016/0006-8993(81)91043-X

Stanfield, A. C., McIntosh, A. M., Spencer, M. D., Philip, R., Gaur, S., and Lawrie, S. M. (2008). Towards a neuroanatomy of autism: a systematic review and meta-analysis of structural magnetic resonance imaging studies. *Eur. Psychiatry* 23, 289–299. doi: 10.1016/j.eurpsy.2007.05.006

Stanley-Cary, C., Rinehart, N., Tonge, B., White, O., and Fielding, J. (2011). Greater disruption to control of voluntary saccades in autistic disorder than Asperger's disorder: evidence for greater cerebellar involvement in autism? *Cerebellum* 10, 70–80. doi: 10.1007/s12311-010-0229-y

Steele, C. J., and Penhune, V. B. (2010). Specific increases within global decreases: a functional magnetic resonance imaging investigation of five days of motor sequence learning. *J. Neurosci.* 30, 8332–8341. doi: 10.1523/JNEUROSCI.5569-09.2010

Stein, J. F. (1986). Role of the cerebellum in the visual guidance of movement. *Nature* 323, 217–221. doi: 10.1038/323217a0

Stein, J. F., and Glickstein, M. (1992). Role of the cerebellum in visual guidance of movement. *Physiol. Rev.* 72, 967–1017. doi: 10.1152/physrev.1992.72.4.967

Stoodley, C. J. (2014). Distinct regions of the cerebellum show gray matter decreases in autism, ADHD, and developmental dyslexia. *Front. Syst. Neurosci.* 8:92. doi: 10.3389/fnsys.2014.00092

Stoodley, C. J., and Limperopoulos, C. (2016). Structure-function relationships in the developing cerebellum: evidence from early-life cerebellar injury and neurodevelopmental disorders. *Semin. Fetal Neonatal Med.* 21, 356–364. doi: 10.1016/j.siny.2016.04.010

Stoodley, C. J., and Schmahmann, J. D. (2009). Functional topography in the human cerebellum: a meta-analysis of neuroimaging studies. *Neuroimage* 44, 489–501. doi: 10.1016/j.neuroimage.2008.08.039

Stoodley, C. J., D'Mello, A. M., Ellegood, J., Jakkamsetti, V., Liu, P., Nebel, M. B., et al. (2017). Altered cerebellar connectivity in autism and cerebellar-mediated rescue of autism-related behaviors in mice. *Nat. Neurosci.* 20, 1744–1751. doi: 10.1038/s41593-017-0004-1

Stoodley, C. J., Valera, E. M., and Schmahmann, J. D. (2012). Functional topography of the cerebellum for motor and cognitive tasks: an fMRI study. *Neuroimage* 59, 1560–1570. doi: 10.1016/j.neuroimage.2011.08.065

Supekar, K., and Menon, V. (2015). Sex differences in structural organization of motor systems and their dissociable links with repetitive/restricted behaviors in children with autism. *Mol. Autism* 6:50. doi: 10.1186/s13229-015-0042-z

Takagi, M., Zee, D. S., and Tamargo, R. J. (1998). Effects of lesions of the oculomotor vermis on eye movements in primate: saccades. *J. Neurophysiol.* 80, 1911–1931. doi: 10.1152/jn.1998.80.4.1911

Takarae, Y., Minshew, N. J., Luna, B., and Sweeney, J. A. (2004). Oculomotor abnormalities parallel cerebellar histopathology in autism. *J. Neurol. Neurosurg. Psychiatry* 75, 1359–1361. doi: 10.1136/jnnp.2003.022491

Takarae, Y., Minshew, N. J., Luna, B., and Sweeney, J. A. (2007). Atypical involvement of frontostriatal systems during sensorimotor control in autism. *Psychiatry Res.* 156, 117–127. doi: 10.1016/j.pscychresns.2007.03.008

Tiemeier, H., Lenroot, R. K., Greenstein, D. K., Tran, L., Pierson, R., and Giedd, J. N. (2010). Cerebellum development during childhood and adolescence: a longitudinal morphometric MRI study. *Neuroimage* 49, 63–70. doi: 10.1016/j.neuroimage.2009.08.016

Townsend, J., Courchesne, E., Covington, J., Westerfield, M., Harris, N. S., Lyden, P., et al. (1999). Spatial attention deficits in patients with acquired or developmental cerebellar abnormality. *J. Neurosci.* 19, 5632–5643. doi: 10.1523/JNEUROSCI.19-13-05632.1999

Travers, B. G., Bigler, E. D., Duffield, T. C., Prigge, M. D. B., Froehlich, A. L., Lange, N., et al. (2017). Longitudinal development of manual motor ability in autism spectrum disorder from childhood to mid-adulthood relates to adaptive daily living skills. *Dev Sci* 20, 10.1111/desc.12401. doi: 10.1111/desc.12401

Tsai, P. T., Rudolph, S., Guo, C., Ellegood, J., Gibson, J. M., Schaeffer, S. M., et al. (2018). Sensitive periods for cerebellar-mediated autistic-like behaviors. *Cell Rep.* 25, 357–367.e4. doi: 10.1016/j.celrep.2018.09.039

Tustison, N. J., Avants, B. B., Cook, P. A., Zheng, Y., Egan, A., Yushkevich, P. A., et al. (2010). N4ITK: improved N3 bias correction. *IEEE Trans. Med. Imaging* 29, 1310–1320. doi: 10.1109/TMI.2010.2046908

Unruh, K. E., Martin, L. E., Magnon, G., Vaillancourt, D. E., Sweeney, J. A., and Mosconi, M. W. (2019). Cortical and subcortical alterations associated with precision visuomotor behavior in individuals with autism spectrum disorder. *J. Neurophysiol.* 122, 1330–1341. doi: 10.1152/jn.00286.2019

Unruh, K. E., McKinney, W. S., Bojanek, E. K., Fleming, K. K., Sweeney, J. A., and Mosconi, M. W. (2021). Initial action output and feedback-guided motor behaviors in autism spectrum disorder. *Mol. Autism* 12:52. doi: 10.1186/s13229-021-00452-8

Vahedi, K., Rivaud, S., Amarenco, P., and Pierrot-Deseilligny, C. (1995). Horizontal eye movement disorders after posterior vermis infarctions. *J. Neurol. Neurosurg. Psychiatry* 58, 91–94. doi: 10.1136/jnnp.58.1.91

Vaillancourt, D. E., Mayka, M. A., and Corcos, D. M. (2006). Intermittent visuomotor processing in the human cerebellum, parietal cortex, and premotor cortex. *J. Neurophysiol.* 95, 922–931. doi: 10.1152/jn.00718.2005

Wang, Z., Magnon, G. C., White, S. P., Greene, R. K., Vaillancourt, D. E., and Mosconi, M. W. (2015). Individuals with autism spectrum disorder show abnormalities during initial and subsequent phases of precision gripping. *J. Neurophysiol.* 113, 1989–2001. doi: 10.1152/jn.00661.2014

Wang, Z., Wang, Y., Sweeney, J. A., Gong, Q., Lui, S., and Mosconi, M. W. (2019). Resting-state brain network dysfunctions associated with visuomotor impairments in autism spectrum disorder. *Front. Integr. Neurosci.* 13:17. doi: 10.3389/fnint.2019.00017

Webb, S. J., Sparks, B. F., Friedman, S. D., Shaw, D. W., Giedd, J., Dawson, G., et al. (2009). Cerebellar vermal volumes and behavioral correlates in children with autism spectrum disorder. *Psychiatry Res.* 172, 61–67. doi: 10.1016/j.pscychresns.2008.06.001

Wechsler, D. (2011). *Wechsler Abbreviated Scale of Intelligence-Second Edition (WASI-II)*. San Antonio, TX: NCS Pearson.

Whitney, E. R., Kemper, T. L., Rosene, D. L., Bauman, M. L., and Blatt, G. J. (2009). Density of cerebellar basket and stellate cells in autism: evidence for a late developmental loss of Purkinje cells. *J. Neurosci. Res.* 87, 2245–2254. doi: 10.1002/jnr.22056

Yu, K. K., Cheung, C., Chua, S. E., and McAlonan, G. M. (2011). Can Asperger syndrome be distinguished from autism? An anatomic likelihood meta-analysis of MRI studies. *J. Psychiatry Neurosci.* 36, 412–421. doi: 10.1503/jpn.100138

Yushkevich, P. A., Piven, J., Hazlett, H. C., Smith, R. G., Ho, S., Gee, J. C., et al. (2006). User-guided 3D active contour segmentation of anatomical structures: significantly improved efficiency and reliability. *Neuroimage* 31, 1116–1128. doi: 10.1016/j.neuroimage.2006.01.015

Conflict of Interest: The authors declare that the research was conducted in the absence of any commercial or financial relationships that could be construed as a potential conflict of interest.

Publisher's Note: All claims expressed in this article are solely those of the authors and do not necessarily represent those of their affiliated organizations, or those of the publisher, the editors and the reviewers. Any product that may be evaluated in this article, or claim that may be made by its manufacturer, is not guaranteed or endorsed by the publisher.

frontiers | Frontiers in Integrative Neuroscience

TYPE Correction
PUBLISHED 09 September 2022
DOI 10.3389/fnint.2022.1020980

OPEN ACCESS

EDITED AND REVIEWED BY
Eric London,
Institute for Basic Research in Developmental Disabilities (IBR), United States

*CORRESPONDENCE
Matthew W. Mosconi
mosconi@ku.edu

RECEIVED 16 August 2022
ACCEPTED 22 August 2022
PUBLISHED 09 September 2022

CITATION
McKinney WS, Kelly SE, Unruh KE, Shafer RL, Sweeney JA, Styner M and Mosconi MW (2022) Corrigendum: Cerebellar volumes and sensorimotor behavior in autism spectrum disorder. *Front. Integr. Neurosci.* 16:1020980. doi: 10.3389/fnint.2022.1020980

Corrigendum: Cerebellar volumes and sensorimotor behavior in autism spectrum disorder

Walker S. McKinney[1,2], Shannon E. Kelly[1,3], Kathryn E. Unruh[1], Robin L. Shafer[1], John A. Sweeney[4], Martin Styner[5] and Matthew W. Mosconi[1,2,3]*

[1]Schiefelbusch Institute for Life Span Studies and Kansas Center for Autism Research and Training (K-CART), University of Kansas, Lawrence, KS, United States, [2]Clinical Child Psychology Program, University of Kansas, Lawrence, KS, United States, [3]Department of Psychology, University of Kansas, Lawrence, KS, United States, [4]Department of Psychiatry and Behavioral Neuroscience, University of Cincinnati College of Medicine, Cincinnati, OH, United States, [5]Department of Psychiatry and Computer Science, University of North Carolina at Chapel Hill, Chapel Hill, NC, United States

KEYWORDS

cerebellum, volumetry, autism spectrum disorder (ASD), sensorimotor, oculomotor, MRI, structure, Crus I

A corrigendum on
Cerebellar volumes and sensorimotor behavior in autism spectrum disorder

by McKinney, W. S., Kelly, S. E., Unruh, K. E., Shafer, R. L., Sweeney, J. A., Styner, M., and Mosconi, M. W. (2022). *Front. Integr. Neurosci.* 16:821109. doi: 10.3389/fnint.2022.821109

In the published article, there was an error. The MRI sequence parameters provided in the original text were incorrect. A correction has been made to **Materials and Methods**, "*MRI Data Acquisition*," Paragraph 1:

"Participants completed a structural MRI scan with a 3T whole-body scanner (Siemens Skyra) and a 32-channel head coil. Participants lay supine with their head stabilized using adjustable padding. A whole-brain T1-weighted (MPRAGE) anatomical scan was acquired across 176 contiguous sagittal slices at 1.200 × 1.055 × 1.055 mm^3 (FOV 176 × 240 × 256 mm^3; matrix 176 × 240 × 256 mm^3; TR = 2.3 s; TE = 2.95 ms; inversion delay to the center k-line 900 ms; flip angle= 9°; pixel bandwidth = 240 Hz; duration 5:12)."

The authors apologize for this error and state that this does not change the scientific conclusions of the article in any way. The original article has been updated.

Publisher's note

frontiers | Frontiers in Integrative Neuroscience

HYPOTHESIS AND THEORY
published: 31 May 2022
doi: 10.3389/fnint.2022.797391

The "Primitive Brain Dysfunction" Theory of Autism: The Superior Colliculus Role

*Rubin Jure**

Centro Privado de Neurología y Neuropsicología Infanto Juvenil WERNICKE, Córdoba, Argentina

A better understanding of the pathogenesis of autism will help clarify our conception of the complexity of normal brain development. The crucial deficit may lie in the postnatal changes that vision produces in the brainstem nuclei during early life. The superior colliculus is the primary brainstem visual center. Although difficult to examine in humans with present techniques, it is known to support behaviors essential for every vertebrate to survive, such as the ability to pay attention to relevant stimuli and to produce automatic motor responses based on sensory input. From birth to death, it acts as a brain sentinel that influences basic aspects of our behavior. It is the main brainstem hub that lies between the environment and the rest of the higher neural system, making continuous, implicit decisions about where to direct our attention. The conserved cortex-like organization of the superior colliculus in all vertebrates allows the early appearance of primitive emotionally-related behaviors essential for survival. It contains first-line specialized neurons enabling the detection and tracking of faces and movements from birth. During development, it also sends the appropriate impulses to help shape brain areas necessary for social-communicative abilities. These abilities require the analysis of numerous variables, such as the simultaneous evaluation of incoming information sustained by separate brain networks (visual, auditory and sensory-motor, social, emotional, etc.), and predictive capabilities which compare present events to previous experiences and possible responses. These critical aspects of decision-making allow us to evaluate the impact that our response or behavior may provoke in others. The purpose of this review is to show that several enigmas about the complexity of autism might be explained by disruptions of collicular and brainstem functions. The results of two separate lines of investigation: 1. the cognitive, etiologic, and pathogenic aspects of autism on one hand, and two. the functional anatomy of the colliculus on the other, are considered in order to bridge the gap between basic brain science and clinical studies and to promote future research in this unexplored area.

Keywords: autism spectrum disorders, superior colliculus (SC), neurodevelopmental disorders, brainstem, early brain development, autism pathogenesis, autism theories

OPEN ACCESS

Edited by:
Susanne Schmid,
Western University, Canada

Reviewed by:
Karl Farrow,
Neuroelectronics Research Flanders, Belgium
Hisao Nishijo,
University of Toyama, Japan

***Correspondence:**
Rubin Jure
rubinjurerj@gmail.com

Received: *18 October 2021*
Accepted: *19 April 2022*
Published: *31 May 2022*

Citation:
Jure R (2022) The "Primitive Brain Dysfunction" Theory of Autism: The Superior Colliculus Role. Front. Integr. Neurosci. 16:797391. doi: 10.3389/fnint.2022.797391

INTRODUCTION

Among the cardinal symptoms of autism spectrum disorder (ASD) are an inability to properly direct gaze and abnormalities in attention to appropriate targets. The superior colliculus (SC) is a brainstem structure with sentinel functions (Merker, 1980), which is also tasked with the ability to redirect both gaze and attention. It also activates emotional and motor networks to produce

responses congruent with the stimuli. To do this, it has widespread connections with structures located throughout the brain. In this article, we set forth the reasoning underlying a new model that places early compromise of collicular function as a central feature of ASD, not only because of these gaze and attention symptoms but also because an early loss of these collicular capabilities leads to improper development of numerous other systems, explaining not only the language and social skill deficits but the full ASD clinical syndrome.

Regardless of their etiology, all neuropsychiatric disorders are syndromes exclusively defined by their clinical manifestations: a cluster of symptoms determined by the compromise of specific functions or neural systems. For example, several etiologies (cerebral infarct, abscess, etc.) affecting specific language networks will result in Broca's aphasia. In two different individuals with the same syndrome, the severity of the symptoms can be very variable, but the more similar their clinical manifestations are, the more similar their pathogenesis will be.

Among all developmental disorders (DD), ASD (or autism) is the most complex because it compromises numerous functions—social, communicative, sensory/motor, emotional, attentional, autonomic, etc. (Tuchman, 2006; American Psychiatric Association, 2013; Eilam-Stock et al., 2014). For this reason, it seems unwise to look for a specific brain area or system responsible for the various clinical manifestations. However, what renders ASD highly coherent is that this heterogeneous cluster of symptoms is present in almost every individual with the syndrome, in spite of their cognitive level- from severe deficiency to high intellectual ability.

Autism spectrum disorder coherence is not explained by etiologic factors because several prenatal or postnatal genetic or non-genetic conditions could result in ASD (Jure, 2019; Martin et al., 2022). Similarly, several autism theories have been proposed, from dysfunctions of sensory, motor, autonomic, attentional, or emotional basic processing (for example abnormal social motivation) to exclusive higher-order compromise (theory of mind, social cognition, executive functions abnormalities, etc.) (see references below). The compromise of a brain hub underlying perceptual, emotional, motor, attentional or cognitive abilities could be the common factor responsible for the repetition of disparate symptoms in most ASD individuals. Additionally, the presence of early brain overgrowth (Courchesne et al., 2007) and abnormalities in the synaptic organization during the first months of life (Vértes and Bullmore, 2015), as well as the timing of clinical presentation circumscribe the search to networks with key innate functions impacting specific aspects of neurodevelopment, while sparing others. This could explain the uneven skills and the coexistence of ASD with high intelligence.

A central aspect of this article is the concept of *consciousness*. There is an intense debate regarding its definition and hence the neural substrate supporting it. The more generalized, corticocentered view, maintains that it is only limited to overt or explicit aspects of reflective self-consciousness, corresponding to an adult human perspective. Some feel that consciousness is *not* the sole preserve of the cerebral cortex. Penfield (1952) based this view on clinical and physiological observations in epilepsy, while more recently, Merker (2007) based his on animal studies and on behaviors of children born without a cerebral cortex. The latter author's proposal includes a continuum of consciousness; the lowest is sustained only by upper brainstem nuclei including the SC, and the highest by the mature human cortex. The former involves the implicit sense of one's own body and the environment in order to select a target and to act due to motivation or emotions. Different degrees of complexity were added during phylogenetic evolution due to the gradual expansion of the telencephalon. These more elaborated perceptual and cognitive characteristics of consciousness reached their highest levels to finally include self-consciousness in great apes and humans, along with the addition of language in the latter. The upper brainstem organization, common to all vertebrates, provides the functional properties not only to support wakefulness but to accomplish basic behaviors in order to survive. These functions dominate the early stages of human development and are central to the theory of mind (Watt, 2007) and to most ASD theories. Additionally, they continue to be essential during all life in order to process the surfeit of covert information provided to the individual and to react automatically whenever necessary (see Merker, 2007 for a thoughtful discussion on this topic). Accordingly, the terms *covert, implicit,* or *automatic* will be used in this article instead of *non-conscious* or *unconscious* attention or behavior.

In the present brain-based framework, previous ASD theories and etiologies will be included as pieces of a more complex puzzle**.** The objective is to analyze how disruptions of the SC might help explain the whole clinical syndrome and its paradoxes.

AUTISM THEORIES

The Role of Vision in ASD

Visual deficits are not included among ASD symptoms (American Psychiatric Association, 2013), and it is well-known that most ASD individuals excel at visual skills. Hence, it seems illogical to point to visual abnormalities as responsible for the syndrome. However, two main facts discussed below contradict this posture: the strong association of congenital blindness (CB) with ASD (Jure et al., 2016) and the fact that most ASD theories are based on the presence of abnormal visual attention and processing.

CB and ASD

Unlike congenital deafness which severely compromises oral language, but is not associated with higher rates of ASD (Jure et al., 1991), total CB conveys a very high prevalence of ASD (Mukaddes et al., 2007; Jure et al., 2016; Kiani et al., 2019). A study comparing children with severe vs. profound congenital visual impairment showed that even the presence of very coarse vision of forms in the first condition (instead of a total lack of vision shown by the second) during the first months of life was a protective factor lowering the presence of developmental setback with autistic-like symptoms (Dale and Sonksen, 2002). *These findings might reflect the importance of very early visual input on social and communicative development.* Additionally,

BOX 1 | Clinical examples of congenital blindness and ASD.

The present author examined a congenitally blind teenage girl with social and communication difficulties and abnormal prosody, but with excellent semantic and syntactic abilities, high level reasoning, and academic skills. Another example (by personal communication) is a social worker with CB who admitted identifying herself in some descriptions of the autistic profile given by a lecturer in a conference about autism. She was also fascinated by the notion *of facial blindness* because "I've been blind from birth and not only have I not seen a face but I have no concept of a face," she added. Another example of the effect of total lack of form vision during the first year of life is the neurodevelopment of two identical twins I followed from infancy until adolescence (same genetic background and environmental conditions). The same etiology: retinopathy of prematurity: provoked total congenital blindness in one of them and partial blindness in the second, with preserved ability to see forms and movements. The first child displays all the myriad of ASD symptoms with severe mood disorders. The second child instead, is empathic, sociable, communicative, cares about his brother, and his mood is usually good and stable. These examples, although anecdotic, reveal the importance of early visual input on the pathogenesis of ASD.

autistic symptoms in CB are not only limited to social and communicative deficits. Stereotypies and repetitive behaviors (Mink and Mandelbaum, 2006), as well as affective disorders (Wigham et al., 2017), are very frequent and very similar in both CB and ASD. Moreover, mood disorders are more common among children and young adults with early and severe visual impairment (Augestad, 2017).

(See **Box 1** for anecdotal but relevant clinical examples of CB and ASD).

Abnormal Visual Attention in ASD

Long before the development of language and social cognition, early life visual attention to faces and movements is supported by a non-canonical, rapid subcortical visual system that accesses the amygdala by way of an SC-pulvinar pathway (Johnson, 2005; McCleery et al., 2007). This stream is predominantly magnocellular and has the ability to automatically detect movement or rapidly changing images. In contrast, the canonical visual route reaches the primary visual cortex *via* the lateral geniculate nucleus (LGN). Although it also receives magnocellular input in two layers, it is predominantly parvocellular, with four layers receiving inputs. While effectively integrated by rich interconnections, the magnocellular system simultaneously processes a great deal of global and dynamic information with a coarse grain. The parvocellular system processes mostly *static,* focused, detailed, and chromatic features of the environment (McCleery et al., 2007; Nassi and Callaway, 2009).

Several well-known theories of ASD point directly or indirectly to a predominance of the parvocellular over the magnocellular visual system*: the Magnocellular Dysfunction Theory* (Milne et al., 2002; McCleery et al., 2007; Laycock et al., 2020), *the Weak Central Coherence (WCC) theory* (Frith and Happé, 1994), and *the Enhanced Perceptual Functioning (EPF) model* (Mottron and Burack, 2001). *The most consistent finding of ASD is an automatic initial attentional bias to local stimuli rather than global processing* (Happé and Frith, 2006; Guy et al., 2016). Typically, healthy individuals automatically perceive the whole picture before explicitly attending to details. A recent meta-analysis review strongly suggests that this pattern is reversed in ASD (Van der Hallen et al., 2015).

There is a weakness regarding diffuse magnocellular dysfunction as responsible for ASD. A generalized magnocellular dysfunction involving both, implicit/subcortical and explicit/cortical magnocellular networks, does not explain why a proportion of individuals with ASD have a normal explicit perception of biologic movements or facial clues and mainly fail in automatic processing (Sato et al., 2010). Additionally, exclusive dysfunction of visual magnocellular functions can explain some, but not all ASD symptoms (Happé and Frith, 2006).

Abnormal Face Processing and Abnormal Social Motivation

Several studies have revealed the presence of abnormal face processing in individuals with ASD (Elgar and Campbell, 2001; Carver and Dawson, 2002; McCleery et al., 2007; Kleinhans et al., 2008; McPartland et al., 2011; Senju et al., 2011; Elsabbagh et al., 2012; Stavropoulos et al., 2018; Morgan and Hills, 2019; Safar et al., 2020; Shephard et al., 2020). *A consistent finding is the presence of abnormalities in the initial, covert perception of faces by subcortical structures* (Sato et al., 2010, 2016; Akechi et al., 2014; Antezana et al., 2016; Naumann et al., 2018; Bathelt et al., 2021). Strong innate behavioral bias neonates share with other vertebrates is the predisposition to follow faces and biological motion, and to pay attention to the gaze of others (Goren et al., 1975; Johnson et al., 1991; Rosa Salva et al., 2015; NIDA-Network et al., 2016). Besides the *innate attraction* to congeners, this process also requires the ability to *recognize* complex images, *decide implicitly* which one to select, and *integrate* internal states with information from a variety of sensory inputs (Chen and Hong, 2018) to finally *activate* premotor and motor commands in order to *perform* the action.

The *social motivation theory of ASD* proposes that dysfunctions of innate social motivational mechanisms affect the development of social cognition later in life. These behaviors are sustained by "experience-expectant"[1] networks (Carver and Dawson, 2002; Chevallier et al., 2012) It has been suggested that developing this capability requires the interaction of several neurotransmitters (oxytocin, dopamine, and glutamate, as well as endogenous opioids) (see references in Chevallier et al., 2012).

The idea that subcortical structures supporting innate social motivation are compromised in ASD was questioned by follow-up studies of children *from 2 months* of age with a high family risk of ASD. These studies found normal visual attention for following faces in these infants (Johnson, 2014; Klin et al., 2015). However, another follow-up study *from birth* revealed that visual preferences for social stimuli strikingly differed between high-risk and low-risk newborns. The authors proposed a U-shaped

[1]Experience-expectant refers to the fact that the average or normal environment provides infants with the necessary input to develop the neural connections to enable the baby to function across these domains.

curve in high risks infants: they started with abnormalities at birth, showed improvement when cortical structures start to mature and take control, and then suffered a regression due to the absence of a normally functioning subcortical mechanism to support the developing cortical areas (NIDA-Network et al., 2016). Prenatal exposure to valproic acid in humans frequently results in ASD (Bescoby-Chambers et al., 2001; Williams et al., 2001; Christianson et al., 2008). In a parallel animal model, it has been shown that visual social orienting mechanisms and social predisposition are selectively abolished in chicks by embryonic exposure to valproic acid (VPA) (Sgadò et al., 2018).

Early postnatal visual experience is necessary to produce the plastic changes required for normal facial processing (Carver and Dawson, 2002) and to shift from subcortical to cortical control (Morton and Johnson, 1991). Specific cortical regions, like the fusiform area normally employed for explicit face processing, may instead be devoted to other tasks depending on the experience and the expertise of the individual (e.g., bird identification or chess scene analysis) (Gauthier et al., 1999; Bilalić, 2016). Notably, activation of the fusiform gyrus and amygdala by cartoon characters, but not to faces, was observed in an autistic boy by fMRI (Grelotti et al., 2005).

Abnormal Attentional ASD Theories

From the first descriptions of ASD to the present, many experts have maintained that early deficits in various attentional aspects have an exponential effect on development, resulting in the full clinical ASD syndrome (see Jure, 2019 and references therein). Early *orienting attention* to biological stimuli is critical for social development and it was found to be abnormal at 7 months in those at risk for ADS (Elison et al., 2013). While overt attention is essentially directed at a single target, cover attention analyzes several stimuli at once. A number of authors have also pointed to deficits in *divided attention during* complex events requiring the *simultaneous* analysis of various factors (Murray et al., 2005; Fletcher-Watson et al., 2008; Jaworski and Eigsti, 2015; Keehn and Joseph, 2016; Unruh et al., 2016; Bolis and Schilbach, 2017; Arora et al., 2022). Social events are the most demanding, as they require simultaneous attention to the internal state of the individual, to the environment, to the behaviors of others, and even to the hidden logic or real intentions behind such behaviors. Skorich et al. (2017) found a negative relationship between autism quotient and shared-attention, which is pivotal for constructing the self-other-object relationship.

Other authors have pointed to *abnormal attention disengagement* as the main factor responsible for ASD (Landry and Bryson, 2004; Elsabbagh et al., 2013; Keehn et al., 2013, 2021). Again, the superior colliculus plays a critical role in shifting attention to a new target.

Abnormal Sensorimotor and Autonomic Processing in ASD

The abnormal response to sensory stimuli in individuals with ASD is highly variable. There is not a single pattern; multiple senses may be involved (auditory, visual, pain, temperature, taste, vestibular, olfactory, and somatosensory) and both hypo- and hypersensitivity have been described (see Rapin, 2006 for a detailed review). The following theories consider abnormal sensorimotor processing as responsible for ASD:

The *Intense World Theory* proposes excessive functioning of microcircuits and enhanced brain functioning as the underlying abnormality responsible for ASD. The animal model of autism used was also valproic acid exposed rat offspring. The authors considered that impaired habituation to sensory stimulation measured *in vivo* by the level of pre-pulse inhibition (PPI) was one of the main features of the hyper-reactivity and enhanced brain functioning in ASD individuals (Markram et al., 2008; Markram and Markram, 2010).

For more than five decades *Multisensory processing abnormalities* have been described in individuals with ASD (Camarata et al., 2020) and proposed as the abnormality responsible for the syndrome (Stevenson et al., 2014; Camarata et al., 2020; Kawakami et al., 2020; Siemann et al., 2020). More recently, a *Bayesian model of ASD* was proposed based on new computational frameworks suggesting that multisensory integration follows Bayesian rules of causal inference (French and DeAngelis, 2020). Palmer et al. (2017) hypothesize that autism is characterized by a greater weighting of sensory information in updating probabilistic representations of the environment. For the authors, this seminal abnormality results in abnormal actions, explaining full-blown ASD syndrome. Bayesian responses are only acquired after repeated exposure to similar events and require an interaction of perceptual, cognitive, and biologic mechanisms (Thaler et al., 2021). Consequently, this ability necessitates a bidirectional (both bottom-up and top-down) postnatal training process using first line, sentinel structures in order to automatically orient the attention to relevant stimuli and ignore non-relevant stimuli.

Integrative theories including motor aspects, such as *the micro-movement perspective theory,* maintain that ASD individuals have an early-life disruption of integration of sensory, motor, and autonomic aspects of the connections between the peripheral and the central nervous systems, which affects the stochastic rhythms of motions (e.g., speech gestures, eyes, facial micro-expressions, head, body, limbs, etc.). This compromises flexible transitions between intentional and spontaneous behaviors (Torres et al., 2013). The logical place for such disruption would be in the brainstem. Impaired acquisition of skilled motor acts, including *dyspraxia,* is frequently found in individuals with ASD, and abnormalities point mainly to a compromise of implicit learning with an excessive reliance on explicit/declarative learning (Gidley Larson et al., 2008). This finding might be indicative of cortically mediated learning, reflecting a more unifocal explicit learning without proper implicit/multifocal support. This may explain the frequent observation of uneven motor skills in this population.

The highest integration is required during dyadic interactions involving motor, emotional, cognitive, conversational, physiological, and neural aspects of *Interpersonal Synchrony.* Development of this capability starts at 2–3-month-old when the infant and mother nonverbally communicate by *intersubjective*, rapid, reciprocal, bidirectional visual-facial, auditory-prosodic, and tactile-gestural means (Schore, 2021). *Atypical interpersonal synchrony* from early life has also been proposed as an early

marker of ASD (Koehne et al., 2016; McNaughton and Redcay, 2020).

Mood Disorders and Alexithymia

There is no pattern of emotional profiles among individuals with ASD. They can vary from a significant lack of reaction to exaggerated behavioral outbursts, and from severe baseline mood disorders to a prominent lack of emotional expressions. What is confirmed is that individuals with ASD are at increased risk of suffering psychiatric conditions during their lifespan, with more prevalence of anxiety and mood disorders (see Rosen et al., 2018 for a review). A related psychiatric disorder, *Alexithymia,* is also highly prevalent among ASD individuals (Kinnaird et al., 2019; Morie et al., 2019). This disorder presents with difficulties in recognizing and expressing a variety of emotions and body sensations, a lack of imagination or fantasy life, and a tendency to focus on external, rather than internal, experiences (Sifneos, 1973). Links between cognitive function, body sensations, affective dimension, alexithymia, empathy, and ASD have been established by several authors (Grynberg et al., 2010; Murphy et al., 2017; Mul et al., 2018). Interestingly, autistic adults have recently described their own interoceptive difficulties as limited awareness of hunger, satiation, or thirst, as well as abnormal awareness or understanding of affective arousal, pain, or illness, and difficulty differentiating benign body signals from signals that represent medical concerns (Trevisan et al., 2021). These symptoms point to very basic, as opposed to higher-order, dysfunction or compromise in the loops that integrate brainstem structures with higher brain areas.

Autonomic and Circadian Dysfunction

Basic neurological functions such as abnormalities in autonomic processing (Hirstein et al., 2001; Eilam-Stock et al., 2014) and circadian dysfunctions (Lorsung et al., 2021) are frequently found in ASD individuals, and these have also been pointed to as responsible for disruptions of emotional/social development. The cluster of abnormalities in autonomic/arousal regulation, sleep-wake homeostasis, and sensorimotor integration during the first months of life, *reflect brainstem involvement* and have been proposed as a very early risk factor for ASD (Burstein and Geva, 2021).

Clinical Paradoxes and IQ Variability

None of the previous theories taken in isolation can explain the myriad of ASD symptoms and they do not clarify some frequent clinical paradoxes. For example, some individuals with confirmed ASD display excellent sports skills or write imaginative tales (author's clinical observations). Additionally, there are several examples of famous athletes, actors, or political leaders with suspected or confirmed ASD (ONGIG, n.d.). While anecdotal, these examples show that at least in some circumstances, sensory/motor integrative skills and/or mental abilities are either spared, or they are different, but not severely compromised. While some would argue that these are just idiosyncratic examples, their presence argues the ASD is not inherently a disorder of higher cerebral functions. In fact, ASD individuals can excel at *any* skill, depending on both, the pattern of their higher-order network losses, and the narrow range of interest the subject displays during their development. The result fosters "hypertrophy" in particular skills to the detriment of others. In fact, well-developed rational and logical abilities and the presence of high IQ levels in some individuals with ASD prompted the theory proposing *Autism as a disorder of high intelligence* (Crespi, 2016). The fact that the presence of superior cognitive skills does not preclude the expression of the full clinical syndrome points to a compromise of more primitive, instead of higher-order cortical networks.

A common factor that is *always abnormal* in ASD is the lack of appropriate development of *primitive behaviors* necessary to respond appropriately depending on the context. These manifestations are not always severe, such as a complete lack of social interest or communication. However, even mildly affected, high functioning, autistic individuals always display at least subtle symptoms, and these can have potentially severe consequences in their lives. It is well-known that they can exhibit a great variety of symptoms, from total lack of fear of strangers or real dangers to generalized fear or severe social anxiety. Mildly affected children will display an innate interest in interacting with others, but they will often do it inappropriately. For example, during a first meeting, they will try to hug, touch, or push the unfamiliar individual. They may not react at all to an aggressor or they might react in an exaggerated fashion to a mild innocent joke. Some do not understand the concept of authority and can treat adults like their peers, but at the same time, they do not know how to play with other children. Although these behaviors also involve higher-order mental abilities, they are universally present in normal children and animals. The latter must differentiate familiar from strange congeners, respect hierarchies, defend themselves and play with their peers in order to develop survival skills from a very early age. This suggests these behaviors are widespread in animals, and so must be part of the normal development of circuitry patterns.

Neurodevelopmental Courses

Another consistent finding of ASD is the timing of onset of clinical manifestations. It occurs before 3 years of age. The usual initial manifestation is a delay or deviation in the emergence of normal social and communicative milestones from the beginning. A significant proportion will show, mostly between 18 and 24 months of life, a pattern of autism *regression,* where they lose early acquired language, social and communicative abilities (Rapin and Tuchman, 2006; Ozonoff and Iosif, 2019). After this initial period of regression, the rest of the evolution is similar to the other DD: a chronic *static* encephalopathy. Most ASD individuals will *partially* improve over time, but their core issues with social and communicative abilities will *remain life-long* and show varying degrees of compromise. A small proportion with *optimal outcomes* (3–20%) will improve significantly, developing acceptable communicative and social abilities in adulthood (Fein et al., 2013). However, even these adults will not enjoy non-predictable or highly demanding social environments that require appropriate spontaneous reactions in quality and timing. *These diverse developmental courses might reflect different pathogenic mechanisms as a result of either, primary abnormalities*

in subcortical structures or abnormal interactions of bridge networks between cortical and subcortical structures.

It is worth noting that all previous developmental courses are replicated in individuals with CB indicating that the absence of vision from birth might share similar pathogenic effects on the developing brain compared with other ASD etiologies (Jure et al., 2016).

Conclusions About ASD Theories and Clinical Manifestations

Autism theories are almost as diverse as autism symptoms. Almost every aspect (perceptive, attentional, autonomic, motor, integrative, emotional, etc.) has been pointed to as the seminal compromise responsible for the full clinical syndrome. This speaks to the significant interdependence between them. Complex behaviors, including socialization and communication, require a highly dynamic balance between these variables, and the dysfunction of one of them will affect the rest. Nevertheless, it is certainly possible that the clustering of ASD symptoms is just an epiphenomenon of a compromise of a brain hub supporting all these functions, as opposed to a cause-effect relationship between them.

We can conclude that the most common aspects of ASD theories are the compromise of implicit mental processes, such as the initial bias in attention to biological events (faces, movements, etc.) or to global instead of local processing, as well as deficits in the automatic integration of simultaneous sensory, emotional, cognitive and motor dimensions. The dysfunction of brainstem structures, which are normally mature at birth may produce pivotal disorders of input-processing-output behaviors, and so might explain several aspects: the full clinical syndrome, the early life manifestations, and the preservation of higher-order cerebral functions resulting in uneven skills.

THE BRAINSTEM AND THE SC

The Primitive Subcortical Brain vs. the Cortical Brain

Every behavior is a motor act requiring the integration of different senses, mostly led by vision, with emotional needs. Brainstem nuclei and loops control the input-processing-output machinery in order to produce primitive behaviors without the involvement of higher neural networks. Among the several subtelencephalic nuclei receiving retinal input, the essential structure to accomplish this process is the tectum, called superior colliculus in mammals (Sewards and Sewards, 2002). Its preservation from the earliest vertebrate to humans bespeaks its irreplaceable role in adaptive behaviors (Basso et al., 2021). From a simple tri-synaptic loop, used to display avoidance or escape responses to looming images in lampreys, its complexity significantly increased during evolution. Along with changes in its cortex-like organization, several collicular-brainstem nuclei loops mediating diverse emotional, autonomic, and hormonal functions developed during phylogenesis (see Isa et al., 2021 for a review on this topic).

Besides the downstream outputs to premotor areas for very fast visuomotor transmission, the SC sends connections to the pulvinar, and other thalamic nuclei, which in turn provide access to the amygdala, striatum, and cerebral cortex. This *retino-colliculo-thalamic* pathway indirectly and simultaneously activates several *visual and non-visual* cortical regions. In turn, the SC receives massive *direct* cortical feedback.

The main visual route in humans is the *retino-geniculate pathway, which transmits* 90% of the retinal input. The dorsal lateral geniculate nucleus (dLGN) is the main nucleus responsible for central, foveal retinal vision. It is devoted to an explicit, detailed, and colorful analysis of the environment. Unlike the SC, the dLGN is *exclusively* visual and only directly reaches the striate visual cortex. Hence, in order to produce a behavior, a *slow* sequential process is initiated to integrate vision with other non-visual cortical regions, evaluate possible actions, make an overtly conscious decision, and finally send a motor command from frontal regions. Although these pathways are highly interconnected and we perceive vision as a unitary process, the retino-colliculo-thalamic pathway mediates covert visuo-motor behaviors, while the retino-geniculate pathway is devoted to detailed overt conscious processing (Isa et al., 2021). There is strong evidence that the human retino-colliculo-thalamic pathway develops much earlier than the retino-geniculo-cortical pathway, and the latter is probably not fully functional until nearly 2 months after birth (Sewards and Sewards, 2002; Bridge et al., 2015).

Emotions and Brainstem Structures

Emotions have a strong and pervasive influence on human behavior as a whole (Schore, 1994; Lerner et al., 2015; Hogeveen et al., 2016; Keltner, 2019), but as we have noted, are not appropriately tied to behavior in ASD. *Primitive emotions* are innate and universal, and they determine orienting biases to environmental phenomena. They also modulate sensory experience, arousal, and autonomic functions, but their ultimate goal is to initiate actions that promote survival in animals and humans (Damasio, 1996; Venkatraman et al., 2017). Being genetically determined, it is not necessary to teach a child a primary emotion like fear, anxiety, anger, joy, or panic (Davis and Montag, 2019). On the other hand, feelings cannot be taught; for example, when it is not innately present, it is a big challenge to teach a child the *motivation* for socialization, communication, or play.

Recent studies in animals and humans disclose that the nuclei and networks which convey primary emotional systems are located in the brainstem (Panksepp and Biven, 2012; Venkatraman et al., 2017; Davis and Montag, 2019). On the other hand, higher cortical networks, which regulate emotions, are *experience-dependent* blank slates at birth that need to be trained by primitive structures and environmental influence (Schore, 1994). Ample evidence in animals and humans that primary emotions do not require the neocortex is reviewed by Davis and Montag (2019). Even primitive structures like the amygdala are dependent on the input of brainstem nuclei. For example, selective ablation of the periaqueductal gray matter (PAG), but not of the amygdala, abolished rage responses in animals (Bailey

and Davis, 1942, 1944). Similarly, exclusive ablation of the SC provoked a total absence of fear of snakes in monkeys (Soares et al., 2017).

The self-sustained and holistic process of brainstem functions explains why neonatally decorticated rats still displayed complex survival/emotional behaviors (Siviy and Panksepp, 1985). These rats were able to reproduce and care for their pups. They also exhibited the same ability to play as control rats and to display aggressive, defensive, or *conditioned* (learned) freezing behaviors. In contrast, rats with small lesions in the parafascicular region of the thalamus significantly reduced play time, motivation, and play solicitation. Evidence in humans with congenital or acquired cerebral lesions also points to subcortical structures acting as substrates for primary emotions (Merker, 2007; Damasio et al., 2013).

The Superior Colliculus

The SC is prepared to perceive relevant external events, mainly biological ones before they reach overt consciousness. The use of canonical pathways from external receptors of each specific sensory modality and then to association and motor cortical areas to accomplish this would be very slow and therefore less useful. The SC superficial layers are exclusively visual and receive direct retinal input from magnocellular and koniocellular neurons (May, 2006; Basso et al., 2021). This visual information is integrated with auditory, somatosensory, and vestibular input within the intermediate/deep layers. In order to react *automatically*, the SC has not only the ability to perceive the stimulus but also to make an implicit decision and finally send the corresponding motor command (Gandhi and Katnani, 2011; Basso and May, 2017; Farrow et al., 2019; Basso et al., 2021). By accurate saccades, it orientates central vision to objects of interest. Then, the canonical visual pathway is activated allowing a detailed analysis of the event. None of the other brain hubs seem to have the key strategic location to function from birth as a first-line monitor and first reactive system (Soares et al., 2017).

At present, it is clear that the SC is not simply a structure for producing reflex movements. It has rich connections with the forebrain through ascending networks and is also well-connected with numerous brainstem nuclei. There is compelling evidence of its role in cognitive, attentional, emotional, and complex, higher-order behaviors (May, 2006; Basso and May, 2017; Basso et al., 2021). This aspect and the fact that it is ready to function at birth as an experience-independent structure is a strong argument in favor of its possible role in neural development. As was previously remarked, late maturing, experience-dependent cortical structures require the information received during the first months of life. Hence, any small abnormality or deviation in SC functions could have significant consequences on neurodevelopment.

The SC Is Responsible for the Initial Global Vision and Facial Detection

Against the traditional view that SC functions are limited to output processes of gaze control, selective attention, and target selection properties, there is evidence for its having an intrinsic *visual perceptive role* in gestalt, coarse rapid object detection, and object identification, as well as in analyzing luminance contrast and motion stimuli (Sewards and Sewards, 2002; Schneider, 2005; Georgy et al., 2016; Chen and Hafed, 2018).

While the pulvinar (Pul) and the LGN receive input from the magnocellular and parvocellular visual system, there is evidence that the SC/Pul pathway is responsible for the automatic *bias* toward magnocellular global processing (Lomber, 2002; Tamietto, 2011; Sato et al., 2016; Petry and Bickford, 2019; Laycock et al., 2020). It has been shown in animals that selective inactivation of the visual superficial layers of the SC during *pattern* discrimination learning reverses the precedence for global visual features that is typical of normal learning (Lomber, 2002).

Findings in favor of the SC/Pul role in automatic alerting or orienting responses are the presence of a *direct subcortical* SC/Pul pathway to the amygdala (Amy) (see above) (Laycock et al., 2020), and the fact that the SC simultaneously triggers visual and *non-visual* sensory and motor cortical structures, allowing a reaction before the stimulus reaches conscious explicit appreciation (Petry and Bickford, 2019). Instead, the information transmitted by the LGN travels first through a series of visual cortical areas, before accessing the Amy, which in turn influences non-visual sensory and motor cortical structures. Most evidence in humans indicates that attentional selection for emotional stimuli is under bottom-up control, even in adults, and is mediated by the SC/Pul/Amy circuits activated by the magnocellular system (Vuilleumier et al., 2003; Vuilleumier, 2015; Mulckhuyse, 2018; McFadyen, 2019; Laycock et al., 2020; McFadyen et al., 2020). Interaction of several subcortical structures plays a key role in multiple aspects of normal face perception during life (Gabay et al., 2014) and it has been demonstrated that the SC, the pulvinar, and the amygdala all support evaluation of facial traits in blindsight (Kinoshita et al., 2019; Ajina et al., 2020). During social interactions, the recording of multiple subtle cues from emotional expressions that depend on the fleeting eye, mouth, face, and body movements are also processed by magno/koniocellular networks (Laycock et al., 2020). An important recent finding is a demonstration that the primate SC houses the first line brain neurons for automatic face detection (∼50 ms after stimulus onset) (Le et al., 2020).

The SC Role in Complex Innate Behaviors

Pivotal work on *sentinel SC functions* was undertaken by Merker in hamsters. Animals with SC lesions demonstrated severe deficits with respect to escape from moving visual threats (Merker, 1980). Several high-density electrode recording studies in optogenetically altered animals, as well as viral or molecular tracing studies, have demonstrated that the SC in rodents mediates a great deal of *innate* behavior, e.g., prey capture (Gahtan, 2005; Hoy et al., 2019), visual avoidance (Dong et al., 2009), and defensive escape, or freezing behaviors (Shang et al., 2015, 2018; Wei et al., 2015; Evans et al., 2018; Reinhard et al., 2019; Isa et al., 2020; Sans-Dublanc et al., 2021). These behaviors are triggered by complex images like body postures, body movements (e.g., attacking or escaping), facial expressions, or eye-related features. Additionally, they are influenced by environmental aspects as well as the emotional state of the animal

(Sewards and Sewards, 2002; da Silva et al., 2013; Rosa Salva et al., 2015; Wei et al., 2015; Dunn et al., 2016; Huang et al., 2017; Ito et al., 2017; Liu et al., 2018; Shang et al., 2018; Lischinsky and Lin, 2019; Zhou et al., 2019; Daviu et al., 2020; Isa et al., 2020; Niu et al., 2020). The networks that mediate these reactions are segregated based on sensory input; as different retinal ganglion cell types record specific visual features of threatening images and activate diverse collicular networks (Gale and Murphy, 2014, 2018; Reinhard et al., 2019), and defined cell types in the SC make distinct contributions to prey capture behaviors (Hoy et al., 2019).

Sensorimotor innate reactions of the SC are further modulated by input from the parabigeminal nucleus (Huda et al., 2020), and from the prefrontal and anterior cingulate cortex (Huda et al., 2020; Tokuoka et al., 2020). The stimulation of different SC descending pathways induces contraversive head/body turns or defense-like behaviors. It is noteworthy that these responses can vary considerably depending on the environment where the animals were tested, so they are context-specific (Isa et al., 2020).

Connections between the substantia nigra (SN) and the SC may play a pivotal role in behaviors driven by *extrinsic motivation* in order to promote survival and reproduction (Comoli et al., 2003; May et al., 2009; Redgrave, 2010; Isa et al., 2020). They are also activated during *intrinsic motivation* triggered by novel stimuli and even by the pleasure of acquiring knowledge or new skills (Fisher et al., 2014; Caligiore et al., 2015). Highly segregated SC loops provoking either defense or approach behaviors also involve the cerebellum, the basal ganglia, and modulatory inputs from *cholinergic* (pedunculopontine nucleus and tegmental nucleus), *noradrenergic* (locus coeruleus), *dopaminergic* (retrorubral area), and *glutaminergic* nuclei (Redgrave, 2010; Comoli et al., 2012), as well as *serotoninergic* cells (raphe nucleus) (Huang et al., 2017). Phylogenetically, all these areas precede the expansion of the cerebral cortex by several 100 millions of years.

In rodents, it has also been shown that visual information from collicular superficial layers is highly *filtered* before reaching the deeper layers in order to develop an increased selectivity for the behaviorally relevant looming stimulus over other innocuous stimuli with similar low-level features; an increasing invariance to the precise location of the threat stimulus; and an increased selectivity for a novel over familiar stimuli (Lee et al., 2020). Additionally, looming images simulating flying predators, cause the SC to stimulate *corticotropin-releasing hormone* (CRH) neurons in the paraventricular nucleus of the hypothalamus, resulting in stress responses and defensive behavior in rodents (Daviu et al., 2020).

Multisensory Integration, Motor Functions, and Orienting Attention: The Role of the SC

After the neonate begins to *experience* repeated multimodal events congruent in time and/or space (visual and auditory), *multisensory/pre-motor single neurons and complex multimodal networks start to appear in the intermediate SC layers*. This training occurs under the double influence of the environment and cortical regions (Alvarado et al., 2008; Stein et al., 2009; Bauer et al., 2012, 2015; Xu et al., 2014; Wang et al., 2020). The deeper SC layers receive whole body somatosensory input with a larger representation of the face. The alignment of visual and sensory maps within the SC layers has been proposed as the functional substrate to create the newborn's minimal intersubjective mind (Pitti et al., 2013). *An interaction between the SC, the PAG, and dopamine systems originating in the midbrain ventral tegmental area has been proposed as the fundamental neural substrate for complex intersubjectivity* (Corrigan and Christie-Sands, 2020).

In order to represent the environment coherently, the brain automatically creates *illusions* of reality. Some illusions are unisensory, while others result from the integration of two senses; for example: when a single flash is presented along with two or more beeps, observers often report seeing two or more flashes (fission illusion). The *McGurck effect* involves visual and auditory fusion (Mcgurk and Macdonald, 1976). *The Ventriloquist effect* apparently adds *semantic congruence* to multisensory/motor integration: we know from previous experience that a voice is produced by lip movements (Wallace et al., 2004; Ursino et al., 2014). Even when we explicitly know that the source of the sound is elsewhere, it is extremely difficult or even impossible to overcome the illusion the dummy speaks in order to find the source of the voice. Evidence indicates that multisensory neurons present on intermediate/deep SC layers play a key role in these phenomena (Stein et al., 2009, 2014; Ursino et al., 2014).

Connections between the SC and the cerebellum provide both the initial command, which generates a saccade and the error signal that ensures saccades remain accurate (Soetedjo et al., 2019). Evidence suggests that *these loops have not only motor but also purely cognitive, functions* which have been linked with ASD and other DD (Sathyanesan et al., 2019). Apparently, several SC brainstem, thalamic, and basal ganglia loops modulate emotional, sensory, and motor variables in order to make automatic decisions in saccade production (Caligiore et al., 2013; Thurat et al., 2015; Solié et al., 2022). Evidence indicates that following *Bayesian* instead of "winner takes all" rules, the motor reaction produced by interacting forces at the SC reflects a saccade choice instead of a simple saccade vector (Basso and May, 2017). Several multisensory, Bayesian, or Hebbian neurocomputational schemes have been proposed to explain the dynamics of the integration required to register the world coherently, and the SC is considered the crucial structure in all of them (see Ursino et al., 2014 for a review).

All these behaviors seem to fit under the concept of *embodied cognition* or *"enaction." This concept* maintains that cognition and language emerge as a result of the active sensorimotor interaction between the agent and its environment (Heinrich et al., 2020), where movements guided by vision play a central role. It also includes the concept of *"autopoietic enactivism"* which means that through active environmental interactions the agent has the ability to self-individuate, self-regulate, self-develop, self-maintain, and reproduce (see Wilson and Foglia, 2017 for a review).

Top-Down Direct Cortical Influence on the SC

Inside the cortex, neurons in all the cortical layers provide input to large pyramidal neurons in the 5th layer in each specialized region of the cerebrum. The descending axons of many of these layer 5 pyramidal neurons establish *direct* connections

with the SC, rendering it functionally an additional cortical layer that is targeted by this cortical outflow pathway (Merker, 2013). For example, recently, it was demonstrated in mice that prefrontal cingulate corticotectal pyramidal neurons enhance saccade planning and visual processing through projections to the SC (Hu et al., 2019).

We can conclude that the SC combines first-line environmental and efference copy signals with the body (from peripheral somatosensory input) and cortical information. In this way, a resonance between the implicit bottom-up reality created at the SC is amalgamated with the colorful, detailed, and dynamic multisensory conscious reality created by higher-order cortical loops. Ultimately, this integration allows a continuous "global best estimate" of sensory, motivational, and motor circumstances in order to act coherently and effectively (Merker, 2013).

Embodied Cognition, the *Self*, and the SC

Dynamic embodiment theories are mainly based on complex *visual stability* achieved by the individual in their environment (Wilson and Foglia, 2017). The SC's integrative analysis of first-line environmental, motor, and higher-order information seems to fulfill the functional requirements to achieve this goal. A thoughtful description of SC functions and its interplay with cortical activity to produce the emergence of visual consciousness under the perspective of the *self* is given by Merker (2013).

The embodied concept also applies to mental abilities. Current evidence suggests that we understand others' emotions and intentions by recreating, at least partially, sensorimotor experiences in our own bodies. In spite of the current consensus and evidence supporting embodied theories, as opposed to body/mind dualism, there is still a debate about the degree of embodiment (Ursino et al., 2014; Wilson and Foglia, 2017). Independent of which neurocomputational scheme is proposed, the SC is considered a key structure for explaining the integration required to register the world coherently (Ursino et al., 2014). It functions as the kernel between the bottom-up input from the body and the environment and the top-down influence of cortical functions.

Plastic and Cognitive Influence of the SC on Normal and Abnormal Neurodevelopment: Neurophysiological Evidence

Animal studies have shown that in early life the SC fosters the creation of Pul-cortical loops that support visual cognition (Bridge et al., 2015). Unlike the dLGN, which matures later (Sewards and Sewards, 2002), the SC is not dependent on postnatal input from cortical areas as it can accomplish *visual sensory functions* in decorticated mice (Shanks et al., 2016). Furthermore, it plays a fundamental role in supporting the neuronal differentiation induced in other structures by retinal input (Alvarado et al., 2021). Through interactions between cell surface molecules and their ligands, the SC develops a series of topographically organized connections (Scicolone et al., 2009; Mendonça et al., 2010; Triplett and Feldheim, 2012; Carr et al., 2013; Chagas et al., 2019). Specific SC mechanisms promote topographic cortical alignment of visuals with somatic input (Triplett et al., 2012). It also acts as a *driver* or *modulator* providing complex motion information to the dLGN, in order to integrate convergent information about stimulus motion, eye movement, and positioning in the visual primary cortex (Bickford et al., 2015).

Summary of SC and Brainstem Functions

The SC and its brainstem loops concentrate several functions necessary to produce behaviors allowing most vertebrates to survive and reproduce. The preservation of this machinery from early vertebrates to humans bespeaks its great efficacy and its irreplaceable character. These functions, triggered mainly by postnatal biological visual input, allow not only for defense, attack, or escaping behaviors, but they also give every creature the sense of self, the ability to differentiate inanimate objects from living beings, to differentiate familiar people from strangers, to respect hierarchies, and to create Bayesian patterns in order to make the right decision at the right time. The lack of *simultaneous* evaluation of several variables of the environment, the self, and other creatures' intentions in order to produce a fairly automatic action with the correct timing is incompatible with self-preservation. This low-level input-output processing is mainly automatic. Perceptual, emotional, and motor aspects cannot be fully separated due to their interdependence. Highly suggestive evidence for this holistic processing is the appearance, very early in life, of individual multisensory/premotor SC neurons with visual, auditory, somatosensory, autonomic, and emotional functions that produce an automatic motor output along with an attendant shift in attention (Meredith et al., 1992; Stein et al., 2009). Accordingly, each action or behavior is preceded by perception and emotions, and a perfect balance between different emotions is necessary in order to make the right decision (for example the mother that, overcoming her own fear, decides to attack a dangerous animal to defend her offspring). We can conclude that the SC and its surrounding structures *are not only responsible for the initial visual bias to global perception, but they also create holistic patterns that involve multisensory-emotional, autonomic, and motor aspects.* As it is difficult to separate between the perceptual, emotional, attentional, and motor theories of autism, it is also difficult to separate the functional confluence of these aspects in the SC.

CORRELATIONS BETWEEN ASD AND SC DISRUPTIONS

The comparison of previous theories, pathogenic and etiologic aspects of ASD with SC functions demonstrate a high level of coincidence (See **Figure 1**). Some of the following points are pivotal aspects of ASD that depend on brain functions that, according to clear scientific evidence, are exclusively performed by the SC. Other symptoms depend on functions in which the SC plays a prominent role, but it is shared by other brain structures. For others, strong evidence of exclusivity is still lacking, but a possible role in development is suspected:

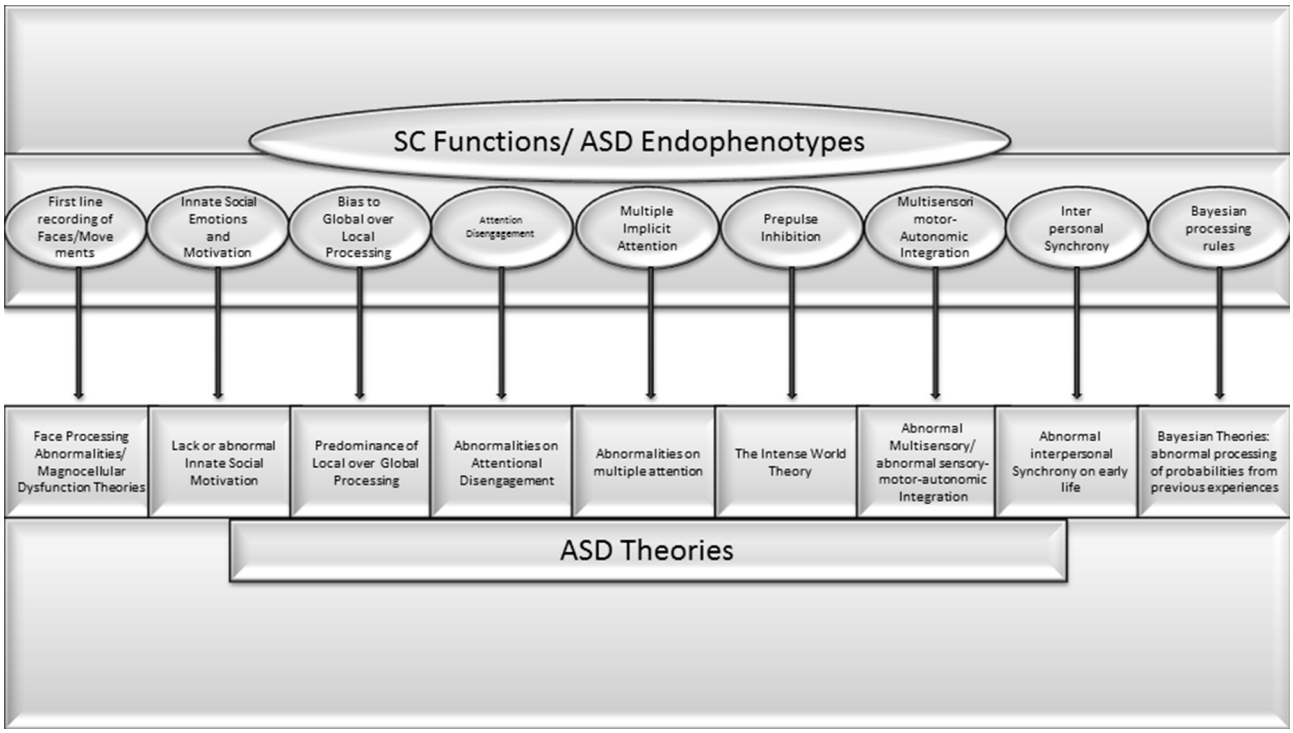

FIGURE 1 | Very high concorndance between SC functions and endophenotypes or pivotal symptoms of ASD theories previously proposed.

- *The atypical automatic bias for global instead local visual processing is the cornerstone of several prominent autism theories* (Van der Hallen et al., 2015). *The superficial visual SC is the exclusive structure responsible for this initial automatic bias to global processing* (Lomber, 2002; Kato et al., 2011).
- *Numerous ASD theories are based on abnormal processing of faces and movements, and abnormal innate social motivation. The SC houses the first line neurons for automatic face recognition* (Le et al., 2020). The lack of responses to faces and biological movement is present from birth in a significant proportion of individuals with ASD (NIDA-Network et al., 2016).
- A very primitive animal behavior is the automatic *response to looming images* representing moving visual threats. In mammals, this function depends *exclusively on input-output processing for SC sentinel functions* (Merker, 1980). *The lack of innate looming-evoked defensive response observed in a significant proportion of children with ASD* and in mice prenatally exposed to valproic acid has been attributed to a dysfunction in the subcortical pathway involving the SC (Hu et al., 2017).[2]
- *Retinocollicular projections* also deserve special attention because *a compromise of these fibers* could be secondary to different nutritional (including a chronic restriction of omega-3 fatty acids), toxic, infectious, hormonal factors, or microglial activation during key developmental periods *resulting in ASD* (Chagas et al., 2020; Sandre et al., 2021).
- Interrupting an ongoing behavior is also essential for social interaction. Several authors have proposed that *abnormal disengagement of visual attention during infancy is the underlying abnormality in ASD* (see above). A specific *subpopulation of disengagement SC neurons* has been described in rodents by Ngan et al. (2015).
- Abnormal response to sensory stimuli and abnormal pre-pulse inhibition (PPI) response were proposed in the *intense world theory* as one of the markers of ASD (see above). Dendrinos et al. (2011) *specifically* linked the compromise of SC parvalbumin containing GABAergic neurons to impaired PPI in rodents prenatally exposed to VPA. More recently, the critical role of the SC was demonstrated in macaques by a frank compromise of PPI to acoustic startle response after bilateral inhibition of collicular deep/intermediate layers (Waguespack et al., 2020).
- *The SC is the main brain hub that integrates sensory, motor, emotional, and autonomic dimensions*. A variety of ASD theories are based on abnormal multisensory functions

[2]A selective compromise with uneven cognitive skills was also observed in one of my patients with ASD secondary to fetal valproate syndrome. He/she spoke fluently with good verbal and visual memory, but displayed severe deficits in socialization, communication and pragmatic abilities. This finding suggests that the compromise of synapses by prenatal valproate exposure is not ubiquitous, but is instead selective and might be related with autistic symptoms dependent on specific SC functions.

(Stevenson et al., 2014; Camarata et al., 2020; Kawakami et al., 2020; Siemann et al., 2020). Motor, autonomic, emotional, and several other variables are included in *the micro-movement perspective theory* (Torres et al., 2013) and the *abnormal interpersonal synchrony theory* (McNaughton and Redcay, 2020). Similarly, *Bayesian theories of ASD* are based on patterns of multisensory integration (French and DeAngelis, 2020). The abnormal synergic activity of multisensory SC neurons with a cascade effect on neurodevelopment has been linked with ASD and dyslexia (Siemann et al., 2020; Wang et al., 2020). Several multisensory, Bayesian, or Hebbian neurocomputational schemes have been proposed to explain the dynamics of the integration required to register the world coherently, and *the SC is considered the integrative hub for all these variables* (see Ursino et al., 2014 for a review).

- The *weak central coherence theory attributes ASD to a reduction in synchronization of high-frequency gamma activity* (Brock et al., 2002). Gamma band abnormalities have been found in individuals with autism during perceptual tasks (Brown et al., 2005), gaze cueing (Richard et al., 2013), and emotional face processing (Safar et al., 2020). *Gamma band synchronization only appears in cortical, SC, and pulvinar regions* (Fries, 2009; Bastos et al., 2015; Bryant et al., 2015; Baranauskas et al., 2016; Le et al., 2019). It is also associated with *cholinergic* (Bryant et al., 2015) and *GABAergic activity* at the SC (Nakamura et al., 2015).
- Postnatal environmental input is essential to activate parvalbumin-positive GABAergic neurons present in different subcortical areas. These neurons orchestrate brain organization promoting an inhibitory-excitatory balance (Takesian and Hensch, 2013). The SC has a high density of GABA, with plastic functions during the perinatal period, and GABA acts as a "pioneer neurotransmitter" responsible for environment-induced synaptic architecture (Grantyn et al., 2011). Early alterations of GABA and glutamate may result in ASD and other DD (Grantyn et al., 2011; Horder et al., 2018; Li et al., 2018b). In fact, *GABA dysfunctions have been proposed as a biomarker for ASD* (Maxwell et al., 2015), *and reduced numbers of GABAergic SC neurons have been associated with autistic-like behavior in knockout mice* (Nakamura et al., 2015).
- The SC contains several subpopulations of parvalbumin-positive, GABAergic neurons, some of which are exclusive inhibitory; but unlike the cortex, it contains *subpopulations of parvalbumin-positive cells with glutamatergic excitatory activity* (Villalobos et al., 2018). Inhibitory (GABAergic) and excitatory (glutamatergic) activities have an influence on the neuroligins responsible for the postnatal postsynaptic balance between AMPA (Ca^{++} excitatory) and GABA (Cl^{-} inhibitory) receptors (Johnston and Blue, 2006). Numerous (∼30) genetic mutations and pathogenic pathways affecting these neuroligins, GABA and AMPA have been linked with ASD (Johnston and Blue, 2006; Trobiani et al., 2020). In animals, *prenatal VPA exposure selectively affects parvalbumin-positive GABAergic neurons of the SC, provoking autistic-like symptomatology* (Dendrinos et al., 2011; Wöhr et al., 2015).
- The *interplay of GABA and serotonin* between the SC and dorsal raphe nucleus translate threatening looming visual signals into defensive responses (Huang et al., 2017), and both neurotransmitters have been linked with ASD pathogenesis (Skuse, 2006; Robertson et al., 2016; Di et al., 2020; Carvajal-Oliveros and Campusano, 2021).
- Other molecules linked with specific behavioral innate approach, defensive, or attack responses triggered by the SC and related to ASD pathogenesis are *acetylcholine* (Tokuoka et al., 2020), *endogenous opioids* (da Silva et al., 2013), *dopamine* (Redgrave, 2010; Solié et al., 2022), *corticotropin-release hormone* (Daviu et al., 2020), *adrenergic SC receptors and norepinephrine* (Iigaya et al., 2012; Li et al., 2018a; London, 2018), and *glutamine* (Barbano et al., 2020).
- *Nitric Oxide* is a key molecule in plastic developing pre-and postnatal periods expressed in the SC (Scheiner et al., 2001; Giraldi-Guimarães et al., 2004) and it is especially linked with Shank3 mutation and ASD (Tripathi et al., 2020).
- Very recently, *the neurexin gene family* has been implicated in ASD and apparently linked with post-synaptic changes. It was found to be *differentially* expressed within specific populations in the larval tectum. *This strongly suggests a potential genetic link between the SC/tectum and ASD* (Martin et al., 2022).
- Lastly, but critically, is the *timing of occurrence of brain changes.* It must precede clinical manifestation within a circumscribed age window from prenatal to early post-natal when subcortical centers shape several brain regions through ascending connections. Synaptic postnatal growth reaches its maximum at 12 months and is followed by a massive pruning during early childhood (Vértes and Bullmore, 2015). An alteration in this balance might be responsible for the early brain overgrowth frequently observed in children with autism (Courchesne et al., 2007), as well as the abnormalities in "growth connectomics"—the organization and reorganization of brain networks during development (Vértes and Bullmore, 2015). Unlike the LGN, the SC is ready at birth to accomplish complex visual functions (Sewards and Sewards, 2002), and likely plays a primary role in the development of cerebral organization during this age window.

DISCUSSION

As was previously mentioned, the lack of association of total congenital deafness and acquired blindness with ASD contrasts sharply with the very high prevalence of ASD in CB. Even children with peripheral (i.e., non-neurological) etiologies of visual impairment that improved from profound to less severe vision compromise after the first year of life show a higher risk of autism regression later (between 15 months and 3 years of age) (Dale and Sonksen, 2002). Additionally, a very high prevalence of ASD has been described in *orphan children with severe environmental deprivation* during the first 6 months of age (Green et al., 2016). The main variable that might explain this difference is the complete lack of early exposition of visual experience, especially faces, human movements, and non-verbal aspects of interaction and communication. Similarly, *a crucial aspect of the present theory is that, in order to result in ASD, SC dysfunction should be*

congenital or acquired very early on, during the first months of life.

It is also worth noting that given all SC connections, the existence of an *exclusive* compromise of its inner structure without an impact on several brainstem and thalamo-cortical structures is not possible. Similarly, it is not possible to compromise any neurotransmitter (GABA, serotonin, etc.) or gene responsible for synaptic changes exclusively in the SC without affecting other structures. However, selective compromise of the retino-colliculi-thalamic or the retino-geniculate pathway is possible due to their relative independence. Considering, hypothetically, that the first network fosters the development of higher-order behaviors dependent on primitive brain functions (including, for example, mental abilities), and the second the higher-order pathway functions *mostly* independent of primitive behaviors, such as logic, reasoning skills, or motor skills that are exclusively human, such as hand dependent abilities. Then, the selective dysfunction of these networks, or the compromise of the interaction between them, might have a great variety or spectrum of cognitive profiles distributed in a continuum, from normal to abnormal behaviors or abilities. These would in turn explain the broad ASD spectrum of clinical manifestations and its superposition with typical individuals in the less affected group.

It is not possible in this discussion to cover all the varieties of ASD symptoms, but the author invites clinicians working with individuals with ASD to use this framework to understand not only the classic symptoms but the paradoxes and the full range of the clinical spectrum, including comorbidities. For example, against the traditional view that oral language emerges first and then fosters neurodevelopment, evidence indicates the contrary. In human babies, the ability to retain and later recreate a sequence of movements is the base of representational play, which emerges shortly before language, with a close correlation between the complexity of representational play and the complexity of language production (McCune and Zlatev, 2015). Simple or deictic communicative gestures like pointing appear near 12 months. These behaviors require motor control and directed attention for triadic interactions (child, object, and other people) for normal function, as well as social/cultural learning, and the understanding that other persons have thoughts and intentions (McCune and Zlatev, 2015). This denotes the importance of early visual attention to social clues and body movements.

Independent of the frequent comorbidity with cognitive deficits and different developmental language disorders (DLD) (Rapin and Allen, 1983; Rapin and Dunn, 2003) abnormalities in these pre-requisites for language development explain several atypical findings, mostly observed in individuals with ASD, and not with DLD without ASD. For example, total attentional neglect to communication and language during the first year of life will result in children obtaining things for themselves or by taking the hand of a caretaker instead of pointing or naming it to get what they want. Subsequently, the lack of discrimination between self and non-self (and its language correlate) could result in echolalic, third person, or rote memory expressions about specific topics like TV commercials, songs, the alphabet, numbers, geometric figures, etc. Patients with ASD monolog about these topics, instead of sharing, in a triadic interaction, a topic of mutual interest. The presence of difficulties referring to events distant in time or space, or problems understanding and expressing narratives (Paolucci, 2020) could be explained by the lack of imaginative play (which is mainly based on images). All this evidence indicates the importance of basic sensorimotor, as well as emotional dimensions, in the development of verbal and non-verbal communication. They also support the theories pointing to embodied language and cognition (see above).

Additionally, SC abnormalities affecting sentinel and integrative sensory-motor and emotional variables might explain abnormalities in automatic reaction to an injury (e.g., a burn) or any dangerous situation that requires innate, primitive reactions (escaping, defense, freezing, etc.). The lack of normal filtering of information by the SC in order to lessen the load of irrelevant detail for the rest of the brain might explain a number of ASD symptoms, such as the abnormal response to sensory stimuli and the great memory for details.

Abnormalities in first-line, automatic, holistic multisensory, autonomic, emotional, and motor representations supported by the SC might affect the creation of Bayesian patterns after repeated expositions to similar events. This dysfunction might explain the difficulty in individuals with ASD to generalize and learn from experience in order to react automatically with the right timing. Also, as the colliculus automatically combines multiple attentional sources, including own-body sensorimotor perception, several external clues, and numerous cortical inputs, it integrates body-mind-environment information. This seems necessary to manage multiple clues and think appropriately about them, as well as to understand one's own body or emotional feelings. Many with ASD suffer deficits in these areas.

As was remarked upon earlier, the coexistence of autistic symptoms with normal or high intelligence in a significant proportion of the spectrum might be explained by the compromise of the primitive brain without affecting higher-order cerebral functions. Developmental motor abnormalities–mainly dyspraxia–frequently observed in ASD individuals could be the result of a different way of motor learning. This learning is more conscious and focal, which explains the presence of disparities, not only in cognitive or sensory areas but also in motor performance.

An improper feedforward and feedback interaction between the primitive brain and higher structures beginning early in life might result in a lack of balance, with the consequent development of hyperactive subcortical circuits. This, in turn, could explain the abnormalities in emotional reactions, excessive anxiety, stereotypies, and obsessive thinking among the symptoms present in ASD.

Several of the neurotransmitters previously mentioned also play a central role in the pathogenesis of other DD. These might explain the ubiquitous presence of one or more comorbidities such as ADHD, learning disabilities, sleep and mood disorders, anxiety, obsessive-compulsive disorders, epilepsy, cognitive deficits, and autonomic abnormalities that are all found in individuals with ASD (Casanova et al., 2020).

FINAL CONCLUSION

Compromise of the SC in ASD was previously proposed by the present author (Jure, 2019). The present publication adds new evidence supporting this hypothesis. It also makes clear the importance of the SC for numerous brainstem structures and loops present in the primitive brain. If there is early collicular dysfunction, this network can act as a bottleneck in the development of social-communicative abilities. Additionally, I have suggested here a new holistic framework of initial bottom-up collicular processing.

An early dysfunction of the primitive brain offers the most unifying theory of ASD pathogenesis. The SC, as the main brainstem hub, accomplishes several primitive functions whose compromise explains not only the core and the accompanying symptoms of ASD, including their usual presentation in clusters, but also the presence of a clinical spectrum, replete with uneven skills, and comorbidities.

Instead of the *exclusively visual* "global" vs. "local" dichotomy, a new framework of information processing is suggested here. The new proposal is that the SC and the networks it activates have a holistic registration of external events that includes multisensory/motor/emotional/autonomic aspects that occur simultaneously and automatically. The SC also helps filter out unnecessary or superfluous details. This kind of processing gives several benefits that are frequently abnormal or absent in ASD individuals.

Disruptions of SC functions may provide the neurologic substrate that encompasses *all* previous theories. Genetic and/or non-genetic prenatal and postnatal etiologic and pathogenic factors may affect the SC and lead to ASD because it is a primary structure for fostering brain plastic changes by epigenetic influence during early postnatal life. This extremely active period shapes the future individual regarding both basic sensory/motor/autonomic aspects, as well as cognitive, social, and emotional higher-order abilities. For this reason, numerous neurotransmitters and neurotrophic and signaling molecules are likely to play a role during this age window, which coincides with the initiation of autistic symptoms. Dysfunction in any of these may play a crucial role in this initiation. This also fits with the findings of genetic and non-genetic compromise of retino-collicular axon guidance formation as pathogenic factors for ASD (Campello-Costa et al., 2000; Lee et al., 2010; Brielmaier et al., 2012; Chagas et al., 2019, 2020). The elusive pathogenesis of ASD, which has not been determined even after decades of research on genes and cortical structures, could lie in the epigenetic and plastic effects that the SC and related brainstem nuclei provoke all over the brain during early life.

To test this theory, future studies need to focus on post-mortem SC observation or non-invasive functional human studies of the colliculus and its targets (e.g., the pulvinar), as well as animal studies undertaken during the critical collicular-driven developmental period. For example, studies regarding the early post-natal activation of subpopulations of SC neurons by specific genes involved in both the development of the SC and the pathogenesis of ASD would be helpful. Developmental changes in subpopulations of GABAergic neurons directly implicated in ASD animal models should also be targeted. It might be useful to develop animal models of ASD in species that show higher levels of social interaction and verbal communication (e.g., chinchillas). Finally, larger prospective studies regarding the development of subtle aspects of social and verbal or non-verbal communicative abilities in individuals with congenital *vs.* acquired blindness are needed.

The references in the present article represent only a small fraction of the indirect evidence of literature supporting the relationship between the SC and different aspects of ASD. Additionally, the SC is only one of the many brainstem nuclei with an influence on neurodevelopment. All of them are highly interconnected. It is possible that the knowledge of their influence on normal and abnormal human development will require new techniques and decades of investigation. Nevertheless, this knowledge might help us to develop more effective therapeutic or preventative tools.

DATA AVAILABILITY STATEMENT

The original contributions presented in the study are included in the article/supplementary material, further inquiries can be directed to the corresponding author.

AUTHOR CONTRIBUTIONS

RJ a child neurologist specialized in neurodevelopmental disorders, provides a Unifying Theory of Autism based on a review of the literature showing new evidence about the role of primitive structures such as the superior colliculus and brainstem related structures on early postnatal brain development.

ACKNOWLEDGMENTS

Special thanks to Prof. Paul May who very generously helped me with scientific aspects and the general organization of the article, and also to my English professor Sara Manzur. I am grateful to Prof. Bjorn Merker who guided me on earlier versions of the manuscript. I dedicate this work to my sons Pablo, Victoria, Leónidas, and to my wife Mary.

REFERENCES

Ajina, S., Pollard, M., and Bridge, H. (2020). The superior colliculus and amygdala support evaluation of face trait in blindsight. *Front. Neurol.* 11, 769. doi: 10.3389/fneur.2020.00769

Akechi, H., Stein, T., Senju, A., Kikuchi, Y., Tojo, Y., Osanai, H., et al. (2014). Absence of preferential unconscious processing of eye contact in adolescents with autism spectrum disorder: unconscious processing of eye contact in ASD. *Autism Res.* 7, 590–597. doi: 10.1002/aur.1397

Alvarado, J. A., Dhande, O. S., Prosseda, P. P., Kowal, T. J., Ning, K., Jabbehdari, S., et al. (2021). Developmental distribution of primary cilia in the

retinofugal visual pathway. *J. Comp. Neurol.* 529, 1442–1455. doi: 10.1002/cne.25029

Alvarado, J. C., Rowland, B. A., Stanford, T. R., and Stein, B. E. (2008). A neural network model of multisensory integration also accounts for unisensory integration in superior colliculus. *Brain Res.* 1242, 13–23. doi: 10.1016/j.brainres.2008.03.074

American Psychiatric Association (Ed.). (2013). *Diagnostic and Statistical Manual of Mental Disorders: DSM-5, 5th ed*. Washington, DC: American Psychiatric Association. doi: 10.1176/appi.books.9780890425596

Antezana, L., Mosner, M. G., Troiani, V., and Yerys, B. E. (2016). Social-Emotional inhibition of return in children with autism spectrum disorder versus typical development. *J. Autism Dev. Disord.* 46, 1236–1246. doi: 10.1007/s10803-015-2661-9

Arora, I., Bellato, A., Gliga, T., Ropar, D., Kochhar, P., Hollis, C., et al. (2022). What is the effect of stimulus complexity on attention to repeating and changing information in autism? *J. Autism Dev. Disord.* 52, 600–616. doi: 10.1007/s10803-021-04961-6

Augestad, L. B. (2017). Mental health among children and young adults with visual impairments: a systematic review. *J. Vis. Impair. Blind.* 111, 411–425. doi: 10.1177/0145482X1711100503

Bailey, P., and Davis, E. W. (1942). Effects of lesions of the periaqueductal gray matter in the cat. *Exp. Biol. Med.* 51, 305–306. doi: 10.3181/00379727-51-13950P

Bailey, P., and Davis, E. W. (1944). Effects of lesions of the periaqueductal gray matter on the macaca mulatta. *J. Neuropathol. Exp. Neurol.* 3, 69–72. doi: 10.1097/00005072-194401000-00006

Baranauskas, G., Svirskis, G., and Tkatch, T. (2016). Spatial synchronization of visual stimulus-evoked gamma frequency oscillations in the rat superior colliculus. *Neuroreport* 27, 203–208. doi: 10.1097/WNR.0000000000000525

Barbano, M. F., Wang, H.-L., Zhang, S., Miranda-Barrientos, J., Estrin, D. J., Figueroa-González, A., et al. (2020). VTA glutamatergic neurons mediate innate defensive behaviors. *Neuron* 107, 368–382.e8. doi: 10.1016/j.neuron.2020.04.024

Basso, M. A., Bickford, M. E., and Cang, J. (2021). Unraveling circuits of visual perception and cognition through the superior colliculus. *Neuron* 109, 918–937. doi: 10.1016/j.neuron.2021.01.013

Basso, M. A., and May, P. J. (2017). Circuits for action and cognition: a view from the superior colliculus. *Ann. Rev. Vis. Sci.* 3, 197–226. doi: 10.1146/annurev-vision-102016-061234

Bastos, A. M., Vezoli, J., Bosman, C. A., Schoffelen, J.-M., Oostenveld, R., Dowdall, J. R., et al. (2015). Visual areas exert feedforward and feedback influences through distinct frequency channels. *Neuron* 85, 390–401. doi: 10.1016/j.neuron.2014.12.018

Bathelt, J., Koolschijn, P. C. M., and Geurts, H. M. (2021). Atypically slow processing of faces and non-faces in older autistic adults. *Autism* 1–15. doi: 10.1177/13623613211065297

Bauer, J., Magg, S., and Wermter, S. (2015). Attention modeled as information in learning multisensory integration. *Neural Networks.* 65, 44–52. doi: 10.1016/j.neunet.2015.01.004

Bauer, J., Weber, C., and Wermter, S. (2012). "A SOM-based model for multi-sensory integration in the superior colliculus," in *The 2012 International Joint Conference on Neural Networks (IJCNN)* (Brisbane, QLD), 1–8. doi: 10.1109/IJCNN.2012.6252816

Bescoby-Chambers, N., Forster, P., and Bates, G. (2001). Foetal valproate syndrome and autism: additional evidence of an association. *Dev. Med. Child Neurol.* 43, 847. doi: 10.1017/S0012162201211542

Bickford, M. E., Zhou, N., Krahe, T. E., Govindaiah, G., and Guido, W. (2015). Retinal and tectal "driver-like" inputs converge in the shell of the mouse dorsal lateral geniculate nucleus. *J. Neurosci.* 35, 10523–10534. doi: 10.1523/JNEUROSCI.3375-14.2015

Bilalić, M. (2016). Revisiting the role of the fusiform face area in expertise. *J. Cogn. Neurosci.* 28, 1345–1357. doi: 10.1162/jocn_a_00974

Bolis, D., and Schilbach, L. (2017). Observing and participating in social interactions: action perception and action control across the autistic spectrum. *Dev. Cogn. Neurosci.* 29, 168–175. doi: 10.1016/j.dcn.2017.01.009

Bridge, H., Leopold, D. A., and Bourne, J. A. (2015). Adaptive pulvinar circuitry supports visual cognition. *Trends Cogn. Sci.* 20, 146–157. doi: 10.1016/j.tics.2015.10.003

Brielmaier, J., Matteson, P. G., Silverman, J. L., Senerth, J. M., Kelly, S., Genestine, M., et al. (2012). Autism-Relevant social abnormalities and cognitive deficits in engrailed-2 knockout mice. *PLoS ONE* 7, e40914. doi: 10.1371/journal.pone.0040914

Brock, J., Brown, C. C., Boucher, J., and Rippon, G. (2002). The temporal binding deficit hypothesis of autism. *Dev. Psychopathol.* 14, 209–224. doi: 10.1017/S0954579402002018

Brown, C., Gruber, T., Boucher, J., Rippon, G., and Brock, J. (2005). Gamma abnormalities during perception of illusory figures in autism. *Cortex* 41, 364–376. doi: 10.1016/S0010-9452(08)70273-9

Bryant, A. S., Goddard, C. A., Huguenard, J. R., and Knudsen, E. I. (2015). Cholinergic control of gamma power in the midbrain spatial attention network. *J. Neurosci.* 35, 761–775. doi: 10.1523/JNEUROSCI.4001-14.2015

Burstein, O., and Geva, R. (2021). The brainstem-informed autism framework: early life neurobehavioral markers. *Front. Integr. Neurosci.* 15, 759614. doi: 10.3389/fnint.2021.759614

Caligiore, D., Mustile, M., Cipriani, D., Redgrave, P., Triesch, J., De Marsico, M., et al. (2015). Intrinsic motivations drive learning of eye movements: an experiment with human adults. *PLoS ONE* 10, e0118705. doi: 10.1371/journal.pone.0118705

Caligiore, D., Pezzulo, G., Miall, R. C., and Baldassarre, G. (2013). The contribution of brain sub-cortical loops in the expression and acquisition of action understanding abilities. *Neurosci. Biobehav. Rev.* 37, 2504–2515. doi: 10.1016/j.neubiorev.2013.07.016

Camarata, S., Miller, L. J., and Wallace, M. T. (2020). Evaluating sensory integration/sensory processing treatment: issues and analysis. *Front. Integr. Neurosci.* 14, 556660. doi: 10.3389/fnint.2020.556660

Campello-Costa, P., Fosse, A. M., Ribeiro, J. C., Paes-De-Carvalho, R., and Serfaty, C. A. (2000). Acute blockade of nitric oxide synthesis induces disorganization and amplifies lesion-induced plasticity in the rat retinotectal projection. *J. Neurobiol.* 44, 371–381. doi: 10.1002/1097-4695(20000915)44:4<371::AID-NEU1>3.0.CO;2-X

Carr, O. P., Glendining, K. A., Leamey, C. A., and Marotte, L. R. (2013). Overexpression of Ten-m3 in the retina alters ipsilateral retinocollicular projections in the wallaby (*Macropus eugenii*). *Int. J. Dev. Neurosci.* 31, 496–504. doi: 10.1016/j.ijdevneu.2013.05.011

Carvajal-Oliveros, A., and Campusano, J. M. (2021). Studying the contribution of serotonin to neurodevelopmental disorders. Can this fly? *Front. Behav. Neurosci.* 14, 601449. doi: 10.3389/fnbeh.2020.601449

Carver, L. J., and Dawson, G. (2002). Development and neural bases of face recognition in autism. *Mol. Psychiatry* 7, S18–S20. doi: 10.1038/sj.mp.4001168

Casanova, M. F., Frye, R. E., Gillberg, C., and Casanova, E. L. (2020). Editorial: comorbidity and autism spectrum disorder. *Front. Psychiatry* 11, 617395. doi: 10.3389/fpsyt.2020.617395

Chagas, L. D. S., Sandre, P. C., Ribeiro e Ribeiro, N. C. A., Marcondes, H., Oliveira Silva, P., Savino, W., et al. (2020). Environmental signals on microglial function during brain development, neuroplasticity, and disease. *Int. J. Mol. Sci.* 21, 2111. doi: 10.3390/ijms21062111

Chagas, L. S., Trindade, P., Gomes, A. L. T., Mendonça, H. R., Campello-Costa, P., Faria Melibeu, A. da, C., et al. (2019). Rapid plasticity of intact axons following a lesion to the visual pathways during early brain development is triggered by microglial activation. *Exp. Neurol.* 311, 148–161. doi: 10.1016/j.expneurol.2018.10.002

Chen, C.-Y., and Hafed, Z. M. (2018). Orientation and contrast tuning properties and temporal flicker fusion characteristics of primate superior colliculus neurons. *Front. Neural Circuits* 12, 58. doi: 10.3389/fncir.2018.00058

Chen, P., and Hong, W. (2018). Neural circuit mechanisms of social behavior. *Neuron* 98, 16–30. doi: 10.1016/j.neuron.2018.02.026

Chevallier, C., Kohls, G., Troiani, V., Brodkin, E. S., and Schultz, R. T. (2012). The social motivation theory of autism. *Trends Cogn. Sci.* 16, 231–239. doi: 10.1016/j.tics.2012.02.007

Christianson, A. L., Chester, N., and Kromberg, J. G. R. (2008). Fetal valproate syndrome: clinical and neuro-developmental features in two sibling pairs. *Dev. Med. Child Neurol.* 36, 361–369. doi: 10.1111/j.1469-8749.1994.tb11858.x

Comoli, E., Coizet, V., Boyes, J., Bolam, J. P., Canteras, N. S., Quirk, R. H., et al. (2003). A direct projection from superior colliculus to substantia nigra for detecting salient visual events. *Nat. Neurosci.* 6, 974–980. doi: 10.1038/nn1113

Comoli, E., Das Neves Favaro, P., Vautrelle, N., Leriche, M., Overton, P. G., and Redgrave, P. (2012). Segregated anatomical input to sub-regions of the rodent superior colliculus associated with approach and defense. *Front. Neuroanat.* 6, 9. doi: 10.3389/fnana.2012.00009

Corrigan, F. M., and Christie-Sands, J. (2020). An innate brainstem self-other system involving orienting, affective responding, and polyvalent relational seeking: some clinical implications for a "deep brain reorienting" trauma psychotherapy approach. *Med. Hypotheses* 136, 109502. doi: 10.1016/j.mehy.2019.109502

Courchesne, E., Pierce, K., Schumann, C. M., Redcay, E., Buckwalter, J. A., Kennedy, D. P., et al. (2007). Mapping early brain development in autism. *Neuron* 56, 399–413. doi: 10.1016/j.neuron.2007.10.016

Crespi, B. J. (2016). Autism as a disorder of high intelligence. *Front. Neurosci.* 10, 300. doi: 10.3389/fnins.2016.00300

da Silva, J. A., de Freitas, R. L., Eichenberger, G. C. D., Maria Padovan, C., and Cysne Coimbra, N. (2013). Chemical neuroanatomical and psychopharmacological evidence that κ receptor-mediated endogenous opioid peptide neurotransmission in the dorsal and ventral mesencephalon modulates panic-like behaviour. *Euro. J. Pharmacol.* 698, 235–245. doi: 10.1016/j.ejphar.2012.07.038

Dale, N., and Sonksen, P. (2002). Developmental outcome, including setback, in young children with severe visual impairment. *Dev. Med. Child Neurol.* 44, 613–622. doi: 10.1111/j.1469-8749.2002.tb00846.x

Damasio, A., Damasio, H., and Tranel, D. (2013). Persistence of feelings and sentience after bilateral damage of the insula. *Cereb. Cortex* 23, 833–846. doi: 10.1093/cercor/bhs077

Damasio, A. R. (1996). The somatic marker hypothesis and the possible functions of the prefrontal cortex. *Philos. Trans. R. Soc. Lund. B. Biol. Sci.* 351, 1413–1420. doi: 10.1098/rstb.1996.0125

Davis, K. L., and Montag, C. (2019). Selected principles of panksepian affective neuroscience. *Front. Neurosci.* 12, 1025. doi: 10.3389/fnins.2018.01025

Daviu, N., Füzesi, T., Rosenegger, D. G., Rasiah, N. P., Sterley, T.-L., Peringod, G., et al. (2020). Paraventricular nucleus CRH neurons encode stress controllability and regulate defensive behavior selection. *Nat. Neurosci.* 23, 398–410. doi: 10.1038/s41593-020-0591-0

Dendrinos, G., Hemelt, M., and Keller, A. (2011). Prenatal VPA exposure and changes in sensory processing by the superior colliculus. *Front. Integrat. Neurosci.* 5, 68. doi: 10.3389/fnint.2011.00068

Di, J., Li, J., O'Hara, B., Alberts, I., Xiong, L., Li, J., et al. (2020). The role of GABAergic neural circuits in the pathogenesis of autism spectrum disorder. *Int. J. Dev. Neurosci.* 80, 73–85. doi: 10.1002/jdn.10005

Dong, W., Lee, R. H., Xu, H., Yang, S., Pratt, K. G., Cao, V., et al. (2009). Visual avoidance in *xenopus* tadpoles is correlated with the maturation of visual responses in the optic tectum. *J. Neurophysiol.* 101, 803–815. doi: 10.1152/jn.90848.2008

Dunn, T. W., Gebhardt, C., Naumann, E. A., Riegler, C., Ahrens, M. B., Engert, F., et al. (2016). Neural circuits underlying visually evoked escapes in larval zebrafish. *Neuron* 89, 613–628. doi: 10.1016/j.neuron.2015.12.021

Eilam-Stock, T., Xu, P., Cao, M., Gu, X., Van Dam, N. T., Anagnostou, E., et al. (2014). Abnormal autonomic and associated brain activities during rest in autism spectrum disorder. *Brain* 137, 153–171. doi: 10.1093/brain/awt294

Elgar, K., and Campbell, R. (2001). Annotation: the cognitive neuroscience of face recognition: implications for developmental disorders. *J. Child Psychol. Psychiatry* 42, 705–717. doi: 10.1111/1469-7610.00767

Elison, J. T., Paterson, S. J., Wolff, J. J., Reznick, J. S., Sasson, N. J., Gu, H., et al. (2013). White matter microstructure and atypical visual orienting in 7-month-olds at risk for autism. *Am. J. Psychiatry* 170, 899–908. doi: 10.1176/appi.ajp.2012.12091150

Elsabbagh, M., Fernandes, J., Jane Webb, S., Dawson, G., Charman, T., and Johnson, M. H. (2013). Disengagement of visual attention in infancy is associated with emerging autism in toddlerhood. *Biol. Psychiatry* 74, 189–194. doi: 10.1016/j.biopsych.2012.11.030

Elsabbagh, M., Mercure, E., Hudry, K., Chandler, S., Pasco, G., Charman, T., et al. (2012). Infant neural sensitivity to dynamic eye gaze is associated with later emerging autism. *Current Biology* 22, 338–342. doi: 10.1016/j.cub.2011.12.056

Evans, D. A., Stempel, A. V., Vale, R., Ruehle, S., Lefler, Y., and Branco, T. (2018). A synaptic threshold mechanism for computing escape decisions. *Nature* 558, 590–594. doi: 10.1038/s41586-018-0244-6

Farrow, K., Isa, T., Luksch, H., and Yonehara, K. (2019). Editorial: the superior colliculus/tectum: cell types, circuits, computations, behaviors. *Front. Neural Circuits* 13, 39. doi: 10.3389/fncir.2019.00039

Fein, D., Barton, M., Eigsti, I.-M., Kelley, E., Naigles, L., Schultz, R. T., et al. (2013). Optimal outcome in individuals with a history of autism. *J. Child Psychol. Psychiatry* 54, 195–205. doi: 10.1111/jcpp.12037

Fisher, S. D., Gray, J. P., Black, M. J., Davies, J. R., Bednark, J. G., Redgrave, P., et al. (2014). A behavioral task for investigating action discovery, selection and switching: comparison between types of reinforcer. *Front. Behav. Neurosci.* 8, 398. doi: 10.3389/fnbeh.2014.00398

Fletcher-Watson, S., Findlay, J. M., Leekam, S. R., and Benson, V. (2008). Rapid detection of person information in a naturalistic scene. *Perception* 37, 571–583. doi: 10.1068/p5705

French, R. L., and DeAngelis, G. C. (2020). Multisensory neural processing: from cue integration to causal inference. *Curr. Opin. Physiol.* 16, 8–13. doi: 10.1016/j.cophys.2020.04.004

Fries, P. (2009). Neuronal gamma-band synchronization as a fundamental process in cortical computation. *Annu. Rev. Neurosci.* 32, 209–224. doi: 10.1146/annurev.neuro.051508.135603

Frith, U., and Happé, F. (1994). Autism: beyond "theory of mind." *Cognition* 50, 115–132. doi: 10.1016/0010-0277(94)90024-8

Gabay, S., Burlingham, C., and Behrmann, M. (2014). The nature of face representations in subcortical regions. *Neuropsychologia* 59, 35–46. doi: 10.1016/j.neuropsychologia.2014.04.010

Gahtan, E. (2005). Visual prey capture in larval zebrafish is controlled by identified reticulospinal neurons downstream of the tectum. *J. Neurosci.* 25, 9294–9303. doi: 10.1523/JNEUROSCI.2678-05.2005

Gale, S. D., and Murphy, G. J. (2014). Distinct representation and distribution of visual information by specific cell types in mouse superficial superior colliculus. *J. Neurosci.* 34, 13458–13471. doi: 10.1523/JNEUROSCI.2768-14.2014

Gale, S. D., and Murphy, G. J. (2018). Distinct cell types in the superficial superior colliculus project to the dorsal lateral geniculate and lateral posterior thalamic nuclei. *J. Neurophysiol.* 120, 1286–1292. doi: 10.1152/jn.00248.2018

Gandhi, N. J., and Katnani, H. A. (2011). Motor functions of the superior colliculus. *Annu. Rev. Neurosci.* 34, 205–231. doi: 10.1146/annurev-neuro-061010-113728

Gauthier, I., Tarr, M. J., Anderson, A. W., Skudlarski, P., and Gore, J. C. (1999). Activation of the middle fusiform "face area" increases with expertise in recognizing novel objects. *Nat. Neurosci.* 2, 568–573. doi: 10.1038/9224

Georgy, L., Celeghin, A., Marzi, C. A., Tamietto, M., and Ptito, A. (2016). The superior colliculus is sensitive to gestalt-like stimulus configuration in hemispherectomy patients. *Cortex* 81, 151–161. doi: 10.1016/j.cortex.2016.04.018

Gidley Larson, J. C., Bastian, A. J., Donchin, O., Shadmehr, R., and Mostofsky, S. H. (2008). Acquisition of internal models of motor tasks in children with autism. *Brain J. Neurol.* 131 (Pt. 11), 2894–2903. doi: 10.1093/brain/awn226

Giraldi-Guimarães, A., Bittencourt-Navarrete, R. E., and Mendez-Otero, R. (2004). Expression of neuronal nitric oxide synthase in the developing superficial layers of the rat superior colliculus. *Braz. J. Med. Biol. Res.* 37, 869–877. doi: 10.1590/S0100-879X2004000600013

Goren, C. C., Sarty, M., and Wu, P. Y. (1975). Visual following and pattern discrimination of face-like stimuli by newborn infants. *Pediatrics* 56, 544–549. doi: 10.1542/peds.56.4.544

Grantyn, R., Henneberger, C., Jüttner, R., Meier, J. C., and Kirischuk, S. (2011). Functional hallmarks of GABAergic synapse maturation and the diverse roles of neurotrophins. *Front. Cell. Neurosci.* 5, 13. doi: 10.3389/fncel.2011.00013

Green, J., Leadbitter, K., Kay, C., and Sharma, K. (2016). autism spectrum disorder in children adopted after early care breakdown. *J. Autism Dev. Disord.* 46, 1392–1402. doi: 10.1007/s10803-015-2680-6

Grelotti, D. J., Klin, A. J., Gauthier, I., Skudlarski, P., Cohen, D. J., Gore, J. C., et al. (2005). FMRI activation of the fusiform gyrus and amygdala to cartoon characters but not to faces in a boy with autism. *Neuropsychologia* 43, 373–385. doi: 10.1016/j.neuropsychologia.2004.06.015

Grynberg, D., Luminet, O., Corneille, O., Grèzes, J., and Berthoz, S. (2010). Alexithymia in the interpersonal domain: a general deficit of empathy? *Pers. Indiv. Diff.* 49, 845–850. doi: 10.1016/j.paid.2010.07.013

Guy, J., Mottron, L., Berthiaume, C., and Bertone, A. (2016). A developmental perspective of global and local visual perception in autism spectrum disorder. *J. Autism Dev. Disord.* 49, 2706–2720. doi: 10.1007/s10803-016-2834-1

Happé, F., and Frith, U. (2006). The weak coherence account: detail-focused cognitive style in autism spectrum disorders. *J. Autism Dev. Disord.* 36, 5–25. doi: 10.1007/s10803-005-0039-0

Heinrich, S., Yao, Y., Hinz, T., Liu, Z., Hummel, T., Kerzel, M., et al. (2020). Crossmodal language grounding in an embodied neurocognitive model. *Front. Neurorobot.* 14, 52. doi: 10.3389/fnbot.2020.00052

Hirstein, W., Iversen, P., and Ramachandran, V. S. (2001). Autonomic responses of autistic children to people and objects. *Proc. R. Soc. Lond. Ser. B Biol. Sci.* 268, 1883–1888. doi: 10.1098/rspb.2001.1724

Hogeveen, J., Salvi, C., and Grafman, J. (2016). 'Emotional intelligence': lessons from lesions. *Trends Neurosci.* 39, 694–705. doi: 10.1016/j.tins.2016.08.007

Horder, J., Petrinovic, M. M., Mendez, M. A., Bruns, A., Takumi, T., Spooren, W., et al. (2018). Glutamate and GABA in autism spectrum disorder—a translational magnetic resonance spectroscopy study in man and rodent models. *Transl. Psychiatry* 8, 106. doi: 10.1038/s41398-018-0155-1

Hoy, J. L., Bishop, H. I., and Niell, C. M. (2019). Defined cell types in superior colliculus make distinct contributions to prey capture behavior in the mouse. *Curr. Biol.* 29, 4130–4138.e5. doi: 10.1016/j.cub.2019.10.017

Hu, F., Kamigaki, T., Zhang, Z., Zhang, S., Dan, U., and Dan, Y. (2019). Prefrontal corticotectal neurons enhance visual processing through the superior colliculus and pulvinar thalamus. *Neuron* 104, 1141–1152.e4. doi: 10.1016/j.neuron.2019.09.019

Hu, Y., Chen, Z., Huang, L., Xi, Y., Li, B., Wang, H., et al. (2017). A translational study on looming-evoked defensive response and the underlying subcortical pathway in autism. *Sci. Rep.* 7, 14755. doi: 10.1038/s41598-017-15349-x

Huang, L., Yuan, T., Tan, M., Xi, Y., Hu, Y., Tao, Q., et al. (2017). A retinoraphe projection regulates serotonergic activity and looming-evoked defensive behaviour. *Nat. Commun.* 8, 14908. doi: 10.1038/ncomms14908

Huda, R., Sipe, G. O., Breton-Provencher, V., Cruz, K. G., Pho, G. N., Adam, E., et al. (2020). Distinct prefrontal top-down circuits differentially modulate sensorimotor behavior. *Nat. Commun.* 11, 6007. doi: 10.1038/s41467-020-19772-z

Iigaya, K., Müller-Ribeiro, F. C. F., Horiuchi, J., McDowall, L. M., Nalivaiko, E., Fontes, M. A. P., et al. (2012). Synchronized activation of sympathetic vasomotor, cardiac, and respiratory outputs by neurons in the midbrain colliculi. *Am. J. Physiol. Regul. Integrat. Comp. Physiol.* 303, R599–R610. doi: 10.1152/ajpregu.00205.2012

Isa, K., Sooksawate, T., Kobayashi, K., Kobayashi, K., Redgrave, P., and Isa, T. (2020). Dissecting the tectal output channels for orienting and defense responses. *Eneuro 7,* ENEURO. 0271–20.2020. doi: 10.1523/ENEURO.0271-20.2020

Isa, T., Marquez-Legorreta, E., Grillner, S., and Scott, E. K. (2021). The tectum/superior colliculus as the vertebrate solution for spatial sensory integration and action. *Curr. Biol.* 31, R741–R762. doi: 10.1016/j.cub.2021.04.001

Ito, S., Feldheim, D. A., and Litke, A. M. (2017). Segregation of visual response properties in the mouse superior colliculus and their modulation during locomotion. *J. Neurosci.* 37, 8428–8443. doi: 10.1523/JNEUROSCI.3689-16.2017

Jaworski, J. L. B., and Eigsti, I.-M. (2015). Low-level visual attention and its relation to joint attention in autism spectrum disorder. *Child Neuropsychol.* 23, 316–331. doi: 10.1080/09297049.2015.1104293

Johnson, M. H. (2005). Subcortical face processing. *Nat. Rev. Neurosci.* 6, 766–774. doi: 10.1038/nrn1766

Johnson, M. H. (2014). Autism: demise of the innate social orienting hypothesis. *Curr. Biol.* 24, R30–R31. doi: 10.1016/j.cub.2013.11.021

Johnson, M. H., Dziurawiec, S., Ellis, H., and Morton, J. (1991). Newborns' preferential tracking of face-like stimuli and its subsequent decline. *Cognition* 40, 1–19. doi: 10.1016/0010-0277(91)90045-6

Johnston, M., and Blue, M. (2006). "Neurobiology of autism," in *Autism: A Neurological Disorder of Early Brain Development*, 1st Edn, eds R. Tuchman and I. Rapin (London: Mac Keith Press), 79–92.

Jure, R. (2019). Autism pathogenesis: the superior colliculus. *Front. Neurosci.* 12, 1029. doi: 10.3389/fnins.2018.01029

Jure, R., Pogonza, R., and Rapin, I. (2016). Autism spectrum disorders (ASD) in blind children: very high prevalence, potentially better outlook. *J. Autism Dev. Disord.* 46, 749–759. doi: 10.1007/s10803-015-2612-5

Jure, R., Rapin, I., and Tuchman, R. F. (1991). Hearing-impaired autistic children. *Dev. Med. Child Neurol.* 33, 1062–1072. doi: 10.1111/j.1469-8749.1991.tb14828.x

Kato, R., Takaura, K., Ikeda, T., Yoshida, M., and Isa, T. (2011). Contribution of the retino-tectal pathway to visually guided saccades after lesion of the primary visual cortex in monkeys: role of retino-tectal pathway in blindsight. *Euro. J. Neurosci.* 33, 1952–1960. doi: 10.1111/j.1460-9568.2011.07729.x

Kawakami, S., Uono, S., Otsuka, S., Yoshimura, S., Zhao, S., and Toichi, M. (2020). Atypical multisensory integration and the temporal binding window in autism spectrum disorder. *J. Autism Dev. Disord.* 50, 3944–3956. doi: 10.1007/s10803-020-04452-0

Keehn, B., and Joseph, R. M. (2016). Slowed search in the context of unimpaired grouping in autism: evidence from multiple conjunction search: slowed visual search in ASD. *Autism Res.* 9, 333–339. doi: 10.1002/aur.1534

Keehn, B., Kadlaskar, G., Bergmann, S., McNally Keehn, R., and Francis, A. (2021). Attentional disengagement and the locus coeruleus – norepinephrine system in children with autism spectrum disorder. *Front. Integr. Neurosci.* 15, 716447. doi: 10.3389/fnint.2021.716447

Keehn, B., Müller, R.-A., and Townsend, J. (2013). Atypical attentional networks and the emergence of autism. *Neurosci. Biobehav. Rev.* 37, 164–183. doi: 10.1016/j.neubiorev.2012.11.014

Keltner, D. (2019). Toward a consensual taxonomy of emotions. *Cogn. Emot.* 33, 14–19. doi: 10.1080/02699931.2019.1574397

Kiani, R., Bhaumik, S., Tyrer, F., Bankart, J., Miller, H., Cooper, S. A., et al. (2019). The relationship between symptoms of autism spectrum disorder and visual impairment among adults with intellectual disability. *Autism Res.* 12, 1411–1422. doi: 10.1002/aur.2138

Kinnaird, E., Stewart, C., and Tchanturia, K. (2019). Investigating alexithymia in autism: a systematic review and meta-analysis. *Euro. Psychiatry* 55, 80–89. doi: 10.1016/j.eurpsy.2018.09.004

Kinoshita, M., Kato, R., Isa, K., Kobayashi, K., Kobayashi, K., Onoe, H., et al. (2019). Dissecting the circuit for blindsight to reveal the critical role of pulvinar and superior colliculus. *Nat. Commun.* 10, 135. doi: 10.1038/s41467-018-08058-0

Kleinhans, N. M., Richards, T., Sterling, L., Stegbauer, K. C., Mahurin, R., Johnson, L. C., et al. (2008). Abnormal functional connectivity in autism spectrum disorders during face processing. *Brain* 131, 1000–1012. doi: 10.1093/brain/awm334

Klin, A., Shultz, S., and Jones, W. (2015). Social visual engagement in infants and toddlers with autism: early developmental transitions and a model of pathogenesis. *Neurosci. Biobehav. Rev.* 50, 189–203. doi: 10.1016/j.neubiorev.2014.10.006

Koehne, S., Hatri, A., Cacioppo, J. T., and Dziobek, I. (2016). Perceived interpersonal synchrony increases empathy: insights from autism spectrum disorder. *Cognition* 146, 8–15. doi: 10.1016/j.cognition.2015.09.007

Landry, R., and Bryson, S. E. (2004). Impaired disengagement of attention in young children with autism. *J. Child Psychol. Psychiatry* 45, 1115–1122. doi: 10.1111/j.1469-7610.2004.00304.x

Laycock, R., Crewther, S. G., and Chouinard, P. A. (2020). Blink and you will miss it: a core role for fast and dynamic visual processing in social impairments in autism spectrum disorder. *Curr. Dev. Disord. Rep.* 7, 237–248. doi: 10.1007/s40474-020-00220-y

Le, Q. V., Le, Q. V., Nishimaru, H., Matsumoto, J., Takamura, Y., Hori, E., et al. (2020). A prototypical template for rapid face detection is embedded in the monkey superior colliculus. *Front. Syst. Neurosci.* 14, 5. doi: 10.3389/fnsys.2020.00005

Le, Q. V., Nishimaru, H., Matsumoto, J., Takamura, Y., Nguyen, M. N., Mao, C. V., et al. (2019). Gamma oscillations in the superior colliculus and pulvinar in response to faces support discrimination performance in monkeys. *Neuropsychologia* 128, 87–95. doi: 10.1016/j.neuropsychologia.2017.10.015

Lee, K. H., Tran, A., Turan, Z., and Meister, M. (2020). The sifting of visual information in the superior colliculus. *Elife* 9, e50678. doi: 10.7554/eLife.50678

Lee, R. H., Mills, E. A., Schwartz, N., Bell, M. R., Deeg, K. E., Ruthazer, E. S., et al. (2010). Neurodevelopmental effects of chronic exposure to elevated levels of pro-inflammatory cytokines in a developing visual system. *Neural Dev.* 5, 2. doi: 10.1186/1749-8104-5-2

Lerner, J. S., Li, Y., Valdesolo, P., and Kassam, K. S. (2015). Emotion and decision making. *Annu. Rev. Psychol.* 66, 799–823. doi: 10.1146/annurev-psych-010213-115043

Li, L., Feng, X., Zhou, Z., Zhang, H., Shi, Q., Lei, Z., et al. (2018a). Stress accelerates defensive responses to looming in mice and involves a locus coeruleus-superior colliculus projection. *Curr. Biol.* 28, 859–871.e5. doi: 10.1016/j.cub.2018.02.005

Li, S., Kumar, T., P., Joshee, S., Kirschstein, T., Subburaju, S., et al. (2018b). Endothelial cell-derived GABA signaling modulates neuronal migration and postnatal behavior. *Cell Res.* 28, 221–248. doi: 10.1038/cr.2017.135

Lischinsky, J. E., and Lin, D. (2019). Looming danger: unraveling the circuitry for predator threats. *Trends Neurosci.* 42, 841–842. doi: 10.1016/j.tins.2019.10.004

Liu, X., Chen, C., Liu, Y., Wang, Z., Huang, K., Wang, F., et al. (2018). Gentle handling attenuates innate defensive responses to visual threats. *Front. Behav. Neurosci.* 12, 239. doi: 10.3389/fnbeh.2018.00239

Lomber, S. G. (2002). Learning to see the trees before the forest: Reversible deactivation of the superior colliculus during learning of local and global visual features. *Proc. Nat. Acad. Sci. U.S.A.* 99, 4049–4054. doi: 10.1073/pnas.062551899

London, E. B. (2018). Neuromodulation and a reconceptualization of autism spectrum disorders: using the locus coeruleus functioning as an exemplar. *Front. Neurol.* 9, 1120. doi: 10.3389/fneur.2018.01120

Lorsung, E., Karthikeyan, R., and Cao, R. (2021). Biological timing and neurodevelopmental disorders: a role for circadian dysfunction in autism spectrum disorders. *Front. Neurosci.* 15, 642745. doi: 10.3389/fnins.2021.642745

Markram, K., and Markram, H. (2010). the intense world theory – a unifying theory of the neurobiology of autism. *Front. Hum. Neurosci.* 4, 224. doi: 10.3389/fnhum.2010.00224

Markram, K., Rinaldi, T., Mendola, D. L., Sandi, C., and Markram, H. (2008). Abnormal Fear conditioning and amygdala processing in an animal model of autism. *Neuropsychopharmacology* 33, 901–912. doi: 10.1038/sj.npp.1301453

Martin, A., Babbitt, A., Pickens, A. G., Pickett, B. E., Hill, J. T., and Suli, A. (2022). Single-Cell RNA sequencing characterizes the molecular heterogeneity of the larval zebrafish optic tectum. *Front. Mol. Neurosci.* 15, 818007. doi: 10.3389/fnmol.2022.818007

Maxwell, C. R., Villalobos, M. E., Schultz, R. T., Herpertz-Dahlmann, B., Konrad, K., and Kohls, G. (2015). Atypical laterality of resting gamma oscillations in autism spectrum disorders. *J. Autism Dev. Disord.* 45, 292–297. doi: 10.1007/s10803-013-1842-7

May, P. J. (2006). The mammalian superior colliculus: laminar structure and connections. *Prog. Brain Res.* 151, 321–378. doi: 10.1016/S0079-6123(05)51011-2

May, P. J., McHaffie, J. G., Stanford, T. R., Jiang, H., Costello, M. G., Coizet, V., et al. (2009). Tectonigral projections in the primate: a pathway for pre-attentive sensory input to midbrain dopaminergic neurons. *Euro. J. Neurosci.* 29, 575–587. doi: 10.1111/j.1460-9568.2008.06596.x

McCleery, J. P., Allman, E., Carver, L. J., and Dobkins, K. R. (2007). Abnormal magnocellular pathway visual processing in infants at risk for autism. *Biol. Psychiatry* 62, 1007–1014. doi: 10.1016/j.biopsych.2007.02.009

McCune, L., and Zlatev, J. (2015). Dynamic systems in semiotic development: the transition to reference. *Cogn. Dev.* 36, 161–170. doi: 10.1016/j.cogdev.2015.09.010

McFadyen, J. (2019). Investigating the subcortical route to the amygdala across species and in disordered fear responses. *J. Exp. Neurosci.* 13, 117906951984644. doi: 10.1177/1179069519846445

McFadyen, J., Dolan, R. J., and Garrido, M. I. (2020). The influence of subcortical shortcuts on disordered sensory and cognitive processing. *Nat. Rev. Neurosci.* 21, 264–276. doi: 10.1038/s41583-020-0287-1

Mcgurk, H., and Macdonald, J. (1976). Hearing lips and seeing voices. *Nature* 264, 746–748. doi: 10.1038/264746a0

McNaughton, K. A., and Redcay, E. (2020). Interpersonal synchrony in autism. *Curr. Psychiatry Rep.* 22, 12. doi: 10.1007/s11920-020-1135-8

McPartland, J. C., Webb, S. J., Keehn, B., and Dawson, G. (2011). Patterns of visual attention to faces and objects in autism spectrum disorder. *J. Autism Dev. Disord.* 41, 148–157. doi: 10.1007/s10803-010-1033-8

Mendonça, H. R., Araújo, S. E. S., Gomes, A. L. T., Sholl-Franco, A., da Cunha Faria Melibeu, A., Serfaty, C. A., et al. (2010). Expression of GAP-43 during development and after monocular enucleation in the rat superior colliculus. *Neurosci. Lett.* 477, 23–27. doi: 10.1016/j.neulet.2010.04.027

Meredith, M. A., Wallace, M. T., and Stein, B. E. (1992). Visual, auditory and somatosensory convergence in output neurons of the cat superior colliculus: multisensory properties of the tecto-reticulo-spinal projection. *Exp. Brain Res.* 88, 181–186. doi: 10.1007/BF02259139

Merker, B. (2007). Consciousness without a cerebral cortex: a challenge for neuroscience and medicine. *Behav. Brain Sci.* 30, 63–81. doi: 10.1017/S0140525X07000891

Merker, B. (2013). The efference cascade, consciousness, and its self: Naturalizing the first person pivot of action control. *Front. Psychol.* 4, 501. doi: 10.3389/fpsyg.2013.00501

Merker, B. H. (1980). *The Sentinel Hypothesis: A Role for the Mammalian Superior Colliculus.*

Milne, E., Swettenham, J., Hansen, P., Campbell, R., Jeffries, H., and Plaisted, K. (2002). High motion coherence thresholds in children with autism. *J. Child Psychol. Psychiatry* 43, 255–263. doi: 10.1111/1469-7610.00018

Mink, J. W., and Mandelbaum, D. E. (2006). "Stereotypies and repetitive behaviors: Clinical assessment and brain basis," in *Autism: A Neurological Disorder of Early Brain Development*, 1st Edn, eds R. Tuchman and I. Rapin (London: Mac Keith Press), 63–78.

Morgan, M., and Hills, P. J. (2019). Correlations between holistic processing, autism quotient, extraversion, and experience and the own-gender bias in face recognition. *PLoS ONE* 14, e0209530. doi: 10.1371/journal.pone.0209530

Morie, K. P., Jackson, S., Zhai, Z. W., Potenza, M. N., and Dritschel, B. (2019). Mood disorders in high-functioning autism: the importance of alexithymia and emotional regulation. *J. Autism Dev. Disord.* 49, 2935–2945. doi: 10.1007/s10803-019-04020-1

Morton, J., and Johnson, M. H. (1991). CONSPEC and CONLERN: a two-process theory of infant face recognition. *Psychol. Rev.* 98, 164–181. doi: 10.1037/0033-295X.98.2.164

Mottron, L., and Burack, J. A. (2001). "Enhanced perceptual functioning in the development of autism," in *The Development of Autism: Perspectives From Theory and Research*, eds J. A. Burack, T. Charman, N. Yirmiya, P. R. Zelazo (Lawrence Erlbaum Associates Publishers), 131–148. Available online at: https://psycnet.apa.org/record/2001-01233-007

Mukaddes, N. M., Kilincaslan, A., Kucukyazici, G., Sevketoglu, T., and Tuncer, S. (2007). Autism in visually impaired individuals. *Psychiatry Clin. Neurosci.* 61, 39–44. doi: 10.1111/j.1440-1819.2007.01608.x

Mul, C., Stagg, S. D., Herbelin, B., and Aspell, J. E. (2018). The feeling of me feeling for you: interoception, alexithymia and empathy in autism. *J. Autism Dev. Disord.* 48, 2953–2967. doi: 10.1007/s10803-018-3564-3

Mulckhuyse, M. (2018). The influence of emotional stimuli on the oculomotor system: a review of the literature. *Cogn. Affect. Behav. Neurosci.* 18, 411–425. doi: 10.3758/s13415-018-0590-8

Murphy, J., Brewer, R., Catmur, C., and Bird, G. (2017). Interoception and psychopathology: a developmental neuroscience perspective. *Dev. Cogn. Neurosci.* 23, 45–56. doi: 10.1016/j.dcn.2016.12.006

Murray, D., Lesser, M., and Lawson, W. (2005). Attention, monotropism and the diagnostic criteria for autism. *Autism* 9, 139–156. doi: 10.1177/1362361305051398

Nakamura, T., Matsumoto, J., Takamura, Y., Ishii, Y., Sasahara, M., Ono, T., et al. (2015). Relationships among parvalbumin-immunoreactive neuron density, phase-locked gamma oscillations, and autistic/schizophrenic symptoms in PDGFR-β knock-out and control mice. *PLoS ONE* 10, e0119258. doi: 10.1371/journal.pone.0119258

Nassi, J. J., and Callaway, E. M. (2009). Parallel processing strategies of the primate visual system. *Nat. Rev. Neurosci.* 10, 360–372. doi: 10.1038/nrn2619

Naumann, S., Senftleben, U., Santhosh, M., McPartland, J., and Webb, S. J. (2018). Neurophysiological correlates of holistic face processing in adolescents with and without autism spectrum disorder. *J. Neurodev. Disord.* 10, 27. doi: 10.1186/s11689-018-9244-y

Ngan, N. H., Matsumoto, J., Takamura, Y., Tran, A. H., Ono, T., and Nishijo, H. (2015). Neuronal correlates of attention and its disengagement in the superior colliculus of rat. *Front. Integrat. Neurosci.* 9, 9. doi: 10.3389/fnint.2015.00009

NIDA-Network, Di Giorgio, E., Frasnelli, E., Rosa Salva, O., Luisa Scattoni, M., Puopolo, M., et al. (2016). Difference in visual social predispositions between newborns at low- and high-risk for autism. *Sci. Rep.* 6, 26395. doi: 10.1038/srep26395

Niu, X., Huang, S., Yang, S., Wang, Z., Li, Z., and Shi, L. (2020). Comparison of pop-out responses to luminance and motion contrasting stimuli of tectal neurons in pigeons. *Brain Res.* 1747, 147068. doi: 10.1016/j.brainres.2020.147068

ONGIG. (n.d.). *Famous People with Autism.* (n.d.). Available online at: https://blog.ongig.com/diversity-and-inclusion/famous-people-with-autism/ (accessed May 28, 2020).

Ozonoff, S., and Iosif, A.-M. (2019). Changing conceptualizations of regression: what prospective studies reveal about the onset of autism spectrum disorder. *Neurosci. Biobehav. Rev.* 100, 296–304. doi: 10.1016/j.neubiorev.2019.03.012

Palmer, C. J., Lawson, R. P., and Hohwy, J. (2017). Bayesian approaches to autism: towards volatility, action, and behavior. *Psychol. Bull.* 143, 521–542. doi: 10.1037/bul0000097

Panksepp, J., and Biven, L. (2012). *The Archaeology of Mind: Neuroevolutionary Origins of Human Emotions, 1st edn*. New York, NY: W. W. Norton.

Paolucci, C. (2020). "A radical enactivist approach to social cognition," in *The Extended Theory of Cognitive Creativity, Vol. 23*, eds A. Pennisi, and A. Falzone (Cham: Springer International Publishing), 59–74. doi: 10.1007/978-3-030-22090-7_4

Penfield, W. (1952). Epileptic automatism and the centrencephalic integrating system. *Res. Publ. Assoc. Res. Nerv. Ment. Dis.* 30, 513–528.

Petry, H. M., and Bickford, M. E. (2019). The second visual system of the tree shrew. *J. Comp. Neurol.* 527, 679–693. doi: 10.1002/cne.24413

Pitti, A., Kuniyoshi, Y., Quoy, M., and Gaussier, P. (2013). Modeling the minimal newborn's intersubjective mind: the visuotopic-somatotopic alignment hypothesis in the superior colliculus. *PLoS ONE* 8, e69474. doi: 10.1371/journal.pone.0069474

Rapin, I. (2006). "Atypical sensory/perceptual responsiveness," in *Autism: A Neurological Disorder of Early Brain Development, 1st edn*, eds R. Tuchman, I. Rapin (London: Mac Keith Press), 202–230.

Rapin, I., and Allen, D. A. (1983). "Developmental language disorders: nosologic considerations," in *Neuropsychology of Language, Reading, and Spelling*,ed U. Kirk (New York, NY: Academic), 155–184. doi: 10.1016/B978-0-12-409680-6.50014-7

Rapin, I., and Dunn, M. (2003). Update on the language disorders of individuals on the autistic spectrum. *Brain Dev.* 25, 166–172. doi: 10.1016/S0387-7604(02)00191-2

Rapin, I., and Tuchman, R. (2006). "Where we are: overview and definitions," in *Autism: A Neurological Disorder of Early Brain Development*, eds R. Tuchman, and I. Rapin (London: Mac Keith Press), 1–18.

Redgrave, P. (2010). Interactions between the midInteractions between the midbrain superior colliculus and the basal ganglia. *Front. Neuroanat.* 4, 132. doi: 10.3389/fnana.2010.00132

Reinhard, K., Li, C., Do, Q., Burke, E. G., Heynderickx, S., and Farrow, K. (2019). A projection specific logic to sampling visual inputs in mouse superior colliculus. *Elife* 8, e50697. doi: 10.7554/eLife.50697.sa2

Richard, A. E., Lajiness-O'Neill, R. R., and Bowyer, S. M. (2013). Impaired prefrontal gamma band synchrony in autism spectrum disorders during gaze cueing. *NeuroReport* 24, 894–897. doi: 10.1097/WNR.0000000000000015

Robertson, C. E., Ratai, E.-M., and Kanwisher, N. (2016). Reduced GABAergic action in the autistic brain. *Curr. Biol.* 26, 80–85. doi: 10.1016/j.cub.2015.11.019

Rosa Salva, O., Mayer, U., and Vallortigara, G. (2015). Roots of a social brain: developmental models of emerging animacy-detection mechanisms. *Neurosci. Biobehav. Rev.* 50, 150–168. doi: 10.1016/j.neubiorev.2014.12.015

Rosen, T. E., Mazefsky, C. A., Vasa, R. A., and Lerner, M. D. (2018). Co-occurring psychiatric conditions in autism spectrum disorder. *Int. Rev. Psychiatry* 30, 40–61. doi: 10.1080/09540261.2018.1450229

Safar, K., Yuk, V., Wong, S. M., Leung, R. C., Anagnostou, E., and Taylor, M. J. (2020). Emotional face processing in autism spectrum disorder: effects in gamma connectivity. *Biol. Psychol.* 149, 107774. doi: 10.1016/j.biopsycho.2019.107774

Sandre, P. C., da Silva Chagas, L., de Velasco, P. C., Galvani, R. G., Dias Fraga, K. Y., Tavares do Carmo, M., et al. (2021). Chronic nutritional restriction of omega-3 fatty acids induces a pro-inflammatory profile during the development of the rat visual system. *Brain Res. Bull.* 174, 366–378. doi: 10.1016/j.brainresbull.2021.07.001

Sans-Dublanc, A., Chrzanowska, A., Reinhard, K., Lemmon, D., Nuttin, B., Lambert, T., et al. (2021). Optogenetic fUSI for brain-wide mapping of neural activity mediating collicular-dependent behaviors. *Neuron* 109, 1888–1905.e10. doi: 10.1016/j.neuron.2021.04.008

Sathyanesan, A., Zhou, J., Scafidi, J., Heck, D. H., Sillitoe, R. V., and Gallo, V. (2019). Emerging connections between cerebellar development, behaviour and complex brain disorders. *Nat. Rev. Neurosci.* 20, 298–313. doi: 10.1038/s41583-019-0152-2

Sato, W., Kochiyama, T., Uono, S., and Toichi, M. (2016). Neural mechanisms underlying conscious and unconscious attentional shifts triggered by eye gaze. *Neuroimage* 124, 118–126. doi: 10.1016/j.neuroimage.2015.08.061

Sato, W., Uono, S., Okada, T., and Toichi, M. (2010). Impairment of unconscious, but not conscious, gaze-triggered attention orienting in asperger's disorder. *Res. Autism Spectr. Disord.* 4, 782–786. doi: 10.1016/j.rasd.2010.02.002

Scheiner, C. A., Kratz, K. E., Guido, W., and Mize, R. R. (2001). Prenatal and postnatal expression of nitric oxide in the developing kitten superior colliculus revealed with NADPH diaphorase histochemistry. *Vis. Neurosci.* 18, 43–54. doi: 10.1017/S0952523801181046

Schneider, K. A. (2005). Visual responses of the human superior colliculus: a high-resolution functional magnetic resonance imaging study. *J. Neurophysiol.* 94, 2491–2503. doi: 10.1152/jn.00288.2005

Schore, A. N. (1994). *Affect Regulation and the Origin of the Self: The Neurobiology of Emotional Development.* Hillsdale, NJ: L. Erlbaum Associates.

Schore, A. N. (2021). The interpersonal neurobiology of intersubjectivity. *Front. Psychol.* 12, 648616. doi: 10.3389/fpsyg.2021.648616

Scicolone, G., Ortalli, A. L., and Carri, N. G. (2009). Key roles of ephs and ephrins in retinotectal topographic map formation. *Brain Res. Bull.* 79, 227–247. doi: 10.1016/j.brainresbull.2009.03.008

Senju, A., Kikuchi, Y., Akechi, H., Hasegawa, T., Tojo, Y., Osanai, H., et al. (2011). Atypical modulation of face-elicited saccades in autism spectrum disorder in a double-step saccade paradigm. *Res. Autism Spectr. Disord.* 5, 1264–1269. doi: 10.1016/j.rasd.2011.01.021

Sewards, T. V., and Sewards, M. A. (2002). Innate visual object recognition in vertebrates: Some proposed pathways and mechanisms. *Comp. Biochem. Physiol. Part Mol. Integr. Physiol.* 132, 861–891. doi: 10.1016/S1095-6433(02)00119-8

Sgadò, P., Rosa-Salva, O., Versace, E., and Vallortigara, G. (2018). Embryonic exposure to valproic acid impairs social predispositions of newly-hatched chicks. *Sci. Rep.* 8, 5919. doi: 10.1038/s41598-018-24202-8

Shang, C., Chen, Z., Liu, A., Li, Y., Zhang, J., Qu, B., et al. (2018). Divergent midbrain circuits orchestrate escape and freezing responses to looming stimuli in mice. *Nat. Commun.* 9, 1232. doi: 10.1038/s41467-018-03580-7

Shang, C., Liu, Z., Chen, Z., Shi, Y., Wang, Q., Liu, S., et al. (2015). A parvalbumin-positive excitatory visual pathway to trigger fear responses in mice. *Science* 348, 1472–1477. doi: 10.1126/science.aaa8694

Shanks, J. A., Ito, S., Schaevitz, L., Yamada, J., Chen, B., Litke, A., et al. (2016). Corticothalamic axons are essential for retinal ganglion cell axon targeting to the mouse dorsal lateral geniculate nucleus. *The Journal of Neuroscience* 36, 5252–5263. doi: 10.1523/JNEUROSCI.4599-15.2016

Shephard, E., Milosavljevic, B., Mason, L., Elsabbagh, M., Tye, C., Gliga, T., et al. (2020). Neural and behavioural indices of face processing in siblings of children with autism spectrum disorder (ASD): a longitudinal study from infancy to mid-childhood. *Cortex* 127, 162–179. doi: 10.1016/j.cortex.2020.02.008

Siemann, J. K., Veenstra-VanderWeele, J., and Wallace, M. T. (2020). Approaches to understanding multisensory dysfunction in autism spectrum disorder. *Autism Res.* 13, 1430–1449. doi: 10.1002/aur.2375

Sifneos, P. E. (1973). The prevalence of 'alexithymic' characteristics in psychosomatic patients. *Psychother. Psychosom.* 22, 255–262. doi: 10.1159/000286529

Siviy, S. M., and Panksepp, J. (1985). Dorsomedial diencephalic involvement in the juvenile play of rats. *Behav. Neurosci.* 99, 1103–1113. doi: 10.1037/0735-7044.99.6.1103

Skorich, D. P., Gash, T. B., Stalker, K. L., Zheng, L., and Haslam, S. A. (2017). Exploring the cognitive foundations of the shared attention mechanism: evidence for a relationship between self-categorization and shared attention across the autism spectrum. *J. Autism Dev. Disord.* 47, 1341–1353. doi: 10.1007/s10803-017-3049-9

Skuse, D. (2006). Genetic influences on the neural basis of social cognition. *Philos. Trans. R. Sock. B Biol. Sci.* 361, 2129–2141. doi: 10.1098/rstb.2006.1935

Soares, S. C., Maior, R. S., Isbell, L. A., Tomaz, C., and Nishijo, H. (2017). Fast detector/first responder: interactions between the superior colliculus-pulvinar pathway and stimuli relevant to primates. *Front. Neurosci.* 1167. doi: 10.3389/fnins.2017.00067

Soetedjo, R., Kojima, Y., and Fuchs, A. F. (2019). How cerebellar motor learning keeps saccades accurate. *J. Neurophysiol.* 121, 2153–2162. doi: 10.1152/jn.00781.2018

Solié, C., Contestabile, A., Espinosa, P., Musardo, S., Bariselli, S., Huber, C., et al. (2022). Superior Colliculus to VTA pathway controls orienting response and influences social interaction in mice. *Nat. Commun.* 13:817. doi: 10.1038/s41467-022-28512-4

Stavropoulos, K. K. M., Viktorinova, M., Naples, A., Foss-Feig, J., and McPartland, J. C. (2018). Autistic traits modulate conscious and nonconscious face perception. *Soc. Neurosci.* 13, 40–51. doi: 10.1080/17470919.2016.1248788

Stein, B. E., Stanford, T. R., and Rowland, B. A. (2009). The neural basis of multisensory integration in the midbrain: its organization and maturation. *Hear. Res.* 258, 4–15. doi: 10.1016/j.heares.2009.03.012

Stein, B. E., Stanford, T. R., and Rowland, B. A. (2014). Development of multisensory integration from the perspective of the individual neuron. *Nat. Rev. Neurosci.* 15, 520–535. doi: 10.1038/nrn3742

Stevenson, R. A., Siemann, J. K., Schneider, B. C., Eberly, H. E., Woynaroski, T. G., Camarata, S. M., et al. (2014). Multisensory temporal integration in autism spectrum disorders. *J. Neurosci.* 34, 691–697. doi: 10.1523/JNEUROSCI.3615-13.2014

Takesian, A. E., and Hensch, T. K. (2013). Balancing plasticity/stability across brain development. *Prog. Brain Res.* 207, 3–34. doi: 10.1016/B978-0-444-63327-9.00001-1

Tamietto, M. (2011). Sentinels in the visual system. *Front. Behav. Neurosci.* 5, 6. doi: 10.3389/fnbeh.2011.00006

Thaler, H., Albantakis, L., and Schilbach, L. (2021). Social cognitive and interactive abilities in autism. *PsyArXiv [Preprint]*. doi: 10.31234/osf.io/et8uv

Thurat, C., N'Guyen, S., and Girard, B. (2015). Biomimetic race model of the loop between the superior colliculus and the basal ganglia: subcortical selection of saccade targets. *Neural Netw.* 67, 54–73. doi: 10.1016/j.neunet.2015.02.004

Tokuoka, K., Kasai, M., Kobayashi, K., and Isa, T. (2020). Anatomical and electrophysiological analysis of cholinergic inputs from the parabigeminal nucleus to the superficial superior colliculus. *J. Neurophysiol.* 124, 1968–1985. doi: 10.1152/jn.00148.2020

Torres, E. B., Brincker, M., Isenhower, R. W., Yanovich, P., Stigler, K. A., Nurnberger, J. I., et al. (2013). Autism: the micro-movement perspective. *Front. Integrat. Neurosci.* 7, 32. doi: 10.3389/fnint.2013.00032

Trevisan, D. A., Parker, T., and McPartland, J. C. (2021). First-Hand accounts of interoceptive difficulties in autistic adults. *J. Autism Dev. Disord.* 51, 3483–3491. doi: 10.1007/s10803-020-04811-x

Tripathi, M. K., Kartawy, M., and Amal, H. (2020). The role of nitric oxide in brain disorders: autism spectrum disorder and other psychiatric, neurological, and neurodegenerative disorders. *Redox Biol.* 34, 101567. doi: 10.1016/j.redox.2020.101567

Triplett, J. W., and Feldheim, D. A. (2012). Eph and ephrin signaling in the formation of topographic maps. *Semin. Cell Dev. Biol.* 23, 7–15. doi: 10.1016/j.semcdb.2011.10.026

Triplett, J. W., Phan, A., Yamada, J., and Feldheim, D. A. (2012). Alignment of multimodal sensory input in the superior colliculus through a gradient-matching mechanism. *J. Neurosci.* 32, 5264–5271. doi: 10.1523/JNEUROSCI.0240-12.2012

Trobiani, L., Meringolo, M., Diamanti, T., Bourne, Y., Marchot, P., Martella, G., et al. (2020). The neuroligins and the synaptic pathway in autism spectrum disorder. *Neurosci. Biobehav. Rev.* 119, 37–51. doi: 10.1016/j.neubiorev.2020.09.017

Tuchman, R (Ed.). (2006). *Autism: A Neurological Disorder of Early Brain Development*. London: MacKeith Press for the International Child Neurology Association.

Unruh, K. E., Sasson, N. J., Shafer, R. L., Whitten, A., Miller, S. J., Turner-Brown, L., et al. (2016). Social orienting and attention is influenced by the presence of competing nonsocial information in adolescents with autism. *Front. Neurosci.* 10, 586. doi: 10.3389/fnins.2016.00586

Ursino, M., Cuppini, C., and Magosso, E. (2014). Neurocomputational approaches to modelling multisensory integration in the brain: a review. *Neural Netw.* 60, 141–165. doi: 10.1016/j.neunet.2014.08.003

Van der Hallen, R., Evers, K., Brewaeys, K., Van den Noortgate, W., and Wagemans, J. (2015). Global processing takes time: a meta-analysis on local–global visual processing in ASD. *Psychol. Bull.* 141, 549–573. doi: 10.1037/bul0000004

Venkatraman, A., Edlow, B. L., and Immordino-Yang, M. H. (2017). The brainstem in emotion: a review. *Front. Neuroanat.* 11, 15. doi: 10.3389/fnana.2017.00015

Vértes, P. E., and Bullmore, E. T. (2015). Annual research review: growth connectomics - the organization and reorganization of brain networks during normal and abnormal development. *J. Child Psychol. Psychiatry* 56, 299–320. doi: 10.1111/jcpp.12365

Villalobos, C. A., Wu, Q., Lee, P. H., May, P. J., and Basso, M. A. (2018). Parvalbumin and GABA microcircuits in the mouse superior colliculus. *Front. Neural Circuits* 12, 35. doi: 10.3389/fncir.2018.00035

Vuilleumier, P. (2015). Affective and motivational control of vision. *Curr. Opin. Neurol.* 28, 29–35. doi: 10.1097/WCO.0000000000000159

Vuilleumier, P., Armony, J. L., Driver, J., and Dolan, R. J. (2003). Distinct spatial frequency sensitivities for processing faces and emotional expressions. *Nat. Neurosci.* 6, 624–631. doi: 10.1038/nn1057

Waguespack, H. F., Aguilar, B. L., Malkova, L., and Forcelli, P. A. (2020). Inhibition of the deep and intermediate layers of the superior colliculus disrupts sensorimotor gating in monkeys. *Front. Behav. Neurosci.* 14, 610702. doi: 10.3389/fnbeh.2020.610702

Wallace, M. T., Roberson, G. E., Hairston, W. D., Stein, B. E., Vaughan, J. W., and Schirillo, J. A. (2004). Unifying multisensory signals across time and space. *Exp. Brain Res.* 158, 252–258. doi: 10.1007/s00221-004-1899-9

Wang, Z., Yu, L., Xu, J., Stein, B. E., and Rowland, B. A. (2020). Experience creates the multisensory transform in the superior colliculus. *Front. Integr. Neurosci.* 14, 18. doi: 10.3389/fnint.2020.00018

Watt, D. F. (2007). Affirmative-action for the brainstem in the neuroscience of consciousness: the zeitgeist of the brainstem as a "dumb arousal" system. *Behav. Brain Sci.* 30, 108–110. doi: 10.1017/S0140525X07001161

Wei, P., Liu, N., Zhang, Z., Liu, X., Tang, Y., He, X., et al. (2015). Processing of visually evoked innate fear by a non-canonical thalamic pathway. *Nat. Commun.* 6, 6756. doi: 10.1038/ncomms7756

Wigham, S., Barton, S., Parr, J. R., and Rodgers, J. (2017). A systematic review of the rates of depression in children and adults with high-functioning autism spectrum disorder. *J. Ment. Health Res. Intellect. Disabil.* 10, 267–287. doi: 10.1080/19315864.2017.1299267

Williams, G., King, J., Cunningham, M., Stephan, M., Kerr, B., and Hersh, J. H. (2001). Fetal valproate syndrome and autism: additional evidence of an association. *Dev. Med. Child Neurol.* 43, 202. doi: 10.1111/j.1469-8749.2001.tb00188.x

Wilson, R. A., and Foglia, L. (2017). "Embodied cognition," in *The Stanford Encyclopedia Philosophy*, ed E. N. Zalta (Spring). Available online at: https://plato.stanford.edu/archives/spr2017/entries/embodied-cognition/

Wöhr, M., Orduz, D., Gregory, P., Moreno, H., Khan, U., Vörckel, K. J., et al. (2015). Lack of parvalbumin in mice leads to behavioral deficits relevant to all human autism core symptoms and related neural

morphofunctional abnormalities. *Transl. Psychiatry* 5, e525. doi: 10.1038/tp.2015.19

Xu, J., Sun, X., Zhou, X., Zhang, J., and Yu, L. (2014). The cortical distribution of multisensory neurons was modulated by multisensory experience. *Neuroscience* 272, 1–9. doi: 10.1016/j.neuroscience.2014.04.068

Zhou, Z., Liu, X., Chen, S., Zhang, Z., Liu, Y., Montardy, Q., et al. (2019). A VTA GABAergic neural circuit mediates visually evoked innate defensive responses. *Neuron* 103, 473–488.e6. doi: 10.1016/j.neuron.2019.05.027

Conflict of Interest: The author declares that the research was conducted in the absence of any commercial or financial relationships that could be construed as a potential conflict of interest.

Publisher's Note: All claims expressed in this article are solely those of the authors and do not necessarily represent those of their affiliated organizations, or those of the publisher, the editors and the reviewers. Any product that may be evaluated in this article, or claim that may be made by its manufacturer, is not guaranteed or endorsed by the publisher.

Advantages of publishing in Frontiers

OPEN ACCESS
Articles are free to read for greatest visibility and readership

FAST PUBLICATION
Around 90 days from submission to decision

HIGH QUALITY PEER-REVIEW
Rigorous, collaborative, and constructive peer-review

TRANSPARENT PEER-REVIEW
Editors and reviewers acknowledged by name on published articles

Frontiers
Avenue du Tribunal-Fédéral 34
1005 Lausanne | Switzerland

Visit us: www.frontiersin.org
Contact us: frontiersin.org/about/contact

REPRODUCIBILITY OF RESEARCH
Support open data and methods to enhance research reproducibility

DIGITAL PUBLISHING
Articles designed for optimal readership across devices

FOLLOW US
@frontiersin

IMPACT METRICS
Advanced article metrics track visibility across digital media

EXTENSIVE PROMOTION
Marketing and promotion of impactful research

LOOP RESEARCH NETWORK
Our network increases your article's readership